RECENT ADVANCES IN ORAL IMMUNITY

EDITED BY: Avi-Hai Hovav, Asaf Wilensky and Jean-Pierre Allam
PUBLISHED IN: Frontiers in Immunology

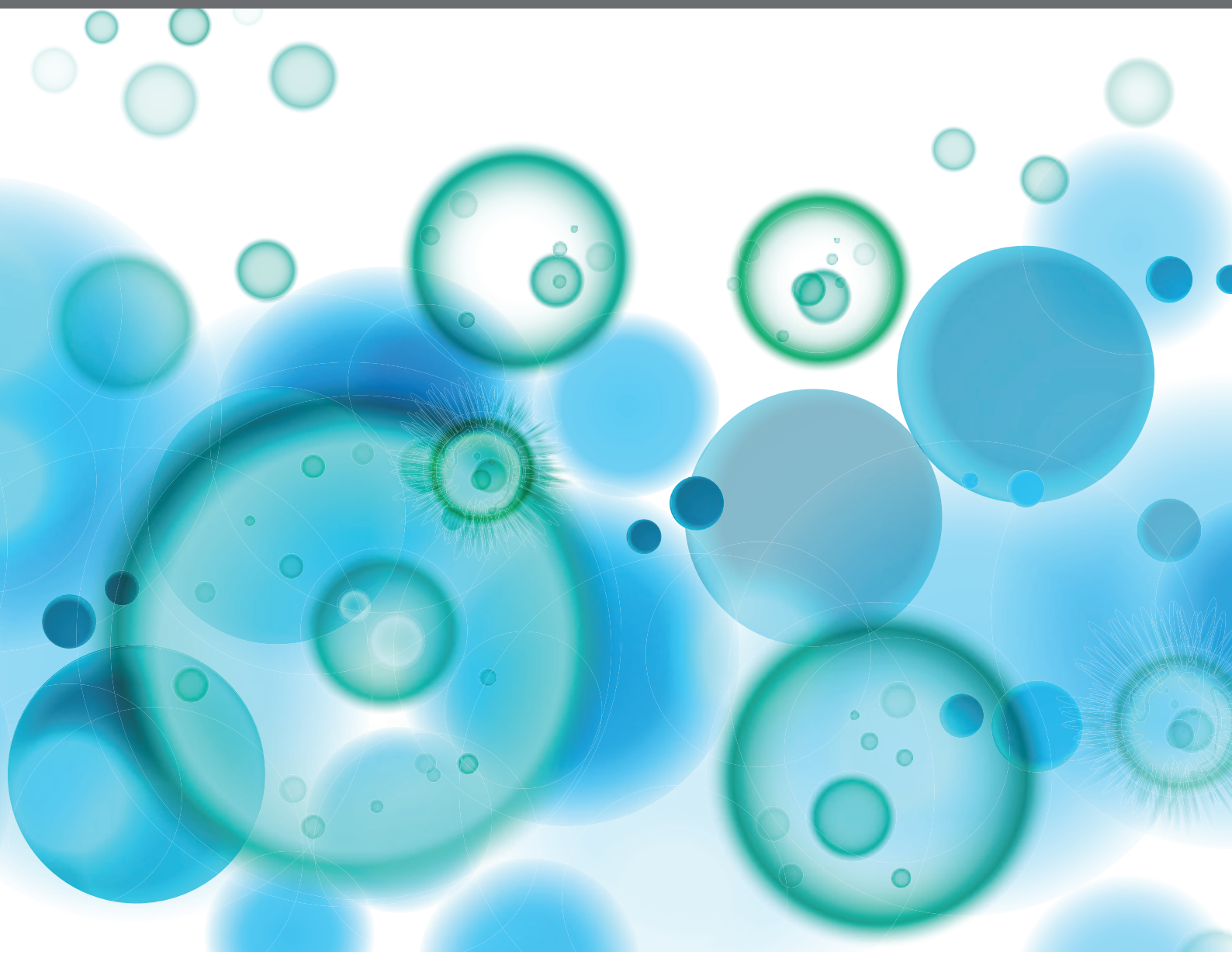

frontiers Research Topics

ISSN 1664-8714
ISBN 978-2-88971-135-2
DOI 10.3389/978-2-88971-135-2

About Frontiers

Frontiers is more than just an open-access publisher of scholarly articles: it is a pioneering approach to the world of academia, radically improving the way scholarly research is managed. The grand vision of Frontiers is a world where all people have an equal opportunity to seek, share and generate knowledge. Frontiers provides immediate and permanent online open access to all its publications, but this alone is not enough to realize our grand goals.

Frontiers Journal Series

The Frontiers Journal Series is a multi-tier and interdisciplinary set of open-access, online journals, promising a paradigm shift from the current review, selection and dissemination processes in academic publishing. All Frontiers journals are driven by researchers for researchers; therefore, they constitute a service to the scholarly community. At the same time, the Frontiers Journal Series operates on a revolutionary invention, the tiered publishing system, initially addressing specific communities of scholars, and gradually climbing up to broader public understanding, thus serving the interests of the lay society, too.

Dedication to Quality

Each Frontiers article is a landmark of the highest quality, thanks to genuinely collaborative interactions between authors and review editors, who include some of the world's best academicians. Research must be certified by peers before entering a stream of knowledge that may eventually reach the public - and shape society; therefore, Frontiers only applies the most rigorous and unbiased reviews.
Frontiers revolutionizes research publishing by freely delivering the most outstanding research, evaluated with no bias from both the academic and social point of view. By applying the most advanced information technologies, Frontiers is catapulting scholarly publishing into a new generation.

What are Frontiers Research Topics?

Frontiers Research Topics are very popular trademarks of the Frontiers Journals Series: they are collections of at least ten articles, all centered on a particular subject. With their unique mix of varied contributions from Original Research to Review Articles, Frontiers Research Topics unify the most influential researchers, the latest key findings and historical advances in a hot research area! Find out more on how to host your own Frontiers Research Topic or contribute to one as an author by contacting the Frontiers Editorial Office: frontiersin.org/about/contact

RECENT ADVANCES IN ORAL IMMUNITY

Topic Editors:
Avi-Hai Hovav, Hebrew University of Jerusalem, Israel
Asaf Wilensky, Hadassah Medical Center, Israel
Jean-Pierre Allam, University Hospital Bonn, Germany

The oral mucosa is a challenging environment from an immunological perspective, containing discrete niches with a unique architecture and function that requires precise adjustment of the immune system. Being the port of entry to the gastrointestinal and respiratory tracts, the oral cavity is also constantly challenged by antigens derived from air and food. Moreover, the oral cavity is the sole tissue of the body harboring a hard surface (i.e. the tooth) that is exposed to the hostile external environment, resulting in the formation of a complex biofilm that has local and systemic effects. To deal with such challenges, the oral immune system aims to prevent the invasion of pathogens/harmful antigens and to tolerate non-pathogenic counterparts in order to maintain homeostasis.

In recent years, numerous studies have addressed these fundamental issues, revealing sophisticated mechanisms engaged by the immune system to maintain oral mucosal homeostasis and to combat various immunological insults. Some of these studies have identified novel immunological mechanisms, emphasizing the uniqueness of the oral immune system and the necessity to further investigate its functions.

Citation: Hovav, A.-H., Wilensky, A., Allam, J.-P., eds. (2021). Recent Advances in Oral Immunity. Lausanne: Frontiers Media SA. doi: 10.3389/978-2-88971-135-2

Table of Contents

frontiers in Immunology

ORIGINAL RESEARCH
published: 18 June 2018
doi: 10.3389/fimmu.2018.01374

Multiple Regulatory Levels of Growth Arrest-Specific 6 in Mucosal Immunity Against an Oral Pathogen

Maria Nassar[1], Yaara Tabib[1], Tal Capucha[1], Gabriel Mizraji[1,2], Tsipora Nir[1], Faris Saba[1], Rana Salameh[1,2], Luba Eli-Berchoer[1], Asaf Wilensky[2], Tal Burstyn-Cohen[1†] and Avi-Hai Hovav[1*†]*

[1] Faculty of Dental Medicine, The Institute of Dental Sciences, Hebrew University, Jerusalem, Israel, [2] Department of Periodontology, Faculty of Dental Medicine, Hadassah Medical Center, Jerusalem, Israel

OPEN ACCESS

Edited by:
Mats Bemark,
University of Gothenburg,
Sweden

Reviewed by:
Claudio Nicoletti,
Università degli Studi di
Firenze, Italy
Gustavo Pompermaier
Garlet, Universidade de
São Paulo, Brazil

***Correspondence:**
Tal Burstyn-Cohen
talbu@ekmd.huji.ac.il;
Avi-Hai Hovav
avihaih@ekmd.huji.ac.il

[†]Co-senior author.

Specialty section:
This article was submitted
to Mucosal Immunity,
a section of the journal
Frontiers in Immunology

Received: 28 March 2018
Accepted: 04 June 2018
Published: 18 June 2018

Citation:
Nassar M, Tabib Y, Capucha T,
Mizraji G, Nir T, Saba F, Salameh R,
Eli-Berchoer L, Wilensky A,
Burstyn-Cohen T and Hovav A-H
(2018) Multiple Regulatory
Levels of Growth Arrest-Specific
6 in Mucosal Immunity
Against an Oral Pathogen.
Front. Immunol. 9:1374.
doi: 10.3389/fimmu.2018.01374

Growth arrest-specific 6 (GAS6) expressed by oral epithelial cells and dendritic cells (DCs) was shown to play a critical role in the maintenance of oral mucosal homeostasis. In this study, we demonstrate that the induction of pathogen-specific oral adaptive immune responses is abrogated in *Gas6*$^{-/-}$ mice. Further analysis revealed that GAS6 induces simultaneously both pro- and anti-inflammatory regulatory pathways upon infection. On one hand, GAS6 upregulates expression of adhesion molecules on blood vessels, facilitating extravasation of innate inflammatory cells to the oral mucosa. GAS6 also elevates expression of CCL19 and CCL21 chemokines and enhances migration of oral DCs to the lymph nodes. On the other hand, expression of pro-inflammatory molecules in the oral mucosa are downregulated by GAS6. Moreover, GAS6 inhibits DC maturation and reduces antigen presentation to T cells by DCs. These data suggest that GAS6 facilitates bi-directional trans-endothelial migration of inflammatory cells and DCs, whereas inhibiting mucosal activation and T-cell stimulation. Thus, the orchestrated complex activity of GAS6 enables the development of a rapid and yet restrained mucosal immunity to oral pathogens.

Keywords: growth arrest-specific 6, infection, oral, mucosa, immunoregulation

INTRODUCTION

The oral cavity is a unique anatomical structure composed of soft and hard tissues, which are continuously exposed to the microbiota. To ensure oral health, the immune system must maintain a symbiotic relationship with the microbiota while preventing invasion of pathogens. This task, however, is not trivial and oral pathogens such as *Porphyromonas gingivalis* can cause a disease by inducing microbial dysbiosis (1). Such an alteration in the composition of oral microbiota results in the development of destructive local immunity, which is associated with systemic adverse complications (2). This demonstrates the delicate equilibrium between the host immune system and microbiota, which likely requires sophisticated mechanisms to maintain a balanced homeostasis.

We recently reported the critical role of growth arrest-specific 6 (GAS6) protein in regulating oral mucosal homeostasis (3). GAS6 and Protein S (PROS1) are ligands of the TYRO3, AXL, and MERTK (TAM) receptor tyrosine kinases (4), which were found to play a role in various biological process including immunoregulation (5). In the oral mucosa, GAS6 and its predominant receptor AXL are expressed by the outermost layers of the epithelium. The expression of GAS6 is induced postnatally by the developing microbiota in a MYD88-dependent fashion (3). GAS6, in turn,

downregulates the activation of epithelial cells, which is required for the establishment of oral mucosal homeostasis. Moreover, GAS6 expressed by dendritic cells (DCs) was found to restrain IL-6 production favoring the generation of T regulatory (Treg) over Th17 cells, further facilitating tolerogenic immune responses against the oral microbiota (3). Whereas these findings highlight a central role of GAS6/AXL signaling in regulating oral mucosal homeostasis, targeting the GAS6/AXL axis by pathogens might induce dysbiosis and subsequent oral pathology. Indeed, *P. gingivalis* is capable of degrading MYD88 in the oral epithelium resulting in a diminished expression of GAS6, AXL, and PROS1 (6). This leads to an oral microbial dysbiosis, elevated production of IFN-α by epithelial cells and temporal "immune paralysis" of the gingiva due to a lack of GAS6 and AXL expression in gingival blood vessels. Furthermore, the unrestrained IFN-α secretion due to the absence of negative regulation by GAS6 and AXL enables the development of excessive Th1-type inflammatory responses which enhance alveolar bone loss (6).

GAS6 thus emerges as a fundamental regulator of oral mucosal immunity at steady state, but also as a potential target for immune dysregulation by oral pathogens. Understanding the precise role of GAS6 during infection is therefore important in order to prevent or modulate local immunity for better protection. Nevertheless, GAS6 is widely expressed by many types of cells in the oral mucosa such as epithelial cells, DCs, and endothelial cells, making it difficult to precisely elucidate its function. This study is aimed at dissecting the mechanisms by which GAS6 engages distinct immunological phases in the oral mucosa upon infection with an oral pathogen.

RESULTS

Diminished Pathogen-Specific Adaptive Immune Responses in *Gas6*$^{-/-}$ Mice

To study the role of GAS6 under inflammatory conditions, we employed the widely used oral infection model causing murine periodontitis. In this model, mice pre-treated with antibiotics are infected three times *via* oral gavage, with the oral pathogen *P. gingivalis* in a carboxymethylcellulose (CMC) solution as a vehicle (**Figure 1A**). To this end, *Gas6*$^{-/-}$ mice and littermate *Gas6*$^{+/+}$ control (WT) mice were infected with *P. gingivalis* or vehicle and analyzed 6 weeks after the last infection. First, we assessed the development of Th1-type immune response by quantifying IFN-γ levels in the supernatants of splenocytes purified from the infected mice and restimulated *ex vivo* with the *P. gingivalis* antigen RgpA. As demonstrated in **Figure 1B**, significant secretion of IFN-γ was detected only in splenocytes of *P. gingivalis*-infected WT mice. Interestingly, besides the inability of restimulated splenocytes of *Gas6*$^{-/-}$ mice to secrete IFN-γ, their baseline secretion of this cytokine was considerably lower in comparison to WT mice. Analyzing *P. gingivalis*-specific antibodies in the serum by ELISA revealed a similar phenomenon. *P. gingivalis*-infected WT mice contained a high circulating antibody titer whereas limited antibody titers were detected in infected and naïve *Gas6*$^{-/-}$ mice (**Figure 1C**). We next examined the induction of oral mucosal immune responses by analyzing the gingiva of the infected mice. Using flow cytometry, we found higher frequencies of CD45^{+} leukocytes in the oral mucosa of *P. gingivalis*-infected WT mice compared to vehicle-treated mice (**Figure 1D**). In *Gas6*$^{-/-}$ mice, on the other hand, no alteration in the percentages of these cells were detected. Further analysis identified an increase in CD4^{+} T cells in the gingiva of infected WT mice, while a fraction of these cells were Treg cells based on their ability to express the transcription factor FOXP3 (**Figures 1E,F**).

The inflammatory responses induced in the gingiva following *P. gingivalis* infection are known to cause alveolar bone loss (7). We therefore quantified residual alveolar bone volume using μCT. Concurring with the above immunological data, a significant loss in the alveolar bone was observed only in *P. gingivalis*-infected WT mice, whereas no loss was found in *Gas6*$^{-/-}$ mice (**Figures 2A,B**). Of note, care should be taken with the interpretation of these results, as GAS6 was reported to play a role in osteoclast activation *in vitro* (8). Nevertheless, the bone loss results were further supported using RT-*q*PCR analysis of RANKL expression (receptor activator of nuclear factor κ-B ligand). This molecule is known to be involved in *P. gingivalis*-induced alveolar bone loss and its expression significantly increased in WT but not *Gas6*$^{-/-}$ mice due to the infection (**Figure 2C**). Taken together, these data demonstrate that GAS6 is essential to elicit *P. gingivalis*-specific adaptive immunity after oral infection.

Differential Regulation of Inflammatory Leukocytes Versus APCs in Infected *Gas6*$^{-/-}$ Mice

To further explore the lack of adaptive immunity in *Gas6*$^{-/-}$ mice, we analyzed early immunological events after infection. For this we infected *Gas6*$^{-/-}$ and WT mice once with *P. gingivalis* to induce an acute inflammation, and examined the development of gingival immune responses in the subsequent days (**Figure 3A**). First, we examined whether the expression of GAS6 and the second TAM ligand, PROS1, in the gingiva is affected by the infection. Using immunofluorescence staining on gingival histological sections and RT-*q*PCR analysis, we found that GAS6 and PROS1 were both upregulated in the oral epithelium (**Figure 3B**). Next, we examined by flow cytometry the content of innate myeloid leukocytes in the gingiva of the infected mice based on the gating strategy described in Figure S1 in Supplementary Material. Three days after the infection, infiltration of CD45^{+} leukocytes, particularly neutrophils and monocytes, into the infected gingiva was seen in WT mice but not in *Gas6*$^{-/-}$ mice (**Figure 3C**). Of note, with regards to monocytes, a significant reduction in this population was observed in the gingiva of infected *Gas6*$^{-/-}$ mice in comparison to the non-infected *Gas6*$^{-/-}$ control group. We then tested gingival MHCII^{+}CD11c^{+} cells representing APCs such as macrophages and DCs, the latter are expected to migrate to the draining lymph node (LN) during the three first days after infection in order to prime T cells and initiate adaptive immunity (9). Surprisingly, unlike neutrophils and monocytes, the frequencies of APCs were not reduced in the gingiva of *Gas6*$^{-/-}$ mice after infection, and in fact, their level markedly increased in the tissue (**Figures 3C,D**). We thus conclude that the absence of GAS6 prevents the infiltration of myeloid leukocytes into the gingiva.

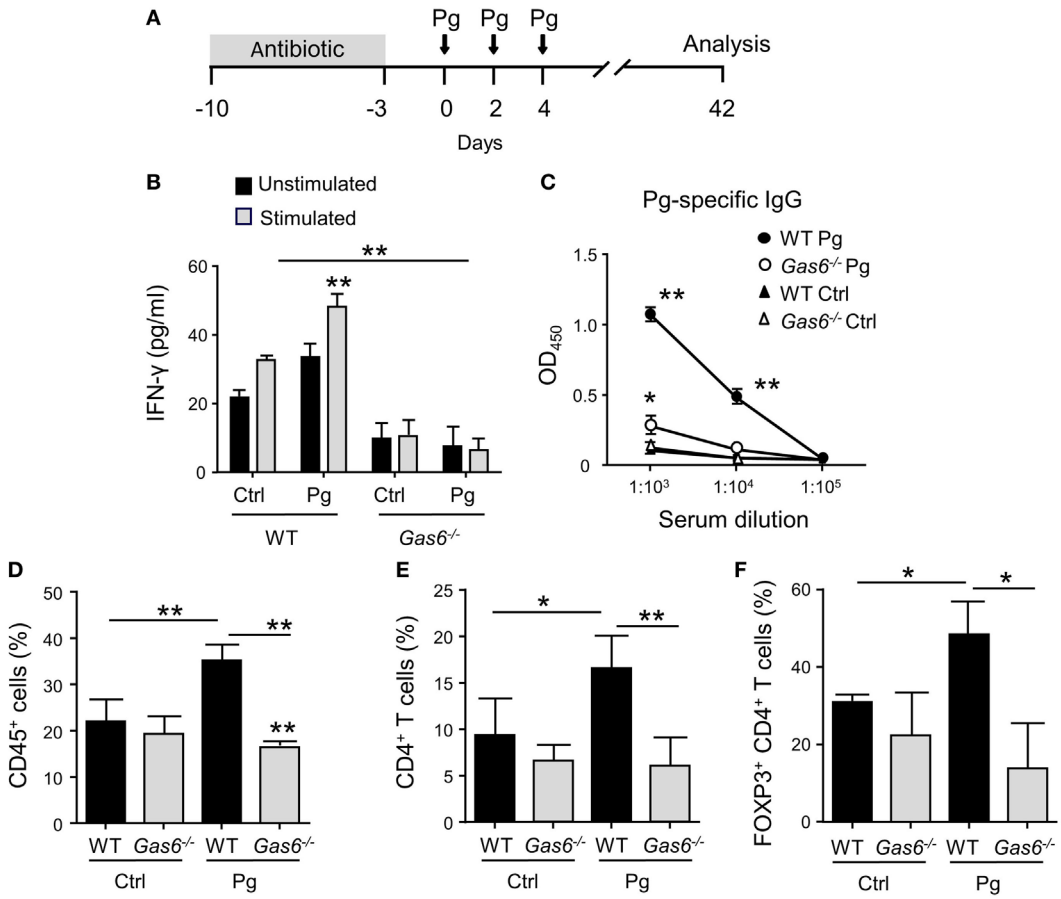

FIGURE 1 | Diminished pathogen-specific adaptive immunity in *Gas6*$^{-/-}$ mice. **(A)** Schematic presentation of the murine periodontitis model used in this study. Antibiotic pre-treated mice were infected *via* oral gavage, three times at 2-day intervals, with 1 × 10^{10} CFU of *Porphyromonas gingivalis* strain 53977 (Pg). Six weeks after the last inoculation, the mice were analyzed. **(B)** IFN-γ production by restimulated splenocytes quantified by ELISA representing the mean value ± SEM (n = 8). **(C)** Pg-specific IgG titers measured by ELISA in the plasma of the mice, representing the mean of OD_{450} values ± SEM (n = 8). **(D–F)** Flow cytometry analysis of the percentages of CD45$^+$ cells **(D)**, CD4$^+$ T cells **(E)**, and FOXP3-expressing CD4$^+$ T regulatory cells **(F)** in the gingival tissues of infected mice (n = 5). Representative data of one out of three independent experiments is shown.

In addition, the increase in the frequency of APCs together with the reduction in the monocyte population, suggests that monocytes might differentiate into APCs in *Gas6*$^{-/-}$ mice upon infection.

The Absence of GAS6 Facilitates Secretion of Pro-Inflammatory Molecules in the Oral Mucosa

The absence of inflammatory cells in the gingiva of infected *Gas6*$^{-/-}$ mice might be due to a diminished production of inflammatory cytokines and chemokines, serving as chemoattractants for these cells. To examine this issue, we measured the gingival expression of the pro-inflammatory cytokines TNF-α and IL-1β as well as the chemokine CCL2. As depicted in **Figure 4A**, upon infection, both WT and *Gas6*$^{-/-}$ mice upregulated the expression of the noted molecules; nevertheless, in *Gas6*$^{-/-}$ mice the expression levels were significantly higher in comparison to WT mice. TNF-α in the serum of *Gas6*$^{-/-}$ infected mice were significantly higher than WT, indicating a systemic reaction to the infection (**Figure 4B**). Furthermore, the percentages of neutrophils in the blood of *Gas6*$^{-/-}$ mice were higher than those detected in infected WT mice or uninfected *Gas6*$^{-/-}$ mice (**Figure 4C**). Collectively, these suggest that GAS6 in the mucosal epithelium downregulates the induction of pro-inflammatory cytokines following infection, implying that its absence should actually facilitate leukocyte infiltration upon infection with *P. gingivalis*.

The Absence of GAS6 Prevents Leukocyte Extravasation Into the Gingiva

Another explanation to the lack of a local innate immune responses in infected *Gas6*$^{-/-}$ mice might be the inability of inflammatory leukocytes to enter the mucosa *via* blood vessels. In this regard, it has been shown that GAS6 is required for leukocytes infiltration in systemic inflammatory models (10). Our previous work also found that GAS6 and its receptor AXL are expressed in arteries of the gingival lamina propria, while repetitive

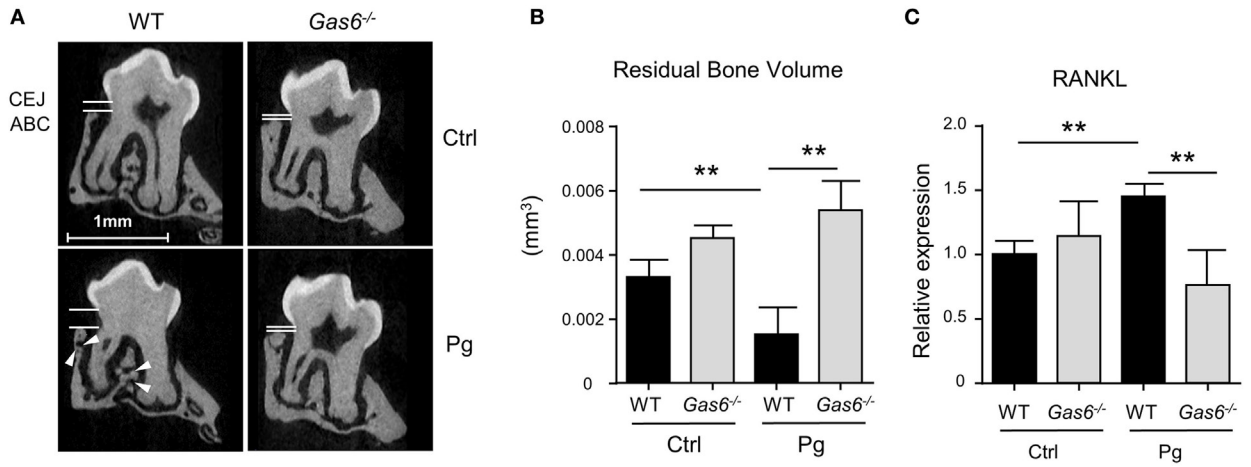

FIGURE 2 | Lack of inflammation-induced bone loss in *Gas6*$^{-/-}$ mice. **(A)** Representative μCT sections of the second upper molar demonstrating the residual bone volume measured from the cemento-enamel junction (CEJ) and alveolar bone crest (ABC). White arrows indicate lesions in the alveolar bone. **(B)** Three-dimensional quantification of the residual alveolar bone. Data are presented as the volume of alveolar bone in the buccal plate and represent the mean of eight mice per group ± SEM. **(C)** Quantification by RT-*q*PCR of the expression levels of RNAKL in the gingiva of infected mice, graphs represent the mean of five mice per group ± SEM. Representative data of one out of two independent experiments is shown.

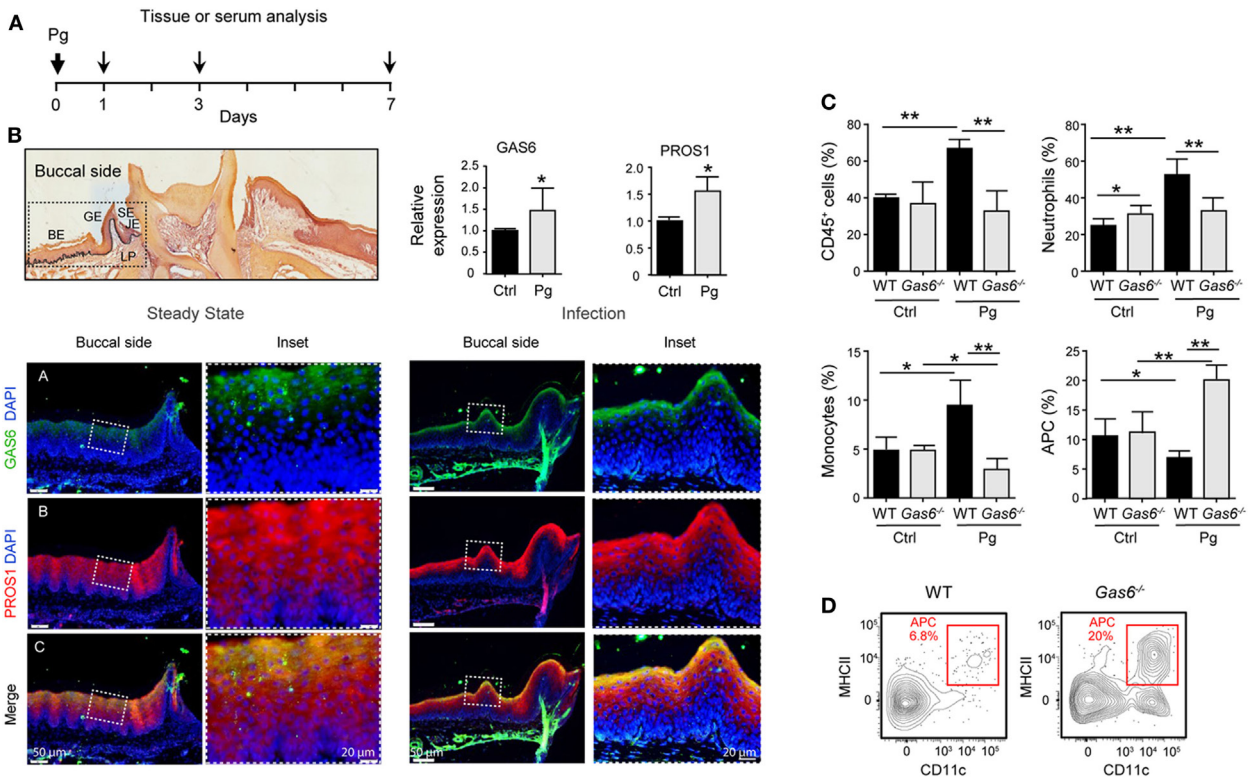

FIGURE 3 | Lack of innate infiltrate in the gingiva of infected *Gas6*$^{-/-}$ mice. **(A)** Schematic presentation of an acute oral infection. Mice were infected once with Pg by oral gavage and analyzed either 1, 3, or 7 days after infection. **(B)** H&E and immunofluorescence stained histological section of the lower jaw and RT-*q*PCR analyses of GAS6 and PROS1 expression in the gingiva of WT mice prior to and 3 days after Pg infection. Bar graphs represent the mean of four mice per group ± SEM. Immunohistochemical staining is shown for GAS6 (green), PROS1 (red) and nuclei are stained with hoechst (blue). Enlarged images of the framed area are shown to the right. **(C)** Percentages of total CD45^{+} cells, neutrophils, monocytes, and APCs in the gingiva 24 h after infection. Bar graphs represent the mean of five mice per group ± SEM. **(D)** Representative FACS plot showing the frequencies of MHCII^{+}CD11c^{+} cells (APCs) in the gingiva of WT and *Gas6*$^{-/-}$ mice 24 h after infection. Representative data of one out of three independent experiments is shown. Abbreviations: BE, buccal epithelium; GE, gingival epithelium; SE, sulcular epithelium; JE, junctional epithelium; LP, lamina propria; GAS6, growth arrest-specific 6.

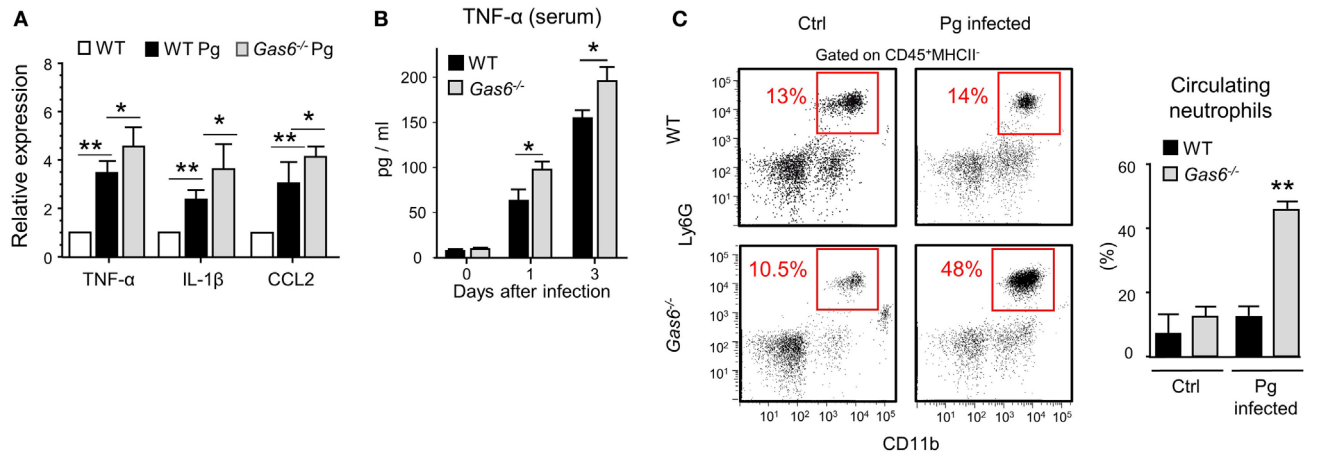

FIGURE 4 | Elevated expression of pro-inflammatory cytokines in *Gas6*$^{-/-}$ mice following infection with Pg. **(A)** Expression levels of TNF-α, IL-1β, and CCL2 in the gingiva 24 h after a single infection with Pg. Data are presented as relative mRNA expression analyzed by RT-*q*PCR and represent the mean of five mice ± SEM. **(B)** Serum levels of TNF-α, on days 0, 1, and 3 days post-infection, measured by ELISA. Graphs represent the mean of five mice ± SEM. Representative data of one out of three independent experiments is shown. **(C)** Peripheral blood samples were collected from naive and infected mice 24 h after infection for flow cytometry analysis. Representative FCAS plots and bar graphs demonstrate the percentages of neutrophils in the blood. Bar graphs represent the mean of five mice per group ± SEM. Representative data of one out of three independent experiments is shown.

infections with *P. gingivalis* down-modulate their expression and prevents innate inflammation (6). We thus examined whether in *Gas6*$^{-/-}$ mice the arrival of innate leukocytes to the oral mucosa is prevented after an acute infection by *P. gingivalis*. First, we analyzed by immunofluorescence analysis the expression of GAS6 and AXL in blood vessels, which were visualized using the CD31-specific antibody (**Figure 5A**). Whereas AXL was found in blood vessels of both naive and infected WT mice, GAS6 was only detected in infected ones. Moreover, the distribution pattern of GAS6 strikingly resembled that of AXL, suggesting that GAS6 might be bound to AXL. To further explore how GAS6 impacts the blood vessels in the oral mucosa under acute inflammatory conditions, we quantified in the gingiva the expression of endothelial adhesion molecules that are known to be upregulated upon infection. As depicted in **Figure 5B**, while expression of P-selectin, ICAM-1, and VCAM-1 were increased in infected WT mice, the expression of these molecules was unchanged by the infection in *Gas6*$^{-/-}$ mice. These findings indicate that GAS6 controls leukocyte infiltration to the gingiva *via* regulating the expression of endothelial adhesion molecules. Nevertheless, since we showed above that the absence of GAS6 resulted in increased production of pro-inflammatory molecules, we analyzed changes in circulating leukocytes at various times after infection. As shown in **Figures 5C,D**, neutrophils and Gr-1^{high} monocytes but not DCs nor Gr-1^{low} monocytes (data not shown) accumulated in the blood of *Gas6*$^{-/-}$ mice 1 and 3 days after infection but returned to normal levels 7 days post-infection. In WT mice, on the other hand, these cells accumulated only in the gingiva during the first 3 days post-infection, returning to basal levels by day 7. Taken together, it can be concluded that GAS6 has opposing roles during bacterial infection. Within the epithelium, upregulation of GAS6 down-modulates the secretion of pro-inflammatory cytokines and chemokines, which are required to induce egression of neutrophils and monocytes from the bone marrow (BM). However, at the same time GAS6 regulates the expression of adhesion molecules in endothelial cells and subsequently prevents leukocyte extravasation into the gingiva.

Migration of Oral DCs to the LNs Is Accelerated by GAS6

The aforementioned data demonstrated that following infection higher frequencies of APCs were found in the gingiva of *Gas6*$^{-/-}$ mice (**Figure 3D**). To examine whether migration of DCs to the LNs was impaired in these mice, we quantified the expression of CCL19 and CCL21, chemokines mediating DC migration to the LNs (11). Using RT-*q*PCR, we found a significant increase in the gingival expression of CCL19 and CCL21 of WT upon infection (**Figure 6A**). By contrast, a reduced expression of both chemokines was detected in *Gas6*$^{-/-}$ mice 1 and 3 days after infection (**Figure 6A**). We next examined whether AXL and GAS6 are expressed on lymphatic endothelial cells (LECs), and if the infection alters their expression pattern. As depicted in **Figure 6B**, at steady state conditions AXL but not GAS6 was expressed by WT LECs that were visualized using staining with anti-LYVE-1 antibody. Upon infection, GAS6 as well as AXL were detected in LECs, suggesting that GAS6 increases permeability similar to blood endothelial cells. These results suggest that DCs might not efficiently migrate to the LNs in infected *Gas6*$^{-/-}$ mice, due to a reduced chemokine production and impaired function of local lymphatic vessels. To address this issue directly, we painted the oral mucosa with an FITC/DBP solution, an approach allowing to track migration of oral DCs into the LNs (FITC-labeled DCs) due to local inflammation induced by the DBP (12). As demonstrated in **Figure 6C**, significantly less FITC-labeled DCs (gated population of CD11c^{intermediate}MHCII^{high} in the LNs) were

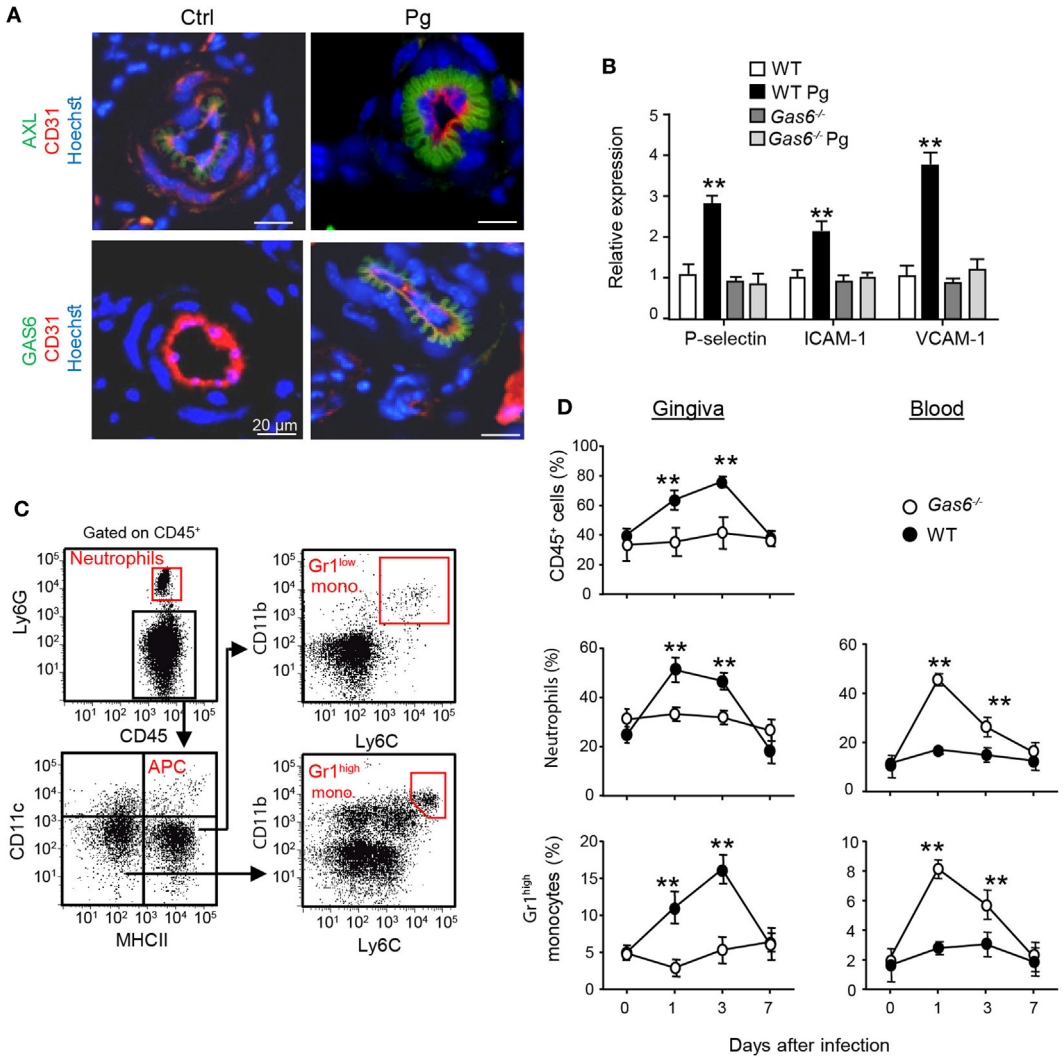

FIGURE 5 | Infiltration of innate leukocytes to the gingiva is blocked in infected *Gas6*$^{-/-}$ mice. **(A)** Immunofluorescence staining of AXL or growth arrest-specific 6 (GAS6) (green), CD31 (red), and hoechst (blue) in gingival lamina propria cross sections of *Pg*-infected and naive WT and *Gas6*$^{-/-}$ mice. Representative images of at least three independent experiments. Scale bars represent 20 µm. **(B)** Expression of P-selectin, ICAM-1, and VCAM-1 in the gingiva of WT and *Gas6*$^{-/-}$ mice 24 h following infection with Pg. Relative mRNA expression levels are presented using RT-*q*PCR analysis representing the mean of five mice per group ± SEM. Representative data of one out of two independent experiments is shown. **(C,D)** Quantification of inflammatory cells in the blood and gingiva following a single infection of WT and *Gas6*$^{-/-}$ mice with Pg. **(C)** Gating strategy to identify neutrophils, APCs, Ly6C^{low}, and Ly6C^{high} monocytes in the blood using flow cytometry analysis. **(D)** Time course analysis of the frequencies of CD45^{+} cells, neutrophils, and Ly6C^{high} monocytes in the blood versus gingiva in WT and *Gas6*$^{-/-}$ mice, representing the mean of five mice per group ± SEM. Representative data of one out of two independent experiments is shown.

detected in *Gas6*$^{-/-}$ compared to WT mice (~50% reduction). No FITC-labeled DCs were found in the population of LN-resident DCs (RLN) or plasmacytoid DCs, confirming that only migratory DCs originating within the oral mucosa were labeled in this assay (Figure S2 in Supplementary Material). Interestingly, despite their reduced migratory levels, DCs of *Gas6*$^{-/-}$ mice, either migratory or RLN DCs, expressed higher levels of MHCII compared to their counterparts in WT mice (**Figure 6C**). Collectively, these data suggest that GAS6 facilitates DC migration to the LNs following infection, contributing to a rapid development of adaptive immunity. The augmentation in MHCII levels on DCs in *Gas6*$^{-/-}$ mice proposes a role for GAS6 also in DC maturation and activation, which led us to explore this possibility.

GAS6 Inhibits DC Maturation and Decreases T-Cell Activation

We previously reported that GAS6 is expressed in DCs and its expression colocalizes with intracellularly expressed MHCII (3). We also have shown that GAS6 had no impact on surface expression levels of MHCII in DCs at steady state. These observations, together with our present finding of elevated MHCII expression after infection, suggest that GAS6 influences DC functions

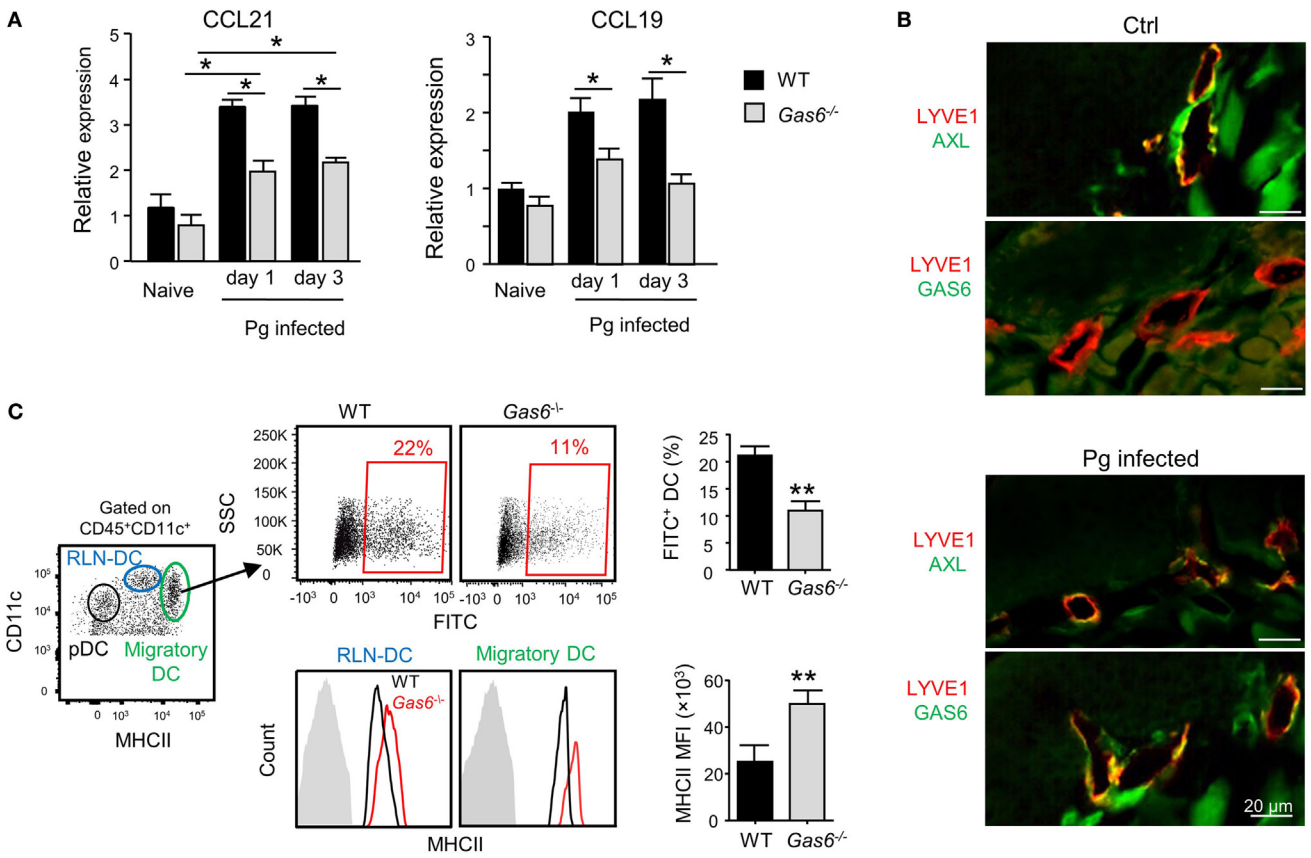

FIGURE 6 | Growth arrest-specific 6 (GAS6) enhances migration of oral dendritic cells (DCs) to the draining lymph nodes (LNs). **(A)** Mice were infected once with Pg and the expression levels of CCL19 and CCL21 chemokines was analyzed in the gingiva using RT-*q*PCR 1 or 3 days later. Data represent the mean of five mice per group ± SEM. **(B)** Immunofluorescence staining of AXL or GAS6 (green) and LYVE1 (red), in gingival lamina propria cross sections of *Pg*-infected and naive WT and *Gas6*$^{-/-}$ mice. Representative images of two independent experiments. **(C)** The oral mucosa of WT and *Gas6*$^{-/-}$ mice were painted with FITC/DBP solution, 2 days later the draining cervical LNs were collected and processed for analysis by flow cytometry. *Left plot*—representative image demonstrating the segregation of CD45^{+}CD11c^{+} cells into distinct DC subsets based on the expression of MHC class II and CD11c (RLN-DC—LN resident DCs; pDC—plasmacytoid DCs). *Upper panel*—representative FACS plots and bar graphs illustrating the percentages of FITC-positive cells among migratory DCs of *Gas6*$^{-/-}$ and WT mice, representing the mean of five mice per group ± SEM. *Lower panel*—representative FCAS histograms showing MHCII expression levels on total migratory DCs and RLN-DCs. Gray histograms represent MHC staining on T cells which do not express MHCII. Bar graphs present the mean florescence intensity (MFI) of MHCII expression on the noted DC populations and represent the mean of five mice per group ± SEM.

under inflammatory conditions. To probe this issue directly, we generated DCs from bone marrow cells (BMDCs) purified from WT and *Gas6*$^{-/-}$ mice, and stimulated them with LPS. Using flow cytometry, we found that MHCII and CD86 expressions were upregulated upon LPS stimulation in both *Gas6*$^{-/-}$ and WT BMDCs; yet, considerably higher levels of these molecules were found in *Gas6*$^{-/-}$ BMDCs (**Figure 7A**). Similar results were obtained in DCs purified from the cervical LNs of WT and *Gas6*$^{-/-}$ mice following LPS stimulation (**Figure 7B**). Interestingly, unlike MHCII and CD86, expression of CCR7 which is required for migration to the LNs was not affected by the absence of GAS6 in LN-purified DCs (**Figure 7B**). Next, we analyzed the ability of DCs to stimulate naive T cells. DCs were enriched from gingiva-draining cervical LNs of *Gas6*$^{-/-}$ and WT mice, and pulsed with MHC class II-restricted $OVA_{223–239}$ or MHC class I-restricted SIINFEKL peptides. The pulsed DCs were then co-cultured for 60 h with CFSE-labeled CD4^{+} OT-II T cells and CD8^{+} OT-I T cells, respectively. A considerable reduction in the CFSE levels was observed by all T cells indicating the capacity of the DCs to induce T-cell proliferation (**Figure 7C**). However, DCs lacking GAS6 had superior capacity to stimulate CD4^{+} T cells as compared to WT mice. Such an effect was not observed for CD8^{+} T cells, which upon stimulation present with proliferation levels equal to either DC population. Furthermore, we measured IFN-γ secretion in the culture supernatants by ELISA and found elevated secretion of this cytokine by CD4^{+} T cells and CD8^{+} T cells in *Gas6*$^{-/-}$ DC cultures in comparison to the WT controls (**Figure 7D**). Taken together, these results demonstrate contrasting roles for GAS6 on DC functions. On one hand, GAS6 expressed by DCs downregulates their maturation and their capability to stimulate T cells. On the other hand, GAS6 enhances the expression of CCL19 and CCL21 in the tissue while not reducing CCR7 expression on activated DCs, thus facilitating DC migration to the LNs and induction of adaptive immunity. This suggests

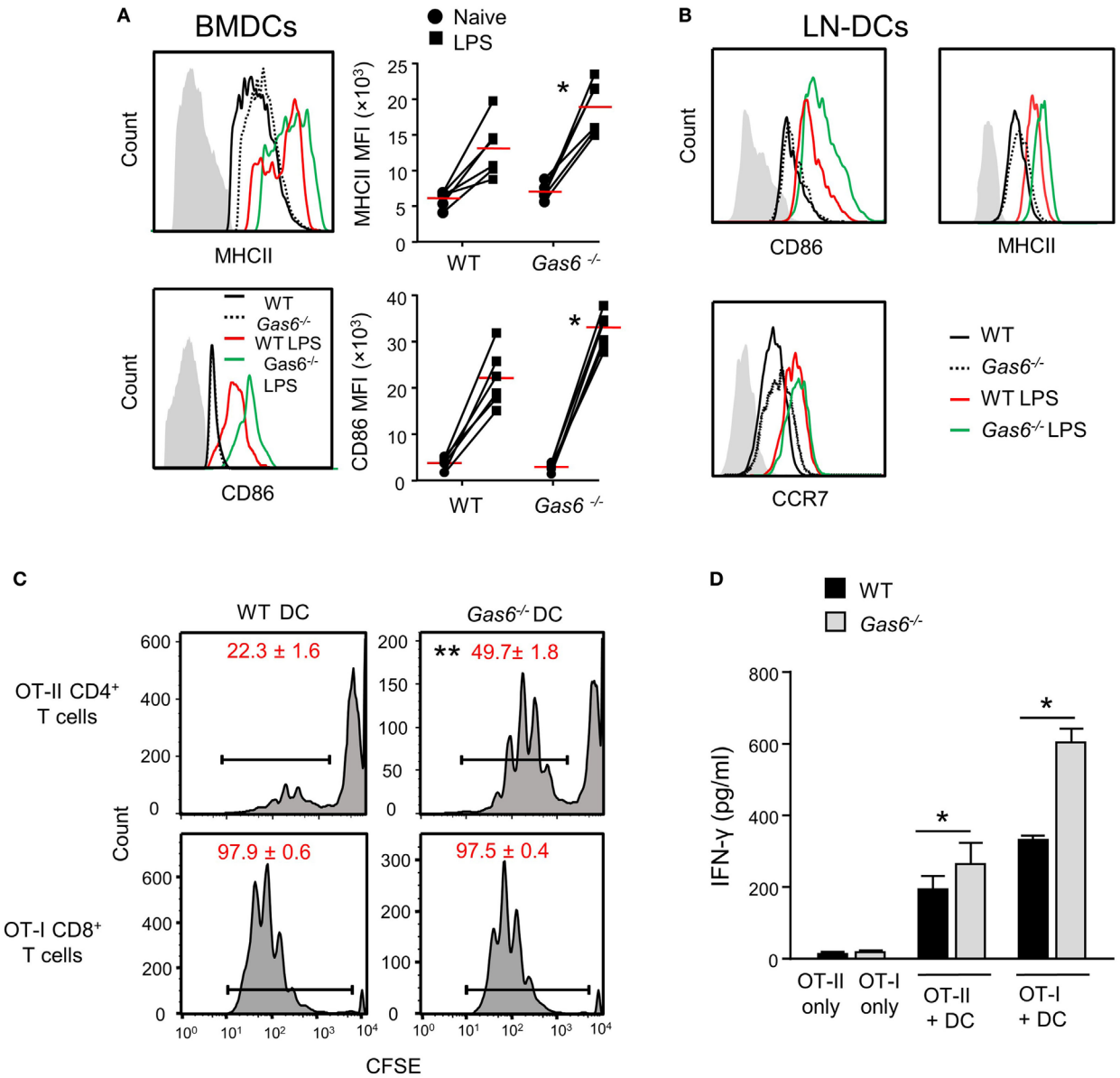

FIGURE 7 | Growth arrest-specific 6 (GAS6) inhibits dendritic cell (DC) maturation and limits T-cell activation by DCs. **(A)** BMDCs generated from WT and *Gas6*$^{-/-}$ mice were stimulated with LPS for 24 h. Representative FACS histograms and graphs demonstrating the expression and mean florescence intensity (MFI) of MHCII (top) and CD86 (bottom) on BMDCs, respectively. Gray histograms represent staining on MHC-negative cells in the culture. **(B)** DCs purified from cervical lymph nodes (LNs) of *Gas6*$^{-/-}$ and WT mice were stimulated with LPS for 24 h. Representative FACS plots demonstrating the expression of CD86, MHCII, and CCR7 are presented. **(C,D)** DCs enriched from cervical LNs of *Gas6*$^{-/-}$ and WT mice were stimulated with LPS and OVA peptides and then co-cultured with naive CFSE-labeled OT-II CD4^{+} T cells or OT-I CD8^{+} T cells. **(C)** Three days post-stimulation the dilution in CFSE levels on the T cells was analyzed by flow cytometry, representative FACS histograms are presented, numbers indicate the mean of three repeats per group ± SEM. **(D)** Bar graphs show the concentrations of IFN-γ secreted to the supernatant by activated CD8^{+} T cells and represent the mean of four repeats per group ± SEM. Representative data of one out of two independent experiments is shown.

that GAS6 accelerates the induction of adaptive immunity by but also restrains its magnitude.

DISCUSSION

In this study, we revealed the complex role of GAS6 in the oral mucosa under inflammatory conditions. Such multifaceted and apparently contrasting activities are likely attributed to the vast expression of GAS6 in various cell types within the oral mucosa. Nonetheless, it can be generalized that GAS6 positively regulates bi-directional trans-endothelial migration of leukocytes into (neutrophils and monocytes) and away (DCs) from the infected mucosa. Conversely, GAS6 negatively regulates the levels of innate and adaptive immune cells recruited to the infection site

(**Figure 8**). Thus, integrating the overall roles of GAS6 upon infection lead us to conclude that GAS6 acts to mount a swift innate immune response and rapid initiation of adaptive immunity, while simultaneously restraining both types of responses.

Oral epithelial cells were shown to express various cytokines and chemokines such as TNF-α, IL-1β, and CCL2 that were upregulated upon infection in our study (13, 14). GAS6 is constitutively expressed in oral epithelial cells and as we recently showed it downregulates the activation of epithelial cells at steady state in order to maintain homeostasis (3). Here, we demonstrate that expression of GAS6 is increased rapidly under inflammatory conditions to inhibit excessive activation of the epithelium, which as we previously reported might have pathological consequences (6). Similar to epithelial cells, GAS6 is also constitutively expressed by macrophages and regulates their steady state function (15). However, upon TLR-mediated activation, expression of GAS6 is decreased enabling the macrophages to mount a potent secretion of pro-inflammatory cytokines and chemokines. These findings further emphasize the versatile functions of GAS6 in immunoregulation and highlight that GAS6 acts in a cell-specific fashion.

Our analysis reveals that GAS6 regulates CCL21 and CCL19 expression in the gingiva and in gingival lymphatic vessels under inflammatory conditions. In contrast to its inhibitory effect on MHCII and CD86 expression on stimulated DCs, GAS6 does not downregulate the expression of their receptor CCR7 on these cells. This demonstrates that the versatile functions of GAS6 in epithelial cells, LECs, and DCs are critically orchestrated to facilitate migration of mature DCs to the LNs *via* the afferent lymphatic vessels (16). To the best of our knowledge, this is the first observation linking GAS6 with activation of the lymphatic system. This lymphatic expression pattern of GAS6 resembles its expression in blood endothelial cells, leading to expression of adhesion molecules. Since LEC also express VCAM-1 and ICAM-1 (17), which were upregulated in the gingiva of infected *Gas6*$^{-/-}$ mice, it is likely that GAS6 also enhances DC migration by enabling endothelial attachment of mature DCs. With regards to chemokine expression, CCL21 is known to be expressed by LECs, and therefore it is likely that GAS6 activates LECs similar to its role on blood endothelial cells. CCL19, on the other hand, is not expressed by LEC but rather by activated DCs, and was proposed to induce their homing to the lymphatics (18). The possibility that in our study GAS6 upregulates CCL19 expression in oral DCs is in line with its incapability to reduce their CCR7 expression (in contrast to the other maturation markers MHCII and CD86), as both CCL19 and CCR7 are required for DC migration to the LNs. In a broader view, the impact of GAS6 on activated DCs suggests that migratory capability (represented by CCL19 and CCR7) and antigen-presentation function (represented by MHCII and CD86) of mature DCs are differentially regulated. In a recent study, PROS1 expressed by T cells was shown to reduce antigen presentation by DCs and to subsequently limit adaptive

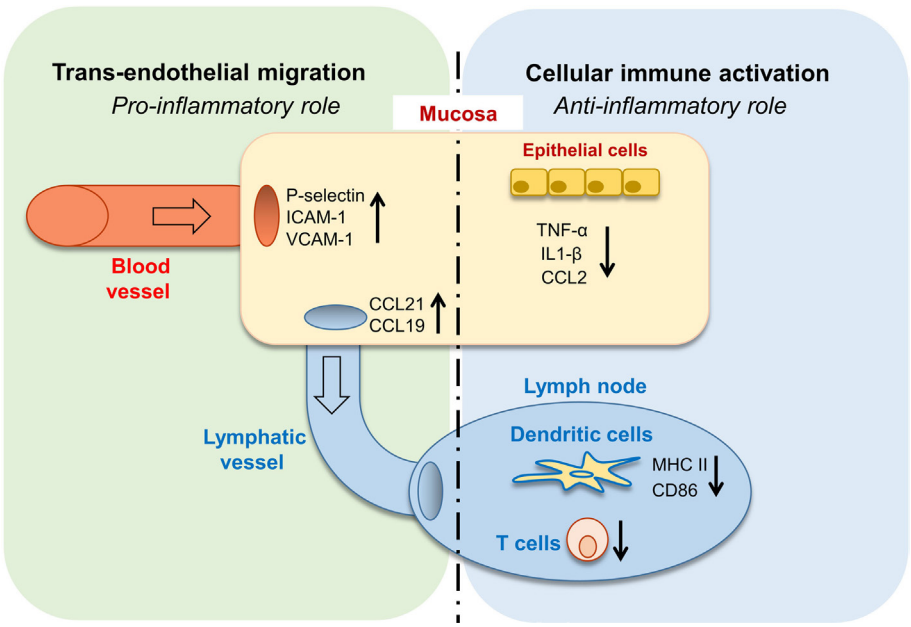

FIGURE 8 | Pro- and anti-inflammatory roles for growth arrest-specific 6 (GAS6) in the oral mucosa. Upon infection, GAS6 facilitates extravasation of neutrophils and Gr1^{high} monocytes to the oral mucosa by upregulating expression of adhesion molecules on blood endothelial cells. GAS6 also enhances migration of mucosal dendritic cells (DCs) to the lymph node by upregulating CCL19/CCL21 expression, chemokines mediating this process *via* interaction with CCR7 on DCs. Both processes involve the GAS6-mediated trans-endothelial migration, indicating its pro-inflammatory function. On the other hand, GAS6 downregulates the production of pro-inflammatory cytokines and chemokines by epithelial cells. In the LN, GAS6 inhibits antigen presentation and T cell activation by DCs, *via* reducing expression of the maturation-associated molecules MHC and CD86. Interestingly, CCR7, an additional molecule associated with DC maturation, is not downregulated by GAS6, thus complementing the upregulation of CCR7 ligands by GAS6 in the mucosa to promote migration. Such apparently opposing roles of GAS6 during infection enable the induction of swift innate inflammatory responses, while facilitating the development of a restrained adaptive immune response.

immunity (19). Here, we showed that DC maturation and antigen presentation is regulated by GAS6 expressed in DCs, thus TAM ligands appear to tightly control adaptive immunity by acting *via* both T cells and DCs.

In vitro stimulation of naive $CD4^+$ T cells but not $CD8^+$ T cells by *Gas6*$^{-/-}$ DCs resulted in a decreased proliferative capacity in comparison to WT DCs. This could be explained by the considerable downregulation of MHCII but not MHCI in *Gas6*$^{-/-}$ DCs upon activation. Nevertheless, in both T cell types, the capability of the cells to secrete IFN-γ was significantly reduced due to the absence of GAS6 in DCs. A recent study has shown that AXL signaling downregulates IL-12 production by DCs (20), a cytokine required for generation of IFN-γ producing T cells (21). In addition, the AXL/GAS6 pathway was shown to diminish IFN-γ expression in NK cells as well as the expression of its master regulator, T-BET (22). T-BET is a transcription factor that is crucial for the induction of Th1-type immune responses and also for cytotoxic $CD8^+$ T cells (23). It is thus possible that GAS6 can regulate T-cell polarization during their priming by DCs.

In summary, this study demonstrates that GAS6 exerts both pro- and anti-inflammatory responses in the oral mucosa to ensure rapid but restrained pathogen-specific immunity. Together with the previously reported capability of GAS6 to control oral homeostasis (3), it can be concluded that GAS6 is a key regulator of the oral mucosal immune system.

MATERIALS AND METHODS

Mice

Gas6$^{-/-}$ (24) and *Gas6*$^{+/+}$ littermate controls (WT) were prepared by crossing *Gas6*$^{-/-}$ mice and C57BL/6 (B6) purchased from Harlan (Rehovot, Israel). The identity of the mice used for experiments was confirmed by genotyping with the following PCR primers: forward-GAGTGCCGTGATTCTGGTC,middle-CCACTAAGG AAACAATAACTG, and reverse-ATCTCTCGTGGGATCATT. The mice were maintained under SPF conditions and analyzed between 8 and 12 weeks of age.

Antibodies and Reagents

The following fluorochrome-conjugated monoclonal antibodies and the corresponding isotype controls were purchased from BioLegend (San Diego, CA, USA): I-A/I-E (M5/114.15.2), CD45.2 (104), CD86 (PO3), Ly6G (1A8), Ly6C (HK1.4), CD3 (17A2), CD11b (M1/70), CD8α (53-6.7), CD4 (GK1.5), FOXP3 (MF-14), and CD11c (N418). CFSE was purchased from Molecular Probes. *E. coli* LPS were purchased from Sigma (Israel).

Isolation and Processing of Gingival Tissue

Gingival tissues were excised, minced, and treated with Collagenase type II (2 mg/ml; Worthington Biochemicals) and DNase I (1 mg/ml; Roche) solution in PBS plus 2% fetal calf serum (FCS) for 25 min at 37°C in a shaker bath. A total of 20 µl of 0.5 M EDTA per 2 ml sample was added to the digested tissues and incubated for an additional 10 min. The cells were washed, filtered with a 70 µm filter, and stained with antibodies as indicated in the text. In some experiments, FOXP3 staining was performed using the FOXP3 Fix/Perm Buffer Set (BioLegend) according to the manufacturer's instructions. The stained samples were run in the LSR II (BD Biosciences) flow cytometer and analyzed using FlowJo software (Tree Star).

Immunofluorescence Staining

The maxilla was fixed overnight at 4°C in 4% paraformaldehyde/PBS solution, and then washed for 1 week in EDTA 0.5 M/PBS that was changed every other day. The tissue was cryopreserved in 30% sucrose (overnight at 4°C), embedded in OCT, and cryosectioned into 10 µm-thick sections. The cross sections, as well as the separated epithelium, were washed three times in PBS, blocked in a blocking buffer (5% FCS, 0.1% Triton X-100 in PBS) for 1 h at room temperature, and incubated with primary antibodies: goat anti-GAS6 (clone sc-1935, Santa Cruz Biotechnology), rabbit anti-PROS1 (clone 2428718, Millipore), rat anti-CD31 (clone 550274, BioLegend), goat anti-AXL (clone sc-1096, Santa Cruz Biotechnology), and rabbit-Anti-LYVE1 (clone-ab14917, Abcam) overnight at 4°C. Following three washing steps in PBS, the samples were incubated with a secondary antibody: donkey anti-goat IgG, donkey anti-rat IgG, or donkey anti-rabbit IgG (Jackson ImmunoResearch) diluted 1:100 in blocking buffer for 1 h at RT, washed three times, stained with hoechst, and mounted. As a negative staining control, primary antibody was omitted and replaced by blocking buffer. Signals were visualized and digital images were obtained using an Olympus BX51 fluorescent microscope mounted with a DP72 (Olympus) camera.

RNA Extraction and RT-*q*PCR

For RNA isolation, the maxilla was homogenized in 1 ml TRI reagent (Sigma) using electric homogenizer, and RNA was extracted according to the manufacturer's instructions. cDNA synthesis was performed using the qScript™ cDNA Synthesis Kit (Quanta-BioSciences Inc™). Real-Time *q*PCR reactions (20 µl volume) were performed using Power SYBR Green PCR Master Mix (Quanta-BioSciences Inc™). The following reaction conditions were used: 10 min at 95°C, 40 cycles of 15 s at 95°C, and 60 s at 60°C. The samples were normalized to the TBP (TATA box binding protein) as control mRNA, by change in cycling threshold (ΔC_T) method and calculated based on $2^{-\Delta\Delta CT}$.

Inflammation-Induced Bone Loss Model

Mice were treated with 0.4% trimethoprim and sulfamethoxazole solution (Resprim; Teva) in the drinking water for 10 days, followed by 3 days without antibiotics. The mice were then infected *via* oral gavage, three times at 2-day intervals, with 1×10^{10} cfu of *P. gingivalis* 53977 in 400 µl of 2% (wt/vol) CMC solution (Sigma). Uninfected mice were treated with the CMC vehicle alone. Six weeks later, the mice were euthanized and the hemi-maxillae were harvested and scanned using µCT (Scanco Medical). 3D alveolar bone loss was quantified as we previously described (9).

Acute Infection With *P. gingivalis*

Mice were infected *via* oral gavage once with 1×10^{10} cfu of *P. gingivalis* 53977 in 400 µl of 2% (wt/vol) CMC solution. At days 1, 3, and 7 post-infection, the gingiva and blood samples were collected from the mice for analysis.

Serum Analysis

Six weeks after infection, blood was drawn from the mice and the sera were stored at −80°C. Ninety-six-well plates (Nunc) were coated overnight at 4°C with 1 µg of *P. gingivalis* 53977 lysate/well in 0.1 M bicarbonate buffer (pH 9). The plates were washed twice with PBS-0.02% Tween 20 and blocked with PBS 10% FCS (2 h at room temperature). Subsequently, mouse serum samples diluted serially in PBS were added to the wells for 3 h incubation at RT. This was followed by four washes in PBS-0.02% Tween 20 and the addition of anti-mouse peroxidases-conjugated IgG, IgG1, and IgG2c antibodies (Jackson ImmunoResearch). After incubation for 2 h at RT, the plates were washed five times and 100 µl/well of tetramethyl benzidine (TMB) solution (Southern Biotech) was added for 5 min, followed by the addition of 100 µl of TMB stop solution (Southern Biotech). Absorption was read at 450 nm using an iMARK microplate reader (Bio-Rad).

T-Cell Activation Assay *Ex Vivo*

Cervical LNs were collected from WT or *Gas6*$^{-/-}$ mice and treated with collagenase type II (1 mg/ml) and DNase I (1 mg/ml) solution in PBS plus 2% FCS for 20 min at 37°C in a shaker bath. 20 µl of 0.5 M EDTA per 2 ml sample was added to the digested LNs and incubated for an additional 10 min. The cells were then washed and filtered. CD11c$^+$ cells were enriched from the digested LNs by positive isolation using MACS MicroBeads according to the manufacturer's instructions (Miltenyi Biotec, Germany). OT-I CD8$^+$ T cells or OT-II CD4$^+$ T cells were purified by negative selection with the EasyStep mouse CD8$^+$ or CD4$^+$ T-cell enrichment kits, respectively, according to the manufacturer's instructions (StemCell Technologies, Canada). The purified T cells were incubated with same volume of 5 mM CFSE in HBSS 10 min at 37°C at a final concentration of 2.5 mM. Labeling was quenched by adding an excess of ice-cold RPMI 1640 complete medium, and cells were washed twice with culture medium. CFSE-labeled OTI CD8$^+$ or OT-II CD4$^+$ T cells (5×10^4/well) were incubated with the enriched CD11c$^+$ cells (1×10^4/well) in 96-well U-bottom plates (Nunc). The SIINFEKL (1 µg/ml) and $OVA_{223–339}$ (1 µg/ml) peptides were added to cultures containing CD8$^+$ or CD4$^+$ T cells, respectively, in the presence of LPS (Sigma) (100 ng/ml). The cultures were then incubated for 60 h, the supernatants were collected and stored at −80°C immediately, and the dilution of CFSE fluorescence in the cell fraction was analyzed using an LSR II instrument.

Preparation and Stimulation of BMDCs

The femur was isolated from the mice, cleaned from soft tissues in RPMI 1640, and soaked in 70% ethanol for 1 min for sterilization. The femur was then washed with sterile PBS and the bone ends was removed by sterile scissors. BM cells eluted from the bone by flushing them several times using sterile syringe filled with RPMI 1640, and the cells were then washed, treated with ACK solution for 3 min on ice, washed again, and counted. BM cells (5×10^5 cells/well) in 24-well plates (Nunc) were cultured with complete RPMI media [450 ml RPMI 1640, 50 ml FCS, 5 ml L-glutamine, 50 µM β-mercaptoethanol, penicillin (100 U/ml), streptomycin (100 µg/ml), and gentamicin (50 µg/ml)] supplemented with GM-SCF (20 ng/ml) for 4 days to induce their differentiation into BMDCs (CD11C$^+$MHCII$^+$). The cultures were then exposed to LPS (Sigma) (100 ng/ml), washed, and stained with the noted antibodies for flow cytometry analysis.

Splenocytes Restimulation and Quantification of IFN-γ Secretion

Splenocytes were prepared from the various groups of mice, plated in a concentration of 1×10^6 cells/well and RgpA (1 µg/ml) was added for 3 days. Supernatants were then collected and the level of IFN-γ in the supernatants was measured using an ELISA MAX mouse IFN-γ kit (BioLegend) according to the manufacturer's instructions. Cytokine levels were determined using standard curves of recombinant cytokines and are expressed as picogram per milliliter.

FITC Painting

FITC (Sigma) was dissolved as a 20% (w/v) solution in DMSO (Sigma-Aldrich) and then diluted to 2% (v/v) FITC solution prepared in acetone and dibutyl phthalate (DBP; 1:1). Mice were painted on both sides of the buccal mucosa 2 days before harvesting the draining LNs.

Statistical Analysis

Data were expressed as mean ± SEM. Statistical tests were performed using one-way analysis of variance and Student's *t* test. $P < 0.05$ was considered significant. $^*P < 0.05$, $^{**}P < 0.005$.

ETHICS STATEMENT

This study was carried out in accordance with the recommendations of the IACUC of the Hebrew University. The protocol was approved by the Hebrew University Institutional Animal Care and Ethics Committee.

AUTHOR CONTRIBUTIONS

MN, AW, TB-C, and A-HH designed the research; MN, GM, YT, TC, and LE-B analyzed the data; MN, GM, TN, FS, RS, and LE-B performed the experiments; A-HH and TB-C wrote the manuscript; AHH and TB-C: funding acquisition.

ACKNOWLEDGMENTS

We would like to thank Prof. Gilad Bachrach for the scientific discussion.

FUNDING

This work was supported by grants from the United States-Israel Binational Science Foundation Grant No. 2015209 to A-HH and Israel Science Foundation Grants No. 1764/12 and 984/12 to TB-C.

SUPPLEMENTARY MATERIAL

The Supplementary Material for this article can be found online at https://www.frontiersin.org/article/10.3389/fimmu.2018.01374/full#supplementary-material.

REFERENCES

1. Hajishengallis G, Liang S, Payne MA, Hashim A, Jotwani R, Eskan MA, et al. Low-abundance biofilm species orchestrates inflammatory periodontal disease through the commensal microbiota and complement. *Cell Host Microbe* (2011) 10:497–506. doi:10.1016/j.chom.2011.10.006
2. Hajishengallis G. Periodontitis: from microbial immune subversion to systemic inflammation. *Nat Rev Immunol* (2015) 15:30–44. doi:10.1038/nri3785
3. Nassar M, Tabib Y, Capucha T, Mizraji G, Nir T, Pevsner-Fischer M, et al. GAS6 is a key homeostatic immunological regulator of host-commensal interactions in the oral mucosa. *Proc Natl Acad Sci U S A* (2017) 114:E337–46. doi:10.1073/pnas.1614926114
4. Lemke G, Rothlin CV. Immunobiology of the TAM receptors. *Nat Rev Immunol* (2008) 8:327–36. doi:10.1038/nri2303
5. Lemke G, Burstyn-Cohen T. TAM receptors and the clearance of apoptotic cells. *Ann N Y Acad Sci* (2010) 1209:23–9. doi:10.1111/j.1749-6632.2010.05744.x
6. Mizraji G, Nassar M, Segev H, Sharawi H, Eli-Berchoer L, Capucha T, et al. *Porphyromonas gingivalis* promotes unrestrained type I interferon production by dysregulating TAM signaling via MYD88 degradation. *Cell Rep* (2017) 18:419–31. doi:10.1016/j.celrep.2016.12.047
7. Genco CA, Van Dyke T, Amar S. Animal models for *Porphyromonas gingivalis*-mediated periodontal disease. *Trends Microbiol* (1998) 6:444–9. doi:10.1016/S0966-842X(98)01363-8
8. Katagiri M, Hakeda Y, Chikazu D, Ogasawara T, Takato T, Kumegawa M, et al. Mechanism of stimulation of osteoclastic bone resorption through Gas6/Tyro 3, a receptor tyrosine kinase signaling, in mouse osteoclasts. *J Biol Chem* (2001) 276:7376–82. doi:10.1074/jbc.M007393200
9. Arizon M, Nudel I, Segev H, Mizraji G, Elnekave M, Furmanov K, et al. Langerhans cells down-regulate inflammation-driven alveolar bone loss. *Proc Natl Acad Sci U S A* (2012) 109:7043–8. doi:10.1073/pnas.1116770109
10. Tjwa M, Bellido-Martin L, Lin Y, Lutgens E, Plaisance S, Bono F, et al. Gas6 promotes inflammation by enhancing interactions between endothelial cells, platelets, and leukocytes. *Blood* (2008) 111:4096–105. doi:10.1182/blood-2007-05-089565
11. Schumann K, Lammermann T, Bruckner M, Legler DF, Polleux J, Spatz JP, et al. Immobilized chemokine fields and soluble chemokine gradients cooperatively shape migration patterns of dendritic cells. *Immunity* (2010) 32:703–13. doi:10.1016/j.immuni.2010.04.017
12. Nudel I, Elnekave M, Furmanov K, Arizon M, Clausen BE, Wilensky A, et al. Dendritic cells in distinct oral mucosal tissues engage different mechanisms to prime CD8+ T cells. *J Immunol* (2011) 186:891–900. doi:10.4049/jimmunol.1002943
13. Eskan MA, Benakanakere MR, Rose BG, Zhang P, Zhao J, Stathopoulou P, et al. Interleukin-1beta modulates proinflammatory cytokine production in human epithelial cells. *Infect Immun* (2008) 76:2080–9. doi:10.1128/IAI.01428-07
14. Takahashi N, Okui T, Tabeta K, Yamazaki K. Effect of interleukin-17 on the expression of chemokines in gingival epithelial cells. *Eur J Oral Sci* (2011) 119:339–44. doi:10.1111/j.1600-0722.2011.00842.x
15. Deng T, Zhang Y, Chen Q, Yan K, Han D. Toll-like receptor-mediated inhibition of Gas6 and ProS expression facilitates inflammatory cytokine production in mouse macrophages. *Immunology* (2012) 135:40–50. doi:10.1111/j.1365-2567.2011.03511.x
16. Sanchez-Sanchez N, Riol-Blanco L, Rodriguez-Fernandez JL. The multiple personalities of the chemokine receptor CCR7 in dendritic cells. *J Immunol* (2006) 176:5153–9. doi:10.4049/jimmunol.176.9.5153
17. Johnson LA, Clasper S, Holt AP, Lalor PF, Baban D, Jackson DG. An inflammation-induced mechanism for leukocyte transmigration across lymphatic vessel endothelium. *J Exp Med* (2006) 203:2763–77. doi:10.1084/jem.20051759
18. Shields JD, Fleury ME, Yong C, Tomei AA, Randolph GJ, Swartz MA. Autologous chemotaxis as a mechanism of tumor cell homing to lymphatics via interstitial flow and autocrine CCR7 signaling. *Cancer Cell* (2007) 11:526–38. doi:10.1016/j.ccr.2007.04.020
19. Carrera Silva EA, Chan PY, Joannas L, Errasti AE, Gagliani N, Bosurgi L, et al. T cell-derived protein S engages TAM receptor signaling in dendritic cells to control the magnitude of the immune response. *Immunity* (2013) 39:160–70. doi:10.1016/j.immuni.2013.06.010
20. Shibata T, Ato M. A critical role of Gas6/Axl signal in allergic airway responses during RSV vaccine-enhanced disease. *Immunol Cell Biol* (2017) 95:906–15. doi:10.1038/icb.2017.61
21. Trinchieri G, Pflanz S, Kastelein RA. The IL-12 family of heterodimeric cytokines: new players in the regulation of T cell responses. *Immunity* (2003) 19:641–4. doi:10.1016/S1074-7613(03)00296-6
22. Park IK, Giovenzana C, Hughes TL, Yu J, Trotta R, Caligiuri MA. The Axl/Gas6 pathway is required for optimal cytokine signaling during human natural killer cell development. *Blood* (2009) 113:2470–7. doi:10.1182/blood-2008-05-157073
23. Sullivan BM, Juedes A, Szabo SJ, Von Herrath M, Glimcher LH. Antigen-driven effector CD8 T cell function regulated by T-bet. *Proc Natl Acad Sci U S A* (2003) 100:15818–23. doi:10.1073/pnas.2636938100
24. Angelillo-Scherrer A, De Frutos P, Aparicio C, Melis E, Savi P, Lupu F, et al. Deficiency or inhibition of Gas6 causes platelet dysfunction and protects mice against thrombosis. *Nat Med* (2001) 7:215–21. doi:10.1038/84667

Conflict of Interest Statement: The submitted work was carried out without the presence of any personal, professional, or financial relationships that could potentially be construed as a conflict of interest.

frontiers in Immunology

ORIGINAL RESEARCH
published: 10 August 2018
doi: 10.3389/fimmu.2018.01804

CCR2 Contributes to F4/80+ Cells Migration Along Intramembranous Bone Healing in Maxilla, but Its Deficiency Does Not Critically Affect the Healing Outcome

*Claudia Cristina Biguetti[1], Andreia Espindola Vieira[2], Franco Cavalla[1,3], Angélica Cristina Fonseca[1], Priscila Maria Colavite[1], Renato Menezes Silva[4], Ana Paula Favaro Trombone[5] and Gustavo Pompermaier Garlet[1]**

[1] Department of Biological Sciences, Bauru School of Dentistry, University of São Paulo, Bauru, Brazil, [2] Institute of Biological Sciences and Health, Federal University of Alagoas, Maceió, Brazil, [3] Department of Conservative Dentistry, School of Dentistry, University of Chile, Santiago, Chile, [4] Department of Endodontics, University of Texas School of Dentistry at Houston, Houston, TX, United States, [5] Department of Biological and Allied Health Sciences, Universidade do Sagrado Coração, Bauru, Brazil

OPEN ACCESS

Edited by:
Asaf Wilensky,
Hadassah Medical Center, Israel

Reviewed by:
Franz E. Weber,
Universität Zürich, Switzerland
Gianluca Matteoli,
KU Leuven, Belgium

***Correspondence:**
Gustavo Pompermaier Garlet
garletgp@usp.br

Specialty section:
This article was submitted to Mucosal Immunity, a section of the journal Frontiers in Immunology

Received: *19 April 2018*
Accepted: *23 July 2018*
Published: *10 August 2018*

Citation:
Biguetti CC, Vieira AE, Cavalla F, Fonseca AC, Colavite PM, Silva RM, Trombone APF and Garlet GP (2018) CCR2 Contributes to F4/80+ Cells Migration Along Intramembranous Bone Healing in Maxilla, but Its Deficiency Does Not Critically Affect the Healing Outcome. Front. Immunol. 9:1804. doi: 10.3389/fimmu.2018.01804

Bone healing depends of a transient inflammatory response, involving selective migration of leukocytes under the control of chemokine system. CCR2 has been regarded as an essential receptor for macrophage recruitment to inflammation and healing sites, but its role in the intramembranous bone healing on craniofacial region remains unknown. Therefore, we investigated the role of CCR2 on F4/80+ cells migration and its consequences to the intramembranous healing outcome. C57BL/6 wild-type (WT) and CCR2KO mice were subjected to upper right incisor extraction, followed by micro-computed tomography, histological, immunological, and molecular analysis along experimental periods. CCR2 was associated with F4/80+ cells influx to the intramembranous bone healing in WT mice, and CCR2+ cells presented a kinetics similar to F4/80+ and CCR5+ cells. By contrast, F4/80+ and CCR5+ cells were significantly reduced in CCR2KO mice. The absence of CCR2 did not cause major microscopic changes in healing parameters, while molecular analysis demonstrated differential genes expression of several molecules between CCR2KO and WT mice. The mRNA expression of TGFB1, RUNX2, and mesenchymal stem cells markers (CXCL12, CD106, OCT4, NANOG, and CD146) was decreased in CCR2KO mice, while IL6, CXCR1, RANKL, and ECM markers (MMP1, 2, 9, and Col1a2) were significantly increased in different periods. Finally, immunofluorescence and FACS revealed that F4/80+ cells are positive for both CCR2 and CCR5, suggesting that CCR5 may account for the remaining migration of the F4/80+ cells in CCR2KO mice. In summary, these results indicate that CCR2+ cells play a primary role in F4/80+ cells migration along healing in intramembranous bones, but its deficiency does not critically impact healing outcome.

Keywords: osteoimmunology, bone histomorphometry, macrophages, bone healing, intramembranous bone

INTRODUCTION

The recruitment of circulating blood monocytes and its transition into macrophages at injured tissues are essential steps of inflammatory immune response and healing processes (1–3). Indeed, macrophages comprise a heterogeneous myeloid cell lineage that participate directly or indirectly in tissue healing by playing a number of functions, such as removing debris and dead cells after injury, as well as producing a large range of growth factors, immunological molecules, and proteolytic enzymes (3–5). However, while these macrophages beneficial contributions to tissue healing are well defined in soft tissue healing (1), soft- and mineralized-tissues substantially differ in their healing processes and outcomes (3).

The bone healing process occurs throughout orchestrated and overlapping phases, starting with a transient inflammatory response that constructively influences subsequent events such as angiogenesis and fibrous connective tissue formation, osteogenic cellular differentiation, and bone formation (6–9). Along bone healing, macrophages are described to be present mainly in the inflammatory phase and are regarded as an important source of pro-inflammatory cytokines (3, 10), which theoretically amplify the recruitment of its own lineage and other immune cells. Indeed, activated macrophages can release multiple mediators, including pro-inflammatory and anti-inflammatory cytokines, and growth factors (11). In this context, the early release of cytokines and growth factors in bone injury sites is associated with a positive intramembranous and endochondral healing outcome (12–14). Moreover, studies suggest that macrophages contribution to bone healing extends beyond earlier inflammatory events and can include the production of growth factors that direct mesenchymal stem cells (MSCs) into osteogenic differentiation (11). Accordingly, macrophages depletion in mice significantly suppresses woven bone deposition and mineralization during bone fracture healing in endochondral bones (15).

It is mandatory to consider that *in vivo* studies concerning macrophages functions in bone healing are predominantly focused on endochondral bone healing following fractures (3, 6, 16). Importantly, endochondral and intramembranous bones have distinctive features, which include substantial differences on healing mechanisms (17). Indeed, while long bone heals *via* endochondral ossification, intramembranous bones (such maxillary alveolar dental socket) healing takes place without cartilage formation (3). Also, while bone fracture sites are usually a sterile milieu, oral tissues surrounding the alveolar bone are under a constant microbial challenge (18). Consequently, the scarce information about macrophage contributions on endochondral bone healing cannot be directly translated to intramembranous bone healing, where its role remains to be determined.

In this context, we previously characterized an alveolar bone healing model after tooth extraction in C57Bl/6 mice, allowing further investigations concerning the role of the immunological system components on intramembranous bone healing (7, 12). Interestingly, a series of macrophage-related growth factors and cytokines, and members of the chemokine family with a potential role in macrophage chemoattraction were found to be upregulated during alveolar bone healing process (7). Specifically, upregulation of the chemokine receptor CCR2, chemokine (C-C motif) receptor 2, and its cognate chemokine (C-C motif) ligand 2 (CCL2) suggests a role for CCR2/CCL2 axis in macrophages migration to bone injury sites (7). Indeed, the chemokine system recruits different leukocytes subsets into the specific microenvironments, where chemokines bind to their respective receptors selectively expressed by each leukocyte subset (19). Exemplifying, while resident macrophages are characterized by the expression of CX3CR1, chemokine receptors CCR2 and CCR5 are expressed by inflammatory monocytes/macrophages and mediate its traffic into injured tissues in response to chemokines such as CCL1, CCL2, and CCL5 (19). CCR2 has been regarded a key player regulating the macrophages influx into injured tissues throughout tissue healing (2, 10). Indeed, CCR2-deficient mice have an impaired recruitment of F4/80+ cells (suggested as macrophages) on different sites of injury (2, 20), including endochondral bones (3, 10), which consequently delays the evolution of the subsequent healing (2). In addition, previous studies demonstrate the F4/80 and CCR2 co-expression in murine macrophages (2), and the association of CCR2 with the migration of F4/80+ cells from blood into inflamed and healing sites (2, 3, 10, 20, 21). Indeed, the majority of F4/80+ cells recruited from blood into inflamed sites are monocytes/macrophages, which co-express CCR2 (2), being the CCR2 targeted disruption associated with decreased F4/80+ cells number of these in injuries sites (2, 3, 10, 20, 21). However, the molecular and cellular mechanisms triggered by CCR2+ cell migration and its impact in the intramembranous bone healing remain unaddressed.

Taking into consideration that bone healing depends of an initial and transient inflammatory response, and that macrophages are key regulators of this process (22), it is reasonable to hypothesize that CCR2 deficiency can reduce F4/80+ cells migration and negatively affect the intramembranous bone healing. Therefore, we investigated the role of CCR2 on F4/80+ cells migration to bone healing sites and its consequences to the subsequent intramembranous bone healing outcome, by means of the CCR2KO and C57Bl/6-wild-type (WT) mice strains comparative analysis using micro-computed tomography (μCT), histological, immunological, and molecular methods.

MATERIALS AND METHODS

Animals

The experimental groups were comprised of 8-week-old male WT C57BL/6 mice and mice with targeted disruption of the CCR2 (CCR2KO, C57BL/6 background), both WT and CCR2KO littermates bred in the animal facilities of USP. Mice were fed with sterile standard solid mice chow (Nuvital, Curitiba, PR, Brazil) and sterile water throughout the study period, except on the first 24 h after surgery, in which diet was crumbled. The experimental groups comprised nine mice (five animals for microscopic analysis and four animals for the PCR array analysis). This study was carried out in strict accordance with the recommendations in the Guide for the Care and Use of Laboratory Animals of the National Institutes of Health. The experimental protocol was

approved by the local Institutional Committee for Animal Care and Use (Committee on Animal Research and Ethics CEEPA-FOB/USP, process #005/2012).

Mice Tooth Extraction Model

The surgical procedures for tooth extraction were performed as described (7). In brief, the animals received general anesthesia by intramuscular administration 80 mg/kg of ketamine chloride (Dopalen, Agribrans do Brasil LTDA) and 160 mg/kg of xylazine chloride (Anasedan, Agribrands do Brasil LTDA) in the proportion 1:1. The upper right incisor was extracted with a dental probe, as previously described (7). After 0 h, 7, 14, and 21 days post tooth extraction, mice were euthanazied and maxillae were harvested. Maxillae for the μCT and histological analyses were fixed in PBS-buffered formalin (10%) solution (pH 7.4) for 48 h at room temperature, subsequently washed overnight in running water and maintained temporarily in alcohol fixative (70% hydrous ethanol) until the conclusion of the μCT analysis, and then decalcified in 4.13% EDTA (pH 7.2) and submitted to histological processing. Samples from maxillae containing only the region of the alveolus were destined to molecular analysis were stored in RNAlater (Ambion, Austin, TX, USA) solutions (7).

μCT Analysis

The maxillae at 0 h, 7, 14, and 21 days post tooth extraction were scanned by the Skyscan 1174 System (Skyscan, Kontich, Belgium) at 50 kV, 800 μA, with a 0.5 mm aluminum filter and 15% beam hardening correction and 180 ° of rotation. Images were captured with a resolution of 14 μm pixel size and reconstructed using the NRecon software. Three-dimensional (3D) images were rendered using CTVox software, and quantitative parameters were assessed using CTAn software following recommended guidelines and a previously μCT characterization (7, 23, 24). Newly formed bone was segmented in a cylindrical region of interest (ROI) covering the entire length of the alveolus (3 mm) and a diameter of 1 mm. The following morphological parameters were assessed: bone volume fraction [Bone Volume/Tissue Volume (BV/TV), %], trabecular thickness (Tb.Th, mm), trabecular number (Tb.N, mm), and trabecular separation (Tb.Sp) (24).

Histology Sample Preparation and Histomorphometric Analysis

After μCT scanning, maxillae were immersed in buffered 4% EDTA for demineralization and processing for embedding in paraffin blocks. Transversal serial 5-μm slices from medial third were cut for histology with H&E staining, picrosirius red, immunohistochemistry, and immunofluorescence. A total of three histological sections from central region of the alveolar socket stained by H&E were used to quantify the following healing components: clot formation, inflammatory infiltrate, connective tissue (collagen fibers, fibroblasts, and blood vessels), bone matrix, osteoblasts, osteoclasts, and other components (empty spaces and bone marrow), as previously described (7). The identification and quantification of healing components was performed by a single calibrated investigator with a binocular light microscope (Olympus Optical Co., Tokyo, Japan) using a 100× immersion objective and a Zeiss kpl 8× eyepiece containing a Zeiss II integration grid (Carl Zeiss Jena GmbH, Jena, Germany) with 100 points in a quadrangular area. The grid image was successively superimposed on 13 histological regions per histological section, totaling 3 sections for each specimen. Only the points coincident with the histological components were considered, and the total number of points was obtained to calculate the area density for each healing component in each section.

Birefringence Analysis

Birefringence analysis was performed with picrosirius-polarization method, to identify and quantify collagen content, as well compare the quality of bone trabeculae matrix as previously described (7). Briefly, four histological from central region of the each alveolar socket were stained with Picrosirius Red Stain, and the images were captured by a polarizing lens coupled to a binocular inverted microscope (Leica DM IRB/E) using a 10× objective. Adobe Photoshop CS6 software was used to delimit the ROI, the socket area filled with new tissue, as well to exclude bony edges of the alveolar margins or residual old bone. The quantification of the intensity of birefringence brightness (pixels^2) was performed using the AxioVision 4.8 software (CarlZeiss) to define total area of green, yellow, and red collagen fibers.

Immunohistochemistry and Immunofluorescence

Histological sections from 0, 7, 14, and 21 days were deparaffinized following standard procedures. For immunohistochemistry, the material was pre-incubated with 3% Hydrogen Peroxidase Block (Spring Bioscience Corporation, CA, USA) and subsequently incubated with 7% NFDM to block serum proteins. The histological sections from both, WT and CCR2 KO mice, were then incubated with anti-CCR2 polyclonal primary antibody (Santa Cruz, #sc-31564), anti-F4/80 (a pan macrophage marker for mice) polyclonal primary antibody (Santa Cruz, #sc-26642), anti-CD68 polyclonal primary antibody (Santa Cruz, #sc-7084), anti-CCR5 polyclonal (Santa Cruz, #sc-6129) at 1:100 concentrations, and with anti-Ly6g-Gr1 polyclonal antibody (Santa Cruz, #sc-168490) and anti-CD3 polyclonal antibody (Santa Cruz, #sc-1127) at 1:50 concentrations, anti-CCR5 polyclonal (Santa Cruz, #sc-6129) at 1:100 concentrations, for 1 h at room temperature. Universal immuno-enzyme polymer method was used, and sections were incubated in immunohistochemical staining reagent for 30 min at room temperature. The identification of antigen–antibody reaction was performed using 3,3′-diaminobenzidine and counterstaining with Mayer's hematoxylin. For control staining of the antibodies, serial sections were treated only with the Universal immuno-enzyme polymer, in a separate preparation. For immunofluorescence, sections from WT at 7 days were rehydrated and retrieved the antigens by boiling the histological slides in 10 mM sodium citrate buffer pH 6 for 30 min at 300°C. Subsequently, the sections were permeabilized with 0.5% Triton X-100 in PBS and blocked with blocking solution (1% bovine

serum albumin diluted in 1× PBS), for 1 h at room temperature. For immunolocalization of CCR2+ CCR5+ macrophages, the sections were incubated with both primary antibodies: anti-CCR2 rabbit monoclonal antimouse (Abcam, #ab203128) and anti-CCR5 goat polyclonal antimouse (Santa Cruz, #sc-6129). All primary antibodies were diluted at 1:100 in blocking solution and incubated over night at 4°C. After repeated washing steps with PBS (3 times, 10 min each wash), the sections were incubated with both secondary antibodies: Alexa Fluor555 goat anti-rabbit secondary antibody (Life Technologies, #A21428) and Alexa Fluor488 donkey anti-goat (Life Technologies, #A11055), diluted at 1:150 in blocking solution, incubated for 2 h at room temperature. Sections were nuclear stained with DAPI (Thermo Fisher Scientific, #D3571) diluted at 3 μM in ddH_2O for 10 min, mounted in with ProLong Gold Antifade Reagent (Invitrogen, #P36930). Imaging was performed in a Nikon Eclipse Ni-U upright fluorescence microscope (Nikon instruments) equipped with a Zyla 5.5 sCMOS camera (Andor).

Quantification of Immunolabeled Cells

The analysis of immunolabeled cells was performed by a single calibrated investigator with a binocular light microscope (Olympus Optical Co., Tokyo, Japan) using a 100× immersion objective, following the similar criteria described previously for histomorphometric analysis in H&E (see Histology Sample Preparation and Histomorphometric Analysis). Briefly, five samples (biological replicate) for each experimental period and strains were used for quantitative analysis. A total of three sections of each sample (technical replicate) containing the central region of the alveolar socket was used to quantify immunolabeled cells for each mentioned target (F4/80, CCR2, CCR5, Ly6g-Gr1, CD3, and CD68). A total of 13 fields (100 points in a quadrangular area) were analyzed using Zeiss II integration grid (100 points) (Carl Zeiss Jena GmbH, Jena, Germany) for each section. Only the points coincident with the immunolabeled cells were considered in cell counting, and the mean for each section was obtained for statistical analysis.

Isolation of F4/80+ Cells From Alveolar Socket and Flow Cytometric Analysis

The isolation and characterization of monocytes/macrophages from the alveolar socket at day 7 post tooth extraction was performed as previously described (25). The alveolar socket tissues from five C57Bl/6 mice were collected at day 7 post tooth extraction, and subsequently were fragmented, weighed, and incubated for 1 h at 37°C, in RPMI-1640 supplemented with $NaHCO_3$, penicillin/streptomycin/gentamycin and liberate blendzyme CI (Roche-F. Hoffmann-La Roche Ltd., Basel, Switzerland). The samples were processed in the presence of 0.05% DNase (Sigma-Aldrich, Steinhein, Germany) using Medimachine (BD Biosciences Pharmingen, San Diego, CA, USA), according to the manufacturer's instructions. The cell viability was assessed by Trypan blue exclusion assay, and the cell count was performed in a hemocytometer, with these data depicted in the manuscript as the total monocyte/macrophage cell count. For flow cytometry analysis, after counting the cells were stained for 20 min at 4°C with the optimal dilution of each antibody; phycoerythrin- and fluorescein isothiocyanate-conjugated antibodies against CCR2, CCR5, and F4/80-anti mouse antibodies, as well with respective isotype controls (BD Biosciences Pharmingen, San Diego, CA, USA), and analyzed by FACScan and CellQuest software (BD Biosciences Pharmingen, San Diego, CA, USA). Results are presented as the number of F4/80+ CCR2+ cells and F4/80+ CCR5+ cells ± SD in the alveolar socket of each mouse.

RealTime PCR Array Reactions

RealTime PCR array reactions were performed as previously described (7). Only hemimaxillae containing the region of the alveolus socket were used as experimental samples, while the hemimaxillae without injury were used as tissue control. Samples were storage in RNA Stabilization Solution (RNAlater®, Thermo Fisher Scientific, Waltham, MA, USA) until RealTime PCR array reactions. The extraction of total RNA from remaining alveolus with 0 h, 7, 14, and 21 days post-extraction from WT and CCR2KO was performed with RNeasyFFPE kit (Qiagen Inc., Valencia, CA, USA) according to the manufacturers' instructions. First, RealTime PCR array was performed from a pool of all experimental time points (0 h, 7, 14, and 21 days), providing targets in which expression variation presented a significant variation compared with the control side. Then, upregulated targets were analyzed regarding their kinetics of expression for specific time points of 0, 7, 14, and 21 days throughout the alveolar bone healing. The integrity of the RNA samples was verified by analyzing 1 μg of total RNA in a 2100Bioanalyzer (Agilent Technologies, Santa Clara, CA, USA) according to the manufacturers' instructions, and the complementary DNA was synthesized using 3 μg of RNA through a reverse transcription reaction (Superscript III, Invitrogen Corporation, Carlsbad, CA, USA). RealTime PCR array was performed in a Viia7 instrument (Life Technologies, Carlsbad, CA, USA) using a custom panel containing targets "Wound Healing" (PAMM-121), "Inflammatory cytokines and receptors" (PAMM-011), and "Osteogenesis" (PAMM-026) (SABiosciences, Frederick, MD, USA) for gene expression profiling. RealTime PCR array data were analyzed by the RT^2 profiler PCR Array Data Analysis online software (SABiosciences, Frederick, MD, USA) for normalizing the initial geometric mean of three constitutive genes (GAPDH, ACTB, and Hprt1) and subsequently normalized by the control group, and expressed as fold change relative to the control group, as previously described (26, 27). Data are expressed as heat map fold change relative to the control group.

Statistical Analysis

Differences among data sets were statistically analyzed by one-way analysis of variance followed by the Tukey multiple comparison post test or Student's *t*-test where applicable. For data that did not fit in the distribution of normality, the Mann–Whitney and Kruskal–Wallis (followed by the Dunn's test) tests were used. The statistical significance of the experiment involving the PCR Array was evaluated by the Mann–Whitney test, and the values tested for correction by the Benjamini–Hochberg procedure (28). Values of $p < 0.05$ were considered statistically significant. All statistical tests were performed using the GraphPad Prism 5.0 software (GraphPad Software Inc., San Diego, CA, USA).

RESULTS

Immunohistochemistry of Inflammatory Infiltrate Throughout Intramembranous Bone Healing in Mice

In the view of the primary role of CCR2 in the migration of monocytes/macrophages into sites of inflammation (29), we used immunohistochemistry to address the presence CCR2+ cells, F4/80+ and CD68+ cells (macrophages), Ly6g-Gr1+ cells (polymorphonuclear leukocyte/neutrophils), and CD3+ cells (lymphocytes) on the site of alveolar bone healing at different time points (0, 7, 14, and 21 days) post tooth extraction in C57Bl/6 WT mice an CCR2KO mice (**Figures 1A–J**). At 0 day time point, there was a peak of Ly6g-Gr1+ cells (**Figure 1I**) observed in the blood clot formed post-extraction in WT and CCR2KO mice, with a significant decrease from 7 to 21 days in C57Bl/6 mice, and with no differences observed among different time points in CCR2KO mice. During the early inflammatory phase (7 days), there was a peak of area density for CCR2+ (**Figure 1F**) and F4/80+ (**Figure 1G**) cells in the granulation tissue and inflammatory infiltrate in the socket of C57BL/6 mice. At 14 days, CCR2+, F4/80+, and CD68+ cells were found in permeating the connective tissue surrounding bone formation areas, while at 21 days, these cells were found predominantly in the bone marrow and surrounding blood vessels (**Figures 1A–C**). The influx of F4/80+ cells was significantly reduced at 7 and 14 days in CCR2KO compared with WT mice ($p < 0.05$) (**Figures 1E,F**). The number of both type of cells, CCR2+ and F4/80+ cells, was significantly decreased ($p < 0.05$) at 14 and 21 days compared with 7 days in C57Bl/6 WT mice (**Figures 1B–D**). No significant differences were observed for CD3+ cells in the WT vs CCR2KO comparisons (**Figure 1**). A different kinetics for Ly6g-Gr1+ and CD68+ cells infiltration was observed in CCR2KO mice compared with WT, with a slight higher number of Ly6g-Gr1+ and CD68+ cells in CCR2KO mice compared with WT at 21 days. However, no significant differences were found between WT vs CCR2KO comparisons in specific time points (**Figures 1H,I**).

μCT Analyses of Intramembranous Bone Healing in WT vs CCR2KO

The sagittal 3D images of maxillae containing socket area (**Figure 2A**) and quantitative assessment of the bone morphological parameters from μCT analysis (**Figure 2B**) did not indicate major differences in the inorganic bone matrix between WT and CCR2KO mice. At the 0 day time point, both WT and CCR2KO mice presented sockets with an absence of hyperdense areas. At 7 days, negligible hyperdense areas were observed from the lateral and apical walls of the extraction sockets, while at 14 and 21 days, hyperdense structures compatible with new trabecular bone were observed filling the entire socket in both, WT and CCR2KO mice (**Figure 2A**). In general, the values of morphological parameters such as volume fraction (BV/TV), trabecular thickness (Tb.Th), and trabecular number (Tb.N) were progressively increased from 7 to 21 days ($p < 0.05$), while the trabecular separation (Tb.Sp) were inversely reduced ($p < 0.05$) in both, WT and CCR2KO mice. Specifically, at 7 days, the Tb.N parameter was significantly lower in the CCR2KO compared with WT mice (**Figure 2B**).

Histological and Birefringence Analysis of Healing Components in WT vs CCR2KO During the Alveolar Bone Healing

Histological analysis demonstrated that the intramembranous bone healing process followed suitable overlapping phases in both strains (WT and CCR2KO), although minor morphological and quantitative differences were observed between them at specific time points (**Figures 3A,B**). Overall, the socket of both (WT and CCR2KO mice) exhibited predominantly blood clot at day 0 (immediately after tooth extraction) with a negligible number of leukocytes. Subsequently, were observed an abundant amount of granulation tissue (blood vessels, fibers from connective tissue, and fibroblasts) with leukocytes infiltration at 7 days, as well as bone formation from remaining bone edges. At 14 days, an intense bone remodeling activity was evidenced by the presence of osteoclasts, while organized matrix surrounding blood vessels and bone marrow were present at 21 days (**Figure 4A**). Comparatively, the absence of CCR2 resulted in an increased area density (%) of fibroblasts at 7 days; blood vessels at 14 days; osteoclasts at 14 and 21 days, osteoblasts; fibers from connective tissue and inflammatory infiltrate at 21 days; in CCR2KO vs WT ($p < 0.05$). On the other hand, CCR2KO showed a reduced area density of osteoblasts at 7 days, fibroblasts, fibers from connective tissue at 14 days; and other components (especially bone marrow) at 21 days ($p < 0.05$; WT vs CCR2KO) (**Figure 4B**). In the birefringence analysis, the new organic matrix consisting predominantly of collagen fibers bundles were found from 7 to 21 days inside the socket in both WT and CCR2KO mice, as evidenced by images under polarized light (**Figure 4A**). The quantitative analysis showed a similar pattern in the matrix maturation dynamics during the time points in both WT and CCR2KO mice (**Figure 4B**). While the area of collagen fibers in green tones (thinner and immature fibers) significantly decreased from 7 to 21 days, collagen fibers emitting yellow and red color spectrum (thicker and mature collagen) increased at these same time points ($p < 0.05$). Of note, CCR2KO mice showed an increased quantity of green fibers (7 days) and yellow fibers (21 days) compared with WT mice ($p < 0.05$). Also, the total amount of collagen fibers bundles (sum of color spectrums) was significantly increased in CCR2KO mice at 21 days ($p < 0.05$ vs WT) (**Figure 4C**).

Differential Gene Expression Between WT vs CCR2KO During the Alveolar Bone Healing

Differential gene expression of several molecules involved in bone healing (i.e., growth factors, bone formation markers, immunological markers, and putative MSC markers) was investigated in CCR2KO and WT strains. We performed an exploratory analysis by RealTime PCR array with a pool from samples of all time points in both WT and CCR2KO mice (**Figure 5**) followed by kinetics of expression analysis for selected targets (**Figure 6**). Of note, the mRNA expression of growth factor

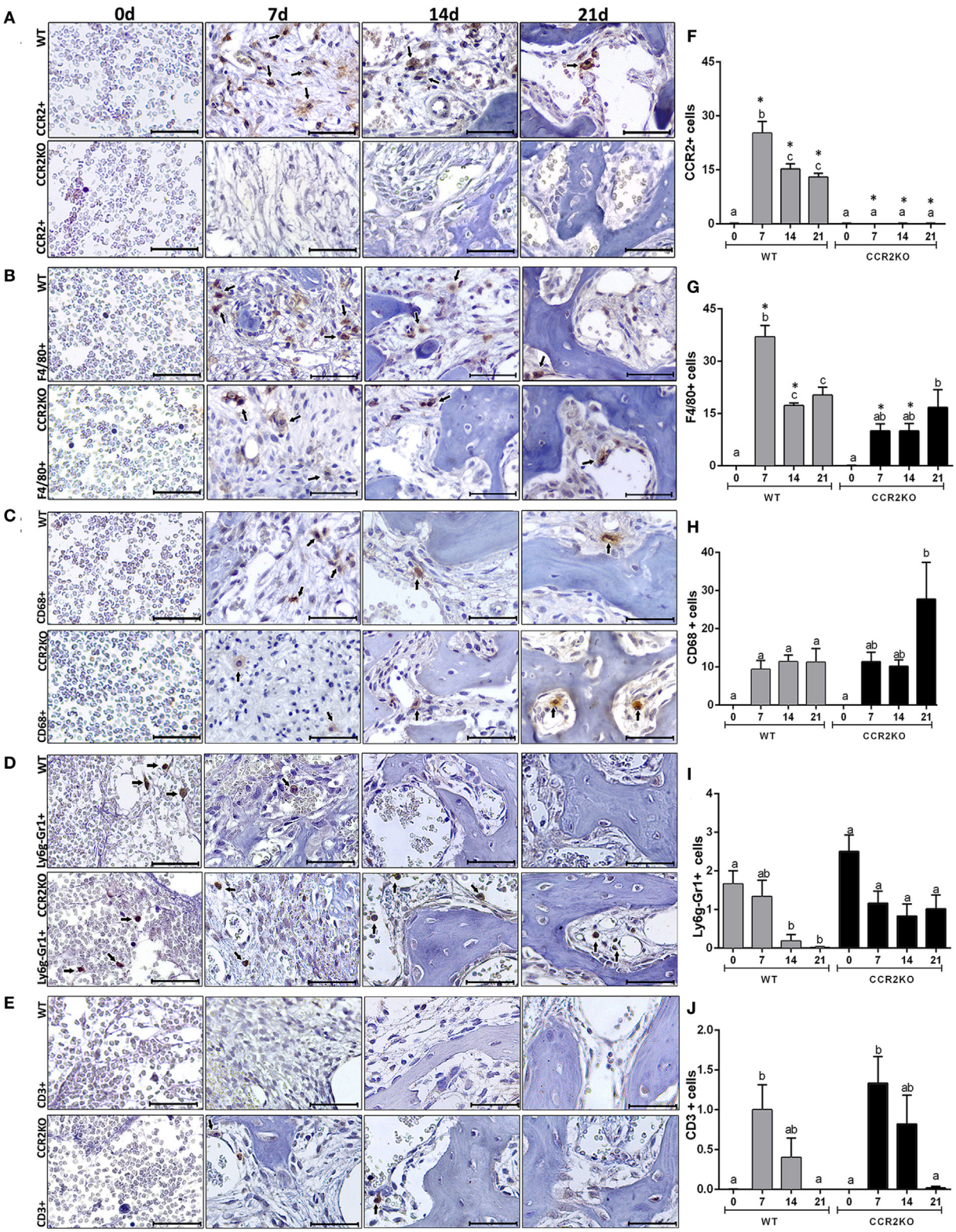

FIGURE 1 | Immunolabeling of inflammatory infiltrate in the intramembranous alveolar bone healing in mice. Representative sections from medial thirds of the socket at 0, 7, 14, and 21 days post tooth extraction with immunolabeling of CCR2+ cells **(A)**, F4/80+ cells **(B)**, CD68+ cells **(C)**, Ly6g-Gr1+ cells **(D)**, and CD3+ cells **(E)** in wild-type (WT) **(A)** and CCR2KO mice **(B)**, as indicated with arrows (scale bar = 100 μm). Quantitative and comparative analysis of CCR2+ cells **(F)**, F4/80+ cells **(G)**, CD68+ cells **(H)**, Ly6g-Gr1+ cells **(I)**, and CD3+ cells **(J)** in WT vs CCR2KO mice at days 0, 7, 14, and 21 post-extraction. Different letters indicate significant differences in each time point ($p < 0.05$); symbol * indicate significant differences between WT vs CCR2KO at the same time point.

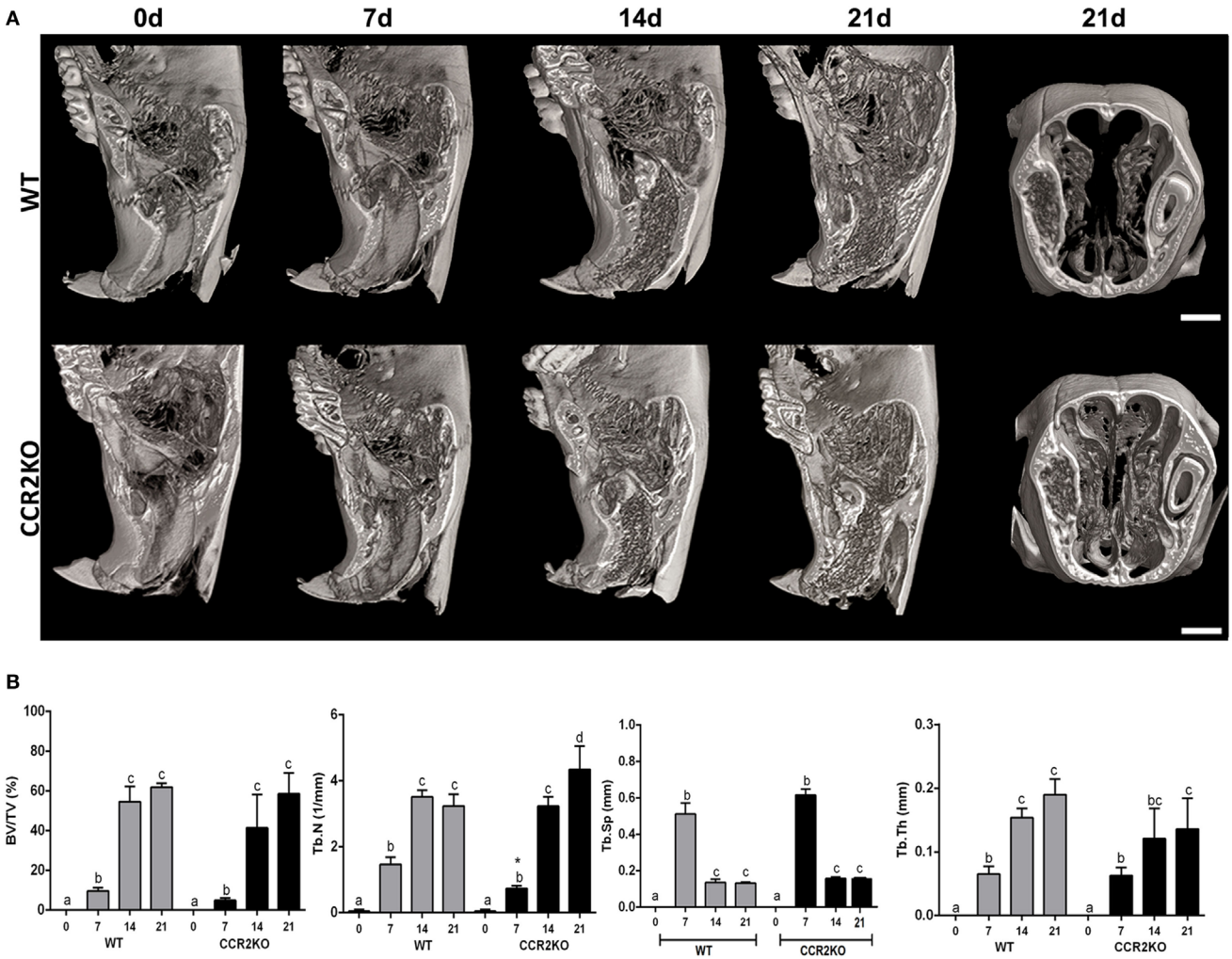

FIGURE 2 | Micro-computed tomography (μCT) analysis along intramembranous bone healing in wild-type (WT) vs CCR2KO mice. Maxillae containing dental sockets post-extraction from WT and CCR2KO mice were scanned with the μCT System (Skyscan 1174; Skyscan, Kontich, Belgium). **(A)** Three-dimensional images obtained by CT-Vox software reveal the socket morphology at 0 h, 7, 14, and 21 days post tooth extraction. **(B)** Morphological parameters such as bone volume fraction (BV/TV, %), trabecular number (Tb.N, 1/mm), trabecular separation (Tb.Sp, mm), and trabecular thickness (Tb.Th, mm) were quantified at 7, 14, and 21 days post tooth extraction. Results are presented as mean and SD to different parameters. Different letters indicate significant differences in each time point ($p < 0.05$); symbol * indicate significant differences between WT vs CCR2KO at the same time point.

TGFB1 and putative MSC markers (CD106, OCT4, NANOG, and CD146) was upregulated in WT mice, with a peak of mRNA levels at 7 days, while those same targets were significantly decreased in CCR2KO at the same time point ($p < 0.05$). Among the bone markers evaluated, the mRNA expression of the early bone formation marker RUNX2 was also significantly reduced in CCR2KO compared with WT mice ($p < 0.05$) at 7 and 14 days, while RANKL was significantly increased in CCR2KO at 21 days (**Figure 6**). For ECM markers, the mRNA levels of Col1a2 and MMP1, MMP2, and MMP9 were increased in CCR2KO mice at 14 and 21 days. Considering immunological markers (cytokines, chemokines, and its receptors), while CCR5 and TNF mRNA levels were decreased in CCR2KO compared with WT, CXCR1 and IL6 were increased in the pooled samples analysis (**Figure 5**) and at 7 days (**Figure 6**). In the kinetics of expression, the TNF, CXCR1, and IL6 mRNA levels peaked at day 7, with a higher expression of TNF in WT mice and a higher expression of CXCR1 and IL6 in CCR2KO mice ($p < 0.05$).

Immunological Analysis of Macrophages Along Intramembranous Bone Healing in WT vs CCR2KO Mice

We used immunohistochemistry to identify and compare the number CCR5+ cells in WT and CCR2KO during alveolar bone healing at different time points (0, 7, 14, and 21 days), as well immunofluorescence and flow cytometry to identify CCR2+ CCR5+ cells in WT mice. CCR5+ cells are present throughout the alveolar bone healing in both, WT and CCR2KO mice

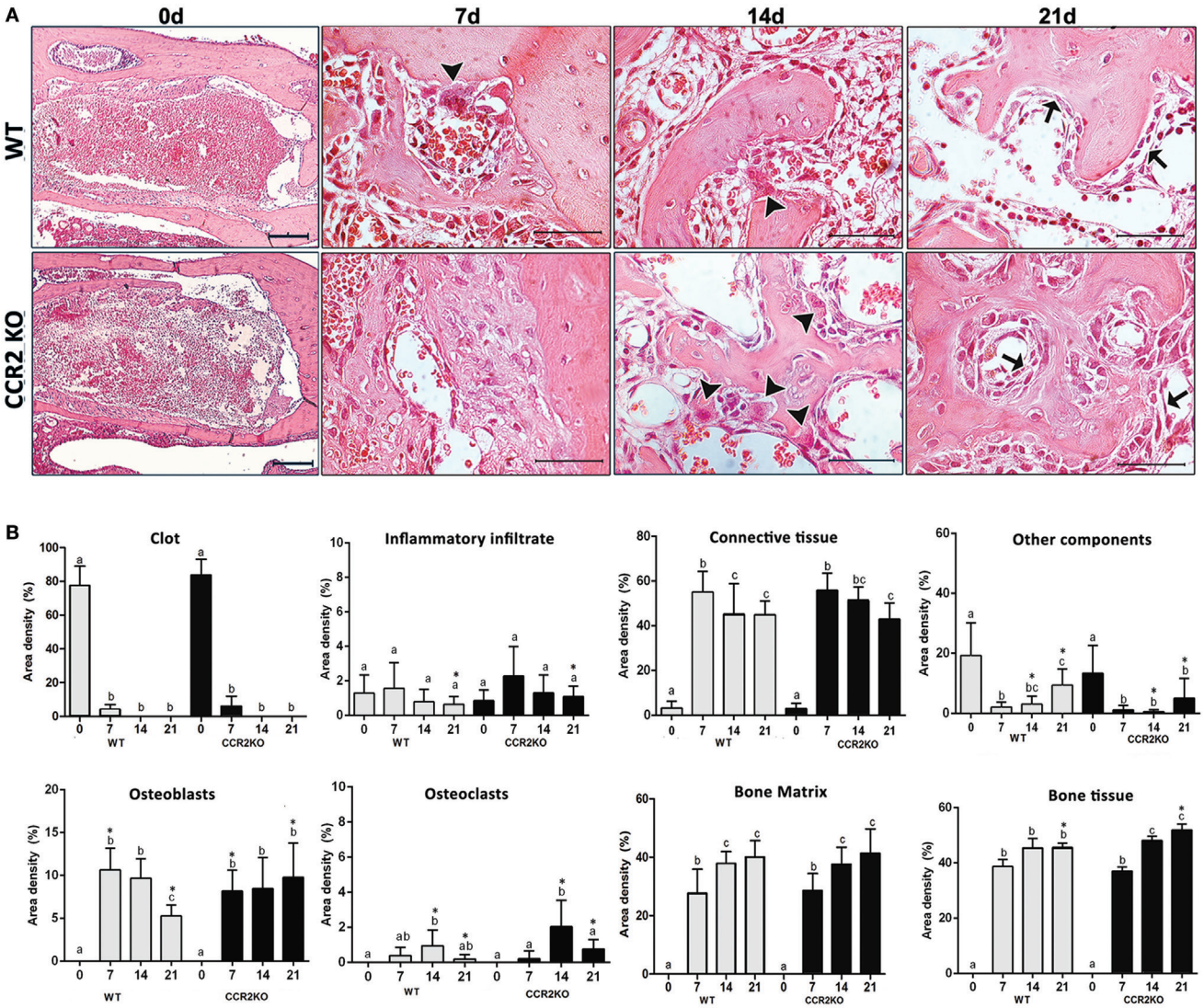

FIGURE 3 | Histological and histomorfometric analysis of healing components during the intramembranous bone healing in wild-type (WT) vs CCR2KO mice. **(A)** Comparative morphology of the healing phases at 0 h, 7, 14, and 21 days post-extraction of upper right incisor, stained with H&E (0 h—10× magnification and bar = 200 μm; 7, 14, and 21 days—40× magnification and bar = 100 μm). **(B)** Results are presented as the mean of area density for each structure measured in each examined group. Different letters indicate significant differences in each time point ($p < 0.05$); symbol * indicates significant differences between WT vs CCR2KO at the same time point (arrowheads = osteoclasts; arrows = osteoblasts).

(**Figure 7A**). However, there was a peak of CCR5+ cells at 7 days in WT mice, while CCR2KO demonstrated a significantly reduced number of these cells ($p < 0.05$) (**Figure 7B**). As evidenced by immunofluorescence at 7 days, CCR2 and CCR5 are co-localized in cell with a suggestive monocyte/macrophage morphology during the alveolar bone healing in C57Bl/6 mice (**Figure 7C**). FACS analyses of F4/80+ cells from alveolar bone healing at 7 days post-extraction in WT mice revealed that 70% of F4/80+ CCR2+ macrophages are also positive for CCR5 (**Figures 7D,E**).

DISCUSSION

Macrophages are among the first immune cells required to trigger and modulate the inflammatory response, and their initial recruitment from circulation into injured tissues is an essential initial event for a proper tissue healing (1–4, 28). In this context, inflammatory macrophages subpopulation is characterized by high levels of CCR2 expression (21, 28–30), and CCR2 and its ligand CCL2 are upregulated along alveolar bone healing (7), suggesting its involvement in macrophages migration throughout the healing events. At this point, contributions of CCR2 in mediating recruitment of blood/medullar monocytes to inflamed tissues has been demonstrated in different models of injury (2, 3, 10), but its specific function on craniofacial bone is repair still unclear (7). Therefore, in this study, we performed a comparative characterization of the alveolar bone healing process in CCR2KO and C57Bl/6-WT mice, to investigate the role of CCR2 in intramembranous bone healing post tooth extraction.

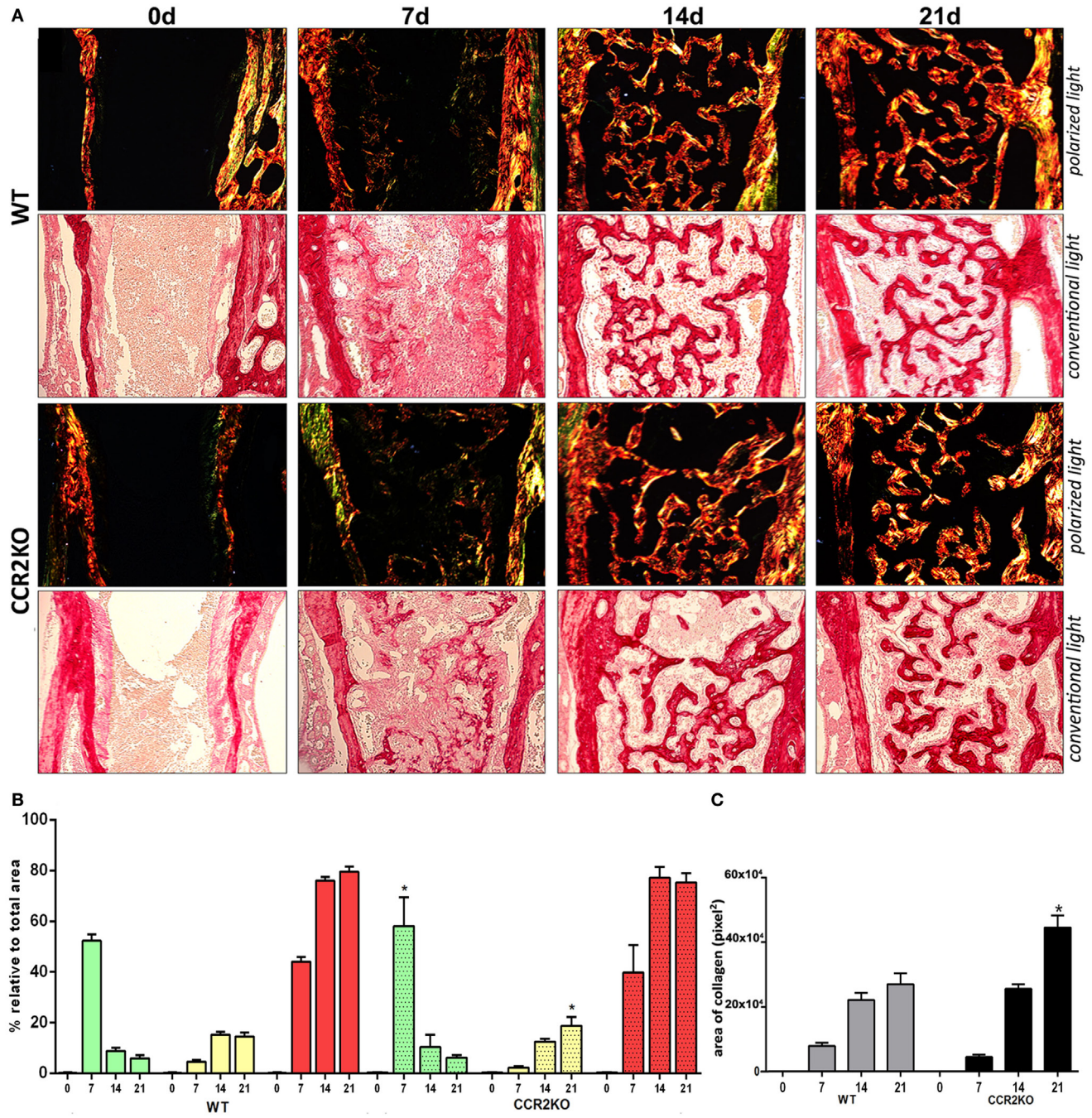

FIGURE 4 | Birefringence analysis of collagen fiber bundles maturation along intramembranous bone healing in wild-type (WT) vs CCR2KO mice. **(A)** Representative sections from medial thirds of the socket stained with Picrosirius red upon polarized and conventional light at 0 h and 7, 14, and 21 days (20× magnification). Green birefringence color indicates thin fibers, while yellow and red colors indicate thick collagen fibers. **(B)** Intensity of birefringence performed using image-analysis software (AxioVision, v. 4.8, CarlZeiss) from each color (%) to quantify thin and thick collagen fibers, as well **(C)** total area of collagen fibers (pixels^2) in WT vs CCR2KO mice. Results are presented as mean and SD of % **(B)** and pixels^2 **(C)**. Symbol * indicates a statistically significant difference ($p < 0.05$) between WT vs CCR2KO at the same time point.

As previously demonstrated by other models of injury in mice, the majority of F4/80+ cells recruited from blood into inflamed sites are monocytes/macrophages, which also exhibit CD11b and CCR2 expression (2). Consequently, the targeted disruption of the CCR2 in CCR2KO mice significantly decreased the number of these F4/80+ cells in cutaneous wounds (2), muscle (20), and endochondral bone injuries (3, 10, 21). In this context, despite the complexity of macrophages

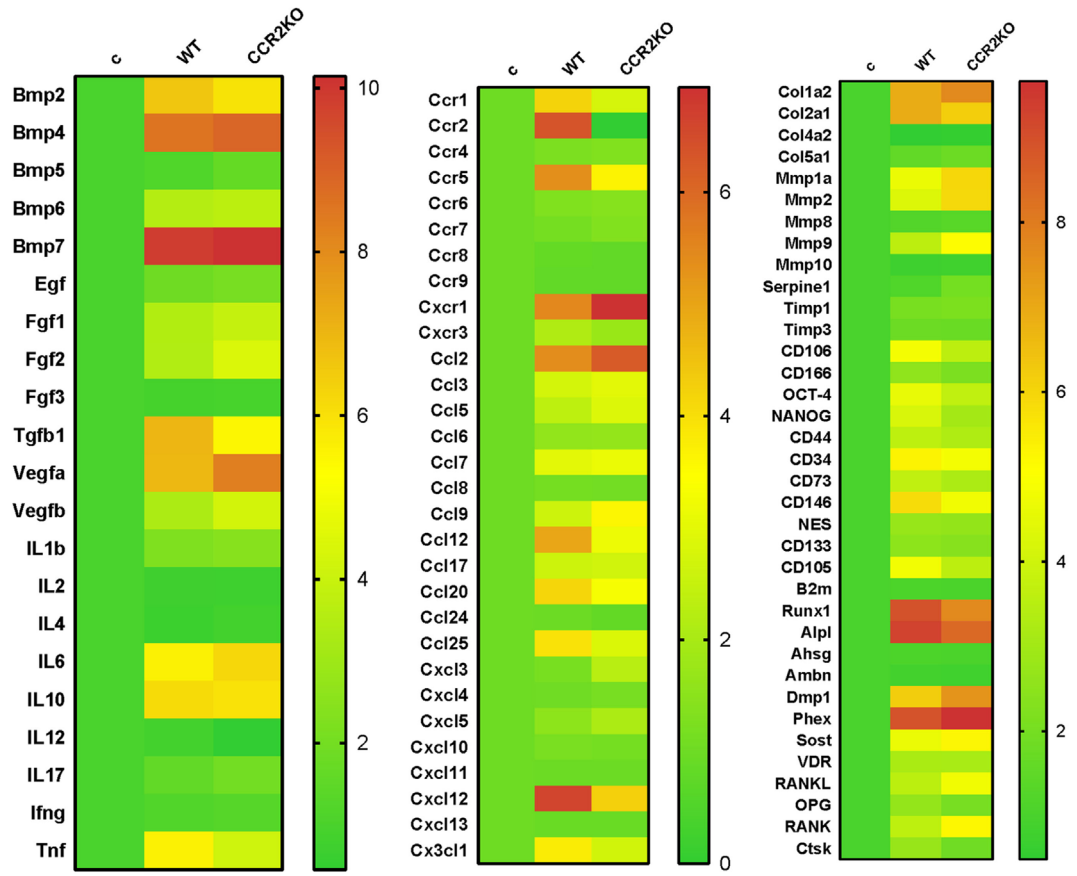

FIGURE 5 | Gene expression patterns in the intramembranous bone healing after tooth extraction in wild-type (WT) vs CCR2KO mice. Molecular analysis of the gene expression patterns in the bone healing was performed with a pool of samples from all the experimental time periods (0, 7, 14, and 21 days) for growth factors, cytokines, chemokines, and chemokine receptors, ECM/repair markers, mesenchymal stem cells, and bone markers. Gene expression was performed by using exploratory analysis by RealTime PCR array, with the VIA7 system (Applied Biosystems, Warrington, UK) and a customized qPCR array comprised of the major targets (Osteogenesis, Inflammatory Cytokines & Receptors, and Wound Healing panels) of the PCR array RT^2 Profiler (SABiosciences/QIAGEN). RealTime PCR array analysis was performed with the VIA7 system (Applied Biosystems, Warrington, UK) using a customized qPCR array comprised of the major targets from the Osteogenesis, Inflammatory Cytokines & Receptors, and Wound Healing panels of the PCR array RT^2 Profiler (SABiosciences/QIAGEN). Results are depicted as the fold increase change (and the SD) in mRNA expression from triplicate measurements in relation to the control samples and normalized by internal housekeeping genes (GAPDH, HPRT, and β-actin).

phenotype, F4/80 has been considered as pan marker for murine macrophages in these specific models of injury. Accordingly, our results initially demonstrate the presence of CCR2+ and F4/80+ cells in the bone healing sites in C57Bl/6 mice, with a peak at inflammatory stage. Interestingly, while F4/80+ cells influx was significantly reduced in CCR2KO mice, suggesting in a cause-and-effect manner the contribution of CCR2 to macrophages migration.

We next investigate if the negative impact of CCR2 deficiency on F4/80+ cells migration was translated into modifications of the subsequent bone healing stages (**Figures 2**–**4**). The μCT analysis demonstrated that absence of CCR2 did not resulted in major changes in the mineralization pattern and bone micro-architecture along alveolar healing in CCR2KO strain (**Figure 2**). Bone mineralization was detected from 7 days in alveolar socket and was gradually increased until the endpoint period (21 days), with important changes on morphological parameters (Tb.Th, Th.Sp, and Th.N) (7), when the alveolar socket is filled whit a thick bone trabeculae and well-defined medullary canals, being such kinetics in accordance with other experimental models in rodents (7, 15, 31). In addition, the histological features of bone healing observed in this study are in accordance to previous description for intramembranous bone healing in mice (7) as well as in humans (32). As well, the birefringence analysis demonstrates a similar evolution in the maturation, organization, and arrangement of collagen fibers inside the alveolar socket in both CCR2KO and WT strains, in accordance with a previous description (7). Taking the μCT and microscopic data together, it is evident that CCR2 deficiency do not impair alveolar bone healing, which is in opposition to endochondral bone healing (6, 10), where CCR2KO mice show a delayed bone formation and maturation during healing. However, as previously mentioned, endochondral and intramembranous bones have fundamental embryological, anatomical, and functional differences (7, 17).

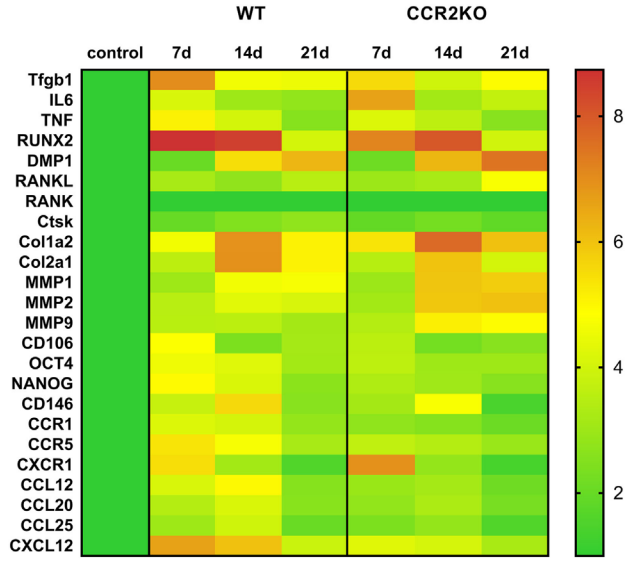

FIGURE 6 | Kinetics of gene expression in the intramembranous bone healing after tooth extraction in wild-type (WT) vs CCR2KO mice. RealTime PCR array pooled from of all the experimental time periods for each strain (WT and CCR2KO mice) was used to identify targets with a significant expression variation for their subsequent analyses in different time points along bone healing post tooth extraction (7, 14, and 21 days). RealTime PCR array analysis was performed with the VIA7 system (Applied Biosystems, Warrington, UK) using a customized qPCR array comprised of the major targets from the Osteogenesis, Inflammatory Cytokines & Receptors, and Wound Healing panels of the PCR array RT^2 Profiler (SABiosciences/QIAGEN). Results are depicted as the fold increase change (and the SD) in mRNA expression from triplicate measurements in relation to the control samples and normalized by internal housekeeping genes (GAPDH, HPRT, and β-actin).

Despite of no major microscopic differences were found between WT and CCR2KO, even by histological analysis, CCR2KO strain presents an impaired resolution of the inflammatory process, as demonstrated by the persistence of higher Ly6g-Gr1+ and CD68+ cells counts until late time points in CCR2KO. Accordingly, the recruitment of neutrophils to fracture sites is also increased in CCR2KO mice compared with WT mice, resulting in an altered composition of inflammatory infiltrate (10). Furthermore, it has been demonstrated that macrophages contribute to promote neutrophil clearance during early resolution phase post liver injury (33), which could explain the persistence of these cells in alveolar sockets of CCR2KO mice.

In the view of the contrasting data regarding CCR2 involvement in intramembranous and endochondral bone healing, we next performed a molecular analysis targeting multiple inflammation and healing related molecules to explore the possible impact of CCR2 lack with a highly sensitive and accurate method. From the molecular viewpoint, CCR2KO mice presented a significantly higher mRNA expression of ECM remodeling markers (Col1a2, Mmp1a, Mmp2, and Mmp9) and at 14 and 21 days, and RANKL at 21 days. On the other hand, mRNA expression of some growth factors (TGFb1) and osteoblast differentiation (Runx-2) markers was downregulated in CCR2KO mice when compared with WT mice (**Figure 6**). Interestingly, while the variation in healing and bone markers expression does not seems to follow a clear (upregulation or downregulation) pattern, the expression of MSC markers (CXCL12, CD106, OCT-4, NANOG, and CD146), presented a homogenous decrease in CCR2KO strain at 7 days (**Figure 6**). Accordingly, CCR2/CCL2 axis is essential for MSCs recruitment in a rib fracture-healing model (6).

However, despite of the molecular differences described between healing sites from CCR2KO and WT strains, it is possible to suggest that such variation was not sufficient to promote significant alteration of the healing phenotype. At this point, we must reinforce that, as previously mentioned, the bone healing is a multi-step process that involves numerous mediators and cell types playing beneficial functions along each healing step (7, 34). In this context, alterations in the migration pattern of a given cell type, suggested as macrophages in this specific case, may be compensate by other elements involved the healing process. Indeed, endothelial cells, MSCs, and other different leukocytes subsets can also release growth factors and immunological mediators involved in many steps of healing, such as angiogenesis, cell proliferation, and resolution of inflammation (35–40). A similar scenario is observed when molecules related to inflammatory cell migration (i.e., inflammatory cytokines and chemokines), where comparatively analyzed during alveolar bone healing in CCR2KO and WT strains. While the expression of some chemokines (CCL12, CCL20, and CCL25), CCR5, and the key inflammatory cytokine TNF expression was decreased in CCR2KO mice at 7 days, the expression of IL6 and CXCR1 (a receptor involved in PMN migration), where significantly higher in CCR2KO strain in the same experimental period, reinforcing that immune system compensatory mechanisms may operate in the absence of CCR2. Accordingly, macrophages are regarded as the major source of TNF during inflammation, where this cytokine plays a pivotal role regulating the pro-inflammatory response (41). However, it has been recognized that IL-6 has many pro-inflammatory functions, such as activation of the immune system, leukocyte chemoattraction (35), and also can contribute to healing processes (14, 37).

In the immunological compensation context, we also must consider that, despite a significant reduction in F4/80+ counts due the lack of CCR2, F4/80+ cells were still present in the bone healing sites in a number enough to support a proper healing outcome. In accordance, in a model of intramembranous bone healing using a model of fracture in tibia, the density of F4/80+ macrophages, as well the bone healing were not compromised by CCR2 deficiency (41). Despite the similar bone healing outcome, at this point, it is important to consider that the reduced F4/80+ cell migration may account for the impaired resolution of the inflammatory process in CCR2KO, which is accordance with the pro-resolutive role of macrophages, which include neutrophil clearance (33). However, when macrophages were aggressively depleted in the site of injury (either using the macrophage-Fas-induced apoptosis or clodronate liposome delivery mouse model), the intramembranous bone healings was drastically impaired in the same tibia fracture model (15). Despite of substantial differences between endochondral long

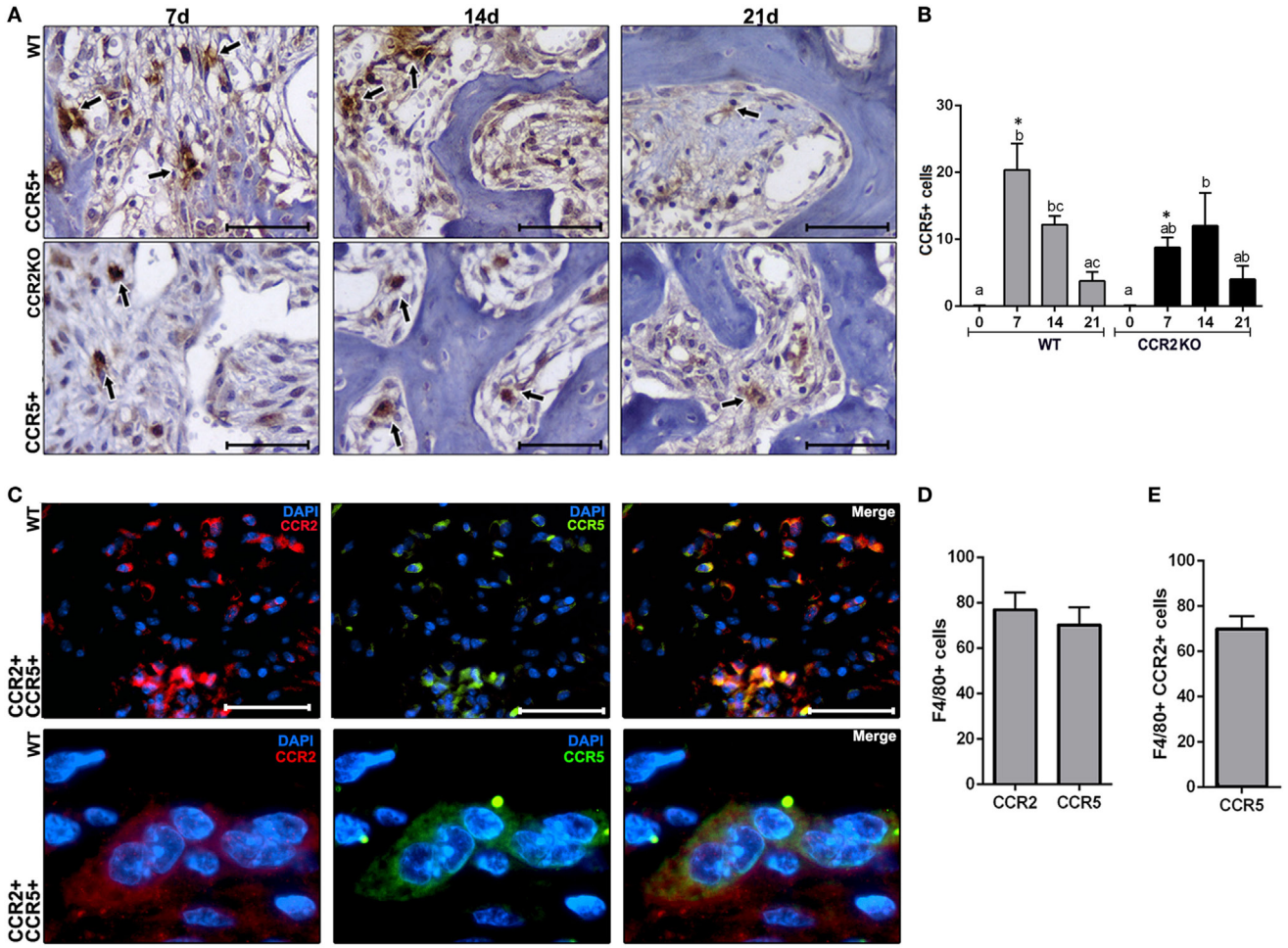

FIGURE 7 | Immunological analysis of CCR2 and CCR5 along intramembranous bone healing in wild-type (WT) vs CCR2KO mice. **(A)** Representative sections from medial thirds of the socket at days 7, 14, and 21 post tooth extraction with immunolabeling for CCR5+ cells in WT and CCR2KO mice (as indicated with arrows) (40× magnification; scale bar = 100 μm). **(B)** Quantitative analysis of CCR5+ cells in WT and CCR2KO mice at days 0, 7, 14, and 21 post-extraction. Different letters indicate significant differences in each time point ($p < 0.05$); symbol * indicate significant differences between WT vs CCR2KO at the same time point. **(C)** Immunocolocalization of CCR2 (TRITC) and CCR5 (fluorescein isothiocyanate) in inflammatory cells at day 7 post tooth extraction in WT mice (100× magnification). **(D,E)** The phenotype of F4/80+ cells from alveolar socket at day 7 post tooth extraction in WT mice, evaluated by flow cytometry, and depicted as the number. Results are presented as mean and SD.

bones and intramembranous craniofacial bones, these evidences suggest that macrophages are not only recruited *via* a CCR2-dependent mechanism.

In this way, the immunological system exhibit intrinsic features that may supply the absence of missing molecules or receptors along inflammatory/immune responses, as the redundancy developed by several cytokines and chemokine/chemokine receptor system (30, 42). Accordingly, immunofluorescence demonstrated a colocalization of CCR2 and CCR5 in macrophages in WT mice, suggesting that macrophages co-express such receptors. Indeed, the FACS analysis confirmed that 70% of F4/80+ CCR2+ cells are also CCR5+ (**Figure 7**) reinforcing the double-positive nature of such cells for CCR2 and CCR5 receptors; which is in line with a previous description that F4/80+ inflammatory macrophages extracted from periodontal tissues are double positive for CCR2 and CCR5 receptors (30). Interestingly, the dual CCR2/CCR5 inhibition with Cenicriviroc significantly inhibited the migration of macrophages in an acute liver injury model (43). Therefore, considering the potential co-expression of CCR2 and CCR5 in F4/80+ cells, the assumption that the dual CCR2/CCR5 inhibition could have a similar effect in bone healing process sounds plausible. In this way, the present results from CCR2KO mice draws the attention to the necessity of future studies with simultaneous inhibition of CCR2 and CCR5 along intramembranous bone healing in craniofacial bones. However, in the view of the potential involvement of other macrophage subsets (which remain to be determined by studies with specific focus in a broad phenotypic analysis of such cell in the healing sites) in intramembranous alveolar bone healing, as well of the other chemokine receptors, additional studies are required to determine the whole contribution of chemokine system to cell migration and its impact in bone healing outcome.

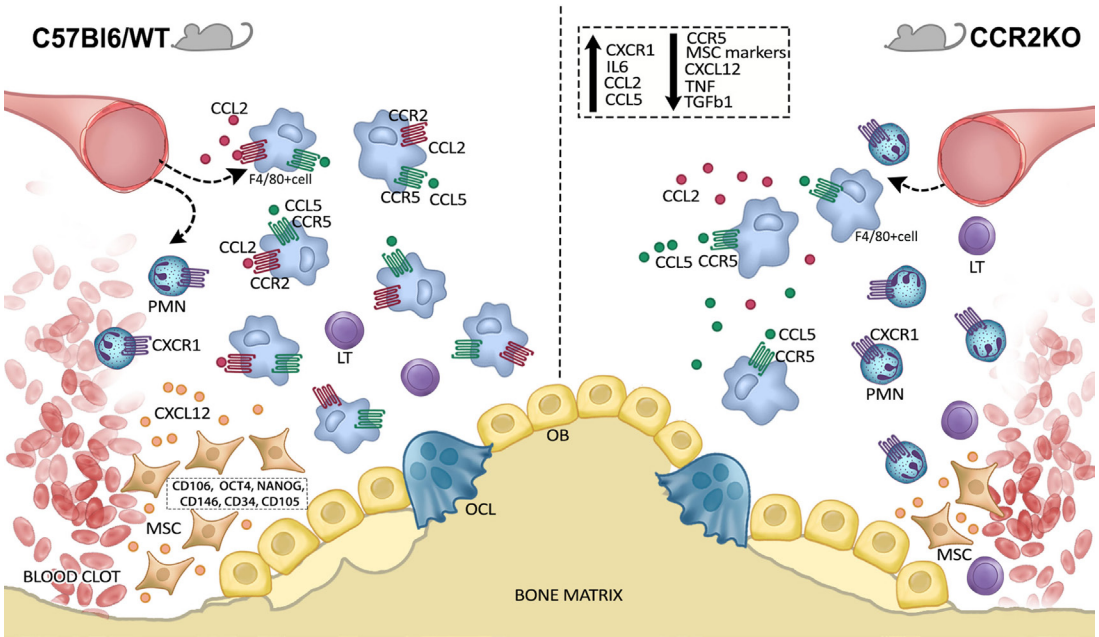

FIGURE 8 | Graphical abstract of CCR2 contributions on F4/80+ cell migration along intramembranous bone healing in maxilla. CCR2 contributes to monocytes/macrophages into alveolar bone injury post tooth extraction, and consequently result in downregulation of mesenchymal stem cell (MSC) markers and growth factors at the healing sites. On the other hand, the migration of the F4/80+ cells in CCR2KO mice it is enough to support the proper healing, in a scenario that can involve compensatory immunological mechanisms.

CONCLUSION

Our results indicate that CCR2 plays an active role on F4/80+ cells migration after alveolar bone injury, and consequently result in downregulation of MSC markers and growth factors at the healing sites (**Figure 8**). However, since CCR2 absence does not significantly impact the outcome of intramembranous bone healing at the endpoint, it is reasonable to suggest that, although reduced, the migration of the F4/80+ cells in CCR2KO mice it is enough to support the proper healing, in a scenario that can involve compensatory immunological mechanisms.

ETHICS STATEMENT

This study was carried out in strict accordance with the recommendations in the Guide for the Care and Use of Laboratory Animals of the National Institutes of Health. The experimental protocol was approved by the local Institutional Committee for Animal Care and Use (Committee on Animal Research and Ethics CEEPA-FOB/USP, process #005/2012).

AUTHOR CONTRIBUTIONS

CB: contributed to acquisition, analysis, and interpretation; drafted manuscript; critically revised manuscript; gave final approval; agreed to be accountable for all aspects of work. AV, FC, and AF: contributed to acquisition, analysis, and interpretation; critically revised manuscript; gave final approval; agreed to be accountable for all aspects of work. PC: contributed to acquisition and analysis; critically revised manuscript; gave final approval; agreed to be accountable for all aspects of work. RS: contributed to conception, contributed to acquisition and interpretation; critically revised manuscript; gave final approval; agreed to be accountable for all aspects of work. AT: contributed to conception and design, contributed to analysis and interpretation; critically revised manuscript; gave final approval; agreed to be accountable for all aspects of work. GG: contributed to conception and design; contributed to acquisition, analysis, and interpretation; drafted manuscript; critically revised manuscript; gave final approval; agreed to be accountable for all aspects of work.

ACKNOWLEDGMENTS

The authors acknowledge Bruno Cavalini Cavenago by his support with μCT; and the technicians Daniele Santi Ceolin, Patrícia de Sá Mortagua Germino, and Tania Mary Cestari for their excellent technical assistance. This work was supported by grants #2012/03636-0 and #2015/24637-3 from São Paulo Research Foundation (FAPESP).

REFERENCES

1. Lucas T, Waisman A, Ranjan R, Roes J, Krieg T, Müller W, et al. Differential roles of macrophages in diverse phases of skin repair. *J Immunol* (2010) 184(7):3964–77. doi:10.4049/jimmunol.0903356
2. Willenborg S, Lucas T, van Loo G, Knipper JA, Krieg T, Haase I, et al. CCR2 recruits an inflammatory macrophage subpopulation critical for angiogenesis in tissue repair. *Blood* (2012) 120(3):613–25. doi:10.1182/blood-2012-01-403386
3. Wu AC, Raggatt LJ, Alexander KA, Pettit AR. Unraveling macrophage contributions to bone repair. *Bonekey Rep* (2013) 2:373–80. doi:10.1038/bonekey.2013.107
4. Brancato SK, Albina JE. Wound macrophages as key regulators of repair: origin, phenotype, and function. *Am J Pathol* (2011) 178(1):19–25. doi:10.1016/j.ajpath.2010.08.003
5. Raggatt LJ, Wullschleger ME, Alexander KA, Wu AC, Millard SM, Kaur S, et al. Fracture healing via periosteal callus formation requires macrophages for both initiation and progression of early endochondral ossification. *Am J Pathol* (2014) 184(12):3192–204. doi:10.1016/j.ajpath.2014.08.017
6. Ishikawa M, Ito H, Kitaori T, Murata K, Shibuya H, Furu M, et al. MCP/CCR2 signaling is essential for recruitment of mesenchymal progenitor cells during the early phase of fracture healing. *PLoS One* (2014) 9(8):e104954. doi:10.1371/journal.pone.0104954
7. Vieira AE, Repeke CE, Ferreira Junior Sde B, Colavite PM, Biguetti CC, Oliveira RC, et al. Intramembranous bone healing process subsequent to tooth extraction in mice: micro-computed tomography, histomorphometric and molecular characterization. *PLoS One* (2015) 10(5):e0128021. doi:10.1371/journal.pone.0128021
8. Claes L, Recknagel S, Ignatius A. Fracture healing under healthy and inflammatory conditions. *Nat Rev Rheumatol* (2012) 8(3):133–43. doi:10.1038/nrrheum.2012.1
9. Vortkamp A, Pathi S, Peretti GM, Caruso EM, Zaleske DJ, Tabin CJ. Recapitulation of signals regulating embryonic bone formation during postnatal growth and in fracture repair. *Mech Dev* (1998) 71(1–2):65–76. doi:10.1016/S0925-4773(97)00203-7
10. Xing Z, Lu C, Hu D, Yu YY, Wang X, Colnot C, et al. Multiple roles for CCR2 during fracture healing. *Dis Model Mech* (2010) 3(7–8):451–8. doi:10.1242/dmm.003186
11. Omar OM, Granéli C, Ekström K, Karlsson C, Johansson A, Lausmaa J, et al. The stimulation of an osteogenic response by classical monocyte activation. *Biomaterials* (2011) 32(32):8190–204. doi:10.1016/j.biomaterials.2011.07.055
12. Gerstenfeld LC, Cho TJ, Kon T, Aizawa T, Cruceta J, Graves BD, et al. Impaired intramembranous bone formation during bone repair in the absence of tumor necrosis factor-alpha signaling. *Cells Tissues Organs* (2001) 169(3):285–94. doi:10.1159/000047893
13. Gerstenfeld LC, Cho TJ, Kon T, Aizawa T, Tsay A, Fitch J, et al. Impaired fracture healing in the absence of TNF-alpha signaling: the role of TNF-alpha in endochondral cartilage resorption. *J Bone Miner Res* (2003) 18(9):1584–92. doi:10.1359/jbmr.2003.18.9.1584
14. Yang X, Ricciardi BF, Hernandez-Soria A, Shi Y, Pleshko Camacho N, Bostrom MP. Callus mineralization and maturation are delayed during fracture healing in interleukin-6 knockout mice. *Bone* (2007) 41(6):928–36. doi:10.1016/j.bone.2007.07.022
15. Alexander KA, Chang MK, Maylin ER, Kohler T, Müller R, Wu AC, et al. Osteal macrophages promote in vivo intramembranous bone healing in a mouse tibial injury model. *J Bone Miner Res* (2011) 26(7):1517–32. doi:10.1002/jbmr.354
16. Schlundt C, El Khassawna T, Serra A, Dienelt A, Wendler S, Schell H, et al. Macrophages in bone fracture healing: their essential role in endochondral ossification. *Bone* (2015) 106:78–89. doi:10.1016/j.bone.2015.10.019
17. Mouraret S, Hunter DJ, Bardet C, Brunski JB, Bouchard P, Helms JA. A pre-clinical murine model of oral implant osseointegration. *Bone* (2014) 58:177–84. doi:10.1016/j.bone.2013.07.021
18. Garlet GP, Sfeir CS, Little SR. Restoring host-microbe homeostasis via selective chemoattraction of Tregs. *J Dent Res* (2014) 93(9):834–9. doi:10.1177/0022034514544300
19. Kothandan G, Gadhe CG, Cho SJ. Structural insights from binding poses of CCR2 and CCR5 with clinically important antagonists: a combined in silico study. *PLoS One* (2012) 7(3):e32864. doi:10.1371/journal.pone.0032864
20. Lu H, Huang D, Saederup N, Charo IF, Ransohoff RM, Zhou L. Macrophages recruited via CCR2 produce insulin-like growth factor-1 to repair acute skeletal muscle injury. *FASEB J* (2011) 25(1):358–69. doi:10.1096/fj.10-171579
21. Sinder BP, Pettit AR, McCauley LK. Macrophages: their emerging roles in bone. *J Bone Miner Res* (2015) 30(12):2140–9. doi:10.1002/jbmr.2735
22. Goodman SC, Letra A, Dorn S, Araujo-Pires AC, Vieira AE, Chaves de Souza L, et al. Expression of heat shock proteins in periapical granulomas. *J Endod* (2014) 40(6):830–6. doi:10.1016/j.joen.2013.10.021
23. Kuroshima S, Kovacic BL, Kozloff KM, McCauley LK, Yamashita J. Intra-oral PTH administration promotes tooth extraction socket healing. *J Dent Res* (2013) 92(6):553–9. doi:10.1177/0022034513487558
24. Bouxsein ML, Boyd SK, Christiansen BA, Guldberg RE, Jepsen KJ, Muller R. Guidelines for assessment of bone microstructure in rodents using micro-computed tomography. *J Bone Miner Res* (2010) 25(7):1468–86. doi:10.1002/jbmr.141
25. Araujo-Pires AC, Vieira AE, Francisconi CF, Biguetti CC, Glowacki A, Yoshizawa S, et al. IL-4/CCL22/CCR4 axis controls regulatory T-cell migration that suppresses inflammatory bone loss in murine experimental periodontitis. *J Bone Miner Res* (2015) 30(3):412–22. doi:10.1002/jbmr.2376
26. Queiroz-Junior CM, Madeira MF, Coelho FM, de Oliveira CR, Cândido LC, Garlet GP, et al. Experimental arthritis exacerbates *Aggregatibacter actinomycetemcomitans*-induced periodontitis in mice. *J Clin Periodontol* (2012) 39(7):608–16. doi:10.1111/j.1600-051X.2012.01886.x
27. Benjamini Y, Hochberg Y. Controlling the false discovery rate: a practical and powerful approach to multiple testing. *J R Stat Soc Series B (Methodol)* (1995) 1(57):11.
28. Volpe S, Cameroni E, Moepps B, Thelen S, Apuzzo T, Thelen M. CCR2 acts as scavenger for CCL2 during monocyte chemotaxis. *PLoS One* (2012) 7(5):e37208. doi:10.1371/journal.pone.0037208
29. Wu AC, Morrison NA, Kelly WL, Forwood MR. MCP-1 expression is specifically regulated during activation of skeletal repair and remodeling. *Calcif Tissue Int* (2013) 92(6):566–75. doi:10.1007/s00223-013-9718-6
30. Repeke CE, Ferreira SB Jr, Claudino M, Silveira EM, de Assis GF, Avila-Campos MJ, et al. Evidences of the cooperative role of the chemokines CCL3, CCL4 and CCL5 and its receptors CCR1+ and CCR5+ in RANKL+ cell migration throughout experimental periodontitis in mice. *Bone* (2010) 46(4):1122–30. doi:10.1016/j.bone.2009.12.030
31. Ebina H, Hatakeyama J, Onodera M, Honma T, Kamakura S, Shimauchi H, et al. Micro-CT analysis of alveolar bone healing using a rat experimental model of critical-size defects. *Oral Dis* (2009) 15(4):273–80. doi:10.1111/j.1601-0825.2009.01522.x
32. Amler MH. The time sequence of tissue regeneration in human extraction wounds. *Oral Surg Oral Med Oral Pathol* (1969) 27(3):309–18. doi:10.1016/0030-4220(69)90357-0
33. Graubardt N, Vugman M, Mouhabed O, Caliari G, Pasmanik-Chor M, Reuveni D, et al. Ly6Chi monocytes and their macrophage descendants regulate neutrophil function and clearance in acetaminophen-induced liver injury. *Front Immunol* (2017) 8:626. doi:10.3389/fimmu.2017.00626
34. Koh TJ, Di Pietro LA. Inflammation and wound healing: the role of the macrophage. *Expert Rev Mol Med* (2011) 13:e23. doi:10.1017/S1462399411001943
35. Gao F, Chiu SM, Motan DA, Zhang Z, Chen L, Ji HL, et al. Mesenchymal stem cells and immunomodulation: current status and future prospects. *Cell Death Dis* (2016) 7:e2062. doi:10.1038/cddis.2015.327
36. Scheller J, Chalaris A, Schmidt-Arras D, Rose-John S. The pro- and anti-inflammatory properties of the cytokine interleukin-6. *Biochim Biophys Acta* (2011) 1813(5):878–88. doi:10.1016/j.bbamcr.2011.01.034
37. Huang YH, Yang HY, Huang SW, Ou G, Hsu YF, Hsu MJ. Interleukin-6 induces vascular endothelial growth factor-C expression via Src-FAK-STAT3 signaling in lymphatic endothelial cells. *PLoS One* (2016) 11(7):e0158839. doi:10.1371/journal.pone.0158839
38. Araujo-Pires AC, Biguetti CC, Repeke CE, Rodini Cde O, Campanelli AP, Trombone AP, et al. Mesenchymal stem cells as active prohealing and immunosuppressive agents in periapical environment: evidence from human and experimental periapical lesions. *J Endod* (2014) 40(10):1560–5. doi:10.1016/j.joen.2014.02.012

39. Parameswaran N, Patial S. Tumor necrosis factor-alpha signaling in macrophages. *Crit Rev Eukaryot Gene Expr* (2010) 20(2):87–103. doi:10.1615/CritRevEukarGeneExpr.v20.i2.10
40. Reinke JM, Sorg H. Wound repair and regeneration. *Eur Surg Res* (2012) 49(1):35–43. doi:10.1159/000339613
41. Batton L, Millard SM, Raggat J, Pettit AR. Osteomacs and bone regeneration. *Curr Osteoporos Rep* (2017) 15(4):385–95. doi:10.1007/s11914-017-0384-x
42. Mack M, Cihak J, Simonis C, Luckow B, Proudfoot AE, Plachý J, et al. Expression and characterization of the chemokine receptors CCR2 and CCR5 in mice. *J Immunol* (2001) 166(7):4697–704. doi:10.4049/jimmunol.166.7.4697
43. Puengel T, Krenkel O, Kohlhepp M, Lefebvre E, Luedde T, Trautwein C, et al. Differential impact of the dual CCR2/CCR5 inhibitor cenicriviroc on migration of monocyte and lymphocyte subsets in acute liver injury. *PLoS One* (2017) 12(9):e0184694. doi:10.1371/journal.pone.0184694

Conflict of Interest Statement: The authors declare that the research was conducted in the absence of any commercial or financial relationships that could be construed as a potential conflict of interest.

frontiers in Immunology

ORIGINAL RESEARCH
published: 15 August 2018
doi: 10.3389/fimmu.2018.01712

Impaired Differentiation of Langerhans Cells in the Murine Oral Epithelium Adjacent to Titanium Dental Implants

Oded Heyman[1], Noam Koren[2], Gabriel Mizraji[1,2], Tal Capucha[2], Sharon Wald[2], Maria Nassar[2], Yaara Tabib[2], Lior Shapira[1], Avi-Hai Hovav[2†] and Asaf Wilensky[1*†]*

[1] Department of Periodontology, Faculty of Dental Medicine, Hebrew University—Hadassah Medical Center, Jerusalem, Israel, [2] Faculty of Dental Medicine, The Institute of Dental Sciences, Hebrew University, Jerusalem, Israel

OPEN ACCESS

Edited by:
Simon Yona, University College London, United Kingdom

Reviewed by:
Clare L. Bennett, University College London, United Kingdom
Alexander Mildner, Max-Delbrück-Centrum für Molekulare Medizin, Helmholtz-Gemeinschaft Deutscher Forschungszentren (HZ), Germany

***Correspondence:**
Avi-Hai Hovav
avihaih@ekmd.huji.ac.il;
Asaf Wilensky
asafw@ekmd.huji.ac.il

†These authors have contributed equally to this work.

Specialty section:
This article was submitted to Antigen Presenting Cell Biology, a section of the journal Frontiers in Immunology

Received: *26 April 2018*
Accepted: *12 July 2018*
Published: *15 August 2018*

Citation:
Heyman O, Koren N, Mizraji G, Capucha T, Wald S, Nassar M, Tabib Y, Shapira L, Hovav A-H and Wilensky A (2018) Impaired Differentiation of Langerhans Cells in the Murine Oral Epithelium Adjacent to Titanium Dental Implants. Front. Immunol. 9:1712. doi: 10.3389/fimmu.2018.01712

Peri-implantitis is a destructive inflammatory process affecting tissues surrounding dental implants and it is considered a new global health concern. Human studies have suggested that the frequencies of Langerhans cells (LCs), the main antigen-presenting cells (APCs) of the oral epithelium, are dysregulated around the implants. Since LCs play a role in regulating oral mucosal homeostasis, we studied the impact of dental titanium implants on LC differentiation using a novel murine model. We demonstrate that whereas the percentage of LC precursors ($CD11c^+MHCII^+$) increased in the peri-implant epithelium, the frequencies of LCs ($CD11c^+MHCII^+EpCAM^+langerin^+$) were significantly reduced. Instead, a population of partially developed LCs expressing $CD11c^+MHCII^+EpCAM^+$ but not langerin evolved in the peri-implant mucosa, which was also accompanied by a considerable leukocyte infiltrate. In line with the increased levels of LC precursors, expression of CCL2 and CCL20, chemokines mediating their translocation to the epithelium, was elevated in the peri-implant epithelium. However, expression of TGF-β1, the major cytokine driving final differentiation of LCs, was reduced in the epithelium. Further analysis revealed that while the expression of the TGF-β1 canonical receptor activing-like kinase (ALK)5 was upregulated, expression of its non-canonical receptor ALK3 was decreased. Since titanium ions releasing from implants were proposed to alter APC function, we next analyzed the impact of such ions on TGF-β1-induced LC differentiation cultures. Concurring with the *in vivo* studies, the presence of titanium ions resulted in the generation of partially developed LCs that express $CD11c^+MHCII^+EpCAM^+$ but failed to upregulate langerin expression. Collectively, these findings suggest that titanium dental implants have the capacity to impair the development of oral LCs and might subsequently dysregulate immunity in the peri-implant mucosa.

Keywords: dental implants, peri-implantitis, Langerhans cells, peri-implant epithelium, langerin

INTRODUCTION

Dental implants provide a successful solution in replacement of missing teeth, with more than two million dental implants are placed annually around the world (1). The use of dental implants brought upon a new disease, peri-implantitis, which became a major health concern worldwide (2–8). A recent epidemiologic review reported that every fifth dental implant eventually develops peri-implantitis during a mean functional loading time of 3.4–11 years (8). Titanium implants

are mostly used for dental rehabilitation; nevertheless, titanium micro-particles were found to be released into peri-implant mucosa and their presence was proposed to alter local mucosal immunity (9–16). Moreover, titanium ions were shown to alter the maturation and migration capabilities of dendritic cells (DCs) differentiated from human monocytes (11). It is thus important to reveal how titanium implants alter oral mucosal immunity, as such knowledge will increase our understanding of the unknown pathogenesis of this new disease together with our capacity to develop therapeutic strategies to prevent dental implant-associated diseases and ultimately failure of the implants.

Langerhans cells (LCs) are a unique type of antigen-presenting cells (APCs) exclusively located in stratified epithelia such as the skin epidermis and the oral mucosa epithelium (17–20). Besides their distinctive anatomical location, LCs can be identified based on their capacity to express high levels of langerin (CD207) and epithelial cell adhesion molecule (EpCAM/CD326). Nevertheless, unlike epidermal LCs that originate from embryonic precursors (21, 22), oral LCs develop at steady state from adult bone marrow (BM) precursors: pre-DCs and monocytes (23). It has been shown recently that differentiation of these two precursors into LCs involves sequential signaling at two separate anatomical locations (24). Upon extravasation from the circulation, LC precursors acquire a $CD11c^{+}MHCII^{+}$ phenotype and later on exposed to bone morphogenetic protein 7 (BMP7), which its expression is restricted to the lamina propria (LP). Interaction of BMP7 with activing-like kinase 3 (ALK3), upregulates the expression of E-cadherin, CCR2, and CCR6 on LC precursors enabling their translocation to the epithelium. Within the epithelium, the precursors are exposed to TGF-β1 that finalizes their differentiation, resulting in an upregulation of EpCAM and later on langerin. This activity of TGF-β1 is considered to involve signaling *via* its canonical receptor ALK5; nevertheless, TGF-β1/ALK3 signaling is also likely to play a role in terminal LC differentiation. Oral LCs can be divided into at least two subsets, $CD103^{+}$LCs and $CD11b^{+}$LCs, which might represent two functionally diverse populations (23). On this regard, LCs were shown to play a regulatory function on oral mucosal immunity at both steady state and inflammatory conditions. Inducible ablation of LCs was shown to alter oral mucosal immunological functions and to induce microbial dysbiosis. Interestingly, oral microbiota also affects LCs development as the absence or decrease in the microbiota resulted in a reduced frequencies of oral LCs, particularly $CD103^{+}$LCs (24). In a setting of infection with the oral pathogen *Porphyromonas gingivalis*, LCs were shown to have a protective function, inducing T regulatory (Treg) cells that inhibit the development of bone destructing Th1 immunity (25).

Given the important role of LCs on oral mucosal immunity, it is very likely that these cells might orchestrate the peri-implant immunological status. It is also possible that the presence of the implant will have some effects on the neighboring LCs. Nevertheless, there is a dispute in the literature regarding the impact of titanium dental implants on oral LCs. Various studies examined LCs in the tissue around dental implants have reported either a reduction or, alternatively, no alteration in the frequencies of these cells (26–30). Whereas such contradicting results could be explained by a variation in tissue sampling, technical approach, or the markers used to identify LCs, they highlight the necessity of an experimental model allowing meticulous analysis of this important topic. Using an experimental murine model, this study was initiated to explore whether and how oral mucosal LCs are regulated by titanium dental implants.

MATERIALS AND METHODS

Mice

BALB/c mice (4–5 week old) were purchased from Harlan (Jerusalem, Israel). All the animals were housed in ventilated cages at room temperature under a 16 h light and 8 h dark cycle and received distilled water and food *ad libitum*. All animal experimental procedures were reviewed and approved by the IACUC of the Hadassah—Hebrew University Medical Center.

Antibodies and Reagents

The following fluorochrome-conjugated monoclonal antibodies and the corresponding isotype controls were purchased from BioLegend (San Diego, CA, USA): CD45.2 (104), I-A/I-E (M5/114.15.2), EpCAM (G8.8), CD11b (M1/70), CD11c (N418), Langerin (4C7), CD205 (NLDC-145), CD103 (2E7), Ly6C (HK1.4), Ly6g (1A8), CD3 (17A2), CD4 (GK1.5), FOXP3 (MF-14), and B220 (RA36B2). Propidium iodide solution was also purchased from BioLegend.

Titanium Implants

Custom-made titanium implants (MIS Implants Technologies Ltd., Israel) were made from Ti6Al4V alloy and were acid etched. The implants length was 1.7 mm and the implant diameter was 0.7 mm at the coronal end and 0.2 mm at the apical end.

Extractions and Implantation

In each experiment, the mice were randomly divided into two groups, implanted and non-implanted. Animals in the first group were designated to receive two titanium implants following the extraction of the left upper molars whereas the mice in the control non-implanted group did not undergo the above-mentioned procedures. In order to ensure minimum interference with the implant osseointegration, the antagonist teeth of the lower jaw were extracted in both groups in order to reduce occlusal masticatory forces. All mice were anesthetized prior to the surgical procedure with an intra-peritoneal injection of ketamine (50 mg/kg) and Xylazine (10 mg/kg). In addition, analgesia was provided by sub-cutaneous injection (Carprofen, 5 mg/ml, 100 µl) and the mice were maintained with sterile soft diet for 1 week. To allow proper wound and bone healing the implants were inserted 4 weeks after teeth extraction, in the sites correlating to the original locations of the first and second molars. Under general anesthesia and analgesia, the osteotomy sites were prepared and the implants were inserted with custom-made driver (MIS Implants Technologies Ltd., Israel) until the implant's threads were completely covered by bone and resistance and stability were achieved. Mice were given antibiotics (5% enrofoloxacin in drinking water) and soft diet for 7 days following implant insertion.

Isolation and Processing of Gingiva and Peri-Implant Mucosa Tissues

The mice were euthanized and a circumference of 1 mm of gingiva around teeth in non-implanted mice, or 1 mm of peri-implant mucosa in implanted mice was harvested and pooled from two to three mice so that a sufficient number of cells were obtained for flow cytometry analysis. These pooled tissues were considered as $n = 1$. Next, the samples were incubated with Dispase II solution (Godo Shusei, Japan) 2 mg/ml in PBS + 2% fetal calf serum (FCS), for 45 min at 37°C. The epithelium was separated by using forceps under a stereoscope, and later on was minced and treated with Collagenase type II (2 mg/ml; Worthington Biochemicals) and DNase I (1 mg/ml; Roche) solution in PBS + 2% FCS for 25 min at 37°C in a shaker bath. A total of 20 µl of 0.5 M EDTA per 2 ml sample was added to the digested tissues and incubated for an additional 10 min. The cells were washed, filtered with a 70-µM filter, and stained with antibodies as indicated in the text. The stained samples were run in the LSR II (BD Biosciences) flow cytometer and analyzed using FlowJo software (Tree Star).

Immunofluorescence Staining

The maxillae were fixed overnight at 4°C in 4% paraformaldehyde/PBS solution, and then washed for 1 week in EDTA 0.5 M/PBS that was changed every other day. Carefully, the implants were taken out in counterclockwise motion without damaging the surrounding tissue. Next, the tissue was cryopreserved in 30% sucrose (overnight at 4°C), embedded in OCT, and cryosectioned into 10-µm-thick sections. The cross sections, as well as the separated epithelium, were washed three times in PBS, blocked in a blocking buffer (5% FCS, 0.1% Triton X-100 in PBS) for 1 h at room temperature, and incubated with primary antibodies: goat anti-langerin (E-17, Santa Cruz Biotechnology), rat anti-MHCII (M5/114.15.2, BioLegend), rabbit anti-TGF-β1 (ab92486 Abcam), and mouse anti-BMP-7 (ab54904 Abcam) overnight at 4°C. Following three washing steps in PBS, the samples were incubated with a secondary antibody: donkey anti-goat IgG, donkey anti-rat IgG, or donkey anti-rabbit IgG (Jackson ImmunoResearch) diluted 1:100 in blocking buffer for 1 h at RT, washed three times, stained with Hoechst, and mounted. Signals were visualized and digital images were obtained using an Olympus BX51 fluorescent microscope mounted with a DP72 (Olympus) camera. The color intensity was calculated using Image J on 8-bit images by countering the specific area of interest. The average pixel intensity was calculated from a pixel histogram representing the color intensity of each pixel. Negative control was achieved by staining the tissue with the same primary antibody using non-compatible secondary antibody.

Picrosirius Red Staining

The cryo cross sections slides were washed once in PBS for 30 min, followed by staining with Weigert's hematoxylin for 8 min. Immediately after, the slides were washed for 10 min in running tap water, followed by staining with Picrosirius red for 1 h in dark. The staining was washed in acidified water that was changed twice and dehydrated for 5 min each time in 100% ethanol that was replaced three times. The slides were then incubated with xylene for 5 min followed by mounting in resinous medium.

RNA Extraction and Quantitative Real-Time PCR (RT-*q*PCR)

For RNA isolation, the peri-implant mucosa and gingiva were separated into submucosa and epithelium layers *via* incubation with Dispase II solution. The different layers were then homogenized in 1 ml TRI reagent (Sigma) using electric homogenizer. After homogenization, the homogenates were centrifuged at 12,000 × *g* for 10 min at 5°C to remove the insoluble material. The clear supernatants were then transferred to fresh tubes and 0.2 ml of chloroform was added to each tube. The tubes were covered tightly, vortexed for 15 s, and left for 10 min at RT. The resulting mixture was centrifuged at 12,000 × *g* for 15 min at 5°C and the colorless upper aqueous phase (containing RNA) was transferred to a fresh tube and 0.5 ml of 2-propanol was added to the tube. The samples stand for 5 min at RT and then centrifuged at 12,000 × *g* for 10 min at 5°C. The RNA precipitate forms a pellet on the side and bottom of the tube. The supernatant was removed and RNA pellet was washed by adding of 1 ml of 75% ethanol per sample, and then centrifuged the samples at 7,500 × *g* for 5 min at 5°C. The RNA pellet was air dried for 5–10 min and an appropriate volume DEPC solution was added. To synthesize cDNA from the RNA pellet, the qScript™ cDNA Synthesis Kit, 95047-100 (Quanta-BioSciences Inc.) was employed. RT-*q*PCR reaction was performed in a 20-µl reaction mixture using Power SYBR Green PCR Master Mix (Quanta-BioSciences Inc.). The following reaction conditions were used: 10 min at 95°C, 40 cycles of 15 s at 95°C and 60 s at 60°C. The samples were normalized to the 18 s as control mRNA, by change in cycling threshold (ΔCT) method and calculated based on $2^{-\Delta CT}$.

Differentiation Cultures of LC-Like Cells

The femur was isolated, cleaned from soft tissues in RPMI 1640 and soaked in 70% ethanol for 1 min for sterilization. The femur was then washed with sterile PBS and the bone ends was removed by sterile scissors. BM cells eluted from the bone by flushing them several times using sterile syringe filled with RPMI 1640, and the cells were then washed, treated with ACK solution for 3 min on ice, washed again and counted. BM cells (5×10^5 cells/well) in 24-well plates (Nunc) were cultured with complete RPMI media [450 ml RPMI 1640, 50 ml FCS, 5 ml L-glutamine, 50 µM β-mercaptoethanol, penicillin (100 U/ml), streptomycin (100 µg/ml), and gentamicin (50 µg/ml)] supplemented with GM-SCF (100 ng/ml), TGF-β1 (10 ng/ml) for 5 days to induce their differentiation into LC-like cells as previously described (31). To examine the impact of Ti ions on LC, we applied Ti standard solution (1,000 µg/ml Ti in H_2O, Sigma), at day 0, in various dilutions to the cultures. The cultures were then washed and stained with the noted antibodies for flow cytometry analysis.

Statistical Analysis

Data were expressed as mean ± SEM. Statistical tests were performed using Student's *t*-test. $p < 0.05$ was considered significant. $^*p < 0.05$, $^{**}p < 0.01$, $^{***}p < 0.001$.

RESULTS

Establishment of Experimental Dental Implant Model in Mice

To study basic immunological and microbial mechanisms involved in the placement of dental implants, a murine model is highly desirable since vast experimental tools and transgenic mice are available. We thus established a novel approach to orally place two titanium dental implants in mice (**Figure 1A**). In this model, the left upper molars were extracted and the mice left to heal for 4 weeks. A custom made titanium implants (MIS Implants Technologies, Israel) were then placed into two sites correlating with the first and second molar sites. As depicted in **Figure 1B**, the total average survival rate of 200 implants located at the posterior maxilla was over 80%. This rate

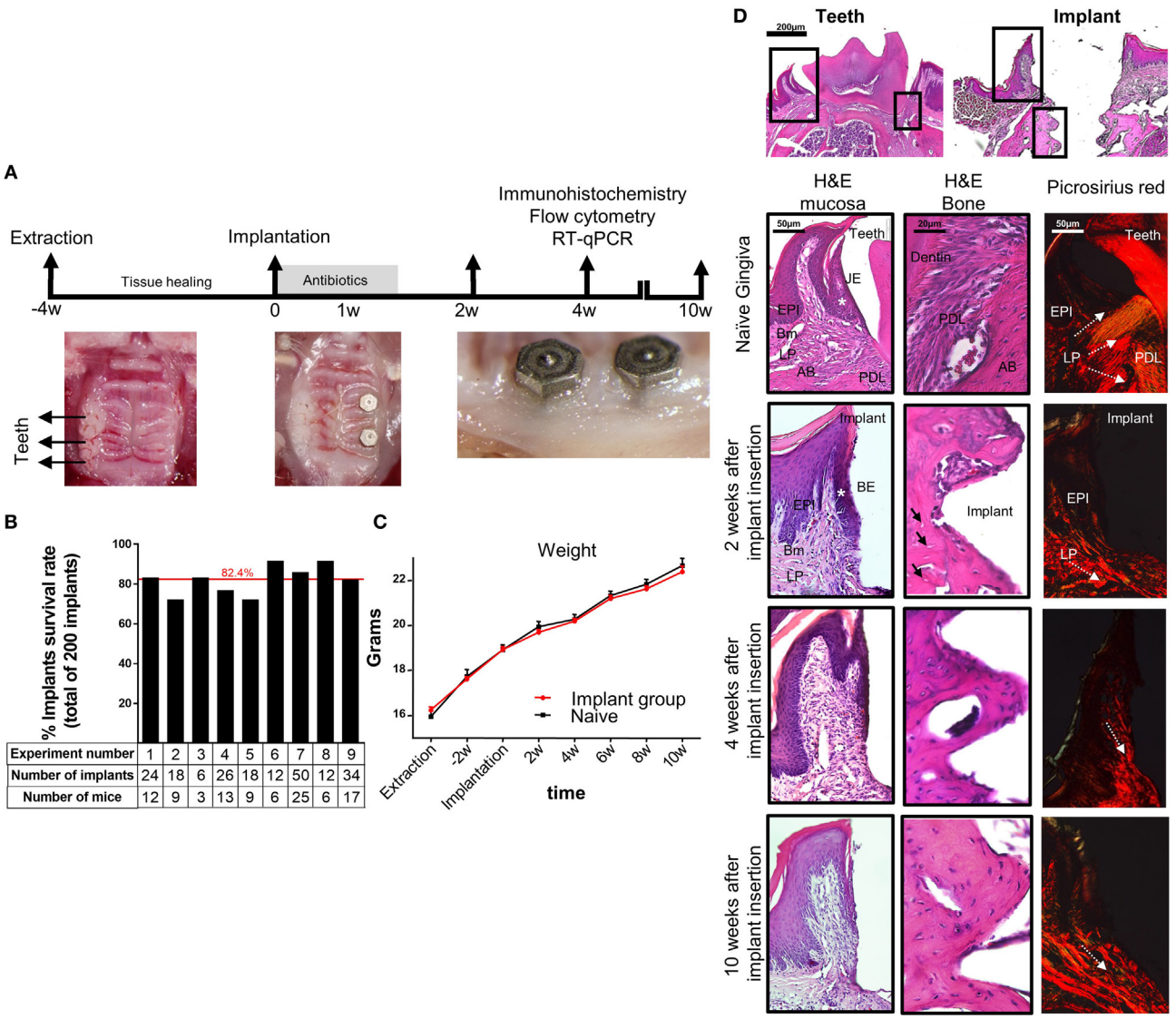

FIGURE 1 | Establishment of a murine model of titanium dental implants. **(A)** Schematic presentation of the experimental setting for insertion of titanium dental implant. Four weeks after tooth extraction two dental implants were inserted in the first and second molar regions of the alveolar bone. The mice were treated for 1 week with antibiotics in the drinking water and soft diet and analyzed 2, 4, and 10 weeks later. **(B)** Bar graph demonstrates the average cumulative survival rate of both implants in nine independent experiments (n = 3–25 implanted mice per experiment). The red line indicates the weighted average mean value. **(C)** Mouse weight in implanted and control mice during 10 weeks post implant insertion, presented as the mean ± SEM (n = 3–25 mice per group). Representative results of one out of four independent experiments are presented. **(D)** Images of H&E and Picrosirius red staining of the gingiva, peri-implant mucosa, and bone taken at 2, 4, and 10 weeks after implant insertion. The upper images visualize the orientation of the tissue with respect to the location of interest presented as squares. White asterisk marks the junctional epithelium (JE) around teeth and its equivalent the barrier epithelium (BE) around implants. Black arrows indicate empty osteocyte lacunae. White dotted arrows specify the collagen bundle orientation in the tissues. Representative results of one out of three independent experiments are presented. In each experiment, at least three mice per group were examined. Abbreviations: EPI, epithelium; Bm, basement membrane; LP, lamina propria; PDL, periodontal ligament; AB, alveolar bone.

is in accordance with the survival rate reported in human studies, emphasizing the efficacy and strength of our experimental model (32, 33). The implanted mice had no significant clinical signs and gained weight in a similar kinetics as the control sex- and aged-matched naïve mice (**Figure 1C**), indicating the mice were in a good health after the implantation. Time course histological analysis of the peri-implant region detected a newly formed bone 2 weeks post-implantation with high number of empty osteocytic lacunas that decreased over time (**Figure 1D**). We next used Picrosirius red staining to evaluate the collagen network in the peri-implant connective tissue. As opposed to the gingiva where the collagen fibers were distributed in a fan-shaped pattern forming a tight seal around teeth, the collagen bundles in the peri-implant tissue were located in parallel to the implant, as previously demonstrated for dental implants in human studies (34) with no remarkable changes later on (**Figure 1D**). Taken together, the described model results in a successful integration of the dental implants and similar histological characteristics as dental implants in humans, thus can be used for further studying how the implants impact local immunity.

Elevated LC Precursors but Reduced Levels of Fully Developed LCs in the Peri-Implant Epithelium

Since previous studies reported opposing results regarding the frequencies of LCs in the peri-implant epithelium, we addressed this issue in our murine system. Epithelial tissues of the peri-implant gingiva were collected 4 weeks after implantation and subjected to flow cytometry analysis (Figure S1 in Supplementary Material). Gingival epithelial tissues from sex- and age-matched naïve mice were used as a control. To identify LCs, the processed epithelial cells were stained with antibodies against CD45, CD11c, MHCII, EpCAM, and langerin, and analyzed based on the gating strategy described in **Figure 2A**. In some experiments, additional staining with CD11b and CD103 antibodies was performed to further separate the LCs to $CD103^+CD11b^{low}$ ($CD103^+$LCs) and $CD11b^+CD103^{neg}$ ($CD11b^+$LCs) subsets as previously reported (23). As demonstrated in **Figure 2B**, elevated percentages of $CD45^+$ leukocytes were detected in the peri-implant epithelium compared to naïve gingiva. Moreover, the frequencies of LC precursors, identified as $CD45^+CD11c^+MHCII^+$ cells, were also significantly increased in the tissue (**Figure 2C**). Nevertheless, despite the increment of their precursors, the frequencies of fully developed LCs in the peri-implant epithelium were considerably reduced (twofold to threefold reduction) in comparison to the control group (**Figure 2D**). Further examination revealed that a large fraction of the $CD45^+CD11c^+MHCII^+$ cells expressed EpCAM but not langerin, and even the mean fluorescence intensity of langerin on the remaining LCs in the peri-implant was lower than control gingival LCs. The reduction in langerin expression was also confirmed using RT-*q*PCR (**Figure 2E**). Importantly, the LC population in the contralateral intact gingiva of the implanted mice was not altered, indicating the confined effect of the implants (Figure S2 in Supplementary Material). We then examined which LC subset is mostly affected by the implant. Since LC numbers in the peri-implant mucosa were too low for such analysis, we gated on $CD45^+CD11c^+MHCII^+EpCAM^+$ cells (i.e., the direct precursors of LCs), and found that $CD103^+$ LCs were mostly affected by the implant (**Figure 2F**).

To further visualize the LCs in the peri-implant epithelium, an immunofluorescence staining on gingival histological cross sections and on whole epithelial layers was executed. Four weeks after implantation, the tissues were prepared from individual mice and stained with antibodies against MHCII and langerin. Concurring with the flow cytometry data, MHCII-positive cells with a morphology of DCs were clearly visualized in the epithelium of both the peri-implant and naïve gingiva epithelium (**Figures 3A,B**). The number of $MHCII^+$ cells was also significantly higher in the peri-implant epithelium in comparison to normal gingiva, and this trend last up at least to 10 weeks post-implantation (**Figure 3C**). On a contrary, langerin-positive cells were very scarce in the peri-implant epithelium, and langerin staining intensity of the residual LCs in this region was much weaker in comparison to control samples (**Figures 3A,B**). The reduction of langerin-positive cells was also detected for at least up to 10 weeks post-implantation (**Figure 3C**). To verify that the lack of langerin-positive cells was not resulting from the surgical procedure performed prior to implant placement, we stained epithelial tissue 4 weeks after tooth extraction just before the implantation. As shown in **Figure 3D**, langerin-positive cells were easily visualized in the epithelium, indicating that langerin-positive cells were normally present in the epithelium prior to the implantation. Collectively, these results suggest that terminal maturation of LCs is impaired in the peri-implant epithelium. The accumulation of $CD45^+CD11c^+MHCII^+EpCAM^+$ LC precursors, representing a transient stage in the development of oral mucosal LCs, proposes that LC differentiation might be dysregulated in the peri-implant epithelium.

Cytokines and Chemokines Mediating the Development of Oral LCs Are Differentially Dysregulated in the Peri-Implant Mucosa

As the aforementioned results suggest that the differentiation of LCs in the peri-implant mucosa is alerted, we next examined the expression of molecules which are known to mediate this process. Expression of TGF-β1 and BMP7, the predominant cytokines instructing LC differentiation, was first analyzed using immunofluorescences staining on gingival cross sections. TGF-β1 expression was detected in the suprabasal epithelia layers of the oral epithelium and also in the sulcular/junctional epithelium (JE) facing the tooth surface (**Figure 4A**). In the peri-implant mucosa, however, expression of TGF-β1 was reduced in the oral epithelium and nearly absent in the barrier epithelium facing the implant (the equivalent of the JE in normal gingiva). Quantification of TGF-β1 staining intensity in several fields of view (**Figure 4B**), or the levels of *Tgf*-β1 mRNA by RT-*q*PCR (**Figure 4C**), further confirmed the reduction in the expression of this cytokine in the epithelium. In contrast to TGF-β1, BMP7 expression which is restricted to the LP (24) was not affected in the peri-implant mucosa (**Figures 4A–C**). Of note, the reduction in TGF-β1 expression was not due to the tooth extraction procedure, since TGF-β1 was comparably expressed in the epithelium

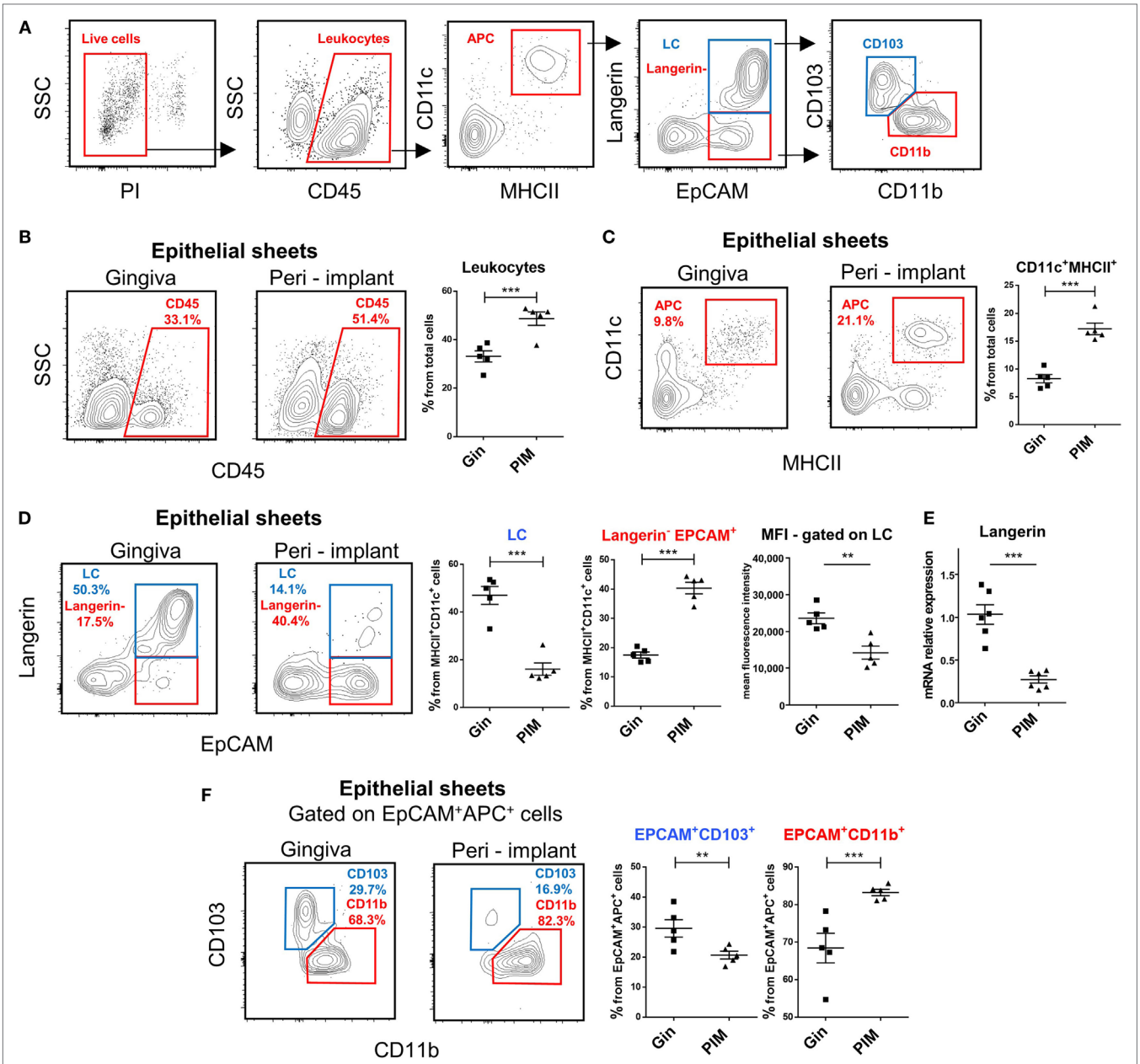

FIGURE 2 | Decreased frequencies of terminally differentiated Langerhans cells (LCs) in the peri-implant epithelium. **(A)** Gating strategy to identify LCs and their precursors in the tissue using flow cytometry. **(B,C)** Frequencies of CD45$^+$ leukocytes **(B)** and CD11c$^+$MHCII$^+$ LC precursors **(C)** in the peri-implant and gingival epithelium 4 weeks after implant insertion. Representative FACS plots and graphs indicates percentages of CD45$^+$ and CD11c$^+$MHCII$^+$ cells from total cells, presented as the mean ± SEM (n = 5 per group, each n represents oral tissues pooled from three individual mice). Data are representative of one out of three independent experiments. **(D)** Expression of langerin and EpCAM on CD11c$^+$MHCII$^+$ cells in the peri-implant and gingival epithelium 4 weeks after implant insertion. Representative facs plots and graphs depicting the percentages of EpCAM$^+$langerin$^+$ (LCs) and EpCAM$^+$langerin^{neg} cells form total CD11c$^+$MHCII$^+$ cells are presented as the mean ± SEM (n = 5 per group). Representative graph illustrate the mean fluorescence intensity (MFI) of langerin expression pre-gated on LCs in peri-implant and gingival epithelium presented as the mean ± SEM (n = 5 per group). **(E)** Quantification of *langerin* mRNA in epithelial tissue prepared from peri-implant and gingival tissues using quantitative real-time PCR. Graph presents the fold change in gene expression normalized to non-implanted mice and presented as the mean ± SEM (n = 6 mice per group). Data are representative of one out of two independent experiments. **(F)** Expression of CD11b and CD103 in epithelial CD11c$^+$MHCII$^+$EpCAM$^+$ cells 4 weeks after implant insertion. Representative FACS plots and graphs illustrating the percentages of the noted subsets presented as the mean ± SEM (n = 5 per group). $^{**}p < 0.01$, $^{***}p < 0.001$.

of both the tooth extraction site and the contralateral intact gingiva (**Figure 4D**). As TGF-β1 and BMP7 were proposed to impact LC development *via* both ALK5 and ALK3 receptors or ALK3 only, respectively (24, 35), the expression of these receptors was also quantified using RT-*q*PCR. As depicted in **Figure 4E**, whereas the mRNA levels of *Alk5* were upregulated in the peri-implant

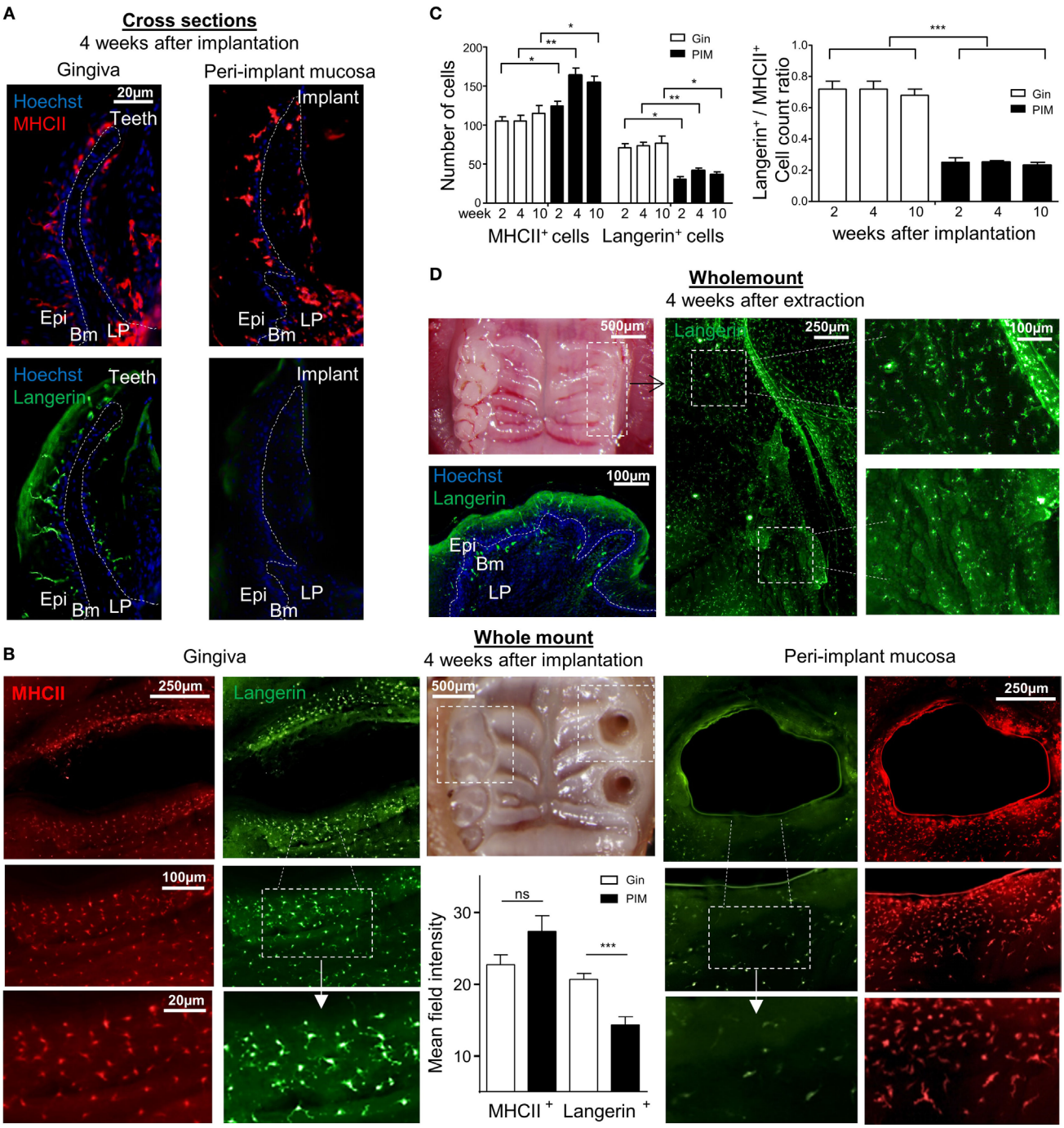

FIGURE 3 | Visualization of langerin and MHCII expression in the peri-implant mucosa. **(A)** Immunofluorescence imaging of the peri-implant and gingival cross sections tissues prepared 4 weeks after implantation stained against MHCII (red), langerin (green), and hoechst (blue) for nuclear visualization. Representative immunofluorescence images of two independent experiments are shown. In each experiment, at least three mice were examined. **(B)** Epithelial layers prepared from peri-implant and gingival tissues 4 weeks after implant insertion, stained for (red), langerin (green), and hoechst (blue). Whole mount immunofluorescence images from one out of two independent experiments are shown, at least three mice were examined in each experiment. Bar graphs represent the mean field staining intensity of langerin and MHCII in the epithelium, shown as the mean ± SEM. The average pixel intensity was calculated for each tissue using ImageJ software by 100 µm circumferential countering the epithelium around implant and teeth (n = 3 mice per group). Representative images of one out of two independent experiments are shown. **(C)** Graphs presents the total numbers of MHCII-positive or langerin-positive cells per a field of view, as well as the relative ratio of the noted cells in epithelial sheets taken 2, 4, and 10 weeks after implant insertion, presented as the mean ± SEM (n = 6 mice per time points). Data of one out of two independent experiments are presented. **(D)** Four weeks after tooth extraction, epithelial tissues were removed from the alveolar process and subjected to immunofluorescence staining as described above. Representative images of one out of two independent experiments are provided, three mice were analyzed in each experiment. *$p < 0.05$, **$p < 0.01$, ***$p < 0.001$.

epithelium compared to normal gingiva epithelium, the levels of *Alk3* mRNA were significantly reduced. Next, mRNA expression of the chemokines *Ccl2* and *Ccl20* was quantified in the epithelium, since we previously reported that these chemokines are differentially expressed in the epithelium and mediate LC recruitment (24, 35). Expression of both cytokines was upregulated in the peri-implant epithelium compared to the control group (**Figure 4E**). Expression of *Gm-csf*, an additional cytokine required for APCs and LCs differentiation, was not modified in the peri-implant epithelium (**Figure 4E**). These results thus

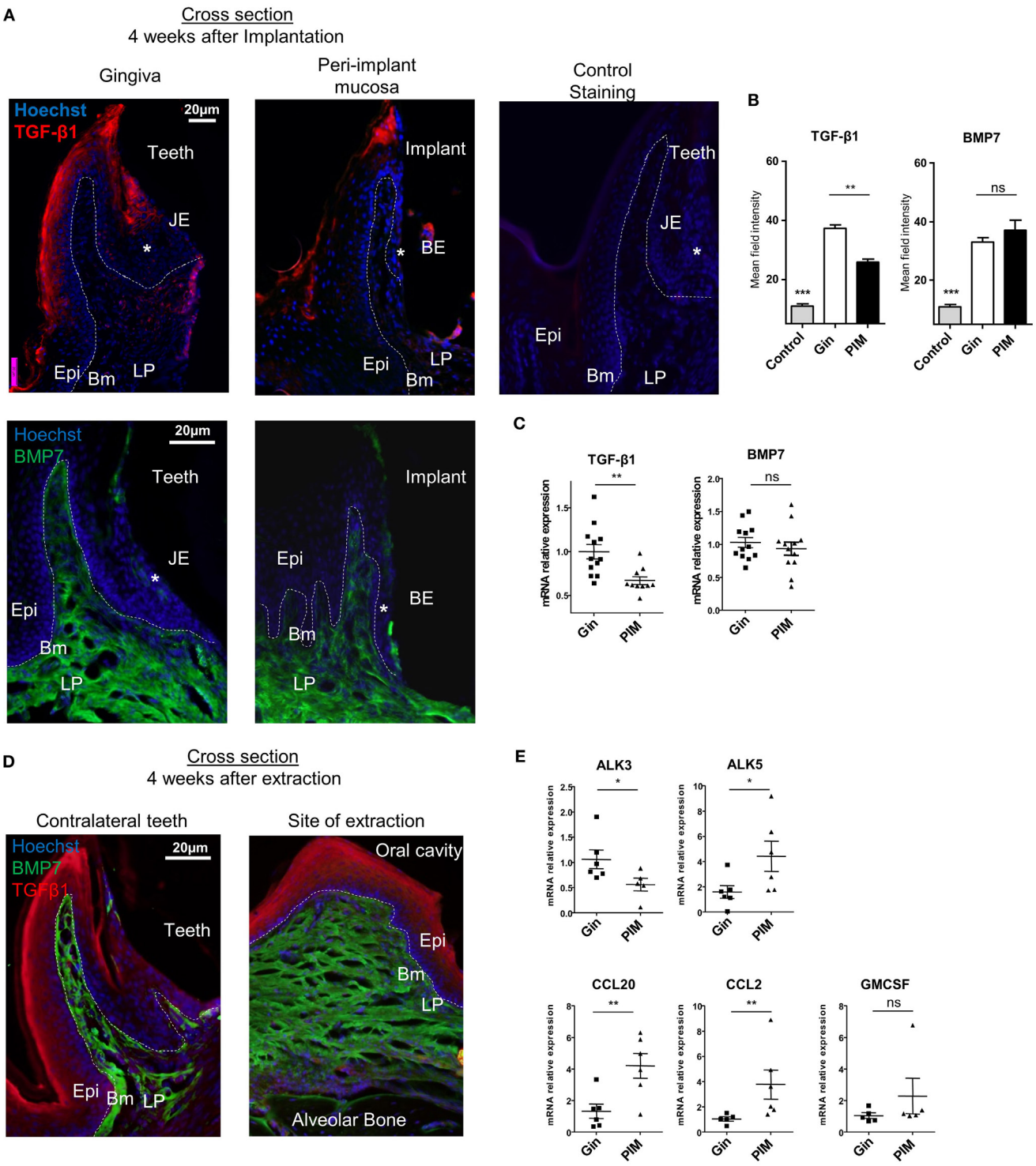

FIGURE 4 | Continued

FIGURE 4 | Dysregulated expression of molecules mediating Langerhans cell differentiation in the peri-implant mucosa. **(A)** Immunofluorescence cross sections of peri-implant and gingival tissues stained 4 weeks after implantation against TGF-β1 (red), bone morphogenetic protein 7 (BMP7) (green), and hoechst (blue). Negative control represents staining with the secondary antibody only. Representative immunofluorescence images of two independent experiments are shown. In each experiment, at least three mice were examined. **(B)** Bar graphs represent the mean field staining intensity of TGF-β1 and BMP7 in the epithelium and submucosa, respectively, shown as the mean ± SEM. The average pixel intensity was calculated for each slide using ImageJ software by countering the epithelium or the submucosa from nine different slides for each group ($n = 3$ mice per group). Representative images of two independent experiments are shown. **(C)** Four weeks after implant insertion, TGF-β1 and BMP7 mRNA expressions were quantified in the epithelium and submucosa, respectively, by RT-*q*PCR. Graph presents the fold change in gene expression normalized to non-implanted mice and presented as the mean ± SEM (at least 10 mice per group were analyzed). Data are representative of two pooled independent experiments. **(D)** Four weeks after teeth extraction, immunofluorescence cross sections of the alveolar process at extraction sites were stained as described in **(A)**. Representative images of one out of two independent experiments are provided, three mice were analyzed in each experiment. **(E)** Graph presents the fold change in gene expression of activing-like kinase 3 (ALK3), ALK5, CCL20, CCL2, and GM-CSF in the epithelium, normalized to non-implanted mice 4 weeks after implantation, presented as the mean ± SEM ($n = 6$ mice per group). Data are representative of one out of two independent experiments. $^{*}p < 0.05$, $^{**}p < 0.01$.

suggest that TGF-β1/ALK5 as well as TGF-β1/ALK3 signaling are dysregulated in peri-implant mucosa. As these singling pathways mediate the differentiation rather than recruitment of LC precursors to the epithelium (24), their dysregulation correlates well with the presence of $CD45^+CD11c^+MHCII^+EpCAM^+$ LC precursors in the epithelium.

Titanium Ions Inhibit the Expression of Langerin on *In Vitro* Generated LC-Like Cells

It has been demonstrated that titanium ions are released from titanium implants (9, 13) and such ions are capable of altering DC function *in vitro* (11, 36). We thus asked whether titanium ions might also modify the differentiation of LC from BM cells, the direct precursors of oral mucosal LCs (23). To induce LC differentiation, BM cells were cultured for 5 days with serum-containing media supplemented with GM-CSF and TGF-β1. Titanium ions were also added to the cultures to examine their capacity to inhibit or modulate LC differentiation. First, we examined the toxicity of various concentrations of titanium ions by quantifying cellular viability in the cultures (Figure S3A in Supplementary Material). Among the various concentrations tested, 5 and 10 ppm of titanium ions resulted in high percentages of live cells >95 and 60%, respectively. In addition, the pH value of the serum-containing differentiation cultures was not affected by the presence of any titanium ions concentration tested (Figure S3B in Supplementary Material). Next, we quantified the generation of LCs by gating on $EpCAM^+DEC205^+$ cells among the $CD11c^+MHCII^+$ population, as these were previously proven to represent LC-like cells (37). Cultures containing GM-CSF + TGF-β1 were able to induce a large fraction of $EpCAM^+DEC205^+$ LC-like cells (**Figure 5A**). Moreover, an additional subset of the $CD11c^+MHCII^+$ cells acquired a phenotype of $EpCAM^+DEC205^{neg}$ cells, a population with a potential to differentiate to LC-like cells (37). The addition of titanium ions to the cultures failed to generate $EpCAM^+DEC205^+$ LC-like cells and only the $EpCAM^+DEC205^{neg}$ population was detected in these cultures. Further characterization revealed that only LC-like cells generated in the absence of titanium ions were able to upregulate langerin expression (**Figure 5B**; Figure S4 in Supplementary Material). The impact of titanium ions on langerin expression was also verified using immunofluorescences analysis by staining the cells with antibody against MHCII and langerin. As depicted in **Figure 5C**, expression of langerin, but not MHCII, on cells derived from titanium ions-containing cultures was greatly reduced compared to control group. To examine whether titanium ions are capable also to alter the activation of the $MHCII^+CD11c^+EpCAM^+$ cells, we employed a different culturing strategy. BM cells were cultured for 3 days with GM-CSF and TGF-β1 and then exposed to titanium ions for 2 days. Higher expression of the co-stimulatory molecules CD86 and CD40 was detected on the surface of $MHCII^+CD11c^+EpCAM^+$ cells, suggesting the titanium ions induce the maturation of these APCs (Figure S5 in Supplementary Material). Next, since titanium ions dysregulates the capacity of BM cells to evolve into LC-like cells, we asked whether titanium implants are capable to alter the differentiation capacity of BM cells systemically rather than locally. For this we isolated BM cells from implanted and naïve mice and cultured them with GM-CSF + TGF-β1. Analysis of the cultures indicated that BM cells from both groups of mice have comparable differentiation capability to LC-like cells (**Figure 5D**). Taken together, these results suggest that titanium ions dysregulate the development of LC-like cells *in vitro*, and preferentially induce cells that are not fully differentiated into LCs but are rather more activated. Moreover, this regulatory function appears to be a local effect rather than systemic, impacting the development of LCs only in areas adjacent to the implant.

High Leukocyte Content in the Peri-Implant Mucosa With No Evidence of an Acute Inflammation

We next analyzed the various leukocytes present in the peri-implant mucosa 4 weeks after implantation. **Figure 6A** demonstrates the gating strategy employed to identify innate and adaptive leukocytes in the peri-implant submucosa and normal gingiva as a control. Higher levels of neutrophils, $Ly6C^{high}$ and $Ly6C^{low}$ monocytes were found in the peri-implant tissue compared to naïve gingiva (**Figure 6B**). Interestingly, the frequencies of $CD11c^+MHCII^+$ APCs in the peri-implant submucosa were significantly lower than those detected in the submucosa of normal gingiva. In correlation with the increased innate cell infiltrate in implanted mice, we also found an elevated expression of *Il-17a, Il-1b, Ifna, Ifnb*, and *Nos2* (iNOS) in the

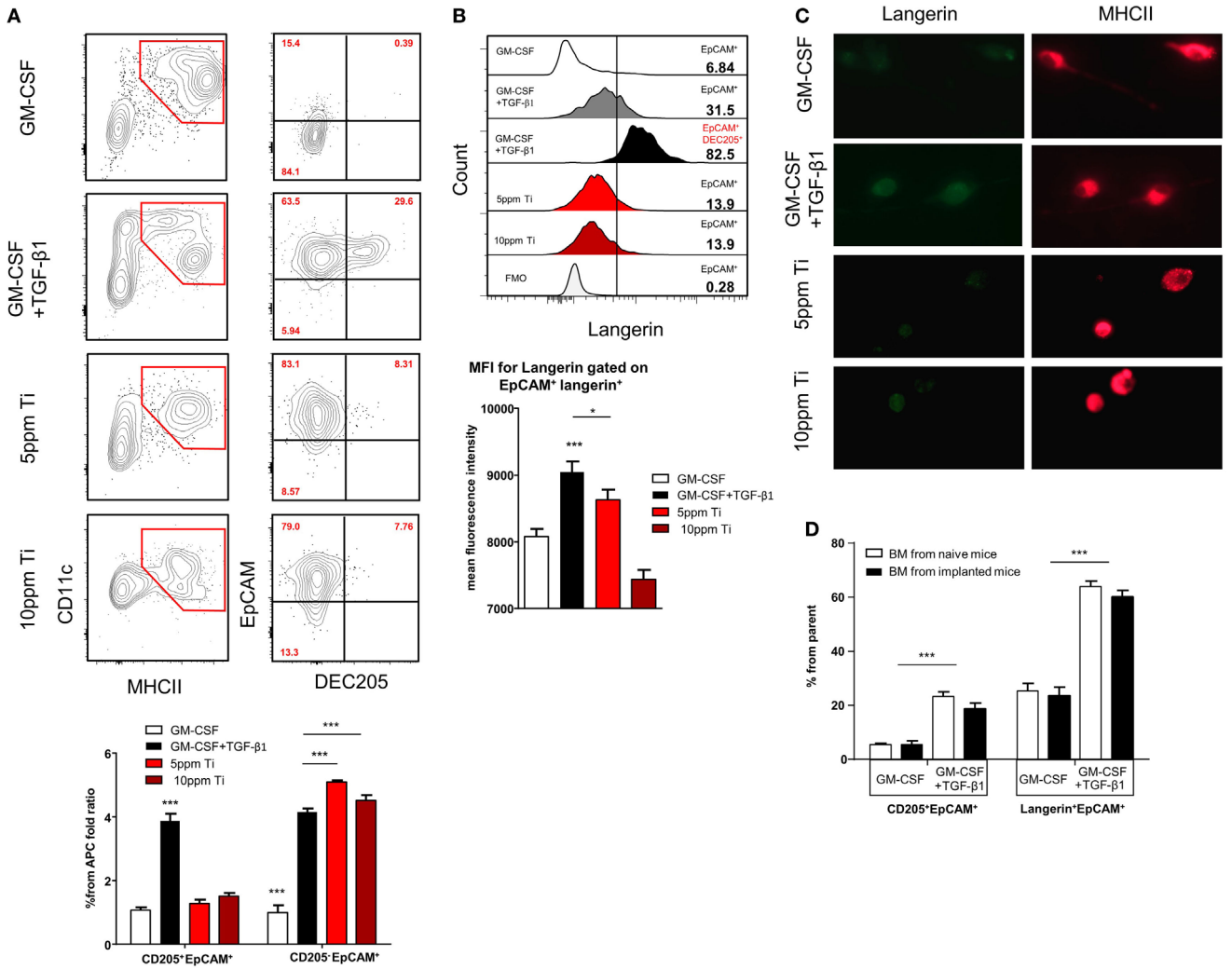

FIGURE 5 | Titanium ions altered *in vitro* differentiation of Langerhans cell (LC)-like cells from BM precursors. **(A)** Frequencies of CD11c^{+}MHCII^{+} cells and LC-like cells (CD11c^{+}MHCII^{+}EpCAM^{+}DEC205^{+}) 5 days after incubation with GM-CSF or TGF-β1 + GM-CSF in the presence or absence of 5 and 10 ppm of Ti ions. Representative FACS plots and graphs indicates the fold change in the percentage of EpCAM^{+}DEC205^{+} (LC-like cells) and EpCAM^{+}DEC205^{neg} cells from total CD11c^{+}MHCII^{+} population (percentages were normalized to the GM-CSF group) presented as the mean ± SEM (n = 6 mice per group). Data are representative of one out of four independent experiments. **(B)** Representative histogram plots illustrate the frequencies of langerin expression on pre-gated EpCAM^{+} and EpCAM^{+}DEC205^{+} cells after 5 days of culture. Bar graph specifies the mean fluorescence intensity (MFI) of langerin expression on pre-gated cells shown as the mean ± SEM (n = 6 mice per group). Data are representative of one out of two independent experiments. **(C)** Cells were collected from the LC differentiation cultures after 5 days and stained against langerin (green) and MHCII (red). Representative immunofluorescence images presenting the expression of langerin and MHCII in each culture condition. Data of one out two independent experiments are shown. **(D)** BM cells purified from implanted and non-implanted mice were cultured with GM-CSF or GM-CSF + TGF-β1 and 5 days later were analyzed by flow cytometry. Bar graph presents the frequencies of LCs-like cells based on the expression of EpCAM, DEC205 an langerin from the CD11c^{+}MHCII^{+} cells representing the mean ± SEM (n = 3 mice per group). Data are representative of one out of two independent experiments *$p < 0.05$, ***$p < 0.001$.

peri-implant mucosa (**Figure 6C**). With regards to adaptive lymphocytes, the percentages of B and T cells were also elevated in the peri-implant mucosa, particularity the CD4^{+} T cell subset. A larger number of these CD4^{+} T cells in the peri-implant mucosa was stained positively to FOXP3, indicating that compared to normal gingiva this tissue contains more Treg cells (**Figure 6D**). Since mucosal homeostasis can be reflected by the ratio of Th17 and Treg cells, we next calculated the relative expression levels of *Il-17a* versus *Foxp3* in the tissue. As shown in **Figure 6E**, the *Il-17A*/*Foxp3* ratio was higher in the peri-implant mucosa in comparison to normal gingiva, indicating that the implant modified tissue homeostasis by increasing inflammatory milieu. We then asked whether such immunological state, recorded 4 weeks after implant placement, represents an acute inflammation in the peri-implant mucosa. To address this question we first quantified the expression of the proinflammatory cytokine

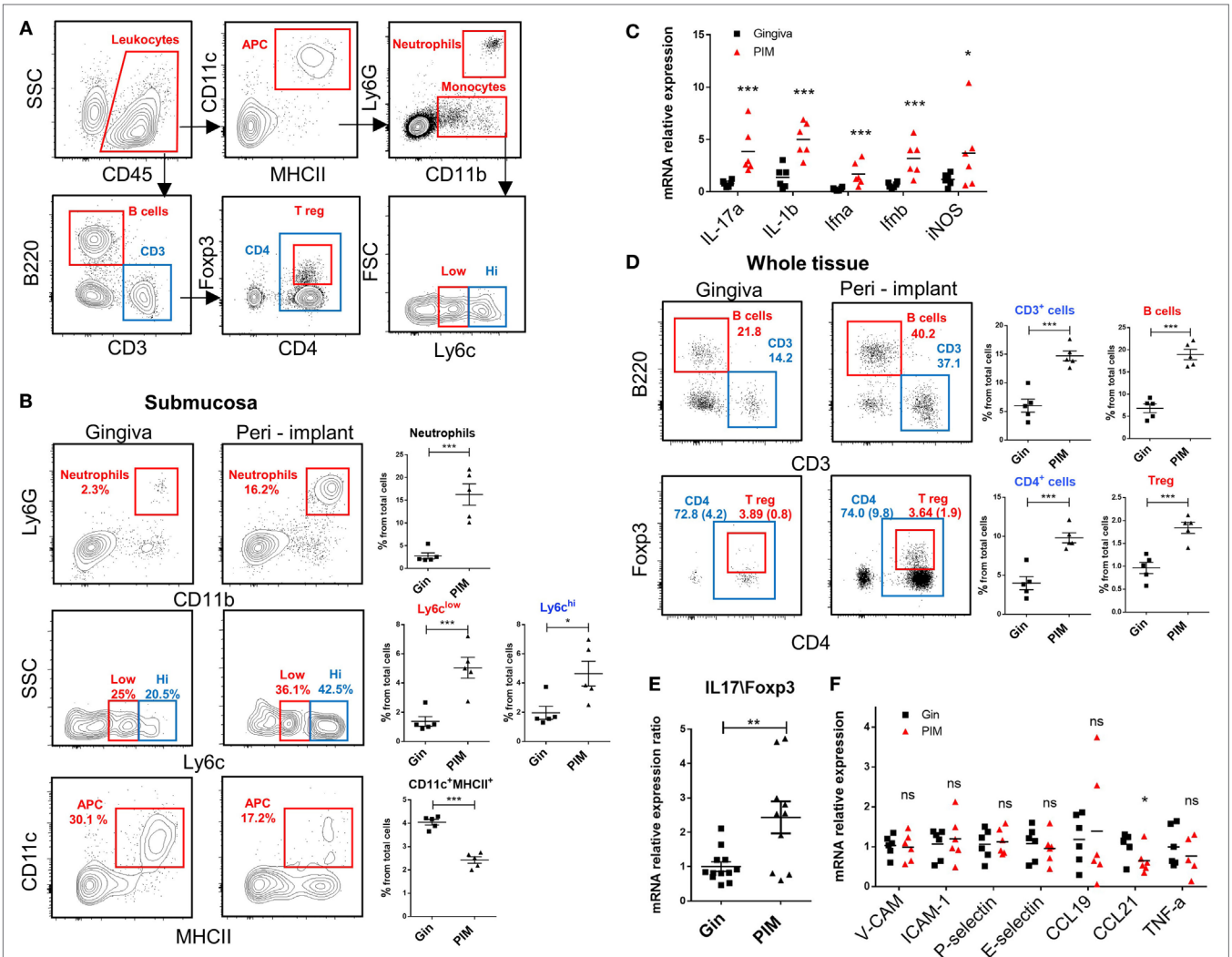

FIGURE 6 | An increased leukocyte infiltrate in the peri-implant mucosa. **(A)** Gating strategy to identify by flow cytometry the noted leukocyte subsets in the tissue. **(B)** Flow cytometry plots illustrate the incidence of neutrophils (Ly6G$^+$CD11b$^+$), monocytes (CD11b$^+$Ly6C$^{high\backslash low}$), antigen-presenting cells CD11c$^+$MHCII$^+$ in the submucosa of the peri-implant and gingiva 4 weeks after implant insertion. Correlating graphs demonstrates the frequencies of the noted immune subsets from the total cell count, presented as the mean ± SEM (n = 5 per group, each n represents tissues pooled from three individual mice). **(C)** mRNA expression levels of proinflammatory cytokines were calculated in the peri-implant epithelium 4 weeks after implant insertion, presented as the mean ± SEM (n = 6 per group, each n represents tissues pooled from three individual mice). **(D)** Frequencies of total lymphocytes (CD3$^+$), B cells (B220$^+$CD3$^-$), T helper cells (CD3$^+$CD4$^+$), and T regulatory (Treg) cells (CD3$^+$CD4$^+$FOXP3$^+$) from the whole peri-implant and gingiva tissues are presented in flow cytometry plots. Frequencies of CD4$^+$ T cells and Treg cells from total cells are provided in brackets within the flow cytometry plots. Graphs indicate the frequency of each cells subset from the total cell population, presented as the mean ± SEM (n = 5 per group, each n represents tissues pooled from three individual mice). Data are representative of one out of two independent experiments. **(E,F)** Four weeks after implant insertion, the mRNA levels of the noted genes were quantified in the peri-implant and gingiva lamina propria using RT-qPCR. **(E)** Ratio of IL-17 and Foxp3 expression level. Data are representative of two independent experiments. **(F)** Graph presents the fold change in gene expression normalized to non-implanted mice and represent the mean ± SEM (n = at least five mice per group). Data are representative of one out of two independent experiments. $^*p < 0.05$, $^{**}p < 0.01$, $^{***}p < 0.001$.

Tnf-a and found comparable levels in the peri-implant mucosa and normal gingiva (**Figure 6F**). Moreover, expression levels of *P-selectin*, *E-selectin*, *Icam-1*, and *Vcam-1*, adhesion molecules that are upregulated on activated endothelium, were similar in both tissues (**Figure 6F**). We also examined the expression of *Ccl21* and *Ccl19*, chemokines mediating migration of DCs to the draining LNs and found reduced levels of *Ccl21* around implants but not *Ccl19* (**Figure 6F**). These results suggest that 4 weeks after implant placement, the peri-implant mucosa contains an elevated leukocyte content, whereas there is no indication to the presence of acute inflammation in the tissue at this time point. With regards to the CD11c$^+$MHCII$^+$ APCs, it is possible that

their reduced frequency in the peri-implant submucosa is due to increased translocation to the epithelium rather then accelerated migration to the LNs.

DISCUSSION

Using a murine model of titanium dental implants, this study shows the absence of fully differentiated LCs in the epithelium of the peri-implant mucosa. We provided both *in vivo* and *in vitro* evidence demonstrating that titanium implants and titanium ions, respectively, are capable of impairing local LC development. As a result, oral LCs expressed EpCAM but failed to upregulate langerin expression, suggesting a partial differentiation of these cells. Previous human studies employing various markers to identify human LCs such as MHCII, CD1a or S-100, reported contradicting results regarding the frequencies of LCs in the peri-implant mucosa (26–28, 30). While the expression kinetics of these markers on human LCs are not clear yet, they are likely to be expressed at different differentiation stages. Thus, it is expected that analysis based on only a single or two markers will provide diverse results.

It has been shown that the first differentiation step of oral LCs is mediated by BMP7/ALK3 signaling, which upregulate expression of E-cadherin, CCR2, and CCR20, enabling the translocation of LC precursors to the epithelium (24). The accumulation of $CD11c^{+}MHCII^{+}EpCAM^{+}$ cells in the peri-implant epithelium suggests that this early differentiation step is intact or even accelerated in implanted mice. In line with this notion, BMP7 expression was not altered in the submucosa, whereas epithelial expression of CCL2 and CCL20 was upregulated. Therefore, titanium implants or titanium ions are considered to impact mainly the second differentiation step of oral LCs that is driven by TGF-β1 in the epithelium. Indeed, expression of TGF-β1 was significantly reduced in the epithelium of the peri-implant mucosa. It is currently unclear how titanium implants or ions regulate TGF-β1 expression, nevertheless, there are indications in human implants and *in vitro* cultures that titanium can modulate TGF-β1 expression (38, 39). Besides TGF-β1, titanium implants were also capable to upregulate expression of its canonical ALK5 receptor while reducing the non-canonical ALK3 receptor. Signaling *via* TGF-β1 and ALK5 was shown to be important for LC homeostasis as it prevents their spontaneous activation and migration to the LNs (40, 41). Concurring with this notion, the upregulation of ALK5 might compensate for the reduced TGF-β1 levels, resulting in the accumulation of the partly developed LCs in the peri-implant epithelium. Yet, TGF-β1/ALK5 signaling is also crucial for efficient differentiation of oral LCs, since differentiation of these cells was shown to be inhibited but not absent in mice lacking ALK5 in $CD11c^{+}$ cells (24). Such ALK5-independent development of oral LCs is likely to be mediated by ALK3 as previously suggested (35). Nevertheless, since ALK3 expression was reduced in the peri-implant epithelium, TGF-β1/ALK5 signaling seems to play the major role in the partial development of the oral LCs. Interestingly, we recently proposed that TGF-β1/ALK3 signaling in the epithelium can mediate langerin expression on oral LCs (24). Accordingly, the reduced expression of both ALK3 and TGF-β1 in the peri-implant epithelium, might explain the lack of langerin expression by local LCs.

In comparison to normal gingiva around teeth, the peri-implant mucosa contains larger infiltrate of innate and adaptive leukocytes 4 weeks after implantation, with no indication to the existence of acute inflammation. An inflammatory infiltrate in the peri-implant mucosa was reported also in clinically healthy implants 6 months after implant insertion (42), which support our findings and also emphasizing the relevance of our model to the clinical situation. Nonetheless, such a phenomenon could simply represent a transitional immunological state of the peri-implant mucosa, which might eventually return to steady state level as in normal gingiva. The gradual reduction in the size of the peri-implant infiltrate that was reported in humans supports this assumption (43). However, it is not clear whether the peri-implant mucosa will indeed reach a "normal" steady state as in the gingiva. This highlights an alternative possibility for the development of an alerted steady state conditions in the peri-implant mucosa. This hypothesis may explain the increased susceptibility of the implant to infection, as based on the Th17/Treg balance, the immunological steady state of the peri-implant is more "inflamed" than normal gingiva. Such condition might eventually lead to a microbial dysbiosis, involving the accumulation of inflammophilic bacteria that will induce disease as we previously reported (44).

The extent of the dysregulation of LC development affects the immune response of the peri-implant mucosa is still unknown. LCs were shown to regulate immunological and microbial homeostasis of the oral mucosa (24), and to play a protective role during infection with an oral pathogen (25). In both cases, LC function was mediated, in part, by their capacity to induce Treg cells that resolve gingival inflammation. Since the Th17/Treg balance is augmented in the peri-implant mucosa compared to normal gingiva, it is likely that the partially differentiated LCs might have reduced capacity to generate Treg cells. The specific decrease in $CD103^{+}$ LCs, a subset that is greatly affected by the microbiota (24), further suggest that the reduction in local LCs might affect the tissue. Nevertheless, further investigation will be required to assess this issue directly.

In summary, the present study provides novel insights into the impact of titanium implant on oral LCs, the major APC subset residing in the epithelium and regulating oral mucosal homeostasis. Besides increasing our understanding on immunological dysfunction associated with insertion of titanium dental implants, this study highlights the sequential differentiation process of oral mucosal LCs. Moreover, it suggests that environmental factors have the capacity to interfere with LC development and subsequently alter oral mucosal homeostasis.

ETHICS STATEMENT

This study was carried out in accordance with the recommendations of "The guide for care and use of laboratory animals," Hebrew University Institutional Animal Care and Ethics Committee. The protocol was approved by the Hebrew University Institutional Animal Care and Ethics Committee.

AUTHOR CONTRIBUTIONS

OH, A-HH, LS, and AW designed the research; OH analyzed the data; OH, NK, GM, TC, SW, MN, and YT performed experiments; A-HH, AW, LS, and OH wrote the manuscript; funding acquisition: AW and A-HH.

ACKNOWLEDGMENTS

We would like to thank MIS Implants Technologies for manufacturing the micro-implants.

FUNDING

This work was supported in part by an internal grant from Hadassah Medical Center and a grant from the Cabakoff foundation to AW, by Israel Science Foundation Grant 766/16 to A-HH and by Israel Science Foundation Grant 2369/18 to AW.

SUPPLEMENTARY MATERIAL

The Supplementary Material for this article can be found online at https://www.frontiersin.org/articles/10.3389/fimmu.2018.01712/full#supplementary-material.

REFERENCES

1. Klinge B, Hultin M, Berglundh T. Peri-implantitis. *Dent Clin North Am* (2005) 49(3):661–76, vii–viii. doi:10.1016/j.cden.2005.03.007
2. Roos-Jansaker AM, Lindahl C, Renvert H, Renvert S. Nine- to fourteen-year follow-up of implant treatment. Part I: implant loss and associations to various factors. *J Clin Periodontol* (2006) 33(4):283–9. doi:10.1111/j.1600-051X.2006.00907.x
3. Zitzmann NU, Berglundh T. Definition and prevalence of peri-implant diseases. *J Clin Periodontol* (2008) (8 Suppl):286–91. doi:10.1111/j.1600-051X.2008.01274.x
4. Koldsland OC, Scheie AA, Aass AM. Prevalence of peri-implantitis related to severity of the disease with different degrees of bone loss. *J Periodontol* (2010) 81(2):231–8. doi:10.1902/jop.2009.090269
5. Zetterqvist L, Feldman S, Rotter B, Vincenzi G, Wennstrom JL, Chierico A, et al. A prospective, multicenter, randomized-controlled 5-year study of hybrid and fully etched implants for the incidence of peri-implantitis. *J Periodontol* (2010) 81(4):493–501. doi:10.1902/jop.2009.090492
6. Sanz M, Chapple IL; Working Group 4 of the VIII European Workshop on Periodontology. Clinical research on peri-implant diseases: consensus report of Working Group 4. *J Clin Periodontol* (2012) 39(Suppl 12):202–6. doi:10.1111/j.1600-051X.2011.01837.x
7. Charalampakis G, Ramberg P, Dahlen G, Berglundh T, Abrahamsson I. Effect of cleansing of biofilm formed on titanium discs. *Clin Oral Implants Res* (2015) 26(8):931–6. doi:10.1111/clr.12397
8. Derks J, Tomasi C. Peri-implant health and disease. A systematic review of current epidemiology. *J Clin Periodontol* (2015) 42(Suppl 16):S158–71. doi:10.1111/jcpe.12334
9. Weingart D, Steinemann S, Schilli W, Strub JR, Hellerich U, Assenmacher J, et al. Titanium deposition in regional lymph nodes after insertion of titanium screw implants in maxillofacial region. *Int J Oral Maxillofac Surg* (1994) 23(6 Pt 2):450–2. doi:10.1016/S0901-5027(05)80045-1
10. Olmedo DG, Duffo G, Cabrini RL, Guglielmotti MB. Local effect of titanium implant corrosion: an experimental study in rats. *Int J Oral Maxillofac Surg* (2008) 37(11):1032–8. doi:10.1016/j.ijom.2008.05.013
11. Chan EP, Mhawi A, Clode P, Saunders M, Filgueira L. Effects of titanium(iv) ions on human monocyte-derived dendritic cells. *Metallomics* (2009) 1(2):166–74. doi:10.1039/b820871a
12. Olmedo DG, Nalli G, Verdu S, Paparella ML, Cabrini RL. Exfoliative cytology and titanium dental implants: a pilot study. *J Periodontol* (2013) 84(1):78–83. doi:10.1902/jop.2012.110757
13. Wachi T, Shuto T, Shinohara Y, Matono Y, Makihira S. Release of titanium ions from an implant surface and their effect on cytokine production related to alveolar bone resorption. *Toxicology* (2015) 327:1–9. doi:10.1016/j.tox.2014.10.016
14. Wilson TG Jr, Valderrama P, Burbano M, Blansett J, Levine R, Kessler H, et al. Foreign bodies associated with peri-implantitis human biopsies. *J Periodontol* (2015) 86(1):9–15. doi:10.1902/jop.2014.140363
15. Pettersson M, Kelk P, Belibasakis GN, Bylund D, Molin Thoren M, Johansson A. Titanium ions form particles that activate and execute interleukin-1beta release from lipopolysaccharide-primed macrophages. *J Periodontal Res* (2017) 52(1):21–32. doi:10.1111/jre.12364
16. Pettersson M, Pettersson J, Molin Thoren M, Johansson A. Release of titanium after insertion of dental implants with different surface characteristics – an ex vivo animal study. *Acta Biomater Odontol Scand* (2017) 3(1):63–73. doi:10.1080/23337931.2017.1399270
17. Romani N, Clausen BE, Stoitzner P. Langerhans cells and more: langerin-expressing dendritic cell subsets in the skin. *Immunol Rev* (2010) 234(1):120–41. doi:10.1111/j.0105-2896.2009.00886.x
18. Merad M, Sathe P, Helft J, Miller J, Mortha A. The dendritic cell lineage: ontogeny and function of dendritic cells and their subsets in the steady state and the inflamed setting. *Annu Rev Immunol* (2013) 31:563–604. doi:10.1146/annurev-immunol-020711-074950
19. Hovav AH. Dendritic cells of the oral mucosa. *Mucosal Immunol* (2014) 7(1):27–37. doi:10.1038/mi.2013.42
20. Wilensky A, Segev H, Mizraji G, Shaul Y, Capucha T, Shacham M, et al. Dendritic cells and their role in periodontal disease. *Oral Dis* (2014) 20(2):119–26. doi:10.1111/odi.12122
21. Chorro L, Sarde A, Li M, Woollard KJ, Chambon P, Malissen B, et al. Langerhans cell (LC) proliferation mediates neonatal development, homeostasis, and inflammation-associated expansion of the epidermal LC network. *J Exp Med* (2009) 206(13):3089–100. doi:10.1084/jem.20091586
22. Hoeffel G, Wang Y, Greter M, See P, Teo P, Malleret B, et al. Adult Langerhans cells derive predominantly from embryonic fetal liver monocytes with a minor contribution of yolk sac-derived macrophages. *J Exp Med* (2012) 209(6):1167–81. doi:10.1084/jem.20120340
23. Capucha T, Mizraji G, Segev H, Blecher-Gonen R, Winter D, Khalaileh A, et al. Distinct murine mucosal Langerhans cell subsets develop from pre-dendritic cells and monocytes. *Immunity* (2015) 43:369–81. doi:10.1016/j.immuni.2015.06.017
24. Capucha T, Koren N, Nassar M, Heyman O, Nir T, Levy M, et al. Sequential BMP7/TGF-beta1 signaling and microbiota instruct mucosal Langerhans cell differentiation. *J Exp Med* (2018) 215(2):481–500. doi:10.1084/jem.20171508
25. Arizon M, Nudel I, Segev H, Mizraji G, Elnekave M, Furmanov K, et al. Langerhans cells down-regulate inflammation-driven alveolar bone loss. *Proc Natl Acad Sci U S A* (2012) 109(18):7043–8. doi:10.1073/pnas.1116770109
26. Maiorano E, Favia G. Langerhans cells in periimplantar gingival tissues: an immunohistochemical study of 14 cases. *Boll Soc Ital Biol Sper* (1994) 70(10–11):257–63.
27. Arvidson K, Fartash B, Hilliges M, Kondell PA. Histological characteristics of peri-implant mucosa around Branemark and single-crystal sapphire implants. *Clin Oral Implants Res* (1996) 7(1):1–10. doi:10.1034/j.1600-0501.1996.070101.x
28. Bullon P, Fioroni M, Goteri G, Rubini C, Battino M. Immunohistochemical analysis of soft tissues in implants with healthy and peri-implantitis condition, and aggressive periodontitis. *Clin Oral Implants Res* (2004) 15(5):553–9. doi:10.1111/j.1600-0501.2004.01072.x
29. Olmedo DG, Paparella ML, Spielberg M, Brandizzi D, Guglielmotti MB, Cabrini RL. Oral mucosa tissue response to titanium cover screws. *J Periodontol* (2012) 83(8):973–80. doi:10.1902/jop.2011.110392

30. Horewicz VV, Ramalho L, dos Santos JN, Ferrucio E, Cury PR. Comparison of the distribution of dendritic cells in peri-implant mucosa and healthy gingiva. *Int J Oral Maxillofac Implants* (2013) 28(1):97–102. doi:10.11607/jomi.2487
31. Tabib Y, Jaber NS, Nassar M, Capucha T, Mizraji G, Nir T, et al. Cell-intrinsic regulation of murine epidermal Langerhans cells by protein S. *Proc Natl Acad Sci U S A* (2018) 115(25):E5736–45. doi:10.1073/pnas.1800303115
32. Becker W, Becker BE, Alsuwyed A, Al-Mubarak S. Long-term evaluation of 282 implants in maxillary and mandibular molar positions: a prospective study. *J Periodontol* (1999) 70(8):896–901. doi:10.1902/jop.1999.70.8.896
33. Tolstunov L. Implant zones of the jaws: implant location and related success rate. *J Oral Implantol* (2007) 33(4):211–20. doi:10.1563/1548-1336(2007)33[211:IZOTJI]2.0.CO;2
34. Glauser R, Schupbach P, Gottlow J, Hammerle CH. Periimplant soft tissue barrier at experimental one-piece mini-implants with different surface topography in humans: a light-microscopic overview and histometric analysis. *Clin Implant Dent Relat Res* (2005) 7(Suppl 1):S44–51. doi:10.1111/j.1708-8208.2005.tb00074.x
35. Yasmin N, Bauer T, Modak M, Wagner K, Schuster C, Koffel R, et al. Identification of bone morphogenetic protein 7 (BMP7) as an instructive factor for human epidermal Langerhans cell differentiation. *J Exp Med* (2013) 210(12):2597–610. doi:10.1084/jem.20130275
36. Zheng X, Mo A, Wang Y, Guo Y, Wu Y, Yuan Q. Effect of FK-506 (tacrolimus) therapy on bone healing of titanium implants: a histometric and biomechanical study in mice. *Eur J Oral Sci* (2017) 125(1):28–33. doi:10.1111/eos.12320
37. Chopin M, Seillet C, Chevrier S, Wu L, Wang H, Morse HC III, et al. Langerhans cells are generated by two distinct PU.1-dependent transcriptional networks. *J Exp Med* (2013) 210(13):2967–80. doi:10.1084/jem.20130930
38. Schierano G, Bellone G, Cassarino E, Pagano M, Preti G, Emanuelli G. Transforming growth factor-beta and interleukin 10 in oral implant sites in humans. *J Dent Res* (2003) 82(6):428–32. doi:10.1177/154405910308200605
39. Mardegan GP, Shibli JA, Roth LA, Faveri M, Giro G, Bastos MF. Transforming growth factor-beta, interleukin-17, and IL-23 gene expression profiles associated with human peri-implantitis. *Clin Oral Implants Res* (2017) 28(7):e10–5. doi:10.1111/clr.12846
40. Kel JM, Girard-Madoux MJ, Reizis B, Clausen BE. TGF-beta is required to maintain the pool of immature Langerhans cells in the epidermis. *J Immunol* (2010) 185(6):3248–55. doi:10.4049/jimmunol.1000981
41. Bobr A, Igyarto BZ, Haley KM, Li MO, Flavell RA, Kaplan DH. Autocrine/paracrine TGF-beta1 inhibits Langerhans cell migration. *Proc Natl Acad Sci U S A* (2012) 109(26):10492–7. doi:10.1073/pnas.1119178109
42. Pongnarisorn NJ, Gemmell E, Tan AE, Henry PJ, Marshall RI, Seymour GJ. Inflammation associated with implants with different surface types. *Clin Oral Implants Res* (2007) 18(1):114–25. doi:10.1111/j.1600-0501.2006.01304.x
43. Tomasi C, Tessarolo F, Caola I, Piccoli F, Wennstrom JL, Nollo G, et al. Early healing of peri-implant mucosa in man. *J Clin Periodontol* (2016) 43(10):816–24. doi:10.1111/jcpe.12591
44. Nassar M, Tabib Y, Capucha T, Mizraji G, Nir T, Pevsner-Fischer M, et al. GAS6 is a key homeostatic immunological regulator of host-commensal interactions in the oral mucosa. *Proc Natl Acad Sci U S A* (2017) 114(3):E337–46. doi:10.1073/pnas.1614926114

Conflict of Interest Statement: The submitted work was carried out without the presence of any personal, professional, or financial relationships that could potentially be construed as a conflict of interest.

The reviewer CB and handling Editor declared their shared affiliation.

frontiers in Immunology

ORIGINAL RESEARCH
published: 23 October 2018
doi: 10.3389/fimmu.2018.02436

Comparative Glycomics of Immunoglobulin A and G From Saliva and Plasma Reveals Biomarker Potential

Rosina Plomp†, Noortje de Haan†, Albert Bondt, Jayshri Murli, Viktoria Dotz and Manfred Wuhrer*

Center for Proteomics and Metabolomics, Leiden University Medical Center, Leiden, Netherlands

The *N*-glycosylation of immunoglobulin (Ig) G, the major antibody in the circulation of human adults, is well known for its influence on antibody effector functions and its alterations with various diseases. In contrast, knowledge on the role of glycans attached to IgA, which is a key immune defense agent in secretions, is very scarce. In this study we aimed to characterize the glycosylation of salivary (secretory) IgA, including the IgA joining chain (JC), and secretory component (SC) and to compare IgA and IgG glycosylation between human plasma and saliva samples to gain a first insight into oral cavity-specific antibody glycosylation. Plasma and whole saliva were collected from 19 healthy volunteers within a 2-h time window. IgG and IgA were affinity-purified from the two biofluids, followed by tryptic digestion and nanoLC-ESI-QTOF-MS(/MS) analysis. Saliva-derived IgG exhibited a slightly lower galactosylation and sialylation as compared to plasma-derived IgG. Glycosylation of IgA1, IgA2, and the JC showed substantial differences between the biofluids, with salivary proteins exhibiting a higher bisection, and lower galactosylation and sialylation as compared to plasma-derived IgA and JC. Additionally, all seven *N*-glycosylation sites, characterized on the SC of secretory IgA in saliva, carried highly fucosylated and fully galactosylated diantennary *N*-glycans. This study lays the basis for future research into the functional role of salivary Ig glycosylation as well as its biomarker potential.

Keywords: *N*-glycan, *O*-glycan, saliva, immunoglobulin G, immunoglobulin A, joining chain, secretory component

OPEN ACCESS

Edited by:
Avi-Hai Hovav,
Hebrew University of Jerusalem, Israel

Reviewed by:
Nicolaas Adrianus Bos,
University Medical Center Groningen, Netherlands
Emma Slack,
ETH Zürich, Switzerland

***Correspondence:**
Noortje de Haan
n.de_haan@lumc.nl

†These authors have contributed equally to this work

Specialty section:
This article was submitted to Mucosal Immunity, a section of the journal Frontiers in Immunology

Received: *31 May 2018*
Accepted: *02 October 2018*
Published: *23 October 2018*

Citation:
Plomp R, de Haan N, Bondt A, Murli J, Dotz V and Wuhrer M (2018) Comparative Glycomics of Immunoglobulin A and G From Saliva and Plasma Reveals Biomarker Potential. Front. Immunol. 9:2436. doi: 10.3389/fimmu.2018.02436

INTRODUCTION

Using saliva for diagnostic purposes has gained increasing popularity due to its various advantages over plasma or serum. First, saliva can be easily and painlessly collected from donors without the need for specialized equipment or training. Second, next to proteins derived from serum (ca. 27% of total salivary proteins), saliva also contains locally produced proteins which might reflect diseases that affect the oral cavity, such as Sjögren's syndrome, or oral cancer (1–3). Saliva assays are already available on the market, e.g., for the detection of antibodies against HIV (1). Moreover, numerous potential salivary protein-, DNA-, RNA-, and small-molecule-based biomarkers for various diseases have been proposed, as recently reviewed (4). Furthermore, two studies using global lectin-based profiling of glycans in saliva revealed associations with breast cancer and Sjögren's syndrome (5, 6).

Glycosylation is a prevalent posttranslational modification which heavily influences the structure and function of proteins, as is well known for plasma-derived immunoglobulin (Ig) G. The glycosylation of the fragment crystallizable (Fc) portion of IgG has been shown to influence binding to Fcγ receptors (FcγRs) and complement factors (7). Moreover, plasma IgG glycosylation has been associated with various diseases and could, therefore, be exploited for diagnostic and therapeutic approaches in the future (8–10). In contrast, for other Igs, such as IgA, less is known about the relationship between their glycosylation and effector functions. Although IgA *N*-glycosylation was shown to influence the IgA transport from circulation to mucosal tissue (11) and the *O*-glycosylation of IgA1 is considered a major factor in the pathogenesis of IgA nephropathy (12), the absence of the Fc *N*-glycosylation of IgA1 had no effect on FcαR binding (13). Site-specific investigation of antibody glycosylation in human samples other than plasma has been limited to cerebrospinal fluid and synovial fluid for IgG (14, 15) and colostrum for IgA (16, 17). The glycosylation of saliva-derived IgG and IgA has only been crudely examined using lectin binding assays, and without a direct comparison to blood (18, 19).

The lack of knowledge about salivary antibody glycosylation is mainly due to the fact that the antibody concentrations are much lower than in plasma, posing a major challenge for their in-depth characterization. Plasma contains approximately 12.5 mg/mL IgG and 2.2 mg/mL IgA, while the concentrations for unstimulated whole saliva are estimated at approximately 0.014 and 0.19 mg/mL for IgG and IgA, respectively (20, 21). Salivary IgG is thought to mainly be derived from circulation, while a minority (<20%) is produced by local plasma cells in gingival lesions or salivary glands (20, 22). In contrast, more than 95% of salivary IgA is produced locally by plasma cells in various glands, where it can form a dimeric complex via the associated joining chain (JC) (23). Secretion of dimeric IgA across the epithelial layer is enabled by the polymeric Ig receptor (pIgR), of which a part remains bound to the IgA and is known as the secretory component (SC). As a consequence, secretory (S)IgA as a complex of dimeric IgA covalently linked to the JC and SC (**Figure 1**), contributes to more than 80% of the salivary IgA pool, as opposed to plasma IgA which is predominantly (∼90%) monomeric (20, 26). In addition, the ratio between IgA1 and IgA2 is dependent on the source of IgA: while saliva contains approximately 35% IgA2, around 20% IgA2 is found in serum (20, 26). In contrast to IgG, which only contains one glycosylation site, or two in case of some IgG3 variants (27), the constant domains of IgA1 and IgA2 contain two up to five potential *N*-glycosylation sites, respectively, and IgA1 carries up to six *O*-glycans in the hinge region (24, 28) (**Figure 1**). In addition, the JC has one and the SC seven *N*-glycosylation sites (**Figure 1**). This further complicates detailed (S)IgA glycosylation analysis. However, in recent years great progress has been made with respect to both measurement sensitivity and data analysis tools in the field of glycoproteomics, facilitating site-specific glycosylation analysis of minute amounts of Igs (29–32).

Here, we developed a method for the analysis of IgG and (S)IgA glycosylation in whole saliva using bead-based affinity chromatography purification, followed by tryptic digestion and analysis with nano liquid chromatography (nanoLC)-electrospray ionization (ESI)-quadrupole time-of-flight (QTOF)-mass spectrometry (MS). The method can be used in a 96-well plate format and was applied to characterize and compare the glycosylation of both IgG and (S)IgA in saliva and plasma of 19 healthy individuals. To the best of our knowledge we are the first to report site-specific glycoprofiling of antibodies in saliva.

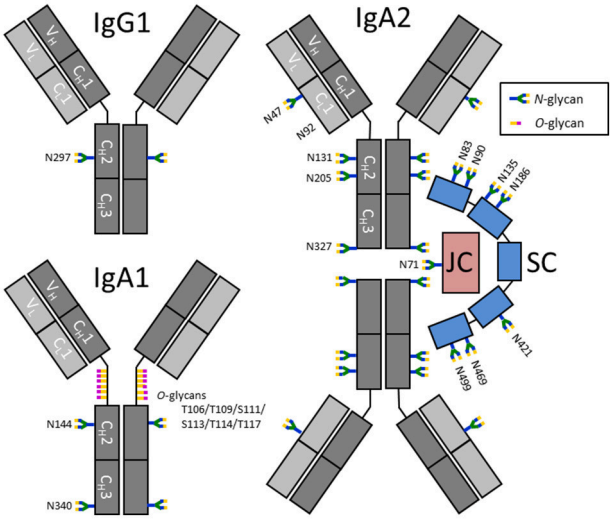

FIGURE 1 | Schematic representation of IgG1, IgA1, and SIgA2 and their glycosylation sites. IgA2 is shown in its dimeric form, in a complex with a joining chain (JC; red) and a secretory component (SC; blue). The JC and SC are covalently linked to IgA by disulfide bonds (not shown). Each Ig monomer is composed of two heavy chains (dark gray) and two light chains (light gray), again connected by disulfide bonds. The chains are further subdivided as constant (C) and variable (V) domains. *N*-glycosylation sites on IgG are indicated by their amino acid number according to the nomenclature used by conventional literature, e.g., (24), while IgA, the JC and SC have UniProt numbering (25). N92 on IgA2 was previously reported to be glycosylated, however, N92 on the IgA2 allotype found in our samples [A2m(1)] was not incorporated in a *N*-glycosylation consensus sequence and was found to be non-glycosylated.

MATERIALS AND METHODS

Collection of Biofluids and Preprocessing

Nineteen healthy donors (18 Caucasians and 1 of South Asian ancestry) were recruited to donate blood and saliva. The study population included 13 females and 6 males, with an average age of 28.4 years (range: 20–42). All donors gave informed consent, and the study was approved by the Medical Ethics Commission of the Leiden University Medical Center (P16.189). Both biofluids were collected between 10:30 a.m. and 12:30 p.m. on the same day. Donors were instructed to rinse their mouth with water an hour prior to collection of saliva and abstain from food and beverages until sample collection was finished. Saliva was collected by unstimulated drooling into a 5-mL Eppendorf tube for approximately 10 min, and immediately frozen at −20°C. Subsequently, 10 mL of venous blood was collected in an EDTA vial. The blood was centrifuged at 3184 × *g*

for 5 min and the clear upper fraction, consisting of plasma, was collected and frozen at −20°C.

Saliva samples underwent a preprocessing step to reduce viscosity: After thawing, the samples were centrifuged at 3184 × *g* at 4°C for 30 min. Four hundred μL of supernatant was collected from each sample and dispersed over four aliquots of 100 μL (for IgG and IgA purification each in duplicate), which were added to a 96-well filter plate with a 10 μm pore frit (Orochem, Naperville, IL). The samples were centrifuged at 200 × *g* for 1 min, and flow-throughs were used for IgG and IgA affinity purification immediately after.

Purification and Digestion of Immunoglobulins From Donor Plasma and Saliva

IgG and IgA were each purified in duplicate on separate plates using affinity bead chromatography, based on a protocol described previously (33). For IgG purification, 15 μL of Protein G Sepharose 4 Fast Flow beads (GE Healthcare, Uppsala, Sweden) were added per well on an Orochem filter plate and washed three times with phosphate-buffered saline (PBS). For IgA purification, the same procedure was followed using 2 μL CaptureSelect IgA Affinity Matrix beads (Thermo Fisher Scientific, Breda, The Netherlands). For IgG purification, either 100 μL of saliva or 2 μL of plasma was added to each well, while 100 μL of saliva or 5 μL of plasma was used for IgA purification. Sample volumes were brought to a total of 200 μL by the addition of PBS. The plates were incubated for 1 h while shaking at 750 rpm with 1.5 mm orbit (Heidolph Titramax 100; Heidolph, Kelheim, Germany) to accommodate binding.

Using a vacuum manifold, the samples were washed three times by adding 400 μL PBS, followed by three times 400 μL of purified water (Purelab Ultra, maintained at 18.2 MΩ; Veolia Water Technologies Netherlands B.V., Ede, The Netherlands). The antibodies were eluted from the beads by adding 100 μL of 100 mM formic acid (Sigma-Aldrich, Zwijndrecht, The Netherlands), incubating for 5 min at 750 rpm, and centrifuging at 100 × *g* for 2 min. Samples were dried for 2 h at 60°C in a vacuum centrifuge.

The IgG samples were resolubilized in 20 μL 50 mM ammonium bicarbonate (Sigma-Aldrich) while shaking for 5 min at 750 rpm. Twenty μL of 0.05 μg/μL tosyl phenylalanyl chloromethyl ketone (TPCK)-treated trypsin (Sigma-Aldrich) in ice-cold purified water was added per well, and the samples were incubated at 37°C overnight.

In contrast to IgG, IgA molecules need to be reduced and alkylated prior to digestion to obtain peptides covering all glycosylation sites. IgA samples were resolubilized in 30 μL 30 mM ammonium bicarbonate, 12.5% acetonitrile (Biosolve, Valkenswaard, the Netherlands) while shaking for 5 min at 750 rpm. Subsequently, 5 μL of 35 mM dithiothreitol (Sigma-Aldrich) was added, followed by 5 min incubation at room temperature on a shaker (750 rpm) and 30 min incubation at 60°C in an oven. After cooling to room temperature, 5 μL of 125 mM iodoacetamide (Sigma-Aldrich) was added and the samples were incubated in the dark while shaking for 30 min. Two μL of 100 mM dithiothreitol was added to quench the iodoacetamide. Finally, 8 μL of 0.08 μg/μL TPCK-treated trypsin in ice-cold purified water was added per well, and the samples were incubated at 37°C overnight. Before LC-MS analysis, IgA and IgG samples derived from plasma were diluted twice and 20-times, respectively, with purified water, whereas saliva-derived samples were not diluted. Assuming no losses and prior concentrations of 12.5 mg/mL plasma IgG, 0.014 mg/mL saliva IgG, 2.2 mg/mL plasma IgA and 0.19 mg/mL saliva IgG (20, 21), the concentrations of the final digests were 0.031, 0.035, 0.110, and 0.380 mg/mL for plasma IgG, saliva IgG, plasma IgA, and saliva IgA, respectively.

Digestion and *N*-Glycan Release of IgA Samples for MS/MS Analysis

For the fragmentation analysis by MS/MS of the IgA glycopeptides, a separate purification and tryptic digestion of IgA was done in triplicate on two saliva samples from two donors from the study described above, a pooled-plasma standard from a minimum of 20 human donors (VisuCon-F Frozen Normal Control Plasma; Affinity Biologicals, Ancaster, Canada), 10 μg of a human plasma-derived IgA standard (Lee Biosolutions, Maryland Heights, MO), and a human colostrum-derived SIgA standard (Athens Research and Technology, Athens, GA). The procedure was similar to what is described above, except that 1 μg trypsin per sample was used instead of 0.64 μg. Twenty μL of trypsin-digested sample was collected and heated to 95°C to inactivate the trypsin. After cooling to room temperature, 1 μL of *N*-glycosidase F (Roche Diagnostics, Mannheim, Germany) was added and the samples were incubated at 37°C overnight. The samples obtained from the pooled-plasma standard were diluted twice and the (S)IgA standard samples thrice with purified water, whereas the saliva-derived samples were not diluted.

NanoLC-ESI-QTOF-MS(/MS) Analysis

IgG and IgA samples were present on separate plates and measured on different days. Each pair of plasma and saliva sample of the same donor was analyzed successively, but the duplicate pair of the same donor was measured at a later time point. Blanks consisting of purified water were run after every 20 samples. Two hundred nL of each sample was injected into an Ultimate 3000 RSLCnano system (Dionex/Thermo Scientific, Breda, the Netherlands) coupled to a quadrupole-TOF-MS (MaXis HD; Bruker Daltonics, Bremen, Germany). The LC system was equipped with an Acclaim PepMap 100 trap column (particle size 5 μm, pore size 100 Å, 100 μm × 20 mm, Dionex/Thermo Scientific) and an Acclaim PepMap C18 nano analytical column (particle size 2 μm, pore size 100 Å, 75 μm × 150 mm, Dionex/Thermo Scientific). A mixture of solvent A (0.1% formic acid in purified water) and solvent B (95% acetonitrile) was applied with a constant flow of 0.7 μL/min using a linear gradient: t(min) = 0, %B = 3; t = 5, %B = 3; t = 35, %B = 53; with washing and equilibration starting at t = 36, %B = 70; t = 38, %B = 70; t = 39, %B = 3; t = 58, %B = 3. The sample was ionized in positive-ion mode using a CaptiveSprayer (Bruker Daltonics) electrospray source at 1300 V. A nanoBooster (Bruker Daltonics) was used to enrich the

nitrogen gas with acetonitrile to enhance ionization efficiency. Mass spectra were acquired with a frequency of 1 Hz and the MS ion detection window was set at mass-to-charge ratio (*m/z)* 550–1800. Fragmentation spectra were recorded with a detection window of *m/z* 50–2800.

Data Processing

LC-MS(/MS) data were first examined manually using DataAnalysis (Bruker Daltonics). Glycopeptides were identified based on their *m/z* and literature (**Supplemental Table S1**) (17, 33–40). In the following, glycosylation site numbering for IgG is based on conventions commonly used in literature, e.g., (24), and for IgA1, IgA2, the JC and the SC, UniProt numbering is used (25) (**Figure 1**). For each glycopeptide cluster, here defined as a group of glycopeptides sharing the same peptide portion, e.g., IgA2 N205, at least one glycopeptide was characterized by MS/MS fragmentation, elucidating the glycan composition and the identity of the peptide (**Supplemental Figure S1**). In order to provide information on the peptide sequence of the IgA glycopeptides, a proteomics analysis (MASCOT Deamon version 2.2.2; Matrix Science, London, UK) was run on the LC-MS/MS data of the *N*-glycosidase F-digested IgA samples, in which the *N*-glycans had been released. The following settings were used: database: SwissProt (2017_09); taxonomy: *Homo sapiens*; enzyme: trypsin; fixed modifications: carbamidomethyl (C); variable modifications: oxidation (M), deamidated (NQ) and Gln➔pyro-Glu (N-term Q); maximal number of missed cleavages: 2; peptide tolerance MS: 0.05 Da; peptide tolerance MS/MS: 0.07 Da (**Supplemental Table S2**). The peptides covering IgA2 N47 and N92 were not recognized by the software, but could still be manually identified (**Supplemental Figure S2**). The proteomics data are available via ProteomeXchange with identifier PXD011228.

For IgA1/2 N340/N327, two different peptide sequences were identified in *N*-glycosidase F-treated samples: the expected LAGKPTHVNVSVVMAEVDGTCY and the truncated LAGKPTHVNVSVVMAEVDGTC, lacking the C-terminal tyrosine, as described before by Bondt et al. (35). Both of these peptides eluted at two different retention times: a minor peak (<20%) first, and a higher peak eluting 1 min later. The same pattern could be seen in samples that were not treated with *N*-glycosidase F. For data analysis, only the higher, later-eluting peak was included, since the lower peak was often of too low signal quality.

LC-MS data were calibrated in DataAnalysis based on a list of the expected *m/z* values of either IgG1 N297 or IgA N205 glycopeptides. The data files were then converted to mzXML format using the MSconvert program from the ProteoWizard 3.0 suite. Alignment of the time axis of the data and extraction of glycopeptide signal intensities, based on sum spectra, was done using the in-house developed LacyTools software, with a list of manually compiled glycopeptides and their retention times as input (29). For signal extraction, area integration was performed within an *m/z* window of ±0.05 Th around each isotopic peak (with the minimum theoretical % of signal intensity covered by the sum of the integrated isotopic peaks at 85%) within an individually specified time window surrounding the retention time. This resulted in background-corrected signal areas for each glycopeptide per charge state {$[M+2H]^{2+}$ to $[M+7H]^{7+}$}. Whether an analyte was present in a sample, was determined based on the signal-to-noise ratio (S/N; > 9), the isotopic pattern quality score (IPQ; < 0.2) and the mass accuracy (<10 ppm deviation) of each signal per charge state. Data of specific glycopeptide clusters were excluded for further processing when either the total number of analytes detected was <50% of the maximum number detected for that cluster, or when the summed absolute intensity of the detected analytes was <5% of the maximum sum observed for that cluster. This assessment was performed separately for samples obtained from saliva or plasma. Subsequently, individual analytes were subjected to quality control criteria to determine which were of sufficient quality for relative quantification. Glycopeptides in specific charge states were included for relative quantification if their signal showed a S/N > 9, IPQ < 0.2 and an absolute mass error <10 ppm in at least 25% of either all plasma or all saliva samples. Finally, all included charge state signals for the same glycopeptide were summed and absolute abundances were corrected for the fraction of isotopes integrated. The glycopeptide signals were normalized on the total signal intensity per glycopeptide cluster, resulting in the relative quantification of each glycopeptide.

Based on the *N*-glycan monosaccharide compositions, glycoforms were categorized as bisected, high-mannose or hybrid, and, in addition, the number of fucoses, galactoses, and sialic acids was determined (**Supplemental Table S1**). This was used for the calculation of several glycosylation features per glycosylation site, based on total-area normalized data. Fucosylation represents the number of fucoses per complex-type *N*-glycan, i.e., sum [(complex-type species with n fucoses)*n]/sum(complex-type species). Bisection represents the fraction of bisected complex-type *N*-glycans, i.e., the sum of all structures presumed to carry a β1-4-linked *N*-acetylglucosamine (GlcNAc) on the innermost mannose, divided by the sum of all complex-type glycoforms. Galactosylation was calculated as the number of galactoses per complex-type *N*-glycan, i.e., sum [(complex-type species with n galactoses)*n]/sum(complex-type species). Sialylation was calculated as the number of sialic acids per complex-type *N*-glycan, i.e., sum [(complex-type species with n sialic acids)*n]/sum(complex-type species). Sialylation/Galactose represents the number of sialic acids per galactose on complex-type species, i.e., sialylation divided by galactosylation. High-mannose represents the fraction of high-mannose type *N*-glycans, i.e., sum of all structures where the core is elongated only by mannoses, while hybrid-type glycans represent the structures that are either hybrid-type or have only one antenna. In addition, for the *O*-glycosylation on IgA1, glycosylation features were defined as follows. #HexNAc represents the number of *N*-acetylhexosamines per *O*-glycopeptide, i.e., sum [(species with n *N*-acetylhexosamines)*n]. #Hex represents the number of hexoses per *O*-glycopeptide, i.e., sum [(species with n hexoses)*n]. #SA represents the number of sialic acids per *O*-glycopeptide, i.e., sum [(species with *n* sialic acids)**n*]. Hex/HexNAc represents the number of hexoses per

N-acetylhexosamine, i.e., #Hex divided by #HexNAc. Finally, SA/Hex represents the number of sialic acids per hexose, i.e., #SA divided by #Hex.

Statistical Analysis

From each duplicate pair of samples, the sample with the higher absolute signal intensity per glycopeptide cluster was used for statistical analyses (**Supplemental Table S3**). The IgG and IgA glycosylation features in plasma and saliva originating from the same donor were compared using the Wilcoxon signed rank test (wilcox.test function from the MASS package) in R [v3.1.2; R Foundation for Statistical Computing, Vienna, Austria (41)] and RStudio (v0.98.1091; RStudio, Inc.; **Supplemental Table S4**). Correlation analysis was performed between the saliva and plasma samples using the cor.test function from the R stats package (use = pairwise.complete.obs, method = spearman) to obtain the correlation coefficient (rho) and associated *p*-value (**Table 1**). The Wilcoxon signed rank test and correlation analysis were only performed when data from at least 11 paired (plasma and saliva from the same donor) samples were available, which was the case for IgG1 N297, IgG2/3 N297, IgG4 N297, IgA2 N205, and IgA2 N47. Bonferroni correction was performed to account for multiple testing, resulting in a *p*-value threshold for significance of 0.05/28 = 0.00179. Graphs were created either in Microsoft Excel 2010 or Graphpad Prism 7.

RESULTS

Paired plasma and saliva samples were collected from 19 healthy donors. From these samples, IgG and IgA were separately purified in duplicate using bead-based affinity chromatography. Samples were trypsin-digested and analyzed by nanoLC-ESI-QTOF-MS. Glycopeptides were identified on the basis of the registered *m/z*, tandem mass spectrometric analyses as well as literature information on immunoglobulin glycosylation (**Supplemental Table S1**, **Supplemental Figure S1, S3**). Glycosylation features were calculated for each glycosylation site of IgG, IgA, JC, and SC (**Supplemental Table S3**).

IgG *N*-Glycosylation

For IgG1 and IgG2/3 N297, 27 different glycan compositions each were quantified in both the plasma and saliva samples, and 13 for IgG4 N297 (**Supplemental Figure S3A**, **Supplemental Table S1A**). IgG1 and IgG4 derived from saliva showed a slightly lower degree of galactosylation and sialylation as compared to plasma (for example, 1.1 and 1.3 times lower medians for IgG1 and IgG4 galactosylation, respectively). In contrast, high-mannose and hybrid-type glycans were more abundant in salivary IgG1 and IgG2/3, as compared to plasma (for example, 2.7 and 3.4 times higher medians for IgG1 and IgG2/3 high-mannose type glycans, respectively; **Figure 2**, **Supplemental Table S4**). For IgG1 and IgG2/3, a significant correlation was observed for the fucosylation, bisection, sialylation and sialylation/galactose between plasma and saliva (**Table 1**), showing the similarities in glycosylation features between the two biofluids to be conserved across the different donors. IgG4 showed similar behavior (**Table 1**).

IgA *N*-Glycosylation

For IgA2 N205 and N47, 15 and 10 different glycoforms were quantified, respectively, in both the saliva and the plasma samples (**Supplemental Figure S3B**, **Supplemental Table S1B**). The *N*-glycans were of the complex-type and mainly diantennary (>98% of total abundance). Two to five-fold differences were observed in the relative abundances of the different glycan types present on plasma- vs. saliva-derived IgA2: salivary *N*-glycans at both N205 and N47 showed a higher degree of bisection and a lower degree of galactosylation, sialylation, and sialylation/galactose (**Figure 2**, **Supplemental Table S4**). None of the tested glycosylation traits on IgA2 showed a significant correlation between plasma and saliva samples (**Table 1**). Of note, for IgA2 *N*-glycosylation site N47 a truncated glycopeptide, i.e., (W)SESGQN$_{47}$VTAR(N), was registered. This peptide features a tryptic *C*-terminal cleavage while the *N*-terminus stems from a chymotryptic cleavage site. The predicted tryptic peptide (K)VFPLSLDSTPQDNVVVACLVQGFFPEPLSVTWSESGQN$_{47}$VTAR(N) was not observed.

The glycopeptides with the peptide moieties LAGKPTHVNVSVVMAEVDGTCY and LAGKPTHVNVSVVMAEVDGTC (truncated; t) were assigned to both IgA1 and IgA2 covering the glycosylation sites N340 and N327, respectively, as these peptide portions are common to both IgA subclasses (**Supplemental Table S2**). The previously reported sequence variant of IgA2 N327, MAGKPTHIN$_{327}$VSVVMAEADGTC(Y), was not observed in our samples, also not with the naturally occurring polymorphisms I326V and A335V (17, 42, 43). The absolute MS signals of the truncated variant were higher in plasma samples, while those relating to the sequence including the *C*-terminal tyrosine were higher in saliva (**Supplemental Table S3**). Twenty-one and eight different glycoforms could be quantified on the full-length and the truncated sequence, respectively (**Supplemental Table S1B**). Furthermore, trends of lower fucosylation (1.4 times lower), galactosylation (2 times lower) and sialylation (5 times lower) and higher bisection (1.7 times higher) in saliva as compared to plasma were observed for IgA1/2 N340/327, but not for IgA1/2 N340/327t (**Figure 2**, **Supplemental Table S4**).

IgA1 N144 and IgA2 N131 share the same tryptic glycopeptide sequence LSLHRPALEDLLLGSEAN$_{144/131}$LTCTLTGLR. While nearly all samples failed to provide data of sufficient quality to derive a glycosylation profile, the three samples which did pass data curation (one from plasma and two from saliva, not paired) showed up to 20% high-mannose type glycans and up to 3% hybrid-type/mono-antennary glycans, in addition to the complex-type *N*-glycans (**Figure 2**). In contrast to other IgA *N*-glycosylation sites, glycans at N144/131 were almost entirely afucosylated (<1% fucosylation; **Supplemental Tables S3, S4**).

For IgA2 N92, in all samples only non-glycosylated peptides with the sequence HYTN$_{92}$PSQDVTVPCPVPPPPPCCHPR [allotype A2m(1)] were observed. Moreover, samples treated with *N*-glycosidase F did not show deamidated forms of this peptide, indicating that no glycosylated variants of N92 were present prior to *N*-glycosidase F digestion (**Supplemental Table S2**).

TABLE 1 | Correlation of derived glycan traits between saliva and plasma samples as shown by the Spearman's correlation coefficient (rho) and associated *p*-values.

				Fucosylation		Bisection		Galactosylation		Sialylation		Sialic acid/galactose	
Protein	**Site**	**Peptide**	**N_{pair}**	**rho**	***p*-value**	**rho**	***p*-value**	**rho**	***p*-value**	**Rho**	***p*-value**	**rho**	***p*-value**
IgG1	N297	EEQYNSTYR	17	0.973	***4.7E-06***	0.877	***< 1E-07***	0.627	0.0084	0.843	***9.7E-07***	0.961	***4.6E-07***
IgG2/3	N297	EEQFNSTFR	17	0.716	***0.0017***	0.936	***< 1E-07***	0.699	0.0025	0.748	***8.4E-04***	0.885	***< 1E-07***
IgG4	N297	EEQFNSTYR	12	NA	NA	0.965	***< 1E-07***	0.706	0.013	0.762	0.0059	0.434	0.16
IgA2	N205	TPLTANITK	16	0.232	0.39	0.474	0.066	−0.0529	0.85	0.191	0.48	0.232	0.39
IgA2	N47	SESGQNVTAR	13	NA	NA	0.412	0.16	−0.242	0.43	0.181	0.55	0.423	0.15

The numbers of included pairs are listed under "N_{pair}." p-values significant after Bonferroni correction are shown in bold ($\alpha = 1.7910^{-3}$). The correlation for IgA1/2 N144/131 and N340/327, JC N71, the SC N-glycosylation and the IgA1 O-glycosylation was not assessed because this data was present in less than 11 paired samples (plasma and saliva from the same individual).

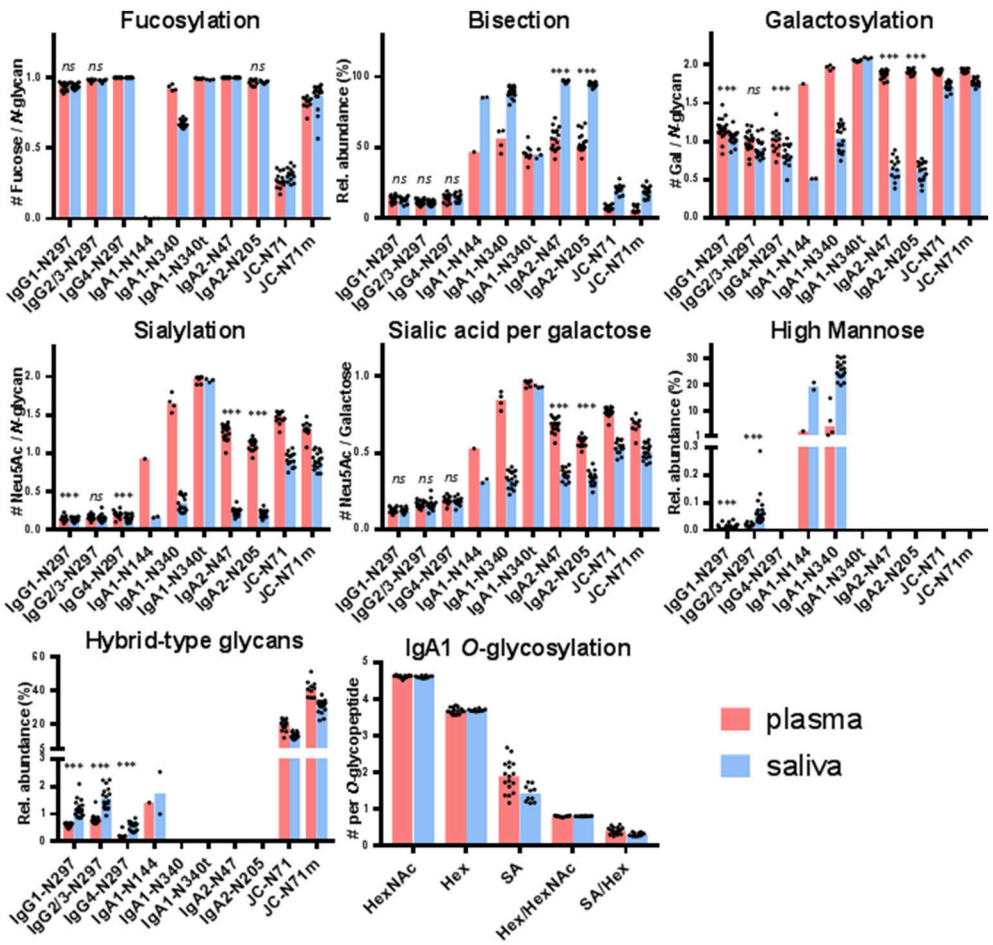

FIGURE 2 | Glycosylation features for each of the glycosylation sites found in IgG, IgA, and the JC. The bar graphs represent the medians per glycosylation site (red for plasma and blue for saliva) and the black dots represent the individual data points for each donor. A Wilcoxon signed rank test was performed between paired samples from plasma and saliva when the total number of pairs was > 10 (**Supplemental Table S4**). Significant differences are denoted by ***, non-significant differences are denoted by *ns*. IgA1-N340t is the *C*-terminally-truncated version of IgA1-N340 and JC-N71m is the miscleavage variant of JC-N71. IgA1-N144 also represents IgA2-N131, and IgA1-N340 and -N340t also represent IgA2-N327 and -N327t.

IgA1 *O*-Glycosylation

The potential *O*-glycosylation sites located within the IgA1 hinge region were part of one large tryptic peptide: HYTNPSQDVTVPCPVPSTPPTPSPSTPPTPSPSCCHPR.

Forty-two *O*-glycopeptides were quantified. The collective glycan composition consisted of two to five hexoses, three to six HexNAcs and zero to five *N*-acetylneuraminic acids, likely distributed over three to six *O*-glycans

(**Supplemental Table S1B**). Only a minor trend of lower (1.4 times lower) salivary *O*-glycan sialylation was observed as compared to plasma (**Figure 2**).

Joining Chain (JC) *N*-Glycosylation

The single *N*-glycosylation site N71 at the JC was observed on two tryptic peptides: EN_{71}ISDPTSPLR (JC N71) and the miscleaved IIVPLNNREN_{71}ISDPTSPLR (JC N71m). In general, this glycosylation site contained a higher fraction of monoantennary and hybrid-type glycans than the IgA constant domain *N*-glycosylation sites (between 20 and 50%; **Supplemental Table S1C**). Furthermore, for this site similar differences between saliva and plasma were observed as for the IgA1 and IgA2 heavy chain *N*-glycosylation sites, namely a higher bisection (3.2 times higher) and lower galactosylation (1.1 times lower) and sialylation (1.7 times lower) in the saliva-derived samples (**Figure 2**, **Supplemental Table S4**). The miscleaved glycopeptides showed a higher abundance of fucosylation as compared to the expected tryptic glycopeptides (3.2 times higher in plasma and 2.9 times higher in saliva; **Figure 2**).

Secretory Component (SC) *N*-Glycosylation

All seven *N*-glycosylation sites of the SC were detected after tryptic digestion of salivary SIgA. Low-intensity signals of SC glycopeptides were also seen in a few plasma samples (**Supplemental Table S3**). *N*-glycans at N135, N186, N421, and N469 were determined to be complex-type and diantennary, furthermore the antennae were fully galactosylated and partially sialylated (**Supplemental Table S1D**, **Supplemental Figure S4**). In addition, on N499, mono-antennary species were identified. The observed glycoforms carried zero to five fucoses, and tandem mass spectrometry indicated the presence of both core and antennary fucosylation (**Figure 3**, **Supplemental Figure S1**). On N135, N469, and N499 between 1 and 4% bisection was observed (**Supplemental Figure S4**). The glycosylation sites N83 and N90 were present on the same tryptic peptide, and the joint glycan composition $H_{10}N_8F_{2-8}S_{0-3}$ indicated that the glycans at these two sites were similar to those on other SC sites.

DISCUSSION

Here we present the first site-specific glycosylation analysis of antibodies in human saliva. IgG and IgA were purified from the plasma and saliva of 19 healthy individuals, and analyzed by LC-MS(/MS). Similar to previous studies on human serum and colostrum IgG or IgA glycosylation which used a comparable analytical methodology (17, 34, 35, 39), we observed glycopeptides covering the *N*-glycosylation sites of IgG1, 2/3 and 4 at N297, IgA1 at N340 and N144, IgA2 at N327, N205 and N131, and of the IgA-associated JC at N71, and the *O*-glycosylation sites in the IgA1 hinge region. We report several non-sialylated glycoforms on the JC that have not been described previously. Moreover, in both plasma and saliva samples we characterized the glycosylation at IgA2 *N*-glycosylation site N47, which had not extensively been described in literature (17, 39). Finally, we provide an overview of the *N*-glycans at all 7 glycosylation sites of the SC in saliva including hitherto unreported molecular species, such as glycoforms with four or five fucoses.

The region surrounding IgA2 N92 is polymorphic and can produce two types of tryptic peptides, $HYTN_{92}$PSQDVTVPC PVPPPPPCCHPR [allotype A2m(1)] and $HYTN_{92}$SSQDVTVP CR [allotype A2m(2)] (44). Since we detected the tryptic IgA2 peptide $HYTN_{92}$PSQDVTVPCPVPPPPPCCHPR in saliva and plasma samples from all individuals included in our study, we conclude that all carry at least one allele of IgA2 allotype A2m(1). This was expected, given that this allele has a frequency of 0.985 in the Caucasian population (44, 45). Allotype A2m(2) peptides were not observed in our samples. Two previous studies reported the NPS sequence on the A2m(1) allotype to be *N*-glycosylated (16, 46), even though the proline following the N92 in A2m(1) does not match the consensus sequence for *N*-glycosylation. Here, however, we found that IgA2 N92 was not glycosylated in either plasma or saliva, in accordance with a previous report on colostrum SIgA (17). In future research also donors expressing the A2m(2) allotype should be included to obtain a complete characterization of IgA glycosylation.

In the current study, we did not detect the (glyco)peptides covering IgA2 N327 when searching for the expected tryptic peptide sequence obtained from UniProt entry IGHA2_HUMAN (P01877) or its naturally occurring variants. However, instead of the methionine in position 319 on IgA2 (25), a leucine was previously reported in allotype A2m(1) (42, 43), resulting in identical peptide sequences for both IgA2 N327 and IgA1 N340. Our observation that all individuals studied expressed IgA2 allotype A2m(1), made us conclude that the glycopeptides that we detected with peptide sequences LAGKPTHVNVSVVMA EVDGTCY and LAGKPTHVNVSVVMAEVDGTC [truncated (35, 47)] represented a mixture of IgA1 N340 and IgA2 N327.

The two differentially cleaved peptide sequences covering N71 of the JC showed a large variation in their glycan fucosylation, with the miscleaved variant having about 3 times higher fucosylation than the expected peptide. This indicates that the core fucose might interfere with tryptic cleavage at R69. Similar differences in fucosylation were found previously (17).

Saliva collection has multiple advantages over the collection of plasma, for example, it is painless and does not require special instrumentation or trained personnel. Specialized devices for saliva collection making use of swabs or chewing on paraffin wax do exist (1, 20). However, we utilized the simplest method, i.e., unassisted, unstimulated drooling, and found that this was sufficient to obtain IgG and IgA for a thorough glycomic analysis. A limitation of the current method might be that only solubilized antibodies were obtained, while the fraction associated to, for example, mucins was precipitated during sample preparation. Furthermore, before saliva can be used as a sample for diagnostics, further research is necessary to evaluate robustness in terms of sample collection mode, time point and sample storage. Finally, although the current method can be performed in a 96-well plate format and has the potential to be automated, for its application in a routine laboratory or diagnostic setting further technological development is required that allows the specific quantification of glycoforms of interest, identified in the discovery phase. Despite the mentioned

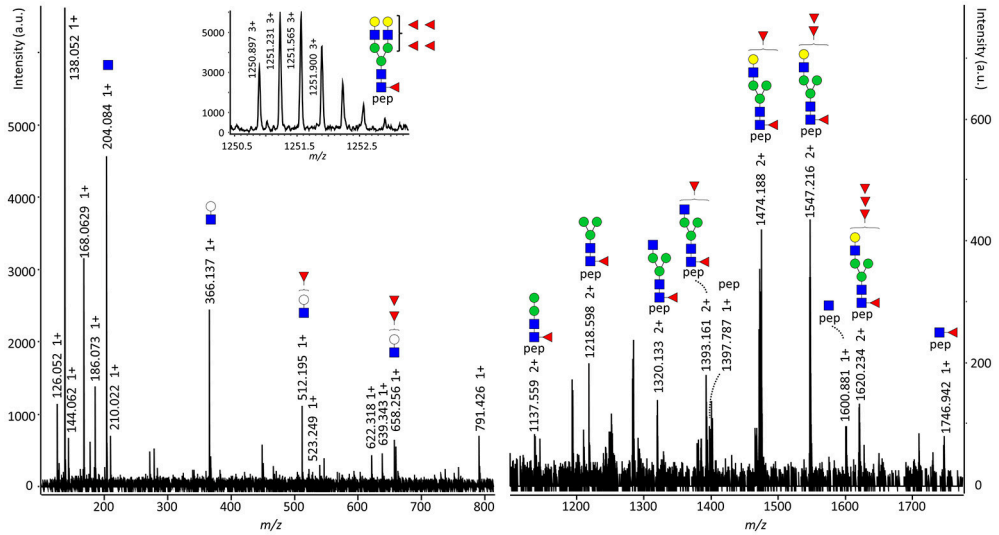

FIGURE 3 | Fragmentation spectrum of SC N469 H5N4F5S0. The parent ions were detected at *m/z* 1250.895 at a retention time of 13.1 min and were assigned as the triply charged variant of [M] = 3749.664 Da, representing SC N469 H5N4F5S0. The structure carries both core and antenna fucosylation, as the former proven by $[M+H]^+$ = 1746.942, representing the peptide sequence $VPGN_{469}VTAVLGETLK$ plus a GlcNAc and a fucose, and the latter by $[M+H]^+$ = 512.195 and 658.256, representing the antenna oxonium ions with one or two fucoses, respectively. pep: $VPGN_{469}VTAVLGETLK$, white circle: hexose, green circle: mannose, yellow circle: galactose, blue square: *N*-acetylglucosamine, red triangle: fucose.

limitations, using saliva Ig glycosylation might have potential in medical research in two different contexts: (i) as a proxy for plasma Ig glycosylation reflecting systemic conditions, and (ii) as a biomarker (panel) or therapeutic target for local perturbations in the oral cavity.

Saliva Ig Glycosylation as Proxy For Plasma Ig Glycosylation

The glycosylation of, in particular, IgG as the most abundant Ig in plasma has been proposed as a biomarker for various physiological and pathological states in multiple large-scale studies (36, 48, 49). Similarly, IgA1 *O*-glycosylation associates with IgA nephropathy, and IgA1 *N*- and *O*-glycosylation showed to alter with pregnancy and rheumatoid arthritis (12, 35, 50). The vast majority of salivary IgG is thought to originate from plasma, and thus differences in glycosylation between plasma- and saliva-derived IgG likely originate from the minority (<20%) of locally produced IgG (20, 22). Here we found salivary IgG at N297 to exhibit a slightly lower galactosylation and sialylation, and a slightly higher abundance of high-mannose and hybrid-type glycans as compared to plasma. However, most IgG glycosylation features, except galactosylation, correlated well between plasma and saliva. This indicates that these features have potential as plasma IgG proxies and, thus, as biomarkers for the systemic health status. Low galactosylation and sialylation of plasma IgG are associated with inflammation and various autoimmune diseases (51, 52). Additionally, galactosylation and sialylation are known to influence the binding of IgG to FcγRs and the C1q protein (7, 53). This suggests that the slight IgG glycosylation differences we found between the two biofluids from healthy individuals may arise from the locally higher inflammatory state in the oral cavity, since it is constantly exposed to pathogens. This aspect should be taken into account when further exploring the use of salivary IgG glycosylation as biomarker for systemic diseases, with special attention regarding possible co-occurring oral inflammatory conditions, such as periodontitis (gum disease). In contrast to IgG, the *N*-glycosylation of IgA was not correlated between plasma and saliva in our study. This is likely due to either the different origin of plasma cells producing the two pools of IgA proteins or to a difference in processing, such as dimerization and J-chain binding, or their translocation through the epithelial cell layer. Our findings in healthy individuals aged between 20 and 42 years suggest that salivary IgA cannot be used as a proxy for plasma IgA *N*-glycosylation.

Saliva Ig Glycosylation as a Biomarker (Panel) or Therapeutic Target for Local Perturbations in the Oral Cavity

Differences of Ig glycosylation in locally produced biofluids can be exploited as biomarkers for local pathological processes. Accordingly, IgG glycosylation in cerebrospinal and synovial fluid from multiple sclerosis and rheumatoid arthritis patients, respectively, revealed biofluid-specific associations with disease (14, 15). In addition, patients with advanced periodontitis were reported to exhibit a lower salivary IgG galactosylation than healthy individuals (18). Our data suggest that salivary IgA *N*-glycosylation analysis also provides a promising tool to detect local glycosylation perturbations in the oral cavity

which might reflect pathological processes. IgA is the most abundant antibody in human saliva, and SIgA is regarded as an important first line of defense against pathogens on mucosal surfaces (11, 20, 21). Interestingly, the *N*-glycosylation profile reported for colostrum-derived SIgA (17) is similar to our data on salivary SIgA, in terms of a high abundance of glycoforms carrying a bisecting GlcNAc, contrary to plasma-derived IgA. This suggests that in healthy individuals, SIgA shares a common *N*-glycosylation profile, whether it originates from the salivary or mammary glands, but differs from the IgA glycosylation profile in circulation. This might be related to the fact that both salivary and milk SIgA enter the gastrointestinal tract via the same route, and can exert similar functions while passing the oral cavity and the gastrointestinal tract.

Salivary IgA and JC showed a considerably higher bisection and lower galactosylation and sialylation at all observed sites of *N*-glycosylation, except for the truncated variants of IgA1 N340 and IgA2 N327 lacking the *C*-terminal tyrosine, which had a similar glycosylation profile in plasma and saliva. Moreover, the truncated version was low-abundant in saliva and highly abundant in plasma. Therefore we hypothesize that the truncated form originates from circulation and is present in saliva due to leakage or transport from circulation (22), while the full-length variant might mainly be produced and secreted locally in the oral cavity. The majority of salivary IgA and JC is produced locally in plasma B cells of the glandular stroma (20, 26). This suggests that changes in the glycosylation machinery of specifically these cells are the cause for the substantial glycosylation differences between plasma and saliva. For example, an upregulation of beta-1,4-*N*-acetylglucosaminyltransferase III (GnT-III/MGAT3) and a downregulation of beta-1,4-galactosyltransferase (B4GalT) and beta-galactoside-alpha-2,6-sialyltransferase (St6Gal) 1 in the glandular stroma B cells could be responsible for the observed differences in IgA *N*-glycosylation. Alternatively, the pIgR-enabled transport of IgA across the epithelium, the dimerization of IgA, and the binding of the J-chain might be selective for certain glycoforms of IgA. However, for the binding to the pIgR this appears unlikely taking into account a previous study which reported that the removal of either the *N*- or *O*-glycans of polymeric IgA had no influence on pIgR-mediated transcytosis (54). An additional explanation for the differences between plasma and salivary IgA glycosylation might be the presence of glycosidases from oral microbiota in saliva that can alter the glycosylation after SIgA secretion (55). Finally, it could be speculated that asialoglycoprotein receptors, which are located primarily in the liver, could alter the overall glycosylation of plasma IgA by specifically removing non-sialylated proteins from circulation (56), thus leading to a higher level of sialylation compared to saliva. However, this would not explain the differences in the levels of bisection between plasma and saliva. The functional consequences of differences in IgA *N*-glycosylation are at this point not well understood: The *N*-glycans on the constant region of IgA do not seem to be essential for FcR binding, in contrast to the ones on IgG (13). However, IgA sialylation has been shown to be required for dectin-1-mediated transport of SIgA across the epithelium of intestinal cells (11). Furthermore, in addition to the Fab-binding sites, SIgA fucosylation and sialylation enable the binding of the antibody to pathogenic bacteria, acting as a decoy to prevent bacterial adhesion to the epithelium and subsequent infection (57–59). Finally, the *C*-terminal *N*-glycan sialic acids have recently been reported to directly inhibit sialic acid-binding viruses like influenza (60).

The fact that we did not find differences between salivary and plasma IgA1 *O*-glycosylation, except for a slight trend of lower sialylation in saliva, is likely due to their inherently different biosynthetic pathways as compared to *N*-glycans, involving distinct glycosyltransferases (61). Additionally, we here evaluated all *O*-glycosylation sites simultaneously at the same glycopeptide, which provides less resolution than analysis on the single-structure level. Thus, it is difficult to judge on the usefulness of IgA *O*-glycosylation as a potential diagnostic biomarker based on our data. However, future investigations should further assess IgA *O*-glycosylation in a specific disease context, since in plasma it has been associated with pathologies, such as IgA nephropathy and Sjögren's syndrome (12, 62, 63).

A comparison of the salivary IgA SC with plasma was not possible, due to insufficient signal intensities of the plasma SC from most individuals in our study, most likely due to its low abundance in plasma. *N*-glycans on the SC have been shown to be crucial for various functional aspects of SIgA (59). For example, SC glycosylation enables the innate protection against mucosal pathogens (64). Furthermore, SC glycans are essential for a correct localization of IgA in the mucosal lining, resulting in protection from bacterial infection in the respiratory tract of mice (65). Because of the important and diverse role of SC glycosylation, future studies should examine whether salivary SC glycosylation is associated with, for example, periodontitis, to explore its potential as a diagnostic biomarker or therapeutic target.

Conclusions

Large differences were found between the glycosylation of plasma- and saliva-derived IgA and its JC, while this was not the case for IgG. This suggests that SIgA, locally produced by plasma B cells in the glandular stroma, differs in glycosylation from IgA of the circulation, that presumably is largely produced by circulating plasma cells, pointing toward distinct regulatory mechanisms. An alternative explanation is that SIgA dimerization or transport into the oral cavity might be glycoform-specific, or that certain IgA-producing B cells, expressing a specific glycosylation repertoire, may be relocated to the glandular stroma after activation. The observed differences between plasma and salivary IgA make biofluid-specific analysis of SIgA glycosylation (including the JC and SC) a promising tool for mucosal disease-related biomarker research. IgG glycosylation, on the other hand, showed a good correlation between plasma and saliva in healthy individuals, indicating that salivary IgG might be a proxy to study plasma IgG in situations where a healthy oral environment can be assumed.

DATA AVAILABILITY STATEMENT

The raw data supporting the conclusions of this manuscript will be made available by the authors, without undue reservation, to any qualified researcher. The mass spectrometry proteomics data have been deposited to the ProteomeXchange Consortium via the PRIDE (66) partner repository with the dataset identifier PXD011228.

AUTHOR CONTRIBUTIONS

RP, VD, and MW designed the study. JM and RP performed sample preparation and experimental analysis. RP and NdH processed data, which were further analyzed by RP, NdH, AB, VD, and MW. NdH and RP drafted the manuscript, which was revised by all authors. All authors approved the final manuscript.

FUNDING

This work was supported by the European Union Seventh Framework Program HighGlycan (278535).

ACKNOWLEDGMENTS

We would like to thank Shivani Kapoerchan and Lisette den Hertog for their help with initial method development. Agnes Hipgrave Ederveen and Carolien Koeleman are acknowledged for their help with running the LC-MS system.

SUPPLEMENTARY MATERIAL

The Supplementary Material for this article can be found online at: https://www.frontiersin.org/articles/10.3389/fimmu.2018.02436/full#supplementary-material

REFERENCES

1. Pfaffe T, Cooper-White J, Beyerlein P, Kostner K, Punyadeera C. Diagnostic potential of saliva: current state and future applications. *Clin Chem.* (2011) 57:675–87. doi: 10.1373/clinchem.2010.153767
2. Hu S, Arellano M, Boontheung P, Wang J, Zhou H, Jiang J, et al. Salivary proteomics for oral cancer biomarker discovery. *Clin Cancer Res.* (2008) 14:6246–52. doi: 10.1158/1078-0432.CCR-07-5037
3. Horsfall AC, Rose LM, Maini RN. Autoantibody synthesis in salivary glands of Sjogren's syndrome patients. *J Autoimmun.* (1989) 2:559–68. doi: 10.1016/0896-8411(89)90189-3
4. Khan RS, Khurshid Z, Yahya Ibrahim Asiri F. Advancing Point-of-Care (PoC) testing using human saliva as liquid biopsy. *Diagnostics* (2017) 7:39. doi: 10.3390/diagnostics7030039
5. Liu X, Yu H, Qiao Y, Yang J, Shu J, Zhang J, et al. Salivary glycopatterns as potential biomarkers for screening of early-stage breast cancer. *EBioMed.* (2018) 28:70–9. doi: 10.1016/j.ebiom.2018.01.026
6. Hall SC, Hassis ME, Williams KE, Albertolle ME, Prakobphol A, Dykstra AB, et al. Alterations in the salivary proteome and N-glycome of Sjögren's syndrome patients. *J Proteome Res.* (2017) 16:1693–705. doi: 10.1021/acs.jproteome.6b01051
7. Dekkers G, Treffers L, Plomp R, Bentlage AEH, de Boer M, Koeleman CAM, et al. Decoding the human immunoglobulin G-glycan repertoire reveals a spectrum of Fc-receptor- and complement-mediated-effector activities. *Front Immunol.* (2017) 8:877. doi: 10.3389/fimmu.2017.00877
8. Albrecht S, Unwin L, Muniyappa M, Rudd PM. Glycosylation as a marker for inflammatory arthritis. *Cancer Biomark* (2014) 14:17–28. doi: 10.3233/CBM-130373
9. Xue J, Zhu LP, Wei Q. IgG-Fc N-glycosylation at Asn297 and IgA O-glycosylation in the hinge region in health and disease. *Glycoconjugate J.* (2013) 30:735–45. doi: 10.1007/s10719-013-9481-y
10. Akmacic IT, Ventham NT, Theodoratou E, Vuckovic F, Kennedy NA, Kristic J, et al. Inflammatory bowel disease associates with proinflammatory potential of the immunoglobulin G glycome. *Inflammatory Bowel Dis.* (2015) 21:1237–47. doi: 10.1097/MIB.0000000000000372
11. Rochereau N, Drocourt D, Perouzel E, Pavot V, Redelinghuys P, Brown GD, et al. Dectin-1 is essential for reverse transcytosis of glycosylated SIgA-antigen complexes by intestinal M cells. *PLoS Biol.* (2013) 11:e1001658. doi: 10.1371/journal.pbio.1001658
12. Novak J, Julian BA, Mestecky J, Renfrow MB. Glycosylation of IgA1 and pathogenesis of IgA nephropathy. *Semin Immunopathol.* (2012) 34:365–82. doi: 10.1007/s00281-012-0306-z
13. Mattu TS, Pleass RJ, Willis AC, Kilian M, Wormald MR, Lellouch AC, et al. The glycosylation and structure of human serum IgA1, Fab, and Fc regions and the role of N-glycosylation on Fcalpha receptor interactions. *J Biol Chem.* (1998) 273:2260–72. doi: 10.1074/jbc.273.4.2260
14. Wuhrer M, Selman MH, McDonnell LA, Kumpfel T, Derfuss T, Khademi M, et al. Pro-inflammatory pattern of IgG1 Fc glycosylation in multiple sclerosis cerebrospinal fluid. *J Neuroinflam.* (2015) 12:235. doi: 10.1186/s12974-015-0450-1
15. Scherer HU, van der Woude D, Ioan-Facsinay A, el Bannoudi H, Trouw LA, Wang J, et al. Glycan profiling of anti-citrullinated protein antibodies isolated from human serum and synovial fluid. *Arthritis Rheumat.* (2010) 62:1620–9. doi: 10.1002/art.27414
16. Huang J, Guerrero A, Parker E, Strum JS, Smilowitz JT, German JB, et al. Site-specific glycosylation of secretory immunoglobulin A from human colostrum. *J Proteome Res.* (2015) 14:1335–49. doi: 10.1021/pr500826q
17. Deshpande N, Jensen PH, Packer NH, Kolarich D. GlycoSpectrumScan: fishing glycopeptides from MS spectra of protease digests of human colostrum sIgA. *J Proteome Res.* (2010) 9:1063–75. doi: 10.1021/pr900956x
18. Stefanovic G, Markovic D, Ilic V, Brajovic G, Petrovic S, Milosevic-Jovcic N. Hypogalactosylation of salivary and gingival fluid immunoglobulin G in patients with advanced periodontitis. *J Periodontol.* (2006) 77:1887–93. doi: 10.1902/jop.2006.060049
19. Carpenter GH, Proctor GB, Shori DK. O-glycosylation of salivary IgA as determined by lectin analysis. *Biochem Soc Transact.* (1997) 25:S659. doi: 10.1042/bst025s659
20. Brandtzaeg P. Secretory immunity with special reference to the oral cavity. *J Oral Microbiol.* (2013) 5:20401. doi: 10.3402/jom.v5i0.20401
21. Mortimer PP, Parry JV. The use of saliva for viral diagnosis and screening. *Epidemiol Infect.* (1988) 101:197–201. doi: 10.1017/S0950268800054108
22. Horton RE, Vidarsson G. Antibodies and their receptors: different potential roles in mucosal defense. *Front Immunol.* (2013) 4:200. doi: 10.3389/fimmu.2013.00200
23. Brandtzaeg P. Presence of J chain in human immunocytes containing various immunoglobulin classes. *Nature* (1974) 252:418–20. doi: 10.1038/252418a0
24. Arnold JN, Wormald MR, Sim RB, Rudd PM, Dwek RA. The impact of glycosylation on the biological function and structure of human immunoglobulins. *Ann Rev Immunol.* (2007) 25:21–50. doi: 10.1146/annurev.immunol.25.022106.141702
25. The UniProt Consortium. UniProt: the universal protein knowledgebase. *Nucleic Acids Res.* (2017) 45:D158–69. Available online at: https://www.uniprot.org/

26. Delacroix DL, Dive C, Rambaud A, Vaerman JP. IgA subclasses in various secretions and in serum. *Immunology* (1982) 47:383–5.
27. Stavenhagen K, Plomp R, Wuhrer M. Site-Specific Protein N- and O-Glycosylation Analysis by a C18-porous graphitized carbon-liquid chromatography-electrospray ionization mass spectrometry approach using pronase treated glycopeptides. *Anal Chem.* (2015) 87:11691–9. doi: 10.1021/acs.analchem.5b02366
28. Zauner G, Selman MH, Bondt A, Rombouts Y, Blank D, Deelder AM, et al. Glycoproteomic analysis of antibodies. *Mol Cell Proteomics* (2013) 12:856–65. doi: 10.1074/mcp.R112.026005
29. Jansen BC, Falck D, de Haan N, Hipgrave Ederveen AL, Razdorov G, Lauc G, et al. LaCyTools: a targeted liquid chromatography-mass spectrometry data processing package for relative quantitation of glycopeptides. *J Proteome Res.* (2016) 15:2198–210. doi: 10.1021/acs.jproteome.6b00171
30. Plomp R, Bondt A, de Haan N, Rombouts Y, Wuhrer M. Recent advances in clinical glycoproteomics of immunoglobulins (Igs). *Mol Cell Proteomics* (2016) 15:2217–28. doi: 10.1074/mcp.O116.058503
31. Ruhaak LR, Xu G, Li Q, Goonatilleke E, Lebrilla CB. Mass spectrometry approaches to glycomic and glycoproteomic analyses. *Chem Rev.* (2018). 118:7886–930. doi: 10.1021/acs.chemrev.7b00732
32. Alocci D, Ghraichy M, Barletta E, Gastaldello A, Mariethoz J, Lisacek F. Understanding the glycome: an interactive view of glycosylation from glycocompositions to glycoepitopes. *Glycobiology* (2018). 28:349–62. doi: 10.1093/glycob/cwy019
33. Bondt A, Rombouts Y, Selman MH, Hensbergen PJ, Reiding KR, Hazes JM, et al. Immunoglobulin G (IgG) Fab glycosylation analysis using a new mass spectrometric high-throughput profiling method reveals pregnancy-associated changes. *Mol Cell Proteomics* (2014) 13:3029–39. doi: 10.1074/mcp.M114.039537
34. Selman MH, Derks RJ, Bondt A, Palmblad M, Schoenmaker B, Koeleman CA, et al. Fc specific IgG glycosylation profiling by robust nano-reverse phase HPLC-MS using a sheath-flow ESI sprayer interface. *J Proteomics* (2012) 75:1318–29. doi: 10.1016/j.jprot.2011.11.003
35. Bondt A, Nicolardi S, Jansen BC, Stavenhagen K, Blank D, Kammeijer GS, et al. Longitudinal monitoring of immunoglobulin A glycosylation during pregnancy by simultaneous MALDI-FTICR-MS analysis of N- and O-glycopeptides. *Sci Rep.* (2016) 6:27955. doi: 10.1038/srep 27955
36. Pucic M, Knezevic A, Vidic J, Adamczyk B, Novokmet M, Polasek O, et al. High throughput isolation and glycosylation analysis of IgG-variability and heritability of the IgG glycome in three isolated human populations. *Mol Cell Proteomics* (2011) 10:M111.010090. doi: 10.1074/mcp.M111. 010090
37. Gomes MM, Wall SB, Takahashi K, Novak J, Renfrow MB, Herr AB. Analysis of IgA1 N-glycosylation and its contribution to FcalphaRI binding. *Biochemistry* (2008) 47:11285–99. doi: 10.1021/bi8 01185b
38. Tarelli E, Smith AC, Hendry BM, Challacombe SJ, Pouria S. Human serum IgA1 is substituted with up to six O-glycans as shown by matrix assisted laser desorption ionisation time-of-flight mass spectrometry. *Carbohydrate Res.* (2004) 339:2329–35. doi: 10.1016/j.carres.2004.07.011
39. Hinneburg H, Stavenhagen K, Schweiger-Hufnagel U, Pengelley S, Jabs W, Seeberger PH, et al. The art of destruction: optimizing collision energies in Quadrupole-Time of Flight (Q-TOF) instruments for glycopeptide-based glycoproteomics. *J Am Soc Mass Spectr.* (2016) 27:507–19. doi: 10.1007/s13361-015-1308-6
40. Flynn GC, Chen X, Liu YD, Shah B, Zhang Z. Naturally occurring glycan forms of human immunoglobulins G1 and G2. *Mol Immunol.* (2010) 47:2074–82. doi: 10.1016/j.molimm.2010.04.006
41. R Core Team. *R: A Language and Environment for Statistical Computing*. Vienna: R Foundation for Statistical Computing (2013).
42. Flanagan JG, Lefranc MP, Rabbitts TH. Mechanisms of divergence and convergence of the human immunoglobulin alpha 1 and alpha 2 constant region gene sequences. *Cell* (1984) 36:681–8.
43. Torano A, Putnam FW. Complete amino acid sequence of the alpha 2 heavy chain of a human IgA2 immunoglobulin of the A2m (2) allotype. *Proc Natl Acad Sci USA.* (1978) 75:966–9. doi: 10.1073/pnas. 75.2.966
44. Tsuzukida Y, Wang CC, Putnam FW. Structure of the A2m(1) allotype of human IgA–a recombinant molecule. *Proc Natl Acad Sci USA.* (1979) 76:1104–8. doi: 10.1073/pnas.76.3.1104
45. Van Loghem E, Wang AC, Shuster J. A new genetic marker of human immunoglobulins determined by an allele at the 2 locus. *Vox Sanguinis* (1973) 24:481–8. doi: 10.1159/000465677
46. Picariello G, Ferranti P, Mamone G, Roepstorff P, Addeo F. Identification of N-linked glycoproteins in human milk by hydrophilic interaction liquid chromatography and mass spectrometry. *Proteomics* (2008) 8:3833–47. doi: 10.1002/pmic.200701057
47. Klapoetke SC, Zhang J, Becht S. Glycosylation characterization of Human IgA1 with differential deglycosylation by UPLC-ESI TOF MS. *J Pharmaceut Biomed Analysis* (2011) 56:513–20. doi: 10.1016/j.jpba.2011.06.010
48. Lauc G, Huffman JE, Pucic M, Zgaga L, Adamczyk B, Muzinic A, et al. Loci associated with N-glycosylation of human immunoglobulin G show pleiotropy with autoimmune diseases and haematological cancers. *PLoS Genet.* (2013) 9:e1003225. doi: 10.1371/journal.pgen.1003225
49. Kristic J, Vuckovic F, Menni C, Klaric L, Keser T, Beceheli I, et al. Glycans are a novel biomarker of chronological and biological ages. *J Gerontol Ser A Biol Sci Med Sci.* (2014) 69:779–89. doi: 10.1093/gerona/glt190
50. Bondt A, Nicolardi S, Jansen BC, Kuijper TM, Hazes JMW, van der Burgt YEM, et al. IgA N- and O-glycosylation profiling reveals no association with the pregnancy-related improvement in rheumatoid arthritis. *Arthritis Research Ther.* (2017) 19:160. doi: 10.1186/s13075-017-1367-0
51. Plomp R, Ruhaak LR, Uh HW, Reiding KR, Selman M, Houwing-Duistermaat JJ, et al. Subclass-specific IgG glycosylation is associated with markers of inflammation and metabolic health. *Sci Rep.* (2017) 7:12325. doi: 10.1038/s41598-017-12495-0
52. Maverakis E, Kim K, Shimoda M, Gershwin ME, Patel F, Wilken R, et al. Glycans in the immune system and The Altered Glycan theory of autoimmunity: a critical review. *J Autoimmunity* (2015) 57:1–13. doi: 10.1016/j.jaut.2014.12.002
53. Quast I, Keller CW, Maurer MA, Giddens JP, Tackenberg B, Wang LX, et al. Sialylation of IgG Fc domain impairs complement-dependent cytotoxicity. *J Clin Investig.* (2015) 125:4160–70. doi: 10.1172/JCI82695
54. Luton F, Hexham MJ, Zhang M, Mostov KE. Identification of a cytoplasmic signal for apical transcytosis. *Traffic* (2009) 10:1128–42. doi: 10.1111/j.1600-0854.2009.00941.x
55. Marsh PD, Do T, Beighton D, Devine DA. Influence of saliva on the oral microbiota. *Periodontol 2000* (2016) 70:80–92. doi: 10.1111/prd.12098
56. Stockert RJ. The asialoglycoprotein receptor: relationships between structure, function, and expression. *Physiol Rev.* (1995) 75:591–609. doi: 10.1152/physrev.1995.75.3.591
57. Falk P, Roth KA, Boren T, Westblom TU, Gordon JI, Normark S. An *in vitro* adherence assay reveals that *Helicobacter pylori* exhibits cell lineage-specific tropism in the human gastric epithelium. *Proc Natl Acad Sci USA.* (1993) 90:2035–9.
58. Schroten H, Stapper C, Plogmann R, Kohler H, Hacker J, Hanisch FG. Fab-independent antiadhesion effects of secretory immunoglobulin A on S-fimbriated *Escherichia coli* are mediated by sialyloligosaccharides. *Infection Immunity* (1998) 66:3971–3.
59. Royle L, Roos A, Harvey DJ, Wormald MR, van Gijlswijk-Janssen D, Redwan el RM, et al. Secretory IgA N- and O-glycans provide a link between the innate and adaptive immune systems. *J Biol Chem.* (2003) 278:20140–53. doi: 10.1074/jbc.M301436200
60. Maurer MA, Meyer L, Bianchi M, Turner HL, Le NPL, Steck M, et al. Glycosylation of human IgA directly inhibits influenza A and other sialic-acid-binding viruses. *Cell Rep.* (2018) 23:90–9. doi: 10.1016/j.celrep.2018.03.027
61. Takahashi K, Raska M, Stuchlova Horynova M, Hall SD, Poulsen K, et al. Enzymatic sialylation of IgA1 O-glycans: implications for studies of IgA nephropathy. *PloS ONE* (2014) 9:e99026. doi: 10.1371/journal.pone.0099026
62. Basset C, Durand V, Mimassi N, Pennec YL, Youinou P, Dueymes M. Enhanced sialyltransferase activity in B lymphocytes from patients with primary Sjogren's syndrome. *Scand J Immunol.* (2000) 51:307–11. doi: 10.1046/j.1365-3083.2000.00692.x
63. Dueymes M, Bendaoud B, Pennec YL, Youinou P. IgA glycosylation abnormalities in the serum of patients with primary Sjogren's syndrome. *Clin Exp Rheumatol.* (1995) 13:247–50.

64. Perrier C, Sprenger N, Corthesy B. Glycans on secretory component participate in innate protection against mucosal pathogens. *J Biol Chem.* (2006) 281:14280–7. doi: 10.1074/jbc.M512958200
65. Phalipon A, Cardona A, Kraehenbuhl JP, Edelman L, Sansonetti PJ, Corthesy B. Secretory component: a new role in secretory IgA-mediated immune exclusion *in vivo*. *Immunity* (2002) 17:107–15. doi: 10.1016/S1074-7613(02)00341-2
66. Vizcaino JA, Csordas A, del-Toro N, Dianes JA, Griss J, Lavidas I, et al. 2016 update of the PRIDE database and its related tools. *Nucleic Acids Res.* (2016) 44:D447–56. doi: 10.1093/nar/gkv1145

Conflict of Interest Statement: The authors declare that the research was conducted in the absence of any commercial or financial relationships that could be construed as a potential conflict of interest.

frontiers in Immunology

ORIGINAL RESEARCH
published: 18 December 2018
doi: 10.3389/fimmu.2018.02963

Mechanism and Prevention of Titanium Particle-Induced Inflammation and Osteolysis

*Michal Eger[1,2], Sahar Hiram-Bab[1], Tamar Liron[1], Nir Sterer[2], Yaron Carmi[3], David Kohavi[2] and Yankel Gabet[1]**

[1] Department of Anatomy and Anthropology, Sackler Faculty of Medicine, Tel Aviv University, Tel Aviv, Israel, [2] Department of Prosthodontics, Goldschleger School of Dental Medicine, Sackler Faculty of Medicine, Tel Aviv University, Tel Aviv, Israel, [3] Department of Pathology, Sackler Faculty of Medicine, Tel Aviv University, Tel Aviv, Israel

The worldwide number of dental implants and orthopedic prostheses is steadily increasing. Orthopedic implant loosening, in the absence of infection, is mostly attributable to the generation of wear debris. Dental peri-implantitis is characterized by a multifactorial etiology and is the main cause of implant failure. It consists of a peri-implant inflammatory lesion that often results in loss of supporting bone. Disease management includes cleaning the surrounding flora by hand instruments, ultrasonic tips, lasers, or chemical agents. We recently published a paper indicating that US scaling of titanium (Ti) implants releases particles that provoke an inflammatory response and osteolysis. Here we show that a strong inflammatory response occurs; however, very few of the titanium particles are phagocytosed by the macrophages. We then measured a dramatic Ti particle-induced stimulation of IL1β, IL6, and TNFα secretion by these macrophages using multiplex immunoassay. The particle-induced expression profile, examined by FACS, also indicated an M1 macrophage polarization. To assess how the secreted cytokines contributed to the paracrine exacerbation of the inflammatory response and to osteoclastogenesis, we treated macrophage/preosteoclast cultures with neutralizing antibodies against IL1β, IL6, or TNFα. We found that anti-TNFα antibodies attenuated the overall expression of both the inflammatory cytokines and osteoclastogenesis. On the other hand, anti-IL1β antibodies affected osteoclastogenesis but not the paracrine expression of inflammatory cytokines, whereas anti-IL6 antibodies did the opposite. We then tested these neutralizing antibodies *in vivo* using our mouse calvarial model of Ti particle-induced osteolysis and microCT analysis. Here, all neutralizing antibodies, administered by intraperitoneal injection, completely abrogated the particle-induced osteolysis. This suggests that blockage of paracrine inflammatory stimulation and osteoclastogenesis are similarly effective in preventing bone resorption induced by Ti particles. Blocking both the inflammation and osteoclastogenesis by anti-TNFα antibodies, incorporated locally into a slow-release membrane, also significantly prevented osteolysis. The osteolytic inflammatory response, fueled by ultrasonic scaling

OPEN ACCESS

Edited by:
Asaf Wilensky,
Hadassah Medical Center, Israel

Reviewed by:
Gustavo Pompermaier Garlet,
University of São Paulo, Brazil
Keith Kirkwood,
University at Buffalo, United States

***Correspondence:**
Yankel Gabet
yankel@tau.ac.il

Specialty section:
This article was submitted to Mucosal Immunity, a section of the journal Frontiers in Immunology

Received: *03 September 2018*
Accepted: *03 December 2018*
Published: *18 December 2018*

Citation:
Eger M, Hiram-Bab S, Liron T, Sterer N, Carmi Y, Kohavi D and Gabet Y (2018) Mechanism and Prevention of Titanium Particle-Induced Inflammation and Osteolysis. Front. Immunol. 9:2963. doi: 10.3389/fimmu.2018.02963

of Ti implants, results from an inflammatory positive feedback loop and osteoclastogenic stimulation. Our findings suggest that blocking IL1β, IL6, and/or TNFα systemically or locally around titanium implants is a promising therapeutic approach for the clinical management of peri-implant bone loss.

Keywords: dental implants, peri-implantitis, macrophages, cytokines, osteoclasts

INTRODUCTION

The prevalence of orthopedic and dental titanium (Ti) implants has increased steadily worldwide. Despite high success rates during the first 10 years (1, 2), orthopedic loosening and oral peri-implantitis remain a major problem for clinicians and constitute a major health problem for the profession. As mentioned, dental peri-implantitis is the main cause of implant failure. The risk of peri-prosthetic complications after 10 years ranges from 20 to 56% (3, 4); however, currently there are no acceptable, standardized protocols for treatment and consequently, recurrence rates remain high (5). Increasing the life expectancy of Ti prostheses is thus a major challenge in orthopedics and oral rehabilitation.

Oral peri-implantitis is believed to have a microbial etiology. However, a strong body of evidence links implant failure to aseptic inflammation around implants due to shedding of debris, Ti ions, and particles (1). Similarly, aseptic loosening of orthopedic implants has been attributed to Ti debris and particles (6). Although Ti prostheses are very biocompatible, these Ti byproducts are far from being bio-inert. Soft tissue biopsies around failing orthopedic (7, 8) and oral (9–11) implants revealed severe inflammatory reactions around aggregates of Ti particles.

We have previously shown that Ti particles released from ultrasonic (US) scaling around dental implants induce a marked inflammatory response in macrophages, with increased expression of pro-inflammatory cytokines, mainly IL1β, IL6, and TNFα. These Ti particles activate osteoclastogenesis *in vitro* and trigger inflammatory bone resorption *in vivo* (12).

Our previous results led us to further investigate the mechanism by which Ti particles entrain bone resorption and to investigate the therapeutic potential of neutralizing antibodies against IL1β, IL6, or TNFα in preventing Ti particle-induced osteolysis.

MATERIALS AND METHODS

All procedures involving animals were carried out in accordance with the guidelines of Tel Aviv University and were approved by the Institutional Animal Care and Use Committee (permit number M-015–047).

Cell Culture

Primary bone marrow-derived macrophages (BMDMs) were isolated from the femora and tibiae of adult C57BL/6J mice (Envigo, Israel), as previously described (13). Briefly, cells were cultured overnight in 6-well dishes at 37°C in a humidified atmosphere with 5% CO_2 in our "standard medium" consisting of alpha-modified Eagle's medium (αMEM, Life Science Technology, NY, USA) and 10% fetal bovine serum (FBS, Rhenium, Ltd, Modi'in, Israel). After 24 h, the non-adherent fraction was cultured in 10-cm non-culture-treated dishes containing standard medium and 100 ng/ml macrophage colony stimulating factor (M-CSF), prepared as previously described (14). The resulting adherent BMDMs were collected after 3 days for the specific assays described below.

Particle Generation

To obtain Ti particles that correspond to the particles shedding from oral implants during routine scaling, we subjected Ti discs that were made from Ti6Al4V (AlphaBio Tec., Petah-Tikva, Israel) to ultrasonic scaling (Newtron Led, Satelec, Acteon, Marignac, France), adjusted to a frequency of 32 kHz. Particles were obtained from discs with a machined (M), sand-blasted and acid-etched (SLA) or sand-blasted (SB) surface topography as described previously (12). When not specified, SLA-derived particles were used. All particles were generated in a sterile environment. Each disc was subjected to US scaling for 60 s in distilled water (ddH2O), then cleaned twice with ethanol, and finally resuspended in distilled water. We previously showed that each 6 mm diameter disc generates ∼2.54 million particles on average. In all our *in vitro* assays and for the preparation of the fibrinogen-thrombin membranes (see below) we used a particle density of 1,293 particles/mm^2.

Environmental Scanning Electron Microscopy (E-SEM)

To examine the cellular response of macrophages to Ti particles, BMDM were seeded on glass slides in a 10-cm plate (10^6 cells per well) and cultured for 24 h in the presence of Ti particles released by the US scaling of SLA-treated discs. Cultures were then visualized by E-SEM. Each field was taken either in backscattered electrons mode (BSE) or secondary electrons (SE) mode to distinguish between extracellular vs. total Ti particles in the culture, respectively.

Protein and Nitric Oxide (NO) Measurements in Conditioned Medium, RNA Isolation, and RT-qPCR

Following a 24–48 h incubation with Ti particles (or LPS or vehicle only), the supernatant was collected and referred to as conditioned medium (CM). Secreted protein amounts of pro- and anti-inflammatory cytokines in CM were measured using a multiplex assay and expressed in MFI units (Multiplex Fluorescent Immunoassay, ProcartaPlex Multiplex Immunoassay, eBioscience, San Diego, CA, USA). NO content was measured using the Griess Reagent System kit (Promega, Madison, WI, USA). After collecting the supernatant, macrophages were washed with sterile PBS, and

RNA was extracted using Tri-RNA Reagent (Favorgen Biotech Corp, Kaohsiung, Taiwan). The 260/280 absorbance ratio was measured to verify the RNA purity and concentration. cDNA was produced using a high-capacity cDNA reverse transcription kit (Invitrogen, Grand Island, NY, USA), and real-time PCR was performed using Kapa SYBR Fast qPCR (Kapa Biosystems, Wilmington, MA, USA) on a StepOne real-time PCR machine (Applied Biosystems, Grand Island, NY, USA). We examined the expression of IL1β, IL6, and TNFα, which are established markers of macrophage inflammation. The primer sets were as follows: F-GAA ATG CCA CCT TTT GAC AGTG and R-TGG ATG CTC TCA TCA GGA CAG for mouse IL1β; F-TAG TCC TTC CTA CCC CAA TTT CC and R-TTG GTC CTT AGC CAC TCC TTC for mouse IL6; and F-TCT TCT CAT TCC TGC TTG TGG and R-GGT CTG GGC CAT AGA ACT GA for mouse TNFα. The reaction was subjected to 40 cycles of amplification using the following program: 95°C for 20 s, 60°C for 20 s, and 72°C for 25 s. The relative mRNA expression levels of the selected genes were normalized to the level of GPDH, which was amplified using the following primers: F-ACC CAG AAG ACT GTG GATG G and R-CAC ATT GGG GGTA GG AACAC.

Osteoclastogenesis Assay

Preosteoclasts, prepared like the BMDMs, were plated in 96-well plates (7,000 cells per well) in standard medium supplemented with 20 ng/ml M-CSF and 50 ng/ml Receptor Activator of Nuclear Factor Kappa-B Ligand (RANKL) (R&D Systems, Minneapolis, MN, USA). On the 3rd day (after 48 h), the medium was replaced by the CM of BMDM, supplemented with RANKL and M-CSF. Where indicated, we also added 2 μg/ml of neutralizing antibodies (Ab) against IL1β (Kineret, anakinra, SOBI, Stockholm, Sweden), IL6-receptor (Actemra, tocilizumab, Roche, San Francisco, CA, USA), or TNFα (Humira, adalimumab, AbbVie Inc., Chicago, IL, USA). These neutralizing Ab, effective in both humans and mice (15–19), are referred to as anti-IL1β, IL6, and TNFα Ab, respectively. On the 4th day, cells were stained using a TRAP kit (Sigma-Aldrich, St. Louis, MO, USA), and multinucleated (>3 nuclei) TRAP-positive cells were defined as osteoclasts. Images were acquired at an original magnification of ×4 (Evos FLC, Life Technologies, MS, USA). The number of osteoclasts and the total osteoclast area were measured using ImageJ software (National Institutes of Health, Bethesda, MD, USA).

Animal Model and Micro-Computed Tomography (μCT)

We used our calvarial model, which was described before (12). Briefly, US-released Ti particles (from M/SLA/SB-treated discs) were incorporated into a fibrinogen-thrombin degradable membrane used as a scaffold to localize the Ti particles. Membranes with no particles or only LPS were prepared as positive and negative controls. As indicated, neutralizing antibodies against TNFα (or saline as control) were incorporated into the membrane together with the Ti particles.

After anesthesia, the skin of 10-week-old C57Bl/6J female mice was shaved and disinfected. The parietal bones of the mice were exposed via a 10-mm incision in the nape area, and the periosteum was removed using a periosteal elevator. The fibrinogen-thrombin membranes were inserted to cover both parietal bones. The surgical incision was then closed using nylon monofilament surgical sutures (5/0). In the sham controls, no membranes were inserted and the incisions were closed. Another control group consisted of inserting an empty fibrinogen-thrombin membrane (with no Ti particles).

To test the therapeutic potential of systemic administration of neutralizing antibodies, we injected antibodies against IL1β, IL6, or TNFα (or saline as control) intraperitoneally 1 day before and once a week (2 mg/kg IL6 and 10 mg/kg TNFα) or daily (10 mg/kg IL1β) after membrane insertion, in accordance with the established clinical procedures (20–23).

All groups comprised a minimum of 6 animals. Animals were euthanized at the indicated post-operative time, and the skull of each mouse was removed, fixed for 24 h in 4% phosphate-buffered formalin, followed by 70% ethanol. All specimens were scanned and analyzed using a μCT system (μCT 50, Scanco Medical AG, Switzerland). Scans were performed at a 10-μm resolution in all three spatial dimensions, with 90 kV energy, 88 μA intensity, and 1,000 projections at a 1,000 m s integration time. The region of interest (ROI) was defined as two 3.7-mm circles in the center of the parietal bones. A custom-made algorithm, based on Image-Processing Language (IPL, Scanco Medical), was developed to isolate the resorption pits, defined as unmineralized pits that were 10 to 40-μm deep on the bone surface (12). Morphometric parameters were determined at the 3D level and included the total volume of bone pits (Pit Resorption Volume, PRV, mm^3) and the bone tissue volume inside ROI (TV, mm^3), which was used to determine the PRV/TV (%).

FACS Analyses

Using our calvarial model, we also determined the effect of Ti particles on macrophage polarization, *in vivo*. The mice received either control membranes (fibrinogen-thrombin only) or membranes including LPS/Ti particles. Mice were euthanized 3 weeks post-op. This time point was chosen to be after the acute inflammatory response induced by the surgery but before the potential resolution of the inflammatory response to the Ti particles. The soft tissue covering the parietal bones was collected and processed using collagenase. Cells were labeled using specific markers (CD11b, Ly6-C, Ly6-G, F4/80, and MHC-II). This panel was used to define macrophages and to differentiate between M1 (CD11b+, Ly6C+, Ly6G+, F4/80+, MHC-II+) and M2 (CD11b+, Ly6C-, Ly6G+, F4/80+, and MHC-II+) polarization (24, 25). Cells were fixed with 1% paraformaldehyde and analyzed on a Gallios flow cytometer (Beckman Coulter, Brea, CA, USA).

RESULTS

Environmental Scanning Electron Microscopy (E-SEM)

To determine whether particles are internalized by the cells, a culture of BMDM and Ti particles was examined by E-SEM (**Figure 1**). Each field was taken either in BSE or SE mode. BSE provides a topographic view of the upper-most layer, which means that the Ti particles seen in this mode

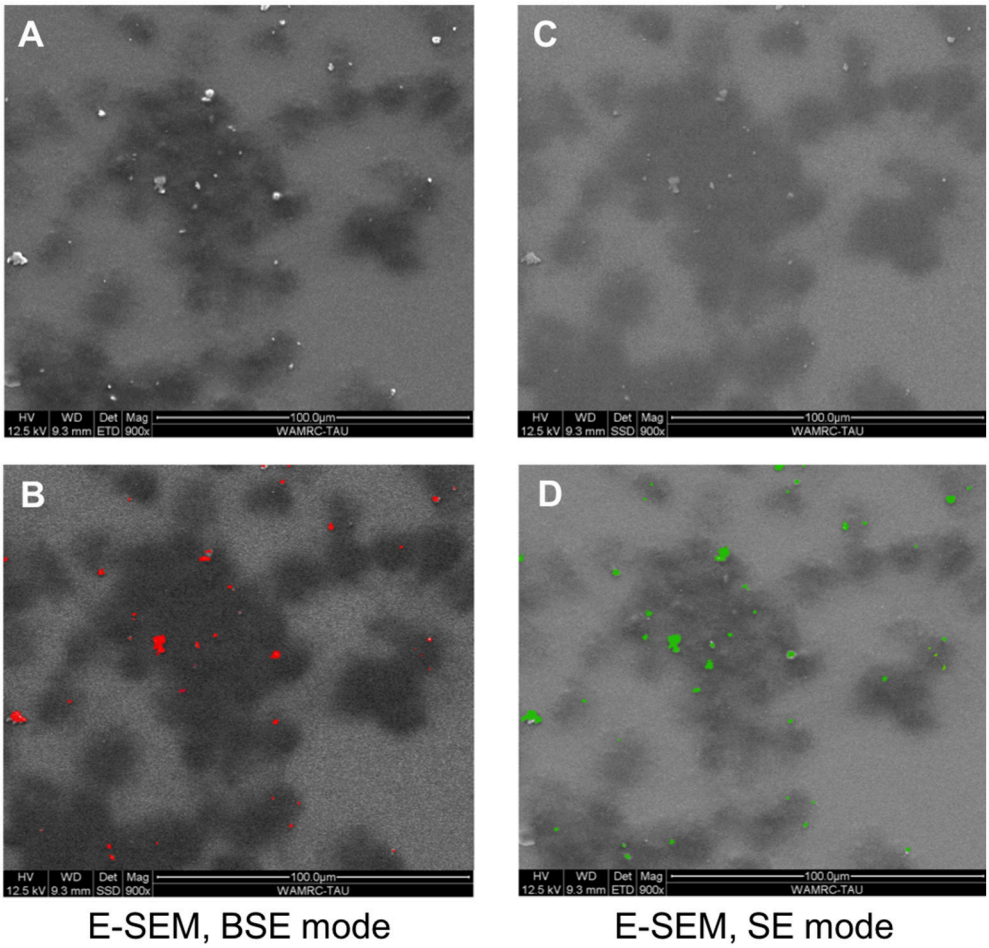

FIGURE 1 | BMDM in the presence of Ti particles, visualized using E-SEM. BMDM were cultured for 24 h in the presence of SLA-derived Ti particles. Each field was taken either in backscattered electrons (BSE) mode or secondary electrons (SE) mode. Dark patches represent macrophages; light-bright dots **(A,C)** are Ti particles. **(B,D)** Color representation of the Ti particles (red in BSE mode, green in SE mode). Note that most particles are outside the cells, as indicated by the similarity between the BSE and SE modes.

were not internalized by the cells but rather, were laid on top of the cell membrane (**Figures 1A,B**). The SE mode is a deep penetrating mode, able to detect all metals in the sample, within or outside the cells (**Figures 1C,D**). Based on the similarity between the two scanning modes (the total number of Ti particles and particles in the upper-most layer), it can be concluded that BMDM failed to internalize most of the US-released Ti particles.

Effect of Ti Particles on Macrophage Polarization

The effect of Ti particles on macrophage polarization was examined *in vivo,* using a mouse calvarial model (12). Either Ti particles (from M/SLA/SB-treated discs) or LPS was incorporated into a fibrinogen-thrombin degradable membrane. Mice were euthanized 3 weeks post-op to examine the macrophages inside the soft tissue covering the parietal bones. Our FACS analysis first gated a CD11b+/F480+/MHC-II+ monocyte/macrophage population, which was further divided into Ly6G-/Ly6C- (Gr1-) non-inflammatory monocytes/macrophages (26), Ly6G+/Ly6C+ M1 and Ly6G+/Ly6C- M2 macrophages (24, 25). Our results show no appreciable difference in the M2 population in either group (**Figure 2**). However, the M1 population was significantly higher in animals exposed to either machined or SLA surface-derived Ti particles. Surprisingly, milder differences were recorded for the SB particles. LPS alone also did not cause an appreciable increase in the M1 macrophage population (**Figure 2**). It is reasonable to assume that the fibrinogen membrane by itself caused some inflammatory changes that masked the differences between LPS and the empty membrane (control).

Cytokine Secretion Profile of Macrophages Exposed to Ti Particles

To further reveal the mechanism underlying the particle-induced inflammatory response, the proteomic profile of

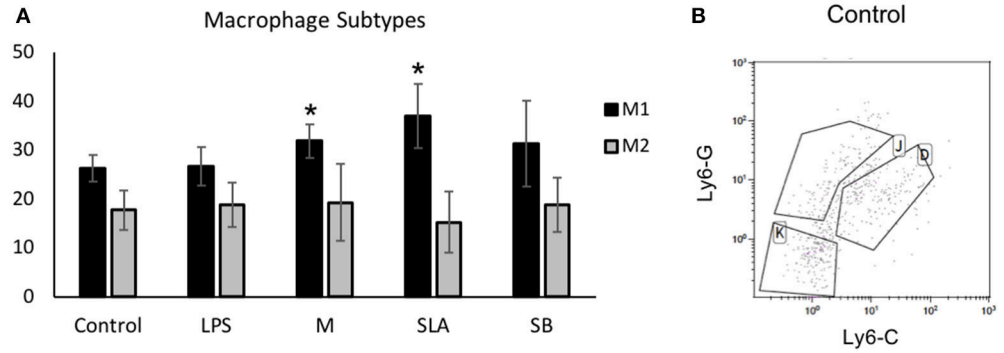

FIGURE 2 | Ti particles induce macrophage polarization *in vivo*: Control fibrin membranes or membranes with either LPS or Ti particles were implanted onto mice calvaria ($n = 5$). Ti particles were obtained from machine (M), SLA or sand-blasted (SB) discs. Mice were euthanized after 3 weeks for soft tissue FACS analysis of macrophage polarization, using specific markers. Results show **(A)** the percentage of gated cells in the macrophages' sub-types, presented as mean ± SD; $^*p < 0.05$ vs. control, 1-way ANOVA. **(B)** Representative FACS plot (K: monocytes, J: M2 and D: M1 macrophages).

macrophages exposed to Ti particles was assessed using the multiplex cytokine kit, after 24 h exposure to either LPS or SLA-derived particles. For most cytokines, the presence of Ti particles induced a 2- to 10-fold elevation in the proinflammatory cytokine levels (**Figure 3**). A modest (∼2-fold) elevation in the anti-inflammatory IL1α and IL10 levels was also found, as well as in IFNγ. With respect to IL1β, IL6, and TNFα, our multiplex analysis showed a marked increase in their levels in the supernatant of macrophages cultured with Ti particles, in line with our previously published RT-qPCR analysis (12). Overall, this cytokine profile is characteristic of an M1 polarization, supporting our findings *in vivo* (**Figure 2**). We also observed a significant increase in NO secretion, which is a hallmark of M1 macrophage polarization (27).

Anti-inflammatory and Anti-osteoclastogenic Effects of Neutralizing Antibodies in BMDM and Preosteoclast Cultures

The concomitant increase in all inflammatory cytokines (**Figure 3**) raised a question regarding a positive paracrine feedback loop that fuels the inflammatory response of the macrophages. To determine whether blocking the paracrine effect of the cytokines secreted in response to Ti particles attenuates the overall inflammatory response of the macrophages, BMDM were cultured in the presence of Ti particles and treated with neutralizing antibodies for IL1β, IL6, or TNFα. Cells were collected after 24 h and changes in the levels of pro-inflammatory cytokines were measured using RT-qPCR. The secretion of IL1β was not affected by either of the neutralizing antibodies in the culture (**Figure 4**). On the other hand, IL6 expression in macrophages reduced significantly in the presence of each of the neutralizing antibodies. In contrast, TNFα expression in the culture was only affected by anti-TNFα antibodies. These findings suggest that the overall inflammatory response to Ti particles not only results from direct contacts between macrophages and Ti particles, but also results from positive feedback induced by paracrine signals.

Next, we tested the potential antagonizing effect of the same neutralizing antibodies on the osteoclastogenic signals emitted by macrophages in the presence of Ti particles. To this end, preosteoclasts cultured under osteoclastogenic conditions for 48 h were supplemented with the CM of BMDM cultured with or without Ti particles. Concomitantly, neutralizing antibodies against IL1β, IL6, or TNFα were added as indicated (**Figure 5**). Cultures were stopped on the 4th day, and the total area covered by multinucleated (>3 nuclei) TRAP-positive osteoclasts was calculated. Treatment with anti-IL6 antibodies did not affect osteoclastogenesis in our culture of isolated preosteoclasts. However, neutralizing antibodies against either IL1β or TNFα suppressed osteoclastogenesis in the presence of CM from BMDM exposed to Ti particles (**Figure 5**).

Dynamics of Ti Particle-Induced Osteolysis

To account for the dynamics of the inflammatory response, we first established the time course of particle-induced osteolysis in our calvarial model. Ti particles released by the US scaling of SLA-treated discs were incorporated into the inserted membranes. A sham group consisted of mice undergoing the same surgical procedure without membrane insertion, which were euthanized after 4 weeks. Mice carrying a Ti particle-loaded membrane were euthanized every 2 weeks to monitor the extent of calvarial resorption using μCT. The results indicate that a dramatic resorption occurred during the first 5 weeks, along with a recovery from the 6th week onward. Of note, the membrane was totally degraded within 4 to 5 weeks; however, the presence of Ti particles was still detected even after 10 weeks (**Figure 6C**). This suggests that the osteolytic response is self-contained and somewhat recovers within 8 weeks after the last insult of Ti particles. Importantly, despite this recovery, the PR volume after 8 and 10 weeks

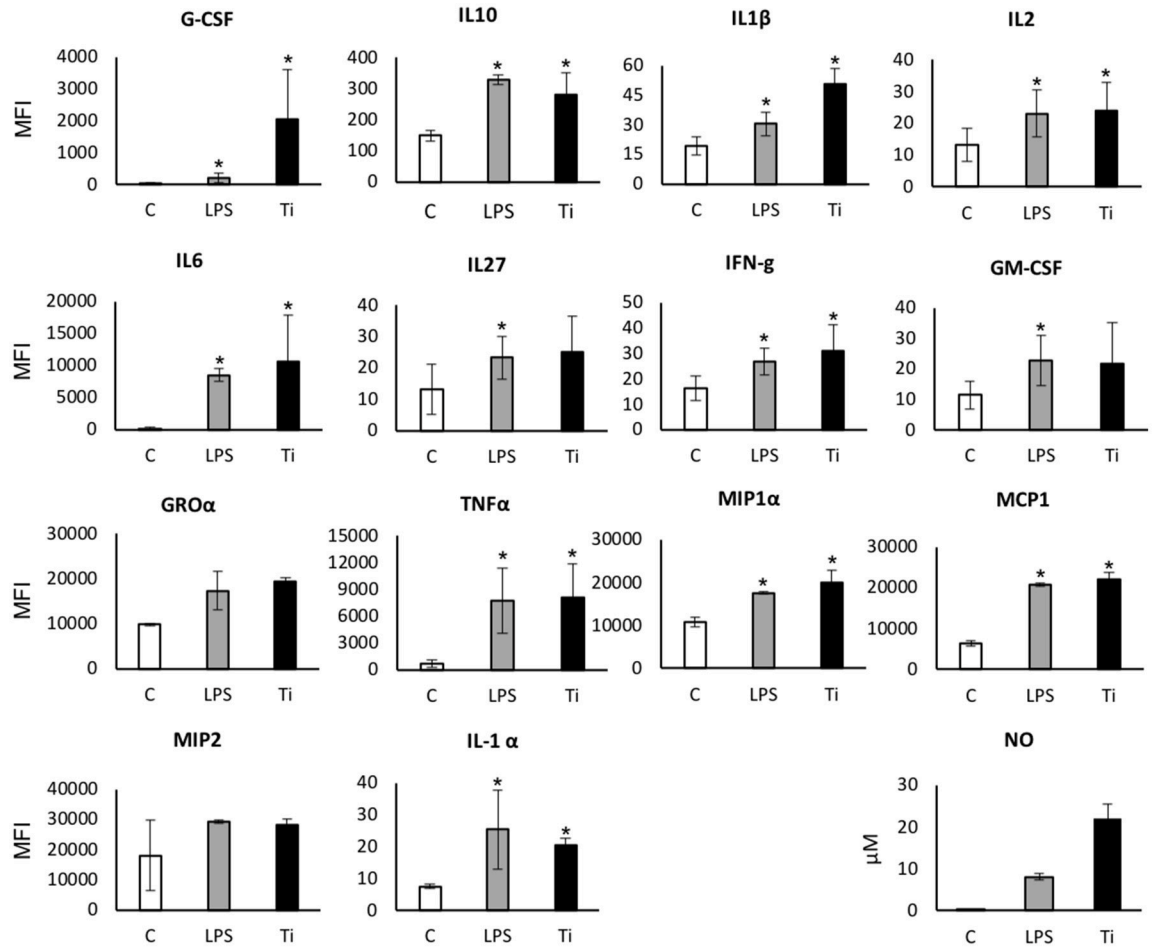

FIGURE 3 | Secreted protein and NO levels in the supernatant of macrophages exposed to LPS/Ti particles. BMDM were cultured in the presence of either LPS or SLA-derived Ti particles. After 24 h, the supernatant was collected and analyzed using multiplex cytokine assay for secreted protein levels, and Griess Reagent System kit for NO. Results are presented as mean Melt Flow Index (MFI) units ±SD, and μM (for NO). $n = 4$. Experiment was repeated once with similar results. *$p < 0.05$ vs. control; non-parametric ANOVA.

remained significantly higher in the Ti than in the sham group.

Based on these results, further treatments were given for 4 weeks. After 4 weeks, the calvariae were collected and processed for μCT.

Therapeutic Potential of Neutralizing Antibodies on Ti Particle-Induced Osteolysis

We repeated the same calvaria model with membranes loaded with SLA-derived Ti-particles. Neutralizing antibodies for IL1β, IL6, or TNFα (or saline as control) were injected intraperitoneally 1 day before, once a week (IL6 and TNFα), or daily (IL1β) after the membrane insertion. As shown in **Figure 7**, each of the 3 neutralizing antibodies had a dramatic, statistically significant effect in preventing particle-induced osteolysis.

Next, we tested the therapeutic potential of topically administered neutralizing antibodies. As a proof-of-concept, we elected to test anti-TNFα neutralizing antibodies incorporated into the membrane together with the Ti particles (**Figure 8**). Importantly, we found that topically-administered neutralizing antibodies significantly suppressed the particle-induced osteolysis (**Figure 8**).

DISCUSSION

In this study, we examined the mechanism by which Ti particles lead to inflammation and bone resorption and tested the therapeutic potential of using specific neutralizing antibodies in preventing particle-induced osteolysis.

Our multiplex analysis revealed an interesting secretion profile of macrophages cultured in the presence of Ti particles. There was a dramatic elevation in the levels of most pro-inflammatory cytokines relative to the modest rise in the anti-inflammatory IL1α and IL10 levels, which may be a compensatory restraining response (28, 29). IFNγ also displayed

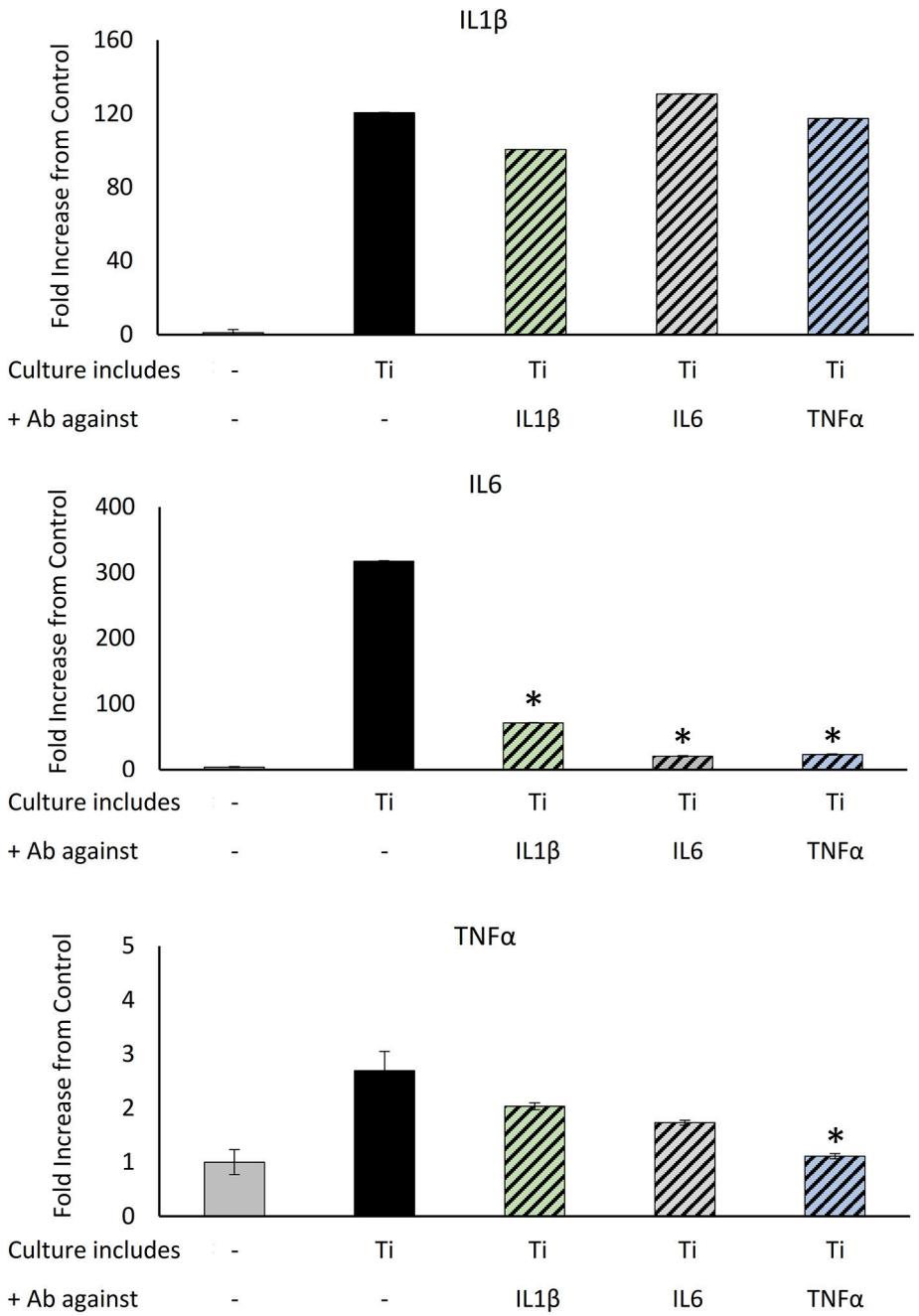

FIGURE 4 | The effect of neutralizing Ab on Ti particle-induced inflammatory response**:** BMDM were cultured for 24 h in the presence of SLA-derived Ti particles released by US with neutralizing Ab for IL1β, IL6, or TNFα. IL1β, IL6, and TNFα expression levels were measured using RT-qPCR, normalized to GAPDH, and expressed as a fold change relative to the control (no particles). Data are shown as the mean ± SD. *$p < 0.05$ vs. Ti, non-parametric ANOVA, $n = 3$.

a significant rise; however, its contribution to the inflammatory response remains unclear, since both pro- and anti-inflammatory actions have been reported for this cytokine (30–32). MIP1α and MCP1 are chemokine proteins (CCL3 and CCL2, respectively). MIP1α is involved in the acute inflammatory state and is responsible for recruitment of polymorphonuclear cells, whereas MCP1 was found in the vicinity of bone resorption sites (33). The latter chemokine may drive osteoclast differentiation in the absence of RANKL (34). With respect to IL1β, IL6, and TNFα, our multiplex analysis revealed a trend very similar to our RT-qPCR analysis reported recently (12), with significantly elevated levels in the supernatant of macrophages cultured with Ti particles. In general, Ti particles induce in macrophages a response similar to that of LPS. The resulting inflammatory

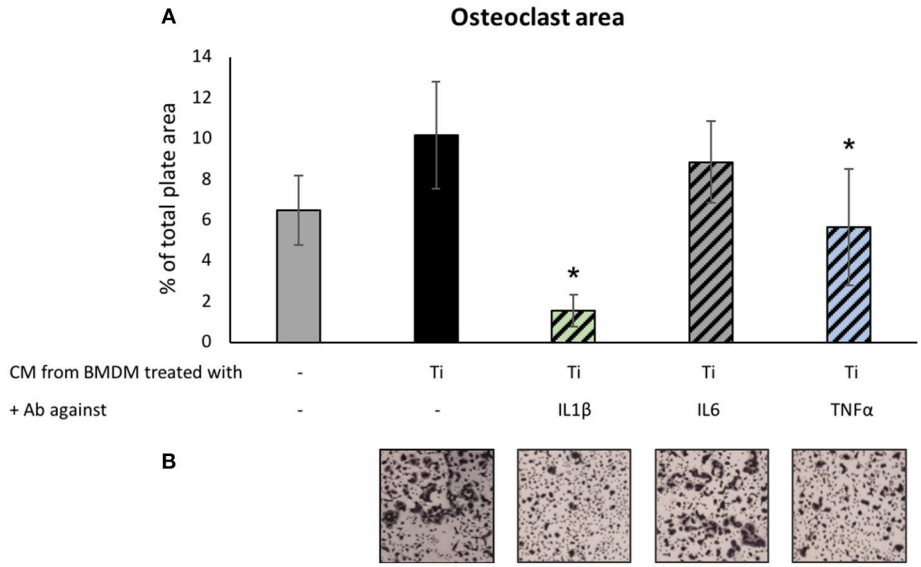

FIGURE 5 | The effect of neutralizing Ab on Ti-particle-induced osteoclastogenesis**:** Preosteoclast cultures under osteoclastogenic conditions for 48 h were supplemented with condition medium (CM, supernatant) of BMDM cultured with or without SLA-derived Ti particles. At the same time, neutralizing antibodies against IL1β, IL6, or TNFα were added as indicated. Cultures were stopped after 36 h. **(A)** Average osteoclast area expressed as mean ± SD, $n = 8$. *$p < 0.05$ vs. Ti, 1-way ANOVA. **(B)** Representative images of TRAP-stained osteoclasts for each condition. Original magnification ×4.

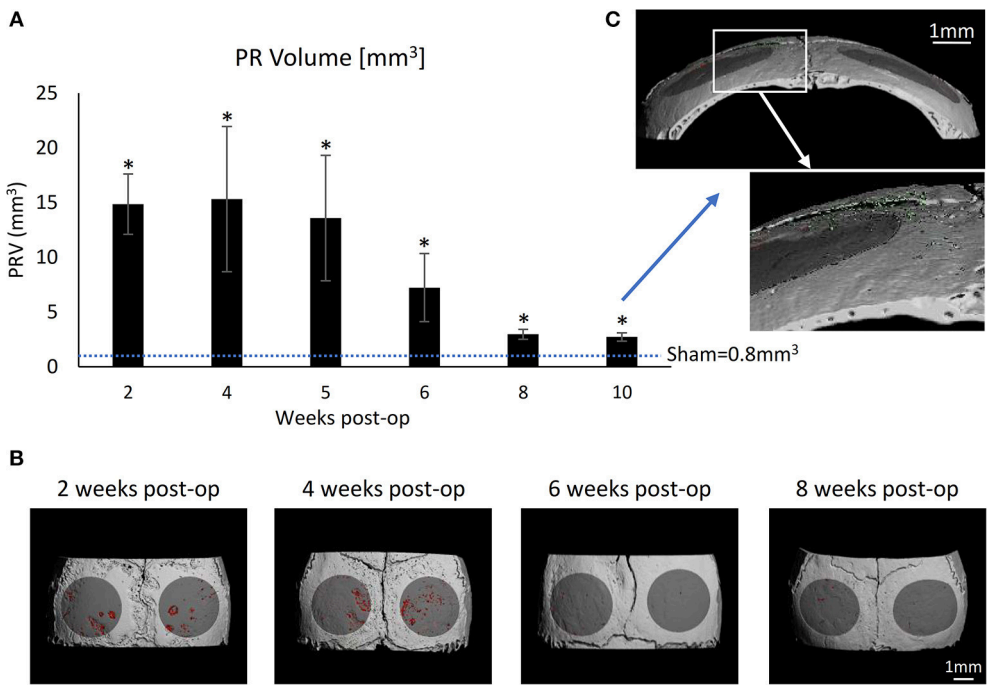

FIGURE 6 | Time-lapse development of particle-induced bone resorption *in vivo***:** Fibrin membranes loaded with SLA-derived Ti particles, were implanted onto mouse calvaria. Mice were euthanized every 2 weeks for μCT analysis to evaluate the dynamic progression of particle-induced osteolysis. **(A)** Pit Resorption Volume (PRV, mm^3); data are expressed as mean ± SD, $n = 5$, *$p < 0.05$ vs. sham (no membrane), non-parametric ANOVA. **(B)** Representative μCT images of the calvaria are shown. The region of interest (ROI) is denoted in dark gray, and the resorption pits are denoted in red. **(C)** High magnification of a sample from the 10-week group indicating the residual Ti particles (green) despite the complete resorption of the membrane.

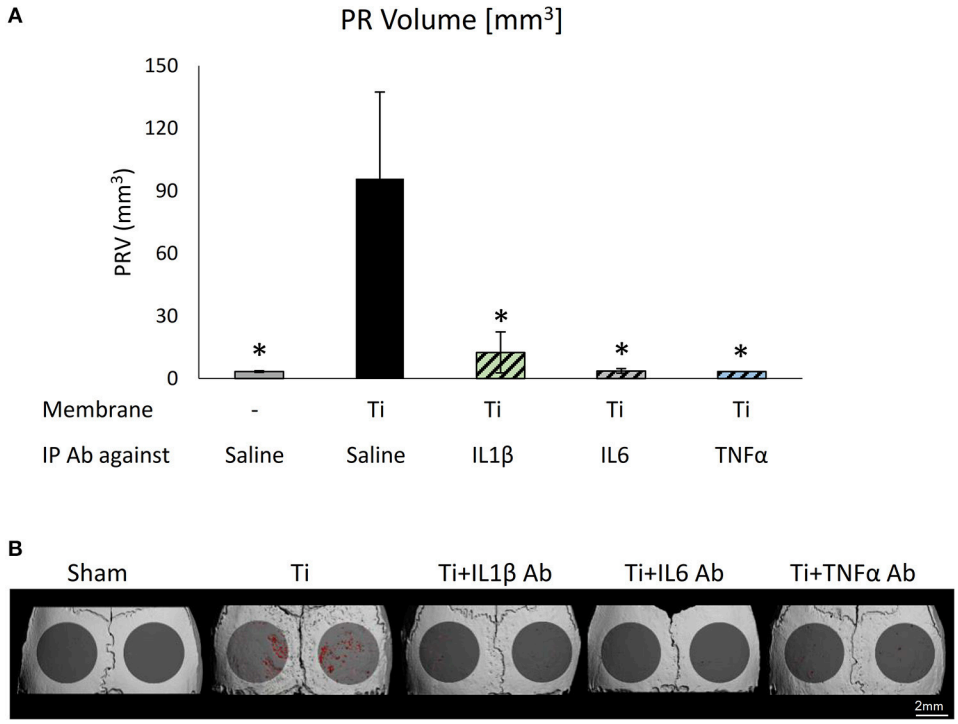

FIGURE 7 | The effect of systemically administering anti-inflammatory neutralizing antibodies on particle-induced osteolysis *in vivo*: Fibrin membranes including SLA-derived Ti particles were implanted onto mouse calvaria. Neutralizing antibodies (Ab) against IL1β, IL6, or TNFα (or saline as control) were injected intraperitoneally (IP) 1 day before, once a week (IL6 and TNFα), or daily (IL1β) after membrane insertion. Mice were euthanized 4 weeks post-op for μCT analysis. **(A)** Pit Resorption Volume (PRV, mm^3), data are expressed as mean ± SD, $n = 6$; $^*p < 0.05$ vs. Ti, 1-way ANOVA. **(B)** Representative μCT images of the calvaria, color-coded as above.

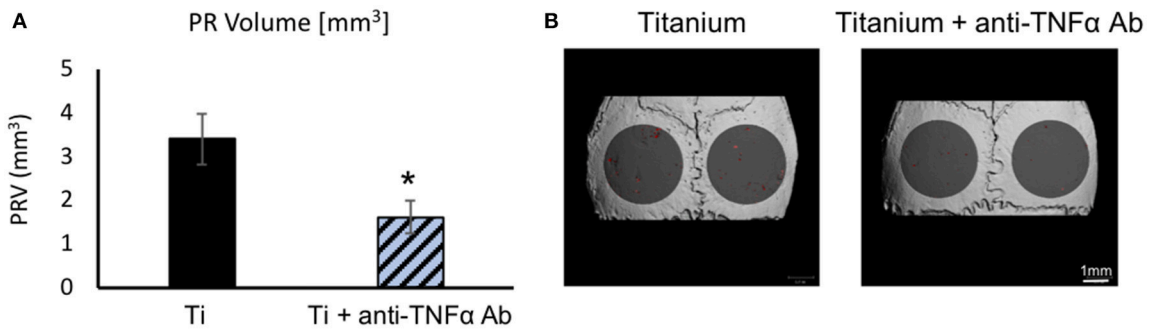

FIGURE 8 | The effect of topically-administered anti-inflammatory neutralizing antibodies on particle-induced osteolysis *in vivo*: Fibrin membranes including Ti particles, together with neutralizing antibodies against TNFα (or saline as control), were implanted onto mouse calvaria. Mice were euthanized 4 weeks post-op for μCT analysis. **(A)** Pit Resorption Volume (PRV, mm^3), data are expressed as mean ± SD, $n = 6$; $^*p = 0.029$ vs. Ti, *t*-test. **(B)** Representative μCT images of the calvaria color-coded as above.

response drives the bone tissue damage mediated by osteoclasts. Together with the FACS, gene expression and secretome profiling on macrophages *in vitro* and *in vivo*, these changes indicate that macrophages undergo an "M1-like" polarization in response to Ti particles. It should be noted however that all our assays were conducted at the early stages of the inflammatory response. The resolving inflammation manifested in the partial tissue repair observed *in vivo* after 6–8 weeks (**Figure 6**), suggests a more dynamic and complex spatio-temporal distribution of M1 and M2 macrophages (27).

Next, we examined how neutralizing antibodies against IL1β, IL6, and TNFα affected Ti particle-induced inflammatory response in macrophages. Importantly, we found that (i) the secretion of IL1β was not affected by either of the neutralizing antibodies, (ii) IL6 expression was significantly decreased by the presence of each of the neutralizing antibodies, and (iii) TNFα expression in culture was only affected by anti-TNFα antibodies. This is in accordance with the notion that both TNFα and IL1β are upstream factors in the inflammatory cascade (35). Indeed, our findings suggest that IL1β expression is independent of the

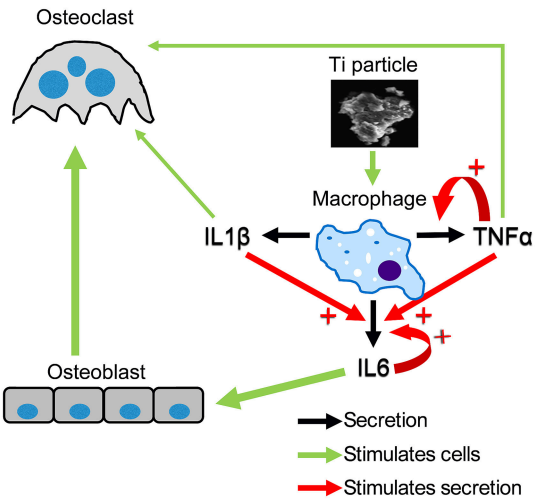

FIGURE 9 | Putative model of the hierarchical roles of IL1β, IL6, and TNFα in particle-induced osteoclastogenesis. This model describes the paracrine and autocrine induction of cytokine secretion by macrophages exposed to SLA-derived Ti particles. The thickness of the green arrows reflects the importance of one pathway over the others.

secretion of IL1β, IL6, and TNFα by neighboring macrophages. In contrast, most IL6 expression by macrophages depends on paracrine signals, including IL1β, IL6, and TNFα. TNFα expression is only partly dependent on these signals, since only blockade of TNFα partly suppressed its own expression. Importantly, we also observed that *in vivo*, blocking any of these 3 cytokines significantly attenuated bone resorption. Based on these observations we propose a model to describe this additive and synergistic interrelationship between these 3 cytokines and the resulting stimulation of osteoclasts, thus inducing bone resorption (**Figure 9**). In this model, blocking IL1β does not affect TNFα expression and vice versa, and blocking IL6 does not affect either IL1β or TNFα expression. Moreover, both IL1β and TNFα directly stimulate osteoclasts while IL6 does so indirectly via the osteoblasts. The latter is suggested by the significant blockade of osteolysis by anti-IL6 antibodies administered *in vivo*, but not *in vitro* in the absence of stromal cells in the cultures. This conclusion is also in line with another study demonstrating that IL6 stimulates osteoclastogenesis via osteoblasts (36). Overall, our model suggests that Ti particles stimulate osteoclastogenesis via 3 pathways, the predominant one being the synergistically increased expression of IL6 by IL1β and TNFα, which in turn stimulates osteoblast-mediated osteoclastogenesis. It is reasonable to assume that both *in vitro* and *in vivo*, not all macrophages are in direct contact with Ti particles. The paracrine effect, depicted here, portrays a chain reaction that could provide the inflammatory signals with an extended range.

We conducted here a time-lapse experiment and evaluated the long-term effects of Ti particles on bone resorption *in vivo* (**Figure 6**). Our data show that the osteolytic response is self-contained and somewhat recovers, although not entirely. After 8 and 10 weeks, the extent of bone residual defects remained significantly higher than in the sham group. Moreover, in clinical settings, a Ti prosthesis is likely to continuously release ions, debris, and particles, thus fueling the inflammatory response, and further aggravating osteolysis.

Previous articles studied different approaches to block the progression of bone resorption. These approaches included promoting apoptosis of osteoclasts, genetic intervention (37, 38) or using bisphosphonates, which caused pathological fractures (39).

In our previous publication, we characterized the size, number, physical and chemical properties of the titanium particles shedding from the surface of rough titanium implant commonly used in contemporary dentistry following ultrasonic scaling (12). Regarding the size, we used an automated cell counter to measure the number and size of the particles shedding from one 6-mm diameter titanium disc with an SLA surface. We found that ultrasonic scaling of each SLA disc generates 2.54 million titanium particles of an average size of 6 to 12 μm. A previous study established that the range of wear debris generated from orthopedic prostheses is between 1 and 30 μm (40). It is thus likely to assume that the cellular and inflammatory responses described in the current study with ultrasonic-generated particles are similar to those observed with wear debris surrounding orthopedic prostheses.

Three main biological strategies were tested to block the chronic inflammatory reaction to orthopedic wear particles, including (i) interference with systemic macrophage trafficking to the local implant site, (ii) modulation of macrophages from an M1 to an M2 phenotype in periprosthetic tissues, and (iii) local inhibition of the transcription factor nuclear factor-kappa B, thereby interfering with the production of pro-inflammatory mediators (38). All three approaches showed promising results in preclinical studies but have not yet been evaluated clinically.

Here we tested three clinically-approved neutralizing antibodies that are prescribed for the management of auto-immune and inflammatory diseases. Anti-IL1β antibodies (Anakinra) are prescribed to rheumatoid arthritis and neonatal-onset multisystem inflammatory disease, anti-IL6 receptor antibodies (Tocilizumab) are administered to treat arthritis and anti-TNFα antibodies (Adalimumab) are effective against rheumatoid arthritis, psoriasis and Crohn's disease (41–43). Our *in vivo* and *in vitro* results showed a clear association between each of these cytokines and the macrophage response to Ti particles. Using our mouse calvarial model, we demonstrated that blocking each of these cytokines prevents Ti particle-induced osteolysis. We further showed that both systemic and local administration are conceptually possible approaches. This preclinical study therefore advocates that neutralizing antibodies be further tested against IL1β, IL6, or TNFα in clinical settings for managing the aseptic loosening of orthopedic prostheses and oral peri-implantitis.

AUTHOR CONTRIBUTIONS

ME, SH-B, TL, NS, YC, DK, and YG: contributed to the design of the research; ME, SH-B, and TL: performed research and contributed to the obtained results; YG and DK: supervised the project; ME and YG: wrote the paper and prepared

it for publication. All authors read and approved the final manuscript.

FUNDING

This work was supported by Israel Science Foundation (ISF) Grants No. 1822/12, 1367/12, and 1086/17 to YG, and a Rothstein-Foundation grant to DK, NS, and YG.

ACKNOWLEDGMENTS

We acknowledge our deepest appreciation to Prof. Sandu Pitaru (Tel Aviv University) for his helpful advices and discussion during this study. This work was carried out in partial fulfillment of the requirements for a Ph.D. degree for ME from the Sackler Faculty of Medicine, Tel Aviv University, Tel Aviv, Israel.

REFERENCES

1. Revell PA. The combined role of wear particles, macrophages and lymphocytes in the loosening of total joint prostheses. *J R Soc Interface* (2008) 5:1263–78. doi: 10.1098/rsif.2008.0142
2. Moraschini V, Poubel LA, Ferreira VF, Barboza Edos S. Evaluation of survival and success rates of dental implants reported in longitudinal studies with a follow-up period of at least 10 years: a systematic review. *Int J Oral Maxillofac Surg*. (2015) 44:377–88. doi: 10.1016/j.ijom.2014.10.023
3. Landgraeber S, Jager M, Jacobs JJ, Hallab NJ. The pathology of orthopedic implant failure is mediated by innate immune system cytokines. *Mediators Inflamm*. (2014) 2014:185150. doi: 10.1155/2014/185150
4. Derks J, Tomasi C. Peri-implant health and disease. A systematic review of current epidemiology. *J Clin Periodontol*. (2015) 42 (Suppl. 16):S158–71. doi: 10.1111/jcpe.12334
5. Esposito M, Grusovin MG, Worthington HV. Interventions for replacing missing teeth: treatment of peri-implantitis. *Cochrane Database Syst Rev*. (2012) 1:CD004970. doi: 10.1002/14651858
6. Fretwurst T, Nelson K, Tarnow DP, Wang HL, Giannobile WV. Is metal particle release associated with peri-implant bone destruction? an emerging concept. *J Dent Res*. (2018) 97:259–65. doi: 10.1177/0022034517740560
7. Scales JT. Black staining around titanium alloy prostheses–an orthopaedic enigma. *J Bone Joint Surg Br*. (1991) 73:534–6.
8. Witt JD, Swann M. Metal wear and tissue response in failed titanium alloy total hip replacements. *J Bone Joint Surg Br*. (1991) 73:559–63.
9. Schlegel KA, Eppeneder S, Wiltfang J. Soft tissue findings above submerged titanium implants–a histological and spectroscopic study. *Biomaterials* (2002) 23:2939–44. doi: 10.1016/S0142-9612(01)00423-9
10. Olmedo DG, Paparella ML, Spielberg M, Brandizzi D, Guglielmotti MB, Cabrini RL. Oral mucosa tissue response to titanium cover screws. *J Periodontol*. (2012) 83:973–80. doi: 10.1902/jop.2011.110392
11. Wilson TGJr, Valderrama P, Burbano M, Blansett J, Levine R, Kessler H, et al. Foreign bodies associated with peri-implantitis human biopsies. *J Periodontol*. (2015) 86:9–15. doi: 10.1902/jop.2014.140363
12. Eger M, Sterer N, Liron T, Kohavi D, Gabet Y. Scaling of titanium implants entrains inflammation-induced osteolysis. *Sci Rep*. (2017) 7:39612. doi: 10.1038/srep39612.
13. Hiram-Bab S, Liron T, Deshet-Unger N, Mittelman M, Gassmann M, Rauner M, et al. Erythropoietin directly stimulates osteoclast precursors and induces bone loss. *FASEB J*. (2015) 29:1890–900. doi: 10.1096/fj.14-259085
14. Takeshita S, Kaji K, Kudo A. Identification and characterization of the new osteoclast progenitor with macrophage phenotypes being able to differentiate into mature osteoclasts. *J Bone Miner Res*. (2000) 15:1477–88. doi: 10.1359/jbmr.2000.15.8.1477
15. Goh AX, Bertin-Maghit S, Ping Yeo S, Ho AW, Derks H, Mortellaro A, et al. A novel human anti-interleukin-1beta neutralizing monoclonal antibody showing *in vivo* efficacy. *MABS* (2014) 6:765–73. doi: 10.4161/mabs.28614
16. Yu D, Ye X, Che R, Wu Q, Qi J, Song L, et al. FGF21 exerts comparable pharmacological efficacy with Adalimumab in ameliorating collagen-induced rheumatoid arthritis by regulating systematic inflammatory response. *Biomed Pharmacother*. (2017) 89:751–60. doi: 10.1016/j.biopha.2017.02.059
17. Zafir-Lavie I, Miari R, Sherbo S, Krispel S, Tal O, Liran A, et al. Sustained secretion of anti-tumor necrosis factor alpha monoclonal antibody from *ex vivo* genetically engineered dermal tissue demonstrates therapeutic activity in mouse model of rheumatoid arthritis. *J Gene Med*. (2017) 19. doi: 10.1002/jgm.2965
18. Hu J, Feng X, Valdearcos M, Lutrin D, Uchida Y, Koliwad SK, et al. Interleukin-6 is both necessary and sufficient to produce perioperative neurocognitive disorder in mice. *Br J Anaesth*. (2018) 120:537–45. doi: 10.1016/j.bja.2017.11.096
19. Wu R, Liu X, Yin J, Wu H, Cai X, Wang N, et al. IL-6 receptor blockade ameliorates diabetic nephropathy via inhibiting inflammasome in mice. *Metabolism* (2018) 83:18–24. doi: 10.1016/j.metabol.2018.01.002
20. Machold KP, Smolen JS. Adalimumab-a new TNF-alpha antibody for treatment of inflammatory joint disease. *Expert Opin Biol Ther*. (2003) 3:351–60. doi: 10.1517/14712598.3.2.351
21. Palframan R, Airey M, Moore A, Vugler A, Nesbitt A. Use of biofluorescence imaging to compare the distribution of certolizumab pegol, adalimumab, and infliximab in the inflamed paws of mice with collagen-induced arthritis. *J Immunol Methods* (2009) 348:36–41. doi: 10.1016/j.jim.2009.06.009
22. Martinez-Fernandez de la Camara C, Hernandez-Pinto AM, Olivares-Gonzalez L, Cuevas-Martin C, Sanchez-Arago M, Hervas D, et al. Adalimumab reduces photoreceptor cell death in a mouse model of retinal degeneration. *Sci Rep*. (2015) 5:11764. doi: 10.1038/srep11764
23. Benny Klimek ME, Sali A, Rayavarapu S, Van der Meulen JH, Nagaraju K. Effect of the IL-1 receptor antagonist kineret(R) on disease phenotype in mdx mice. *PLoS ONE* (2016) 11:e0155944. doi: 10.1371/journal.pone.0155944
24. Nahrendorf M, Swirski FK, Aikawa E, Stangenberg L, Wurdinger T, Figueiredo JL, et al. The healing myocardium sequentially mobilizes two monocyte subsets with divergent and complementary functions. *J Exp Med*. (2007) 204:3037–47. doi: 10.1084/jem.20070885
25. Rider P, Carmi Y, Guttman O, Braiman A, Cohen I, Voronov E, et al. IL-1alpha and IL-1beta recruit different myeloid cells and promote different stages of sterile inflammation. *J Immunol*. (2011) 187:4835–43. doi: 10.4049/jimmunol.1102048
26. Geissmann F, Jung S, Littman DR. Blood monocytes consist of two principal subsets with distinct migratory properties. *Immunity* (2003) 19:71–82. doi: 10.1016/S1074-7613(03)00174-2
27. Murray PJ. Macrophage polarization. *Annu Rev Physiol*. (2017) 79:541–66. doi: 10.1146/annurev-physiol-022516-034339
28. Fiorentino DF, Zlotnik A, Mosmann TR, Howard M, O'Garra A. IL-10 inhibits cytokine production by activated macrophages. *J Immunol*. (1991) 147:3815–22.
29. Baseler WA, Davies LC, Quigley L, Ridnour LA, Weiss JM, Hussain SP, et al. Autocrine IL-10 functions as a rheostat for M1 macrophage glycolytic commitment by tuning nitric oxide production. *Redox Biol*. (2016) 10:12–23. doi: 10.1016/j.redox.2016.09.005
30. Allen JB, Bansal GP, Feldman GM, Hand AO, Wahl LM, Wahl SM. Suppression of bacterial cell wall-induced polyarthritis by recombinant gamma interferon. *Cytokine* (1991) 3:98–106.
31. Wahl SM, Allen JB, Ohura K, Chenoweth DE, Hand AR. IFN-gamma inhibits inflammatory cell recruitment and the evolution of bacterial cell wall-induced arthritis. *J Immunol*. (1991) 146:95–100.
32. Muhl H, Pfeilschifter J. Anti-inflammatory properties of pro-inflammatory interferon-gamma. *Int Immunopharmacol*. (2003) 3:1247–55. doi: 10.1016/S1567-5769(03)00131-0
33. Cook DN. The role of MIP-1 alpha in inflammation and hematopoiesis. *J Leukoc Biol*. (1996) 59:61–6.

34. Kim MS, Day CJ, Morrison NA. MCP-1 is induced by receptor activator of nuclear factor-{kappa}B ligand, promotes human osteoclast fusion, and rescues granulocyte macrophage colony-stimulating factor suppression of osteoclast formation. *J Biol Chem*. (2005) 280:16163–9. doi: 10.1074/jbc.M412713200
35. Rider P, Carmi Y, Cohen I. Biologics for targeting inflammatory cytokines, clinical uses, and limitations. *Int J Cell Biol*. (2016) 2016:9259646. doi: 10.1155/2016/9259646
36. Udagawa N, Takahashi N, Katagiri T, Tamura T, Wada S, Findlay DM, et al. Interleukin (IL)-6 induction of osteoclast differentiation depends on IL-6 receptors expressed on osteoblastic cells but not on osteoclast progenitors. *J Exp Med*. (1995) 182:1461–8.
37. Wang H, Jia TH, Zacharias N, Gong W, Du HX, Wooley PH, et al. Combination gene therapy targeting on interleukin-1beta and RANKL for wear debris-induced aseptic loosening. *Gene Ther*. (2013) 20:128–35. doi: 10.1038/gt.2012.1
38. Goodman SB, Gibon E, Pajarinen J, Lin TH, Keeney M, Ren PG, et al. Novel biological strategies for treatment of wear particle-induced periprosthetic osteolysis of orthopaedic implants for joint replacement. *J R Soc Interface* (2014) 11:20130962. doi: 10.1098/rsif.2013.0962
39. Orozco C, Maalouf NM. Safety of bisphosphonates. *Rheum Dis Clin North Am*. (2012) 38:681–705. doi: 10.1016/j.rdc.2012.09.001
40. Schmiedberg SK, Chang DH, Frondoza CG, Valdevit AD, Kostuik JP. Isolation and characterization of metallic wear debris from a dynamic intervertebral disc prosthesis. *J Biomed Mater Res*. (1994) 28:1277–88. doi: 10.1002/jbm.820281105
41. Mertens M, Singh JA. Anakinra for rheumatoid arthritis. *Cochrane Database Syst Rev*. (2009) CD005121. doi: 10.1002/14651858.CD005121.pub3
42. Kearsley-Fleet L, Beresford MW, Davies R, De Cock D, Baildam E, Foster HE, et al. Short-term outcomes in patients with systemic juvenile idiopathic arthritis treated with either tocilizumab or anakinra. *Rheumatology* (2018). doi: 10.1093/rheumatology/key262. [Epub ahead of print].
43. Murray E, Ellis A, Butylkova Y, Skup M, Kalabic J, Garg V. Systematic review and network meta-analysis: effect of biologics on radiographic progression in rheumatoid arthritis. *J Comp Eff Res*. (2018). doi: 10.2217/cer-2017-0106

Conflict of Interest Statement: The authors declare that the research was conducted in the absence of any commercial or financial relationships that could be construed as a potential conflict of interest.

frontiers in Immunology

REVIEW
published: 14 February 2019
doi: 10.3389/fimmu.2019.00208

Oral Mucosal Epithelial Cells

Sabine Groeger and Joerg Meyle*

Department of Periodontology, Justus-Liebig-University of Giessen, Giessen, Germany

Cellular Phenotype and Apoptosis: The function of epithelial tissues is the protection of the organism from chemical, microbial, and physical challenges which is indispensable for viability. To fulfill this task, oral epithelial cells follow a strongly regulated scheme of differentiation that results in the formation of structural proteins that manage the integrity of epithelial tissues and operate as a barrier. Oral epithelial cells are connected by various transmembrane proteins with specialized structures and functions. Keratin filaments adhere to the plasma membrane by desmosomes building a three-dimensional matrix.

Cell-Cell Contacts and Bacterial Influence: It is known that pathogenic oral bacteria are able to affect the expression and configuration of cell-cell junctions. Human keratinocytes up-regulate immune-modulatory receptors upon stimulation with bacterial components. Periodontal pathogens including *P. gingivalis* are able to inhibit oral epithelial innate immune responses through various mechanisms and to escape from host immune reaction, which supports the persistence of periodontitis and furthermore is able to affect the epithelial barrier function by altering expression and distribution of cell-cell interactions including tight junctions (TJs) and adherens junctions (AJs).
In the pathogenesis of periodontitis a highly organized biofilm community shifts from symbiosis to dysbiosis which results in destructive local inflammatory reactions.

Cellular Receptors: Cell-surface located toll like receptors (TLRs) and cytoplasmatic nucleotide-binding oligomerization domain (NOD)-like receptors (NLRs) belong to the pattern recognition receptors (PRRs). PRRs recognize microbial parts that represent pathogen-associated molecular patterns (PAMPs).
A multimeric complex of proteins known as inflammasome, which is a subset of NLRs, assembles after activation and proceeds to pro-inflammatory cytokine release.

Cytokine Production and Release: Cytokines and bacterial products may lead to host cell mediated tissue destruction. Keratinocytes are able to produce diverse pro-inflammatory cytokines and chemokines, including interleukin (IL)-1, IL-6, IL-8 and tumor necrosis factor (TNF)-α. Infection by pathogenic bacteria such as *Porphyromonas gingivalis* (*P. gingivalis*) and *Aggregatibacter actinomycetemcomitans* (*A. actinomycetemcomitans*) can induce a differentiated production of these cytokines.

Immuno-modulation, Bacterial Infection, and Cancer Cells: There is a known association between bacterial infection and cancer. Bacterial components are able to up-regulate immune-modulatory receptors on cancer cells. Interactions of bacteria

OPEN ACCESS

Edited by:
Asaf Wilensky,
Hadassah Medical Center, Israel

Reviewed by:
Denis Francis Kinane,
Geneva University Hospitals (HUG), Switzerland
Bruno G. Loos,
Academic Centre for Dentistry Amsterdam (ACTA), Netherlands
Georgios N. Belibasakis,
Karolinska Institute (KI), Sweden

****Correspondence:***
Sabine Groeger
sabine.e.groeger@dentist.med.uni-giessen.de

Specialty section:
This article was submitted to Mucosal Immunity, a section of the journal Frontiers in Immunology

Received: *03 September 2018*
Accepted: *23 January 2019*
Published: *14 February 2019*

Citation:
Groeger S and Meyle J (2019) Oral Mucosal Epithelial Cells. Front. Immunol. 10:208. doi: 10.3389/fimmu.2019.00208

with tumor cells could support malignant transformation an environment with deficient immune regulation.

The aim of this review is to present a set of molecular mechanisms of oral epithelial cells and their reactions to a number of toxic influences.

Keywords: oral epithelial cells, differentiation, receptors, cytokines, immuno-modulation, infection, cancer

INTRODUCTION

The oral mucosal epithelium is a barrier that separates the underlying tissues from their environment. It consists of two layers, the surface stratified squamous epithelium and the deeper lamina propria. In keratinized oral mucosa, the epithelium is composed of the four layers stratum basale, stratum spinosum, stratum granulosum, and stratum corneum. In nonkeratinised epithelium, the stratum basale is followed by the stratum filamentosum and the stratum distendum. In the oral mucosa distinct phenotypes are differentiated, lining mucosa, masticatory mucosa, and specialized mucosa (1). Lining mucosa is localized over mobile structures such as soft palate, cheeks, lips, alveolar mucosa, vestibular fornix and floor of the mouth and is extensible and loosely bound to adjacent structures by an elastin rich connective tissue and has a non-keratinizing squamous epithelium. Masticatory mucosa is the rigid and tough protecting cover of the gingiva and the hard palate, tightly bound by dense connective tissue to the underlying bone. This epithelium is keratinized. Specialized mucosa is located on the dorsum of the tongue, shows a keratinized epithelium and includes lingual papillae and taste buds as specialized structures (2).

Junctional epithelium (JE) maintains the direct attachment to the tooth surface. The basal cells of the JE are attached to the connective tissue by the external basal lamina while the suprabasal cells are anchored to the tooth surface by an internal basal lamina that is produced by the JE. JE contains fewer cell-junctions as the oral gingival epithelium, but well developed gap junctions and some small adherens junctions can be detected (2). The JE has wide intercellular spaces, is highly permeable for water-soluble substances and serves as the primary pathway for the transmigration of polymorph nuclear leukocytes (3, 4). JE does not exhibit phenotypic stratification, but the outermost cells appear elongated and align with their long axis parallel to tooth surface (3).

The oral epithelial barrier is the outcome of numerous structural and functional protein interactions resulting in the ability to respond to a various exogenous, possibly toxic, influences. Squamous epithelia possess structural properties like stratification and cornification of the keratinocytes and specific cell-to-cell interactions to maintain its barrier function. It is now recognized that epithelial cells are not passive bystanders, but rather are metabolically active and capable of reacting to external stimuli by synthesizing a number of cytokines, adhesion molecules, growth factors, chemokines, and matrix-metalloproteases (5). Gingival tissues provide defense to resist frictional forces of mastication as well as to defend the soft tissues against chemical or microbial challenge (3).

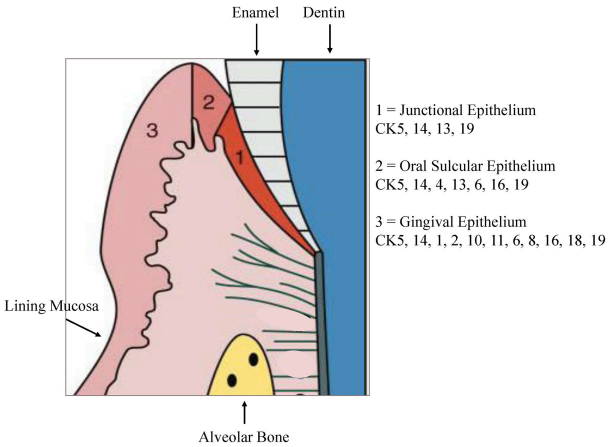

FIGURE 1 | Cytokeratin distribution patterns. Cytokeratin (CK) distribution patterns in oral epithelia. Modified according to Pöllänen et al. (6).

CELLULAR PHENOTYPE AND APOPTOSIS OF ORAL EPITHELIAL CELLS

The stratified epithelium of the oral mucosa belongs, together with the epithelium of the skin, to the most protective and resistant epithelia. It is composed of two layers, first epithelial cells with a basement membrane and second an underlying connective tissue, the *lamina propria* (4). The gingiva is combined of epithelial and connective tissues forming a collar of masticatory mucosa attached to the teeth and the alveolar bone. Gingival epithelium constitutes of a stratified squamous keratinized epithelium while the oral sulcular epithelium appears to be stratified and non-keratinized (**Figure 1**).

The non-keratinized JE shows no true phenotypic stratification (3). In contrast to the ortho-keratinized epidermis of the skin, oral epithelia normally express all three major differentiation patterns of keratinocytes. As an anatomical and functional unit, the gingival keratinization pattern shows variations that origin partly from adaptive processes of the tissue to the special site around fully erupted teeth. A keratinized epithelium similar to the epidermis is exhibited in regions that encounter masticatory and other mechanical forces. The muco-gingival junction designates the boundary of the gingiva from the movable alveolar mucosa and the mucosa of the floor of the mouth. The floor of the mouth and the buccal part need to be flexible for speech, swallowing or chewing and are covered with a lining mucosa that doesn't keratinize. The specialized mucosa on the dorsum of the tongue includes a number of papillae and

is covered by an epithelium, which may be either keratinized or non-keratinized. Under physiological conditions, the barrier of polarized epithelia allows regulated paracellular fluxes of solutes and nutrients as well as the collection of antigens and surveillance by mucosal immune cells. During inflammation, this protective mechanism may be compromised by different stimuli originating from both sides of the epithelial barrier.

Cytokeratins

Keratins are one major component of the epithelial cytoskeleton. They belong to the intermediate filament group of cytoskeletal proteins. A gene family of approximately 30 members encode keratins. They have a common structure composed of about 310-amino-acid central o-helical rod domain flanked by non-helical end-domains which are highly variable in sequence and structure (7). Based on the amino acid sequence and charge the keratin proteins are divided into two groups, acidic type I keratins including keratins K9-K20 and the basic or neutral type II keratins including K1–K8. Two keratin proteins, one type I and one type II, are always co-expressed and build heteropolymers to form the 10-nm keratin intermediate filaments (Ifs) that are part of the cytoskeleton. In the basal proliferative layer the keratin pair K5/K14 is expressed in stratified epithelia. Keratin 19 is detectable in simple epithelia and basal cells of non-keratinizing epithelia (8, 9). The keratin pair that is expressed in the post-mitotic layers of differentiating suprabasal cells differs depending on the localization. Cytokeratin distribution is highly specific and varies with type of epithelium, site, differentiation grade, so keratin expression is a sensitive and specific marker of differentiation in epithelial cells (10). Gingival and epidermal tissues as examples for cornifying epithelia, the keratins K1 and K10 are present while epithelia of buccal mucosa or esophagus K4 and K13 are the mainly expressed keratins (11). Suprabasal epithelial cells of the hard palate and gingiva furthermore express K2, designated as K2p in contrast to the epidermal K2e. The genes of K2p and K2e are related but separate (12). Other than the keratin pattern expressed from the attached gingiva some specialized epithelial cells within the gingiva show a distinct keratin pattern. The sulcular epithelium and cells of the gingival margin express K4 and K13. In contrast, the junctional epithelium adjacent to the tooth surface synthesizes K8, K13, K16, K18, and K19 (11, 13). **Figure 1** shows the regional cytokeratin distribution pattern of the gingiva. Oral epithelia can exhibit one of 2 patterns of epithelial maturation, (1) they keratinize thus the mucosa matures by formation of a surface layer of keratin. This includes orthokeratinization which refers to the absence of nuclei in the superficial layer of scales on maturation and parakeratinization which designates the retention of pyknotic nuclei in the surface layer of squames during maturation (14). Nonkeratinization is the second possibility which means maturation with absence of a keratin layer which denotes that the nuclei remain, with scarce keratin filaments, in the cytoplasm of the most superficial cells (15). Depending on the functional demands, different types of keratinization are present in the gingival tissue. Oral gingival epithelium is keratinized while the sulcular and junctional epithelia (JE) as well as the lining mucosa are not keratinized (14).

Keratin filament assembly starts by parallel association. One type I chain form a paired dimer with its type II counterpart, two dimers associate in an antiparallel fashion to a tetramer. Two tetramers connect laterally resulting in a protofilament, from which eight are twisted into a rope building the keratin filament. Each keratin filament therefore possesses a cross section of 32 individual α helical coils. The polypeptide chains are further stabilized by strong lateral hydrophobic interactions. Bundled keratin filaments are associated to macromolecular networks that are oriented radial in the cytoplasm (2, 16). The regional specificity of keratin expression may be attributed to intrinsic specialization of regional keratinocyte stem cells. Disorders in keratin may be genetic or acquired. Numerous keratin mutations were identified as cause of several skin and mucosal disorders. Abnormal keratinization is part of several oral diseases. This topic is reviewed by Rao et al. (17).

The Gingival Epithelial Barrier

Biofilms differentially modulate the epithelial cellular immune response based on their properties and composition. The bacterial biofilm located on the tooth surface and in the gingival crevice is considered as the primary causative agent involved in the pathogenesis of gingivitis and periodontitis and involves polymicrobial synergy and dysbiosis (18). Dysbiosis is based on the relative abundance of different bacterial species compared to their low presence in health, causing a modification of host–microbe interactions that can mediate destructive inflammation and bone loss (19, 20).

Keystone pathogens, such as *Porphyromonas gingivalis* (*P. gingivalis*), are able to subvert host response and promote breakdown of the homeostatic state, while further bacterial species show properties of pathobionts that can trigger destructive inflammation including both innate and adaptive immune response (21, 22). In addition the onset of gingivitis and periodontitis requires a susceptible host governing the complex inflammatory interactions.

Keratinocytes of the gingival epithelium form a barrier against bacterial infection and invasion (23). They are interconnected by a number of specialized transmembrane molecular complexes, among them cell-cell junctions comprising tight junctions adherens junctions, and gap junctions (**Figure 2**).

Normal expression of these molecular complexes in the gingival tissues is essential for maintaining epithelial integrity. Once integrity is disturbed by biofilm-derived noxious influences, the associated bacteria may invade into the deeper periodontal tissues, triggering an inflammatory response. Thus these cell-cell connections are a crucial part of the innate immune response to resist microbial and toxic challenge.

Structure and Function of Tight Junctions (TJ)

Tight junctions are complex protein structures, forming a belt like pattern among neighboring cells, encircling cells at the apical side of the lateral membrane (25). One of the major functions of the TJ complex is to form a barrier to regulate the passage through the paracellular pathway of water, ions, solutes and other small molecules (26–28). The structure of TJs appears as a string

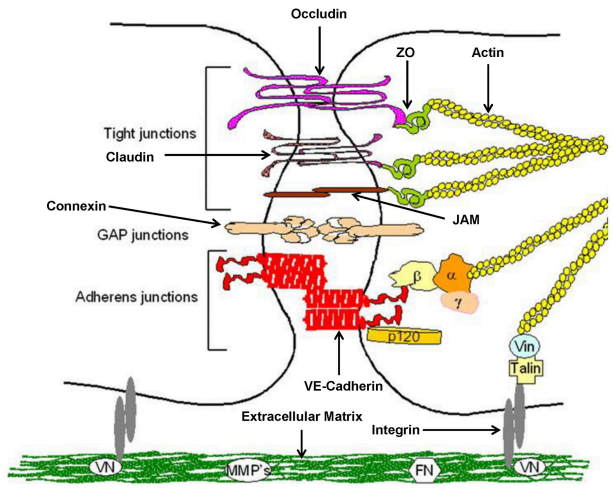

FIGURE 2 | Structure of epithelial cell-cell contacts. Model of cellular junctions, modified according to Metha and Malik (24). Arrangement of junctions comprising tight junctions, adherens junctions, gap junctions, and integrin. Occludin, claudins, and junctional adhesion molecules (JAMs) required for tight junctions, whereas vascular endothelial (VE)-cadherin forms adherens junctions. Connexins are part of gap junctions. The extracellular domains of occludin, claudins, and VE-cadherin maintain cell-cell contacts. Intracellular domains provide junctional stability linking to the actin cytoskeleton via catenins (β,β-catenin, α,α-catenin; γ,γ-catenin; p120, p120-catenin) or zonula occludens-1 protein (ZO-1). Gap junctions are responsible for fast exchange of information by low-molecular-mass second messengers such as Ca^{2+} and IP_3 between contiguous cells. Integrin receptors link endothelial cells with the extracellular matrix (ECM) through matrix proteins like fibronectin (FN) or vitronectin (VN). The cytosolic domains of integrins are linked to the actin cytoskeleton through the proteins talin and vinculin (Vin), involved in integrin-mediated signaling.

of continuous particles inlaid into the membrane, forming TJ strands. The strand is a fibril-like structure built by the assembly of claudin and tight junction–associated MARVEL proteins (TAMPs). TAMPS are composed of the tight junction-associated MAL = myelin and lymphocyte domain and the MARVEL = related proteins for vesicle trafficking and membrane link domain. The assembled structure represents the functional unit of TJs, formed by adjacent plasma membranes (29, 30).

A number of different signaling and trafficking molecules, that regulate cell differentiation, proliferation and polarity, are coordinated by TJs (31, 32). TJ topology consists of three protein domains, a helical transmembrane domain, a cytosolic scaffolding domain and cytosolic tail featuring cellular signaling. TJ strands are formed by the transmembrane proteins, a class that consists of multiple integral membrane proteins, including the groups of tissue- and cell-specific claudins, (29, 33) the TAMP family and the junction adhesion molecules (JAMs). The structure of claudin includes four transmembrane domains, two extracellular domains forming two loops, in which the N-terminus and C-terminus are located intracellularly. Claudins fulfill barrier properties (30, 34, 35) and are able to regulate the gate function as paracellular tight junction channels (PTJC). Their biological and physical properties are comparable to traditional ion channels (36). They also include occludin into the junctions (29). In adjacent mouse liver cells it was shown that various members of the claudin family form homophilic or heterophilic polymers. Furthermore, claudins may form paired strands to the membrane of adjacent cells (37). Differences in barrier properties between cell types are probably caused by different combinations of claudins (38).

The TAMP family includes MARVEL D1, also called occludin, MARVEL D2 (tricellulin) and MARVEL D3 protein. These molecules possess four transmembrane domains and two extracellular loops, similar to claudin (39, 40). It is not clear whether occludin composed strands have the same functions as strands formed by claudins but *in vitro* and *in vivo* studies demonstrated that occludin is of importance in TJ barrier function and intercellular adhesive interactions (39, 41–43). Claudin 1 and occludin were detected in the gingival but not in the sulcular and junctional epithelium. Furthermore, it was found that the adherens junction proteins P-cadherin and α-catenin are detectable in all three epithelia while E-cadherin was not present in junctional epithelium (44). The expression of claudin-4 was detected in the human oral squamous cell carcinoma epithelial cell line H413 (45) and in immortalized human gingival keratinocytes (46). Genetic investigations of adhesion proteins in stratified multi-layered gingival epithelial cell cultures showed strong expression of claudin-4, claudin-1, JAM-1, claudin-25, claudin-17, occludin and claudin-12 (47). Occludin is able to associate with different signaling molecules such as the non-receptor tyrosine kinase c-Yes, atypical protein kinase C (aPKC) and phosphoinositide 3-kinase (PI3K), as well as protein phosphatases 2A and 1 and appears to have signal transmitter functions (48, 49).

MARVEL D2 (also called tricellulin) is detectable at the tricellular contact sites. It is assembled to strands that form a tubular structure vertical to the bicellular TJ belt (50). It probably controls the flow of macromolecules but it is also needed for TJ organization. In the mouse mammalian epithelial cell line Eph4 tricellulin knock-out led to impairment of the structure of bicellular and tricellular contacts (51). The third TAMP, MARVEL D3, is expressed in many epithelial cells and its function was found not to be essential for TJ formation (52).

The members of the junctional adhesion molecule family (JAM), JAM-A, JAM-B, JAM-4, JAM-L and coxsackie and adenovirus receptor (CAR) belong to the immunoglobulin superfamily. JAMs seem to be less important for the regulation of the junctional structure, but rather contribute to adhesion and signaling. Studies mostly focused on the junctional role of JAM-A, that was shown to be localized to claudin-based tight junction fibrils in epithelial cells (53). JAM-A protein contains two extracellular immunoglobulin-like loops, a single transmembrane and a cytoplasmic domain ending in a PDZ binding motif that has been reported to interact with AF-6/afadin and zonula occludens protein (ZO)-1 (54) and ZO-2 (55). CAR appears to be a cell adhesion molecule that contributes to the formation of cell–cell contacts. In cultured epithelial cells, CAR molecules on adjacent cells form homotypic interactions (56). CAR is locally concentrated in TJs at the most apical regions of the lateral surfaces of polarized epithelial cells and its overexpression in cultured polarized cells increased TER (57),

while soluble CAR and anti-CAR antibodies were shown to disrupt TJs, (56) suggesting that CAR is involved in the barrier function of TJs.

All members of the cytosolic scaffolding proteins have one or multiple post synaptic density proteins (PSD95), drosophila disc large tumor suppressor (Dlg1) domains, and zonula occludens-1 protein (PDZ) domains. They are able to bind to various integral membrane proteins like claudins, occludin or JAMs and also can bind to actin filaments. In this manner they connect TJ to the actin filaments and stabilize the protein complexes. An increasing number of PDZ containing proteins is known including membrane associated guanylate kinase (MAGUK)-like proteins, protein associated with Lin7 (Pals1), AF-6/afadin, atypical protein kinase C (aPKC), isotype-specific interacting protein (ASIP), partitioning-defective protein 3 (PAR-3), multi-PDZ protein 1 (MUPP1) and protein associated with tight junctions (PATJ) (58). These scaffolding proteins seem to be important for the organization and localization of TJs because blockade of PDZ domains results in poorly organized TJs that in consequence are distributed to other areas (59). Zonula occludens (ZO) proteins belong to the MAGUK family and include the three members ZO-1 (60), ZO-2 (61), and ZO-3 (62). Through their three PDZ domains ZO proteins interact with several proteins such as claudins, MARVEL D1 or JAMs and F-actin. This association with multiple proteins makes the formation of large complexes possible which are linking the cytoskeleton to the TJ strands (58).

The barrier function and structure of TJs is regulated by intracellular signaling proteins which include protein kinase A, protein kinase C, Rho kinase, myosin light chain kinase, GTPase Rab13, tyrosin kinase and mitogen activated protein kinase. All these proteins are not specific for TJs but essential for their establishment and function. The signal transduction of TJs is reviewed in Takano et al. (63). Further reviews are available addressing TJ physiology and function (64), regulation (65) and the specific components such as tricellular tight junctions (66). In gingival tissue, TJs were observed only in the granular and cornified layer, were they did not form complex strands, in contrast to cultured gingival keratinocytes *in vitro* that showed a largely extended framework of TJ strands (67).

Measurement of the transepithelial electrical resistance (TER) is a method for investigations of the permeability of mucosal barriers *in vitro* and alterations of TER values are directly related to the integrity and function of the paracellular occluding barrier (68, 69). TER measurements are a useful tool to assess integrity of tight junctions. The strength of the transmucosal resistance is closely related to the number of junctional strands and junctional tightness (70). This correlation was demonstrated in primary human gingival keratinocytes (**Figure 3**) (67). The development of TER depends on the intracellular Ca^{2+} concentration (72).

Immortalized human gingival keratinocytes (IHGK) (73, 74) used in a 3D culture model, were infected with gingipain-producing *P. gingivalis* strains and a RGP/KGP defect mutant (75). This caused a significant decrease of TER after 24 h by the gingipain producing strains, but not by the defect mutant. Investigations of tight junction proteins in the same experimental setting using immunostaining revealed

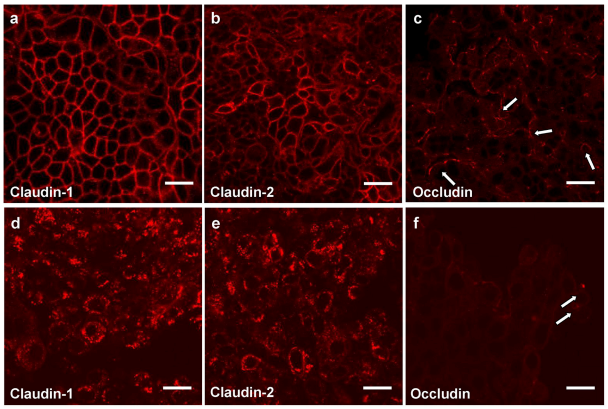

FIGURE 3 | Tight junction proteins of primary keratinocytes after infection with *P. gingivalis*. Immunostaining of the tight junction proteins in primary human gingival keratinocytes, claudin 1 **(a,d)** claudin 2 **(b,e)** and occludin **(c,f)**; **(a–c)** cells in culture medium; **(d–f)** cells infected apically plus basolaterally with *Pophyromonas gingivalis* (*P. gingivalis*) W83 (MOI 10^4) for 4 h. Arrows **(e,f)** show curved occludin strains in the walls of non-infected cells, in infected cells the arrows point to occludin aggregations, scale bar = 20 μm (71).

infection-induced alterations in claudin-1, claudin-2 and in occludin expressions. After infection the typical chicken wire pattern of claudin-1 and claudin-2 (**Figures 3a,b**) disappeared and the proteins formed conglomerates (**Figures 3d,e**). The curved strands of occludin present in the control assays (**Figure 3c**) were degraded as well (**Figure 3f**). Soluble virulence factors such as gingipains disrupt the epithelial barrier *in vitro*, which is correlated with the disintegration of junctional cell-cell complexes. Invasion and damage of the epithelial layer by infective agents is an important step and may result in bacterial invasion and destruction of the underlying connective tissue.

The results of this study give some insights into the initial stages of oral bacterial infections leading to gingivitis and periodontitis.

A further mechanism besides damage may be active internalization of epithelial adhesion complexes. In intestinal epithelial cells (T84 cells), IFN-γ induces a process of TJ protein internalization (claudin-1, occludin, JAM-A) by micropinocytosis, which results in leakage of the epithelial layer (76). Guo et al. (77) determined the impact of *P. gingivalis*, *P. gingivalis* LPS and eATP on TJ proteins in an oral epithelial cell culture model. Quantified real time polymerase chain reaction (RT-PCR), immunostaining and immunoblots of gene and protein expression in TJs revealed that *P. gingivalis* infection led to temporary upregulation of the genes encoding occludin, claudin- 1, and claudin-4 but not JAM-A, claudin-15, or ZO-1, while *P. gingivalis* LPS increased claudin-1, claudin-15, and ZO-1 and decreased occludin, JAM-A, and claudin-4. Significant upregulation of tight junction proteins was demonstrated when cells were pretreated with eATP. These results indicate that *P. gingivalis* induced early defense mechanisms of the host. *P. gingivalis* LPS stimulates the destruction of the epithelial barrier more potently than *P. gingivalis*. ATP stimulation further increased the effect on TJ proteins after

P. gingivalis infection and LPS-induced disruption of epithelial integrity (77).

Structure and Function of Adherens Junctions (AJ)

The adherens junctions (AJs) or zonula adherens, intermediate junction, or "belt desmosome," are a defining feature of all epithelia, forming apical localized structures of adhesion closely aligned to the membranes of neighboring epithelial cells, that play an essential role in the regulation of the junctional complex. AJs are protein complexes that appear at cell–cell junctions in epithelial and endothelial tissues. Their localization is more basal than tight junctions. AJs are like bands that encircle the cell (zonula adherens) or appear as attachment spots to the extracellular matrix (adhesion plaques). The cell-to-cell adhesion sites are composed of cadherins which are connected to the actin cytoskeleton by catenins and other constituents like actinin and vinculin (78). AJs are formed by homophilic binding of the extracellular cadherin domains in a calcium-dependent manner. The cell-to cell apposition is maintained and reinforced by the homophilic interactions of single-pass transmembrane E-Cadherin (E-Cad) molecules. This process is stabilized by accumulating a tight network of actin filaments and by linking molecules that fix E-Cad clusters on the inner cytoskeleton (79). The E-Cad cytoplasmic domain consists of the β-catenin (β-Cat) interacting with p120-catenin (p120-Ctn). β-Cat associates with α-Catenin (α-Cad), maintaining the link to the actin cytoskeleton. Cadherin directly binds to β-catenin or plakoglobin, followed by binding to α-catenin that afterwards binds to vinculin, α-actinin, ZO-1 and actin (80). Also α-Cat is able to interact with further actin-binding proteins such as formin, AF6/afadin, or EPLIN (81). Nectin and its associated AF6/afadin protein L-afadin occurs concentrated at AJs (82). The transmembrane protein vezatin is localized at sites of cadherin-based cell-to-cell adhesion in cultured cells and anchors myosin VIIa to the cadherin-catenin complex (83). Due to their dynamic structure, adherens junctions physically connect adjacent epithelial cells, bridge intercellular adhesive contacts to the cytoskeleton, and are involved in the definition of each cell's apical–basal axis. E-Cads as well as catenins are substrates of phosphatases and kinases that are key regulators of AJs and modify the interactions between the proteins enabling them to regulate the interaction grade between E-Cad and the catenin complex and their concentrations in the membrane, which is essential for the modulation of adhesive strength and AJ remodeling [reviewed in (84)].

As a result of proteolytic disruption by putative periodontal pathogens such as *P. gingivalis* E-Cads are affected in periodontitis (85, 86). *P. gingivalis* is able to produce a variety of proteolytic enzymes, including eight endopeptidases and numerous exopeptidases (87). Gingipains are extracellular cysteine proteinases, which can impair endothelial cell adhesion (88, 89). Gingipains are also able to enhance collagenolysis by inducing matrix metalloproteinases of the host. Sheets et al. (90) also demonstrated cleavage of cellular receptors. The cleavage of adherence junction proteins (shown in HOK-16 cells) affects N-cadherin, VE-cadherin, β-integrin and reduces the adhesion of the cells to the extracellular matrix proteins (91). This may result in the detachment of the endothelial cells.

Bacterial Adhesion and Invasion Into Epithelial Cells Are Pathological Processes Which Are Also Able to Disrupt the Epithelial Barrier in Periodontitis

It was shown that *P. gingivalis* fimbriae bind to cellular α5β1-integrin, which mediates bacterial adherence to host cells (92–94). Cellular integrins are heterodimeric receptors for extracellular matrix proteins and are essentially involved in cellular physiological processes that are related to metabolism, activation, differentiation, motility, and proliferation (95). These functions depend on the α5β1-integrin binding to its ligand fibronectin (96).

P. gingivalis can degrade cellular signaling molecules and inactivate a variety of cellular functions, which are important for healing and regeneration as well as homeostatic properties of periodontal tissues (91, 97–99).

Invasion of epithelial cells disrupts the epithelial barrier and the intracellular pathogens affect cellular functions by the usage of dynamin, actin fibers, microtubules, PI3K, and lipid rafts of the host cells.

Intracellular localization enables pathogens to penetrate deep into tissues by spreading from cell to cell, a process that seems to be mediated by membrane protrusions based on actin polymerization. This avoids the need of bacterial release into the extracellular space, i.e., periodontal pathogens like *P. gingivalis* spread in between cells without entering the extracellular space which may allow colonization of oral tissues avoiding revelation to the humoral immune response (86).

The importance of junctional proteins in the immune response to bacterial biofilms has been demonstrated by Belibasakis et al. (47). The group investigated the effects of a 10-species subgingival biofilm model on gene expression of all known cellular contacts (tight junctions, desmosomes, gap junctions and adherens junctions), and evaluated the involvement of the 3 "red-complex" species [*P. gingivalis, Treponema denticola* (*T. denticola*), and *Tannerella forsythia* (*T. forsythia*)] in a multi-layered gingival epithelial cell culture. The results of this study showed different effects on the junctional expression of the 2 biofilm (BF) models (one with and one without the "red complex"). It was found that BF including the "red complex" did not affect the expression of any of the studied tight junction genes. Absence of the "red complex" (RC) from the biofilm resulted in significantly higher Claudin-4 expression compared to the control after 3 and 24 h. Assessment of gene expression of desmosomes, adherens junctions, and gap junction proteins in response to biofilms without the "red complex" resulted in up-regulated desmocollin-2 expression after 3 h while the "red complex" including biofilm did not induce this effect. After 24 h, this expression was significantly downregulated by both biofilm variants. After 3 h of biofilm challenge, the gene expression of none of the investigated junctional adapter proteins

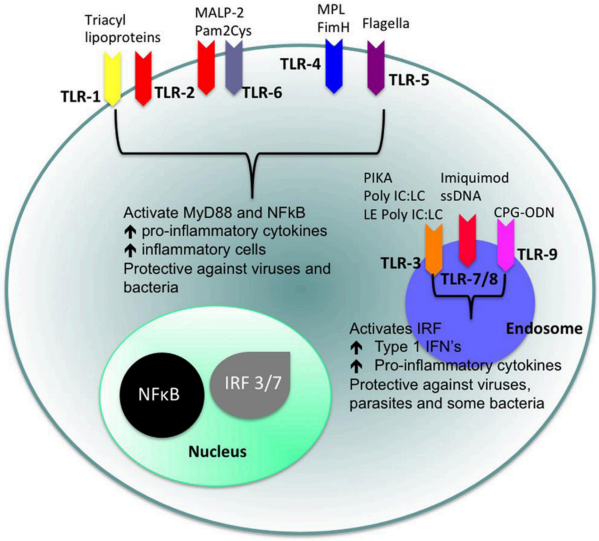

FIGURE 4 | Cellular location of toll like receptors (TLRs) and the identity of their ligands/agonists. The stimulation of surface TLRs (TLR-2, TLR-4, and TLR-5) with appropriate ligands results in the activation of nuclear factor (NF)-κB. The ensuing increase in levels of pro-inflammatory cytokines and the influx of inflammatory cells then provides an environment, which protects against both virus and bacterial challenge. Activation of intracellular TLRs (TLR-3, TLR-7, TLR-8, and TLR-9) leads to interferon regulating factor (IRF) activation and the production of Type 1 interferons (IFNs) and pro-inflammatory cytokines, again providing an environment not conducive for pathogens (100).

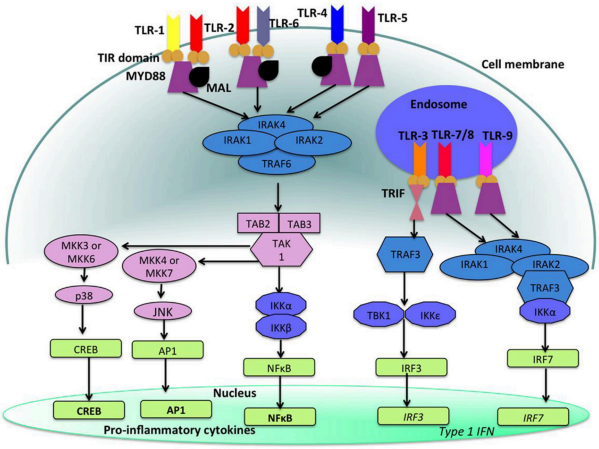

FIGURE 5 | Toll like receptor (TLR)-signaling pathways. TLR-4, TLR-5, and the heterodimers TLR-1/TLR-2 and TLR-2/TLR-6 are located on the cell surface where they are activated by the appropriate ligand. Conversely, TLR-3, TLR-7, TLR-8, and TLR-9 are located within endosomal compartments of the cell and recognize microbial and viral nucleic acids. Stimulation of TLR-1/TLR-2, TLR-2/TLR-6, TLR-4, and TLR-5 leads to the engagement of myeloid differentiation primary response protein (MyD88) and MYD88-adapter-like protein (MAL) with the toll/interleukin-1 receptor (TIR) domain-containing adapter proteins. This stimulates downstream signaling pathways that involve the interactions between IL-1R-associated kinases (IRAKs) and the adapter molecules tumor necrosis factor (TNF) receptor-associated factors (TRAFs) and activates mitogen-activated protein kinases (MAPKs) JUN N-terminal kinases (JNK) and p38. Activation of these kinases leads to the activation of transcriptional factors such as nuclear factor-κB (NF-κB), cyclic adenosine mono phosphate (AMP)-responsive element binding protein (CREB), and activator protein-1 (AP-1). A major consequence of activation of surface TLRs is the induction of pro-inflammatory cytokines. Activation of TLR-7, TLR-8, and TLR-9 also leads to the engagement of MyD88, MAL, IRAKs, and NF-κB inhibitor kinase (IKK)α, however, interferon-regulatory factors (IRFs) are activated, which leads to the production of type 1 interferons (IFN). Stimulation of TLR-3 results in the association of TIR domain-containing adapter protein inducing IFNβ (TRIF). This leads to the downstream signaling of TNF receptor-associated factors (TRAFs) and IKK leading to the activation of IRF3 and the production of type 1 IFNs (100).

was regulated while after 24 h, the expression of desmoplakin and plakoglobin were down-regulated in response to both biofilms (47).

CELLULAR RECEPTORS

Toll-Like Receptors (TLRs)

Toll-like receptors (TLRs) (**Figures 4**, **5**) belong to the best characterized family of cellular effectors for the detection of pathogens (101). TLRs are widely expressed in eukaryotic cells. They are trans-membrane proteins that recognize molecular structures classified as "pathogen associated molecular patterns" (PAMPs) and thus belong to the pattern recognition receptors (PRRs). These patterns are present in nearly all types of microorganisms (102). Toll-like receptors contain a horseshoe-shaped extracellular leucine-rich repeat (LRR) and an intra-cytoplasmic toll/IL-1R (TIR) domain that are connected by a single trans-membrane domain. The LRR domain is responsible for ligand recognition and intracellular signal transfer is maintained by the TIR domain. TLRs represent not only the most important but also one of the first mechanisms in immune-defense against fungal, bacterial and viral pathogens. After binding the TLR downstream signaling pathway is activated playing an important role in innate and adaptive immune responses. In the oral cavity a great number of microorganisms is constantly present, therefore expression and function of TLRs is essential for the maintenance of oral tissue homeostasis.

In humans, currently 10 TLRs have been identified, including extracellular as well as intracellular receptors. All exhibit a number of specific ligands, except for the orphan receptor TLR10, where the specific ligand has yet not been discovered (101, 103). TLR1, TLR2, TLR4, TLR5, TLR6, and TLR10 are expressed on the cell surface for recognition of extracellular microorganisms and ligands. TLR3, TLR7, TLR8, and TLR9 are intracellularly localized in the cytosolic endosomal compartment, binding microorganisms and ligands which passed the membrane of the host cell (104). **Figure 4** shows the location of TLRs and the identity of their ligands/agonists. TLR11 has been identified in the human genome but does not translate into a protein, because its open reading frame contains a stop codon (105). TLR2 forms heterodimers with TLR1 or TLR6 and recognizes peptidoglycan, lipopeptide and lipoproteins while lipopolysaccharide of Gram-negative bacteria is the specific ligand of TLR4 (106, 107). TLR3 recognizes double-stranded RNA (dsRNA), TLR 5 can detect bacterial flagellin, TLR7 and

TLR8 were shown to recognize imidazoquinilins and single-stranded RNA and TLR9 detects bacterial and viral DNA over their cytosine and guanine basepairing (108–113). LRR binding by ligands induces conformational changes of TIR resulting in interactions between TIR domains of adjacent TLRs and binding of additional adaptor proteins that are needed for the initiation of the intracellular signaling cascade. The most important adaptor molecules are the myeloid differentiation factor 88 (MyD88), the MyD88 adaptor-like (Mal) (TIR domain-containing adaptor protein, TIRAP), the TIR domain-containing adaptor protein inducing interferon-β (TRIF) (TIR-containing adaptor molecule, TICAM as synonym) and the TRIF-related adaptor molecule (TRAM) (114–119). TLR signaling can be negatively regulated by a variety of inhibitory molecules, including the toll-interacting protein (Tollip), interleukin-1 receptor (IL-1R) associated protein kinase (IRAK)-M, the sterile a- and HEAT-Armadillo- motif-containing protein (SARM), and the B cell adaptor or PI3K (BCAP), which inhibit downstream phases in the TLR- dependent signaling cascades. IL-1R associated protein kinases (IRAKs) IRAK4, IRAK1, and IRAK2 are activated by MyD88 followed by activation of tumor necrosis factor receptor-associated factor 6 (TRAF6) and RIP, that proceed by activation of transforming growth factor (TGF)-β-activated kinase 1 (TAK1) and TAK1-binding protein (TAB1, TAB2, and TAB3) complex (120–123). Subsequently, gene expression regulatory factors of the mitogen activated protein kinases (MAPK) family (ERK, JNK, p38) and NF-kB are activated, regulating cell survival and proliferation, and induce immune cell activation, production of pro-/anti-inflammatory mediators (cytokines and chemokines), interferons, and anti-microbial products. Activation of the intracellularly located TLR7, TLR8, and TLR9 is forwarded through MyD88 as well, but can also initiate TRAF6, IRAK4, and TRAF3-dependent activation of IRF7, which translocates to the nucleus and induces the production of type-I interferon (114, 124).

Figure 5 shows the signaling pathways of TLRs. mRNA of all 10 TLRs was detected in oral epithelial cells, but the actual expression and cellular localization of TLR proteins varies and is inducible. TLR2 is highly expressed in the basal layer of the gingival epithelium, levels are lower in the superficial layers that are more exposed to microorganisms and environmental influences. Apart from the detection of colonizing microorganisms in the superficial part of the epithelium, this may be regarded as a mechanism that facilitates TLR-depending inflammatory response only when pathogens are recognized in the basal layer. For TLR1, TLR3, TLR4, TLR5, and TLR9 a similar expression pattern was demonstrated (125, 126). The expression of TLR7 and TLR8 shows the same pattern in healthy and inflamed tissue. TLR2 and TLR4 expression is increased in acute and persistent gingival inflammation, though stimulation with TLR agonists did not induce production of pro-inflammatory cytokines, but β-defensin-2 generation in epithelial cells, and thus favored local downstream immune response (127).

Under chronic inflammatory conditions such as periodontitis in contrast to the TLR2 upregulation expression of TLR4 decreased, which may prevent from inflammatory exacerbation, i.e., tissue and bone destruction through containment of the inflammatory response (128). It was demonstrated that human healthy and inflamed oral tissues express TLR2, TLR4, NOD1 and NOD2 molecules, where cell-surface localizations of TLR2 and TLR4 could be more clearly detected in the inflamed than in healthy gingiva. It was furthermore demonstrated that human oral epithelial cell lines HSC-2, HO-1-u-1, and KB cells as well as primary cultured oral epithelial cells constitutively express TLR2, TLR4, NOD1, and NOD2. Stimulation of these cells with TLR and NOD agonists caused up-regulation of the antimicrobial peptide β-defensin (129). Oral epithelial cells, in contrast to colonic epithelial cells, did not secrete cytokines such as IL-8, monocyte chemoattractant protein-1 (MCP-1), granulocyte colony stimulating factor (G-CSF), granulocyte macrophage colony-stimulating factor (GM-CSF), and vascular endothelial growth factor (VEGF) after stimulation with bacterial components but upregulated expression of peptidoglycan recognition proteins (PGRPs), a further family of pattern recognition molecules (130, 131). These results suggest that part of the cells are desensitized to prevent tissue destruction over excessive innate immune responses to bacterial stimuli, because cells and bacteria interact constitutively (130, 131).

In periodontitis an abnormal immune response known as a "hyper-responsive" phenotype was demonstrated by investigations of peripheral blood leukocytes that were stimulated with TLR2 and TLR4 agonists. The stimulation resulted in elevated levels of pro-inflammatory cytokines produced by leukocytes that were derived from patients with localized aggressive periodontitis. This altered immune response may result in rapid loss of connective tissue and periodontal attachment as well as alveolar bone, which could result in early tooth loss already in young individuals (132). A cross-sectional study examined the role of epigenetic regulation, specifically DNA methylation status, of genes in the TLR pathway in patients with localized aggressive periodontitis (LAP). Peripheral blood stimulated with *Escherichia coli* (*E. coli*) LPS was analyzed for DNA methylation of seven TLR signaling genes. At specific CpG positions in LAP patients compared to healthy controls, differences in the methylation status were observed, as well as between severe and moderate LAP. Individuals with moderate LAP presented hypermethylation of both the upregulating and downregulating genes, while severe LAP presented hypomethylation of these genes. The methylation status correlated with an increased pro-inflammatory cytokine profile in LAP patients suggesting that epigenetic modifications in TLR signaling may modulate disease progression and tissue destruction (133).

A meta-analysis assessing the association between TLR4 polymorphisms and chronic periodontitis (CP) detected an association between TLR4C > G (rs7873784) allele and CP in Asians (134). The association between TLR4 polymorphisms and gastric cancer was investigated in the meta-analysis by Jin et al. (134). This group detected an increased gastric cancer risk in TLR4 + 896A/G and TLR4 + 1196C/T polymorphism in a Caucasian population (135).

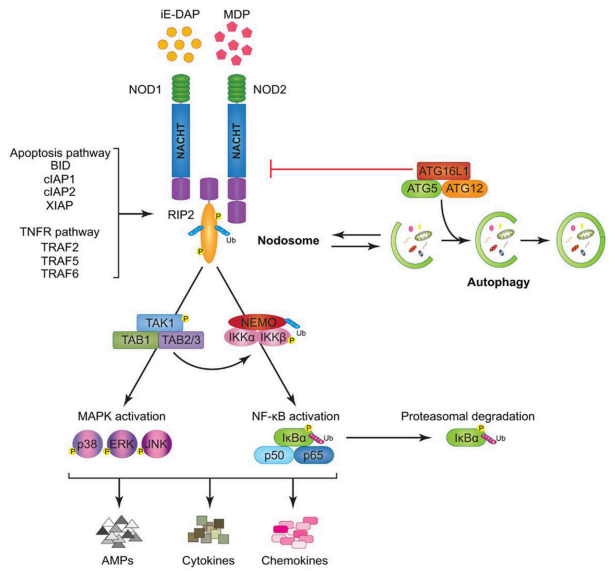

FIGURE 6 | Model of Nucleotide-binding oligomerization domain-containing protein (NOD)1 and NOD2 signaling cascades. NOD1 and NOD2 recognize bacterial peptidoglycans (PGNs), (iE-DAP), and muramyl dipeptide (MDP), respectively. Following ligand sensing the NODs recruit their common adaptor receptor-interacting serine/threonine-protein kinase (RIP)2 by caspase activation and recruitment domains (CARD)–CARD interactions and induce RIP2 to undergo phosphorylation. The members of the tumor necrosis factor receptor-associated factor (TRAF) family (TRAF2, TRAF5, and TRAF6), the inhibitor of apoptosis (IAP) family (XIAP, cIAP1, and cIAP2), and the B-cell lymphoma (BCL)2 family (BID) bind to RIP2 and facilitate its ubiquitination allowing the recruitment of transforming growth factor-β-activated kinase (TAK)1 and ubiquitinated nuclear factor (NF-κB) essential modulator (NEMO) to the nodosome. On one hand, NEMO instigates activation of the canonical NF-κB pathway by phosphorylating NF-κB inhibitor kinase (IKK)α and IKKβ, by inducing nuclear factor of kappa light polypeptide gene enhancer in B-cells inhibitor alpha (IκBα) phosphorylation and proteasomal degradation, and by freeing p50 and p65 NF-κB subunits. On the other hand, transforming growth factor-β-activated kinase 1 (TAK1) recruits, transforming growth factor-β-activated kinase binding protein (TAB)1 and TAB2/3 inducing both (p38, extracellular-signal Regulated Kinases = ERK, and JUN N-terminal kinases = JNK) mitogen activated protein kinases (MAPK) and NF-κB activation. Stimulation of both arms culminates in the induction of anti-microbial peptides (AMPs), cytokines, and chemokines. The formation of the nodosome promotes autophagy and conversely, a fully functional autophagy machinery helps in signal transduction through the nodosome. Autophagy-related protein (ATG)16L1 along with ATG5 and ATG12 is required for autophagosome formation, however, independently of its autophagy functions, ATG16L1 negatively regulates NOD/RIP2 signaling (136).

Nucleotide-Binding Oligomerization Domain Receptors (NODs)

Nucleotide-binding oligomerization domain receptors (NODs) (**Figure 6**) are cytosolic pattern recognition molecules that bind to peptidoglycan (PGN), a component of bacterial cell walls. They belong to the NOD-like receptor (NLRs) family including also NACHT-LRR (leucine-rich repeat) and pyrin-domain-containing proteins (NALPs), neuronal apoptosis inhibitor factors (NAIPs), and ICE-protease activating factor (IPAF) (137–139). The NOD1 ligand is PGN-derived γ-D-glutamylmesodiaminopimelicacid (iE-DAP) while muramyl dipeptide (MDP) is a NOD2 ligand (140, 141). MDP is detectable in Gram-negative and also in Gram-positive bacterial PGN, while iE-DAP is present in Gram-negative bacterial PGN and in PGN of particular Gram-positive bacteria such as *Bacillus subtilis* and *Listeria monocytogenes* (142). Hence, NOD1 is particularly involved in recognizing components from Gram-negative bacterial cell walls, while NOD2 can sense both (143, 144). A number of different cell types including oral epithelial cells express NOD1 that plays an essential role in innate immune responses (127, 129, 145). NOD1 binding and downstream signaling elicits an inflammatory reaction, inducing the production of cytokines, chemokines and antimicrobial peptides. Among these products, some are pro-inflammatory, such as interleukin (IL)-6, IL-8, tumor necrosis factor (TNF)-α and human beta defensin (hBD)-2, while others have immuno-regulatory or antimicrobial properties, such as interferon (IFN)-γ and human β-defensin-1 (hBD-1).The effects of iE-DAP on cytokine production have also been investigated with conflicting results: while it was reported that iE-DAP stimulated various human epithelial cells to produce anti-microbial peptides, but not pro-inflammatory cytokines like IL-6 and IL-8 (127, 129, 131, 145), it was also shown in human intestinal epithelial cells and dental pulp fibroblasts that NOD1 activation induces the production of pro-inflammatory cytokines (127, 142, 146–148).

In a human oral mucosal epithelial cell line (Leuk-1) upon stimulation activation of NOD1, receptor-interacting serine/threonine-protein kinase 2 (RIP2) and P-NF-κB was demonstrated, which was significantly inhibited by pretreatment of the cells with cigarette smoke extract (CSE). The suppressive effect of CSE on NOD1 expression was reversed following iE-DAP treatment. Combination of CSE stimulation with iE-DAP treatment prevented the further enhancement of RIP2 and P-NF-κB levels, i.e., iE-DAP reversed the inhibitory effect of CSE on NOD1 expression and prevented the over-activation of RIP2 and P-NF-κB due to CSE exposure. CSE furthermore upregulated levels of IL-6, IL-8, and TNF-α and downregulated IFN-γ level while iE-DAP enhanced the levels of IL-6, TNF-α, and IFN-γ, indicating that iE-DAP augmented gene expression and release of IL-6, TNF-α, and IFN-γ in Leuk-1 cells but diminished the mRNA level of IL-8 without affecting the production of IL-8 at protein level. These results indicate that iE-DAP is able to antagonize CSE-mediated effects on NOD1 expression and downstream signaling to a certain extent (149). In **Figure 6** a model of NOD1 and NOD2 signaling cascades is depicted.

Protease-Activated Receptors (PARs)

Protease-activated receptors (PARs) are a family of G-protein-coupled receptors (GPCRs) that include four members, PAR-1, PAR-2, PAR-3, and PAR-4, that play an important role in wound healing, inflammation, hemostasis, thrombosis, cancer progression, and embryonic development (150). PARs are activated by proteolytic cleavage of the N-terminal extracellular sequence of the receptors by a proteinase. This cleavage exposes a new N-terminal sequence, operating as a tethered ligand which, after binding to the receptor, initiates multiple signaling cascades

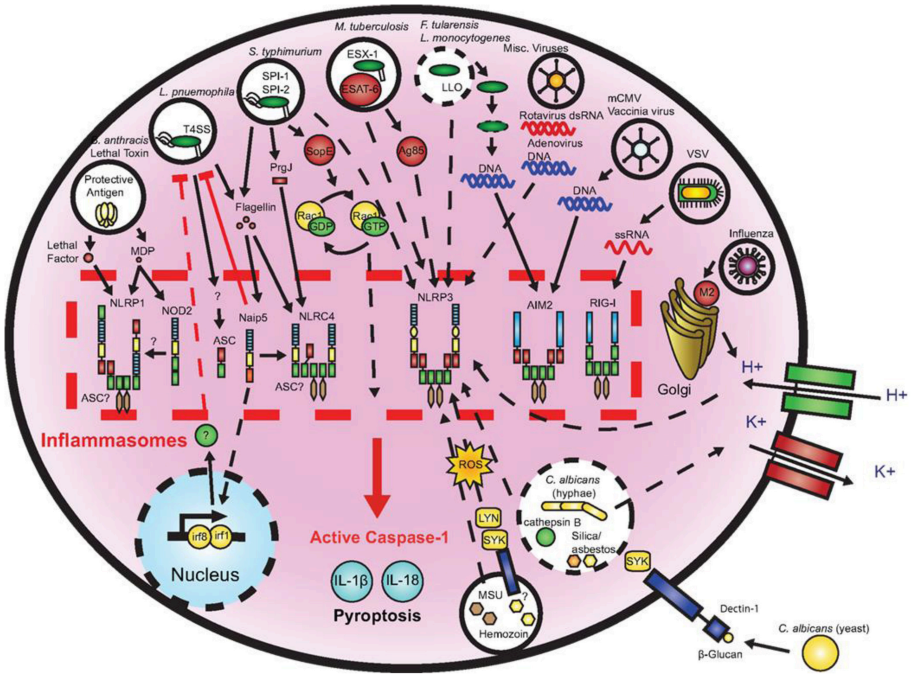

FIGURE 7 | Microbial activation of the inflammasomes. Pathogenic microorganisms activate the inflammasomes through multiple agonists and pathways. *Salmonells typhimurium (S. typhimurium)*, *Legionells pneumophila (L. pneumophila)*, and *Mycobacterium tuberculosis* (*M. tuberculosis*) reside within the host cell phagosome and are capable of activating inflammasomes through secreted flagellin, effectors, or undefined NACHT, LRR, and PYD domains-containing protein (NLRP)3 agonists. NACHT = NAIP, neuronal apoptosis inhibitor protein; C2TA, class 2 transcription activator, of the MHC; HET-E, heterokaryon incompatibility; TP1, telomerase-associated protein 1; LRR, leucine-rich repeat; PYD, PYRIN domain. *Francisella tularensis* (*F. tularensis*) and *Listeria monocytogenes* (*L. monocytogenes*), which escape the phagosome activate absent in melanoma (AIM)2 that senses cytosolic deoxyribonucleic acid (DNA). *Bacillus anthracis* (*B. anthracis*) lethal toxin activates the NLRP1 inflammasome. *Candida. albicans* (*C. albicans*) and hemozoin activate NLRP3 through Spleen tyrosine kinase (SYK) signaling. Viral-mediated inflammasome activation is heavily dependent on the detection of nucleic acids by NLRP3, AIM2, and retinoic acid-inducible gene (RIG)-I. Dotted lines indicate signaling through an unknown mechanism (161).

(151–153). Although all PARs show the same mechanism of function, it has been demonstrated that different PARs can be activated by different proteinases and show diverse distributions and biological activities (154). One main activator of PAR-1, PAR-2, and PAR-3 is thrombin, further essential activators of PAR-1 comprise activated protein C (APC) and matrix metalloproteinase-1 (MMP-1). Trypsin and human mast cell tryptase activate PAR-2 while trypsin and cathepsin G activate PAR-4. Analysis of the downstream signaling responses after activation of PARs revealed that PAR-1, PAR-2, and PAR-4 may signal autonomously, while PAR-3 rather seem to be a co-receptor for PAR-1 and PAR-4 (155–158). PARs are expressed in a number of different cell types and it has been suggested that they influence physiological processes, such as growth, development, inflammation, tissue repair, and pain. In gingival epithelial cells (GEC) the presence of PAR-1,-2 and 3 mRNA and protein expression could be demonstrated while PAR-4 was not detected. Pre-incubation of the cells with *P. gingivalis* supernatant containing proteolytic activity, induced PAR-2 mRNA up-regulation. In contrast, PAR-1 and -3 were down-regulated. The authors concluded from these results that GECs recognize *P. gingivalis* by PARs and mediate innate immunity cell responses (159). PARs, NODs, and TLR were found to exhibit a complex interplay. In silencing experiments it was shown that knock-out of one receptor type may affect the others. GEC with silenced PAR-1 and -2 reacted with up-regulated NOD1 and NOD2 expression upon stimulation with *P. gingivalis* or *Fusobacterium nucleatum* (*F. nucleatum*). Expression of TLR2 decreased after infection with *P. gingivalis* when PAR2 was knocked down but was not affected after stimulation with *F. nucleatum*, while TLR4 expression was increased after PAR2 silencing and subsequent stimulation with *F. nucleatum*. *F. nucleatum* activates TLR4, while *P. gingivalis*, due to its unique LPS structure, is able to utilize TLR2 and shut down TLR4. These data suggest that if PAR receptors are absent, expression of TLRs is modified in response to bacteria following their activation level. PRRs can function as substitute in epithelial immune-response to bacterial challenge. These responses show variations depending on the properties of the bacterial stimuli (160).

Inflammasomes

One further mechanism of the immune system to initialize a pro-inflammatory response is the so called inflammasome (**Figures 7**, **8**), a protein complex composed as multimer which develops in the cytoplasm participating in the immune response to pathogenic microbes or danger signals. The

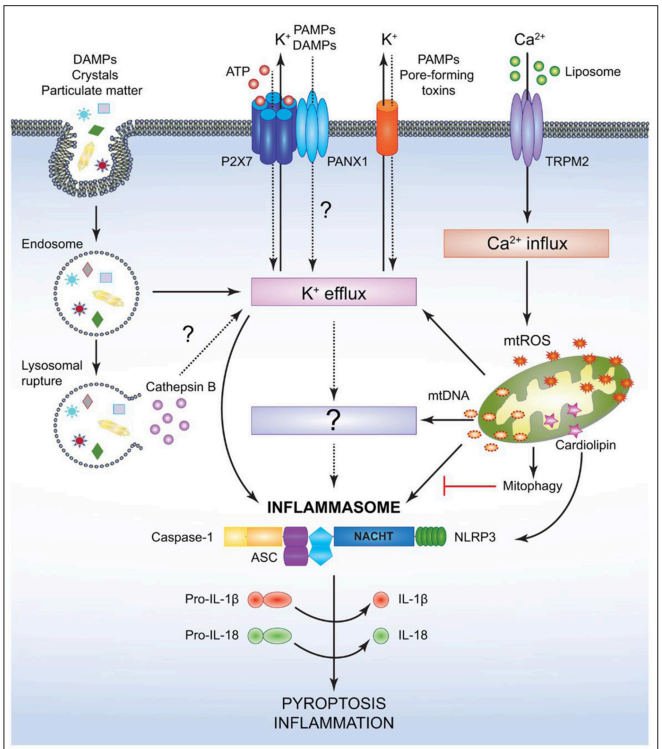

FIGURE 8 | Mechanism for canonical NACHT, LRR and PYD domains-containing protein (NLRP)3- inflammasome activation. NACHT = NAIP, neuronal apoptosis inhibitor protein; C2TA, class 2 transcription activator, of the MHC; HET-E, heterokaryon incompatibility; TP1, telomerase-associated protein 1; LRR, leucine-rich repeat; PYD, PYRIN domain. Various pathogen associated molecular patterns (PAMPs) and damage associated molecular patterns (DAMPs) provide the signal 2 required to assemble and activate the NLRP3 inflammasome comprised of NLRP3, apoptosis-associated speck-like protein (ASC), and caspase-1. Although the precise mechanism leading to NLRP3 activation is still controversial, it is speculated that potassium ion K^+ efflux may be the common cellular response that triggers inflammasome activation. However, this notion has not been fully verified and it is possible that an unidentified or intermediate adaptor may be required for transmitting signals between K^+ efflux and the NLRP3 inflammasome. Crystals and particulate DAMPs enter the cell via endocytosis directly inducing K^+ efflux and NLRP3-inflammasome formation. In addition, the endo- lysosomes carrying these DAMPs undergo lysosomal rupture and release cathepsin B, which acts as an intracellular DAMP and can induce K^+ efflux. However, contradicting studies indicate that lysosomal rupture may cause K^+ efflux and inflammasome activation even in the absence of cathepsin B. Adenosin triphosphate (ATP) binds to the P2X purinoceptor 7 (P2X7) receptor on the cell membrane and causes opening of the annexin 1 (PANX1) channels allowing K^+ efflux and influx of any PAMPs and DAMPs present in the extracellular space. PAMPs such as pore-forming toxins activate the NLRP3 inflammasome and facilitate K^+ efflux. Liposomes instigate Ca^{2+} influx through opening of (TRPM2) channels. Accumulation of excessive Ca^{2+} in the cytosol causes mitochondrial dysfunction and release of mitochondrial reactive oxygen species (mtROS) and oxidized mitochondrial deoxyribonucleic acid (mtDNA), which may activate the NLRP3 inflammasome either directly or by inducing K^+ efflux. Clearance of distressed mitochondria by mitophagy serves to evade such inflammasome activation. Mitochondrial cardiolipin binds to NLRP3 and is required for the NLRP3-inflammasome activation. Following NLRP3-inflammasome assembly, caspase-1 undergoes proximity driven proteolytic cleavage and further processes pro-interleukin (IL)-18 and pro-IL-1β into their mature active forms. Activation of the NLRP3-caspase-1 axis results in inflammation and pyroptotic cell death (136).

inflammasome induces the production and secretion of mature pro-inflammatory cytokines, IL-1β and IL-18 eventually leading to pyroptosis, a special kind of cell death (162–165). Inflammasomes can be grouped into canonical and noncanonical pathways (162, 164–167). Typically, a functional canonical inflammasome complex consists of a nucleotide-binding domain leucine-rich repeat (NLR) protein, an adaptor molecule apoptosis-associated speck-like protein containing a CARD (ASC) domain, and caspase-1 (167). The composition of the upstream regulators and specific molecules of the inflammasome depends on the type of the danger signals and the microbial inducers (164). The best characterized NLR, the pyrin domain containing 3 (NLRP3) inflammasome (**Figure 8**) for example is activated by extracellular adenosine triphosphate (eATP) danger signaling by the purinic receptor 2X7 (P2X7) and reactive oxygen species (ROS). Infection with bacterial pathogens can induce the NLRP3 inflammasome. Specific activation of the absent in melanoma (AIM)2 inflammasome is triggered by sensing double-stranded DNA in the cytosol while the IL-1β-converting enzyme (ICE) protease-activating factor (IPAF) inflammasome is activated by Gram-negative bacteria (e.g., *Salmonella typhimurium*, *Shigella flexneri*, *Legionella pneumophila*, and *Pseudomonas aeruginosa*) which have type III or IV secretion systems (164). In gingival epithelial cells *F. nucleatum* also activates the NLRP3 inflammasome, which in turn activates caspase-1 and stimulates secretion of mature IL-1β (168).

P. gingivalis is able to inhibit the innate immune response using a nucleoside-diphosphate kinase (NDK) after stimulation with extracellular (e)ATP. The danger signal eATP binds to P2X7 receptors leading to activation of the inflammasome and caspase-1. Thus, exposure of gingival epithelial cells (GECs) to wild-type *P. gingivalis* was demonstrated to result in blockade of ATP-induced caspase-1 activation while NDK-deficient *P. gingivalis* showed fewer effects.

P. gingivalis NDK was shown to modify release of high-mobility group protein B1 (HMGB1), another pro-inflammatory danger signal, which, in non-infected cells, remains linked to chromatin. Infection with wild-type or NDK-deficient *P. gingivalis* induced release of HMGB1 from the nucleus to the cytosol. HMGB1 was delivered to the extracellular space when non-infected GECs were stimulated with ATP. HMGB1 was released in higher extend, when ATP-treated cells were infected with NDK-deficient mutants instead of wild-type *P. gingivalis*. These results suggest that NDKs are significantly involved in inhibiting P2X7-dependent inflammasome activation and HMGB1 release from bacterially infected GECs (169).

A multitude of inflammasomes exists, which can be activated by varying mechanisms resulting in the maturation and secretion of pro-inflammatory cytokines (170, 171). Extracellular ATP, one of the first activators that was discovered to induce NLRP3 inflammasome formation, is considered to belong to the group of endogenous damage-associated molecular patterns (DAMPs) released by dying or injured cells (172, 173). It exhibits minor presence in healthy tissues, but may increase to high micromolar concentrations at inflamed sites following tissue

damage (174). Studies demonstrated that eATP caused caspase-1 activation that was followed by IL-1β release (175, 176). Yilmaz et al. (177) revealed that LPS-treated or infected gingival epithelial cells (GECs) did not secrete IL-1β unless they were stimulated with eATP and that eATP did not alter NLRP3 or apoptosis-associated speck like protein (ASC) expression in *P. gingivalis* infected gingival epithelial cells. NLRP10 is the smallest human NLR protein. It is different from the other NLR proteins because of its lack of the leucine-rich repeat domain, which is involved in ligand sensing or binding. Upon infection with two periodontal pathogens, *T. forsythia* and *F. nucleatum* the human oral epithelial cell line HOK-16B reacted with up-regulated mRNA and protein expression of NLRP10 while infection with *Streptococcus oralis* (*S. oralis*) did not induce this effect. These results demonstrate that NLRP10 up-regulation in HOK-16B cells is pathogen-specific (178). **Figure 7** demonstrates microbial activation of the inflammasomes.

CYTOKINE PRODUCTION AND RELEASE

Interleukin (IL)-8 response of gingival epithelial cells after exposure to different multispecies biofilms was differentially regulated (179). Characterization of the whole secretome after biofilm challenge with species of the red complex demonstrated that more proteins were downregulated than up-regulated (180).

Keratinocytes are able to produce a variety of cytokines such as IL-1, IL-6, IL-8, and tumor necrosis factor (TNF)-α. They maintain normal homeostatic mechanisms and can induce proliferative effects upon injury. Mucosal cytokines may have pro-inflammatory as well as anti-inflammatory functions. An imbalance in the cytokine levels can support inflammatory diseases. Cytokines provide a paracrine (between adjacent cells), an endocrine (cells at distant sites) and an autocrine (intercellular) cell-to-cell communication system. Cytokines, based on different functions, origins, and chemical structures, are classified into the following groups: ILs, TNFs, chemokines, colony-stimulating factors (CSF), interferons (IFNs), and growth factors (GF). Cytokines share a multitude of activities and functions (pleiotropic and redundant), thus they could be classified in more than one group. IL-3 for example may also be classified in the CSF group (181). The IL-1 cytokines (IL-1α, IL-1β, and IL-1Ra) are important in regulation of immune response and inflammation because they induce the expression of many effector proteins, e.g., cytokines/chemokines, nitric oxide synthetase, and MMPs (182).

The immortalized human oral epithelial cell line OKF6-TERT2 responds to co-incubation with *in vitro* cultured biofilms of single- and mixed-bacterial species consisting of *P. gingivalis*, *F. nucleatum, Aggregatibacter actinomycetemcomitans* (*A. actinomycetemcomitans*) and *Streptococcus mitis* (*S. mitis*) with increased expression of mRNA for IL-8, C-X-C motif chemokine ligand 3 (CXCL3), CXCL1, IL-1, IL-6, CSF-2, and TNF-α. The response was biggest after stimulation with mixed-species biofilms (183).

The chemokine IL-8 shows crucial importance in oral health because it supports the transition of activated immune cells into and through gingival tissues, and promotes immune cell adhesion, tissue remodeling, and angiogenesis (184). IL-8 is increased in the saliva of patients with oral carcinomas. It could probably be a biomarker for the detection of oral and oropharyngeal squamous cell carcinomas (185). In patients with severe periodontitis, IL-8 was also detected in high levels in crevicular fluid at healthy sites (186). Schueller et al. investigated the basal release levels of IL-8, and linked it to the bacterial community, personal oral hygiene and nutrition in persons with a healthy gingival situation (187). It was shown that the basal IL-8 release was between 9.9 and 98.2 pg/ml, and bacterial biofilms were distinctive for healthy oral microbiota. An association between basal IL-8 levels and the oral microbiota was detected, suggesting a link between oral bacteria and the inflammatory state. A link between nutrition, personal oral hygiene, oral microbiota and IL-8 levels was also reported. The identification of indicator bacteria in healthy subjects with high levels of IL-8 release was regarded as important as they possibly are promising indicators for the onset of oral diseases (187). Fujimura et al. (188), reported that the hemophoric hemoglobin receptor (HbR), that binds hemoglobin and captures porphyrin and heme (*P. gingivalis* needs iron to grow), in interaction with host cells, affected cellular signal transduction of these cells, followed by inhibited differentiation of osteoclasts from bone marrow macrophages (188). The IL-8 inducing function of HbR from host epithelial cells was demonstrated to be maintained by activation of cellular signal transduction. Increased expression of IL-8 by gingival epithelial cells was induced by HbR in a dose dependent manner. This process is associated with activation of p38 MAPK and Erk1/2 using silencing (si)RNAs and inhibitors (189).

IL-33 belongs to the IL-1 cytokine family and is constitutively expressed in the nuclei of epithelial and endothelial cells (190). Epithelial cell-derived IL-33 augments T helper cell (Th)2 cytokine-mediated inflammatory immune response upon bacterial challenge (191). IL-33 was detected in inflamed gingival epithelium from chronic periodontitis patients. Enhanced IL-33 expression induced by *P. gingivalis* was detected in the cytoplasm of human gingival epithelial cells *in vitro*. In contrast, *P. gingivalis* fimbriae, lipopolysaccharide or lipopeptide did not induce this effect. Inhibition of *P. gingivalis* proteases (gingipains) blocked IL-33 mRNA induction. Also the *P. gingivalis* gingipain-null mutant KDP136 did not up-regulate IL-33 expression. Silencing of PAR-2 and inhibition of phospholipase C, p38 and NF-κB restrained the *P. gingivalis* induced IL-33 expression. These results indicate activation of the PAR-2/IL-33 axis in human gingival epithelial cells by *P. gingivalis* via a gingipain-dependent mechanism (192).

The angiopoietin-like protein (ANGPTL), belongs to a family of eight secreted glycoproteins, but doesn't bind to the tyrosine kinase with immunoglobulin-like and EGF-like domains (Tie)2 angiopoietin receptor or to the related protein Tie1, and, classified as orphan ligand, appears to exhibit biological functions different from angiopoietins (193–195). ANGPTL2 manages tissue homeostasis by induction of inflammation and angiogenesis (194, 196). Elevated ANGPTL2 concentrations are present in gingival crevicular fluid (GCF)

from chronic periodontitis patients and stimulation with *P. gingivalis* LPS up-regulated ANGPTL2 mRNA and protein levels in gingival squamous cell carcinoma Ca9-22 cells. Recombinant human ANGPTL2 caused augmented IL-1β, IL-8, TNF-α mRNA and protein levels in Ca9-22 cells. Silencing of ANGPTL2 and blocking antibodies against the ANGPTL receptor integrin α5β1 inhibited the IL-1β, IL-8, and TNF-α mRNA and protein up-regulation, which suggests that ANGPTL secretion induces inflammatory cytokines in gingival epithelial cells through an autocrine loop. Thus, a new inflammatory cytokine induction cascade featuring sequential *P. gingivalis* LPS-ANGPTL2-integrin α5β1 activation was detected which might be responsible for periodontal destructive processes induced by gingival epithelial cells. Thus ANGPTL2 participates in the pathogenesis of periodontitis and may promote continuous chronic inflammation (197).

An immortalized human gingival cell line reacted with enhanced IL-8 and IL-6 mRNA concentrations and supported phosphorylation of ERK and p38 MAP kinase upon infection with *A. actinomycetemcomitans* (198).

A. actinomycetemcomitans, a member of the taxonomic family *Pasteurellaceae,* has been related to the development of aggressive periodontitis and may also promote chronic periodontitis (199–201). Amongst other pathogenic members of the periodontal biofilm, *A. actinomycetemcomitans* produces various substances that are able to damage cells and tissues in a direct or indirect manner. As a member of the oral biofilm this bacterium is known to express complex operons for two cytotoxins, leukotoxin (Lkt) and cytolethal distending toxin (Cdt) (202, 203). These toxins are able to impair the host's immune response and thus may promote the pathogenesis of periodontitis (204). Human gingival epithelial cells (HGECs) were stimulated with 50 clinical strains and 7 reference strains of *A. actinomycetemcomitans*, including various serotypes and non-serotypeable strains, strains from deep or shallow pockets, and reference serotype strains, and investigated for the expression of IL-1β, IL-6, IL-8, and TNF-α mRNAs. Results showed that IL-8 mRNA was strongly up-regulated after stimulation with clinically obtained *A. actinomycetemcomitans* and also with reference strains. Serotype f induced the highest expression in comparison to the other serotypes. The JP2-like leukotoxin promoter gene and non-serotypeable (NS) 1 and NS2 caused lesser IL-8 induction compared to serotypeable strains, and IL-8 up-regulation after stimulation with clinical strains from deep pockets showed also significantly lower levels than those isolated from shallow pockets. These results indicate that JP2-like leukotoxin NS1 and NS2 from clinical isolates of *A. actinomycetemcomitans,* obtained from deep pockets, are able to affect neutrophil function by lowering the IL-8 responses, which results in immunosuppression that may support virulence and survival of these bacteria (205).

Influence of *Treponema denticola*

T. denticola is a Gram-negative anaerobic oral spirochete that is known as a member of periodontal pathogens and is associated with chronic periodontitis (206, 207). It possesses a variety of virulence factors including dentilisin, an active cell-surface-located protease that cleaves at phenylalanyl/alanyl and prolyl/alanyl bonds, trypsin-like protease activity and the capability for motility and chemotaxis via periplasmic flagella [for Review see Dashper et al. (208)].

On primary gingival epithelial cells it has been demonstrated that *T. denticola* fails to induce IL-8 production that can't be explained by IL-8 degradation, as a protease mutant that does not degrade IL-8 also didn't induce IL-8 production. *T. denticola* furthermore failed to promote transcription of IL-8 and hβD-2 mRNA. This impaired epithelial cell response to *T. denticola* suggests contribution to the pathogenesis of periodontitis by deficient chemotaxis initiation of neutrophils into the periodontal pocket (209). The mechanism of IL-8 suppression by *T. denticola* was investigated using immortalized human gingival epithelial (HOK-16B) cells. Dentisilin degraded TNF-α, an IL-8-inducing cytokine, suggesting modulation of IL-8 (210). In monocytes derived from human peripheral blood mononuclear cells the role of *T. denticola* periplasmic flagella (PF) was investigated. Stimulation of the innate immune response via PAMPs revealed, that flagella-exhibiting wild type *T. denticola* induced the production of the cytokines TNF-α, IL-1, IL-6, IL-10, and IL-12 over activation of nuclear factor (NF)-κB through toll like receptor (TLR)2. These results suggest that *T. denticola* activates the innate immune response in a TLR2-dependent way and that flagella are involved as key bacterial components (211).

The IL-17 family, consisting of IL-17A–IL-17F, plays an important role in host defense against microbial challenge and has also been demonstrated to be crucial in pathogenesis of periodontitis (212). Initially IL-17A was regarded as a cytokine exclusively expressed by Th17 cells (213) but subsequent studies revealed that other cellular sources are capable to express IL-17A, including γδ T cells, natural killer cells, neutrophils, eosinophils, mast cells and macrophages (212). In gingival tissues of periodontitis patients (214–217) presence of IL-17 producing cells correlates with severity of inflammation in periodontitis lesions (218). Furthermore, elevated IL-17A levels were detected in GCF of patients with periodontitis. The IL-17A levels are reduced after non-surgical therapy (219, 220). Awang et al. (221) analyzed clinical linkage between cytokines of the IL-17 family and periodontitis and the biological effect of IL-17A and IL-17E using *in vitro* model systems. According to their studies serum, saliva and GCF IL-17A levels are increased in periodontitis patients and correlate with the clinical parameters attachment loss, pocket depth and bleeding on probing. Periodontitis patients exhibit lower IL-17E serum levels and the IL-17A-IL-17E ratio in serum also correlates positively with clinical parameters. *In vitro*, IL-17E suppressed IL-17A and *P. gingivalis* induced chemokine-expression by inhibiting phosphorylation of the NF-kB p65 subunit, which indicated that in the pathogenesis of periodontitis the serum IL-17A-IL-17E ratio might be a marker of disease severity while IL-17E is opposing IL-17A. IL-17E produced by oral keratinocytes may down-regulate IL-17A in the periodontium (221).

IMMUNO-MODULATION, BACTERIAL INFECTION AND CANCER CELLS

Role of Growth Arrest-Specific 6 (GAS6)

The growth arrest-specific 6 (GAS6) and Protein S (PROS1) are ligands of the tyrosin-protein kinase receptor (TYRO)3, AXL, and proto-oncogene (MERTK or TAM) receptor tyrosine kinases (222), which are involved in a number of biological processes including immune regulation (223). GAS6 is constitutively expressed in oral epithelial cells and was shown to downregulate epithelial activation at equilibrium state in order to sustain homeostasis (224). In the oral mucosa, the superficial layers of the epithelium express GAS6 together with its predominant receptor AXL. After birth GAS6 expression is induced in a MYD88-dependent way by the developing microbiota. GAS6 expressed by dendritic cells (DCs) was shown to inhibit IL-6 production by supporting development of T regulatory (Treg) cells and diminishing Th17 cell generation. This provides a more tolerogenic immunological environment for the oral microbiota (224). GAS6/AXL signaling seems to play a crucial role in the regulation of homeostasis in the oral mucosa. Thus, pathogens affecting the GAS6/AXL axis might generate a dysbiotic state and subsequent oral pathology. The induction of oral adaptive immune responses by specific pathogens is abolished in *Gas6*−/− mice and GAS6 is able to induce simultaneously pro- and anti-inflammatory regulatory pathways after mice were infected with *P. gingivalis*. GAS6 not only upregulates the expression of adhesion molecules in blood vessels which supports extravasation of immune cells belonging to the innate immune response, it also increases the expression of CCL19 and CCL21 chemokines and thus supports oral DCs to migrate to the lymph nodes. In addition the expression of the pro-inflammatory molecules P-selectin, intercellular adhesion molecule 1 (ICAM-1), and vascular cell adhesion molecule 1 (VCAM-1) in the oral mucosa is downregulated by GAS6. Furthermore, GAS6 blocks DC maturation and decreases antigen presentation by DCs to T cells. The authors concluded that GAS6 facilitates migration of inflammatory cells and DCs through the endothelium in both directions, while T-cell stimulation and activation of the mucosa is inhibited. This highly regulated activity of GAS6 supports a rapid but still moderate mucosal immunity to oral pathogens (225).

Bacterial Infection and Cancer Cells

Evidence suggests an increased risk for cancer in chronic infections and inflammation. Bacterial infections and carcinogenesis seem to be connected (226). Periodontitis, one of the most common chronic human inflammatory diseases, is caused by microorganisms in the oral biofilm that trigger local inflammation. Periodontitis induces epithelial proliferation and apical migration along the root surface of the tooth and leads to a constant release of inflammatory cytokines, growth factors, prostaglandins, and enzymes, which all of them are closely associated with the development of cancer (226). In previous studies by Tezal et al. (226, 227) it was reported that the assumed association between periodontitis and oral neoplasms is significant. High PD-L1 expression has been linked to different types of human malignancies like lung cancer, pancreatic cancer, oral cancer, kidney cancer, breast and gastric cancer (228, 229). Head and neck cancer belongs to the 10 most frequent cancers worldwide (230). About 95% of the cases are of the squamous cell carcinoma (SCC) type. Tumors can only grow if their tissue environment provides them with a milieu that sustains their growth and spread. Alterations of tissue homeostasis by infection or inflammation can compromise stromal structural integrity and support tumorigenesis (231).

Programmed death ligand 1 (PD-L1, also called B7-H1) belongs to the B7 family and plays an important role in the regulation of cell-mediated immune response (232, 233). PD-L1 mediated signals are essential in co-signaling of T cell activation and tolerance (234). PD-L1 signals are also able to downregulate T cell functions and survival (228, 235). Modification of immune responses in cancer sites is a crucial mechanism that is linked to immune evasion of tumors. In the tumor microenvironment PD-L1 and programmed death receptor 1 (PD-1) may interact and induce tumor-protective mechanisms by activation of multiple specific pathways including ligation of PD-1 by PD-L1 on antigen specific T cells. This in turn may lead to functional anergy and/or apoptosis of these effector T cells. Ligation of PD-1 by PD-L1 possibly promotes tolerance and directly protects the tumor from apoptosis by reverse signaling through PD-L1 (228, 236, 237). It was demonstrated that *P. gingivalis* W83 up-regulates PD-L1 in oral cancer cells and in primary as well as in immortalized human gingival keratinocytes (238). High levels of PD-L1 were demonstrated in invasive oral squamous carcinoma cells (239). Also, positive PD-L1 expression was detected in tissue samples of oral squamous cell carcinomas *ex vivo* (240). Membrane proteins of *P. gingivalis* are responsible for the up-regulation while cytosolic proteins failed to induce PD-L1 (241). Primary human gingival keratinocytes (PHGK) and oral squamous cell carcinoma (SCC-25) cells up-regulated a number of inflammation-related genes upon infection with *P. gingivalis* membranes, amongst them members of the downstream NF-κB signaling pathway, TLR signaling and MAPK pathways. These data not only suggest that *P. gingivalis* membrane induces a pro-inflammatory response in malignant and non-malignant oral epithelial cells, but also indicates a possible link between infection and oral carcinomas, since p38 MAPK and MEK4-JNK1 signaling pathways were shown to be involved in context of tumor microenvironment and the control of cancer growth (242).

In a Chinese population an increased risk for head and neck carcinomas in individuals with oral submucous fibrosis, oral leukoplakia and repetitive dental ulcers was demonstrated suggesting a strong association between these diseases and cancer (243). Also patients with colorectal cancer carry strains of *F. nucleatum* in the cancerous lesions. *F. nucleatum* is one of the most densely colonized bacterial species in the oral cavity and known to be associated with periodontitis (244). The effect of oral pathogens on the development of oral tumors was investigated by Hoppe et al. (245). Stimulation of oral tumor cells with *P. gingivalis* led to increased cell proliferation while in contrast, *A. actinomycetemcomitans* promoted cell death. Bacteria as well as anti-microbial peptides induced diverse

effects on the transcription levels of the oncogenic defensin genes and epidermal growth factor receptor (EGFR) signaling. The primary impact of the two oral pathogens were opposite on the proliferation behavior of oral tumor cells. In contrast, both induced similar secondary effects on the proliferation rate by modulating the extend of oncogenic important α-defensin gene expression. Human defensins differently modify epidermal growth factor receptor signaling, supporting the assumption that these anti-microbial peptides are possible ligands of EGFR. Interaction of these two molecules may cause the modification of the proliferative behavior of oral tumor cells (245). A newly established model of long term infection by stimulating human immortalized oral epithelial cells (HIOECs) with *P. gingivalis* at a low multiplicity of infection (MOI) for 5–23 weeks was used to investigate possible alterations in tumors. Persistent infection with *P. gingivalis* induced changes in cell morphology, enhanced proliferative capability and promoted cell migratory and invasive properties. Furthermore, tumor-related genes including GAS6 and PD-L1 that possibly act as key regulators in transformation from non-cancerous to tumor cells were upregulated as a reaction to long-term exposure of *P. gingivalis*. The authors concluded that *P. gingivalis* is able to support tumorigenic characteristics of HIOECs, suggesting that chronic *P. gingivalis* infection possibly represents a risk factor for oral cancers (246). Using a newly-established murine oral tumorigenesis model that is associated with periodontitis, it was reported that chronic bacterial infection supports development of OSCC, inducing enhanced signaling of the IL-6- signal transducer and activator of transcription 3 (STAT3) pathway. The results indicate that periodontal pathogens like *P. gingivalis* and *F. nucleatum* promote tumorigenesis by interacting directly with oral epithelial cells through TLR2. Furthermore, these pathogens stimulate the proliferation of human OSCC and induce expression of molecular key factors that take part in tumorigenesis, such as STAT3, that becomes activated in response to interferons, EGF, IL-5, IL-6, and cyclin D1, which is required for progression through the G1 phase of the cell cycle and induces cell migration. These findings represent a function of oral bacteria in the mechanism of chemically induced OSCC tumorigenesis (247).

The epithelial–mesenchymal transition (EMT) is critical in the conversion of normal epithelial cells into carcinoma cells during carcinogenesis. Downregulation of E-cadherin and up-regulation of N-cadherin and the transcription factors zinc finger protein SNAI1 (=Snail), SNAI2 (=Slug) and zinc finger e-box-binding homeobox (Zeb)1 are typical markers for this conversion (248). In a newly established long term infection *in vitro* model Lee et al. (249) demonstrated that primary oral epithelial cells after 120 h of infection with *P. gingivalis* develop an EMT phenotype including decrease of E-cadherin and increase of Slug, Snail, and Zeb1 expression. Infection of primary rat epithelial cell cultures with periodontal pathogens for 8 days caused an enhanced percentage of vimentin-positive cells, 20% after stimulation with *P. gingivalis* and 30% after infection with *F. nucleatum*. Furthermore, the periodontal pathogens induced augmented activation of Snail and the electrical impedance in comparison with unexposed controls of the cultures was reduced. The capability of the cells to migrate was extended as reaction to bacterial stimulation, demonstrated by the number of migrating cells and scratch-wound closure rates. In conclusion, persistent stimulation of primary rat oral keratinocyte cultures to periodontal pathogens elicited EMT-like properties, which indicates that this process may promote loss of epithelial integrity (250).

CONCLUSIONS

The composition of the gingival epithelial barrier is quite complex since its structure composes of a huge number of different molecules. Keratins are the major component of the keratinizing stratified epithelial cytoskeleton. Depending on localization and function different epithelia express a distinct cytokeratin pattern. In order to sustain their function, stratified epithelia, including the oral mucosa, have to sustain tight cell-cell adhesion in the viable cells that involves intercellular tight and adherens junctions which connect to the actin cytoskeleton. Oral tissue immune response is able to recognize microbial infection and colonization and is able to manage it. The epithelial cells express a number of pattern recognition receptors, including TLRs, NOD1, NOD2 and PARs and are able to assemble different kinds of inflammasomes and express a variety of pro-inflammatory cytokines and chemokines. Resident oral bacteria permanently influence epithelial host cells. Depending on their composition biofilms differentially modify cellular immune responses of the epithelium. Major periodontal pathogens like *P. gingivalis* possess a number of different strategies to escape from innate immunity and survive in the tissues, which affects the epithelial barrier by modifying the expression and integrity of the different cell-cell junctions.

The balanced immune-inflammatory state of the host with its biofilm in health may be disturbed by distinct species, such as *P. gingivalis* and *F. nucleatum* that are able to destroy this equilibrium, causing a dysbiotic microbiota (251). Chronic infections and persistent inflammation are associated with an increased risk of cancer. Persisting bacterial agents may induce up-regulation of immune-inhibitory receptors which in turn facilitate the ability of cancer cells to evade from anti-tumor immune responses of the host. Furthermore, long term infection possibly supports carcinogenesis by regulating gene expressions of the infected epithelial cells in a way that leads to development into a phenotype indicating cellular transformation from normal to cancerous.

AUTHOR CONTRIBUTIONS

SG wrote the manuscript. JM corrected the manuscript and assisted in writing.

REFERENCES

1. Gartner LP. Oral anatomy and tissue types. *Semin Dermatol.* (1994) 13:68–73.
2. Garant PR. *Oral Cells and Tissues*. Illinois, IL: Quintessence Publishing Co., Inc. (2003).
3. Schroeder HE, Listgarten MA. The gingival tissues: the architecture of periodontal protection. *Periodontol* (1997)13:91–120.
4. Squier CA, Kremer MJ. Biology of oral mucosa and esophagus. *J Natl Cancer Inst Monogr.* (2001) 29:7–15.
5. Groeger SE, Meyle J. Epithelial barrier and oral bacterial infection. *Periodontol* (2015) 69:46–67. doi: 10.1111/prd.12094
6. Pollanen MT, Salonen JI, Uitto VJ. Structure and function of the tooth-epithelial interface in health and disease. *Periodontol* (2003) 31:12–31. doi: 10.1034/j.1600-0757.2003.03102.x
7. Steinert PM, Roop DR. Molecular and cellular biology of intermediate filaments. *Annu Rev Biochem.* (1988) 57:593–625.
8. Moll R, Franke WW, Schiller DL, Geiger B, Krepler R. The catalog of human cytokeratins: patterns of expression in normal epithelia, tumors and cultured cells. *Cell* (1982) 31:11–24. doi: 10.1016/0092-8674(82)90400-7
9. Su L, Morgan PR, Lane EB. Protein and mRNA expression of simple epithelial keratins in normal, dysplastic, and malignant oral epithelia. *Am J Pathol.* (1994) 145:1349–57.
10. Moll R, Divo M, Langbein L. The human keratins: biology and pathology. *Histochem Cell Biol.* (2008) 129:705–33. doi: 10.1007/s00418-008-0435-6
11. Dale BA, Salonen J, Jones AH. New approaches and concepts in the study of differentiation of oral epithelia. *Crit Rev Oral Biol Med.* (1990) 1:167–90. doi: 10.1177/10454411900010030201
12. Collin C, Ouhayoun JP, Grund C, Franke WW. Suprabasal marker proteins distinguishing keratinizing squamous epithelia: cytokeratin 2 polypeptides of oral masticatory epithelium and epidermis are different. *Differentiation* (1992) 51:137–48. doi: 10.1111/j.1432-0436.1992.tb00690.x
13. Mackenzie IC, Rittman G, Gao Z, Leigh I, Lane EB. Patterns of cytokeratin expression in human gingival epithelia. *J Periodontal Res.* (1991) 26:468–78. doi: 10.1111/j.1600-0765.1991.tb01797.x
14. Berkovitz BKB HG, Moxham BJ. *Oral Anatomy, Histology and Embryology*. Edinbergh: Elsevier limited. (2009).
15. Nanci A. Ten *Cate's Oral Histology, Development, Structure and Function*. Mosby, MO: Elsevier Mosby (2008).
16. Alberts B JA, Lewis J, Raff M, Roberts K, Walter P. *Molecular Biology of the Cell*. New York, NY: Garland Science (2002).
17. Rao RS, Patil S, Ganavi BS. Oral cytokeratins in health and disease. *J Contemp Dent Pract.* (2014) 15:127–36. doi: 10.5005/jp-journals-10024-1502
18. Hajishengallis G, Lamont RJ. Beyond the red complex and into more complexity: the polymicrobial synergy and dysbiosis (PSD) model of periodontal disease etiology. *Mol Oral Microbiol.* (2012) 27:409–19. doi: 10.1111/j.2041-1014.2012.00663.x
19. Abusleme L, Dupuy AK, Dutzan N, Silva N, Burleson JA, Strausbaugh LD, et al. The subgingival microbiome in health and periodontitis and its relationship with community biomass and inflammation. *ISME J.* (2013) 7:1016–25. doi: 10.1038/ismej.2012.174
20. Hajishengallis G, Darveau RP, Curtis MA. The keystone-pathogen hypothesis. *Nat Rev Microbiol.* (2012) 10:717–25. doi: 10.1038/nrmicro2873
21. Hajishengallis G. Immunomicrobial pathogenesis of periodontitis: keystones, pathobionts, and host response. *Trends Immunol.* (2014) 35:3–11. doi: 10.1016/j.it.2013.09.001
22. Hajishengallis G. The inflammophilic character of the periodontitis-associated microbiota. *Mol Oral Microbiol.* (2014) 29:248–57. doi: 10.1111/omi.12065
23. Presland RB, Jurevic RJ. Making sense of the epithelial barrier: what molecular biology and genetics tell us about the functions of oral mucosal and epidermal tissues. *J Dent Educ.* (2002) 66:564–74.
24. Mehta D, Malik AB. Signaling mechanisms regulating endothelial permeability. *Physiol Rev.* (2006) 86:279–367. doi: 10.1152/physrev.00012.2005
25. Niessen CM. Tight junctions/adherens junctions: basic structure and function. *J Invest Dermatol.* (2007) 127:2525–32. doi: 10.1038/sj.jid.5700865
26. Anderson JM. Molecular structure of tight junctions and their role in epithelial transport. *News Physiol Sci.* (2001) 16:126–30.
27. Tsukita S, Furuse M, Itoh M. Multifunctional strands in tight junctions. *Nat Rev Mol Cell Biol.* (2001) 2:285–93. doi: 10.1038/35067088
28. Dejana E. Endothelial cell-cell junctions: happy together. *Nat Rev Mol Cell Biol.* (2004) 5:261–70. doi: 10.1038/nrm1357
29. Furuse M, Fujita K, Hiiragi T, Fujimoto K, Tsukita S. Claudin-1 and -2: novel integral membrane proteins localizing at tight junctions with no sequence similarity to occludin. *J Cell Biol.* (1998) 141:1539–50. doi: 10.1083/jcb.141.7.1539
30. Furuse M, Sasaki H, Fujimoto K, Tsukita S. A single gene product, claudin-1 or−2, reconstitutes tight junction strands and recruits occludin in fibroblasts. *J Cell Biol.* (1998) 143:391–401. doi: 10.1083/jcb.143.2.391
31. Matter K, Aijaz S, Tsapara A, Balda MS. Mammalian tight junctions in the regulation of epithelial differentiation and proliferation. *Curr Opin Cell Biol.* (2005) 17:453–8. doi: 10.1016/j.ceb.2005.08.003
32. Kohler K, Zahraoui A. Tight junction: a co-ordinator of cell signalling and membrane trafficking. *Biol Cell* (2005) 97:659–65. doi: 10.1042/BC20040147
33. Tsukita S, Furuse M. Overcoming barriers in the study of tight junction functions: from occludin to claudin. *Genes Cells* (1998) 3:569–73. doi: 10.1046/j.1365-2443.1998.00212.x
34. Furuse M, Hata M, Furuse K, Yoshida Y, Haratake A, Sugitani Y, et al. Claudin-based tight junctions are crucial for the mammalian epidermal barrier: a lesson from claudin-1-deficient mice. *J Cell Biol.* (2002) 156:1099–111. doi: 10.1083/jcb.200110122
35. Tsukita S, Furuse M. Claudin-based barrier in simple and stratified cellular sheets. *Curr Opin Cell Biol.* (2002) 14:531–6. doi: 10.1016/S0955-0674(02)00362-9
36. Tang VW, Goodenough DA. Paracellular ion channel at the tight junction. *Biophys J.* (2003) 84:1660–73. doi: 10.1016/S0006-3495(03)74975-3
37. Furuse M, Sasaki H, Tsukita S. Manner of interaction of heterogeneous claudin species within and between tight junction strands. *J Cell Biol.* (1999) 147:891–903. doi: 10.1083/jcb.147.4.891
38. Furuse M. Knockout animals and natural mutations as experimental and diagnostic tool for studying tight junction functions *in vivo*. *Biochim Biophys Acta* (2009) 1788:813–9. doi: 10.1016/j.bbamem.2008.07.017
39. Furuse M, Hirase T, Itoh M, Nagafuchi A, Yonemura S, Tsukita S, et al. Occludin: a novel integral membrane protein localizing at tight junctions. *J Cell Biol.* (1993) 123(6 Pt 2):1777–88. doi: 10.1083/jcb.123.6.1777
40. Muresan Z, Paul DL, Goodenough DA. Occludin 1B, a variant of the tight junction protein occludin. *Mol Biol Cell* (2000) 11:627–34. doi: 10.1091/mbc.11.2.627
41. Shen L, Turner JR. Actin depolymerization disrupts tight junctions via caveolae-mediated endocytosis. *Mol Biol Cell* (2005) 16:3919–36. doi: 10.1091/mbc.e04-12-1089
42. Utech M, Mennigen R, Bruewer M. Endocytosis and recycling of tight junction proteins in inflammation. *J Biomed Biotechnol.* (2010) 2010:484987. doi: 10.1155/2010/484987
43. Yu AS, McCarthy KM, Francis SA, McCormack JM, Lai J, Rogers RA, et al. Knockdown of occludin expression leads to diverse phenotypic alterations in epithelial cells. *Am J Physiol Cell Physiol.* (2005) 288:C1231–41. doi: 10.1152/ajpcell.00581.2004
44. Hatakeyama S, Yaegashi T, Oikawa Y, Fujiwara H, Mikami T, Takeda Y, et al. Expression pattern of adhesion molecules in junctional epithelium differs from that in other gingival epithelia. *J Periodontal Res.* (2006) 41:322–8. doi: 10.1111/j.1600-0765.2006.00875.x
45. Ye P, Yu H, Simonian M, Hunter N. Expression patterns of tight junction components induced by CD24 in an oral epithelial cell-culture model correlated to affected periodontal tissues. *J Periodontal Res.* (2014) 49:253–9. doi: 10.1111/jre.12102
46. Groeger S, Jarzina F, Windhorst A, Meyle J. Influence of retinoic acid on human gingival epithelial barriers. *J Periodontal Res.* (2016) 51:748–57. doi: 10.1111/jre.12351
47. Belibasakis GN, Kast JI, Thurnheer T, Akdis CA, Bostanci N. The expression of gingival epithelial junctions in response to subgingival biofilms. *Virulence* (2015) 6:704–9. doi: 10.1080/21505594.2015.1081731
48. Chen YH, Lu Q, Goodenough DA, Jeansonne B. Nonreceptor tyrosine kinase c-Yes interacts with occludin during tight junction formation

in canine kidney epithelial cells. *Mol Biol Cell* (2002) 13:1227–37. doi: 10.1091/mbc.01-08-0423
49. Seth A, Sheth P, Elias BC, Rao R. Protein phosphatases 2A and 1 interact with occludin and negatively regulate the assembly of tight junctions in the CACO-2 cell monolayer. *J Biol Chem.* (2007) 282:11487–98. doi: 10.1074/jbc.M610597200
50. Ikenouchi J, Furuse M, Furuse K, Sasaki H, Tsukita S. Tricellulin constitutes a novel barrier at tricellular contacts of epithelial cells. *J Cell Biol.* (2005) 171:939–45. doi: 10.1083/jcb.200510043
51. Krug SM, Amasheh S, Richter JF, Milatz S, Gunzel D, Westphal JK, et al. Tricellulin forms a barrier to macromolecules in tricellular tight junctions without affecting ion permeability. *Mol Biol Cell* (2009) 20:3713–24. doi: 10.1091/mbc.e09-01-0080
52. Raleigh DR, Marchiando AM, Zhang Y, Shen L, Sasaki H, Wang Y, et al. Tight junction-associated MARVEL proteins marveld3, tricellulin, and occludin have distinct but overlapping functions. *Mol Biol Cell* (2010) 21:1200–13. doi: 10.1091/mbc.e09-08-0734
53. Itoh M, Sasaki H, Furuse M, Ozaki H, Kita T, Tsukita S. Junctional adhesion molecule (JAM) binds to PAR-3: a possible mechanism for the recruitment of PAR-3 to tight junctions. *J Cell Biol.* (2001) 154:491–7. doi: 10.1083/jcb.200103047
54. Ebnet K, Schulz CU, Meyer Zu, Brickwedde MK, Pendl GG, Vestweber D. Junctional adhesion molecule interacts with the PDZ domain-containing proteins AF-6 and ZO-1. *J Biol Chem.* (2000) 275:27979–88. doi: 10.1074/jbc.M002363200
55. Monteiro AC, Sumagin R, Rankin CR, Leoni G, Mina MJ, Reiter DM, et al. JAM-A associates with ZO-2, afadin, and PDZ-GEF1 to activate Rap2c and regulate epithelial barrier function. *Mol Biol Cell* (2013) 24:2849–60. doi: 10.1091/mbc.e13-06-0298
56. Cohen CJ, Shieh JT, Pickles RJ, Okegawa T, Hsieh JT, Bergelson JM. The coxsackievirus and adenovirus receptor is a transmembrane component of the tight junction. *Proc Natl Acad Sci USA.* (2001) 98:15191–6. doi: 10.1073/pnas.261452898
57. Walters RW, Freimuth P, Moninger TO, Ganske I, Zabner J, Welsh MJ. Adenovirus fiber disrupts CAR-mediated intercellular adhesion allowing virus escape. *Cell* (2002) 110:789–99. doi: 10.1016/S0092-8674(02)00912-1
58. Zhang GH, Wu LL, Yu GY. Tight junctions and paracellular fluid and ion transport in salivary glands. *Chin J Dent Res.* (2013) 16:13–46.
59. McCarthy KM, Francis SA, McCormack JM, Lai J, Rogers RA, Skare IB, et al. Inducible expression of claudin-1-myc but not occludin-VSV-G results in aberrant tight junction strand formation in MDCK cells. *J Cell Sci.* (2000) 113(Pt 19):3387–98.
60. Stevenson BR, Siliciano JD, Mooseker MS, Goodenough DA. Identification of ZO-1: a high molecular weight polypeptide associated with the tight junction (zonula occludens) in a variety of epithelia. *J Cell Biol.* (1986) 103:755–66. doi: 10.1083/jcb.103.3.755
61. Gumbiner B, Lowenkopf T, Apatira D. Identification of a 160-kDa polypeptide that binds to the tight junction protein ZO-1. *Proc Natl Acad Sci USA.* (1991) 88:3460–4. doi: 10.1073/pnas.88.8.3460
62. Haskins J, Gu L, Wittchen ES, Hibbard J, Stevenson BR. ZO-3, a novel member of the MAGUK protein family found at the tight junction, interacts with ZO-1 and occludin. *J Cell Biol.* (1998) 141:199–208. doi: 10.1083/jcb.141.1.199
63. Takano K, Kojima T, Sawada N, Himi T. Role of tight junctions in signal transduction: an update. *EXCLI J.* (2014) 13:1145–62.
64. Anderson JM, Van Itallie CM. Physiology and function of the tight junction. *Cold Spring Harb Perspect Biol.* (2009) 1:a002584. doi: 10.1101/cshperspect.a002584
65. Turner JR, Buschmann MM, Romero-Calvo I, Sailer A, Shen L. The role of molecular remodeling in differential regulation of tight junction permeability. *Semin Cell Dev Biol.* (2014) 36:204–12. doi: 10.1016/j.semcdb.2014.09.022
66. Furuse M, Izumi Y, Oda Y, Higashi T, Iwamoto N. Molecular organization of tricellular tight junctions. *Tissue Barriers* (2014) 2:e28960. doi: 10.4161/tisb.28960
67. Meyle J, Gultig K, Rascher G, Wolburg H. Transepithelial electrical resistance and tight junctions of human gingival keratinocytes. *J Periodontal Res.* (1999) 34:214–22. doi: 10.1111/j.1600-0765.1999.tb02244.x
68. Gumbiner B, Simons K. A functional assay for proteins involved in establishing an epithelial occluding barrier: identification of a uvomorulin-like polypeptide. *J Cell Biol.* (1986) 102:457–68. doi: 10.1083/jcb.102.2.457
69. Staddon JM, Herrenknecht K, Smales C, Rubin LL. Evidence that tyrosine phosphorylation may increase tight junction permeability. *J Cell Sci.* (1995) 108(Pt 2):609–19.
70. Claude P. Morphological factors influencing transepithelial permeability: a model for the resistance of the zonula occludens. *J Membr Biol.* (1978) 39:219–32. doi: 10.1007/BF01870332
71. Groeger S, Doman E, Chakraborty T, Meyle J. Effects of *Porphyromonas gingivalis* infection on human gingival epithelial barrier function *in vitro*. *Eur J Oral Sci.* (2010) 118:582–9. doi: 10.1111/j.1600-0722.2010.00782.x
72. Palant CE, Duffey ME, Mookerjee BK, Ho S, Bentzel CJ. Ca2+ regulation of tight-junction permeability and structure in Necturus gallbladder. *Am J Physiol.* (1983) 245:C203–12. doi: 10.1152/ajpcell.1983.245.3.C203
73. Huibregtse JM, Beaudenon SL. Mechanism of HPV E6 proteins in cellular transformation. *Semin Cancer Biol.* (1996) 7:317–26.
74. Groeger S, Michel J, Meyle J. Establishment and characterization of immortalized human gingival keratinocyte cell lines. *J Periodontal Res.* (2008) 43:604–14. doi: 10.1111/j.1600-0765.2007.01019.x
75. Shi Y, Ratnayake DB, Okamoto K, Abe N, Yamamoto K, Nakayama K. Genetic analyses of proteolysis, hemoglobin binding, and hemagglutination of *Porphyromonas gingivalis*. Construction of mutants with a combination of rgpA, rgpB, kgp, and hagA. *J Biol Chem.* (1999) 274:17955–60.
76. Bruewer M, Utech M, Ivanov AI, Hopkins AM, Parkos CA, Nusrat A. Interferon-gamma induces internalization of epithelial tight junction proteins via a macropinocytosis-like process. *FASEB J.* (2005) 19:923–33. doi: 10.1096/fj.04-3260com
77. Guo W, Wang P, Liu ZH, Ye P. Analysis of differential expression of tight junction proteins in cultured oral epithelial cells altered by *Porphyromonas gingivalis*, *Porphyromonas gingivalis* lipopolysaccharide, and extracellular adenosine triphosphate. *Int J Oral Sci.* (2018) 10:e8. doi: 10.1038/ijos.2017.51
78. Provost E, Rimm DL. Controversies at the cytoplasmic face of the cadherin-based adhesion complex. *Curr Opin Cell Biol.* (1999) 11:567–72. doi: 10.1016/S0955-0674(99)00015-0
79. Baum B, Georgiou M. Dynamics of adherens junctions in epithelial establishment, maintenance, and remodeling. *J Cell Biol.* (2011) 192:907–17. doi: 10.1083/jcb.201009141
80. Imamura Y, Itoh M, Maeno Y, Tsukita S, Nagafuchi A. Functional domains of alpha-catenin required for the strong state of cadherin-based cell adhesion. *J Cell Biol.* (1999) 144:1311–22. doi: 10.1083/jcb.144.6.1311
81. Abe K, Takeichi M. EPLIN mediates linkage of the cadherin catenin complex to F-actin and stabilizes the circumferential actin belt. *Proc Natl Acad Sci USA.* (2008) 105:13–9. doi: 10.1073/pnas.0710504105
82. Mandai K, Nakanishi H, Satoh A, Obaishi H, Wada M, Nishioka H, et al. A novel actin filament-binding protein with one PDZ domain localized at cadherin-based cell-to-cell adherens junction. *J Cell Biol.* (1997) 139:517–28. doi: 10.1083/jcb.139.2.517
83. Kussel-Andermann P, El-Amraoui A, Safieddine S, Nouaille S, Perfettini I, Lecuit M, et al. Vezatin, a novel transmembrane protein, bridges myosin VIIA to the cadherin-catenins complex. *EMBO J.* (2000) 19:6020–9. doi: 10.1093/emboj/19.22.6020
84. Coopman P, Djiane A. Adherens junction and E-cadherin complex regulation by epithelial polarity. *Cell Mol Life Sci.* (2016) 73:3535–53. doi: 10.1007/s00018-016-2260-8
85. Nakagawa I, Inaba H, Yamamura T, Kato T, Kawai S, Ooshima T, et al. Invasion of epithelial cells and proteolysis of cellular focal adhesion components by distinct types of *Porphyromonas gingivalis* fimbriae. *Infect Immun.* (2006) 74:3773–82. doi: 10.1128/IAI.01902-05
86. Yilmaz O, Verbeke P, Lamont RJ, Ojcius DM. Intercellular spreading of *Porphyromonas gingivalis* infection in primary gingival epithelial cells. *Infect Immun.* (2006) 74:703–10. doi: 10.1128/IAI.74.1.703-710.2006
87. Potempa J, Banbula A, Travis J. Role of bacterial proteinases in matrix destruction and modulation of host responses. *Periodontol* (2000) 24:153–92. doi: 10.1034/j.1600-0757.2000.2240108.x
88. Bedi GS, Williams T. Purification and characterization of a collagen-degrading protease from *Porphyromonas gingivalis*. *J Biol Chem.* (1994) 269:599–606.

89. Chen Z, Casiano CA, Fletcher HM. Protease-active extracellular protein preparations from *Porphyromonas gingivalis* W83 induce N-cadherin proteolysis, loss of cell adhesion, and apoptosis in human epithelial cells. *J Periodontol.* (2001) 72:641–50. doi: 10.1902/jop.2001.72.5.641
90. Sheets SM, Potempa J, Travis J, Fletcher HM, Casiano CA. Gingipains from *Porphyromonas gingivalis* W83 synergistically disrupt endothelial cell adhesion and can induce caspase-independent apoptosis. *Infect Immun.* (2006) 74:5667–78. doi: 10.1128/IAI.01140-05
91. Hintermann E, Haake SK, Christen U, Sharabi A, Quaranta V. Discrete proteolysis of focal contact and adherens junction components in *Porphyromonas gingivalis*-infected oral keratinocytes: a strategy for cell adhesion and migration disabling. *Infect Immun.* (2002) 70:5846–56. doi: 10.1128/IAI.70.10.5846-5856.2002
92. Amano A. Molecular interaction of *Porphyromonas gingivalis* with host cells: implication for the microbial pathogenesis of periodontal disease. *J Periodontol.* (2003) 74:90–6. doi: 10.1902/jop.2003.74.1.90
93. Nakagawa I, Amano A, Kuboniwa M, Nakamura T, Kawabata S, Hamada S. Functional differences among FimA variants of *Porphyromonas gingivalis* and their effects on adhesion to and invasion of human epithelial cells. *Infect Immun.* (2002) 70:277–85. doi: 10.1128/IAI.70.1.277-285.2002
94. Tsuda K, Amano A, Umebayashi K, Inaba H, Nakagawa I, Nakanishi Y, et al. Molecular dissection of internalization of *Porphyromonas gingivalis* by cells using fluorescent beads coated with bacterial membrane vesicle. *Cell Struct Funct.* (2005) 30:81–91. doi: 10.1247/csf.30.81
95. Huttenlocher A, Ginsberg MH, Horwitz AF. Modulation of cell migration by integrin-mediated cytoskeletal linkages and ligand-binding affinity. *J Cell Biol.* (1996) 134:1551–62. doi: 10.1083/jcb.134.6.1551
96. Cox EA, Sastry SK, Huttenlocher A. Integrin-mediated adhesion regulates cell polarity and membrane protrusion through the Rho family of GTPases. *Mol Biol Cell* (2001) 12:265–77. doi: 10.1091/mbc.12.2.265
97. Kato T, Kawai S, Nakano K, Inaba H, Kuboniwa M, Nakagawa I, et al. Virulence of *Porphyromonas gingivalis* is altered by substitution of fimbria gene with different genotype. *Cell Microbiol.* (2007) 9:753–65. doi: 10.1111/j.1462-5822.2006.00825.x
98. Lamont RJ, Yilmaz O. In or out: the invasiveness of oral bacteria. *Periodontol* (2002) 30:61–9. doi: 10.1034/j.1600-0757.2002.03006.x
99. Amano A. Disruption of epithelial barrier and impairment of cellular function by *Porphyromonas gingivalis*. *Front Biosci.* (2007) 12:3965–74. doi: 10.2741/2363
100. Mifsud EJ, Tan AC, Jackson DC. TLR agonists as modulators of the innate immune response and their potential as agents against infectious disease. *Front Immunol.* (2014) 5:79. doi: 10.3389/fimmu.2014.00079
101. Sasai M, Yamamoto M. Pathogen recognition receptors: ligands and signaling pathways by Toll-like receptors. *Int Rev Immunol.* (2013) 32:116–33. doi: 10.3109/08830185.2013.774391
102. Akira S, Sato S. Toll-like receptors and their signaling mechanisms. *Scand J Infect Dis.* (2003) 35:555–62. doi: 10.1080/00365540310015683
103. Kawai T, Akira S. TLR signaling. *Semin Immunol.* (2007) 19:24–32. doi: 10.1016/j.smim.2006.12.004
104. Cario E, Brown D, McKee M, Lynch-Devaney K, Gerken G, Podolsky DK. Commensal-associated molecular patterns induce selective toll-like receptor-trafficking from apical membrane to cytoplasmic compartments in polarized intestinal epithelium. *Am J Pathol.* (2002) 160:165–73. doi: 10.1016/S0002-9440(10)64360-X
105. Zhang D, Zhang G, Hayden MS, Greenblatt MB, Bussey C, Flavell RA, et al. A toll-like receptor that prevents infection by uropathogenic bacteria. *Science* (2004) 303:1522–6. doi: 10.1126/science.1094351
106. Poltorak A, He X, Smirnova I, Liu MY, Van Huffel C, Du X, et al. Defective LPS signaling in C3H/HeJ and C57BL/10ScCr mice: mutations in Tlr4 gene. *Science* (1998) 282:2085–8. doi: 10.1126/science.282.5396.2085
107. Takeuchi O, Sato S, Horiuchi T, Hoshino K, Takeda K, Dong Z, et al. Cutting edge: role of toll-like receptor 1 in mediating immune response to microbial lipoproteins. *J Immunol.* (2002) 169:10–4. doi: 10.4049/jimmunol.169.1.10
108. Alexopoulou L, Holt AC, Medzhitov R, Flavell RA. Recognition of double-stranded RNA and activation of NF-kappaB by Toll-like receptor 3. *Nature* (2001) 413:732–8. doi: 10.1038/35099560
109. Bauer S, Kirschning CJ, Hacker H, Redecke V, Hausmann S, Akira S, et al. Human TLR9 confers responsiveness to bacterial DNA via species-specific CpG motif recognition. *Proc Natl Acad Sci USA.* (2001) 98:9237–42. doi: 10.1073/pnas.161293498
110. Hayashi F, Smith KD, Ozinsky A, Hawn TR, Yi EC, Goodlett DR, et al. The innate immune response to bacterial flagellin is mediated by Toll-like receptor 5. *Nature* (2001) 410:1099–103. doi: 10.1038/35074106
111. Hemmi H, Kaisho T, Takeuchi O, Sato S, Sanjo H, Hoshino K, et al. Small anti-viral compounds activate immune cells via the TLR7 MyD88-dependent signaling pathway. *Nat Immunol.* (2002) 3:196–200. doi: 10.1038/ni758
112. Hemmi H, Takeuchi O, Kawai T, Kaisho T, Sato S, Sanjo H, et al. A Toll-like receptor recognizes bacterial DNA. *Nature* (2000) 408:740–5. doi: 10.1038/35047123
113. Jurk M, Heil F, Vollmer J, Schetter C, Krieg AM, Wagner H, et al. Human TLR7 or TLR8 independently confer responsiveness to the antiviral compound R-848. *Nat Immunol.* (2002) 3:499. doi: 10.1038/ni0602-499
114. Fitzgerald KA, Palsson-McDermott EM, Bowie AG, Jefferies CA, Mansell AS, Brady G, et al. Mal (MyD88-adapter-like) is required for Toll-like receptor-4 signal transduction. *Nature* (2001) 413:78–83. doi: 10.1038/35092578
115. Fitzgerald KA, Rowe DC, Barnes BJ, Caffrey DR, Visintin A, Latz E, et al. LPS-TLR4 signaling to IRF-3/7 and NF-kappaB involves the toll adapters TRAM and TRIF. *J Exp Med.* (2003) 198:1043–55. doi: 10.1084/jem.20031023
116. Horng T, Barton GM, Medzhitov R. TIRAP: an adapter molecule in the Toll signaling pathway. *Nat Immunol.* (2001) 2:835–41. doi: 10.1038/ni0901-835
117. Medzhitov R, Preston-Hurlburt P, Kopp E, Stadlen A, Chen C, Ghosh S, et al. MyD88 is an adaptor protein in the hToll/IL-1 receptor family signaling pathways. *Mol Cell* (1998) 2:253–8. doi: 10.1016/S1097-2765(00)80136-7
118. Oshiumi H, Matsumoto M, Funami K, Akazawa T. Seya T. TICAM-1, an adaptor molecule that participates in Toll-like receptor 3-mediated interferon-beta induction. *Nat Immunol.* (2003) 4:161–7. doi: 10.1038/ni886
119. Yamamoto M, Sato S, Hemmi H, Hoshino K, Kaisho T, Sanjo H, et al. Role of adaptor TRIF in the MyD88-independent toll-like receptor signaling pathway. *Science* (2003) 301:640–3. doi: 10.1126/science.1087262
120. Akira S, Yamamoto M, Takeda K. Role of adapters in Toll-like receptor signalling. *Biochem Soc Trans.* (2003) 31(Pt 3):637–42. doi: 10.1042/bst0310637
121. Gohda J, Matsumura T, Inoue J. Cutting edge: TNFR-associated factor (TRAF) 6 is essential for MyD88-dependent pathway but not toll/IL-1 receptor domain-containing adaptor-inducing IFN-beta (TRIF)-dependent pathway in TLR signaling. *J Immunol.* (2004) 173:2913–7. doi: 10.4049/jimmunol.173.5.2913
122. Kondo T, Kawai T, Akira S. Dissecting negative regulation of Toll-like receptor signaling. *Trends Immunol.* (2012) 33:449–58. doi: 10.1016/j.it.2012.05.002
123. Meylan E, Burns K, Hofmann K, Blancheteau V, Martinon F, Kelliher M, et al. RIP1 is an essential mediator of Toll-like receptor 3-induced NF-kappa B activation. *Nat Immunol.* (2004) 5:503–7. doi: 10.1038/ni1061
124. Chen HC, Zhan X, Tran KK, Shen H. Selectively targeting the toll-like receptor 9 (TLR9)–IRF 7 signaling pathway by polymer blend particles. *Biomaterials* (2013) 34:6464–72. doi: 10.1016/j.biomaterials.2013.05.016
125. Beklen A, Hukkanen M, Richardson R, Konttinen YT. Immunohistochemical localization of Toll-like receptors 1–10 in periodontitis. *Oral Microbiol Immunol.* (2008) 23:425–31. doi: 10.1111/j.1399-302X.2008.00448.x
126. Semlali A, Witoled C, Alanazi M, Rouabhia M. Whole cigarette smoke increased the expression of TLRs, HBDs, and proinflammory cytokines by human gingival epithelial cells through different signaling pathways. *PLoS ONE* (2012) 7:e52614. doi: 10.1371/journal.pone.0052614
127. Uehara A, Fujimoto Y, Fukase K, Takada H. Various human epithelial cells express functional Toll-like receptors, NOD1 and NOD2 to produce anti-microbial peptides, but not proinflammatory cytokines. *Mol Immunol.* (2007) 44:3100–11. doi: 10.1016/j.molimm.2007.02.007
128. Promsudthi A, Poomsawat S, Limsricharoen W. The role of Toll-like receptor 2 and 4 in gingival tissues of chronic periodontitis subjects with type 2 diabetes. *J Periodontal Res.* (2014) 49:346–54. doi: 10.1111/jre.12112

129. Sugawara Y, Uehara A, Fujimoto Y, Kusumoto S, Fukase K, Shibata K, et al. Toll-like receptors, NOD1, and NOD2 in oral epithelial cells. *J Dent Res.* (2006) 85:524–9. doi: 10.1177/154405910608500609
130. Uehara A, Sugawara S, Tamai R, Takada H. Contrasting responses of human gingival and colonic epithelial cells to lipopolysaccharides, lipoteichoic acids and peptidoglycans in the presence of soluble CD14. *Med Microbiol Immunol.* (2001) 189:185–92. doi: 10.1007/s004300100063
131. Uehara A, Sugawara Y, Kurata S, Fujimoto Y, Fukase K, Kusumoto S, et al. Chemically synthesized pathogen-associated molecular patterns increase the expression of peptidoglycan recognition proteins via toll-like receptors, NOD1 and NOD2 in human oral epithelial cells. *Cell Microbiol.* (2005) 7:675–86. doi: 10.1111/j.1462-5822.2004.00500.x
132. Shaddox L, Wiedey J, Bimstein E, Magnuson I, Clare-Salzler M, Aukhil I, et al. Hyper-responsive phenotype in localized aggressive periodontitis. *J Dent Res.* (2010) 89:143–8. doi: 10.1177/0022034509353397
133. Shaddox LM, Mullersman AF, Huang H, Wallet SM, Langaee T, Aukhil I. Epigenetic regulation of inflammation in localized aggressive periodontitis. *Clin Epigenetics* (2017) 9:94. doi: 10.1186/s13148-017-0385-8
134. Jin SH, Guan XY, Liang WH, Bai GH, Liu JG. TLR4 polymorphism and periodontitis susceptibility: a meta-analysis. *Medicine* (2016) 95:e4845. doi: 10.1097/MD.0000000000004845
135. Zhou Q, Wang C, Wang X, Wu X, Zhu Z, Liu B, et al. Association between TLR4 (+896A/G and +1196C/T) polymorphisms and gastric cancer risk: an updated meta-analysis. *PLoS ONE* (2014) 9:e109605. doi: 10.1371/journal.pone.0109605
136. Saxena M, Yeretssian G. NOD-like receptors: master regulators of inflammation and cancer. *Front Immunol.* (2014) 5:327. doi: 10.3389/fimmu.2014.00327
137. Becker CE, O'Neill LA. Inflammasomes in inflammatory disorders: the role of TLRs and their interactions with NLRs. *Semin Immunopathol.* (2007) 29:239–48. doi: 10.1007/s00281-007-0081-4
138. Martinon F, Tschopp J. NLRs join TLRs as innate sensors of pathogens. *Trends Immunol.* (2005) 26:447–54. doi: 10.1016/j.it.2005.06.004
139. Ting JP, Kastner DL, Hoffman HM. CATERPILLERs, pyrin and hereditary immunological disorders. *Nat Rev Immunol.* (2006) 6:183–95. doi: 10.1038/nri1788
140. Girardin SE, Boneca IG, Carneiro LA, Antignac A, Jehanno M, Viala J, et al. Nod1 detects a unique muropeptide from gram-negative bacterial peptidoglycan. *Science* (2003) 300:1584–7. doi: 10.1126/science.1084677
141. Inohara N, Ogura Y, Fontalba A, Gutierrez O, Pons F, Crespo J, et al. Host recognition of bacterial muramyl dipeptide mediated through NOD2. Implications for Crohn's disease. *J Biol Chem.* (2003) 278:5509–12. doi: 10.1074/jbc.C200673200
142. Chamaillard M, Hashimoto M, Horie Y, Masumoto J, Qiu S, Saab L, et al. An essential role for NOD1 in host recognition of bacterial peptidoglycan containing diaminopimelic acid. *Nat Immunol.* (2003) 4:702–7. doi: 10.1038/ni945
143. Inohara C, McDonald C, Nunez G. NOD-LRR proteins: role in host-microbial interactions and inflammatory disease. *Annu Rev Biochem.* (2005) 74:355–83. doi: 10.1146/annurev.biochem.74.082803.133347
144. Strober W, Murray PJ, Kitani A, Watanabe T. Signalling pathways and molecular interactions of NOD1 and NOD2. *Nat Rev Immunol.* (2006) 6:9–20. doi: 10.1038/nri1747
145. Uehara A, Takada H. Synergism between TLRs and NOD1/2 in oral epithelial cells. *J Dent Res.* (2008) 87:682–6. doi: 10.1177/154405910808700709
146. Hirao K, Yumoto H, Takahashi K, Mukai K, Nakanishi T, Matsuo T. Roles of TLR2, TLR4, NOD2, and NOD1 in pulp fibroblasts. *J Dent Res.* (2009) 88:762–7. doi: 10.1177/0022034509341779
147. Lee YY, Chan CH, Hung SL, Chen YC, Lee YH, Yang SF. Up-regulation of nucleotide-binding oligomerization domain 1 in inflamed human dental pulp. *J Endod.* (2011) 37:1370–5. doi: 10.1016/j.joen.2011.06.008
148. Zhou S, Yu P, Guan L, Xing A, Liu S, Xiong Q, et al. NOD1 expression elicited by iE-DAP in first trimester human trophoblast cells and its potential role in infection-associated inflammation. *Eur J Obstet Gynecol Reprod Biol.* (2013) 170:318–23. doi: 10.1016/j.ejogrb.2013.04.011
149. Gao Y, Jiang W, Qian Y, Zhou Q, Jiang H, Wang X, et al. NOD1 agonist iE-DAP reverses effects of cigarette smoke extract on NOD1 signal pathway in human oral mucosal epithelial cells. *Int J Clin Exp Med.* (2015) 8:12519–28.
150. Gieseler F, Ungefroren H, Settmacher U, Hollenberg MD, Kaufmann R. Proteinase-activated receptors (PARs) - focus on receptor-receptor-interactions and their physiological and pathophysiological impact. *Cell Commun Signal.* (2013) 11:86. doi: 10.1186/1478-811X-11-86
151. Bunnett NW. Protease-activated receptors: how proteases signal to cells to cause inflammation and pain. *Semin Thromb Hemost.* (2006) 32(Suppl. 1):39–48. doi: 10.1055/s-2006-939553
152. Knecht W, Cottrell GS, Amadesi S, Mohlin J, Skaregarde A, Gedda K, et al. Trypsin IV or mesotrypsin and p23 cleave protease-activated receptors 1 and 2 to induce inflammation and hyperalgesia. *J Biol Chem.* (2007) 282:26089–100. doi: 10.1074/jbc.M703840200
153. Lourbakos A, Chinni C, Thompson P, Potempa J, Travis J, Mackie EJ, et al. Cleavage and activation of proteinase-activated receptor-2 on human neutrophils by gingipain-R from *Porphyromonas gingivalis*. *FEBS Lett.* (1998) 435:45–8. doi: 10.1016/S0014-5793(98)01036-9
154. Coughlin SR, Camerer E. PARticipation in inflammation. *J Clin Invest.* (2003) 111:25–7. doi: 10.1172/JCI17564
155. Camerer E, Huang W, Coughlin SR. Tissue factor- and factor X-dependent activation of protease-activated receptor 2 by factor VIIa. *Proc Natl Acad Sci USA.* (2000) 97:5255–60. doi: 10.1073/pnas.97.10.5255
156. Cottrell GS, Amadesi S, Grady EF, Bunnett NW. Trypsin IV, a novel agonist of protease-activated receptors 2 and 4. *J Biol Chem.* (2004) 279:13532–9. doi: 10.1074/jbc.M312090200
157. Ishihara H, Connolly AJ, Zeng D, Kahn ML, Zheng YW, Timmons C, et al. Protease-activated receptor 3 is a second thrombin receptor in humans. *Nature* (1997) 386:502–6. doi: 10.1038/386502a0
158. Sambrano GR, Huang W, Faruqi T, Mahrus S, Craik C, Coughlin SR. Cathepsin G activates protease-activated receptor-4 in human platelets. *J Biol Chem.* (2000) 275:6819–23. doi: 10.1074/jbc.275.10.6819
159. Zhang D, Li S, Hu L, Sheng L, Chen L. Modulation of protease-activated receptor expression by *Porphyromonas gingivalis* in human gingival epithelial cells. *BMC Oral Health* (2015) 15:128. doi: 10.1186/s12903-015-0105-8
160. Chung WO, An JY, Yin L, Hacker BM, Rohani MG, Dommisch H, et al. Interplay of protease-activated receptors and NOD pattern recognition receptors in epithelial innate immune responses to bacteria. *Immunol Lett.* (2010) 131:113–9. doi: 10.1016/j.imlet.2010.02.006
161. Skeldon A, Saleh M. The inflammasomes: molecular effectors of host resistance against bacterial, viral, parasitic, and fungal infections. *Front Microbiol.* (2011) 2:15. doi: 10.3389/fmicb.2011.00015
162. Martinon F, Burns K, Tschopp J. The inflammasome: a molecular platform triggering activation of inflammatory caspases and processing of proIL-beta. *Mol Cell* (2002) 10:417–26. doi: 10.1016/S1097-2765(02)00599-3
163. Said-Sadier N, Ojcius DM. Alarmins, inflammasomes and immunity. *Biomed J.* (2012) 35:437–49. doi: 10.4103/2319-4170.104408
164. Schroder K, Tschopp J. The inflammasomes. *Cell* (2010) 140:821–32. doi: 10.1016/j.cell.2010.01.040
165. Yilmaz O, Lee KL. The inflammasome and danger molecule signaling: at the crossroads of inflammation and pathogen persistence in the oral cavity. *Periodontol* (2015) 69:83–95. doi: 10.1111/prd.12084
166. Akhter A, Caution K, Abu Khweek A, Tazi M, Abdulrahman BA, Abdelaziz DH, et al. Caspase-11 promotes the fusion of phagosomes harboring pathogenic bacteria with lysosomes by modulating actin polymerization. *Immunity* (2012) 37:35–47. doi: 10.1016/j.immuni.2012.05.001
167. van de Veerdonk FL, Netea MG, Dinarello CA, Joosten LA. Inflammasome activation and IL-1beta and IL-18 processing during infection. *Trends Immunol.* (2011) 32:110–6. doi: 10.1016/j.it.2011.01.003
168. Bui FQ, Johnson L, Roberts J, Hung SC, Lee J, Atanasova KR, et al. *Fusobacterium nucleatum* infection of gingival epithelial cells leads to NLRP3 inflammasome-dependent secretion of IL-1beta and the danger signals ASC and HMGB1. *Cell Microbiol.* (2016) 18:970–81. doi: 10.1111/cmi.12560
169. Johnson L, Atanasova KR, Bui PQ, Lee J, Hung SC, Yilmaz O, et al. *Porphyromonas gingivalis* attenuates ATP-mediated inflammasome activation and HMGB1 release through expression of a nucleoside-diphosphate kinase. *Microbes Infect.* (2015) 17:369–77. doi: 10.1016/j.micinf.2015.03.010

170. Creagh EM. Caspase crosstalk: integration of apoptotic and innate immune signalling pathways. *Trends Immunol.* (2014) 35:631–40. doi: 10.1016/j.it.2014.10.004
171. Eldridge MJ, Shenoy AR. Antimicrobial inflammasomes: unified signalling against diverse bacterial pathogens. *Curr Opin Microbiol.* (2015) 23:32–41. doi: 10.1016/j.mib.2014.10.008
172. Bauernfeind F, Ablasser A, Bartok E, Kim S, Schmid-Burgk J, Cavlar T, et al. Inflammasomes: current understanding and open questions. *Cell Mol Life Sci.* (2011) 68:765–83. doi: 10.1007/s00018-010-0567-4
173. Ferrari D, Pizzirani C, Adinolfi E, Lemoli RM, Curti A, Idzko M, et al. The P2X7 receptor: a key player in IL-1 processing and release. *J Immunol.* (2006) 176:3877–83. doi: 10.4049/jimmunol.176.7.3877
174. Michaud M, Martins I, Sukkurwala AQ, Adjemian S, Ma Y, Pellegatti P, et al. Autophagy-dependent anticancer immune responses induced by chemotherapeutic agents in mice. *Science* (2011) 334:1573–7. doi: 10.1126/science.1208347
175. Perregaux DG, McNiff P, Laliberte R, Conklyn M, Gabel CA. ATP acts as an agonist to promote stimulus-induced secretion of IL-1 beta and IL-18 in human blood. *J Immunol.* (2000) 165:4615–23. doi: 10.4049/jimmunol.165.8.4615
176. Sanz JM, Di Virgilio F. Kinetics and mechanism of ATP-dependent IL-1 beta release from microglial cells. *J Immunol.* (2000) 164:4893–8.
177. Yilmaz O, Sater AA, Yao L, Koutouzis T, Pettengill M, Ojcius DM. ATP-dependent activation of an inflammasome in primary gingival epithelial cells infected by *Porphyromonas gingivalis*. *Cell Microbiol.* (2010) 12:188–98. doi: 10.1111/j.1462-5822.2009.01390.x
178. Lee SJ, Choi BK. Involvement of NLRP10 in IL-1alpha induction of oral epithelial cells by periodontal pathogens. *Innate Immun.* (2017) 23:569–77. doi: 10.1177/1753425917722610
179. Belibasakis GN, Thurnheer T, Bostanci N. Interleukin-8 responses of multi-layer gingival epithelia to subgingival biofilms: role of the "red complex" species. *PLoS ONE* (2013) 8:e81581. doi: 10.1371/journal.pone.0081581
180. Bostanci N, Bao K, Wahlander A, Grossmann J, Thurnheer T, Belibasakis GN. Secretome of gingival epithelium in response to subgingival biofilms. *Mol Oral Microbiol.* (2015) 30:323–35. doi: 10.1111/omi.12096
181. Feliciani C, Gupta AK, Sauder DN. Keratinocytes and cytokine/growth factors. *Crit Rev Oral Biol Med.* (1996) 7:300–18. doi: 10.1177/10454411960070040101
182. Dinarello CA. The IL-1 family and inflammatory diseases. *Clin Exp Rheumatol.* (2002) 20(5 Suppl. 27):S1–13.
183. Ramage G, Lappin DF, Millhouse E, Malcolm J, Jose A, Yang J, et al. The epithelial cell response to health and disease associated oral biofilm models. *J Periodontal Res.* (2017) 52:325–33. doi: 10.1111/jre.12395
184. Campbell LM, Maxwell PJ, Waugh DJ. Rationale and means to target pro-inflammatory interleukin-8 (CXCL8) signaling in cancer. *Pharmaceuticals* (2013) 6:929–59. doi: 10.3390/ph6080929
185. St John MA, Li Y, Zhou X, Denny P, Ho CM, Montemagno C, et al. Interleukin 6 and interleukin 8 as potential biomarkers for oral cavity and oropharyngeal squamous cell carcinoma. *Arch Otolaryngol Head Neck Surg.* (2004) 130:929–35. doi: 10.1001/archotol.130.8.929
186. Goutoudi P, Diza E, Arvanitidou M. Effect of periodontal therapy on crevicular fluid interleukin-6 and interleukin-8 levels in chronic periodontitis. *Int J Dent.* (2012) 2012:362905. doi: 10.1155/2012/362905
187. Schueller K, Riva A, Pfeiffer S, Berry D, Somoza V. Members of the oral microbiota are associated with IL-8 release by gingival epithelial cells in healthy individuals. *Front Microbiol.* (2017) 8:416. doi: 10.3389/fmicb.2017.00416
188. Fujimura Y, Hotokezaka H, Ohara N, Naito M, Sakai E, Yoshimura M, et al. The hemoglobin receptor protein of porphyromonas gingivalis inhibits receptor activator NF-kappaB ligand-induced osteoclastogenesis from bone marrow macrophages. *Infect Immun.* (2006) 74:2544–51. doi: 10.1128/IAI.74.5.2544-2551.2006
189. Fujita Y, Nakayama M, Naito M, Yamachika E, Inoue T, Nakayama K, et al. Hemoglobin receptor protein from *Porphyromonas gingivalis* induces interleukin-8 production in human gingival epithelial cells through stimulation of the mitogen-activated protein kinase and NF-kappaB signal transduction pathways. *Infect Immun.* (2014) 82:202–11. doi: 10.1128/IAI.01140-12
190. Moussion C, Ortega N, Girard JP. The IL-1-like cytokine IL-33 is constitutively expressed in the nucleus of endothelial cells and epithelial cells *in vivo*: a novel "alarmin"? *PLoS ONE* (2008) 3:e3331. doi: 10.1371/journal.pone.0003331
191. Paul WE, Zhu J. How are T(H)2-type immune responses initiated and amplified? *Nat Rev Immunol.* (2010) 10:225–35. doi: 10.1038/nri2735
192. Tada H, Matsuyama T, Nishioka T, Hagiwara M, Kiyoura Y, Shimauchi H, et al. *Porphyromonas gingivalis* gingipain-dependently enhances IL-33 production in human gingival epithelial cells. *PLoS ONE* (2016) 11:e0152794. doi: 10.1371/journal.pone.0152794
193. Kadomatsu T, Endo M, Miyata K, Oike Y. Diverse roles of ANGPTL2 in physiology and pathophysiology. *Trends Endocrinol Metab.* (2014) 25:245–54. doi: 10.1016/j.tem.2014.03.012
194. Kim I, Moon SO, Koh KN, Kim H, Uhm CS, Kwak HJ, et al. Molecular cloning, expression, and characterization of angiopoietin-related protein. angiopoietin-related protein induces endothelial cell sprouting. *J Biol Chem.* (1999) 274:26523–8. doi: 10.1074/jbc.274.37.26523
195. Santulli G. Angiopoietin-like proteins: a comprehensive look. *Front Endocrinol.* (2014) 5:4. doi: 10.3389/fendo.2014.00004
196. Kubota Y, Oike Y, Satoh S, Tabata Y, Niikura Y, Morisada T, et al. Cooperative interaction of Angiopoietin-like proteins 1 and 2 in zebrafish vascular development. *Proc Natl Acad Sci USA.* (2005) 102:13502–7. doi: 10.1073/pnas.0501902102
197. Ohno T, Yamamoto G, Hayashi JI, Nishida E, Goto H, Sasaki Y, et al. Angiopoietin-like protein 2 regulates *Porphyromonas gingivalis* lipopolysaccharide-induced inflammatory response in human gingival epithelial cells. *PLoS ONE* (2017) 12:e0184825. doi: 10.1371/journal.pone.0184825
198. Imai H, Fujita T, Kajiya M, Ouhara K, Yoshimoto T, Matsuda S, et al. Mobilization of TLR4 into lipid rafts by aggregatibacter actinomycetemcomitans in gingival epithelial cells. *Cell Physiol Biochem.* (2016) 39:1777–86. doi: 10.1159/000447877
199. Armitage GC. Comparison of the microbiological features of chronic and aggressive periodontitis. *Periodontol* (2010) 53:70–88. doi: 10.1111/j.1600-0757.2010.00357.x
200. Darveau RP. Periodontitis: a polymicrobial disruption of host homeostasis. *Nat Rev Microbiol.* (2010) 8:481–90. doi: 10.1038/nrmicro2337
201. Taubman MA, Valverde P, Han X, Kawai T. Immune response: the key to bone resorption in periodontal disease. *J Periodontol.* (2005) 76(11 Suppl.):2033–41. doi: 10.1902/jop.2005.76.11-S.2033
202. Lally ET, Golub EE, Kieba IR, Taichman NS, Rosenbloom J, Rosenbloom JC, et al. Analysis of the *Actinobacillus actinomycetemcomitans* leukotoxin gene. Delineation of unique features and comparison to homologous toxins. *J Biol Chem.* (1989) 264:15451–6.
203. Mayer MP, Bueno LC, Hansen EJ, DiRienzo JM. Identification of a cytolethal distending toxin gene locus and features of a virulence-associated region in *Actinobacillus actinomycetemcomitans*. *Infect Immun.* (1999) 67:1227–37.
204. Feng Z, Weinberg A. Role of bacteria in health and disease of periodontal tissues. *Periodontol* (2006) 40:50–76. doi: 10.1111/j.1600-0757.2005.00148.x
205. Pahumunto N, Chotjumlong P, Makeudom A, Krisanaprakornkit S, Dahlen G, Teanpaisan R. Pro-inflammatory cytokine responses in human gingival epithelial cells after stimulation with cell wall extract of *Aggregatibacter actinomycetemcomitans* subtypes. *Anaerobe* (2017) 48:103–9. doi: 10.1016/j.anaerobe.2017.08.001
206. Simonson LG, Goodman CH, Bial JJ, Morton HE. Quantitative relationship of *Treponema denticola* to severity of periodontal disease. *Infect Immun.* (1988) 56:726–8.
207. Socransky SS, Haffajee AD, Cugini MA, Smith C, Kent RL Jr. Microbial complexes in subgingival plaque. *J Clin Periodontol.* (1998) 25:134–44.
208. Dashper SG, Seers CA, Tan KH, Reynolds EC. Virulence factors of the oral spirochete *Treponema denticola*. *J Dent Res.* (2011) 90:691–703. doi: 10.1177/0022034510385242
209. Brissette CA, Pham TT, Coats SR, Darveau RP, Lukehart SA. Treponema denticola does not induce production of common innate immune mediators

from primary gingival epithelial cells. *Oral Microbiol Immunol.* (2008) 23:474–81. doi: 10.1111/j.1399-302X.2008.00452.x
210. Jo AR, Baek KJ, Shin JE, Choi Y. Mechanisms of IL-8 suppression by *Treponema denticola* in gingival epithelial cells. *Immunol Cell Biol.* (2014) 92:139–47. doi: 10.1038/icb.2013.80
211. Ruby J, Martin M, Passineau MJ, Godovikova V, Fenno JC, Wu H. Activation of the innate immune system by *Treponema denticola* periplasmic flagella through toll-like receptor 2. *Infect Immun.* (2018) 86: e00573-17. doi: 10.1128/IAI.00251-18
212. Gu C, Wu L, Li X. IL-17 family: cytokines, receptors and signaling. *Cytokine* (2013) 64:477–85. doi: 10.1016/j.cyto.2013.07.022
213. Yao Z, Painter SL, Fanslow WC, Ulrich D, Macduff BM, Spriggs MK et al. Human IL-17: a novel cytokine derived from T cells. *J Immunol.* (1995) 155:5483–6.
214. Adibrad M, Deyhimi P, Ganjalikhani Hakemi M, Behfarnia P, Shahabuei M, Rafiee L. Signs of the presence of Th17 cells in chronic periodontal disease. *J Periodontal Res.* (2012) 47:525–31. doi: 10.1111/j.1600-0765.2011.01464.x
215. Beklen A, Ainola M, Hukkanen M, Gurgan C, Sorsa T, Konttinen YT. MMPs, IL-1, and TNF are regulated by IL-17 in periodontitis. *J Dent Res.* (2007) 86:347–51. doi: 10.1177/154405910708600409
216. Cardoso CR, Garlet GP, Crippa GE, Rosa AL, Junior WM, Rossi MA, et al. Evidence of the presence of T helper type 17 cells in chronic lesions of human periodontal disease. *Oral Microbiol Immunol.* (2009) 24:1–6. doi: 10.1111/j.1399-302X.2008.00463.x
217. Konermann A, Beyer M, Deschner J, Allam JP, Novak N, Winter J, et al. Human periodontal ligament cells facilitate leukocyte recruitment and are influenced in their immunomodulatory function by Th17 cytokine release. *Cell Immunol.* (2012) 272:137–43. doi: 10.1016/j.cellimm.2011.10.020
218. Allam JP, Duan Y, Heinemann F, Winter J, Gotz W, Deschner J, et al. IL-23-producing CD68(+) macrophage-like cells predominate within an IL-17-polarized infiltrate in chronic periodontitis lesions. *J Clin Periodontol.* (2011) 38:879–86. doi: 10.1111/j.1600-051X.2011.01752.x
219. Buduneli N, Buduneli E, Kutukculer N. Interleukin-17, RANKL, and osteoprotegerin levels in gingival crevicular fluid from smoking and non-smoking patients with chronic periodontitis during initial periodontal treatment. *J Periodontol.* (2009) 80:1274–80. doi: 10.1902/jop.2009.090106
220. Vernal R, Dutzan N, Chaparro A, Puente J, Antonieta Valenzuela M, Gamonal J. Levels of interleukin-17 in gingival crevicular fluid and in supernatants of cellular cultures of gingival tissue from patients with chronic periodontitis. *J Clin Periodontol.* (2005) 32:383–9. doi: 10.1111/j.1600-051X.2005.00684.x
221. Awang RA, Lappin DF, MacPherson A, Riggio M, Robertson D, Hodge P, et al. Clinical associations between IL-17 family cytokines and periodontitis and potential differential roles for IL-17A and IL-17E in periodontal immunity. *Inflamm Res.* (2014) 63:1001–12. doi: 10.1007/s00011-014-0776-7
222. Lemke G, Rothlin CV. Immunobiology of the TAM receptors. *Nat Rev Immunol.* (2008) 8:327–36. doi: 10.1038/nri2303
223. Lemke G, Burstyn-Cohen T. TAM receptors and the clearance of apoptotic cells. *Ann NY Acad Sci.* (2010) 1209:23–9. doi: 10.1111/j.1749-6632.2010.05744.x
224. Nassar M, Tabib Y, Capucha T, Mizraji G, Nir T, Pevsner-Fischer M, et al. GAS6 is a key homeostatic immunological regulator of host-commensal interactions in the oral mucosa. *Proc Natl Acad Sci USA.* (2017) 114:E337–46. doi: 10.1073/pnas.1614926114
225. Nassar M, Tabib Y, Capucha T, Mizraji G, Nir T, Saba F, et al. Multiple regulatory levels of growth arrest-specific 6 in mucosal immunity against an oral pathogen. *Front Immunol.* (2018) 9:1374. doi: 10.3389/fimmu.2018.01374
226. Tezal M, Sullivan MA, Reid ME, Marshall JR, Hyland A, Loree T, et al. Chronic periodontitis and the risk of tongue cancer. *Arch Otolaryngol Head Neck Surg.* (2007) 133:450–4. doi: 10.1001/archotol.133.5.450
227. Tezal M, Grossi SG, Genco RJ. Is periodontitis associated with oral neoplasms? *J Periodontol.* (2005) 76:406–10. doi: 10.1902/jop.2005.76.3.406
228. Dong H, Strome SE, Salomao DR, Tamura H, Hirano F, Flies DB, et al. Tumor-associated B7-H1 promotes T-cell apoptosis: a potential mechanism of immune evasion. *Nat Med.* (2002) 8:793–800. doi: 10.1038/nm730
229. Wu P, Wu D, Li L, Chai Y, Huang J. PD-L1 and survival in solid tumors: a meta-analysis. *PLoS ONE* (2015) 10:e0131403. doi: 10.1371/journal.pone.0131403
230. Siegel R, Naishadham D, Jemal A. Cancer statistics, 2013. *CA Cancer J Clin.* (2013) 63:11–30. doi: 10.3322/caac.21166
231. Grivennikov SI, Greten FR, Karin M. Immunity, inflammation, and cancer. *Cell* (2010) 140:883–99. doi: 10.1016/j.cell.2010.01.025
232. Dong H, Zhu G, Tamada K, Chen L. B7-H1, a third member of the B7 family, co-stimulates T-cell proliferation and interleukin-10 secretion. *Nat Med.* (1999) 5:1365–9. doi: 10.1038/70932
233. Freeman GJ, Long AJ, Iwai Y, Bourque K, Chernova T, Nishimura H, et al. Engagement of the PD-1 immunoinhibitory receptor by a novel B7 family member leads to negative regulation of lymphocyte activation. *J Exp Med.* (2000) 192:1027–34. doi: 10.1084/jem.192.7.1027
234. Wang S, Chen L. T lymphocyte co-signaling pathways of the B7-CD28 family. *Cell Mol Immunol.* (2004) 1:37–42.
235. Subudhi SK, Zhou P, Yerian LM, Chin RK, Lo JC, Anders RA, et al. Local expression of B7-H1 promotes organ-specific autoimmunity and transplant rejection. *J Clin Invest.* (2004) 113:694–700. doi: 10.1172/JCI19210
236. Azuma T, Yao S, Zhu G, Flies AS, Flies SJ, Chen L. B7-H1 is a ubiquitous antiapoptotic receptor on cancer cells. *Blood* (2008) 111:3635–43. doi: 10.1182/blood-2007-11-123141
237. Duraiswamy J, Kaluza KM, Freeman GJ, Coukos G. Dual blockade of PD-1 and CTLA-4 combined with tumor vaccine effectively restores T-cell rejection function in tumors. *Cancer Res.* (2013) 73:3591–603. doi: 10.1158/0008-5472.CAN-12-4100
238. Groeger S, Domann E, Gonzales JR, Chakraborty T, Meyle J. B7-H1 and B7-DC receptors of oral squamous carcinoma cells are upregulated by *Porphyromonas gingivalis*. *Immunobiology* (2011) 216:1302–10. doi: 10.1016/j.imbio.2011.05.005
239. Hirai M, Kitahara H, Kobayashi Y, Kato K, Bou-Gharios G, Nakamura H, et al. Regulation of PD-L1 expression in a high-grade invasive human oral squamous cell carcinoma microenvironment. *Int J Oncol.* (2017) 50:41–8. doi: 10.3892/ijo.2016.3785
240. Groeger S, Howaldt HP, Raifer H, Gattenloehner S, Chakraborty T, Meyle J. Oral squamous carcinoma cells express B7-H1 and B7-DC receptors *in vivo*. *Pathol Oncol Res.* (2017) 23:99–110. doi: 10.1007/s12253-016-0100-7
241. Groeger S, Jarzina F, Mamat U, Meyle J. Induction of B7-H1 receptor by bacterial cells fractions of Porphyromonas gingivalis on human oral epithelial cells. *Immunobiology* (2017) 222:137–147. doi: 10.1016/j.imbio.2016.10.011
242. Groeger S, Jarzina F, Domann E, Meyle J. *Porphyromonas gingivalis* activates NFkappaB and MAPK pathways in human oral epithelial cells. *BMC Immunol.* (2017) 18:1. doi: 10.1186/s12865-016-0185-5
243. Li S, Lee YC, Li Q, Chen CJ, Hsu WL, Lou PJ, et al. Oral lesions, chronic diseases and the risk of head and neck cancer. *Oral Oncol.* (2015) 51:1082–7. doi: 10.1016/j.oraloncology.2015.10.014
244. Komiya Y, Shimomura Y, Higurashi T, Sugi Y, Arimoto J, Umezawa S, et al. Patients with colorectal cancer have identical strains of *Fusobacterium nucleatum* in their colorectal cancer and oral cavity. *Gut* (2018). doi: 10.1136/gutjnl-2018-316661. [Epub ahead of print].
245. Hoppe T, Kraus D, Novak N, Probstmeier R, Frentzen M, Wenghoefer M, et al. Oral pathogens change proliferation properties of oral tumor cells by affecting gene expression of human defensins. *Tumour Biol.* (2016) 37:13789–98. doi: 10.1007/s13277-016-5281-x
246. Geng F, Liu J, Guo Y, Li C, Wang H, Wang H, et al. Persistent exposure to *Porphyromonas gingivalis* promotes proliferative and invasion capabilities, and tumorigenic properties of human immortalized oral epithelial cells. *Front Cell Infect Microbiol.* (2017) 7:57. doi: 10.3389/fcimb.2017.00057
247. Binder Gallimidi A, Fischman S, Revach B, Bulvik R, Maliutina A, Rubinstein AM, et al. Periodontal pathogens *Porphyromonas gingivalis* and *Fusobacterium nucleatum* promote tumor progression in an oral-specific chemical carcinogenesis model. *Oncotarget* (2015) 6:22613–23. doi: 10.18632/oncotarget.4209
248. Bolos V, Peinado H, Perez-Moreno MA, Fraga MF, Esteller M, Cano A. The transcription factor Slug represses E-cadherin expression and induces epithelial to mesenchymal transitions: a comparison with Snail and E47 repressors. *J Cell Sci.* (2003) 116(Pt 3):499–511. doi: 10.1242/jcs.00224

249. Lee J, Roberts JS, Atanasova KR, Chowdhury N, Han K, Yilmaz O. Human primary epithelial cells acquire an epithelial-mesenchymal-transition phenotype during long-term infection by the oral opportunistic pathogen, *Porphyromonas gingivalis*. *Front Cell Infect Microbiol.* (2017) 7:493. doi: 10.3389/fcimb.2017.00493
250. Abdulkareem AA, Shelton RM, Landini G, Cooper PR, Milward MR. Potential role of periodontal pathogens in compromising epithelial barrier function by inducing epithelial-mesenchymal transition. *J Periodontal Res.* (2018) 53:565–74. doi: 10.1111/jre.12546
251. Meyle J, Chapple I. Molecular aspects of the pathogenesis of periodontitis. *Periodontol* (2015) 69:7–17. doi: 10.1111/prd.12104
252. Paster BJ, Boches SK, Galvin JL, Ericson RE, Lau CN, Levanos VA, et al. Bacterial diversity in human subgingival plaque. *J Bacteriol.* (2001) 183:3770–83. doi: 10.1128/JB.183.12.3770-3783.2001
253. van Winkelhoff AJ, Loos BG, van der Reijden WA, van der Velden U. *Porphyromonas gingivalis, Bacteroides forsythus* and other putative periodontal pathogens in subjects with and without periodontal destruction. *J Clin Periodontol.* (2002) 29:1023–8. doi: 10.1034/j.1600-051X.2002.291107.x
254. Tatakis DN, Kumar PS. Etiology and pathogenesis of periodontal diseases. *Dent Clin North Am.* (2005) 49:491–516. doi: 10.1016/j.cden.2005.03.001
255. Ji S, Kim Y, Min BM, Han SH, Choi Y. Innate immune responses of gingival epithelial cells to nonperiodontopathic and periodontopathic bacteria. *J Periodontal Res.* (2007) 42:503–10. doi: 10.1111/j.1600-0765.2007.00974.x
256. Guo W, Wang P, Liu Z, Yang P, Ye P. The activation of pyrin domain-containing-3 inflammasome depends on lipopolysaccharide from *Porphyromonas gingivalis* and extracellular adenosine triphosphate in cultured oral epithelial cells. *BMC Oral Health* (2015) 15:133. doi: 10.1186/s12903-015-0115-6
257. Moore WE, Moore LV. The bacteria of periodontal diseases. *Periodontol* (1994) 5:66–77. doi: 10.1111/j.1600-0757.1994.tb00019.x
258. Kumagai Y, Yagishita H, Yajima A, Okamoto T, Konishi K. Molecular mechanism for connective tissue destruction by dipeptidyl aminopeptidase IV produced by the periodontal pathogen *Porphyromonas gingivalis*. *Infect Immun.* (2005) 73:2655–64. doi: 10.1128/IAI.73.5.2655-2664.2005
259. Holt SC, Kesavalu L, Walker S, Genco CA. Virulence factors of *Porphyromonas gingivalis*. *Periodontol* (1999) 20:168–238. doi: 10.1111/j.1600-0757.1999.tb00162.x
260. Birkedal-Hansen H, Taylor RE, Zambon JJ, Barwa PK, Neiders ME. Characterization of collagenolytic activity from strains of Bacteroides gingivalis. *J Periodontal Res.* (1988) 23:258–64. doi: 10.1111/j.1600-0765.1988.tb01369.x
261. Soolari AS, Champagne C, Punzi JS, Amar S, Van Dyke TE. Serum modulation of neutrophil response to *Porphyromonas gingivalis* LPS in periodontal disease. *J Int Acad Periodontol.* (1999) 1:101–9.
262. Kesavalu L, Ebersole JL, Machen RL, Holt SC. *Porphyromonas gingivalis* virulence in mice: induction of immunity to bacterial components. *Infect Immun.* (1992) 60:1455–64.
263. Amano A, Nakagawa I, Okahashi N, Hamada N. Variations of *Porphyromonas gingivalis* fimbriae in relation to microbial pathogenesis. *J Periodontal Res.* (2004) 39:136–42. doi: 10.1111/j.1600-0765.2004.00719.x
264. Jotwani R, Cutler CW. Fimbriated *Porphyromonas gingivalis* is more efficient than fimbria-deficient P. gingivalis in entering human dendritic cells *in vitro* and induces an inflammatory Th1 effector response. *Infect Immun.* (2004) 72:1725–32.
265. Preshaw PM, Schifferle RE, Walters JD. *Porphyromonas gingivalis* lipopolysaccharide delays human polymorphonuclear leukocyte apoptosis *in vitro*. *J Periodontal Res.* (1999) 34:197–202. doi: 10.1111/j.1600-0765.1999.tb02242.x
266. Hamada N, Watanabe K, Sasakawa C, Yoshikawa M, Yoshimura F, Umemoto T. Construction and characterization of a fimA mutant of *Porphyromonas gingivalis*. *Infect Immun.* (1994) 62:1696–704.
267. Grenier D. Inactivation of human serum bactericidal activity by a trypsinlike protease isolated from *Porphyromonas gingivalis*. *Infect Immun.* (1992) 60:1854–7.
268. Njoroge T, Genco RJ, Sojar HT, Hamada N, Genco CA. A role for fimbriae in *Porphyromonas gingivalis* invasion of oral epithelial cells. *Infect Immun.* (1997) 65:1980–4.
269. Lamont RJ, Chan A, Belton CM, Izutsu KT, Vasel D, Weinberg A. *Porphyromonas gingivalis* invasion of gingival epithelial cells. *Infect Immun.* (1995) 63:3878–85.
270. Yilmaz O, Watanabe K, Lamont RJ. Involvement of integrins in fimbriae-mediated binding and invasion by *Porphyromonas gingivalis*. *Cell Microbiol.* (2002) 4:305–14. doi: 10.1046/j.1462-5822.2002.00192.x
271. Watanabe K, Yamaji Y, Umemoto T. Correlation between cell-adherent activity and surface structure in *Porphyromonas gingivalis*. *Oral Microbiol Immunol.* (1992) 7:357–63. doi: 10.1111/j.1399-302X.1992.tb00636.x
272. Shah HN, Gharbia SE, Kowlessur D, Wilkie E, Brocklehurst K. Isolation and characterization of gingivain, a cysteine proteinase from *Porphyromonas gingivalis* strain W83. *Biochem Soc Trans.* (1990) 18:578–9. doi: 10.1042/bst0180578
273. Wolburg H, Lippoldt A. Tight junctions of the blood-brain barrier: development, composition and regulation. *Vascul Pharmacol.* (2002) 38:323–37. doi: 10.1016/S1537-1891(02)00200-8

Conflict of Interest Statement: The authors declare that the research was conducted in the absence of any commercial or financial relationships that could be construed as a potential conflict of interest.

frontiers in Immunology

ORIGINAL RESEARCH
published: 27 February 2019
doi: 10.3389/fimmu.2019.00330

Persistence of *Candida albicans* in the Oral Mucosa Induces a Curbed Inflammatory Host Response That Is Independent of Immunosuppression

*Florian R. Kirchner[1], Katharina Littringer[2], Simon Altmeier[1], Van Du T. Tran[3], Franziska Schönherr[1], Christina Lemberg[1], Marco Pagni[3], Dominique Sanglard[4], Nicole Joller[2] and Salomé LeibundGut-Landmann[1]**

[1] Section of Immunology, Vetsuisse Faculty, University of Zurich, Zurich, Switzerland, [2] Institute of Experimental Immunology, University of Zurich, Zurich, Switzerland, [3] Vital-IT Group, Swiss Institute of Bioinformatics, Lausanne, Switzerland, [4] Institute of Microbiology, University of Lausanne and University Hospital Center, Lausanne, Switzerland

Controlled immune activation in response to commensal microbes is critical for the maintenance of stable colonization and prevention of microbial overgrowth on epithelial surfaces. Our understanding of the host mechanisms that regulate bacterial commensalism has increased substantially, however, much less data exist regarding host responses to members of the fungal microbiota on colonized surfaces. Using a murine model of oropharyngeal candidiasis, we have recently shown that differences in immune activation in response to diverse natural isolates of *Candida albicans* are associated with different outcomes of the host-fungal interaction. Here we applied a genome-wide transcriptomic approach to show that rapid induction of a strong inflammatory response characterized by neutrophil-associated genes upon *C. albicans* colonization inversely correlated with the ability of the fungus to persist in the oral mucosa. Surprisingly, persistent fungal isolates showed no signs of a compensatory regulatory immune response. By combining RNA-seq data, genetic mouse models, and co-infection experiments, we show that attenuation of the inflammatory response at the onset of infection with a persistent isolate is not a consequence of enhanced immunosuppression. Importantly, depletion of regulatory T cells or deletion of the immunoregulatory cytokine IL-10 did not alter host-protective type 17 immunity nor did it impair fungal survival in the oral mucosa, indicating that persistence of *C. albicans* in the oral mucosa is not a consequence of suppressed antifungal immunity.

Keywords: *Candida albicans*, oropharyngeal candidiasis, immune regulation, persistence, IL-17, IL-10, regulatory T cells

OPEN ACCESS

Edited by:
Avi-Hai Hovav,
Hebrew University of Jerusalem, Israel

Reviewed by:
Julian Naglik,
King's College London, United Kingdom
Pushpa Pandiyan,
Case Western Reserve University, United States

***Correspondence:**
Salomé LeibundGut-Landmann
salome.leibundgut-landmann@uzh.ch

Specialty section:
This article was submitted to Mucosal Immunity, a section of the journal Frontiers in Immunology

Received: *29 September 2018*
Accepted: *08 February 2019*
Published: *27 February 2019*

Citation:
Kirchner FR, Littringer K, Altmeier S, Tran VDT, Schönherr F, Lemberg C, Pagni M, Sanglard D, Joller N and LeibundGut-Landmann S (2019) Persistence of Candida albicans in the Oral Mucosa Induces a Curbed Inflammatory Host Response That Is Independent of Immunosuppression. Front. Immunol. 10:330. doi: 10.3389/fimmu.2019.00330

INTRODUCTION

Opportunistic infections with fungi are an increasing cause of morbidity and mortality worldwide. *C. albicans* is one of the most important disease-causing fungi in humans. It is found as a commensal in the human gastrointestinal and genital tracts with a large proportion of healthy individuals being carriers, but it may become pathogenic under certain conditions. Disease symptoms range from mild to severe superficial infections of the oral and vaginal mucosae, the

skin and the nails, affecting millions of people worldwide (1–5). More rarely, *C. albicans* causes systemic diseases associated with high mortality rates (6). The development of *C. albicans* mucosal infections is mainly attributed either to defects in host cellular immunity, including those resulting from primary or secondary immunodeficiency, or to changes in the normal microbiota that may be caused by antibiotic treatment (3, 5). Defects in epithelial barrier integrity are also associated with infections, highlighting the importance of intact epithelial function for preventing fungal entry into the tissue (7). In addition to host factors, *C. albicans* infections may be favored by increased expression of virulence attributes of the fungus. Genetic variations within the species of *C. albicans* that result in phenotypic diversity within the fungus have been found to modulate its pathogenicity at epithelial surfaces and systemically (8–12). The decision between *C. albicans* commensalism and disease is thus the result of a fine balance between fungal virulence and host defense mechanisms.

The experimental model of oropharyngeal candidiasis (OPC) in mice has been widely used to study the interaction of *C. albicans* with the host at mucosal surfaces *in vivo* (13). It allowed unraveling antifungal immune mechanisms against *C. albicans*, such as the interleukin 17 (IL-17)-pathway (14), and to explore the pathogenicity of *C. albicans* mutants at the mucosal surface (15, 16).

Using the common laboratory strain SC5314 for infection in this model only partially reflects the situation of OPC in humans (where *C. albicans* is a commensal). In wild type mice, this highly virulent *C. albicans* isolate is rapidly cleared from the oral mucosa (17). However, we have recently shown that depending on the fungal isolate, the murine oral mucosa can be colonized with *C. albicans* for a prolonged period of time without immunosuppression of the host (12), thus mimicking the situation in humans.

Our initial investigations of the differences between acute and persistent OPC in mice have revealed major differences in the host response that was induced by different isolates of *C. albicans* (12). Most strikingly, the differential degree of inflammation that was triggered by virulent strains (such as strain SC5314) compared to persistent strains (such as strain 101) correlated with the differential outcome of infection (12). However, the basis of the differential host response triggered by different strains remains unclear.

Here, we applied an unbiased genome-wide approach to obtain a comprehensive view on the host response to two functionally divergent fungal strains and to assess differences in the host response that might modulate the balance between fungal persistence and rapid clearance. Moreover, we addressed whether persistent *C. albicans* had a propensity to trigger an immunosuppressive response in the host that might be responsible for the curbed immune activation and in turn allow prolonged colonization in the host.

MATERIALS AND METHODS

Mice

Foxp3-GFP.KI x *Il10*-Thy1.1 reporter mice (18, 19), DEREG mice (20) and *Il10*$^{-/-}$ mice (21) were obtained from Vijay Kuchroo (Brigham and Women's Hospital, Harvard Medical School, Boston, MA, USA), Manfred Kopf (ETH Zurich, Switzerland), and the Swiss Immunological Mouse Repository, respectively and bred at the Laboratory Animal Service Center (University of Zürich, Switzerland). Wildtype (WT) C57BL/6J mice were purchased from Janvier Elevage. All mice were kept in specific pathogen-free conditions and used in sex- and age-matched groups at 6–15 weeks of age. DEREG mice were treated with 1 μg diphtheria toxin i.p. on day 11 and 13 post-infection. Where indicated, 0.125 mg anti-CD25 antibody (clone PC-61.5.3, BioXCell) or the corresponding isotype control were administered i.p. per mouse 7 days prior to infection.

Fungal Strains and OPC Infection Model

C. albicans strains SC5314 (22) and 101 (12) were grown in YPD medium at 30°C and 180 rpm for 15–18 h. Mice were infected sublingually with 2.5×10^6 *C. albicans* yeast cells as described (23), without immunosuppression. In co-infection experiments, mice were infected with 1.25×10^6 yeast cells of each strain, i.e., with a total of 2.5×10^6 yeast cells. For determination of the fungal burden, the tongue of euthanized animals was removed, homogenized in sterile 0.05% NP40 in H_2O for 3 min at 25 Hz using a Tissue Lyzer (Qiagen) and serial dilutions were plated on YPD agar containing 100 μg/ml Ampicillin. Infection of mice with strain 101 resulted in detectable fungal loads in the tongue and in the feces for >60 days, in some mice >1 year.

Preparation of Tongue Epithelial Sheets and RNA Isolation

The tongue was cut in half to obtain the dorsal part, which was then freed from muscle tissue with a scalpel and floated on PBS containing 2.86 mg/ml dispase II (Roche) for 60 min with the epithelial side facing upwards to separate the epithelial tissue from the lamina propria. Epithelial sheets were incubated in RNAlater (Sigma-Aldrich) for 1 min immediately after isolation and then grinded in liquid N_2. Three epithelial sheets were pooled for the generation of each RNA-seq replicate and two replicates were generated.

RNA isolation from epithelial sheets was done by combining two phase separations and DirectZol™ RNA MiniPrep kit (Zymo Research) as described (24). DNase treatment was performed off-column using the DNA-free™ Kit (Life Technologies). RNA integrity was determined using a 2100 Bioanalyzer system (Agilent Technologies) according to the manufacturer's instructions. Samples were only included in the study if the RNA integrity value (RIN) was above 7.5 and no obvious degradation was observed.

Preparation of cDNA Libraries and Sequencing

cDNA libraries were generated using the SureSelect multiplexed sequencing kit with strand-specific RNA library preparation for Illumina (Agilent Technologies) according to the manufacturer's instructions. In brief, mRNA was purified using poly(A) beads, fragmented and double-stranded cDNA with ligated adapters was generated. The library was amplified using primers that match the adapters. During this step, RNA-seq indexes were inserted

into the libraries for multiplexing. The collected double-strand cDNA was then amplified and indexed in a separate PCR. RNA quality, fragment size, and cDNA concentration were determined using a fragment analyzer automated CE system (Advanced Analytical) and a Qubit fluorometer (Invitrogen).

cDNA libraries were subjected to cluster generation using the Illumina TruSeq PE cluster kit v3 reagents and sequenced on the Illumina HiSeq 2500 system with TruSeq SBS kit v3 reagents at the Lausanne Genomic Technologies Facility (LGTF).

RNA-Seq Data Analysis

RNA-seq purity-filtered reads were adapter- and quality-trimmed with *cutadapt* (v1.2.1) (25) and filtered for low complexity with *seq_crumbs* (v0.1.8) (https://bioinf.comav.upv.es/seq_crumbs). After alignment against the mouse genome GRCm38.p4 using STAR (v2.4.2a), *htseq-count* (v0.5.4p3) (26) was used to summarize the number of read counts per gene locus. Genes with counts fewer than one per million in all samples were removed from the statistical analysis, yielding 13,855 remaining genes. Data normalization and differential expression analysis were performed in R (v3.2.2) as follows. Normalization of read count data was performed with the *edgeR* package using the TMM (trimmed mean of M-values) method (27). Normalized read count data was transformed to log2-counts with the *voom* transformation (28). A linear model was applied to the transformed data using the *limma* package (29) on all conditions, all in duplicates. The contrasts representing the difference between the infected and naïve conditions were studied, including conditions at 9 h, 1 day, 3 days, 7 days post-infection with strains SC5314 and 101, respectively. *P*-values produced from the differential analysis were adjusted using Benjamini & Hochberg correction (30). Genes were considered to be differentially regulated if their expression was altered by a factor of at least 2-fold with adjusted p-values < 0.05 (false discovery rate, FDR). Gene Ontology (GO) enrichment analysis was done with the *topGO* package (version 2.32.0) using the *fisher* statistic and *weight01* algorithm. This analysis was restricted to all GO terms that are offspring of GO:0002376 (immune system processes) and to genes that are differentially regulated in at least one contrast. An additional enrichment analysis was performed with the *MetaCore*^{TM} software (Thomson Reuters, https://clarivate.com/products/metacore) on all GO terms belonging to biological process. Heat maps and hierarchical clustering were generated with the *Morpheus* software (Broad Institute, https://software.broadinstitute.org/morpheus) using the distance of one minus Pearson correlation and the average linkage mode. The data analyzed here are accessible under the NCBI BioProject accession number PRJNA491801.

RNA Isolation From Total Tongue and Quantitative RT-PCR

Isolation of total RNA from bulk tongues was carried out according to standard protocols using TRI Reagent® (Sigma Aldrich). cDNA was generated by RevertAid reverse transcriptase (Thermo Fisher). Quantitative PCR was performed using SYBR Green (Roche) and a QuantStudio 7 Flex (Life Technologies) instrument. The primers used for qPCR are listed in **Table S1**. All qRT-PCR assays were performed in duplicate and the relative expression (rel. expr.) of each gene was determined after normalization to β-actin transcript levels.

Preparation of Lymph Node Cells for T Cell and Treg Analysis by Flow Cytometry

Cervical lymph nodes were removed and single cell suspensions were prepared by digestion with DNase I (2.4 mg/ml, Roche) and Collagenase I (2.4 mg/ml, Invitrogen) in PBS for 15 min at 37°C. For inducing cytokine production by primed T cells, 10^6 cervical lymph node cells were re-stimulated for 6 h with 1×10^5 MutuDC1940 cells (31) pulsed with 2.5×10^5/ml heat-killed *C. albicans* or left unpulsed. Brefeldin A (10 μg/ml, AppliChem) was added for the last 5 h to inhibit the secretory pathway. Intracellular IL-17 and IFN-γ production was then analyzed by flow cytometry.

Preparation of Tongue Cells for Flow Cytometry

For quantification of neutrophils, tongues were removed and digested with DNase I (2.4 mg/ml, Roche), and Collagenase IV (4.8 mg/ml) in PBS for 45 min at 37°C. For analysis of Tregs, mice were anesthetized with a sublethal dose of Ketamin (100 mg/kg), Xylazin (20 mg/kg), and Acepromazin (2.9 mg/kg) and perfused by injection of PBS into the right heart ventricle prior to removing the tongue. Tongues were cut in half and the underlying muscle tissue was carefully removed using a scalpel. The remaining tongue tissue was cut into small pieces and digested with DNase I (2.4 mg/ml, Roche), Collagenase IV (2.4 mg/ml) and in some case Trypsin (1 mg/ml) in PBS for 45 min at 37°C. Single cell suspensions were obtained by passing the digested tissue through a 70 μm strainer using icecold PBS supplemented with 1% FCS and 2 mM EDTA and then stained for flow cytometry.

Flow Cytometry

Single cell suspensions of tongue and lymph nodes were stained in PBS supplemented with 1% FSC, 5 mM EDTA, and 0.02% NaN_3. LIVE/DEAD Near IR stain (Life Technologies) was used for exclusion of dead cells. The antibodies for surface and intracellular cytokine staining are listed in **Table S2**. For intracellular cytokine staining, cells were fixed and permeabilized using BD Cytofix/Cytoperm reagent (BD Biosciences) and subsequently incubated in Perm/Wash buffer (BD Biosciences). All extracellular and intracellular staining steps were carried out on ice.

For intranuclear Foxp3 staining, cells were fixed/permeabilized for 40 min at RT using the Foxp3 Staining Buffer Set (eBioscience) and subsequently stained for 40 min at RT in BD Perm/Wash buffer (BD Biosciences), Cells were acquired on a FACS Gallios (Beckman Coulter), a SP6800 Spectral Analyzer (Sony) or a BD LSRFortessa (BD Biosciences). The data were analyzed with FlowJo software (FlowJo LLC). The gating of the flow cytometric data was performed according to the guidelines for the use of flow cytometry and cell sorting in immunological studies (32), including pre-gating on viable and single cells for analysis. Absolute cell numbers of lymphoid

cell populations were calculated based on a defined number of counting beads (BD Biosciences, Calibrite Beads), which were added to the samples before flow cytometric acquisition.

Histology

For histology, tissue was fixed in 4% PBS-buffered paraformaldehyde overnight and embedded in paraffin. Sagittal sections (9 μm) were stained with Periodic-acidic Schiff (PAS) reagent and counterstained with Haematoxilin and mounted with Pertex (Biosystem, Switzerland) according to standard protocols. Images were acquired with a digital slide scanner (NanoZoomer 2.0-HT, Hamamatsu) and analyzed with NDP.view2.

RESULTS

The Host Response to *C. albicans* Strain 101 Is Delayed Compared to Strain SC5314

To obtain genome-wide information about the host response to *C. albicans* in the oral mucosa, we performed a transcriptomic analysis. We used the two functionally distinct *C. albicans* strains SC5314 and 101 to assess strain-specific differences between acute and persistent infection in mice at 9 h, 1 day, 3 days and 7 days post-infection. To enrich for host tissue in direct contact with the fungus, we isolated epithelial sheets from the tongue by dispase II-mediated digestion of the basal membrane. Epithelial sheets were strongly enriched for epithelial cells compared to the proportion found in the bulk tongue, but they also contained tissue-resident and infiltrated immune cells as evidenced by histology and flow cytometry (**Figure S1**).

Epithelial sheets were subjected to RNA isolation, cDNA library generation and sequencing. Analysis of the number of differentially expressed genes over time in comparison to uninfected conditions revealed a rapid onset of the transcriptional response to the virulent strain SC5314 between 9 and 24 h post-infection, whereas a slower kinetic was observed after infection with the persistent strain 101, which started rising after day 1 post-infection and increased continuously until day 7 post-infection (**Figures 1A–C**). Interestingly, in case of strain SC5314, the number of differentially expressed genes increased until day 3 post-infection (**Figures 1A–C**), even though the fungal burden is known to decline rapidly at this time point for this specific isolate (33). The genes differentially expressed on day 3 post-infection largely differed from those regulated earlier (**Figure S2**). Finally, by day 7, only very few genes were changed in comparison to uninfected controls (**Figures 1A–C**, **Figure S2**) indicating that homeostasis was rapidly restored after clearance of strain SC5314.

Quantitative and Qualitative Differences in the Host Response to Virulent and Persistent OPC

Given the delayed response observed to the persistent strain 101 compared to the virulent strain SC5314, we were interested whether the two responses were qualitatively comparable, regardless of kinetics of the observed changes. While a large number of genes were selectively regulated by SC5314, there was also a considerable overlap between the two responses, whereby most co-regulated genes were delayed by one to two time points in case of strain 101 (**Figure S2**). Likewise, at the level of the regulated biological processes, as defined at the level of gene ontology, there was a good concordance of the response to the two fungal strains, again with slower kinetics and lower FDR in case of strain 101 (**Figure S3**). The processes that were most strongly induced early after infection comprised those linked to antimicrobial response and immunity, while on day 3 post-infection with strain SC5314, metabolic processes dominated. The processes that were most strongly repressed by both strains comprised those linked to development and negative regulation of signaling (**Figure S3**).

Among the immune system processes that were most significantly regulated by strain SC5314, some were found to have a comparably high FDR in the response to strain 101, including GO terms linked to chemotaxis and cell migration. This strain-specific difference was also reflected at the level of the genes that were annotated to these processes: genes encoding for the neutrophil chemokines CXCL1, CXCL2, and CXCL5 as well as IL-1β were strongly induced in response to SC5314 on day 1 post-infection, but very poorly in response to 101 at any time point analyzed (**Figure 2**). Even after 60 days of infection, when mice were still highly colonized with strain 101, expression of these factors remained as low as in uninfected controls (**Figures S4A–B**). This was consistent with the curbed recruitment of neutrophils to the tongue infected with strain 101 in comparison to strain SC5314 (12). In some mice, strain 101 persisted for over 1 year without causing inflammation or triggering neutrophil recruitment (**Figures S4C–E**).

Among the genes annotated to immune system processes that were significantly regulated (FDR $<$ 0.05), we observed many that were regulated to a comparable degree by both fungal strains, including genes associated with the IL-17 pathway (**Figure 2**). Conserved induction of the IL-17 pathway by both fungal strains was also confirmed at the level of IL-17 target genes, including those coding for S100a8, S100a9, Lipocalin 2, β-defensin-3, and β-defensin-1. They reached highest expression levels on day 1–3 post-infection in case of strain SC5314, and on day 3–7 in case of strain 101, respectively (**Figure 2**). *Defb3* and *Defb1* genes were an exception to this pattern as their expression did not rise before day 3 in either condition (**Figure 2**). Overall, this confirmed what we previously observed in response to these two fungal strains (**Figure S4F**) (12).

C. albicans Strain 101 Does Not Actively Suppress the Host Response at the Onset of Infection

In search of an explanation for the delayed and more limited host response to strain 101 in comparison to strain SC5314, we examined whether expression of immune regulatory and immunosuppressive genes that might curb the inflammatory response predominated during infection with strain 101. Surprisingly, such genes were not found to be significantly induced in the RNA-seq data set by any of the two strains.

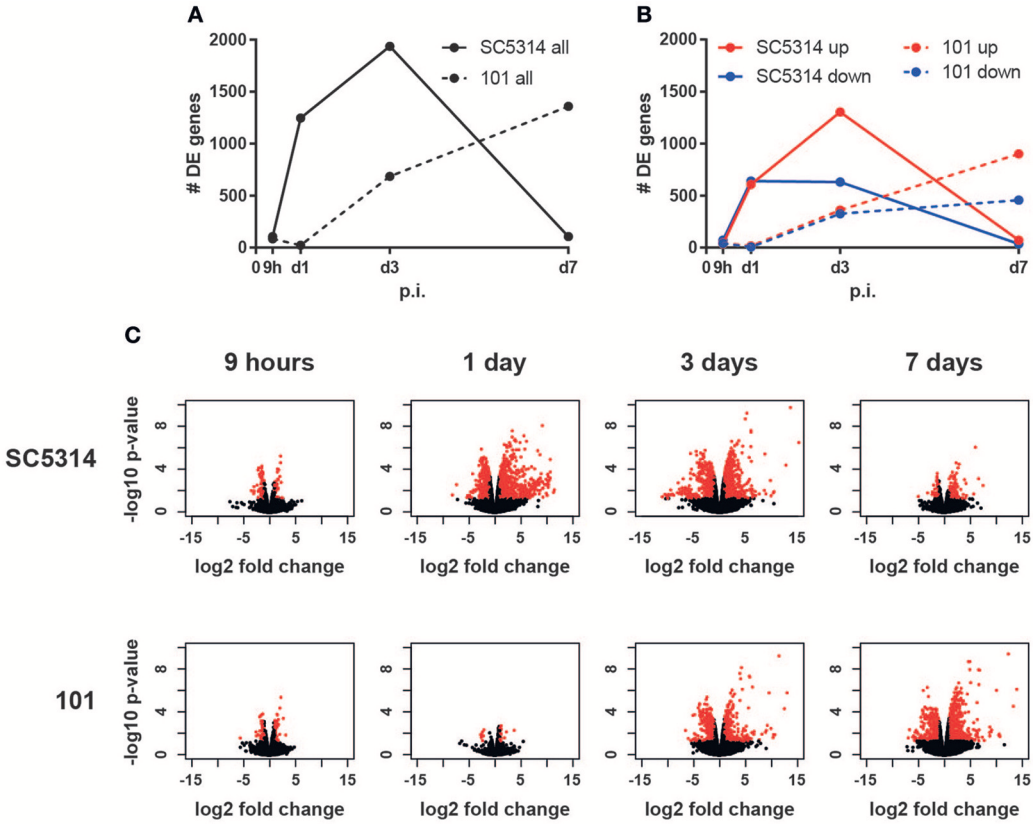

FIGURE 1 | The host response to *C. albicans* strain 101 is delayed compared to strain SC5314. Epithelial sheet from *C. albicans* strain SC5314- and strain 101-infected WT mice were subjected to RNA-seq analysis. **(A)** Graph showing the total number of differentially expressed (DE) genes at the indicated time points compared to naïve controls. **(B)** Separate display of the up- and down-regulated genes at the indicated time points. **(C)** Volcano plots displaying the fold changes and the FDR of all genes detected in each condition separately. Genes with FDR $<$ 0.05 and fold change $<$ -2 or $>$ 2 are marked in red.

Moreover, in a GO process enrichment analysis, processes associated with immune regulation such as "negative regulation of immune response" or "negative regulation of immune system processes" were not altered significantly. This was also consistent with the absence of an increase in IL-10 or TGF-β transcript levels by RT-qPCR in epithelial sheets (**Figure 3A**). This analysis may not have captured the full spectrum of the antifungal response, as the epithelial sheets used for RNA isolation and sequencing/RT-qPCR do not represent the full complexity of the mucosal immune system and some cells may have been lost during preparation of the epithelial sheets (and others might act at a distance). We therefore quantified IL-10 and TGF-β expression levels in the bulk tongue of 101-infected compared to naïve mice (**Figure 3B**).

We further looked at regulatory T cells (Tregs) and whether they contribute to suppression of the early host response to strain 101. Immune suppression might be undetectable at the RNA level as transcriptional changes may occur in rare cell populations that are lost in resolution in the whole tissue. Tregs are more abundant in the oral mucosa compared to other organs (34). Detection of lymphocytes in the tongue is challenging due to the small number of cells and the high degree of autofluorescence of this tissue (37, 38). Using a refined protocol of tissue preparation and flow cytometry we were able to detect a small number of Foxp3$^+$ T cells in the tongue which were present at comparable frequencies in naïve and infected animals (**Figures 3C–D**). Moreover, depletion of Tregs prior to infection (**Figure S5**) did not alter the kinetics of the epithelial response to strain 101 or allow expression of inflammatory genes such as those regulating the neutrophil response (**Figure 3E**), nor did it affect the fungal load (**Figure 3F**). This indicates that Tregs are not responsible for the limited and delayed host response at the onset of persistent OPC.

Finally, we tested the capacity of strain 101 to suppress the host response in the oral mucosa with an unbiased approach using a co-infection experiment for which we infected mice with a 1:1 mix of strain 101 and strain SC5314. We questioned whether the presence of strain 101 would lead to a reduced overall host response in the tongue due to a dominant regulatory response. This was however not the case: the induction of a rapid inflammatory response was as efficient after co-infection as after infection with strain SC5314 alone. The recruitment of neutrophils to the site of infection as well as the induction of *Il17f* and *S100a9*, two of the most strongly induced genes

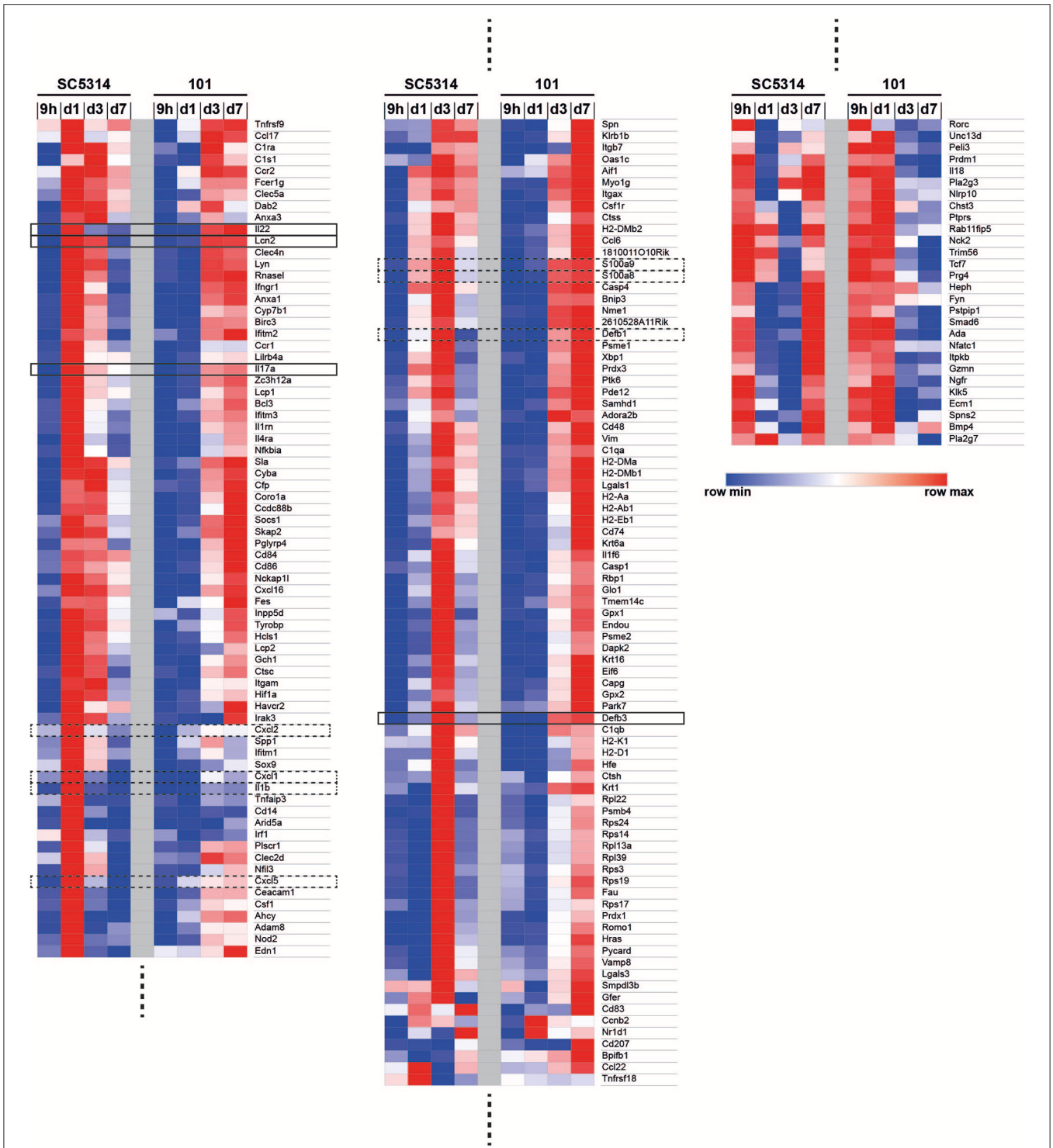

FIGURE 2 | Co-regulated and differentially regulated genes in the mucosal response to strains 101 and SC5314. The GO term enrichment analysis on genes that are differentially regulated in at least one contrast for the 62 GO terms that are offspring of GO: 0002376 (immune system processes) with $p < 0.05$ yielded 182 genes. Genes were ordered by hierarchical clustering of their log2 fold changes, which are displayed in a heat map with a row-scaling color scheme.

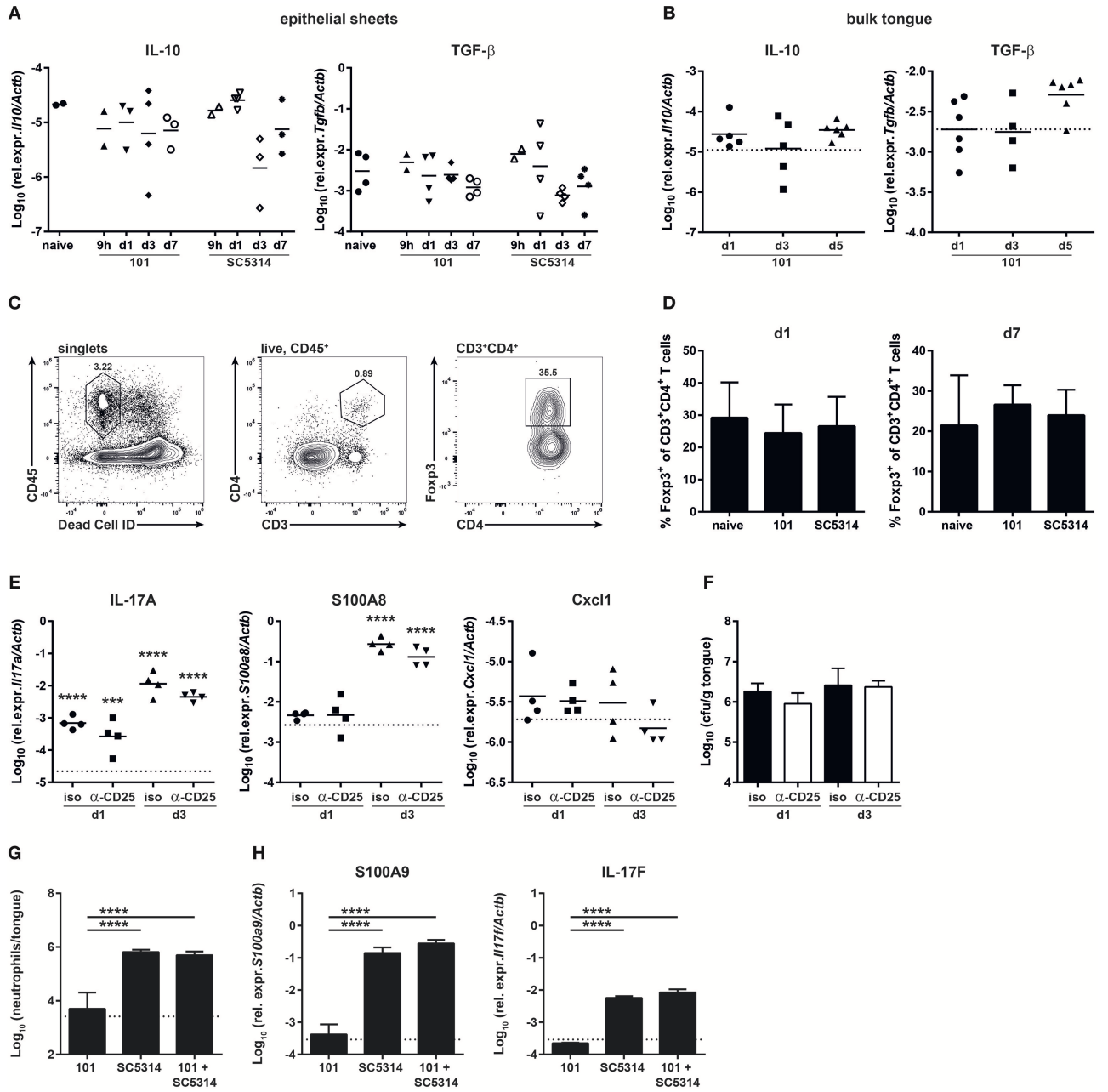

FIGURE 3 | The persistent strain 101 does not suppress the antifungal host response. **(A,B)** Relative expression of *Il10* (left) and *Tgfb1* transcripts (right) in epithelial sheets **(A)** or in bulk tongue tissue **(B)** of mice that were infected with strain 101 or SC5314 for the indicated period of time. Each symbol represents a pool of epithelial sheets from three animals each **(A)** or a single mouse **(B)**. The geomean of each group is indicated. Data are pooled from two independent experiments each. **(C,D)** % Foxp3$^+$ Tregs within the viable CD45$^+$CD3$^+$CD4$^+$ population in the tongue of mice that were infected with strain 101 or SC5314 for the indicated period of time. Representative FACS plots and the gating strategy are shown in C, summary plots showing the mean + SD of data pooled from two independent experiments with 3–4 animals per group are shown in D. **(E,F)** Mice were treated with anti-CD25 or isotype control antibody prior to infection with strain 101. Relative expression of *Il17a* (left), *S100a8* (middle), and *Cxcl1* (right) **(E)** and tongue fungal loads **(F)** in the bulk tongue tissue at the indicated time point after infection are shown. In **(E)**, each symbol represents a single animal, The geomean of each group is indicated. The dotted line represents transcript levels in naïve animals (mean of 8 animals). In **(F)**, each bar is the geomean + SD of 4 animals per group. **(G,H)** WT mice were infected sublingually with a 1:1 mixture of strain 101 and strain SC5314 or with each strain alone. Tongues were harvested on day 1 post-infection and analyzed for the infiltration of Ly6G$^+$Ly6C^{lo}CD11b$^+$ neutrophils by flow cytometry **(G)** and for the expression of *S100a9* and *Il17f* **(H)** transcript by RT-qPCR. Data are the mean + SD of 3–4 mice per group. Graphs display data representative of one out of two independent experiments. The dotted line represents the detection limit. Statistics were calculated using one-way ANOVA. In **(E)**, statistics compare infected to naïve groups. ***$p < 0.001$, ****$p < 0.0001$.

by SC5314 on day 1 post-infection, was comparable in both conditions (**Figures 3G–H**). These data show that strain 101 is not actively repressing the antifungal host-response and that fungal persistence is not a consequence of suppressed immune activation.

The Treg Compartment Is Normal During Persistent *C. albicans* Infection

Albeit with delay and more restricted in comparison to strain SC5314, *C. albicans* strain 101 does induce a pronounced immune response in the host, characterized by a prominent IL-17 signature. While induction of the type 17 response does not lead to clearance of strain 101 from the oral mucosa, IL-17 signaling is essential for controlling persistence and preventing fungal overgrowth (12). Importantly, unlike infection with strain SC5314, the type 17 response to strain 101 infection is maintained over a prolonged period of time (**Figures 4A,B**). Given the potential of type 17 immunity to cause immunopathology and provoke tissue damage (35), tight regulation by mechanisms such as those mediated by Tregs might be necessary.

We thus turned to the analysis of Tregs at later time points of infection to assess their role during persistent colonization of the oral mucosa with *C. albicans*. Treg numbers did not change significantly over the course of 3 weeks of infection and there was also no difference in Treg frequencies between strain 101 and strain SC5314-infected mice (**Figures 4C,D**). Treg frequencies remained unchanged even after 100 days of *C. albicans* colonization with strain 101 (data not shown). We also examined possible functional differences in Tregs in the different settings. Tregs are characterized by the expression of co-inhibitory receptors. We have shown previously that Tim-3 expression is induced on Tregs in a type 17-polarized environment (36) and this was also observed here (**Figure 4E**). Differences in Tim-3 expression by Tregs were detected on day 7 post-infection, but were lost at later time points (**Figures 4E,F**). The expression of other co-inhibitory receptors remained unchanged during the course of OPC with either strain of *C. albicans* (**Figures 4E,F**).

Next we assessed IL-10 expression by Tregs, a key effector molecule of these cells with a central role in preventing inflammation-mediated tissue damage. IL-10 is very difficult to track by intracellular staining and flow cytometry. Therefore, we made use of *Il10*-Thy1.1 reporter mice (18). These mice also contain a GFP-reporter for Foxp3 (19), making the need for intranuclear staining of Foxp3 dispensable. Infecting these mice with *C. albicans* revealed a strong expression of IL-10 by $Foxp3^+$ cells and to a lesser degree by $Foxp3^-$ cells (**Figures 4G,H**). However, again no significant differences in IL-10 production were observed between Tregs from naïve and infected animals, if anything, there was a trend toward higher IL-10 in SC5314 infected mice (**Figures 4G,H**).

Next, we analyzed IL-10 production by Tregs in the tongue. A prominent fraction of those also expressed IL-10, as assessed by the Thy1.1 reporter (**Figures 4I,J**). In addition, we detected some IL-10 expression by Foxp3-negative T cells. Albeit with some variation, these populations were detected in all samples analyzed, including the naïve tongue and that of animals infected with either strain of *C. albicans* (**Figures 4I,J**).

Tregs and IL-10 Are Not Required for *C. albicans* Persistence in the Murine Oral Mucosa

Although we did not observe significant changes in the Treg compartment during *C. albicans* colonization of the oral mucosa, the Tregs present might still modulate the antifungal host response to *C. albicans* and thereby contribute to fungal persistence in the oral mucosa. We therefore examined DEREG mice (20) in which Tregs can be ablated by means of diphtheria toxin injection. We chose to initiate Treg depletion at a time point when stable fungal colonization and burden-regulating IL-17 immunity was already established (**Figure 5A**). To our surprise, we did not observe any significant changes in the degree and the quality of the effector T cell response to *C. albicans* (**Figure 5B**) or in the growth of the fungus on the mucosa (**Figure 5C**) upon Treg depletion.

Because IL-10 production was not limited to the Treg compartment, we also assessed the impact of IL-10 itself on the antifungal response and on *C. albicans* colonization levels separately by means of IL-10-deficient mice (21). Similarly to what we observed under Treg-depleting conditions, IL-10 deficiency did not affect the extent or the quality of the *C. albicans*-specific Th17 response in animals infected with strain 101 (**Figure 5D**). Consistent with this, fungal loads in the tongue were also unchanged in IL-10 knockout mice compared to WT controls (**Figure 5E**). Together, these findings indicate that immune regulation by Tregs and IL-10 is dispensable for persistent *C. albicans* colonization of the oral mucosa.

DISCUSSION

Immunoregulatory mechanisms such as those mediated by Tregs and IL-10 are essential for maintaining tolerance and preventing excessive immune responses to commensal microbes. In this study we analyzed the role of immune regulation during *C. albicans* colonization. Our data indicate that fungal persistence in the oral mucosa is not associated with immunosuppression that would blunt a strong host response and prevent rapid fungal elimination at the onset of infection, as it is observed during OPC with the highly virulent strain SC5314. Rather, the failure of strain 101 to induce an early inflammatory response appears to result from intrinsic properties of the strain and how it interacts with the host and in particular with the epithelium.

The epithelial response to *C. albicans* in turn instructs the extent of neutrophil trafficking to the site of infection (39). The fungal determinants that are responsible for the strain-specific differences at the interface with the epithelium and that underlie the differential behavior in contact with the host may comprise differences in filamentation (40), tissue invasion (12), and the production of virulence factors such as the recently identified peptide toxin candidalysin (15). Candidalysin has been linked to mucosal immune activation and neutrophil recruitment (15,

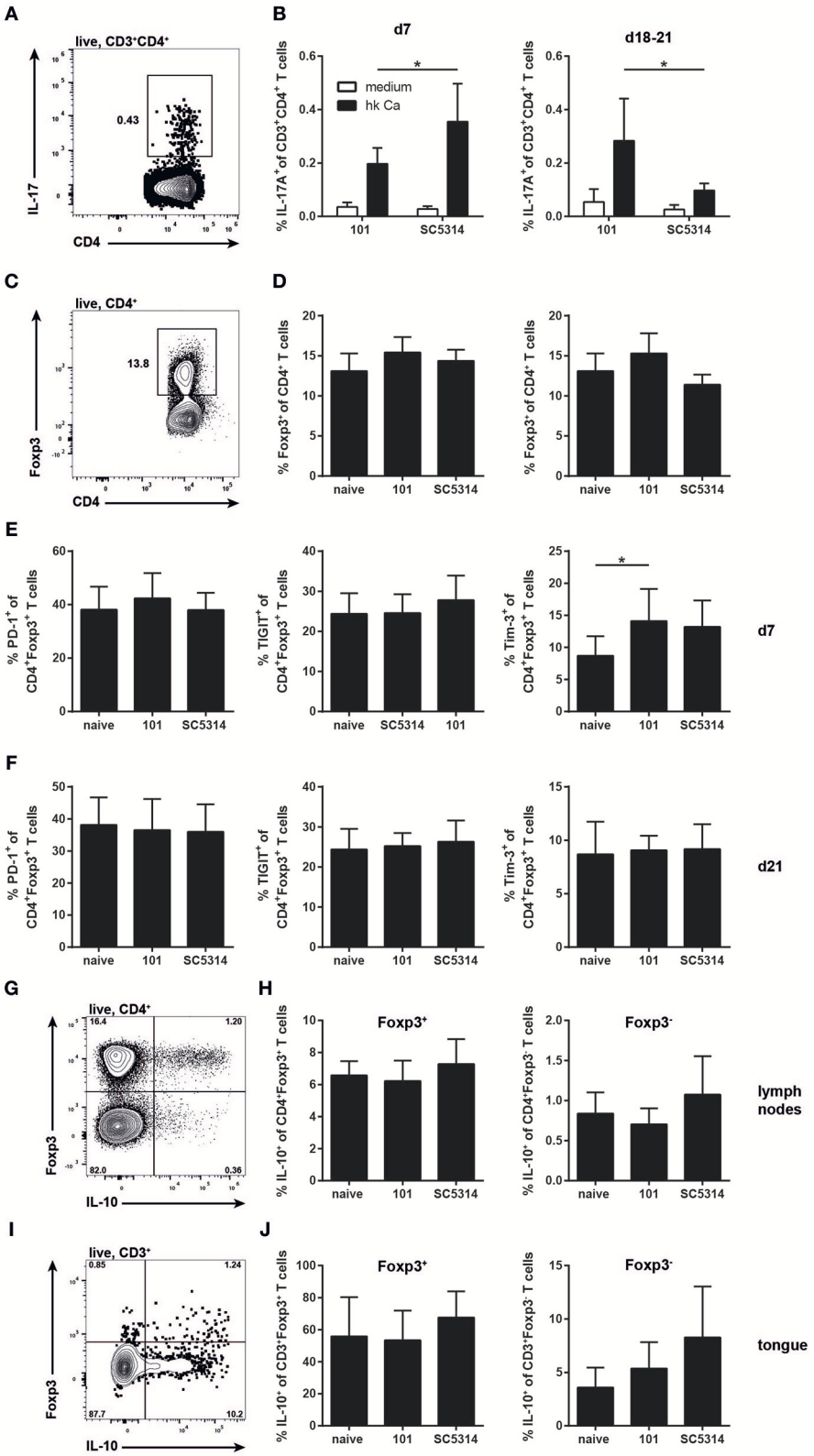

FIGURE 4 | The Treg response during persistent colonization of the oral mucosa with *C. albicans*. **(A–F)** WT mice were sublingually infected with strain 101 or SC5314 and cervical lymph node cells were analyzed on day 7 or day 18–21 as indicated. **(A,B)** Lymph node cells were re-stimulated with MutuDC1940 cells that were pulsed with heat-killed *C. albicans* or left unpulsed for 5 h in the presence of Brefeldin A. IL-17A production by $CD3^+CD4^+$ cells was analyzed by intracellular

(Continued)

FIGURE 4 | cytokine staining and flow cytometry. **(C,D)** The frequency of Foxp3-expressing cells within the $CD4^+$ lymphocyte compartment was assessed by flow cytometry. **(E,F)** PD-1, TIGIT, and Tim-3 expression by $CD4^+Foxp3^+$ Treg cells was analyzed by flow cytometry. (**G–J**) *Il10*-Thy1.1 reporter mice were sublingually infected with strain 101 or SC5314 or left naive. IL-10 expression by $Foxp3^+$ Tregs and $Foxp3^-$ effector T cells was assessed in the cervical lymph nodes **(G,H)** and in the tongue **(I,J)** on day 21 post-infection by flow cytometry. Cells were pregated on $CD90^+CD4^+$ **(G,H)** or on $CD45.2^+CD3^+$ **(I,J)**, respectively. Representative FACS plots are shown in (A, C, G, I); summary plots with data pooled from at least 2 experiments with 6–9 animals per infected group and 3–4 animals per naive group are shown in (B, D–F, H, J), with the exception of the right plot in **(D)**, where data are from a single experiment with 3 animals per group. In B, Statistics were calculated using *t*-test. In **(D–F, H, J)**, statistics were calculated using one-way ANOVA. $*p < 0.05$.

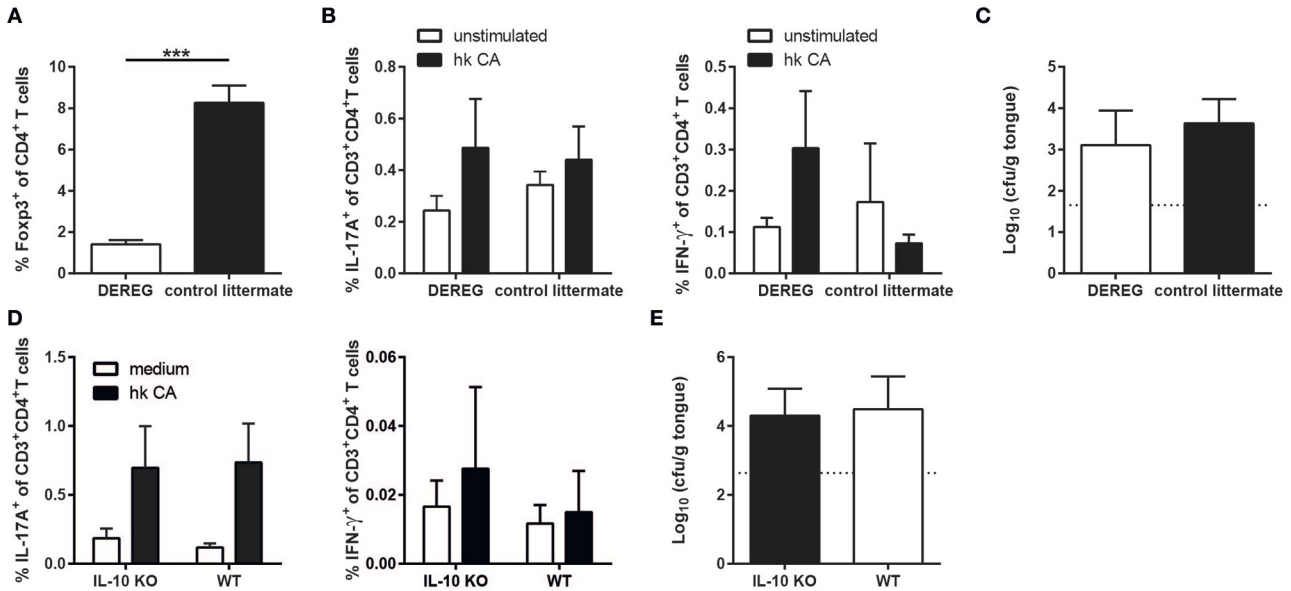

FIGURE 5 | The absence of Tregs or IL-10 does not compromise persistence of strain 101 in the oral epithelium. **(A–C)** DEREG mice and control littermates were sublingually infected with *C. albicans* strain 101 and treated with diphtheria toxin on day 11 and 13 after the antifungal response was fully established. One day after the last treatment, the mice were sacrificed for analysis. **(A)** Treg depletion efficiency was analyzed in the cervical lymph nodes by flow cytometry. Data are the % of $Foxp3^+$ cells within the population of $CD4^+$ viable cells. **(B)** Lymph node cells were re-stimulated with MutuDC1940 cells that were pulsed with heat-killed *C. albicans* or left unpulsed for 5 h in the presence of Brefeldin A. IL-17A (left) and IFN-γ (right) production by $CD3^+CD4^+$ cells was analyzed by intracellular cytokine staining and flow cytometry. **(C)** The fungal burden was determined by plating tongue homogenates on YPD agar. Each bar represents the mean + SD of 3 to 4 mice per group. Data are from one out of two independent experiments. **(D,E)** IL-10-deficient mice and WT controls were sublingually infected with *C. albicans* strain 101 and analyzed on day 9 post-infection. **(D)** Lymph node cells were re-stimulated and analyzed for IL-17 (left) and IFN-γ (right) production as in B. **(E)** Tongue fungal burdens were analyzed as in C. Each bar represents the mean + SD of 8–9 mice per group pooled from two independent experiments. Statistics were calculated using unpaired t-Test. $***p < 0.001$.

41) with an important contribution of IL-1 family cytokine-dependent chemokine induction (39, 42, 43). Our previous work has shown reduced expression of the ECE1 gene (which encodes for candidalysin) by strain 101 in contact with epithelial cells (12), and this difference to strain SC5314 may at least in part be responsible for the observed interspecies differences. The identification of relevant fungal factors underlying the differential host response is subject of ongoing research.

Induction of an inflammatory response by the highly virulent *C. albicans* strain SC5314 in epithelial cells and tissues has been observed in previous transcriptomic studies (44–47). However, our study is the first, to our knowledge, that assesses the kinetics of the transcriptional response to two functionally distinct *C. albicans* isolates in the murine oral mucosa *in vivo*. While host genes associated with the neutrophil response are differentially regulated during infection with strains SC5314 and 101, many other immune genes including those linked to the IL-17 pathway, are expressed to comparable levels in response to the two *C. albicans* strains under investigation, albeit with delay in case of strain 101. By day 3, IL-17 and related cytokines are expressed at comparable levels in both SC5314- and 101-infected tongues. Similarly, Th17 differentiation was indistinguishable after day 7 post-infection. The differential activation of the epithelial-inflammatory response and the IL-17 pathway by strain 101 underlines the notion that the two host pathways constitute two distinct modules of the antifungal response in the oral mucosa that are regulated largely independently. It also supports our earlier observation that the recruitment of neutrophils to the infected epithelium is not compromised in absence of IL-17 signaling (33), and strong IL-17 induction in response to strain 101 on the other hand is not sufficient for bringing neutrophils to the site of infection (12).

The uncoupling of the IL-17 pathway from the epithelial/neutrophil response is also consistent with our

recent finding that induction of IL-17 is instructed by dendritic cells and in particular by the Langerin$^+$ subset of dendritic cells that have the unique property in the *C. albicans*-infected oral mucosa to co-produce the three major IL-17-instructing cytokines IL-23, IL-1, and IL-6 (37). The IL-17 response may be further modulated via epithelial sensing of *C. albicans* and IL-1 family cytokines that are released from the epithelium in response to candidalysin in case of infection with strain SC5314 (42, 43).

β-defensin-3 is a prominent target gene of IL-17 and it was proposed to act as the major antifungal effector molecule during OPC (48). Strong induction in response to both strains SC5314 and 101 was confirmed in our RNA-seq analysis. However, surprisingly, β-defensin-3 expression was delayed when compared to the kinetics of IL-17 induction in case of SC5314. It reached its maximum levels only by day 3 post-infection when the fungus was already nearly cleared from the oral mucosa. Together with the observation that the lack of β-defensin-3 resulted in a slightly less severe loss of fungal control than IL-17 signaling deficiency (48), this suggests that additional IL-17-dependent antimicrobial effector molecules are likely involved.

Based on the observation that the IL-17 pathway is crucial for regulating fungal growth independently of the fungal isolate (12), it is surprising that strain 101 is able to resist the continuously activated IL-17-mediated immunity and to persist in the oral mucosa. Its predominant localization to the stratum corneum may limit its exposure to host immune effectors. Further, it is surprising that the prolonged IL-17 response does not trigger signs of tissue damage despite the strong pro-inflammatory potential of the cytokine. The IL-17 pathway can drive severe immunopathology in barrier tissues under certain conditions, as seen for instance in the skin of psoriatic patients and in murine models of psoriasis (49, 50). Th17 cells have been divided in different subtypes that differ in their pathogenic potential (51). Here, we show that a small proportion of all T helper cells in the lymph nodes and in the tongue of mice infected with strain SC5314 or 101 do express IL-10. However, a comprehensive analysis of the cytokine profile of *C. albicans*-specific Th17 cells during persistent and acute OPC remains to be determined in the future.

The generation of Th17 cells was proposed to be supported by Tregs. This might be through the provision of TGF-β (19, 52, 53), but also through the consumption of IL-2, which negatively regulates Th17 differentiation (54). As such, Pandiyan et al. showed in an adoptive transfer system that co-transfer of Tregs with effector T cells enhances Th17 differentiation in response to *C. albicans* (55). In our study, depletion of Tregs in wild type mice did not affect the induction of *C. albicans*-specific Th17 cells, nor did it affect already established type 17 immunity when Tregs were depleted at a later time point of persistent colonization. Similar results were also obtained in mice lacking IL-10, one of the key regulatory cytokines and a potent suppressor of Th17 cells (56). Together, our data thus indicate that immune regulation does not make an essential contribution to the balance of a protective non-pathological Th17 response and fungal persistence in our model.

In conclusion, our study indicates that the attenuated host response to *C. albicans* strain 101 is well-tared to allow fungal persistence in the oral mucosa by preventing elimination of the fungus but also uncontrolled fungal overgrowth as well as avoiding the development of immunopathology.

ETHICS STATEMENT

All mouse experiments described in this study were conducted in strict accordance with the guidelines of the Swiss Animal Protection Law and were performed under protocols approved by the Veterinary office of the Canton Zurich, Switzerland (license number 201/2012 and 183/2015). All efforts were made to minimize suffering and ensure the highest ethical and human standards.

AUTHOR CONTRIBUTIONS

FRK, KL, SA, NJ, and SL-L: conceptualization; SA and DS: methodology; FRK, KL, SA, FS, and CL: investigation; FRK, KL, SA, VDTT, FS, and CL: formal analysis; NJ, DS, and SL-L: validation and project administration; FRK, KL, VDTT, and SL-L: visualization; MP, NJ, DS, and SL-L: funding acquisition; MP, NJ, and SL-L; supervision; FRK and SL-L: writing-original draft; KL, SA, VDTT, NJ, and DS: writing-review and editing.

ACKNOWLEDGMENTS

We would like to thank Manfred Kopf, Vijay Kuchroo and Casey Weaver for mice; the staff of the Laboratory Animal Service Center of University of Zurich for animal husbandry; the Lausanne Genomic Technologies Facility for sequencing; and members of the LeibundGut-lab and the Joller-lab for helpful advice and discussions. This work was supported by the Swiss National Science Foundation (grant CRSII3_141848 to MP, DS, and SL-L, grant PP00P3_150663 to NJ), the Promedica Foundation (to SL-L), the Fonds zur Förderung des akademischen Nachwuchses of the Zurich University Association (to SL-L.) and the European Research Council (grant 677200 to NJ).

SUPPLEMENTARY MATERIAL

The Supplementary Material for this article can be found online at: https://www.frontiersin.org/articles/10.3389/fimmu.2019.00330/full#supplementary-material

Figure S1 | Characterization of tongue epithelial sheets. Epithelial sheets were isolated from infected tongues as described in the Methods and analyzed by microscopy after periodic acid-Schiff staining **(A)** or digested with trypsin to obtain single cell suspensions and analyzed by flow cytometry **(B)** for their composition. In **(A)**, the black arrow indicates epithelial cells; the white arrow indicates cellular infiltrates; the white arrow head indicates *C. albicans* hyphae. The numbers indicate the % of cells in each gate. The representative data shown are from strain SC5314-infected animals.

Figure S2 | Overlap of differentially expressed genes at different time points and by the different strains of *C. albicans*. Venn diagrams showing the number of differentially expressed genes in tongue epithelial sheets at each time point after infection with *C. albicans* strain SC5314 **(A)** or strain 101 **(B)**. **(C)** Venn diagram

showing the differentially expressed genes on day 1 and 3 after infection with strain SC5314 and on day 3 and 7 after infection with strain 101, respectively, i.e., the conditions with the highest number of gene expression activity. The numbers in the overlapping areas refer to the number of genes that were co-regulated in the respective conditions.

Figure S3 | The host response to *C. albicans* in the tongue is dominated by changes in the immune response and metabolic processes. The heat maps show the upregulated **(A)** and downregulated **(B)** GO processes with the smallest FDR. The heat map was arranged by hierarchical clustering using the distance of one minus Pearson correlation and the average linkage mode.

Figure S4 | Transcriptional response to *C. albicans* strain 101 during persistent oral infection. **(A,B)** Mice were infected with strain 101 for 60 days. Relative expression of *Cxcl1* (left), *Cxcl2* (middle), and *Cxcl5* transcripts (right) in the bulk tongue tissue **(A)** and cfu in the feces **(B)** are shown. Each symbol represents one animal. The geomean of each group is indicated. **(C–E)** Mice were infected with strain 101 for 12–14 months. The fungal load in the feces **(C)** and in the tongue **(D)** are shown. **(E)** shows representative tongue histology stained with PAS from one of the still highly colonized mice. **(F)** Relative expression of *S100a8* (left), *Lcn2* (middle), and *Defb1* transcripts (right) in the tongue of mice were infected with strains 101 or SC5314 for the indicated period of time. Each symbol represents one animal. The geomean of each group is indicated. Dotted line: geomean of a naive control group. Data are pooled from two independent experiments each, except for fecal cfu in **(C)**, which are from one experiment only. Statistics were calculated using one-way ANOVA (comparison of infected to naïve groups). $^{*}p < 0.05$, $^{**}p < 0.01$, $^{***}p < 0.001$, $^{****}p < 0.0001$.

Figure S5 | Treg Depletion. % $Foxp3^{+}$ cells within the splenic $CD4^{+}CD3^{+}$ population of mice treated with anti-CD25 antibody or isotype control as indicated.

Table S1 | Oligonucleotides used in this study.

Table S2 | Antibodies used in this study.

REFERENCES

1. Brown GD, Denning DW, Gow NA, Levitz SM, Netea MG, White TC. Hidden killers: human fungal infections. *Sci Transl Med.* (2012) 4:165rv13. doi: 10.1126/scitranslmed.3004404
2. de Repentigny L, Lewandowski D, Jolicoeur P. Immunopathogenesis of oropharyngeal candidiasis in human immunodeficiency virus infection. *Clin Microbiol Rev.* (2004) 17:729–59, table of contents. doi: 10.1128/CMR.17.4.729-759.2004
3. Goncalves B, Ferreira C, Alves CT, Henriques M, Azeredo J, Silva S. Vulvovaginal candidiasis: epidemiology, microbiology and risk factors. *Crit Rev Microbiol.* (2016) 42:905–27. doi: 10.3109/1040841X.2015.1091805
4. Kirkpatrick CH. Chronic mucocutaneous candidiasis. *Pediatr Infect Dis J.* (2001) 20:197–206. doi: 10.1097/00006454-200102000-00017
5. Puel A, Cypowyj S, Marodi L, Abel L, Picard C, Casanova JL. Inborn errors of human IL-17 immunity underlie chronic mucocutaneous candidiasis. *Curr Opin Allergy Clin Immunol.* (2012) 12:616–22. doi: 10.1097/ACI.0b013e328358cc0b
6. Pfaller MA, Diekema DJ. Epidemiology of invasive candidiasis: a persistent public health problem. *Clin Microbiol Rev.* (2007) 20:133–63. doi: 10.1128/CMR.00029-06
7. Struck MF, Gille J. Fungal infections in burns: a comprehensive review. *Ann Burns Fire Disasters.* (2013) 26:147–53.
8. Odds FC, Bougnoux ME, Shaw DJ, Bain JM, Davidson AD, Diogo D, et al. Molecular phylogenetics of *Candida albicans*. *Eukaryot Cell.* (2007) 6:1041–52. doi: 10.1128/EC.00041-07
9. MacCallum DM, Castillo L, Nather K, Munro CA, Brown AJ, Gow NA, et al. Property differences among the four major *Candida albicans* strain clades. *Eukaryot Cell.* (2009) 8:373–87. doi: 10.1128/EC.00387-08
10. Hirakawa MP, Martinez DA, Sakthikumar S, Anderson MZ, Berlin A, Gujja S, et al. Genetic and phenotypic intra-species variation in *Candida albicans*. *Genome Res.* (2015) 25:413–25. doi: 10.1101/gr.174623.114
11. Marakalala MJ, Vautier S, Potrykus J, Walker LA, Shepardson KM, Hopke A, et al. Differential adaptation of *Candida albicans in vivo* modulates immune recognition by dectin-1. *PLoS Pathog.* (2013) 9:e1003315. doi: 10.1371/journal.ppat.1003315
12. Schönherr FA, Sparber F, Kirchner FR, Guiducci E, Trautwein-Weidner K, Gladiator A, et al. The intraspecies diversity of C. albicans triggers qualitatively and temporally distinct host responses that determine the balance between commensalism and pathogenicity. *Mucosal Immunol.* (2017) 10:1335–50. doi: 10.1038/mi.2017.2
13. Hohl TM. Overview of vertebrate animal models of fungal infection. *J Immunol Methods.* (2014) 410:100–12. doi: 10.1016/j.jim.2014.03.022
14. Sparber F, LeibundGut-Landmann S. Interleukin 17-mediated host defense against *Candida albicans*. *Pathogens.* (2015) 4:606–19. doi: 10.3390/pathogens4030606
15. Moyes DL, Wilson D, Richardson JP, Mogavero S, Tang SX, Wernecke J, et al. Candidalysin is a fungal peptide toxin critical for mucosal infection. *Nature.* (2016) 532:64–8. doi: 10.1038/nature17625
16. Swidergall M, Solis NV, Lionakis MS, Filler SG. EphA2 is an epithelial cell pattern recognition receptor for fungal beta-glucans. *Nat Microbiol.* (2018) 3:53–61. doi: 10.1038/s41564-017-0059-5
17. Gladiator A, Wangler N, Trautwein-Weidner K, LeibundGut-Landmann S. Cutting edge: IL-17-secreting innate lymphoid cells are essential for host defense against fungal infection. *J Immunol.* (2013) 190:521–5. doi: 10.4049/jimmunol.1202924
18. Maynard CL, Harrington LE, Janowski KM, Oliver JR, Zindl CL, Rudensky AY, et al. Regulatory T cells expressing interleukin 10 develop from Foxp3+ and Foxp3- precursor cells in the absence of interleukin 10. *Nat Immunol.* (2007) 8:931–41. doi: 10.1038/ni1504
19. Bettelli E, Carrier Y, Gao W, Korn T, Strom TB, Oukka M, et al. Reciprocal developmental pathways for the generation of pathogenic effector TH17 and regulatory T cells. *Nature.* (2006) 441:235–8. doi: 10.1038/nature04753
20. Lahl K, Loddenkemper C, Drouin C, Freyer J, Arnason J, Eberl G, et al. Selective depletion of Foxp3+ regulatory T cells induces a scurfy-like disease. *J Exp Med.* (2007) 204:57–63. doi: 10.1084/jem.20061852
21. Kuhn R, Lohler J, Rennick D, Rajewsky K, Muller W. Interleukin-10-deficient mice develop chronic enterocolitis. *Cell.* (1993) 75:263–74. doi: 10.1016/0092-8674(93)80068-P
22. Odds FC, Brown AJ, Gow NA. *Candida albicans* genome sequence: a platform for genomics in the absence of genetics. *Genome Biol.* (2004) 5:230. doi: 10.1186/gb-2004-5-7-230
23. Solis NV, Filler SG. Mouse model of oropharyngeal candidiasis. *Nat Protoc.* (2012) 7:637–42. doi: 10.1038/nprot.2012.011
24. Amorim-Vaz S, Tran Vdu T, Pradervand S, Pagni M, Coste AT, Sanglard D. RNA enrichment method for quantitative transcriptional analysis of pathogens *in vivo* applied to the fungus *Candida albicans*. *MBio* (2015) 6:e00942-15. doi: 10.1128/mBio.00942-15
25. Martin M. Cutadapt removes adapter sequences from high-throughput sequencing reads. *EMBnet.journal* (2011) 17:10–2. doi: 10.14806/ej.17.1.200
26. Anders S, Pyl PT, Huber W. HTSeq–a Python framework to work with high-throughput sequencing data. *Bioinformatics.* (2015) 31:166–9. doi: 10.1093/bioinformatics/btu638
27. Robinson MD, Oshlack A. A scaling normalization method for differential expression analysis of RNA-seq data. *Genome Biol.* (2010) 11:R25. doi: 10.1186/gb-2010-11-3-r25
28. Law CW, Chen Y, Shi W, Smyth GK. voom: precision weights unlock linear model analysis tools for RNA-seq read counts. *Genome Biol.* (2014) 15:R29. doi: 10.1186/gb-2014-15-2-r29
29. Smyth GK. limma: Linear Models for Microarray Data. In: Gentleman R, Carey VJ, Huber W, Irizarry RA, Dudoit S, Editors. *Bioinformatics and Computational Biology Solutions Using R and Bioconductor. Statistics for Biology and Health.* New York, NY: Springer (2005). p. 397–420.

30. Benjamini Y, Hochberg Y. Controlling the false discovery rate: a practical and powerful approach to multiple testing. *J R Stat Soc Ser B*. (1995) 57:289–300. doi: 10.1111/j.2517-6161.1995.tb02031.x
31. Fuertes Marraco SA, Grosjean F, Duval A, Rosa M, Lavanchy C, Ashok D, et al. Novel murine dendritic cell lines: a powerful auxiliary tool for dendritic cell research. *Front Immunol.* (2012) 3:331. doi: 10.3389/fimmu.2012.00331
32. Cossarizza A, Chang HD, Radbruch A, Akdis M, Andra I, Annunziato F, et al. Guidelines for the use of flow cytometry and cell sorting in immunological studies. *Eur J Immunol.* (2017) 47:1584–797. doi: 10.1002/eji.201646632
33. Trautwein-Weidner K, Gladiator A, Nur S, Diethelm P, LeibundGut-Landmann S. IL-17-mediated antifungal defense in the oral mucosa is independent of neutrophils. *Mucosal Immunol*. (2015) 8:221–31. doi: 10.1038/mi.2014.57
34. Park JY, Chung H, DiPalma DT, Tai X, Park JH. Immune quiescence in the oral mucosa is maintained by a uniquely large population of highly activated Foxp3(+) regulatory T cells. *Mucosal Immunol.* (2018) 11:1092–102. doi: 10.1038/s41385-018-0027-2
35. Eyerich K, Dimartino V, Cavani A. IL-17 and IL-22 in immunity: driving protection and pathology. *Eur J Immunol.* (2017) 47:607–14. doi: 10.1002/eji.201646723
36. Littringer K, Moresi C, Rakebrandt N, Zhou X, Schorer M, Dolowschiak T, et al. Common features of regulatory T cell specialization during Th1 responses. *Front Immunol*. (2018) 9:1344. doi: 10.3389/fimmu.2018.01344
37. Sparber F, Dolowschiak T, Mertens S, Lauener L, Clausen BE, Joller N, et al. Langerin+ DCs regulate innate IL-17 production in the oral mucosa during *Candida albicans*-mediated infection. *PLoS Pathog.* (2018) 14:e1007069. doi: 10.1371/journal.ppat.1007069
38. Sparber F, LeibundGut-Landmann S. Assessment of immune responses to fungal infections: identification and characterization of immune cells in the infected tissue. *Methods Mol Biol.* (2017) 1508:167–82. doi: 10.1007/978-1-4939-6515-1_8
39. Altmeier S, Toska A, Sparber F, Teijeira A, Halin C, LeibundGut-Landmann S. IL-1 coordinates the neutrophil response to *C. albicans* in the oral mucosa. *PLoS Pathog.* (2016) 12:e1005882. doi: 10.1371/journal.ppat.1005882
40. Moyes DL, Runglall M, Murciano C, Shen C, Nayar D, Thavaraj S, et al. A biphasic innate immune MAPK response discriminates between the yeast and hyphal forms of *Candida albicans* in epithelial cells. *Cell Host Microbe*. (2010) 8:225–35. doi: 10.1016/j.chom.2010.08.002
41. Richardson JP, H.Willems ME, Moyes DL, Shoaie S, Barker KS, Tan SL, et al. Candidalysin drives epithelial signaling, neutrophil recruitment, and immunopathology at the vaginal mucosa. *Infect Immun.* (2017) 86:IAI.00645-17. doi: 10.1128/IAI.00645-17
42. Verma AH, Richardson JP, Zhou C, Coleman BM, Moyes DL, Ho J, et al. Oral epithelial cells orchestrate innate type 17 responses to *Candida albicans* through the virulence factor candidalysin. *Sci Immunol.* (2017) 2:eaam8834. doi: 10.1126/sciimmunol.aam8834
43. Verma AH, Zafar H, Ponde NO, Hepworth OW, Sihra D, Aggor FEY, et al. IL-36 and IL-1/IL-17 drive immunity to oral candidiasis via parallel mechanisms. *J Immunol.* (2018) 201:627–34. doi: 10.4049/jimmunol.1800515
44. Bruno VM, Shetty AC, Yano J, Fidel PL Jr, Noverr MC, Peters BM. Transcriptomic analysis of vulvovaginal candidiasis identifies a role for the NLRP3 inflammasome. *MBio*. (2015) 6:e00182-15 doi: 10.1128/mBio.00182-15
45. Conti HR, Shen F, Nayyar N, Stocum E, Sun JN, Lindemann MJ, et al. Th17 cells and IL-17 receptor signaling are essential for mucosal host defense against oral candidiasis. *J Exp Med*. (2009) 206:299–311. doi: 10.1084/jem.20081463
46. Liu Y, Shetty AC, Schwartz JA, Bradford LL, Xu W, Phan QT, et al. New signaling pathways govern the host response to *C. albicans* infection in various niches. *Genome Res*. (2015) 25:679–89. doi: 10.1101/gr.187427.114
47. Moyes DL, Shen C, Murciano C, Runglall M, Richardson JP, Arno M, et al. Protection against epithelial damage during *Candida albicans* infection is mediated by PI3K/Akt and mammalian target of rapamycin signaling. *J Infect Dis*. (2014) 209:1816–26. doi: 10.1093/infdis/jit824
48. Conti HR, Bruno VM, Childs EE, Daugherty S, Hunter JP, Mengesha BG, et al. IL-17 receptor signaling in oral epithelial cells is critical for protection against oropharyngeal candidiasis. *Cell Host Microbe*. (2016) 20:606–17. doi: 10.1016/j.chom.2016.10.001
49. Hawkes JE, Chan TC, Krueger JG. Psoriasis pathogenesis and the development of novel targeted immune therapies. *J Allergy Clin Immunol.* (2017) 140:645–53. doi: 10.1016/j.jaci.2017.07.004
50. van der Fits L. Mourits S, Voerman JS, Kant M, Boon L, Laman JD, Cornelissen F, et al. Imiquimod-induced psoriasis-like skin inflammation in mice is mediated via the IL-23/IL-17 axis. *J Immunol*. (2009) 182:5836–45. doi: 10.4049/jimmunol.0802999
51. McGeachy MJ, Bak-Jensen KS, Chen Y, Tato CM, Blumenschein W, McClanahan T, et al. TGF-beta and IL-6 drive the production of IL-17 and IL-10 by T cells and restrain T(H)-17 cell-mediated pathology. *Nat Immunol*. (2007) 8:1390–7. doi: 10.1038/ni1539
52. Mangan PR, Harrington LE, O'Quinn DB, Helms WS, Bullard DC, Elson CO, et al. Transforming growth factor-beta induces development of the T(H)17 lineage. *Nature*. (2006) 441:231–4. doi: 10.1038/nature04754
53. Veldhoen M, Hocking RJ, Atkins CJ, Locksley RM, Stockinger B. TGFbeta in the context of an inflammatory cytokine milieu supports *de novo* differentiation of IL-17-producing T cells. *Immunity*. (2006) 24:179–89. doi: 10.1016/j.immuni.2006.01.001
54. Laurence A, Tato CM, Davidson TS, Kanno Y, Chen Z, Yao Z, et al. Interleukin-2 signaling via STAT5 constrains T helper 17 cell generation. *Immunity*. (2007) 26:371–81. doi: 10.1016/j.immuni.2007.02.009
55. Pandiyan P, Conti HR, Zheng L, Peterson AC, Mathern DR, Hernandez-Santos N, et al. CD4(+)CD25(+)Foxp3(+) regulatory T cells promote Th17 cells *in vitro* and enhance host resistance in mouse *Candida albicans* Th17 cell infection model. *Immunity*. (2011) 34:422–34. doi: 10.1016/j.immuni.2011.03.002
56. Huber S, Gagliani N, Esplugues E, O'Connor W Jr, Huber FJ, Chaudhry A, et al. Th17 cells express interleukin-10 receptor and are controlled by Foxp3(-) and Foxp3+ regulatory CD4+ T cells in an interleukin-10-dependent manner. *Immunity*. (2011) 34:554–65. doi: 10.1016/j.immuni.2011.01.020
57. Huang XR, Chung AC, Wang XJ, Lai KN, Lan HY. Mice overexpressing latent TGF-beta1 are protected against renal fibrosis in obstructive kidney disease. *Am J Physiol Renal Physiol.* (2008) 295:F118–27. doi: 10.1152/ajprenal.00021.2008
58. Overbergh L, Giulietti A, Valckx D, Decallonne R, Bouillon R, Mathieu C. The use of real-time reverse transcriptase PCR for the quantification of cytokine gene expression. *J Biomol Tech*. (2003) 14:33–43.
59. Ivanov II, McKenzie BS, Zhou L, Tadokor CE, Lepelley A, Lafaille JJ, et al. The orphan nuclear receptor RORgammat directs the differentiation program of proinflammatory IL-17+ T helper cells. *Cell*. (2006) 126:1121–33. doi: 10.1016/j.cell.2006.07.035
60. Kundu P, Ling TW, Korecka A, Li Y, D'Arienzo R, Bunte RM, et al. Absence of intestinal PPARgamma aggravates acute infectious colitis in mice through a lipocalin-2-dependent pathway. *PLoS Pathog.* (2014) 10:e1003887. doi: 10.1371/journal.ppat.1003887
61. Kolar SS, Baidouri H, Hanlon S, McDermott AM. Protective role of murine beta-defensins 3 and 4 and cathelin-related antimicrobial peptide in *Fusarium solani* keratitis. *Infect Immun.* (2013) 81:2669–77. doi: 10.1128/IAI.00179-13

Conflict of Interest Statement: SA currently works for Novartis but on a different topic and the data are restricted to his previous role in the LeibundGut-lab.

The remaining authors declare that the research was conducted in the absence of any commercial or financial relationships that could be construed as a potential conflict of interest.

frontiers in Immunology

REVIEW
published: 16 April 2019
doi: 10.3389/fimmu.2019.00728

Aggregatibacter actinomycetemcomitans (*Aa*) Under the Radar: Myths and Misunderstandings of *Aa* and Its Role in Aggressive Periodontitis

Daniel H. Fine, Amey G. Patil and Senthil K. Velusamy*

Department of Oral Biology, Rutgers School of Dental Medicine, Newark, NJ, United States

Aggregatibacter actinomycetemcomitans (Aa) is a low-abundance Gram-negative oral pathobiont that is highly associated with a silent but aggressive orphan disease that results in periodontitis and tooth loss in adolescents of African heritage. For the most part *Aa* conducts its business by utilizing strategies allowing it to conceal itself below the radar of the host mucosal immune defense system. A great deal of misinformation has been conveyed with respect to *Aa* biology in health and disease. The purpose of this review is to present misconceptions about *Aa* and the strategies that it uses to colonize, survive, and evade the host. In the process *Aa* manages to undermine host mucosal defenses and contribute to disease initiation. This review will present clinical observational, molecular, and interventional studies that illustrate genetic, phenotypic, and biogeographical tactics that have been recently clarified and demonstrate how *Aa* survives and suppresses host mucosal defenses to take part in disease pathogenesis. At one point in time *Aa* was considered to be the causative agent of Localized Aggressive Periodontitis. Currently, it is most accurate to look at *Aa* as a community activist and necessary partner of a pathogenic consortium that suppresses the initial host response so as to encourage overgrowth of its partners. The data for *Aa's* activist role stems from molecular genetic studies complemented by experimental animal investigations that demonstrate how *Aa* establishes a habitat (housing), nutritional sustenance in that habitat (food), and biogeographical mobilization and/or relocation from its initial habitat (transportation). In this manner *Aa* can transfer to a protected but vulnerable domain (pocket or sulcus) where its community activism is most useful. *Aa*'s "strategy" includes obtaining housing, food, and transportation at no cost to its partners challenging the economic theory that "there ain't no such thing as a free lunch." This "strategy" illustrates how co-evolution can promote *Aa's* survival, on one hand, and overgrowth of community members, on the other, which can result in local host dysbiosis and susceptibility to infection.

Keywords: *A. actinomycetemcomitans*, leukotoxin, habitat, nutritional sustenance, biogeographical mobilization, aggressive periodontitis

OPEN ACCESS

Edited by:
Cecil Czerkinsky, Institut National de la Santé et de la Recherche Médicale (INSERM), France

Reviewed by:
Richard Lamont, University of Louisville, United States
Gill Diamond, University of Florida, United States

****Correspondence:***
Daniel H. Fine
finedh@sdm.rutgers.edu

Specialty section:
This article was submitted to Mucosal Immunity, a section of the journal Frontiers in Immunology

Received: *18 October 2018*
Accepted: *19 March 2019*
Published: *16 April 2019*

Citation:
Fine DH, Patil AG and Velusamy SK (2019) Aggregatibacter actinomycetemcomitans (Aa) Under the Radar: Myths and Misunderstandings of Aa and Its Role in Aggressive Periodontitis. Front. Immunol. 10:728. doi: 10.3389/fimmu.2019.00728

INTRODUCTION

Ever since 1976 when it was discovered that *Aggregatibacter actinomycetemcomitans* (ne Actinobacillus) was associated with Aggressive Periodontitis in adolescents there have been many attempts to understand its relationship to disease (1, 2). *A. actinomycetemcomitans* (*Aa*) was first reported by Klinger in 1912 where he described a previously unknown Gram-negative microorganism that was found in actinomycotic lesions associated with Actinomyces, hence the latin word "comitans" in common with Actinomyces (3). In addition to its association with aggressive periodontitis, *Aa* has been implicated as an organism associated with a variety of systemic diseases including but not limited to; infectious endocarditis, brain abscesses, and chest wall abscesses (4). While initially it was thought that *Aa* was the cause of localized aggressive periodontitis (LAgP) (5) current research suggests that *Aa* is implicated as an important and perhaps necessary constituent of a consortium of microorganisms related to disease (6). What follows is a review that focuses on major trends that have supported, and in some cases misrepresented the role of *Aa* in the LAgP disease process. The review will divide *Aa*'s role in the disease process into several steps that are required for this specific microorganism to participate in an infection that attacks the periodontal attachment apparatus and bone. In this review the disease provoking process has been divided into four steps as follows; Step 1: colonization above the gum-line, Step 2: integration and survival in the biofilm milieu, Step 3: migration to a new setting below the gumline, and Step 4: suppression of the mucosal host defenses below the gum-line. Many of these steps have been clarified in recent years by harmonizing; (a) clinical observational studies in humans (7), (b) studies using molecular approaches (8), and (c) interventional/experimental studies in animal models (9). As a result it is now possible to put forward a narrative that illustrates how *Aa* can actively participate in the disease process.

MISCONCEPTION 1: *AA* IS A LATE COLONIZER

Clinical

In seminal experiments in the mid-1960's it became clear that dental plaque/biofilm formation is due to synchronized events that begin with deposition of salivary proteins above the gumline on the native tooth surface, followed by accumulation of Streptococcal species onto the glycoprotein layer set down on the enamel (10). In the first 2-days following plaque deposition on the tooth surface streptococcal species can amount to up to 90% of the tooth related microbiota followed by actinomyces species. These pioneer colonizers form parallel arrays, perpendicular to the tooth surface interspersed by lactate utilizing Veillonella (11). Over a 3-week period the composition of plaque changes from a predominantly Gram-positive aerobic Streptococcal microbiota to a mixed Gram positive and Gram negative facultatively anaerobic flora containing streptococci, *Actinomyces* sp, *Veillonella* sp, *Fusobacteria* sp, vibrios, spirochetes, and others (12).

Early on there were controversies related to *Aa*'s attachment properties (8). These disputes were due to the fact that ATCC laboratory strains were used in early studies that focused on *Aa* attachment (13). When these lab strains were investigated they failed to demonstrate the natural aggregative tendency of *Aa,* and thus *Aa* was shown to adhere poorly (13). This concept was re-inforced by Kolenbrander and associates who studied co-aggregation and suggested that *Aa* was a poor colonizer since, the ATCC strain Y4 only coaggregated with *Fusobacteria nucleatum,* the universal coaggregator (14, 15). These coaggregation/microbial interactions have, with the exception of *Aa*, been shown, for the most part, to play a critical role in plaque chronology (15). Thus, it was suggested that *Aa* was a late colonizer incapable of participation in early plaque formation (16).

Molecular

The first evidence to strengthen support for *Aa*'s adherence properties were shown by comparing attachment of laboratory strains to clinical isolates derived from the same parental strain (17). Lessons learned from these comparisons led to an understanding of how to maintain the clinical adherent phenotype in the laboratory, which led to the discovery of the Widespread Colonization Island (WCI) (13, 18). The WCI discovered in 2001 consists of a 14 gene operon and was shown to contain the *flp, tad,* and *rcp* genes that are intimately related to attachment to abiotic surfaces, aggregation, and tight adherence (18–20). This genomic island was present in many pathogenic strains including; *Yersinia pestis*, *Haemophilus ducreyi*, *Psuedomonas aeroginosa*, *Bordetella pertussis*, *Caulobacter crescentus*, *Salmonella enterica*, *Eschericia coli,* and all Archea sequenced to date (19). The discovery of the WCI undoubtedly influenced the change in the genus name from *Actinobacillus* to *Aggregatibacter* and demonstrated how important attachment was for survival of even the most primitive species (21). The fact that so many pathobionts contain the functional portion of this island attest to the importance of adherence in their persistence (**Figure 1**).

The specificity of *Aa*'s binding was illustrated by the fact that *Aa* obtained from pre-dentate children showed a high degree of tissue and species specificity (23, 24). In addition, *Aa* strains from parent and child often showed the same genotype demonstrating patterns of vertical transmission (25).

The studies described above were further supported by the discovery of an outer membrane adhesin, Aae, which showed specificity for oral epithelium (26). Unlike the WCI, Aae bound to its receptor on buccal epithelial cells (BECs) in a highly specific, dose dependent manner, that was saturable and thus achieved a plateau where no further binding was attainable (27). This data coupled with the finding that the Aae adhesin showed selective binding to BECs obtained from humans and old world primates but did not bind to BECs obtained from dogs, cats, pigs, goats etc., demonstrated a high level of species and tissue specificity (28). Further, subsequent reports revealed that *Aa* moved from tissue to teeth after teeth erupted depicting the direction of movement within specific oral domains (28, 29).

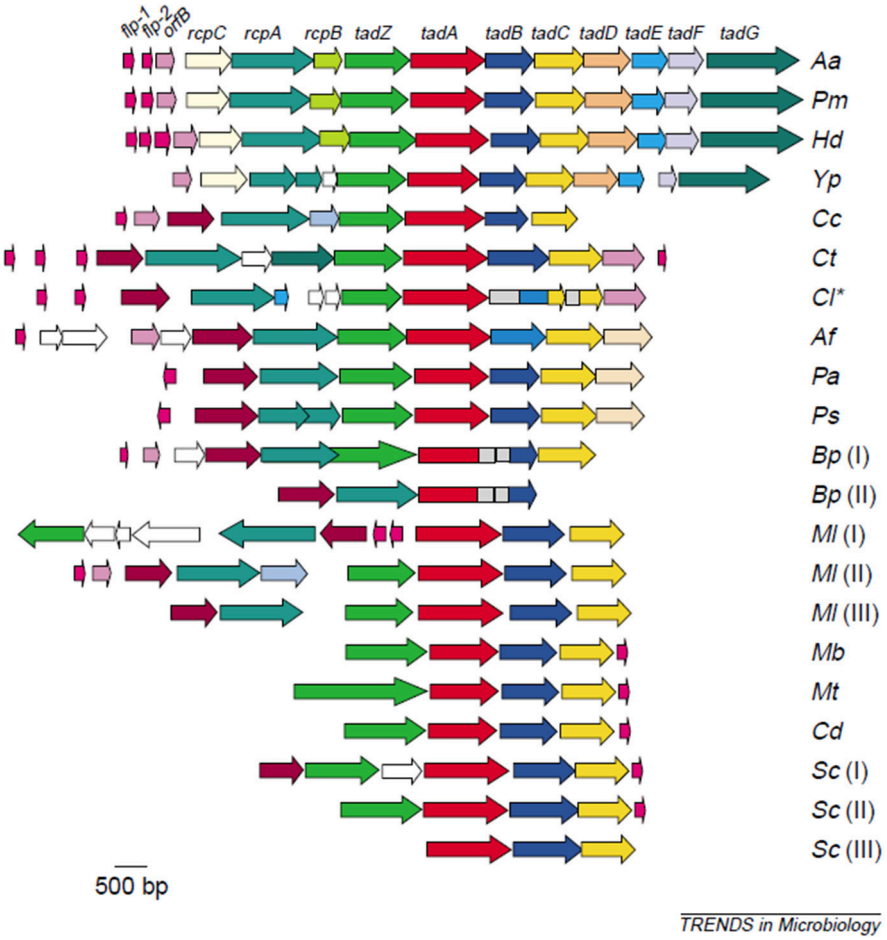

FIGURE 1 | Illustration of the widespread colonization island (WCI). WCI consists of a 14 gene operon seen in its complete genetic composition in *(Aa) Aggregatibacter actinomycetemcomitans, (Pm)Pasteurella multocida, (Hd) Haemophilus ducreyi.* Remainder of microbes have a portion of the WCI: *(Yp)Yersinia pestis. (Cc) Caulobacter crescentus, (Ct) Chlorobium tepidum, (Cl) Chlorobium limicola, (Af) Acidithiobacillus ferooxidans, (Pa) Pseudomonas aeruginosa, (Ps) P. syringae, (Bp) Bordetella pertussis* [two clusters], *(Ml) Mesorhizobium loti* [three clusters], *(Mb) Mycobacterium bovis, (Mt) M. tuberculosis, (Cd) Corynebacterium diphtheriae, (Sc) Streptomyces coelicolor* [three custers]. This island is responsible for binding to abiotic surfaces and is present in many pathobionts and in all Archae sequenced to date (22).

In a clear contrast to the non-specificity of the binding to abiotic surfaces via the WCI, binding of *Aa* via outer membrane adhesins were shown to be highly specific. *Aa* therefore has the capacity for both specific and non-specific mechanisms of adherence in the oral cavity.

Experimental

The difficulty in changing the initial perception that *Aa* was a poor colonizer was due to the fact that it was hard to demonstrate that *Aa* was seen in the early stages of plaque formation. Clinical proof that *Aa* was a hardy colonizer was elusive because; (1) *Aa* was rarely found in plaque isolated from healthy individuals (5, 7), and (2) when *Aa* was isolated from periodontally diseased individuals it aggregated (13, 20). After isolation from clinical sites, *Aa* had a characteristic rough colonial texture that clumped on subculture and was highly adherent to abiotic surfaces. However, after repeated passage in the laboratory *Aa* reverted to a smooth colonial morphology that did not clump and was minimally adherent (13) (see **Figure 1**) This rough to smooth conversion fit the description of phase variation demonstrated by several pathogens that change from rough to smooth (*Neisseria*) enhancing their pathogenic strategy (30). However, in studies of *Aa*, this shift was seen *in-vitro* (12) but was not seen *in-vivo* in animal models and thus has been proposed to be a laboratory artifact (31).

To characterize *Aa* in humans it was necessary to survey over 100 adolescents in order to select 5 individuals who had *Aa* on buccal epithelial cells (BECs) and on tooth surfaces, and 5 individuals who had *Aa* only on tooth surfaces, as compared to 3 individuals who did not have *Aa* in their oral cavity (32). Stents were fabricated for these subjects and hydroxyapatite (HA) squares or discs were inserted into the stent. The stents were placed into the mouths of these subjects and HA squares were removed 5 min, 1, 4, 6, and 7 h after placement. Following

HA square removal the square was sonicated, and the bacteria removed from the HA square after sonication were plated for determination of total bacteria, *streptococcal* spp., *Actinomyces* spp and *Aa* colonies (**Figure 2**). In these experiments subjects who had *Aa* on their BECs, were found to have *Aa* on HA squares within 6 h after the start of the *in-vivo* experiment, however none of those with *Aa* on teeth alone showed *Aa* on the HA squares (32). In a parallel series of *in-vitro* experiments, pre-treatment of BECs with *Aa* where shown to have been colonized by *Aa*. Reaction of these *Aa* colonized BECs with sterile/untreated HA squares in a test tube showed that *Aa* migrated and attached to the HA squares *in-vitro*. In contrast, HA squares pre-treated with *Aa* showed that *Aa* attached avidly to HA squares *in-vitro*. However, when these HA treated squares were reacted with untreated/uncontaminated BECs in a test tube, *Aa* attached to HA did not migrate to BECs. Results showed that while *Aa* was incapable of moving from HA to BECs, *Aa* was quite capable of moving from BECs to HA. These *in-vivo* and *in-vitro* experiments clearly demonstrated the difference in the kinetics of *Aa* attached to BECs via specific adhesin/receptor interactions that are reversible, as compared to linear and irreversible, non-specific aggregative adherence mediated by *flp*, *tad*, and *rcp* genes that facilitate *Aa's* attachment to HA (32).

Confirmation of the early plaque formation of *Aa* came from a little known experiment conducted in 1976 by Kilian and Rolla where these investigators set out to study the dietary impact of sucrose on *Streptococcus mutans* colonization in a Rhesus monkey model (33). In these experiments it was clearly shown that sucrose influenced early colonization of *S. mutans*, but unintentionally it was also demonstrated that *Aa*, a member of the commensal flora in these monkeys, was found on teeth within 3 h following thorough oral debridement of these Rh monkeys.

Conclusions

Current data indicates that *Aa* can colonize tooth surfaces above the gum-line and that this is an early event. In the section below we will describe how *Aa* can compete for nutritional elements with a multitude of rival bacteria in order to survive.

MISCONCEPTION 2: NUTRITIONAL FASTIDIOUS NATURE OF *AA*

Clinical

Aa has been characterized as a fastidious microbe that requires CO_2, serum, and specific carbohydrates such as glucose for its growth (34). It has been reported that *Aa* has a mandatory requirement for 5% CO_2 for primary isolation, and that its growth is purported to be boosted by addition of serum (34). The difficult recovery of the microbe from potentially diseased sites throughout the body has been attributed to *Aa's* **f**astidious nature and its slow and inconsistent growth after initial isolation. These characteristics have suggested that the organism is difficult to isolate from human sites and difficult to grow in the laboratory. These features coupled with the aggregative nature of the microbe when grown in the laboratory has made quantitative assessment of the microbe problematic. Further, these features have discouraged a more intense investigation of the genetic traits of *Aa* (13). More recently genetic methodologies have made it easier to do quantitative assessment of the microbe from individual periodontal sites of interest.

Molecular

In 2007, Brown and Whiteley demonstrated that *Aa* preferentially metabolizes lactate over other more readily available carbon sources such as glucose and fructose due to novel exclusion methods controlled by phosphoenol pyruvate-dependent phosphtranferase systems (35). Reduced levels of lactate appeared to limit *Aa*'s ability to grow and in the presence of high glucose consuming competitors such as Streptococci, *Aa* was shown to thrive. It was proposed that *Aa*'s survival was due to reduced competition with fast-growing and abundant members of the pioneer plaque flora such as Streptococci that utilized glucose as their carbon source. Further proof was obtained by creation of a lactic acid dehydrogenase deficient strain of *Aa* that fully ablated *Aa* growth (36). Results were also supported by the fact that lactate added to chemically defined media and/or the addition of lactate producing Streptococci caused increased growth of *Aa* in multi-community co-culture biofilms.

Moreover, Stacy et al. (37) showed that the toxic elements (H_2O_2) produced by co-culture with *S. gordonii* were overcome by the up-regulation *katA, apiA,* and *dspB* genes that protect *Aa* from the destructive effects of H_2O_2. These *in-vitro* reductionist models (and *in-vivo* dual species mouse studies) have been substantiated in human and primate models that examined both supra and sub gingival plaque (38).

Experimental

Supragingival plaque communities were examined in an interventional/experimental Rhesus (Rh) primate model (9). With respect to *Aa*, Rh primates are unique in that the overwhelming majority of healthy primates harbor *Aa* in their supragingival plaque (9). This consistent presence of *Aa* in supragingival plaque allows for examination of *Aa*'s role in early plaque formation (9). By using a modification of a specific correlation analysis (39) we were able to substantiate and extend the observations of the Whiteley group (38). This network analysis allowed us to select the top 50 microbes by means of operational taxonomic units via 16S RNA identification. Selecting *Aa* as the node in the analysis of the 16 Rh monkeys with fully formed plaque biofilms, we were able to show that several key lactate producing species including streptococci, *Leptotrichia,* and *Abiotrophia* as well as *Veillonella* (a microbe with a strict lactate requirement) were highly associated with the hyper-leukotoxin producing strain of *Aa* (**Table 1**). This was true at baseline and 4-weeks after plaque reformed after thorough debridement (40). Calculation of lactate availability favored the growth and survival of *Aa* in a real-world environment [(39); **Figure 3**].

Conclusion

Molecular and experimental Rh primate models support the concept that *Aa* preferentially associates with lactate producing species which enables *Aa* to survive by limiting its competition for glucose as a carbon source used by other pioneer colonizers. The Rh primate model support and extend the findings of the Whiteley group in a real world competitive natural model.

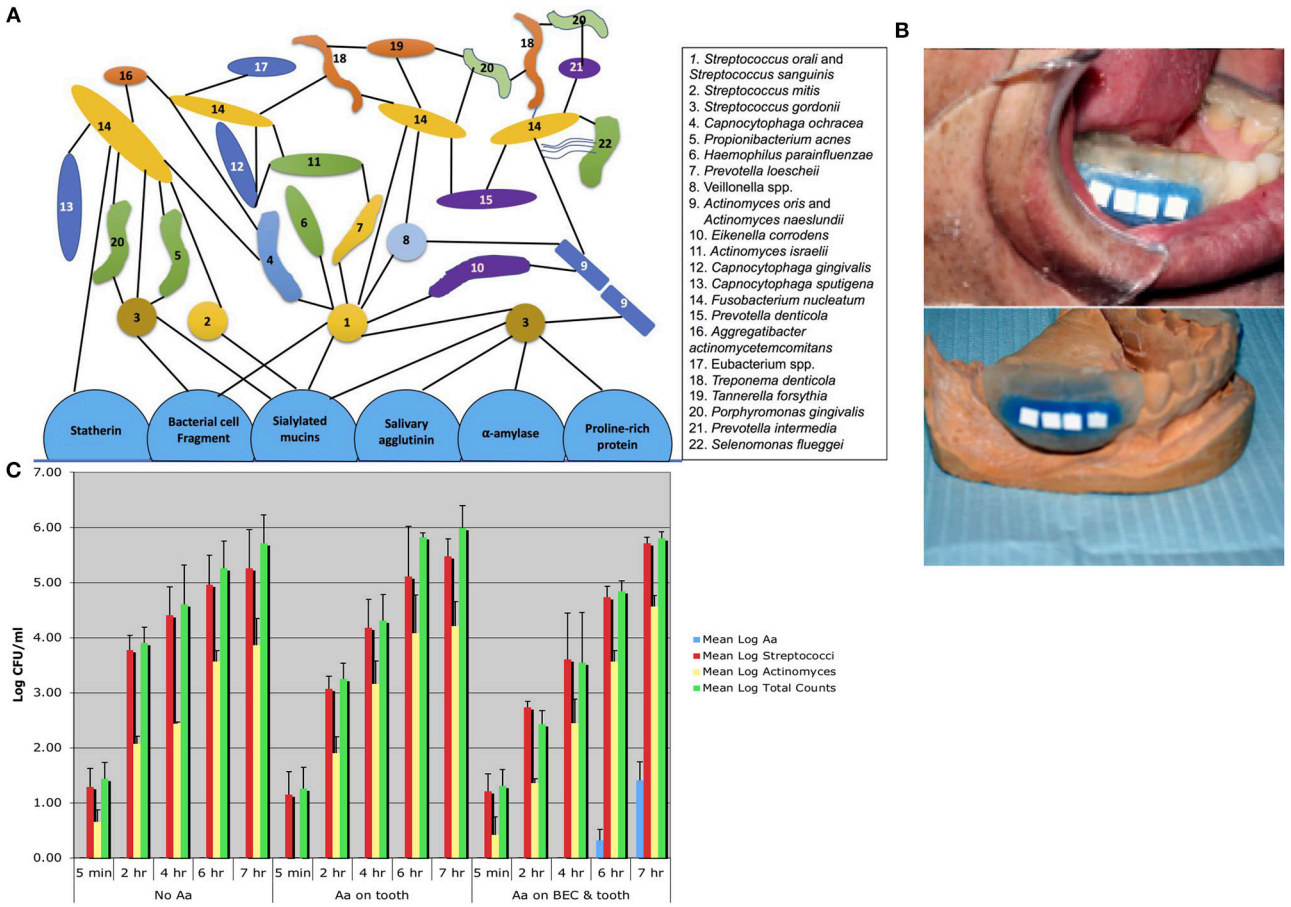

FIGURE 2 | Diagram of plaque biofilm topography and chronology contrasted to *in-vivo* studies illustrating *Aa* colonization. Diagram shows pioneer colonizers closest to tooth surface and late colonizers on outer border of plaque geography [Adpated from Kolenbrander et al. (16)]. Note that *Aa* #16 in this figure is depicted as a late colonizer attached to *Fusobacterium nucleatum* **(A)**. Picture of stent fabricated for human volunteers containing Hydroxyapatite (HA) squares used for the capture of oral microorganisms that show early binding in subjects who harbor *Aa* **(B)**. Bar graph showing three panels 5 min to 7 h. First panel on left represents bacteria found over the 7 h period in subjects who had no *Aa* (controls). Middle panel shows subjects who had *Aa* on tooth surface only where no *Aa* is found on HA squares. Panel on right shows subjects with *Aa* on buccal cells and teeth, where *Aa* has migrated from buccal cells to HA squares and is detected on square at 6 and 7 h time-point **(C)** [Adapted from Fine et al. (32)].

MISCONCEPTION 3: A HIGHLY AGGREGATIVE NON-MOTILE MICROBE CANNOT ESCAPE FROM ITS BIOFILM HABITAT

Clinical

After a great deal of research it became obvious that *Aa* aggregates avidly in its "native" state. This dramatic phenotype led to the question as to how *Aa* could be trapped in one location and migrate to another. Without this capability to migrate, *Aa* would have to be designated as a pathobiont with biogeographically limited capabilities (13).

The importance of the transfer of *Aa* from a position above the gum-line to the cul de sac shaped sulcus below the gum-line is critical for transition from health to disease. The subgingival habitat differs significantly from the domain seen above the gum-line. The subgingival domain is anaerobic, filled with a serum transudate derived from vessels contained in the subjacent connective tissue. The junctional epithelium (JE) forms the base of the sulcus and borders the tooth surface. The "V" shaped structure of the sulcus surrounds the tooth. The left side of the V is the junctional epithelium (JE) derived from reduced enamel epithelium, remnants of the enamel organ (41), while the right side of the V is sulcular epithelium derived from oral epithelial tissue precursors.

These JE cells are one to two layers thick and are extremely permeable to outward flow of serum and cells. Directly beneath the basement membrane of the JE is a dense vascular network (42). Within 3–4 days after abstaining from brushing, microbial plaque lines the outer portion of the JE. Cells within the JE (Langerhan-type antigen presenting cells) sample members of dense multispecies indigenous flora that are pressed up against its periphery and move these components into subjacent lymphatic vessels. The broad ability of cells associated with innate immunity

TABLE 1 | Estimation of lactate availability comparing Veillonella to lactate producers.

	Wild Type- RhAa3			RhAa-Itx P530		
Genus	**Wk 1 OTUs**	**Wk 2 OTUs**	**Wk 4 OTUs**	**Wk 1 OTUs**	**Wk 2 OTUs**	**Wk 4 OTUs**
Abiotrophia	3,915	1,662	12,778	3,136	627	2,654
Leptotrichia	227	2,422	6,002	147	1,915	863
Streptococci	3,255	18,750	70,261	7,359	14,658	6,591
Total: Producers (P)	7,397	22,834	89,001	10,642	17,200	10,108
Veillonella- Utilizers (U)	3,718	13,689	35,861	1,355	3,395	381
Ratio: P/U	2/1	1.67/1	2.5/1	7.85/1	5.1/1	26.5/1

OTUs: Operational Taxonomic Units; Wk: Week; Ratio: Producers/Utilizers.

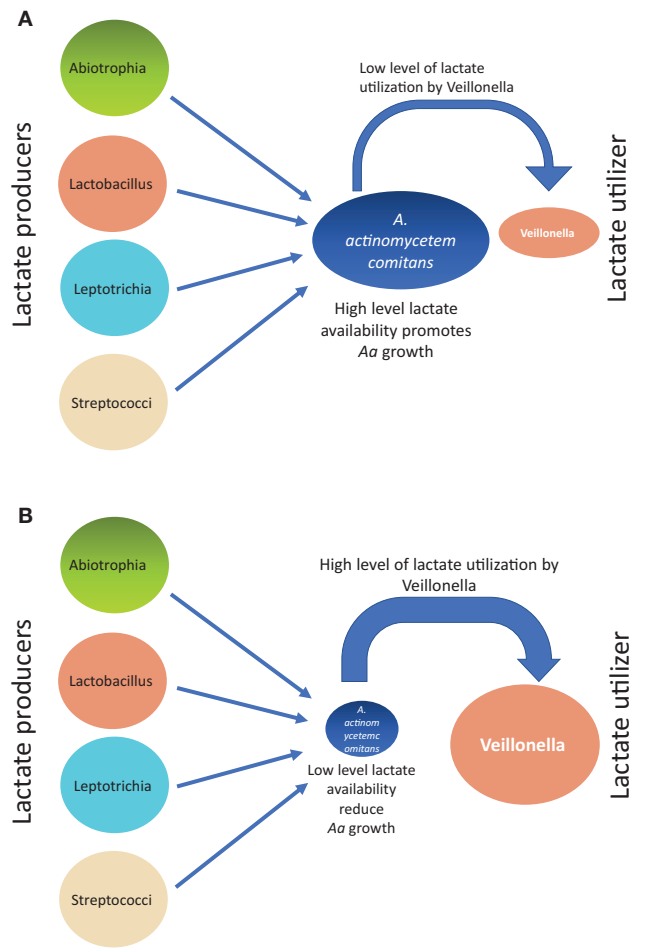

FIGURE 3 | Diagram illustrating how growth of *Aa* can be influenced from associations of lactate producers (LP) as compared to lactate utilizers(LU) in Rh primate plaque studies. Panel on top **(A)** illustrates the scenario describing relative *Aa* growth when there is a low level of lactate utilization by Veillonella. Panel on bottom **(B)** illustrates the scenario describing relative *Aa* growth when there is a high level of lactate utilization by Veillonella leaving a low level of lactate available for *Aa* consumption.

that display pattern recognition receptors (PRRs) are designed to identify pathogen associated molecular patterns (PAMPs) present on the surface of persistent microbial contaminants of the JE. This local subgingival biofilm results in intracellular signaling pathways causing gene transcription and responsiveness in the tissue underlying the JE (43). These antigen presenting cells then migrate to the regional lymph vessels. After presenting these antigens to lymphocytes in the regional lymph nodes, the lymphocytes become sensitized and ultimately make their way back from the node to the locus of infection, the sulcus, where they confront the marauding plaque bacteria. This movement to and fro is guided by cytokines and particularly by ICAM and VCAM receptors. Repopulation of sensitized cells can take anywhere from 7 to 14 days after bacterial contact with the JE (44).

These highly orchestrated events represent a skeletal description of the interaction of the innate and acquired immune responsiveness. However, prior to this series of events a more primitive response occurs. Here almost immediately after the microbial assault the bacterial components make their way to the underlying vasculature initiating the complement cascade and migration of polymorphonuclear leukocytes (PMNs) to the sulcus to protect against the bacterial onslaught. Thus, within 2–3 days after abstinence from oral hygiene, marauding bacteria are confronted by a wall of complement and PMNs that line the outer border of the sulcus (45).

Molecular

Aggregation is a double-edged sword, on one hand it forms a shield and protects the biofilm mass from antimicrobial agents and other environmental challenges. However, on the other hand, aggregation limits the ability of the microbe to mobilize and move away from danger. Dispersin B (dspB) is a hexosaminidase that attacks hexosamine containing matrix polysaccharides that consist of a N-acetyl –D- glucosamine residues (46). dsp B was first discovered in *Aa* in 2003 by Kaplan et al. (47). Kaplan developed two dramatic experiments that exemplified how an organism whose main phenotype is aggregation could migrate and escape from its captivity (48). In the first experiment in an enlarged tissue culture dish, a single mother colony of *Aa* was carefully inoculated at one side of the plate and then 3 days later the daughter colonies had migrated away from the mother colony at what was calculated as a distance of over 2,500 human miles (47). The migration was due to the rupture of the

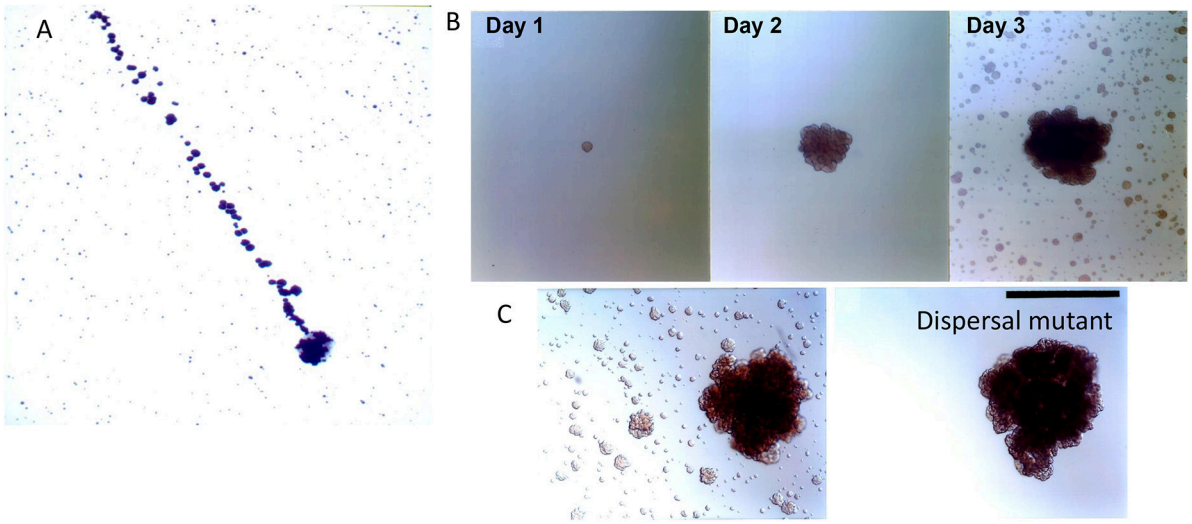

FIGURE 4 | Biofilm dispersion by *Aa.* Illustration of dispersal of daughter colonies (top of panel **A**) derived from initial mother colony (bottom area of panel **A**). Distance covered by calculation of the 1 micron size of *Aa* is estimated at 2,500 human miles calculating the distance from location of *Aa* at bottom to location of *Aa* on top of panel **(A)** [Modified from Kaplan et al. (47)]. Depiction of colonies adhering to capillary pipette immersed in broth containing *Aa* after 1, 2, and 3 days of *Aa* incubation. Note the satellite colonies of *Aa* seen in broth surrounding capillary pipette after 3 days of growth **(B)**. Panel C depicting the wild type parental strain containing *dspB* as compared to the transposon mutant. Note that the mutation has affected the presence of satellite colonies as seen in right panel. Left panel shows wild type Aa expressing dispersen **(B)** and showing satellite colonies **(C)** [Modified from Kaplan et al. (49)].

biofilm membrane and the explosive projection of *Aa* to a distant site (48).

In a second series of experiments *Aa* was allowed to grow on capillary pipettes immersed into a broth containing *Aa* (48). *Aa* colonized the pipette leaving the surrounding broth clear of cells. Three days later satellite colonies derived from those cells adhering to the pipette were found in the surrounding broth. Using transposon mutagenesis, the gene responsible for producing the satellite colonies was interrupted and identified as an enzyme called dispersin B (**Figure 4**). The fact that the enzymes had specificity for a polysaccharide substrate, PGA substantiated the finding. The 3 dimensional structure of the enzyme and the substrate it disrupted illustrated the process, its function, and how its discovery provided a new model of transportation and mobilization for *Aa* (48).

Experimental

In a series of elegant experiments Stacy et al. illustrated the biological relevance of dspB. Using a dual species biofilm model consisting of *Aa* and *S. gordonii* it was demonstrated that lactate, the preferred carbon source for *Aa,* was provided by *S. gordonii* (50). Further *S. gordonii* was also responsible for producing H_2O_2 that could be toxic to *Aa.* Stacy et al. showed that in the presence of excessive levels of H_2O_2 *Aa* up-regulated genes such as; *katA*, responsible for catalase, which can neutralize H_2O_2 (50). However, in times when H_2O_2 was produced in excessive levels, *Aa* up-regulated *dspB* permitting *Aa* to move away (likely subgingivally) to avoid the toxic effects of H_2O_2. Thus, *dspB* provides a survival mechanism for *Aa* when it confronts environment stress (the Stacy experiments) or when it lives in an environment where nutritional stress occurs such as seen in the Kaplan experiments (48, 50).

Conclusion

The discovery of *dspB* has provided a mechanism for mobility leading to protection. *Aa* has figured out how to have the best of both worlds; nutritional convenience by virtue of its close association with lactate producing species and locomotion away from products such as H_2O_2 formed by these same lactate producing species in order to avoid the hazardous conditions created by these species (**Figure 4**).

MISCONCEPTION 4: *AA* IS THE CAUSATIVE AGENT IN LAGP: OVERCOMING HOST RESTRICTIONS (SUPPRESSING HOST DEFENSES)

Clinical

Several early studies suggested that *Aa* was the causative agent responsible for LAgP. The association of *Aa* with disease was re-inforced by the fact that *Aa* possessed leukotoxin that killed white blood cells as well as other virulence attributes that gave biological plausibility to *Aa* as a causative agent. Several recent studies have been performed examining microbes related to the development and progression of LAgP (6, 51, 52). These studies attest to the relevance of *Aa* in this disease, however, its role with respect to causation is challenged (6) and although *Aa* is necessary for disease it needs partners. In the case where the more virulent higher leukotoxic *Aa* strain was found, the association of *Aa* with causation may be more relevant (51, 52). To the greatest extent early studies isolated plaque from previously diseased sites and therefore the cause and effect relationship was open to question (5). The first major study to examine subjects going from health to disease was a study showing that African

American adolescents who carry *Aa* show a greater relationship to disease as it progresses (7). These findings were extended in studies by Haubek et al. who in another longitudinal study showed an increased relative risk for the JP2 strain (the hyper-leukotoxin –producing strain of *Aa*) although there was a much reduced relative risk shown for the non-JP2 strain (the moderate leukotoxic strain of *Aa*). These studies suffered from the fact that only *Aa* and no other microbe was examined in the plaque matrix.

The first longitudinal study to examine *Aa* relative to the overall commensal flora going from relative health to disease was done in 2013**.** This study was an observational longitudinal human study that was designed to detect progression from health to disease in African American or Hispanic adolescents (6). Of over one-thousand subjects screened, 63 *Aa*-positive and 72 *Aa*-negative students, who were initially periodontally healthy, were selected to follow for a 2–3 years observational period. Out of the 135 students enrolled in the longitudinal study 16 students and 18 sites developed bone loss over 2–3 years (6). Using the HOMIM technology 5 microbes were highly associated with disease prior to detection of bone loss. Of the 700 taxa followed, *Aa*, *S. parasanguinis* and *Filifactor alocis* were most highly related to sites that developed disease as compared to sites in the same individuals that had *Aa* and remained healthy. The association of this consortium occurred 6 months prior to bone loss with a sensitivity of 89% and a specificity of 99% (6). Cross-sectional studies examining subjects with LAgP, healthy housemates, and healthy others, also from African American backgrounds found similar constellations of microbes (53). Other cross-sectional studies from other ethnicities have found distinctly different combinations of microorganisms (54). The association of *Aa* with *S. parasanguinis* is consistent with the findings of the Whiteley group and supports the concept of nutritional interdependency since *S. gordonii* and *S. parasanguinis* provide lactate and have similar physiological properties (35). The 2013 study is the first report of such an association in the subgingival region of a site that was healthy and developed aggressive periodontitis.

Molecular

Leukotoxin (Ltx) was discovered in 1977 by Taichman and was first biochemically characterized by Baehni et al. (55) and Tsai et al. (56) as a toxin that kills leukocytes and lymphocytes (55–57). The genetics of Ltx was determined almost simultaneously by Lally et al. and Kolodrubetz et al. in (58, 59) and the difference between the minimally toxic and highly toxic strains were illustrated in clinical studies by Haubek et al. (51). The fact that the toxin was both secreted and membrane bound was first determined by Kachlany et al. in (60). The importance of the promoter region in elevated toxin production is still ongoing (61). Thus far, all bacteria that show this toxin have been implicated in disease, particularly infectious disease caused by a multispecies consortium (27). It is our belief that the toxin neutralizes the local mucosal immune response to enable other bacteria to overgrow.

ApiA was first discovered in 1999 as one of six Outer Membrane Proteins [OMPs] (44) thought to play some role in the pathogenesis of Aggressive Periodontitis. Initially ApiA was called OMP 29 and then Omp 34 when heat treated (62). However, it appears as if this 100 mw OMP autotransporter exists as a trimer that has multiple functions. The phenotypic characteristics of ApiA include; adhesion, invasion, and complement resistance. As for complement resistance, based on the work of Asakawa et al. it appears as if factor H binding occurs somewhere between 100 and 200 amino acids in the 295 ApiA amino acid protein (63). While invasion and adhesion appear to occur in separate regions of the protein this trimeric autotransporter/multifunctional protein plays a significant role in *Aa*'s survival and immune resistance as demonstrated by its upregulation during environmental stress and turbulence (as described below).

Experimental

While all studies do not support the role of *Aa* in LAgP almost all studies of adolescents of African or Middle Eastern descent do support this observation (64). Moreover, studies that do claim a role for *Aa* suggest that the JP2 type hyper-leukotoxin producing strain is more virulent (65). The most likely explanation for these discrepancies can be placed on geographic, ethnic, and genetic differences in susceptibility and in exposure to bacteria. However, relative to populations exposed and sensitive to *Aa,* we are much closer to understanding how the microbe affects the disease process as follows.

Shortly after plaque development changes occur in the JE. These changes make the JE more vulnerable to penetration by microbial antigens that border the basement membrane creating a standing osmotic gradient that causes changes in the connective tissue vasculature subjacent to the bacterial/epithelial barrier. Sampling of these antigens by antigen presenting cells causes stagnation of blood flow in these vessels, leukocyte margination, pavementing of leukocytes, and then diapedesis due to chemotactic signals guiding PMNs to mobilize in the direction of the overwhelming microbial burden bordering the epithelial barrier (45).

The first element that confronts this microbial burden is a serum exudate that consists of complement and PMNs that can kill bacteria either directly or indirectly. Complement appears to act directly on the cell wall of bacteria, punching holes in the membrane resulting in cell lysis (66). PMNs can engulf and degrade microbes at a rapid rate. *Aa* is equipped with strategies to neutralize these two potent host innate defense systems. Not only does *Aa* possess ApiA, a complement effector molecule, and leukotoxin, a toxin that kills PMNs, but it has been shown that, under stress, these genes are up-regulated as a defense against these host elements (67).

In the experimental model described below the association of the up-regulation of Ltx expression when *Aa* is under stress was shown in a model that examined an erythromycin resistant strain of *Aa* challenged by high doses of erythromycin [Er] (67). The Er challenged cells showed increased biofilm formation and up-regulation of 4 genes; *flp, pga, ltx, and tfox*, in the Er resistant *Aa* strain. This up-regulation showed an unexpected but previously demonstrated linkage between *ltx*, *pga* and *flp* expression when *Aa* was under stress (67).

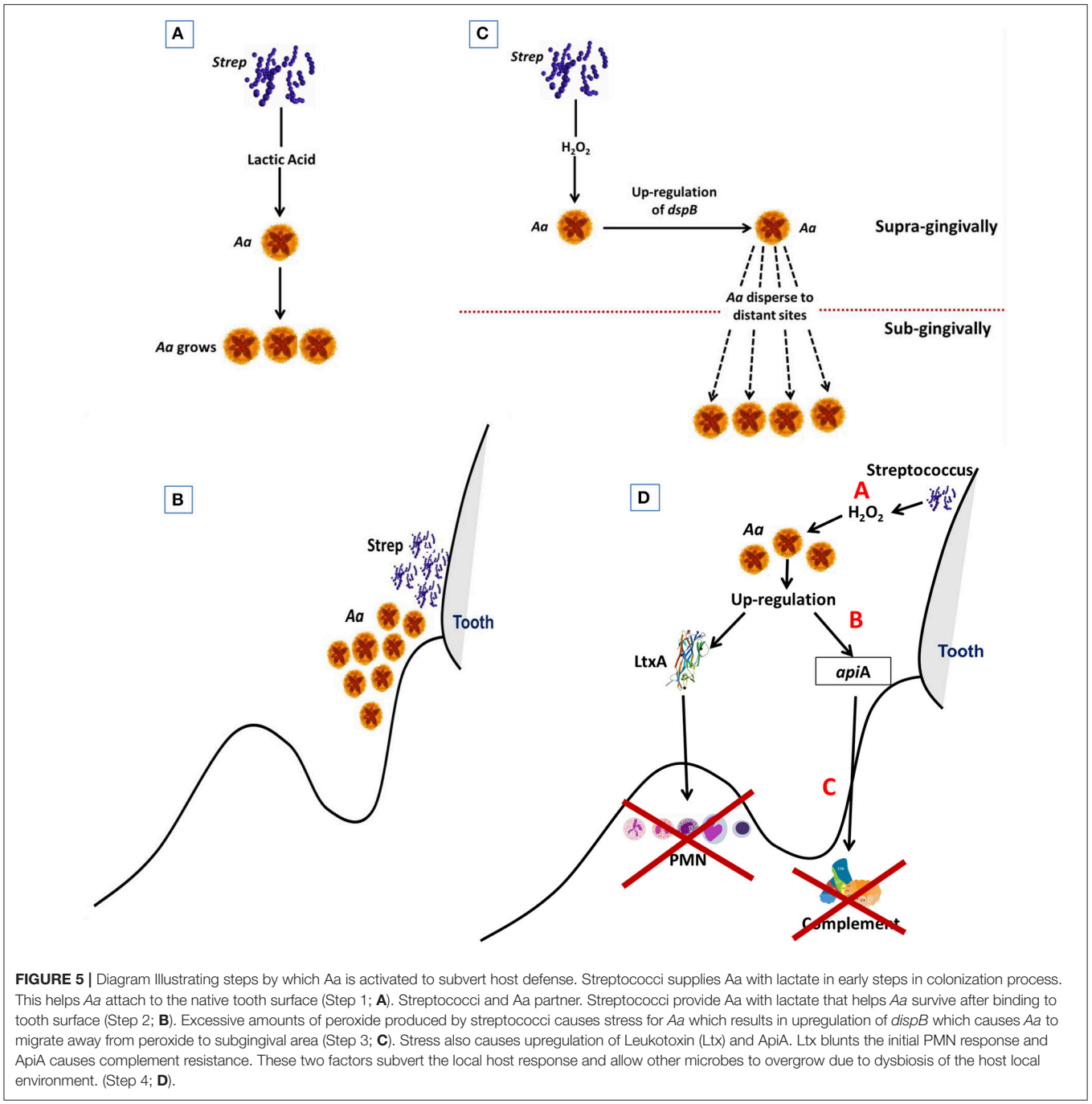

FIGURE 5 | Diagram Illustrating steps by which Aa is activated to subvert host defense. Streptococci supplies Aa with lactate in early steps in colonization process. This helps *Aa* attach to the native tooth surface (Step 1; **A**). Streptococci and Aa partner. Streptococci provide Aa with lactate that helps *Aa* survive after binding to tooth surface (Step 2; **B**). Excessive amounts of peroxide produced by streptococci causes stress for *Aa* which results in upregulation of *dispB* which causes *Aa* to migrate away from peroxide to subgingival area (Step 3; **C**). Stress also causes upregulation of Leukotoxin (Ltx) and ApiA. Ltx blunts the initial PMN response and ApiA causes complement resistance. These two factors subvert the local host response and allow other microbes to overgrow due to dysbiosis of the host local environment. (Step 4; **D**).

Two host innate elements that appear to be related to disease susceptibility in studies of limited but well-defined subjects with LAgP are lactoferrin and PMN functionality (68, 69). Thus, both lactoferrin (Lf) and PMN differences have been observed in African American adolescents (69, 70). In the case of Lf, a single nucleotide polymorphism in the N-terminal- antimicrobial region of Lf appears to have an impact on oral microbial constituents aside from *Aa* in these populations (71). This Lf activity could potentially increase vulnerability to LAgP by altering microbial growth and survival although susceptibility appears to vary based on ethnicity (71). Further, these adolescents appear to have Lf containing minimal iron that permits *Aa* to colonize with greater efficiency as compared to controls who have Lf with high iron content (72). With respect to PMNs, reduced chemotaxis appears to be due to primed PMNs resulting in hyperactive PMN responsiveness, impaired phagocytosis, and overproduction of superoxide (73). In combination these alterations in innate immunity could potentiate disease susceptibility.

Conclusion

Early in the disease process *Aa* is confronted with potent host defense systems consisting of a wall of PMNs and a high concentration of complement, both of these host defense elements can destroy *Aa* and other potential pathobionts. Alteration of these host defense systems could permit *Aa* to survive. Nevertheless, these defense systems while altered still exist and put stress on *Aa* and other members of the flora. Responding to the stress *Aa* produces agents that can neutralize host defenses to enable other microbes in the region to survive and as such acts as a useful participant in local host dysbiosis (**Figure 5**). In this respect *Aa* could be designated as a keystone pathogen (74).

OVERALL CONCLUSIONS

Molecular and experimental models conclusively demonstrate that *Aa* is an early colonizer, co-colonizing with other early colonizers who produce lactate. *Aa* can then migrate away from stressful challenges to a more protected subgingival domain by up-regulation of *dspB*. Facing the challenge of an innate subgingival response, *Aa* can up-regulate complement resistance genes and leukotoxin production to modulate the local host immune response in order to allow for an overgrowth of a consortium of pathobionts. Working together the consortium can overwhelm the natural resistance of the local host innate defense response and produce inflammatory cytokines that can result in connective tissue and bone loss and derangement of the attachment apparatus. It is still to be proven whether this scenario is unique to the non-JP2 strain of *Aa* or if this is a general strategy used to provoke local disease. This working hypothesis can be applied to other combinations of microbes that can operate under differing circumstances in populations distinct from the African American adolescents studied in Localized Aggressive Periodontitis.

AUTHOR CONTRIBUTIONS

All authors listed have made a substantial, direct and intellectual contribution to the work, and approved it for publication.

ACKNOWLEDGMENTS

The author would like to thank Dr (s). D. Figurski, S. Kachlany, P. Planet, J. Kaplan and N. Rammasubbu for their unwavering commitment to achieving a better understanding of the role of Aa in disease. There have been many manuscripts that were not included in this review due to the focused nature of the review and I therefore would like to take this opportunity to apologize to those who have devoted time and effort to our understanding of this area but who I failed to acknowledge due to the limited scope of this review. I would also like to extend my appreciation to the NIH for their support over the years in the form of several grants including; DE017968, DE021172, DE016306.

REFERENCES

1. Slots J. The predominant cultivable organisms in juvenile periodontitis. *Scand J Dent Res.* (1976) 84:1–10. doi: 10.1111/j.1600-0722.1976.tb00454.x
2. Newman MG, Socransky SS, Savitt ED, Propas DA, Crawford A. Studies of the microbiology of periodontosis. *J Periodontol.* (1976) 47:373–79. doi: 10.1902/jop.1976.47.7.373
3. Klinger R. Untersuchungen uber,enschliche aktinomykose. *Centralblat Bacteriol.* (1912) 1912:191–200.
4. Kaplan AH, Weber DJ, Oddone EZ, Perfect JR. Infection due to *Actinobacillus actinomycetemcomitans*: 15 cases and review. *Rev Infect Dis.* (1989) 11:46–63. doi: 10.1093/clinids/11.1.46
5. Zambon JJ. Actinobacillus actinomycetemcomitans in human periodontal disease. *J Clin Periodontol.* (1985) 12:1–20. doi: 10.1111/j.1600-051X.1985.tb01348.x
6. Fine DH, Markowitz K, Fairlie K, Tischio-Bereski D, Ferrendiz J, Furgang D, et al. A consortium of *Aggregatibacter actinomycetemcomitans*, *Streptococcus parasanguinis*, and *Filifactor alocis* is present in sites prior to bone loss in a longitudinal study of localized aggressive periodontitis. *J Clin Microbiol.* (2013) 51:2850–61. doi: 10.1128/JCM.00729-13
7. Fine DH, Markowitz K, Furgang D, Fairlie K, Ferrandiz J, Nasri C, et al. *Aggregatibacter actinomycetemcomitans* and its relationship to initiation of localized aggressive periodontitis: longitudinal cohort study of initially healthy adolescents. *J Clin Microbiol.* (2007) 45:3859–69. doi: 10.1128/JCM.00653-07
8. Fives-Taylor PM, Meyer DH, Mintz KP, Brissette C. Virulence factors of *Actinobacillus actinomycetemcomitans. Periodontol 2000.* (1999) 20:136–67. doi: 10.1111/j.1600-0757.1999.tb00161.x
9. Fine DH, Karched M, Furgang D, Sampathkumar V, Velusamy S, Godboley D. Colonization and persistence of labeled and "foreign" strains of inoculated into the mouths of rhesus monkeys. *J Oral Biol.* (2015) 2:1. doi: 10.13188/2377-987X.1000005
10. Ritz HL. Microbial population shifts in developing human plaque. *Archs Oral Biol.* (1967) 12:1561–8. doi: 10.1016/0003-9969(67)90190-2
11. Listgarten MA. The structure of dental plaque. *Periodontol 2000.* (1994) 5:52–65. doi: 10.1111/j.1600-0757.1994.tb00018.x
12. Moore LV, Moore WE, Cato EP, Smibert RM, Burmeister JA, Best AM, et al. Bacteriology of human gingivitis. *J Dent Res.* (1987) 66:989–95. doi: 10.1177/00220345870660052401
13. Fine DH, Furgang D, Schreiner HC, Goncharoff P, Charlesworth J, Ghazwan G, et al. Phenotypic variation in *Actinobacillus actinomycetemcomitans* during laboratory growth: implications for virulence. *Microbiology.* (1999) 145 (Pt 6):1335–47. doi: 10.1099/13500872-145-6-1335
14. Kolenbrander P, Andersen RA, Moore LVH. Coaggregation of *Fusobacterium nucleatum*, *Selenomonas flueggei*, *Selenomonas infelix*, *Selenomonas noxia*, and *Selenomonas sputigena* with strains from 11 genera of oral bacteria. *Infect Immun.* (1989) 57:3194–203.
15. Kolenbrander PE, Palmer RJ Jr, Rickard AH, Jakubovics NS, Chalmers NI, Diaz PI. Bacterial interactions and successions during plaque development. *Periodontol 2000.* (2006) 42:47–79. doi: 10.1111/j.1600-0757.2006.00187.x
16. Kolenbrander PE, Palmer RJ Jr, Periasamy S, Jakubovics NS. Oral multispecies biofilm development and the key role of cell-cell distance. *Nat Rev Microbiol.* (2010) 8:471–80. doi: 10.1038/nrmicro2381
17. Rosan B, Slots J, Lamont RL, Listgarten MA, Nelson GM. *Actinobacillus actinomycetemcomitans* fimbriae. *Oral Microbiol Immunol.* (1988) 3:58–63. doi: 10.1111/j.1399-302X.1988.tb00082.x
18. Planet PJ, Kachlany SC, DeSalle R, Figurski DH. Phylogeny of genes for secretion of NTPases: identification of the widespread tadA subfamily and development of a diagnostic key for gene classification. *Proc Natl Acad Sci USA.* (2001) 98:2503–08. doi: 10.1073/pnas.051436598
19. Planet PJ, Kachlany SC, Fine DH, DeSalle R, Figurski DH. The widespread colonization island of *Actnobacillus actinomycetemcomitans. Nat Genet.* (2003) 34:193–98. doi: 10.1038/ng1154

20. Haase EM, Zmuda JL, Scannapieco FA. Identification of rough-colony-specific outer membrane proteins in *Actinobacillus actinomycetemcomitans*. *Infect Immun.* (1999) 67:2901–08.
21. Norskov-Lauritsen N, Kilian M. Reclassification of *Actinobacillus actinomycetemcomitans*, *Haemophilus paraphrophilus* and *Heamophilus segnis* as *Aggregatibacter actinomycetemcomitans* gen. nov., comb. nov., *Aggregatibacter aphrophilus* comb. nov. and *Aggregatibacter segnis* comb. nov., and emended description of *Aggregatibacter aphrophilus* to include V factor-dependent and V factor-independent isolates. *Int J Syst Evol Microbiol.* (2006) 56:2135–46. doi: 10.1099/ijs.0.64207-0
22. Kachlany SC, Planet PJ, DeSalle R, Fine DH, Figurski DH. Genes for tight adherence of *Actinobacillus actinomycetemcomitans*: from plaque to plague to pond scum. *Trends Microbiol.* (2001) 9:429–37. doi: 10.1016/S0966-842X(01)02161-8
23. Lamell CW, Griffen AL, McClellan DL, Leys EJ. Acquisition and colonization stability of *Actinobacillus actinomycetemcomitans* and *Porphyromonas gingivalis* in children. *J Clin Microbiol.* (2000) 38:1196-69.
24. Tanner AC, Milgrom PM, Kent RL, Mokeem SA, Page RC, Riedy CA, et al. The microbiota of young children from tooth and tongue samples. *J Dent Res.* (2002) 81:53–7. doi: 10.1177/002203450208100112
25. Asikainen S, Chen C, Slots J. Likelihood of transmitting *Actinobacillus actinomycetemcomitans* and *Porphyromonas gingivalis* in families with periodontitis. *Oral Microbiol Immunol.* (1996) 11:387–94. doi: 10.1111/j.1399-302X.1996.tb00200.x
26. Rose JE, Meyer DH, Fives-Taylor PM. Aae, an autotransporter involved in adhesion of actinobaciillus actinomyctemcomitans to epithelial cells. *Infect Immun.* (2003) 71:2384–93. doi: 10.1128/IAI.71.5.2384-2393.2003
27. Fine DH, Kaplan JB, Kachlany SC, Schreiner HC. How we got attached to *Actinobacillus actinomycetemcomitans*: a model for infectious diseases. *Periodontol 2000.* (2006) 42:114–57. doi: 10.1111/j.1600-0757.2006.00189.x
28. Fine DH, Velliyagonder K, Furgang D, Kaplan JB. The *Actinobacillus actinomycetemcomitans* autotransporter adhesin Aae exhibits specificity for buccal epithelial cells from humans and old world primates. *Infect Immun.* (2005) 73:1947–53. doi: 10.1128/IAI.73.4.1947-1953.2005
29. Van Winkelhoff AJ, Boutaga K. Transmission of periodontal bacteria and models of infection. *J Clin Periodontal.* (2005) 32:16–27. doi: 10.1111/j.1600-051X.2005.00805.x
30. van der Woude MW, Baumler AJ. Phase and antigenic variation in bacteria. *Clin Microbiol Rev.* (2004) 17:581–611. doi: 10.1128/CMR.17.3.581-611.2004
31. Schreiner HC, Sinatra K, Kaplan JB, Furgang D, Kachlany SC, Planet PJ, et al. Tight-adherence genes of Actinobacillus actinomycetemcomitans are required for virulence in a rat model. *Proc Natl Acad Sci USA.* (2003) 100:7295–300. doi: 10.1073/pnas.1237223100
32. Fine DH, Markowitz K, Furgang D, Velliyagounder K. *Aggregatibacter actinomycetemcomitans* as an early colonizer of oral tissues: epithelium as a reservoir? *J Clin Microbiol.* (2010) 48:4464–73. doi: 10.1128/JCM.00964-10
33. Kilian M, Rolla G. Initial colonization of teeth in monkeys as related to diet. *Infect Immun.* (1976) 14:1022–7.
34. Slots J. elective medium for isolation of *Actinobacillus actinomycetems*. *J Clin Microbiol.* (1982) 15:606–9.
35. Brown SA, Whiteley M. A novel exclusion mechanism for carbon resource partitioning in *Aggregatibacter actinomycetemcomitans*. *J Bacteriol.* (2007) 189:6407–14. doi: 10.1128/JB.00554-07
36. Brown SA, Whiteley M. Characterization of the L-lactate dehydrogenase from *Aggregatibacter* actinomycetemcomitans. *PLoS ONE.* (2009) 4:e7864. doi: 10.1371/journal.pone.0007864
37. Stacy A, Everett J, Jorth P, Trivedi U, Rumbaugh KP, Whiteley M. Bacterial fight-and-flight responses enhance virulence in a polymicrobial infection. *Proc Natl Acad Sci USA*. (2014) 111:7819–24. doi: 10.1073/pnas.1400586111
38. Ramsey MM, Rumbaugh KP, Whiteley M. Metabolite cross-feeding enhances virulence in a model polymicrobial infection. *PLoS Pathog.* (2011) 7:e1002012. doi: 10.1371/journal.ppat.1002012
39. Faust K, Raes J. CoNet app: inference of biological association networks using Cytoscape. *F1000Res*. (2016) 5:1519. doi: 10.12688/f1000research.9050.1
40. Fine D, Velusamy SK, Sampathkumar V, Paster BJ. *Lactate and Leukotoxin Promote Colonization of Aggregatibacter in Rhesus Monkeys.* London, UK: International Association of Dental Research (2018).
41. Schroeder HE, Listgarten MA. Fine structure of the developing epithelial attachment to teeth. *Monogr Dev Biol.* (1971) 2:1–134.
42. Schroeder HE, Listgarten MA. The gingival tissues: the architecture of periodontal protection. Periodontol 2000. (1997) 13:91-120. doi: 10.1111/j.1600-0757.1997.tb00097.x
43. Janeway CA Jr, Medzhitov R. Innate immune recognition. *Ann Rev Immunol.* (2002) 20:197–216. doi: 10.1146/annurev.immunol.20.083001.084359
44. Ebersole JL, Dawson D, Emecan-Huja P, Nagarajan R, Howard K, Grady ME, et al. The periodontal war: microbes and immunity. *Periodontol 2000*. (2017) 75:52–115. doi: 10.1111/prd.12222
45. Page RC, Schroeder HE. Pathogenesis of inflammatory periodontal disease. A summary of current work. *Lab Invest.* (1976) 34:235–49.
46. Ramasubbu N, Thomas LM, Ragunath C, Kaplan JB. Structural analysis of dispersin B, a biofilm-releasing glycoside hydrolase from the periodontopathogen *Actinobacillus actinomycetemcomitans*. *J Mol Biol.* (2005) 349:475–86. doi: 10.1016/j.jmb.2005.03.082
47. Kaplan JB, Meyenhofer MF, Fine DH. Biofilm growth and detachment of *Actinobacillus actinomycetemcomitans*. *J Bacteriol.* (2003) 185:1399–404. doi: 10.1128/JB.185.4.1399-1404.2003
48. Kaplan JB. Biofilm dispersal: mechanisms, clinical implications and potential therapeutic uses. *J Dent Res.* (2010) 89:205–18. doi: 10.1177/0022034509359403
49. Kaplan JB, Ragunath C, Ramasubbu N, Fine DH. Detachment of Actinobacillus actinomycetemcomitans biofilm cells by an endogenous β-hexosaminidase activity. J Bacteriol. (2003) 185:4693–8. doi: 10.1128/JB.185.16.4693-4698.2003
50. Stacy A, McNally L, Darch SE, Brown SP, Whiteley M. The biogeography of polymicrobial infection. *Nat Rev Microbiol.* (2016) 14:93–105. doi: 10.1038/nrmicro.2015.8
51. Haubek D, Poulsen K, Westergaard J, Dahlen G, Kilian M. Highly toxic clone of *Actinobacillus actinomycetemcomitans* in geographically widespread cases of juvenile periodontitis in adolescents of African origin. *J Clin Microbiol.* (1996) 34:1576–8.
52. Burgess D, Huang H, Harrison P, Aukhil I, Shaddox L. *Aggregatibacter actinomycetemcomitans* in African Americans with localized aggressive periodontitis. *JDR Clin Trans Res.* (2017) 2:249–57. doi: 10.1177/2380084417695543
53. Shaddox LM, Huang H, Lin T, Hou W, Harrison PL, Aukhil I, et al. Microbiological characterization in children with aggressive periodontitis. *J Dent Res*. (2012) 91:927–33. doi: 10.1177/0022034512456039
54. Li Y, Feng X, Zhang L, Ruifang L, Shi D, Wang X, et al. Oral microbiome in chinese patients with aggressive periodontitis and their family members. *J Clin Periodontol.* (2015) 42:1015–23. doi: 10.1111/jcpe.12463
55. Baehni P, Tsai CC, Taichman NS, McArthur WP. Interaction of inflammatory cells and oral microorganisms. V. Electron microscopic and biochemical study on the mechanisms of release of lysosomal constituents from human polymorphonuclear leukocytes exposed to dental plaque. *J Periodontal Res.* (1978) 13:333–48. doi: 10.1111/j.1600-0765.1978.tb00188.x
56. Tsai CC, McArthur WP, Baehni PC, Hammond BF, Taichman NS. Extraction and partial characterization of a leukotoxin from a plaque-derived Gram-negative microorganism. *Infect Immun.* (1979) 25:427–39.
57. Taichman NS, Tsai CC, Baehni PC, Stoller N, McArthur WP. Interaction of inflammatory cells and oral microorganisms. IV. *In vitro* release of lysosomal constituents from polymorphonuclear leukocytes exposed to supragingival and subgingival bacterial plaque. *Infect Immun.* (1977) 16:1013–23.
58. Lally ET, Golub EE, Kieba IR, Taichman NS, Rosenblum J, Rosenblum JC, et al. Analysis of the Actinobacillus actinomycetemcomitans leukotoxin gene. *J Biol Chem.* (1989) 264:15451–6.
59. Koldrubetz D, Dailey T, Ebersole J. Cloning and expression of the leukotoxin gene from *Actinobacillus actinomycetemcomitans. Infect Immun.* (1989) 57:1465–9.
60. Kachlany SC, Fine DH, Figurski DH. Secretion of RTX leukotoxin by *Actinobacillus actinomycetemcomitans. Infect Immun.* (2000) 68:6094–100. doi: 10.1128/IAI.68.11.6094-6100.2000
61. Sampathkumar V, Velusamy SK, Godboley D, Fine DH. Increased leukotoxin production: Characterization of 100 base pairs within the 530 base pair

leukotoxin promoter region of Aggregatibacter actinomycetemcomitans. *Sci Rep.* (2017) 7:1887. doi: 10.1038/s41598-017-01692-6
62. Komatsuzawa H, Kawai T, Wilson ME, Taubman MA, Sugai M, Suginaka H. Cloning of the gene encoding the Actinobacillus actinomycetemcomitans serotype b OmpA-like outer membrane protein. *Infect Immun.* (1999) 67: 942–45.
63. Asakawa R, Komatsuzawa H, Goncalves RB, Izumi S, Fujiwara T, Nakano Y, et al. Outer membrane protein 100, a versatile virulence factor of *Actinobacillus actinomycetemcomitans. Mol Microbiol.* (2003) 50:1125–39. doi: 10.1046/j.1365-2958.2003.03748.x
64. Fine DH, Patil AG, Loos BG. Classification and diagnosis of aggressive periodontitis. *J Periodontol.* (2018) 89(Suppl. 1):S103–19. doi: 10.1002/JPER.16-0712
65. Haubek D, Ennibi OK, Poulsen K, Vaeth M, Poulsen S, Kilian M. Risk of aggressive periodontitis in adolescent carriers of the JP2 clone of Aggregatibacter (Actinobacillus) actinomycetemcomitans in Morocco: a prospective longitudinal cohort study. *Lancet.* (2008) 371:237–42. doi: 10.1016/S0140-6736(08)60135-X
66. Bostanci N, Bao K, Li X, Maekawa T, Grossmann J, Panse C, et al. Interaction of inflammatory cells and oral microorganisms. V. Electron microscopic and biochemical study on the mechanisms of release of lysosomal constituents from human polymorphonuclear leukocytes exposed to dental plaque. *J Proteome Res.* (2018) 17:3153–75. doi: 10.1021/acs.jproteome.8b00263
67. Narayanan AM, Ramsey MM, Stacy A, Whiteley M. Defining genetic fitness determinants and creating genomic resources for an oral pathogen. *Appl Environ Microbiol.* (2017) 83:14. doi: 10.1128/AEM.00797-17
68. Van Dyke TE, Zinney W, Winkel K, Taufiq A, Offenbacher S, Arnold RR. Neutrophil function in localized juvenile periodontitis. Phagocytosis, superoxide production and specific granule release. *J Periodontol.* (1986) 57:703–8. doi: 10.1902/jop.1986.57.11.703
69. Fine DH, Furgang D, Beydouin F. Lactoferrin iron levels are reduced in saliva of patients with localized aggressive periodontitis. *J Periodontol.* (2002) 73:624–30. doi: 10.1902/jop.2002.73.6.624
70. Kantarci A, Oyaizu K, Van Dyke TE. Neutrophil-mediated tissue injury in periodontal disease pathogenesis: findings from localized aggressive periodontitis. *J Periodontol.* (2003) 74:66–75. doi: 10.1902/jop.2003.74.1.66
71. Fine DH. Lactoferrin: a roadmap to the borderland between caries and periodontal disease. *J Dent Res.* (2015) 94:768–76. doi: 10.1177/0022034515577413
72. Fine DH, Furgang D. Lactoferrin iron levels affect attachment of Actinobacillus actinomycetemcomitans to buccal epithelial cells. *J Periodontol.* (2002) 73:616–23. doi: 10.1902/jop.2002.73.6.616
73. Fredman G, Oh SF, Ayilavarapu S, Hasturk H, Serhan CN, Van Dyke TE. Impaired phagocytosis in localized aggressive periodontitis: rescue by Resolvin E1. *PLoS ONE.* (2011) 6:e24422. doi: 10.1371/journal.pone.0024422
74. Hajishengallis G, Darveau RP, Curtis MA. The keystone-pathogen hypothesis. *Nat Rev Microbiol.* (2012) 10:717–25. doi: 10.1038/nrmicro2873

Conflict of Interest Statement: The authors declare that the research was conducted in the absence of any commercial or financial relationships that could be construed as a potential conflict of interest.

frontiers in Immunology

ORIGINAL RESEARCH
published: 30 April 2019
doi: 10.3389/fimmu.2019.00933

BET Bromodomain Inhibitors Suppress Inflammatory Activation of Gingival Fibroblasts and Epithelial Cells From Periodontitis Patients

Anna Maksylewicz[1†], Agnieszka Bysiek[1†], Katarzyna B. Lagosz[1], Justyna M. Macina[1], Malgorzata Kantorowicz[2], Grzegorz Bereta[1], Maja Sochalska[1], Katarzyna Gawron[1], Maria Chomyszyn-Gajewska[2], Jan Potempa[1,3] and Aleksander M. Grabiec[1]**

[1] Department of Microbiology, Faculty of Biochemistry, Biophysics and Biotechnology, Jagiellonian University, Kraków, Poland, [2] Department of Periodontology and Oral Medicine, Faculty of Medicine, Jagiellonian University Medical College, Kraków, Poland, [3] Department of Oral Immunology and Infectious Diseases, University of Louisville School of Dentistry, Louisville, KY, United States

BET bromodomain proteins are important epigenetic regulators of gene expression that bind acetylated histone tails and regulate the formation of acetylation-dependent chromatin complexes. BET inhibitors suppress inflammatory responses in multiple cell types and animal models, and protect against bone loss in experimental periodontitis in mice. Here, we analyzed the role of BET proteins in inflammatory activation of gingival fibroblasts (GFs) and gingival epithelial cells (GECs). We show that the BET inhibitors I-BET151 and JQ1 significantly reduced expression and/or production of distinct, but overlapping, profiles of cytokine-inducible mediators of inflammation and bone resorption in GFs from healthy donors (*IL6*, *IL8*, *IL1B*, *CCL2*, *CCL5*, *COX2,* and *MMP3*) and the GEC line TIGK (*IL6*, *IL8*, *IL1B*, *CXCL10*, *MMP9*) without affecting cell viability. Activation of mitogen-activated protein kinase and nuclear factor-κB pathways was unaffected by I-BET151, as was the histone acetylation status, and new protein synthesis was not required for the anti-inflammatory effects of BET inhibition. I-BET151 and JQ1 also suppressed expression of inflammatory cytokines, chemokines, and osteoclastogenic mediators in GFs and TIGKs infected with the key periodontal pathogen *Porphyromonas gingivalis*. Notably, *P. gingivalis* internalization and intracellular survival in GFs and TIGKs remained unaffected by BET inhibitors. Finally, inhibition of BET proteins significantly reduced *P. gingivalis*-induced inflammatory mediator expression in GECs and GFs from patients with periodontitis. Our results demonstrate that BET inhibitors may block the excessive inflammatory mediator production by resident cells of the gingival tissue and identify the BET family of epigenetic reader proteins as a potential therapeutic target in the treatment of periodontal disease.

Keywords: periodonditis, BET bromodomain, gingival fibroblast, gingival epithelial cell, porphyromonas gingivalis, I-BET151, chronic inflammation

OPEN ACCESS

Edited by:
Asaf Wilensky,
Hadassah Medical Center, Israel

Reviewed by:
Whasun Oh Chung,
University of Washington, United States
Joerg Meyle,
University of Giessen, Germany

***Correspondence:**
Jan Potempa
jan.potempa@uj.edu.pl
Aleksander M. Grabiec
aleksander.grabiec@uj.edu.pl

[†]These authors have contributed equally to this work

Specialty section:
This article was submitted to Mucosal Immunity, a section of the journal Frontiers in Immunology

Received: *02 September 2018*
Accepted: *11 April 2019*
Published: *30 April 2019*

Citation:
Maksylewicz A, Bysiek A, Lagosz KB, Macina JM, Kantorowicz M, Bereta G, Sochalska M, Gawron K, Chomyszyn-Gajewska M, Potempa J and Grabiec AM (2019) BET Bromodomain Inhibitors Suppress Inflammatory Activation of Gingival Fibroblasts and Epithelial Cells From Periodontitis Patients. Front. Immunol. 10:933. doi: 10.3389/fimmu.2019.00933

INTRODUCTION

Periodontitis is an inflammatory disease of the periodontium caused by microbial imbalance (dysbiosis) and the anaerobic bacterium *Porphyromonas gingivalis* plays a central role in driving the chronic inflammation (1). Oral pathogen interaction with gingival cells and infiltrating immune cells leads to a local immune response which fails to eradicate the invading bacteria which are equipped with sophisticated mechanisms of immune evasion. If unresolved, ongoing inflammation leads to periodontal ligament degradation, bone resorption and eventual tooth loss (2). Resident cells of the gingival tissue, including gingival epithelial cells (GECs) and gingival fibroblasts (GFs), represent the first line of defense against oral pathogens and are considered an important component of the innate immune system (3, 4). However, their chronic activation due to persistent interaction with oral bacteria, which involves the secretion of large quantities of cytokines, chemokines, matrix-degrading enzymes, and prostaglandins, significantly contributes to periodontitis pathogenesis (5).

Expression of inflammatory mediators is tightly regulated by epigenetic mechanisms, among which reversible acetylation of histone proteins plays a critical role. Importantly, pathological changes in histone acetylation and in expression of histone-modifying enzymes, histone acetyltransferases (HATs) and histone deacetylases (HDACs), have been identified in periodontitis patients and in a mouse model of periodontal disease (6, 7). Bromodomain proteins, 46 of which have been identified in the human genome, recognize ε-N-lysine acetylation motifs on histone tails and regulate the formation of acetylation-dependent chromatin complexes that are required for transcription (8). In particular, the ubiquitously expressed proteins BRD2, BRD3, BRD4, which belong to the bromodomain and extraterminal domain (BET) family, play distinct roles in coupling histone acetylation to gene transcription (9), including transcriptional activation of inflammatory genes (10). BET proteins are critical regulators of transcriptional elongation and cell division, and dysregulation of BET protein function, such as pathogenic chromosomal BRD4 translocations, has been identified in oncological conditions (11). BET proteins have thus emerged as potential therapeutic targets, and compounds targeting their tandem bromodomains are currently being evaluated in clinical trials (12).

The discovery of specific BET inhibitors acting as acetylated histone mimetics, I-BET151, and JQ1 (13, 14), has not only allowed for therapeutic targeting of BET proteins in cancer, but also provided insight into contributions of bromodomain-containing proteins to the pathogenesis of inflammatory disorders that are associated with an altered epigenetic landscape (15). BET inhibitors suppress lipopolysaccharide (LPS)- and cytokine-induced expression of inflammatory cytokines and chemokines in monocytes and macrophages *in vitro* and *in vivo*, and protect mice from lethal endotoxic shock and sepsis (16, 17). Inhibition of BET proteins also ameliorates inflammation and resulting pathology in animal models of several inflammatory diseases, including rheumatoid arthritis (RA), graft-vs. host disease and multiple sclerosis (18–20). Surprisingly, despite extensive efforts toward understanding bromodomain protein function in health and disease, little is still known about the role of BET proteins in the pathogenesis of periodontitis. The only study available to date demonstrated that the BET inhibitor JQ1 ameliorates gingival inflammation and alveolar bone destruction in *P. gingivalis*-induced experimental periodontitis in mice (21). In this model, the therapeutic effects of BET inhibition were attributed to diminished inflammatory cytokine production by macrophages and reduced osteoclast formation (21). However, the influence of JQ1 on other cell types involved in periodontitis pathogenesis has not been tested. In the present study, we investigated the effects of the BET bromodomain inhibitors I-BET151 and JQ1 on inflammatory and antimicrobial responses of resident cells of the gingival tissue, GFs and GECs, in the context of infection with the periodontal pathogen *P. gingivalis*.

MATERIALS AND METHODS

Subjects, Cell Isolation, and Culture

Gingival tissue specimens for primary cell isolation were collected from healthy individuals undergoing orthodontic treatment ($n = 9$) and from patients with chronic periodontitis ($n = 5$) at the Department of Periodontology and Oral Medicine, Faculty of Medicine, Jagiellonian University Medical College in Kraków, Poland. This study was approved by and carried out in accordance with the recommendations of the Bioethical Committee of the Jagiellonian University in Kraków, Poland (permit numbers 122.6120.337.2016 and KBET/310/B/2012). All subjects gave written informed consent in accordance with the Declaration of Helsinki. Clinical characteristics of patients included in the study are shown in **Supplementary Table 1**.

The epithelial layer was separated enzymatically by treatment with dispase at 4°C overnight (o/n) and subjected to three rounds of digestion with trypsin (BioWest) for 10 min at 37°C. After centrifugation, the obtained GECs were suspended in keratinocyte growth medium (KGM-Gold, Lonza) and cultured in 6-well plates until confluence. GFs were isolated from the remaining connective tissue by digestion with 0.1% collagenase I (Invitrogen) at 37°C o/n. Cells were then vigorously pipetted, washed in PBS, suspended in Dulbecco's modified Eagle's medium (DMEM, Lonza) supplemented with 10% fetal bovine serum (FBS, EuroClone), 50 U/ml penicillin/streptomycin and 50 U/ml gentamicin, and cultured in T75 flasks. Cells were cultured in the presence of 10 μg/ml nystatin until passage 2 to prevent fungal contamination. The isolation procedure and the homogeneity of GF cultures have been standardized and described previously (22). GECs were used for experiments at passage 2 and GFs were used between passages 4 and 9. Telomerase-immortalized gingival keratinocytes (TIGKs, RRID:CVCL_M095) were kindly provided by Prof. Richard J Lamont (University of Louisville School of Dentistry) (23) and were cultured in KGM-Gold. One day prior to and during experiments, GFs were cultured in antibiotic-free DMEM containing 2% FBS, whereas TIGKs and primary GECs were cultured in antibiotic-free KGM-Gold.

Bacterial Culture and Cell Infection

Porphyromonas gingivalis wild-type strain ATCC 33277 was grown on blood agar plates as described elsewhere (24). After anaerobic culture for 5–7 days at 37°C, bacteria were inoculated into brain–heart infusion (BHI) broth (Becton Dickinson) supplemented with 0.5 mg/ml L-cysteine, 10 μg/ml hemin and 0.5 μg/ml vitamin K, and cultured o/n in an anaerobic chamber (85% N_2, 10% CO_2, and 5% H_2). Bacteria were then washed in PBS, resuspended in fresh BHI broth at optical density $(OD)_{600nm} = 0.1$ and cultured for ∼20 h. A bacterial suspension at $OD_{600nm} = 1$ [corresponding to 10^9 colony-forming units (CFU)/ml] in PBS was prepared and used for experiments. In some experiments, bacteria were heat-inactivated by 30 min incubation at 60°C or were treated with specific gingipain inhibitors KYT-1 and KYT-36 (Peptide Institute Inc.). 1μM KYT-1 and KYT-36 were incubated with bacteria for 20 min at 37°C prior to infection and were added to culture media for the duration of infection.

RNA Isolation and Quantitative (q)PCR

GFs and TIGKs were seeded at 2.5×10^5 cells per well in 12-well plates and after o/n culture were treated with DMSO [0.005% (V/V)] (BioShop), 1 μM I-BET151 (TargetMol) or 1 μM JQ1 (Abcam) for 30 min followed by stimulation with TNF, IL-1β (10 ng/ml, both from BioLegend) or infection with *P. gingivalis* at a multiplicity of infection (MOI) of 100 for 4 h. In some experiments, protein synthesis was blocked with 10 μg/ml cycloheximide (CHX, TargetMol). Total RNA was isolated using an EZ-10 Spin Column Total RNA Minipreps Super Kit (Bio-Basic), quantified using a Nanodrop spectrophotometer (Thermo Scientific) and equivalent amounts of RNA (500–1,000 ng) were converted to cDNA using a High-Capacity cDNA Reverse Transcription Kit (Applied Biosystems). qPCR reactions were performed on a CFX96 Touch™ Real-Time PCR Detection System (BIO-RAD) using PowerUp SybrGreen PCR mix (Applied Biosystems) and primers (Genomed S.A.) listed in **Supplementary Table 2**. The data were analyzed using the CFX Manager (BIO-RAD) and changes in mRNA expression were calculated relative to RPLP0 (ribosomal protein lateral stalk subunit P0) expression using the ΔΔCT method unless otherwise indicated.

ELISA

GFs and TIGKs were seeded at 5.0×10^4 cells per well in 48-well plates and after o/n culture were treated with DMSO [0.005% (V/V)], I-BET151 or JQ1 (both at 100 nM−1 μM) for 30 min before stimulation with TNF or IL-1β (10 ng/ml), or infection with heat-inactivated or KYT-treated *P. gingivalis* for 24 h. Alternatively, after treatment with inhibitors, GFs were infected with *P. gingivalis* at an MOI of 100 for 1 h. Cells were then washed 3 times with PBS and cultured in fresh medium containing DMSO, I-BET151, or JQ1 for another 24 h prior to collection of supernatants. Cell-free culture supernatants were collected and concentrations of IL-6, IL-8, CCL2, and CCL20 were determined using ELISA MAX kits (BioLegend) according to the manufacturer's instructions. Absorbance was measured using an Infinite M200 microplate reader (Tecan).

Measurement of Cell Viability

Cell viability was assessed using the MTT (3-(4,5-dimethylthiazol-2-yl)-2,5-diphenyltetrazolium bromide, Sigma-Aldrich) reduction assay as described previously (25).

Immunoblotting

Cell lysates were prepared in 1x Laemmli's buffer (2% SDS, 10% glycerol, 125 mM Tris-HCl, pH 6.8) and protein content was quantitated using the Bradford assay (BioShop). In some experiments, cells treated with the HDAC inhibitor suberoylanilide hydroxamic acid (SAHA, 5 μM) (Abcam) were used as a positive control. Equivalent amounts of protein were resolved by electrophoresis on 10 or 15% polyacrylamide gels and transferred to the Immobilon-P^{SQ} PVDF membranes (Millipore). Membranes were then blocked in 2% milk (BioShop) in TBS containing 0.1% Tween-20 (BioShop) (TBS/T), and incubated at 4°C o/n with primary antibodies recognizing acetylated lysine, acetyl-histone 3 (Ac-H3), H3, IκBα, phospho (p)-p38, p-ERK, p-p65 (all from Cell Signaling Technology), or tubulin (clone DM1A, Sigma-Aldrich). After washing in TBS/T, membranes were incubated with horseradish peroxidase (HRP)–conjugated anti-mouse or anti-rabbit Ig secondary antibodies (Dako) and developed with a Clarity Western ECL Substrate (BIO-RAD). Visualization was performed using a ChemiDocMP Imaging System and the ImageLab software (BIO-RAD).

Measurement of Bacterial Internalization and Survival—Colony-Forming Assay

Cells were treated with 0.005% (V/V) DMSO or 1 μM I-BET151 in triplicate wells for 20 h prior to infection with *P. gingivalis* at an MOI of 100 for 1 h. Cells were then washed 3 times with PBS and were either lysed immediately in sterile distilled water for 20 min or cultured in fresh medium containing DMSO or I-BET151 for another 24 h before lysis. Cell lysates were serially diluted and 10μl of each dilution was plated in duplicate on blood agar plates and cultured for 5–7 d anaerobically at 37°C. Bacterial colonies were counted and the data were expressed as CFU per cell.

Statistical Analyses

Data are presented as the mean +SEM. In studies of primary GFs and GECs, n's represent cell lines from individual donors/patients, while in TIGK studies n's refer to independent experiments. Parametric tests were used for comparisons between groups (ratio paired *t*-test or one-way ANOVA followed by Bonferroni multiple comparison test, where appropriate). $p < 0.05$ were considered statistically significant.

RESULTS

BET Inhibitors Suppress Cytokine-Induced Inflammatory Activation of GFs and TIGKs

We initiated this study by investigating whether BET bromodomain proteins are involved in GF inflammatory activation in response to cytokines that are present in the inflamed gingival tissue. Primary GFs from healthy individuals were stimulated with TNF or IL-1β in the presence of the BET inhibitor I-BET151. BET inhibition significantly suppressed

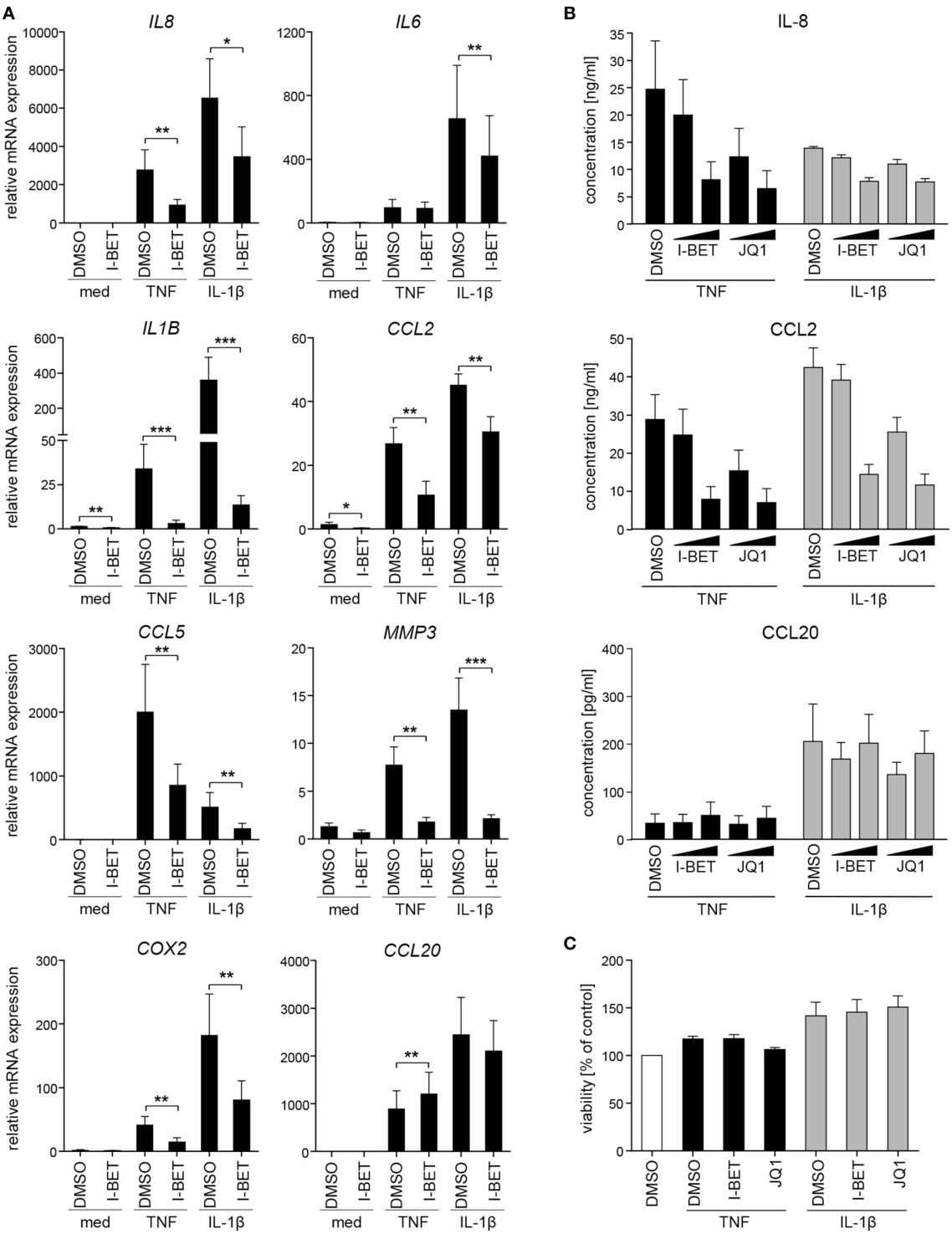

FIGURE 1 | BET inhibitors suppress cytokine-induced gingival fibroblast (GF) inflammatory activation without affecting cell viability. **(A)** Relative mRNA expression of *IL8*, *IL6*, *IL1B*, *CCL2*, *CCL5*, *MMP3*, *COX2,* and *CCL20* in GFs treated with DMSO or 1 μM I-BET151 for 30 min prior to simulation with TNF or IL-1β (both at 10 ng/ml) for 4 h analyzed by qPCR (mean + SEM; $n = 4$–5). $^{*}P < 0.05$, $^{**}P < 0.01$, $^{***}P < 0.001$; ratio paired *t*-test. **(B)** IL-8, CCL2, and CCL20 production by GFs treated with DMSO or I-BET151 or JQ1 at two different concentrations (100 nM and 1 μM) for 30 min prior to simulation with TNF or IL-1β (both 10 ng/ml) for 24 h determined by ELISA (mean concentration + SEM; $n = 5$). **(C)** Viability of GFs ($n = 3$) treated with DMSO, I-BET151, or JQ1 (both at 1 μM) for 30 min prior to simulation with 10 ng/ml TNF or IL-1β for 24 h assessed using MTT assay and presented as % of control + SEM.

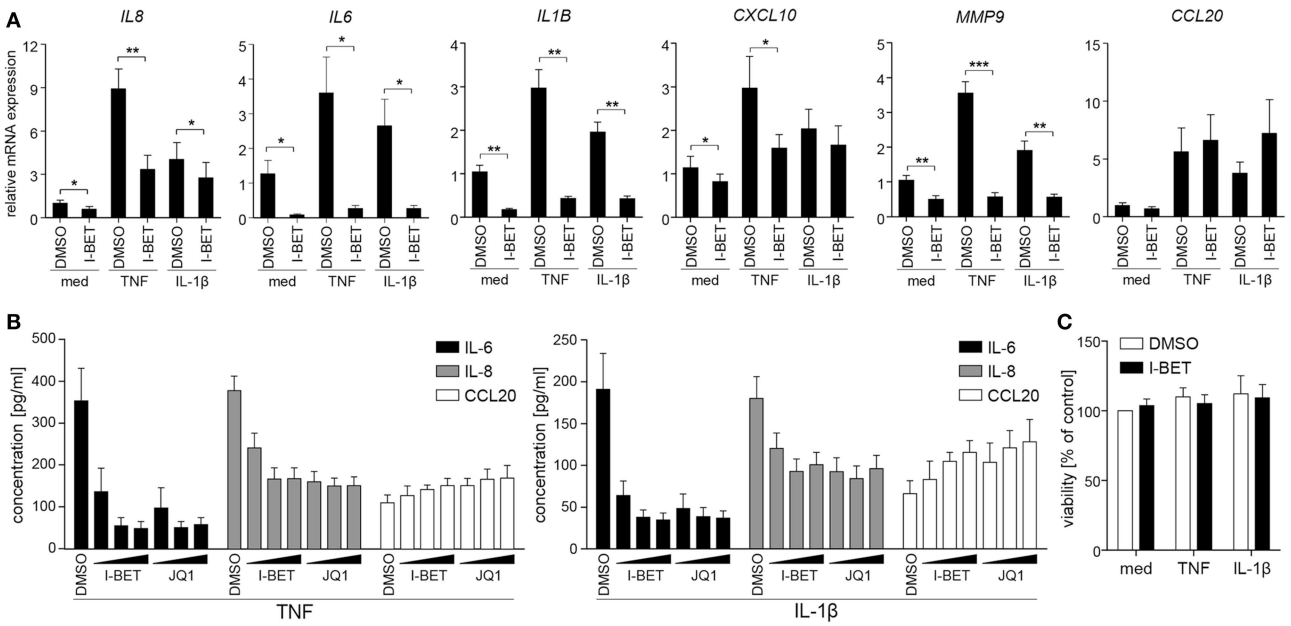

FIGURE 2 | BET inhibitors reduce cytokine-induced inflammatory mediator production by telomerase-immortalized gingival keratinocytes (TIGKs) without affecting cell viability. **(A)** Relative mRNA expression of *IL8*, *IL6*, *IL1B*, *CXCL10*, *MMP9,* and *CCL20* in TIGKs treated with DMSO or 1 μM I-BET151 for 30 min prior to simulation with TNF or IL-1β (both at 10 ng/ml) for 4 h determined by qPCR (mean + SEM; $n = 4$–5). $^{*}P < 0.05$, $^{**}P < 0.01$, $^{***}P < 0.001$; ratio paired *t*-test. **(B)** IL-6, IL-8, and CCL20 production by TIGKs treated with DMSO or increasing concentrations (100 nM, 500 nM, and 1 μM) of I-BET151 or JQ1 for 30 min followed by simulation with 10 ng/ml TNF (left panel) or 10 ng/ml IL-1β (right panel) for 24 h measured by ELISA (mean concentration + SEM; $n = 5$). **(C)** Viability of TIGKs ($n = 3$) treated with DMSO or 1 μM I-BET151 for 30 min prior to simulation with TNF or IL-1β (both 10 ng/ml) for 24 h analyzed using MTT assay and shown as % of control + SEM.

cytokine-induced mRNA expression of a broad range of inflammatory mediators involved in the pathogenesis of periodontitis, including *IL8*, *IL1B*, *CCL2*, *CCL5*, *MMP3*, and *COX2* (**Figure 1A**). Interestingly, some selectivity of I-BET151 effects on GF gene expression was noted, as I-BET151 suppressed IL-1β-, but not TNF-induced *IL6* expression, and, surprisingly, promoted expression of the antimicrobial chemokine *CCL20* in response to TNF stimulation. In the absence of inflammatory stimulation, I-BET151 significantly reduced mRNA levels of *IL1B* and *CCL2*, whereas expression of other mediators included in our analyses remained unaffected (**Figure 1A**). Next, to test if effects of BET inhibition on mRNA expression translate into changes in protein levels, we treated GFs with I-BET151 or a chemically unrelated BET inhibitor, JQ1, prior to 24 h cytokine stimulation. Both compounds dose-dependently suppressed TNF- and IL-1β-induced IL-8 and CCL2 production, reaching up to 70% inhibition at 1 μM. JQ1 displayed more potent inhibitory activity, significantly suppressing IL-8 and CCL2 secretion already at 100 nM (**Figure 1B**). In contrast, BET inhibition had no significant effects on agonist-induced CCL20 production, though a trend toward increased CCL20 secretion in the presence of TNF stimulation was noted (**Figure 1B**), consistent with mRNA data. To exclude the possibility that the observed effects of BET inhibitors on GF activation could be attributed to compound cytotoxicity, GFs were exposed to I-BET151 or JQ1 in the presence of cytokine stimulation for 24 h. Both compounds had negligible effects on cell viability as determined using the MTT reduction assay (**Figure 1C**).

To verify whether BET inhibitors similarly modulate inflammatory responses of GECs, we utilized TIGKs, an immortalized cell line derived from healthy donor GECs that closely mimics primary cell responses (23). TNF and IL-1β stimulation upregulated a cluster of inflammatory mediators in TIGKs that was distinct from, but partly overlapping with that observed in GFs. I-BET151 treatment significantly suppressed cytokine-induced mRNA expression of *IL8*, *IL6*, *IL1B*, *CXCL10,* and *MMP9* (**Figure 2A**). Interestingly, BET inhibition reduced not only inducible, but also basal levels of these transcripts. Similar to observations in GFs, BET inhibition had limited effect on *CCL20* expression. Interestingly, the sensitivity of individual genes to transcriptional suppression by I-BET151 differed between the two analyzed cell types: while I-BET151 reduced cytokine-induced *IL6* mRNA accumulation by >90% in TIGKs (**Figure 2A**), it had modest effects on *IL6* expression in GFs (**Figure 1A**), indicating differential requirements for BET proteins in transcriptional induction of the same gene in two different cell types. The observed effects of BET inhibition were next confirmed at the protein level. I-BET151 and JQ1 dose-dependently reduced IL-6 and IL-8 accumulation in cell culture supernatants, whereas CCL20 production was moderately induced (**Figure 2B**). Maximum suppression of IL-6 and IL-8 production by BET inhibitors was achieved at 100-500 nM, suggesting that TIGKs might be more sensitive to

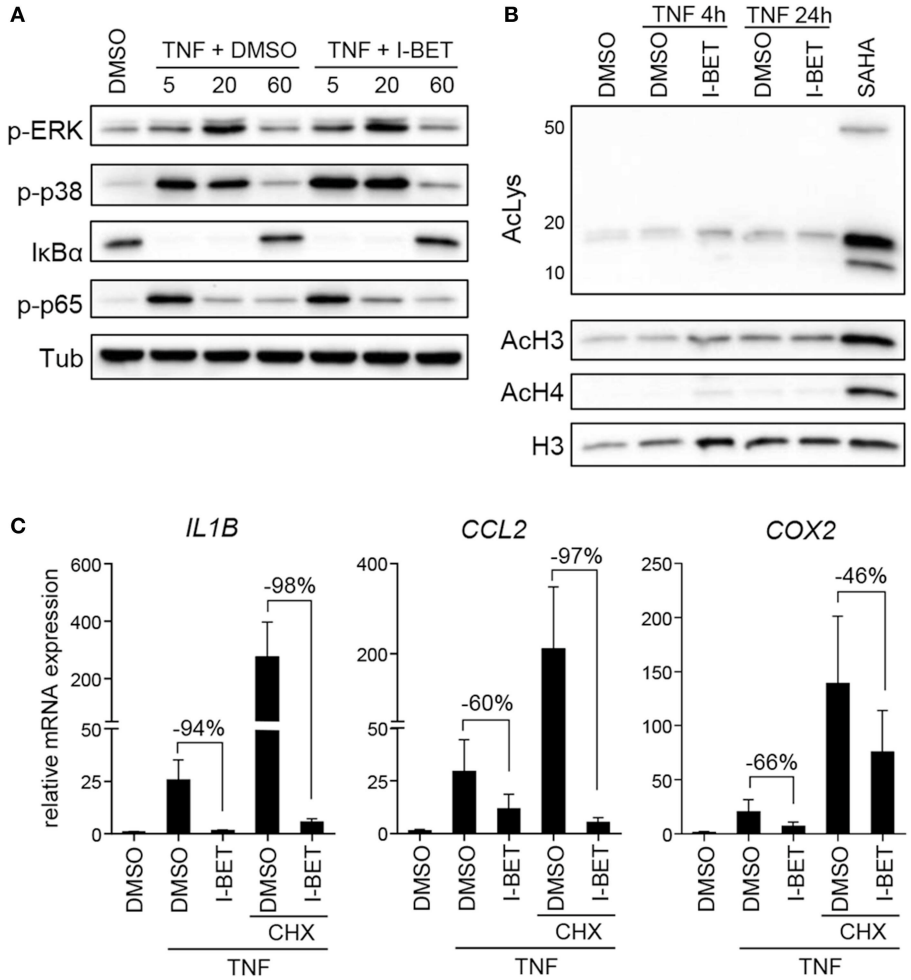

FIGURE 3 | I-BET151 has no effect on MAPK and NFκB activation in gingival fibroblasts (GFs) and new protein synthesis is not required for inflammatory gene suppression by I-BET151. **(A)** Western blot analysis of phospho (p)-ERK, p-p38, IκBα, p-p65(Ser536), and tubulin (Tub) in total cell lysates of GFs after 30 min treatment with DMSO or 1 μM I-BET151 followed by stimulation with 10 ng/ml TNF for 5, 20, or 60 min. **(B)** Western blot analysis of total acetylated lysine (AcLys), acetyl-histone H3(Lys18) (AcH3), acetyl-H4(Lys8) (AcH4), and total H3 in cell lysates of GFs treated with DMSO or 1 μM I-BET151 for 30 min prior to TNF (10 ng/ml) stimulation for 4 or 24 h. Cells treated with SAHA for 4 h were used as a positive control for lysine hyperacetylation. Data representative of 2–3 independent experiments are shown in **(A,B)**. **(C)** Relative mRNA expression of *IL1B*, *CCL2,* and *COX2* in GFs treated with DMSO or 1 μM I-BET151 in the presence or absence of cycloheximide (CHX) for 30 min prior to simulation with 10 ng/ml TNF for 4 h analyzed by qPCR (mean + SEM; $n = 4$; % of suppression compared to DMSO control are depicted in each graph).

low concentrations of BET inhibitors compared to GFs. In line with previous observations in GFs, I-BET151, and JQ1 had no effect on TIGK viability (**Figure 2C**).

BET Inhibitors Have No Effect on Inflammatory Signaling Pathway Activation in GFs and Do Not Require New Protein Synthesis for Gene Suppression

Inhibition or silencing of BET proteins regulates gene expression not only through disruption of interactions between bromodomains and acetylated histones at individual gene promoters, but also by affecting acetylation-dependent signaling pathways, including mitogen-activated protein kinase (MAPK) and NF-κB signaling (26, 27). We therefore analyzed the effects of BET inhibition on TNF-induced activation of signaling pathways critical for inflammatory cell activation and on protein acetylation status. Treatment of primary GFs from healthy donors with I-BET151 had no effect on p38 and extracellular signal-regulated kinase (ERK) MAPK activation, degradation of IκBα and phosphorylation of p65 NFκB subunit (**Figure 3A**). I-BET151 also failed to affect histone H3 and H4 acetylation, as well as the levels of total acetylated lysine detected in cellular lysates (**Figure 3B**), excluding the possibility that BET inhibitors could affect GF activation through off-target effects on HATs or HDACs. Finally, we tested whether BET inhibitors could affect gene expression indirectly by induction of gene repressors in GFs. I-BET151 suppressed *IL1B*, *CCL2,* and *COX2*

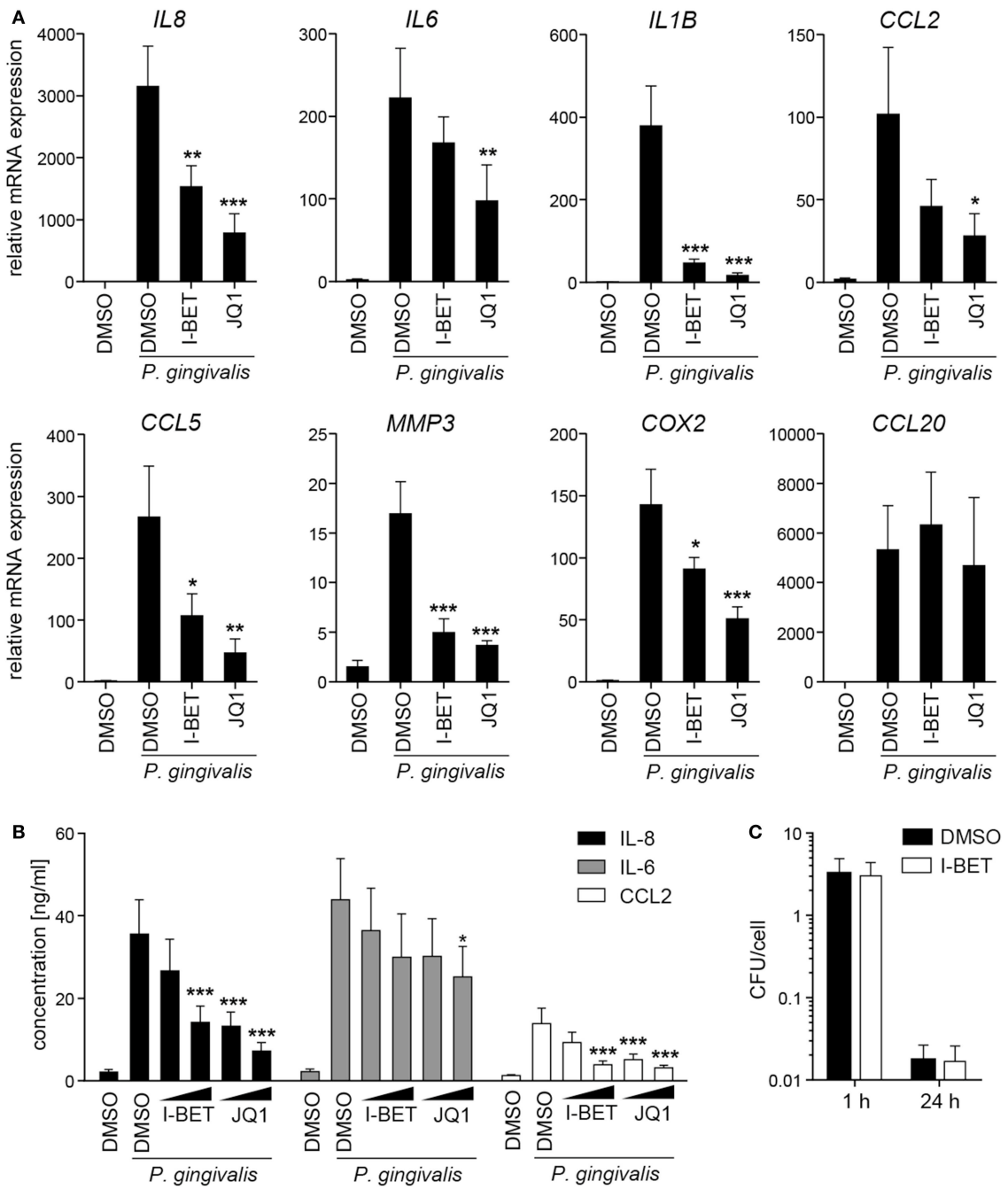

FIGURE 4 | BET inhibitors suppress production of inflammatory mediators by gingival fibroblasts (GFs) infected with *P. gingivalis*. **(A)** qPCR analysis of relative mRNA expression of *IL8*, *IL6*, *IL1B*, *CCL2*, *CCL5*, *MMP3*, *COX2,* and *CCL20* in GFs treated with DMSO, I-BET151 or JQ1 (both at 1 μM) for 30 min prior to infection with *P. gingivalis* (MOI = 100) for 4 h (mean + SEM; $n = 5$–6). **(B)** Production of IL-8, IL-6 and CCL2 by GFs exposed to DMSO or I-BET151 or JQ1 at two different concentrations (100 nM and 1 μM) for 30 min before *P. gingivalis* infection (MOI = 100) for 1 h, followed by washing and 24 h culture in fresh medium containing DMSO or BET inhibitors (mean concentration + SEM; $n = 5$–6). **(A,B)** $^{*}P < 0.05$, $^{**}P < 0.01$, $^{***}P < 0.001$; one-way ANOVA followed by Bonferroni multiple comparison test. **(C)** Intracellular survival of *P. gingivalis* in GFs treated with DMSO or 1 μM I-BET151 for 20 h prior to infection with *P. gingivalis* (MOI = 100) for 1 h determined by colony-forming assay immediately (1 h) or 24 h post-infection. Data are presented as mean colony-forming units (CFU)/cell + SEM of 4 independent experiments.

expression both in the absence or presence of the protein synthesis inhibitor CHX (**Figure 3C**). Suppression of *IL6* and *IL8* by I-BET151 in TNF-stimulated TIGKs was also unaffected by CHX (**Supplementary Figure 1**), indicating that *de novo* synthesis of repressor proteins is not necessary for suppression of inflammatory mediators by BET inhibitors in both cell types.

BET Inhibitors Suppress Inflammatory Mediator Production by GFs and TIGKs Infected With *P. gingivalis*

In periodontal disease, *P. gingivalis* directly interacts with and invades resident cells of the gingival tissue, which not only contributes to the chronicity of inflammation, but also facilitates bacterial spreading to deeper tissues. To analyze the role of BET proteins in GF and TIGK activation and antimicrobial responses, cells were treated with I-BET151 or JQ1 prior to infection with *P. gingivalis*. In primary GFs from healthy donors, induction of inflammatory mediator expression by *P. gingivalis* was comparable to, or even higher than that observed following cytokine stimulation, and BET inhibition significantly suppressed bacteria-induced upregulation of *IL8*, *IL1B*, *CCL2*, *CCL5*, *MMP3*, and *COX2*, but not *CCL20* (**Figure 4A**). In line with previous observations, JQ1 was more potent in blocking gene induction than I-BET151. Although the kinetics of mRNA induction by *P. gingivalis* differed between individual genes, I-BET151 uniformly reduced *IL8, IL1B, CCL2, and CCL5* expression at 4 and 24 h post-infection (**Supplementary Figure 2**). Production of IL-8 and CCL2 protein by *P. gingivalis*-infected GFs was also dose-dependently reduced by both BET inhibitors, whereas suppression of IL-6 production was less pronounced (**Figure 4B**). Next, to test whether BET inhibitors affect cellular response to *P. gingivalis* infection, GFs were treated with I-BET151 for 20h prior to infection with *P. gingivalis* for 1 h, and the presence of live bacteria in cell lysates was determined using the colony-forming assay. I-BET151 had no effect on the numbers of bacteria detected in GFs immediately and 24 h post-infection (**Figure 4C**), indicating that BET proteins are not involved in internalization and elimination of intracellular *P. gingivalis* by GFs.

Infection of TIGKs with *P. gingivalis* also led to transcriptional upregulation of a set of inflammatory genes largely overlapping with that induced by cytokines (**Figure 5A**). I-BET151 treatment significantly reduced mRNA levels of *IL8*, *IL6*, *IL1B*, *COX2,* and *CXCL10*, while leaving *CCL20* expression unaffected (**Figure 5A**). I-BET151 and JQ1 also significantly reduced TIGK IL-6 and IL-8 production induced by exposure to heat-inactivated *P. gingivalis*. Both compounds inhibited IL-6 and IL-8 secretion by ∼85 and 40%, respectively, already at 100 nM (**Figure 5B**). A similar degree of IL-6 and IL-8 inhibition by BET inhibitors was observed in TIGKs infected with live *P. gingivalis* in the presence of gingipain inhibitors that were used to eliminate the potential confounding factor of cytokine degradation by bacterial proteases (data not shown). Importantly, BET inhibitor effects were restricted to inflammatory gene transcription as treatment with I-BET151 for 20h prior to infection failed to affect *P. gingivalis* internalization by TIGKs (**Figure 5C**), consistent with previous observations in GFs. Collectively, these results demonstrate that BET inhibitors suppress production of a broad range inflammatory mediators by GFs and GECs without affecting *P. gingivalis* internalization and survival within the infected cells.

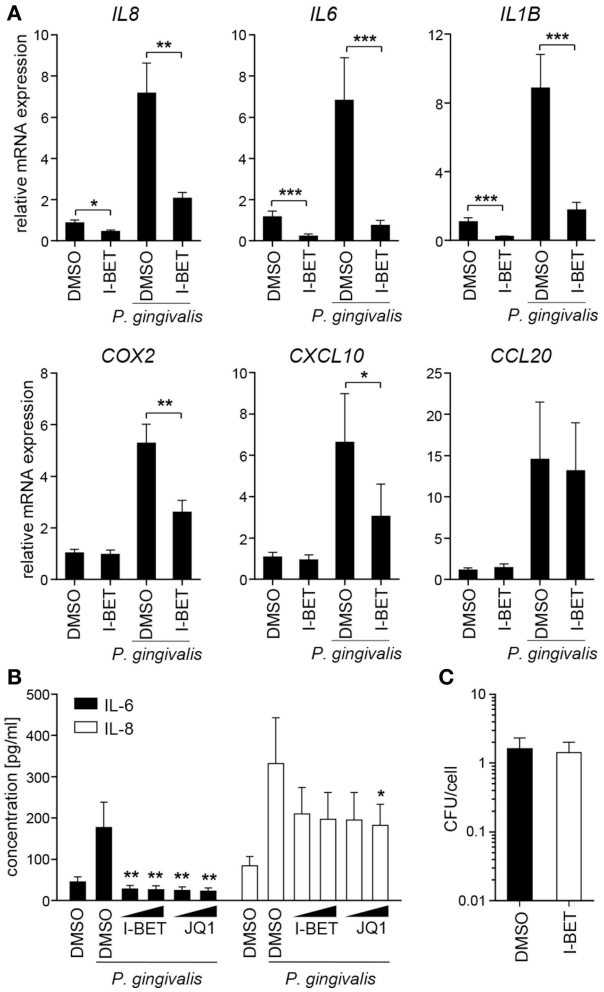

FIGURE 5 | BET inhibitors block inflammatory activation of telomerase-immortalized gingival keratinocytes (TIGKs) infected with *P. gingivalis*. **(A)** Relative mRNA expression of *IL8*, *IL6*, *IL1B*, *COX2*, *CXCL10,* and *CCL20* in TIGKs cultured for 30 min with DMSO or I-BET151 (1 μM) followed by 4 h infection with *P. gingivalis* (MOI = 100) determined by qPCR (mean + SEM; $n = 4$–5). $^{*}P < 0.05$, $^{**}P < 0.01$, $^{***}P < 0.001$; ratio paired *t*-test. **(B)** Production of IL-6 and IL-8 by TIGKs treated with DMSO or I-BET151 or JQ1 at two different concentrations (100 nM and 1 μM) for 30 min prior to infection with heat-inactivated *P. gingivalis* (MOI = 100) for 24 h (mean concentration + SEM; $n = 4$). $^{*}P < 0.05$, $^{**}P < 0.01$; one-way ANOVA followed by followed by Bonferroni multiple comparison test. **(C)** Intracellular survival of *P. gingivalis* in TIGKs treated with DMSO or 1 μM I-BET151 for 20 h before infection with *P. gingivalis* (MOI = 100) for 1 h determined by colony-forming assay immediately after infection. Results are presented as mean colony-forming units (CFU)/cell + SEM of 4 independent experiments.

BET Inhibitors Reduce Inflammatory Gene Expression in GFs and GECs From Patients With Periodontitis

GFs present in the inflamed gingival tissue in periodontitis patients display an activated phenotype and hyperresponsiveness to *P. gingivalis* infection *in vitro* (28, 29). We therefore examined whether GFs isolated from patients with periodontitis were

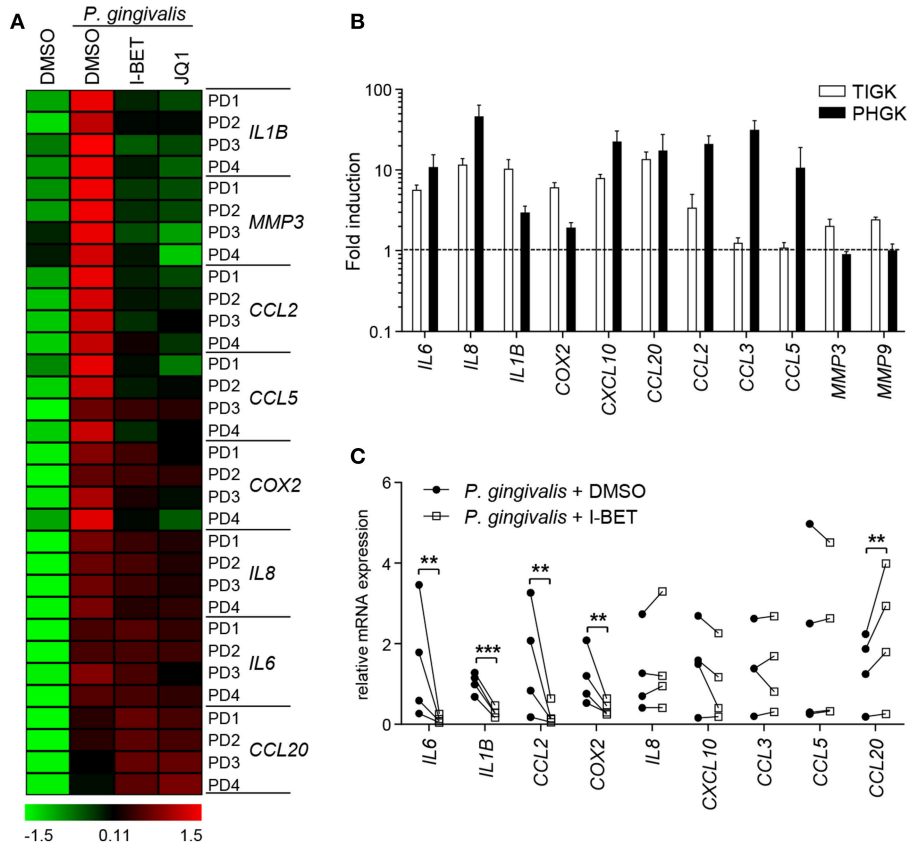

FIGURE 6 | Gingival fibroblasts (GFs) and gingival epithelial cells (GECs) from periodontitis patients are sensitive to the anti-inflammatory activity of BET inhibitors. **(A)** Primary GFs from patients with periodontitis were treated with DMSO, I-BET151 or JQ1 (both at 1 μM) for 30 min prior to infection with *P. gingivalis* (MOI = 100) for 4 h and mRNA levels of inflammatory mediators were determined by qPCR. Data for individual patients (PD1–PD4) are presented on a heat map as row *Z*-scores calculated from ΔCt values relative to a housekeeping gene (RPLP0). **(B)** Comparison of inflammatory mediator induction in TIGKs and primary GECs from periodontitis patients after 4 h infection with *P. gingivalis* (MOI = 100) (mean fold induction compared to uninfected cells + SEM; $n = 3$ for TIGKs vs. $n = 3$ GEC lines from individual patients (PD1, PD2, PD5). **(C)** qPCR analysis of mRNA levels of inflammatory mediators in primary GECs from patients with periodontitis (PD1, PD2, PD3, PD5) treated with DMSO or 1 μM I-BET151 for 30 min followed by infection with *P. gingivalis* (MOI = 100) for 4 h. Symbols represent relative expression values from individual patients ($n = 4$). $^{**}P < 0.01$, $^{***}P < 0.001$; ratio paired *t*-test.

resistant to the anti-inflammatory effects of BET inhibitors. The degree of suppression of *IL8*, *IL1B*, *CCL2*, *CCL5*, *MMP3*, and *COX2* caused by I-BET151 or JQ1 in *P. gingivalis*-infected GFs from periodontitis patients was comparable to that observed in healthy donor GFs (**Figure 6A**). JQ1, but not I-BET151, moderately reduced *IL6* mRNA levels, consistent with observations in GFs from healthy individuals, while *CCL20* expression was upregulated by both BET inhibitors (**Figure 6A**). Next, to assess the sensitivity of GECs from periodontitis patients to BET inhibitors, we first compared the inflammatory gene expression profile induced by *P. gingivalis* in TIGKs and primary GECs. While a shared cluster of genes that included *IL6*, *IL8*, *IL1B*, *COX2*, *CXCL10*, *CCL20,* and *CCL2* was upregulated by *P. gingivalis* in both types of cells, we also noted some differential responses. The chemokines *CCL3* and *CCL5* were selectively induced in GECs, but not in TIGKs, whereas expression of the metalloproteinases *MMP3* and *MMP9* was upregulated upon *P. gingivalis* infection only in TIGKs (**Figure 6B**). Treatment of primary GECs from periodontitis patients with I-BET151 prior to *P. gingivalis* infection resulted in significant suppression of *IL6*, *IL1B*, *CCL2,* and *COX2*. However, in contrast to TIGKs, *IL8,* and *CXCL10* mRNA levels were not affected by BET inhibition, whereas *CCL20* expression was consistently induced (**Figure 6C**). Together, these observations suggest that BET proteins play a key role in regulating inflammatory mediator expression in GFs and GECs in response to an oral pathogen.

DISCUSSION

A severe form of periodontitis affects approximately 10% of the human population, leading to inevitable tooth loss if left untreated, and is strongly associated with increased risk of developing systemic diseases, including RA, atherosclerosis and cancer (1, 30). Non-surgical treatment strategies conventionally used to treat periodontitis, scaling and root planing, or root surface debridement, focus solely on reducing bacterial challenge, but in many patients are insufficient to fully resolve

chronic inflammation. Because of that, there is a growing need for identifying novel therapeutic strategies ameliorating the host inflammatory response that could be used as an adjunct to conventional treatment (31). The identification of anti-inflammatory properties of HDAC and BET inhibitors has generated great interest in the therapeutic potential of targeting epigenetic mechanisms in many inflammatory and infectious disorders, including periodontitis (32–34). Indeed, pharmacological modulators of histone acetylation protected against pathology in animal models of periodontal disease (21, 35). In particular, the BET inhibitor JQ1 has shown potent anti-inflammatory and bone-protective activity (21). Here, we show for the first time that BET bromodomain proteins are important regulators of resident gingival cell activation in response to *P. gingivalis* and inflammatory cytokines, and that small molecule BET inhibitors suppress production of cytokines, chemokines, and other mediators of inflammation by GFs and GECs from periodontitis patients.

Destruction of the gingival connective tissue, periodontal ligament, and alveolar bone in periodontitis is a consequence of a futile attempt by the host immune response to eradicate microbial pathogens (2). Resident gingival cells contribute to this vicious circle of chronic inflammation by secreting a plethora of inflammatory mediators, including cytokines (IL-6, IL-1β), chemokines (IL-8, CCL2, CCL5, CXCL10, CCL20), matrix-degrading enzymes (MMP1, MMP3, MMP9), and prostaglandins (5). Elevated levels of these mediators are present in gingival tissue and/or gingival crevicular fluid from periodontitis patients, correlating with disease severity (5, 36, 37), and studies in animal models show that genetic ablation or pharmacological targeting of IL-6 or IL-1β ameliorates pathology in experimental periodontitis (38). Our data provide evidence that BET proteins are required for transcriptional induction of key inflammatory molecules in GFs and GECs infected with *P. gingivalis* and thus represent a potential therapeutic target for modulation of the host immune response. Although quantitative differences in the sensitivity of individual genes to BET inhibition were noted, our observations are consistent with the broad anti-inflammatory activity of BET inhibitors reported in synovial fibroblasts and in airway epithelial cells (39, 40). While our data suggest that suppression of GF and GEC inflammatory activation by BET inhibitors is stimulus-independent, future studies should analyze the role of BET proteins in gingival cell response to a complex dental biofilm containing other oral pathogens, such as *Fusobacterium nucleatum*, *Tanerella forsythia,* and *Treponema denticola*. In this regard it is noteworthy that JQ1 attenuated gastric inflammation and immune cell infiltration in mice infected with *Helicobacter pylori* (41), indicating its immunosuppressive potential in chronic infections caused by Gram-negative pathogenic bacteria.

BET proteins regulate cellular activation not only at the gene promoter level, but also through chromatin-independent mechanisms. BRD4 binds acetylated lysine-310 of the p65 NF-κB subunit, enhancing its transcriptional activity and thus acting as a coactivator of NF-κB-dependent genes (26). In macrophages, BRD4 also modulates NF-κB signaling through translational control of IκBα resynthesis (42), whereas in endothelial cells BET inhibition blocks early events in NF-κB activation as well as p38 and JNK MAPK phosphorylation (27). These mechanisms are, however, cell type-specific and apparently not operational in GFs based on our analyses of MAPK, IκBα, and NF-κB p65 activation. While it remains to be determined if BET inhibition also fails to affect NF-κB transcriptional activity and binding to specific gene promoters in GFs, our findings are consistent with studies of synovial fibroblasts from RA patients demonstrating the lack of effect of I-BET151 on NF-κB and MAPK signaling pathways (40). We also show that *de novo* synthesis of repressor proteins is not required for suppression of inflammatory genes by I-BET151 in GFs and GECs, in line with observations in human macrophages (17). Collectively, these results argue against indirect or signaling pathway-dependent effects of BET inhibition in gingival cells and suggest that interference with direct interaction of BET proteins with acetylated histones at gene promoters is most likely responsible for the observed suppression of inflammatory mediator transcriptional induction. Although potential off-target effects of BET inhibitors cannot be ruled out based on our studies, extensive screening of these compounds failed to identify any significant effects on non-BET protein targets (13, 43).

Among the analyzed inflammatory genes, expression of *CCL20* was selectively upregulated by I-BET151 and JQ1 in some experimental conditions, particularly in GECs. CCL20 may play a dual role in periodontitis. As a chemoattractant for immature dendritic cells and Th17 cells, CCL20 may contribute to the chronicity of inflammation by facilitating immune cell recruitment and accumulation (37). On the other hand, CCL20 displays direct microbicidal activity against Gram-positive and Gram-negative bacteria through its antimicrobial regions structurally related to human β-defensin-2 (44). *CCL20* induction by BET inhibitors could therefore facilitate bacterial elimination by innate immune mechanisms. It remains to be verified if CCL20 exerts antimicrobial activity against *P. gingivalis* or other oral pathogens, and whether this mechanism is operational in the inflamed gingival tissue during periodontitis. While the exact role of bromodomain proteins in CCL20 regulation has yet to be investigated, HDAC inhibitors have also been shown to promote CCL20 production by GECs and intestinal epithelial cells (45, 46), suggesting a critical role for histone acetylation in CCL20 transcriptional regulation that requires detailed studies at the gene promoter level.

The idea that BET inhibitors may display clinical activity in periodontal disease is also supported by recent evidence that N-methyl-2-pyrrolidone (NMP), a component of dental barrier membranes used in dental procedures, displays bromodomain inhibitory activity (47). While initially thought to lack biological activity, it was later discovered that NMP displays anti-inflammatory and anti-osteoclastogenic activity similar to the effects of BET inhibitors (48, 49). The efficacy of NMP-based dental barrier membranes in periodontal tissue regeneration could therefore be partly attributed to their ability to inhibit BET bromodomains (50), a possibility that should be addressed in future studies directly comparing NMP and BET inhibitor activity in periodontitis models. These observations, together with the results of our study and the initial proof of principle obtained in an animal model (21), indicate that specific targeting

of epigenetic reader proteins from the BET family may block the excessive inflammatory mediator production by multiple cell types important in the pathogenesis of periodontitis and reduce the significant morbidity associated with periodontal disease.

ETHICS STATEMENT

This study was approved by and carried out in accordance with the recommendations of the Bioethical Committee of the Jagiellonian University in Kraków, Poland (permit numbers 122.6120.337.2016 and KBET/310/B/2012). All subjects gave written informed consent in accordance with the Declaration of Helsinki.

AUTHOR CONTRIBUTIONS

AM, AB, KBL, JMM, and GB contributed to research design, performed experiments, and analyzed data. MK obtained all clinical materials and analyzed clinical records. MS, KG, MC-G, and JP contributed to research design, data interpretation, and writing the manuscript. AMG designed the study, analyzed and interpreted the data, and wrote the manuscript. All authors contributed to manuscript revision, read and approved the submitted version.

FUNDING

AMG was supported by the National Science Centre, Poland (POLONEZ fellowship 2015/19/P/NZ7/03659; this project has received funding from the European Union's Horizon 2020 research and innovation programme under the Marie Skłodowska-Curie grant agreement No. 665778). MS was supported by the Foundation for Polish Science (Homing/2016-1/9). JP is supported by grants from National Science Center, Poland (UMO-2018/30/A/NZ5/00650) and NIH/NIDCR, US (R01 DE 022597).

ACKNOWLEDGMENTS

We thank Dr. Pawel A. Kabala (University Medical Center Utrecht, The Netherlands) for assistance in heat map preparation and Dr. Kris A. Reedquist (University Medical Center Utrecht, The Netherlands) for critical reading of the manuscript.

SUPPLEMENTARY MATERIAL

The Supplementary Material for this article can be found online at: https://www.frontiersin.org/articles/10.3389/fimmu.2019.00933/full#supplementary-material

REFERENCES

1. Hajishengallis G. Periodontitis: from microbial immune subversion to systemic inflammation. *Nat Rev Immunol.* (2014) 15:30–44. doi: 10.1038/nri3785
2. Hajishengallis G, Lamont RJ. Breaking bad: manipulation of the host response by *Porphyromonas gingivalis*. *Eur J Immunol.* (2014) 44:328–38. doi: 10.1002/eji.201344202
3. Benakanakere M, Kinane DF. Innate cellular responses to the periodontal biofilm. *Front Oral Biol.* (2012) 15:41–55. doi: 10.1159/000329670
4. Bautista-Hernández LA, Gómez-Olivares JL, Buentello-Volante B, Bautista-de Lucio VM. Fibroblasts: the unknown sentinels eliciting immune responses against microorganisms. *Eur J Microbiol Immunol.* (2017) 7:151–7. doi: 10.1556/1886.2017.00009
5. Yucel-Lindberg T, Båge T. Inflammatory mediators in the pathogenesis of periodontitis. *Expert Rev Mol Med.* (2013) 15:e7. doi: 10.1017/erm.2013.8
6. Martins MD, Jiao Y, Larsson L, Almeida LO, Garaicoa-Pazmino C, Le JM, et al. Epigenetic modifications of histones in periodontal disease. *J Dent Res.* (2016) 95:215–22. doi: 10.1177/0022034515611876
7. Cantley MD, Dharmapatni AA, Algate K, Crotti TN, Bartold PM, Haynes DR. Class I and II histone deacetylase expression in human chronic periodontitis gingival tissue. *J Periodontal Res.* (2016) 51:143–51. doi: 10.1111/jre.12290
8. Filippakopoulos P, Knapp S. The bromodomain interaction module. *FEBS Lett.* (2012) 586:2692–704. doi: 10.1016/j.febslet.2012.04.045
9. LeRoy G, Rickards B, Flint SJ. The double bromodomain proteins Brd2 and Brd3 couple histone acetylation to transcription. *Mol Cell.* (2008) 30:51–60. doi: 10.1016/j.molcel.2008.01.018
10. Hargreaves DC, Horng T, Medzhitov R. Control of inducible gene expression by signal-dependent transcriptional elongation. *Cell.* (2009) 138:129–45. doi: 10.1016/j.cell.2009.05.047
11. Prinjha RK, Witherington J, Lee K. Place your BETs: the therapeutic potential of bromodomains. *Trends Pharmacol Sci.* (2012) 33:146–53. doi: 10.1016/j.tips.2011.12.002
12. Andrieu G, Belkina AC, Denis GV. Clinical trials for BET inhibitors run ahead of the science. *Drug Discov Today Technol.* (2016) 19:45–50. doi: 10.1016/j.ddtec.2016.06.004
13. Filippakopoulos P, Qi J, Picaud S, Shen Y, Smith WB, Fedorov O, et al. Selective inhibition of BET bromodomains. *Nature.* (2010) 468:1067–73. doi: 10.1038/nature09504
14. Mirguet O, Lamotte Y, Donche F, Toum J, Gellibert F, Bouillot A, et al. From ApoA1 upregulation to BET family bromodomain inhibition: discovery of I-BET151. *Bioorg Med Chem Lett.* (2012) 22:2963–7. doi: 10.1016/j.bmcl.2012.01.125
15. Belkina AC, Denis GV. BET domain co-regulators in obesity, inflammation and cancer. *Nat Rev Cancer.* (2012) 12:465–77. doi: 10.1038/nrc3256
16. Nicodeme E, Jeffrey KL, Schaefer U, Beinke S, Dewell S, Chung C-W, et al. Suppression of inflammation by a synthetic histone mimic. *Nature.* (2010) 468:1119–23. doi: 10.1038/nature09589
17. Chan CH, Fang C, Qiao Y, Yarilina A, Prinjha RK, Ivashkiv LB. BET bromodomain inhibition suppresses transcriptional responses to cytokine-Jak-STAT signaling in a gene-specific manner in human monocytes. *Eur J Immunol.* (2015) 45:287–97. doi: 10.1002/eji.201444862
18. Bandukwala HS, Gagnon J, Togher S, Greenbaum JA, Lamperti ED, Parr NJ, et al. Selective inhibition of CD4+ T-cell cytokine production and autoimmunity by BET protein and c-Myc inhibitors. *Proc Natl Acad Sci USA.* (2012) 109:14532–7. doi: 10.1073/pnas.1212264109
19. Mele DA, Salmeron A, Ghosh S, Huang H-R, Bryant BM, Lora JM. BET bromodomain inhibition suppresses TH17-mediated pathology. *J Exp Med.* (2013) 210:2181–90. doi: 10.1084/jem.20130376
20. Sun Y, Wang Y, Toubai T, Oravecz-Wilson K, Liu C, Mathewson N, et al. BET bromodomain inhibition suppresses graft-versus-host disease after allogeneic bone marrow transplantation in mice. *Blood.* (2015) 125:2724–8. doi: 10.1182/blood-2014-08-598037
21. Meng S, Zhang L, Tang Y, Tu Q, Zheng L, Yu L, et al. BET Inhibitor JQ1 blocks inflammation and bone destruction. *J Dent Res.* (2014) 93:657–62. doi: 10.1177/0022034514534261
22. Gawron K, Ochała-Kłos A, Nowakowska Z, Bereta G, Łazarz-Bartyzel K, Grabiec AM, et al. TIMP-1 association with collagen type I overproduction in hereditary gingival fibromatosis. *Oral Dis.* (2018) 24:1581–90. doi: 10.1111/odi.12938
23. Moffatt-Jauregui CE, Robinson B, de Moya AV, Brockman RD, Roman AV, Cash MN, et al. Establishment and characterization of a telomerase

immortalized human gingival epithelial cell line. *J Periodontal Res.* (2013) 48:713–21. doi: 10.1111/jre.12059
24. Gawron K, Bereta G, Nowakowska Z, Lazarz-Bartyzel K, Lazarz M, Szmigielski B, et al. Peptidylarginine deiminase from *Porphyromonas gingivalis* contributes to infection of gingival fibroblasts and induction of prostaglandin E2 -signaling pathway. *Mol Oral Microbiol.* (2014) 29:321–32. doi: 10.1111/omi.12081
25. Grabiec AM, Korchynskyi O, Tak PP, Reedquist KA. Histone deacetylase inhibitors suppress rheumatoid arthritis fibroblast-like synoviocyte and macrophage IL-6 production by accelerating mRNA decay. *Ann Rheum Dis.* (2012) 71:424–31. doi: 10.1136/ard.2011.154211
26. Huang B, Yang X-D, Zhou M-M, Ozato K, Chen L-F. Brd4 coactivates transcriptional activation of NF-kappaB via specific binding to acetylated RelA. *Mol Cell Biol.* (2009) 29:1375–87. doi: 10.1128/MCB.01365-08
27. Huang M, Zeng S, Zou Y, Shi M, Qiu Q, Xiao Y, et al. The suppression of bromodomain and extra-terminal domain inhibits vascular inflammation by blocking NF-κB and MAPK activation. *Br J Pharmacol.* (2017) 174:101–15. doi: 10.1111/bph.13657
28. Scheres N, Laine ML, Sipos PM, Bosch-Tijhof CJ, Crielaard W, de Vries TJ, et al. Periodontal ligament and gingival fibroblasts from periodontitis patients are more active in interaction with *Porphyromonas gingivalis*. *J Periodontal Res.* (2011) 46:407–16. doi: 10.1111/j.1600-0765.2011.01353.x
29. Baek KJ, Choi Y, Ji S. Gingival fibroblasts from periodontitis patients exhibit inflammatory characteristics *in vitro*. *Arch Oral Biol.* (2013) 58:1282–92. doi: 10.1016/j.archoralbio.2013.07.007
30. Eke PI, Thornton-Evans GO, Wei L, Borgnakke WS, Dye BA, Genco RJ. Periodontitis in US Adults: National Health and Nutrition Examination Survey 2009-2014. *J Am Dent Assoc.* (2018) 149:576–88 e6. doi: 10.1016/j.adaj.2018.04.023
31. Preshaw PM. Host modulation therapy with anti-inflammatory agents. *Periodontol 2000.* (2018) 76:131–49. doi: 10.1111/prd.12148
32. Grabiec AM, Potempa J. Epigenetic regulation in bacterial infections: targeting histone deacetylases. *Crit Rev Microbiol.* (2018) 44:336–50. doi: 10.1080/1040841X.2017.1373063
33. Grabiec AM, Tak PP, Reedquist KA. Function of histone deacetylase inhibitors in inflammation. *Crit Rev Immunol.* (2011) 31:233–63. doi: 10.1615/CritRevImmunol.v31.i3.40
34. Tough DF, Tak PP, Tarakhovsky A, Prinjha RK. Epigenetic drug discovery: breaking through the immune barrier. *Nat Rev Drug Discov.* (2016) 15:835–53. doi: 10.1038/nrd.2016.185
35. Cantley MD, Bartold PM, Marino V, Fairlie DP, Le GT, Lucke AJ, et al. Histone deacetylase inhibitors and periodontal bone loss. *J Periodontal Res.* (2011) 46:697–703. doi: 10.1111/j.1600-0765.2011.01392.x
36. Franco C, Patricia H-R, Timo S, Claudia B, Marcela H. Matrix metalloproteinases as regulators of periodontal inflammation. *Int J Mol Sci.* (2017) 18:1–12. doi: 10.3390/ijms18020440
37. Sahingur SE, Yeudall WA. Chemokine function in periodontal disease and oral cavity cancer. *Front Immunol.* (2015) 6:214. doi: 10.3389/fimmu.2015.00214
38. Graves D. Cytokines that promote periodontal tissue destruction. *J Periodontol.* (2008) 79:1585–91. doi: 10.1902/jop.2008.080183
39. Khan YM, Kirkham P, Barnes PJ, Adcock IM. Brd4 is essential for IL-1β-induced inflammation in human airway epithelial cells. *PLoS ONE.* (2014) 9:e95051. doi: 10.1371/journal.pone.0095051
40. Klein K, Kabala PA, Grabiec AM, Gay RE, Kolling C, Lin L-L, et al. The bromodomain protein inhibitor I-BET151 suppresses expression of inflammatory genes and matrix degrading enzymes in rheumatoid arthritis synovial fibroblasts. *Ann Rheum Dis.* (2016) 75:422–9. doi: 10.1136/annrheumdis-2014-205809
41. Chen J, Wang Z, Hu X, Chen R, Romero-Gallo J, Peek RM, et al. BET Inhibition attenuates helicobacter pylori-induced inflammatory response by suppressing inflammatory gene transcription and enhancer activation. *J Immunol.* (2016) 196:4132–42. doi: 10.4049/jimmunol.1502261
42. Bao Y, Wu X, Chen J, Hu X, Zeng F, Cheng J, et al. Brd4 modulates the innate immune response through Mnk2-eIF4E pathway-dependent translational control of IκBα. *Proc Natl Acad Sci USA.* (2017) 114:E3993–4001. doi: 10.1073/pnas.1700109114
43. Dawson MA, Prinjha RK, Dittman A, Giotopoulos G, Bantscheff M, Chan W-I, et al. Inhibition of BET recruitment to chromatin as an effective treatment for MLL-fusion leukaemia. *Nature.* (2011) 478:529–33. doi: 10.1038/nature10509
44. Yang D, Chen Q, Hoover DM, Staley P, Tucker KD, Lubkowski J, et al. Many chemokines including CCL20/MIP-3alpha display antimicrobial activity. *J Leukoc Biol.* (2003) 74:448–55. doi: 10.1189/jlb.0103024
45. Yin L, Chung WO. Epigenetic regulation of human β-defensin 2 and CC chemokine ligand 20 expression in gingival epithelial cells in response to oral bacteria. *Mucosal Immunol.* (2011) 4:409–19. doi: 10.1038/mi.2010.83
46. Sim J-R, Kang S-S, Lee D, Yun C-H, Han SH. Killed whole-cell oral cholera vaccine induces CCL20 secretion by human intestinal epithelial cells in the presence of the short-chain fatty acid, butyrate. *Front Immunol.* (2018) 9:55. doi: 10.3389/fimmu.2018.00055
47. Philpott M, Yang J, Tumber T, Fedorov O, Uttarkar S, Filippakopoulos P, et al. Bromodomain-peptide displacement assays for interactome mapping and inhibitor discovery. *Mol Biosyst.* (2011) 7:2899–908. doi: 10.1039/c1mb05099k
48. Ghayor C, Correro RM, Lange K, Karfeld-Sulzer LS, Grätz KW, Weber FE. Inhibition of osteoclast differentiation and bone resorption by N-methylpyrrolidone. *J Biol Chem.* (2011) 286:24458–66. doi: 10.1074/jbc.M111.223297
49. Shortt J, Hsu AK, Martin BP, Doggett K, Matthews GM, Doyle MA, et al. The drug vehicle and solvent N-methylpyrrolidone is an immunomodulator and antimyeloma compound. *Cell Rep.* (2014) 7:1009–19. doi: 10.1016/j.celrep.2014.04.008
50. Hogg SJ, Johnstone RW, Shortt J. Letter to the Editor, "BET inhibitor JQ1 blocks inflammation and bone destruction". *J Dent Res.* (2015) 94:229. doi: 10.1177/0022034514557673

Conflict of Interest Statement: The authors declare that the research was conducted in the absence of any commercial or financial relationships that could be construed as a potential conflict of interest.

frontiers in Immunology

REVIEW
published: 25 June 2019
doi: 10.3389/fimmu.2019.01403

Distal Consequences of Oral Inflammation

Joanne E. Konkel[1,2]*, *Conor O'Boyle*[1] and *Siddharth Krishnan*[1,2]

[1] Faculty of Biology, Medicine and Health, Manchester Academic Health Science Centre, Lydia Becker Institute of Immunology and Inflammation, University of Manchester, Manchester, United Kingdom, [2] Manchester Collaborative Centre for Inflammation Research (MCCIR), University of Manchester, Manchester, United Kingdom

Periodontitis is an incredibly prevalent chronic inflammatory disease, which results in the destruction of tooth supporting structures. However, in addition to causing tooth and alveolar bone loss, this oral inflammatory disease has been shown to contribute to disease states and inflammatory pathology at sites distant from the oral cavity. Epidemiological and experimental studies have linked periodontitis to the development and/or exacerbation of a plethora of other chronic diseases ranging from rheumatoid arthritis to Alzheimer's disease. Such studies highlight how the inflammatory status of the oral cavity can have a profound impact on systemic health. In this review we discuss the disease states impacted by periodontitis and explore potential mechanisms whereby oral inflammation could promote loss of homeostasis at distant sites.

Keywords: periodontitis, adaptive immunity, innate immunity, antigen mimicry, innate cell training, inflammation, commensal bacteria

OPEN ACCESS

Edited by:
Avi-Hai Hovav,
Hebrew University of Jerusalem, Israel

Reviewed by:
Gustavo Pompermaier Garlet,
University of São Paulo, Brazil
Nurcan Buduneli,
Ege University, Turkey

***Correspondence:**
Joanne E. Konkel
joanne.konkel@manchester.ac.uk

Specialty section:
This article was submitted to Mucosal Immunity, a section of the journal Frontiers in Immunology

Received: *21 October 2018*
Accepted: *03 June 2019*
Published: *25 June 2019*

Citation:
Konkel JE, O'Boyle C and Krishnan S (2019) Distal Consequences of Oral Inflammation. Front. Immunol. 10:1403. doi: 10.3389/fimmu.2019.01403

Barrier sites such as the mouth, gut and skin are interfaces between our inside bodies and the outside world. Maintaining their integrity is crucial to survival. Each barrier has unique requirements and must perform its physiological function whilst maintaining control of commensal microbes and responding to environmental insults and pathogen invasion. The immune system critically promotes barrier integrity in the face of these challenges and is carefully tailored to barrier environments, creating highly-specialized immuno-surveillance networks that police these sites. One area of intense research focus is to understand how tissue-specific signals balance immunity and regulation at barrier sites (1, 2). Elucidating these mechanisms is essential to develop tissue-specific therapies for disease. One barrier at which appropriate immune control frequently fails is the oral barrier. Breakdown of balanced immune responses at the gingiva, a key oral barrier, leads to periodontitis, the most common chronic inflammatory disease of humans, affecting ∼50% of the UK population (3). This prevalent disease undermines the tooth-supporting tissues, the periodontium, resulting in impaired dentition and tooth loss.

Specific bacteria have long been thought to drive development of periodontitis (4), however, more recent data indicates that diverse microbial communities are associated with disease (5). Although, triggered in response to the local microbiota, key to the development of periodontitis pathology are defects in the well-balanced inflammatory reactions occurring at the oral barrier. For example alterations in neutrophil recruitment and function as well as increases in T-helper 17 (Th17) cells have been shown to be key in periodontitis development (6–8). Detailed insight and understanding the pathogenesis of periodontitis is vital, as not only does this chronic disease affect a substantial proportion of the global population, but periodontitis has been associated with the initiation, exacerbation, and pathogenesis of a plethora of other inflammatory diseases.

Indeed, recurring inflammation at the oral barrier has been shown to adversely affect systemic health, which may be especially important in individuals with pre-existing conditions. Periodontitis has been routinely associated with a multitude of diseases, ranging from inflammatory to infectious,

as well as developmental, cardiovascular, and neurodegenerative conditions. Although aberrant immune responses, heightened inflammation, and oral bacteria are frequently proposed to explain these associations, the exact contribution of periodontitis to the etiology and/or progression of systemic disease is unclear in most instances. What is clear, however, is that pathology in the oral cavity can lead to potentially deleterious consequences for the rest of the body. In this review we will briefly discuss the diseases that have been associated with periodontitis as well as outlining the possible mechanisms by which periodontal inflammation could mediate its deleterious effects at distal body sites. We aim to cover the key mechanisms that have already been suggested but will additionally highlight novel mechanisms by which periodontitis could affect distal inflammatory diseases; taking lessons from inflammation occurring at extra-oral sites.

FROM HEARTS AND MINDS TO JOINTS; THE REACHES OF PERIODONTITIS

To date, perhaps the condition most strongly linked with periodontitis is cardiovascular disease (CVD). An association between periodontitis and CVD was first reported 20 years ago (9). Since, periodontitis has been consistently reported in both epidemiological and experimental studies to have a role in the development and progression of atherosclerotic cardiovascular disease (10–12). Periodontal treatment may also reduce the prevelance of CVD (13), or, at the very least, mitigate some of the risk factors, by improving endothelial function (14), or lowering inflammatory markers (15, 16). Most frequently it is periodontal bacteria that have been proposed to drive CVD, as bacterial species isolated from atherosclerotic plaques are thought to be derived from the oral cavity (17). In particular, viable periodontal bacteria such as *Porphyromonas gingivalis, Streptococcus sanguis, Aggregatibacter actinomycetemcomitans,* and *Tannerella forsythia* have been isolated from atheromas (18–20). These oral microbes are proposed to exert atherogenic effects by accumulating at sites of plaque development and modulating local vascular inflammation (21), with *P. gingivalis* specifically reported to exacerbate atherosclerosis in animal models (22).

As periodontitis is causally linked to CVD, periodontitis is also by association often linked with cerebrovascular disease (23–26), a link that remains uncertain from recent evidence in experimental studies (27). Some epidemiological studies propose that dental infections, including periodontitis, increase the risk of stroke (28–30), although not all indicate an increased risk (31). Periodontal bacteria and their products are associated with systemic inflammation and platelet aggregation, which are known contributors of increased brain damage post-stroke (32).

In addition to CVD, substantial epidemiological and pre-clinical evidence indicates a role for periodontitis in the pathogenesis of rheumatoid arthritis (RA) (33–35). For decades, a link between periodontitis and RA has been proposed, with evidence suggesting that periodontitis can exacerbate or initiate RA, and vice versa. Current models for RA induction include the "two-hit" model; "one" where tolerance is broken and "two" where pathology is established/amplified; periodontitis could contribute to either and/or both of these steps. Recent evidence lends credence to the suggestion that periodontitis could represent the second hit, promoting inflammation and specifically driving RA pathology. Indeed, individuals with chronic RA have a higher incidence of periodontitis, and similarly, the prevalence of RA is higher in periodontitis patients (34). Moreover, RA patients with persistent periodontitis are less responsive to conventional therapeutic interventions (36) and periodontitis treatment can reduce the severity of RA (37). Animal models have also clearly indicated that RA is exacerbated by periodontitis (35, 38). Most research to date has focused on the roles of periodontal bacteria in driving the inflammatory consequences of periodontitis in RA; in fact, DNA from periodontal microbes have been detected in human synovial fluid during RA (33). In particular, *P. gingivalis* has been isolated from joints and is thought to drive RA pathology through molecular mimicry which promotes pathogenic self-reactive T cells that exacerbate disease (discussed further in the next section) (39). Given the pathogenic potential of anaerobic bacteria such as *P. gingivalis*, it is unsurprising therefore that antibacterial treatments (such as ornidazole, ievofloxacin, and clarithromycin) also lessen the severity of RA (40–42), implying oral bacteria could be an important driver of rheumatoid pathology.

More recent evidence has also implicated periodontitis with an increase in cognitive decline in Alzheimer's disease (AD) (43–45). In particular, periodontitis contributed to a six-fold increase in cognitive decline in AD patients which was independent of baseline cognitive state, again possibly driven by modulation of the patients' inflammatory state (46). Pre-clinical findings support this association, highlighting that periodontal bacteria can gain access to the brain in genetically-susceptible mice, contribute directly to pathology by promoting neuroinflammation (47–49), and kill neurons through the activity of extracellular proteases (45).

Given that periodontitis represents an inflammatory disease of the oral mucosa, it is perhaps not surprising that periodontitis is associated with driving pathology at other mucosal surfaces, most notably the gut (50) and the lung (51). Considering that the oral cavity is the access point to both respiratory and gastrointestinal (GI) tracts, it is conceivable that oral inflammation could affect the lung or GI environments. In particular, periodontitis has been proposed to exacerbate inflammatory bowel disease and colorectal cancer. Elevated levels of periodontal bacteria increase the risk of developing pre-cancerous gastric lesions (52), and the oral-derived *Fusobacterium nucleatum* has been shown to directly promote colorectal cancer (53, 54). In addition to potential oncogenic effects, oral bacteria are proposed to contribute to the inflammatory pathology in inflammatory bowel disease (IBD) (50). Patients with IBD are reported to have higher prevalence and extent of periodontitis compared to healthy individuals (55, 56). However, despite some preclinical evidence indicating a possible role for periodontal bacteria in the gut (57, 58), as with the other diseases already discussed, a direct causal association between periodontitis and IBD has not been established. With regard to periodontitis and lung pathologies, while the current evidence is perhaps circumstantial, some clinical and pre-clinical studies have found that periodontal

bacteria are capable of directly contributing to lung pathology; *A. actinomycetemcomitans* can cause pulmonary infections of humans either alone or in tandem with *Actinomyces* species (59). Furthermore, *P. gingivalis* has also been isolated with the opportunistic pathogen, *Pseudomonas aeruginosa* in tracheal aspirates from patients with chronic obstructive pulmonary disease (60), and in mice, *P. gingivalis* and *Treponema denticola* have been reported to exacerbate lung pathology (61).

In addition to the aforementioned associations between periodontitis and systemic diseases, there is also some evidence linking periodontitis with obesity (62), diabetes (63), non-alcoholic steatohepatitis (64, 65), and pregnancy complications (66, 67). Periodontitis is more prevalent in diabetics and obese individuals (62, 63) and may contribute to metabolic dysregulation (68, 69). In relation to pregnancy, periodontal bacteria have been implicated in low birth weight, premature birth, and miscarriage (66, 67). Indeed, both *F. nucleatum* and *P. gingivalis* have been shown to colonize the placenta and thought to drive inflammation which is associated with fetal loss in both human and mouse studies (66, 70).

Despite a wealth of information associating periodontitis with adverse impacts on systemic health, evidence causally tying periodontitis to disease development and/or progression is lacking. This is due to a number of issues. In particular presence of oral disease is typically under-reported in individuals with severe health conditions. Unless oral parameters are explicit readouts of an otherwise non-oral disease, then they are likely not considered, and therefore frequently not examined; limiting useful evidence. Nevertheless, multiple animal studies have identified a number of mechanisms by which periodontal inflammation mediates potentially deleterious consequences at body sites away from the oral cavity.

MECHANISMS IDENTIFIED; HOW PERIODONTITIS COMPLICATES DISEASE PROCESSES AT DISTAL SITES

Most of the evidence linking periodontitis and systemic disease centers around the physical dissemination of periodontal bacteria and/or immunogenic factors via the circulation (71, 72). Chronic inflammation coupled with a richly vascularized periodontium leads to ulceration of the oral epithelial barrier, and consequently, greater access for pathogenic microbes and their products to the bloodstream. Generally, the chronic systemic distribution of oral bacteria-derived products converges at the point of an altered state of immunity, achieved either through subversion of host defenses, or prolonged and/or enhanced inflammatory responses. These changes are thought to amplify the overall threat that periodontitis poses to the host (**Figure 1**).

The Virulence of Periodontal Bacteria; Contributions to Systemic Disease

The ability of oral bacteria to invade and thrive in non-oral sites could unbalance homeostatic tissue responses in their new home and potentially contribute to disease. Since oral pathogens thrive within anaerobic periodontal pockets (73), the virulence factors that enable successful oral colonization may also render them capable of thriving at other sites. Indeed, prominent oral pathogenic bacteria including *F. nucleatum*, *P. gingivalis*, and *A. actinomycetemcomitans* have been detected in a multitude of extra-oral tissue sites, including the lung, heart, gut, placenta, and inflamed joints (33, 47, 49, 51, 66, 74, 75). Furthermore, all aforementioned species are capable of invading epithelial and endothelial cells (76), and specifically, *A. actinomycetemcomitans* can spread to neighboring cells, disseminating via membrane-bound vacuoles endocytosed by adjacent host cells (74). Indeed, even a site like the brain, with a restrictive blood-brain barrier, is not protected from invasion by oral bacteria; oral *Treponema* spirochetes have been found in human AD brains and in branches of the trigeminal nerves, indicating a potential route of access to the demented brain (77). In addition to a remarkable invasiveness potential, periodontal bacteria possess an extensive suite of virulence factors which facilitate colonization at extra-oral sites; fimbriae, adhesion molecules, and capsules are just some components of an arsenal that equip oral bacteria with the capability to persist outside the periodontium (78).

Periodontal bacteria also utilize sophisticated immune subversion mechanisms which can undermine the host response and thereby enable persistence at extra-oral sites, and include evasion of complement-mediated killing (79, 80), disarming leukocyte responses (81, 82), inhibition of lymphocyte activity (83), and modulation of toll-like receptor (TLR) signaling (81). The details of the immune evasion strategies employed by oral bacteria are beyond the scope of the current review, but have been well-outlined previously (78). While most evidence to date has been carried out in the context of the oral cavity, some studies have endeavored to address whether these subversive strategies can be employed at extra-oral sites, mostly in the context of atherosclerosis (84–86). In a similar regard, recent evidence from both pre-clinical models and human patients, suggest that oral bacteria can "hijack" immune cells (87, 88), enabling systemic dissemination from oral foci while simultaneously evading killing.

Independently of employing direct immune evasion strategies, periodontal bacteria also disrupt homeostatic processes, which has the potential to adversely impact systemic health. In this regard, *P. gingivalis* and *S. sanguis* can induce platelet aggregation (89, 90), which may contribute to an increased risk of infarction. *P. gingivalis* is also capable of modifying low-density lipoprotein which promotes foam cell formation (91, 92), a pathogenic feature of atherosclerotic disease. Extracellular proteases from *P. gingivalis* can kill neurons *in vitro*, thereby aggravating cognitive dysfunction in mouse models of AD (45), and in the context of metabolic disease, *P. gingivalis* can promote glucose intolerance and insulin resistance in mice fed a diabetogenic diet (57). In the gut environment, *F. nucleatum* can bind to oncogenic cells via its Fap2 protein, promoting colorectal cancer (53). In addition, oral *Klebsiella* species have been shown to promote T-helper 1 inflammatory responses in the gut, contributing to GI inflammation in mice (50). In all these cases tissue homeostasis is disrupted potentially laying the foundation for disease initiation and/or further amplification.

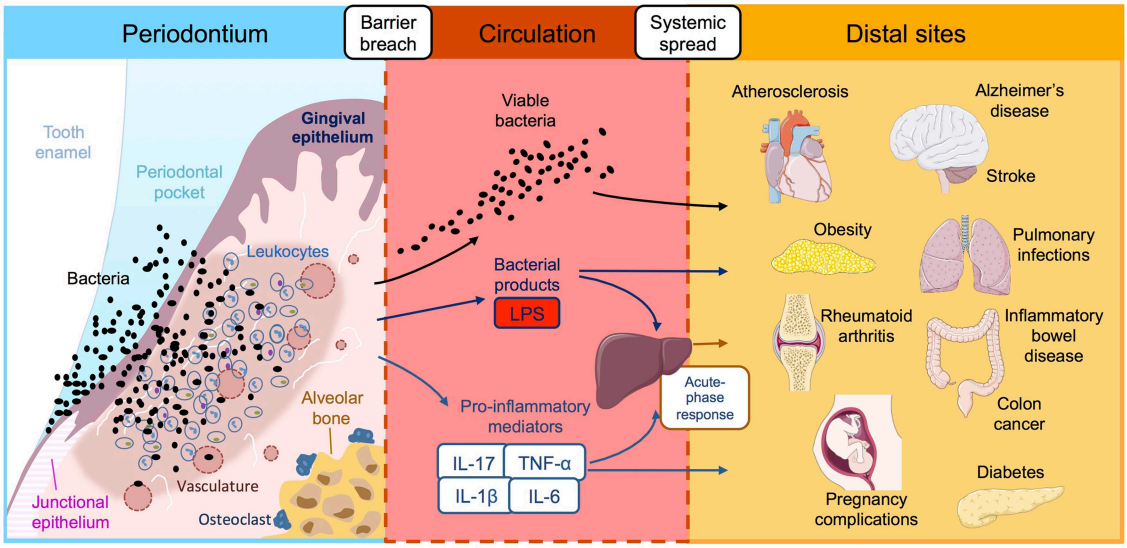

FIGURE 1 | Reported associations between periodontitis and systemic diseases. Periodontitis is initiated by ulceration of the gingival epithelium, bacterial invasion and influx of immune cells, leading to inflammatory damage to the periodontal tissues and destruction of the supporting alveolar bone. This chronic inflammatory reaction leads to leakage of bacterial products, host inflammatory factors and pathogenic oral bacteria into the bloodstream where they are transported to distal tissue sites. Once in the systemic circulation, periodontially-derived products have the potential to adversely affect a multitude of systemic diseases, either directly *in situ* or indirectly via amplification of the systemic inflammatory response. LPS, lipopolysaccharide; IL, interleukin; TNF-α tumor necrosis factor-alpha.

Well-documented within the oral cavity (78), inter-species microbial synergy could support oral bacteria survival at sites outside the oral cavity. Although further research is needed, studies have postulated a role for extra-oral microbial synergy by periodontal bacteria; for example *P. gingivalis* promotes the ability of *P. aeruginosa* to invade and persist in respiratory epithelial cells *in vitro* (93, 94), and the temporal dynamics of *F. nucleatum* and *P. gingivalis* colonization which mutually benefits survival in the oral cavity are also posited to do the same in the gut and contribute to colorectal tumorigenesis (95).

It is important to note, that while the aforementioned strategies relate to viable bacteria promoting their own persistence at extra-oral sites, chronic presence of oral bacteria in the systemic compartment will provoke an immune response, regardless of viability. This undoubtedly escalates the burden that host defenses are tasked with as large numbers of oral commensals are transported into the bloodstream during periodontitis. This may explain why chronic bacteremia as a result of periodontitis poses an important threat, especially when periodontal pathogens themselves are usually found in low numbers (73).

Leakage of Microbial and Host Factors

While destruction of the oral basement membrane facilitates increased leakage of microbes from the periodontium, so too are locally-produced host and microbial factors flushed into the systemic circulation. Furthermore, dental procedures (scaling, extractions, root planning etc.) as well as habitual brushing, flossing, and mastication all increase the rate of blood contamination (96) and in turn, aggravate the systemic inflammatory response. In this regard, lipopolysaccharide (LPS) from Gram negative bacteria such as *P. gingivalis* has been given the most attention. Although more weakly immunogenic than it's *E. coli* counterpart, blood-borne LPS from *P. gingivalis* can induce inflammation *in vivo* (97–99) and can also directly contribute to the pathogenesis of atherosclerosis in pre-clinical models (100–102). In patients with severe periodontitis, even gentle mastication can lead to elevated LPS in the circulation (71), and, when taken together, suggests that systemic leakage of oral-derived LPS is an important determinant of further complications outside the periodontium.

In addition to microbial factors, chronic oral inflammation can also result in sustained and increased levels of host inflammatory mediators in the circulation, which is a trigger for the acute-phase response. Indeed, the acute-phase reactants, interleukin (IL)-6, C-reactive protein (CRP), haptoglobin, fibrinogen, serum amyloid A, and serum amyloid P are elevated in periodontitis patients (103–107). Prolonged or excessive activation of the acute-phase response is associated with systemic pathology such as sepsis and ischaemia-reperfusion injury (108–110), as well as cardiovascular disease (111). As such, one way in which periodontitis could contribute to systemic disease may be via modulation of the acute phase response.

Moreover, there are reports of serum increases in levels of the pro-inflammatory cytokines IL-6 (105), IFN-γ (112), as well as TNF-α and IL-17 in patients with generalized aggressive periodontitis (113, 114); findings from animal models of periodontitis also support a heightened systemic inflammatory profile (58, 115, 116). Sustained elevation of inflammatory cytokines in the serum is a well-documented driver of cerebrovascular and cardiovascular disease in humans and in animal models (105, 117, 118). Although evidence directly

tying periodontitis to systemic disease via increased circulating cytokines is lacking, some studies, both clinical and pre-clinical, have reported that periodontitis-induced increases in serum IL-6 and CRP levels can lead to endothelial dysfunction (115, 119). Thus, transit of immunomodulatory factors from an inherently leaky oral focus of inflammation into the circulation could potentially alter the course of systemic disease progression and represents a potential avenue by which periodontitis could contribute to pathology at distal sites.

Antigen Mimicry

In general, periodontal bacteria can actively modulate the innate immune response and their products can provoke the inflammatory response, whether this is at oral or extra-oral sites. Aberrant immunity represents a general explanation for the adverse effects of periodontitis on systemic diseases, but perhaps the most robust evidence for a direct role of periodontal bacteria in a specific disease setting is the ability of *P. gingivalis* to promote RA pathology via molecular mimicry (39, 120, 121). Citrullination of peptides, and consequent autoantibody generation, is a pathogenic hallmark of RA, and importantly occurs prior to disease onset as well as correlating strongly with disease severity (122). *P. gingivalis* is unique in that it can citrullinate proteins via its own enzyme, peptidylarginine-deiminase (PAD), and therefore is a direct contributor to the production of pathogenic antibodies, driving auto-reactive T cells to promote inflammatory synovial destruction (39, 120, 121). In this regard, PAD-deficient *P. gingivalis* strains fail to exacerbate RA severity in mice (39). More recently, *A. actinomycetemcomitans* has also been shown to promote citrullination of peptides. Here, rather than possessing enzymatic capacity themselves, *A. actinomycetemcomitans* has been shown to trigger dysregulated activation of citrullinating enzymes in neutrophils (123).

P. gingivalis has also been reported to elicit antigen mimicry in the context of CVD and pregnancy complications. Cross-reactive bacterial epitopes mimic host cardiolipin and induce specific autoantibodies that have been associated with atherosclerotic thrombosis and adverse pregnancy outcomes (70, 124). Moreover, elevated levels of cardiolipin-specific antibodies are found in the gingival crevicular fluid and serum of periodontitis patients (124, 125). Antigen mimicry is further suggested to link oral and atherosclerotic disease through the cross-reactivity of heat-shock proteins (HSPs) with oral bacterial components (126). HSPs are associated with enhanced atherosclerotic development (127) and *P. gingivalis* GroEL proteins are highly homologous to HSP60 (126, 128) and thus capable of contributing to disease pathology.

Aberrant Immune Responses

In addition to chronic systemic elevation of host inflammatory mediators, specific changes in host immunity have been reported to link periodontitis and distal diseases. This point is nicely illustrated in studies where genetic alterations in host immunity confer an increased risk to RA in the presence of a periodontitis-dependent stimulus. Specifically, in human-leukocyte antigen (HLA)-DRβ1 humanized mice, which are susceptible to RA, exposure to oral *P. gingivalis* results in the generation of anti-citrullinated protein antibodies; something which does not occur in wild-type mice (129). This suggests that changes in the host immune response can underpin the systemic impact of periodontitis.

In a similar sense, changes in inflammatory genes can not only confer susceptibility to periodontitis, but can also account for the increased risk of adverse systemic effects due to periodontitis. IL-17 is a major driver of disease in periodontitis (130), RA (131), as well as type I diabetes mellitus (132). Indeed, genetic polymorphisms in IL-17A have been suggested to enhance the impact of periodontitis on type I diabetes (133), indicating that a failure of adequate host immunity during periodontitis can lead to worsening of other non-oral diseases.

IL-17 is also implicated in mediating the crosstalk between periodontitis and RA. *P. gingivalis* induced periodontitis enhances the severity of articular injury during experimental arthritis; this aggravation of arthritis did not occur in IL-17RA-deficient mice (134). Additionally, the levels of IL-17 produced in response to *P. gingivalis* and *Prevotella nigrescens* correlates with the intensity of arthritic bone destruction (135). Furthermore, IL-17 can promote even more distant effects outside gingiva and joint, as mice with experimental RA orally-infected with *P. gingivalis* have raised serum IL-17 levels, increased Th17 cells in mesenteric lymph nodes, and exhibit shifts in the composition of the gut microbiome (136). Together, these studies indicate that IL-17 may be a mediator of the deleterious effects of periodontitis at distant sites, aggravating pathology in a number of disease contexts. Nevertheless, it is important to remember that during periodontitis, elevated production of IL-17 is due to Th17 cells, cells which produce IL-17 in direct response to the dysbiotic microbiota (130). Thus, even if aberrant host immunity is ultimately the driver of local and systemic pathology, this only occurs because of microbial signals. For example, in the absence of TLR2 in antigen-presenting cells, Th17-dependent IL-17 production is impeded, highlighting that initial microbial sensing is an important initiator of dysregulated host immunity in periodontitis (135).

Altered innate immune responses during periodontitis have also been suggested to mediate some dangerous crosstalk between oral and extra-oral sites. Neutrophils play key roles in local periodontitis pathology (137), and also in multiple disease states in which periodontitis is associated (134, 138). Neutrophil responses during periodontitis could promote systemic exacerbations, especially in the context of RA, since neutrophils release PADs and neutrophil extracellular traps (which contain chromatin and granular contents to bind and kill pathogens) which citrullinate proteins in the joints (138). Furthermore, the neutrophil-recruiting complement component C5a is produced during periodontitis and has been shown to exacerbate RA progression (139). In addition to altered neutrophil responses, there is also evidence to suggest that aberrant monocyte responses can promote systemic dysfunction. Specifically, ligature-induced periodontitis in rats alters circulating monocytes, rendering them more adherent to aortic vascular endothelial cells via VCAM-1 binding, and

thereby increasing the risk of atherosclerosis (140). Periodontitis-activated monocytes could also prime Th17 cells for enhanced IL-17 production (141), suggesting that a dysregulated interplay between innate and adaptive immune networks may contribute to the risk of complications at distant sites.

Ultimately, systemic complications due to periodontitis are the product of crosstalk from the host as well as microbes. Untangling the exact contribution of each component has so far been extremely difficult and complicated by recent evidence suggesting that periodontitis can drive changes in the composition of the gut microbiome (58, 142). Gut dysbiosis in itself is well-known to cause profound changes in host immunity, and consequently is a contributor to a range of diseases (143). Thus, not only can periodontitis directly lead to dysregulated host immunity, but it can alter microbial communities locally as well as distally and indirectly impact immune responses. This emphasizes the complex nature of how periodontitis can affect systemic diseases. It is important to reiterate that even though we have described specific instances whereby altered host immunity or microbial activities clearly predispose to detrimental systemic effects, they are only one part of the overall picture. Adverse distal effects of periodontitis are most likely the result of a dynamic interplay between microbial signals and aberrant host responses.

INTER-ORGAN IMMUNITY; LONG RANGE CONTROL OF IMMUNE RESPONSES

As outlined above, in the setting of periodontitis, oral microbes themselves, their products, or indeed, host immune mediators are all capable of eliciting changes to systemic immunity, by amplifying inflammation, subverting innate immune defenses, and promoting autoimmunity; all of which have the net effect of promoting systemic complications and disease development. Despite this, the idea that inflammation at one site can lead to alterations in immune responsiveness at another is not new, and indeed has been demonstrated in a number of settings away from the oral cavity. In particular, in 1978 the idea of the common mucosal immunologic system was proposed (144), suggesting mucosal sites communicate to protect the body from pathogenic challenge. Subsequently, increasing evidence has emerged suggesting that immune activation at one mucosal compartment directly impacts immunity at a distal mucosal site (145–148). The oral mucosal barriers of the mouth would certainly form a constituent of these collective mucosae, and thus immunological cross-talk between the oral barrier and distant mucosal sites has perhaps long been proposed in healthy if not in pathological settings. In addition to this mucosa-to-mucosa cross-talk, inflammation at non-oral barrier sites has also been associated with rheumatoid arthritis and joint pain, skin inflammation, as well as pathologies of the central nervous system (CNS). Thus, that inflammation at one site can effect inflammatory processes at another is not unexpected, but periodontitis is unique in the plethora of pathologies it has been reported to impact; perhaps a result of the inherent leakiness of the oral barrier.

Thus, far we have discussed possible mechanisms of cross-talk which have already been shown to contribute to how oral inflammation promotes a plethora of systemic diseases. Taking our cues from data that does not examine the oral barrier; we will now discuss immunological mechanisms that have been described whereby inflammation at one site affects immune control at another. We will outline possible mechanisms that periodontitis could hijack to exacerbate inflammation at distal sites such as the CNS and bone marrow, discussing studies that do not focus on periodontitis but other settings of acute, chronic or mucosal barrier inflammation. Exploring established and emerging concepts we will consider the relevance of these long-range signals to the distal inflammatory effects mediated by periodontitis (**Figure 2**).

POSSIBLE MECHANISMS BY WHICH PERIODONTITIS COULD CONTRIBUTE TO DISTAL DISEASES

Cytokine Communication

As already discussed, the levels of certain cytokines have been shown to increase in the serum of periodontitis patients. Some of these elevated inflammatory cytokines could be mediating distal effects in the bone marrow. A number of studies have implicated cytokines such as IL-12, granulocyte-macrophage colony-stimulating factor (GM-CSF), thymic stromal lymphopoietin (TSLP), and IL-17 as candidates that can mediate long-range signals that influence the fundamental process of haematopoiesis (149–155). For example, produced in the gastrointestinal tract during inflammation, IL-12 is also detected within the blood and can be sensed in the bone marrow, modulating immune cell output. Monocytes primed for regulatory functions are generated upon instruction by natural killer (NK) cells in the bone marrow which sense inflammation-driven systemic IL-12 and release interferon (IFN)-γ (150). In line with this cytokines such as GM-CSF and TSLP have also been shown to mediate effects distal from their site of generation during settings of auto-inflammation. In another example, Siracusa et al. (155) reported that systemic TSLP can elicit extramedullary haematopoiesis in the spleen. This resulted in the expansion of progenitors with an intrinsic preference to differentiate into granulocytes; these immune cells promoted the development of allergic airway inflammation. Such studies demonstrate that localized inflammation results in the systemic elevation of cytokines that feed-back to the bone-marrow, subsequently altering the quality and/or quantity of the immune cells generated.

In conjunction with relaying signals to the bone marrow, systemic cytokines could directly modulate other distal tissues such as the CNS. It has been recently demonstrated that a gut-initiated Th17 response is capable of inducing cognitive decline through the effects of systemic IL-17 on the cerebrovasculature, inducing endothelial dysfunction (152). As cytokine levels are altered systemically in periodontitis, impacts of these on bone marrow output, as well as the CNS, could be easily envisaged and future work should examine changes to these compartments in patients and in pre-clinical models of periodontitis. With

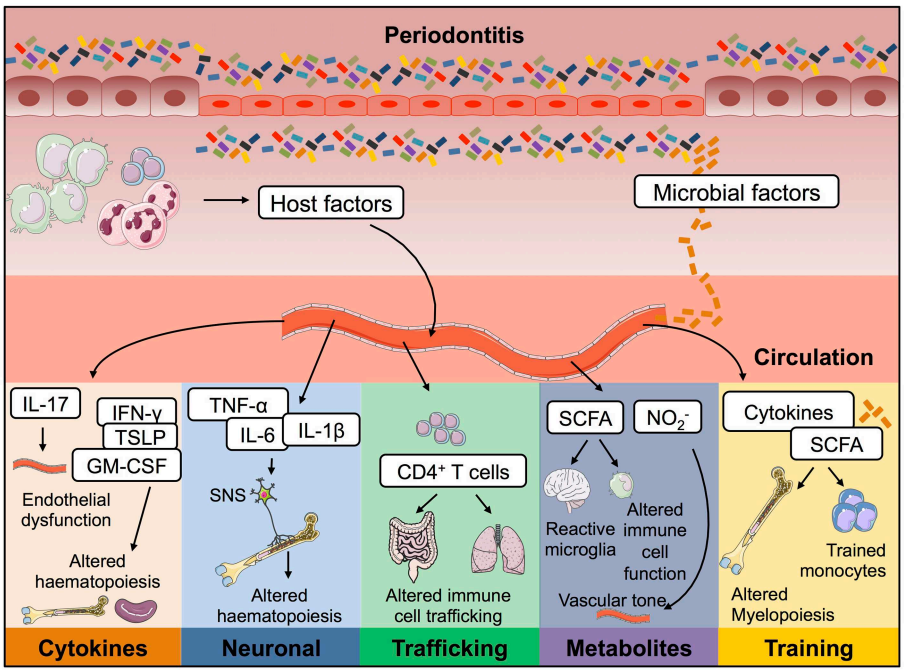

FIGURE 2 | Possible mechanisms by which periodontitis contributes to inflammation at distal tissue locations. During oral inflammation both host- and microbial-derived factors could contribute to inflammatory pathology at extra-oral sites. Passage into the blood stream would give these immune-modulators access to a plethora of body compartments and therefore mediate effects on many body systems. Periodontitis could therefore contribute to the pathophysiology of other diseases in the following ways; (i) lead to endothelial dysfunction; (ii) drive changes to haematopoiesis; (iii) promote activation of T cells capable of trafficking to other mucosal barriers; (iv) result in changes to circulating immuno-modulatory microbial-derived metabolites; and (v) cause innate immune cell training. IL, interleukin; TNF-α, tumor necrosis factor α; PGE_2, prostaglandin E_2; SCFA, short chain fatty acids; NO_2^- nitrite.

specific relation to changes to the bone marrow compartment, such fundamental alterations in immune cells could explain why periodontitis can impact the pathogenesis of such a variety of other diseases.

Neuronal Signals

As well as cytokines, neuronal signals, particularly those of the autonomic nervous system have also emerged as critical regulators that can relay long-range signals to the haematopoietic compartment during homeostasis and inflammation (156–160). As a result, it becomes essential to consider the role of these neuronal pathways during periodontal inflammation as their activation could well-contribute to the systemic inflammatory effects of this disease.

The concept of neuro-immune cross-talk has emerged from elegant demonstrations of the dynamic interactions between the nervous and immune systems in both homeostasis and non-periodontal disease that has reformed our understanding of these seemingly disparate systems (161–170). A number of studies have demonstrated that the bone marrow haematopoietic compartment receives rich sympathetic innervation (156, 171, 172) and that adrenergic signaling is critical in modulating haematopoietic output (156, 173), its circadian oscillations (171), aging (157) and ability to regenerate in contexts of injury (158). For example, the interaction of noradrenaline with the β_2 adrenergic receptor have been shown to be indispensable for Granulocyte colony-stimulating factor (G-CSF)-mediated mobilization of haematopoietic stem and progenitor cells (HSPC), through the downregulation of the bone marrow anchor, CXCL12 (156). The ability of the sympathetic nervous system to exert diverse effects on the bone marrow haematopoietic niche stems from the transduction of signals via distinct β-adrenergic receptor sub-types (157, 171, 173). Intriguingly, the capacity of the autonomic nervous system to tune the bone marrow HSPC compartment is not restricted to neuronal signals. Non-myelinating schwann cells in the bone marrow are thought to play an integral role in maintaining HSPCs and their quiescence through their ability to contact HSPCs and activate latent transforming growth factor (TGF-β) (174). These networks are also thought to be important in disease as inflammation could disrupt the neuro-immune crosstalk. Indeed, there is a large body of evidence that has implicated sympathetic over-activation following ischaemic stroke in driving alterations in systemic immunity (175–177), in part, mediated through alterations in haematopoiesis in the bone marrow (159).

The ability of the nervous system to shape immune function is not limited to effects on haematopoiesis as neuropeptides derived from the enteric nervous system have also emerged as key players that shape immune function in health and disease (170, 178–183). Critical in driving group 2 innate lymphoid cell (ILC2)-mediated type 2 inflammation, the neuropeptide,

neuromedin U has been shown to augment type-2 responses and therefore amplify allergic inflammation (182, 183). Recently, cytokines have emerged as candidates that are capable of directing immune function through effects on the nervous system (184). In this context it can be postulated that inflammation could modulate immune functions through alterations in neuronal signaling mediated by cytokines. As a result, it can be envisaged that the systemic leakage of cytokines during periodontal disease could engage autonomic and enteric neuronal circuits in the gut or bone marrow that could exacerbate systemic inflammation.

Trained Innate Immunity

Thus, far, we have considered how cytokine and neuronal signals altered in periodontal disease may mediate immune changes that could contribute to altered inflammatory responses at non-oral sites. Here, we shall delve into a more fundamental concept, how the sequence of signals experienced by innate cells are critical in directing their effector function, a concept historically confined to the realms of adaptive immunity. Although this has yet to be explored in settings of periodontitis, we shall discuss how through its myriad of effects, periodontal disease could subvert evolutionarily conserved pathways that serve to enhance and diversify the repertoire of innate responses to pathogenic challenges.

Traditionally it is considered that innate immune cells, such as monocytes, acquire effector functions upon recruitment to inflammatory sites, experiencing local signals that drive functional adaptation and local differentiation. However, it has now emerged that the terminal effector function of mononuclear phagocytes can be imprinted by infection, injury-driven cytokines or microbe-derived metabolites in distal tissues such as the bone marrow, altering the monocyte compartment as a whole (150, 185, 186). These studies add to the growing body of evidence (187) that illustrates the concept of trained innate immunity, a primitive means to tune the monocyte network to protect against pathogenic challenges.

Recent studies have illustrated that innate immunity can be trained to protect against subsequent challenges through the emergence of short-lived distinct myeloid populations that have a modulated, usually enhanced capacity to respond to pathogenic challenges. For example, monocytes, whilst one of the first responders to infection or injury possess an intrinsic inability to initiate pathogenic-specific responses like T cells or take on sub-specializations like tissue-specific macrophages (188, 189). In order to facilitate an expeditious and effective immune response during infection, it is thought that the host replaces the monocyte compartment as a whole through targeted alterations in haematopoiesis involving epigenetic rewiring (150, 186, 190, 191). Critically, it is distinct from emergency haematopoiesis which occurs in response to infection (192) as it tunes immunity by altering the functional responsiveness of the innate cells, specifically monocytes, generated.

Although trained immunity can have a positive effect in settings of infection, alterations in innate cell function could well mediate disastrous consequences in settings of auto-inflammation and specifically, contribute to the distal effects of periodontitis. Diverse stimuli have been shown to be capable of imparting monocyte training, including metabolites such as short chain fatty acids (SCFAs) (185) and mevalonate (193), and infection-driven cytokines such as IFN-γ (150). Whilst it is thought that this immune "memory" is maintained through distinct alterations in haematopoiesis (190), intriguingly, innate immune cells are capable of being trained at multiple stages, from the point of genesis (150, 185, 190) to the point of maturity (194). For example, studies (150, 185, 190) have shown that microbial products such as β-glucan or SCFAs and cytokines such as IFN-γ can modulate myelopoiesis resulting in the production of altered myeloid precursors as a means to imprint immunity against pathogens or in response to inflammation at mucosal sites such as the lung or gut. Whilst mature monocytes can also be trained by similar stimuli such as β-glucan, the training is thought to be epigenetically imprinted and consequently confers an enhanced capacity to respond to subsequent pathogenic challenges (194, 195). Unlike alterations in haematopoiesis, epigenetic signatures serve to impart immune "memory" to mature cells that have exited the haematopoietic developmental programme. It can thus be inferred that these mechanisms act in synergy, modulating developing as well as mature monocytes, replacing the monocyte compartment of the host.

It is conceivable that the systemic dissemination of cytokines, microbial products, and metabolites that occurs during periodontitis, could drive innate immune cell training. Unlike the changes to global haematopoiesis discussed in the previous sections, periodontitis could drive fundamental changes to monocyte function, resulting in the specification of immunogenic phenotypes in monocytes generated in the bone marrow. This could have catastrophic consequences as the generation of trained innate immune cells with altered immunogenic potential could well be a key driver of aberrant inflammation at extra-oral sites. Indeed alterations in peripheral blood monocytes have been noted in periodontitis patients (196–199), potentially suggesting innate immune cell training occurs in this disease. Whether trained epigenetic changes underpin these altered functions remains to be determined. Such fundamental changes to immune cell function, if they do occur in periodontitis, would likely impact subsequent and on-going immune processes, irrespective of their anatomical location.

Trafficking of Activated T Cells

Usually a consequence of alterations in the cytokine milieu, altering immune cell trafficking is also an effective means to modulate immunity at a distal site. This concept also contributes to the idea of a common mucosal immune system, extending immune responses beyond compartmentalized tissues (200, 201). For example, it has emerged that infection-driven inflammation in the lung is capable of instructing $CCR9^{+}CD4^{+}$ T cell recruitment from the lungs to the gut (145). This recruitment of activated T cells to the gut resulted in intestinal injury and dysbiosis, driven by production of IFN-γ and IL-17A. Thus, T cells primed at one mucosal site could drive pathology when found at another. Moreover, intra-nasal delivery of antigens is capable of inducing protective immunity against an enteric

Salmonella challenge by activating lung dendritic cells (DCs) that promote the homing of $CD4^+$ T cells to the gastrointestinal tract through the up-regulation of the integrin α4β7 and CCR9 (146), again highlighting lymphocyte trafficking between mucosal barriers.

In fact, when considering the cross-talk between the oral barrier and distal tissues, it is particularly salient to probe mucosal sites, after all it is well-established that oral vaccination induces protective immunity at distal mucosal barriers (147, 202, 203), indicating responses primed orally are effectively recalled at other barriers. Indeed many antigens encountered in the oral cavity, including those of both food- and bacterial-origin, are subsequently seen in the gastrointestinal tract or lung. As exposure to these antigens will change during oral inflammation, it raises the possibility that altered T cell priming and trafficking could link periodontitis with diseases of the gut and lung.

Commensal Bacterial Metabolites

It is now well-established that commensal-derived signals play crucial roles in shaping both local immune networks at barrier surfaces, as well as distal tissue sites like the brain (1). This is a relationship that is fraught with peril as a nuanced system of checks and balances are required to limit invasive flora whilst restraining overtly inflammatory responses and allowing the host to reap the benefits of housing a commensal community. As a consequence of this intimate host-microbe relationship, it is unsurprising that shifts in the microbial communities inhabiting barrier surfaces are associated with disease states during inflammation, injury and aging (204–207). In this context, metabolites generated by the gastrointestinal microbial community have been demonstrated to calibrate homeostatic and anti-microbial immune networks *in situ* (208–211). Importantly, not only are these metabolites important for shaping local gastrointestinal intestinal immunity but studies have illustrated that microbe-derived metabolites are capable of being deployed as long-range signals, modulating inflammation at distal sites such as the CNS (212–214) and lung (185, 215, 216). These commensal-derived keystone metabolites thus calibrate immune responsiveness and alteration in the systemic levels of these products has been shown to contribute to immune dysfunction. A number of studies have shown that microbial metabolites from the gut such as the SCFA butyrate play an important role in limiting pathology and promoting the resolution of pulmonary infections through diverse effects on innate and adaptive immunity (185, 217–219). Although not studied to anywhere near the same extent, shifts in the oral commensal community could also contribute to systemic inflammation through the alteration of key metabolites. Focusing on SCFA, the oral commensal community has been shown to shift toward a more butyrate producing community during inflammation (220–223). Whether this leads to subsequent changes in systemic SCFA has yet to be explored, but if so would likely impact peripheral immunity. In addition a key metabolite generated by oral commensals is nitrite, as the oral community reduces nitrates (224–226), generating this metabolite which has vasoactive effects (227–229). Thus, changes in the oral bacterial community during periodontitis could impact systemic levels of nitrite which would have profound effects on systemic vascular tone (229). These concepts await exploration in the context of periodontal disease but again could contribute to the systemic pathologies that are associated with periodontitis.

CONCLUDING REMARKS

Data from pre-clinical animal models and epidemiological studies indicate strong associations between the presence of periodontitis and amplification of plethora of diseased states ranging from joint inflammation to cognitive decline. Despite this, only a few detailed mechanisms have emerged outlining how periodontitis mediates these deleterious effects. As discussed in this review, it is not difficult to envisage possible periodontitis-induced mediators that could be driving distal inflammatory consequences; what remains now is to better delineate these mechanisms and definitively establish cause-and-effect relationships during periodontitis. This can be achieved through well-designed animal experiments utilizing cutting-edge technologies to establish systemic and tissue-specific changes during periodontitis. Moreover, large scale, well-powered, human studies should be undertaken to assess the impact of periodontitis treatment on extra-oral disease pathology. This should be done alongside the careful clinical evaluation of oral parameters in patients with diseases associated with periodontitis, to generate detailed insight into the oral health of these patients. Better understanding of the cross-talk between the oral barrier and distal sites could support a step-change in the clinical treatment of many diseases. Not only could oral health parameters be employed to stratify patients and/or monitor disease progression but in some cases it may emerge that aggressive intervention to improve oral health could mediate dramatic improvements in a plethora of life-limiting diseases.

AUTHOR CONTRIBUTIONS

CO reviewed data and wrote the sections regarding the systemic consequences of periodontitis and already postulated mechanisms driving these consequences. SK reviewed data and wrote the sections regarding possible mechanisms whereby periodontitis drives its systemic inflammatory risks. JK supervised the review process, wrote, and compiled the manuscript.

ACKNOWLEDGMENTS

Work in the authors' laboratory was supported by the BBSRC (BB/M025977/1) and Arthritis Research UK. We acknowledge Servier Medical Art for artistic templates. We thank Drs. John Grainger and Flora McClure for critical review of this manuscript.

REFERENCES

1. Belkaid Y, Naik S. Compartmentalized and systemic control of tissue immunity by commensals. *Nat Immunol*. (2013) 14:646–53. doi: 10.1038/ni.2604
2. Moutsopoulos NM, Konkel JE. Tissue-specific immunity at the oral mucosal barrier. *Trends Immunol*. (2018) 39:276–87. doi: 10.1016/j.it.2017.08.005
3. White DA, Tsakos G, Pitts NB, Fuller E, Douglas GVA, Murray JJ, et al. Adult Dental Health Survey 2009: common oral health conditions and their impact on the population. *Br Dent J*. (2012) 213:567–72. doi: 10.1038/sj.bdj.2012.1088
4. Socransky SS, Haffajee AD. Periodontal microbial ecology. *Periodontol 2000*. (2005) 38:135–87. doi: 10.1111/j.1600-0757.2005.00107.x
5. Hajishengallis G, Lamont RJ. Beyond the red complex and into more complexity: the polymicrobial synergy and dysbiosis (PSD) model of periodontal disease etiology. *Mol Oral Microbiol*. (2012) 27:409–19. doi: 10.1111/j.2041-1014.2012.00663.x
6. Hajishengallis G, Moutsopoulos NM, Hajishengallis E, Chavakis T. Immune and regulatory functions of neutrophils in inflammatory bone loss. *Semin Immunol*. (2016) 28:146–58. doi: 10.1016/j.smim.2016.02.002
7. Moutsopoulos NM, Konkel J, Sarmadi M, Eskan MA, Wild T, Dutzan N, et al. Defective neutrophil recruitment in leukocyte adhesion deficiency type I disease causes local IL-17-driven inflammatory bone loss. *Sci Transl Med*. (2014) 6:229ra40. doi: 10.1126/scitranslmed.3007696
8. Dutzan N, Abusleme L, Bridgeman H, Greenwell-Wild T, Zangerle-Murray T, Fife ME, et al. On-going mechanical damage from mastication drives homeostatic Th17 cell responses at the oral barrier. *Immunity*. (2017) 46:133–47. doi: 10.1016/j.immuni.2016.12.010
9. Beck J, Garcia R, Heiss G, Vokonas PS, Offenbacher S. Periodontal disease and cardiovascular disease. *J Periodontol*. (1996) 67:1123–37. doi: 10.1902/jop.1996.67.10s.1123
10. Kuramitsu HK, Qi M, Kang IC, Chen W. Role for periodontal bacteria in cardiovascular diseases. *Ann Periodontol*. (2001) 6:41–7. doi: 10.1902/annals.2001.6.1.41
11. Gendron R, Grenier D, Maheu-Robert LF. The oral cavity as a reservoir of bacterial pathogens for focal infections. *Microbes Infect*. (2000) 2:897–906. doi: 10.1016/S1286-4579(00)00391-9
12. Beck JD, Offenbacher S. Systemic effects of periodontitis : epidemiology and cardiovascular disease. *J Periodontol*. (2005) 76:2089–100. doi: 10.1902/jop.2005.76.11-S.2089
13. Peng CH, Yang YS, Chan KC, Kornelius E, Chiou JY, Huang CN. Periodontal treatment and the risks of cardiovascular disease in patients with type 2 diabetes: a retrospective cohort study. *Intern Med*. (2017) 56:1015–21. doi: 10.2169/internalmedicine.56.7322
14. Tonetti MS, D'Aiuto F, Nibali L, Donald A, Storry C, Parkar M, et al. Treatment of periodontitis and endothelial function. *N Engl J Med*. 356:911–20. doi: 10.1056/NEJMoa063186
15. Offenbacher S, Beck JD, Moss K, Mendoza L, Paquette DW, Barrow DA, et al. Results from the Periodontitis and Vascular Events (PAVE) study: a pilot multicentered, randomized, controlled trial to study effects of periodontal therapy in a secondary prevention model of cardiovascular disease. *J Periodontol*. (2009) 80:190–201. doi: 10.1902/jop.2009.080007
16. Paraskevas S, Huizinga JD, Loos BG. A systematic review and meta-analyses on C-reactive protein in relation to periodontitis. *J Clin Periodontol*. (2008) 35:277–90. doi: 10.1111/j.1600-051X.2007.01173.x
17. Koren O, Spor A, Felin J, Fåk F, Stombaugh J, Tremaroli V, et al. Human oral, gut, and plaque microbiota in patients with atherosclerosis. *Proc Natl Acad Sci USA*. (2011) 108:4592–8. doi: 10.1073/pnas.1011383107
18. Haraszthy VI, Zambon JJ, Trevisan M, Zeid M, Genco RJ. Identification of periodontal pathogens in atheromatous plaques. *J Periodontol*. (2000) 71:1554–60. doi: 10.1902/jop.2000.71.10.1554
19. Kozarov E V, Dorn BR, Shelburne CE, Dunn WA, Progulske-Fox A. Human atherosclerotic plaque contains viable invasive *Actinobacillus actinomycetemcomitans* and *Porphyromonas gingivalis*. *Arterioscler Thromb Vasc Biol*. (2005) 25:e17–8. doi: 10.1161/01.ATV.0000155018.67835.1a
20. Herrera RL, Kozarov D, Reyes L, Herrera D, Kozarov E, Rold An S, et al. Periodontal bacterial invasion and infection: contribution to atherosclerotic pathology. *J Clin Periodontol*. (2013) 40:S30–50. doi: 10.1111/jcpe.12079
21. Genco RJ, Van Dyke TE. Reducing the risk of CVD in patients with periodontitis. *Nat Rev Cardiol*. (2010) 7:479–80. doi: 10.1038/nrcardio.2010.120
22. Gibson FC, Hong C, Chou HH, Yumoto H, Chen J, Lien E, et al. Innate immune recognition of invasive bacteria accelerates atherosclerosis in apolipoprotein E-deficient mice. *Circulation*. (2004) 109:2801–6. doi: 10.1161/01.CIR.0000129769.17895.F0
23. Dorfer CE, Becher H, Ziegler CM, Kaiser C, Lutz R, Jorss D, et al. The association of gingivitis and periodontitis with ischemic stroke. *J Clin Periodontol*. (2004) 31:396–401. doi: 10.1111/j.1600-051x.2004.00579.x
24. Grau AJ, Becher H, Ziegler CM, Lichy C, Buggle F, Kaiser C, et al. Periodontal disease as a risk factor for ischemic stroke. *Stroke*. (2004) 35:496–501. doi: 10.1161/01.STR.0000110789.20526.9D
25. Joshipura KJ, Hung HC, Rimm EB, Willett WC, Ascherio A. Periodontal disease, tooth loss, and incidence of ischemic stroke. *Stroke*. (2003) 34:47–52. doi: 10.1161/01.STR.0000052974.79428.0C
26. Elter JR, Offenbacher S, Toole JF, Beck JD. Relationship of periodontal disease and edentulism to stroke/TIA. *J Dent Res*. (2003) 82:998–1001. doi: 10.1177/154405910308201212
27. O'Boyle C, Haley MJ, Lemarchand E, Smith CJ, Allan SM, Konkel JE, et al. Ligature-induced periodontitis induces systemic inflammation but does not alter acute outcome after stroke in mice. *Int J Stroke*. (2019). doi: 10.1177/1747493019834191. [Epub ahead of print].
28. Kweider M, Lowe GD, Murray GD, Kinane DF, McGowan DA. Dental disease, fibrinogen and white cell count; links with myocardial infarction? *Scott Med J*. (1993) 38:73–4. doi: 10.1177/003693309303800304
29. Syrjanen J, Peltola J, Valtonen V, Iivanainen M, Kaste M, Huttunen JK. Dental infections in association with cerebral infarction in young and middle-aged men. *J Intern Med*. (1989) 225:179–84. doi: 10.1111/j.1365-2796.1989.tb00060.x
30. Grau AJ, Buggle F, Ziegler C, Schwarz W, Meuser J, Tasman AJ, et al. Association between acute cerebrovascular ischemia and chronic and recurrent infection. *Stroke*. (1997) 28:1724–9. doi: 10.1161/01.STR.28.9.1724
31. Howell TH, Ridker PM, Ajani UA, Hennekens CH, Christen WG. Periodontal disease and risk of subsequent cardiovascular disease in U.S. male physicians. *J Am Coll Cardiol*. (2001) 37:445–50. doi: 10.1016/S0735-1097(00)01130-X
32. Dénes A, Ferenczi S, Kovács KJ. Systemic inflammatory challenges compromise survival after experimental stroke via augmenting brain inflammation, blood- brain barrier damage and brain oedema independently of infarct size. *J Neuroinflammation*. (2011) 8:164. doi: 10.1186/1742-2094-8-164
33. Ogrendik M. Rheumatoid arthritis is an autoimmune disease caused by periodontal pathogens. *Int J Gen Med*. (2013) 6:383–6. doi: 10.2147/IJGM.S45929
34. Ogrendik M. Rheumatoid arthritis is linked to oral bacteria:etiological association. *Mod Rheumatol*. (2009) 19:453–6. doi: 10.3109/s10165-009-0194-9
35. Bartold PM, Marino V, Cantley M, Haynes DR. Effect of Porphyromonas gingivalis-induced inflammation on the development of rheumatoid arthritis. *J Clin Periodontol*. (2010) 37:405–11. doi: 10.1111/j.1600-051X.2010.01552.x
36. Savioli C, Ribeiro ACM, Fabri GMC, Calich AL, Carvalho J, Silva C a, et al. Persistent periodontal disease hampers anti-tumor necrosis factor treatment response in rheumatoid arthritis. *JCR J Clin Rheumatol*. (2012) 1. doi: 10.1097/RHU.0b013e31825828be
37. Silvestre F, Silvestre-Rangil J, Bagán L, Bagán J-V. Effect of nonsurgical periodontal treatment in patients with periodontitis and rheumatoid arthritis: a systematic review. *Med Oral Patol Oral y Cir Bucal*. (2016) e349–54. doi: 10.4317/medoral.20974
38. Cantley MD, Haynes DR, Marino V, Bartold PM. Pre-existing periodontitis exacerbates experimental arthritis in a mouse model. *J Clin Periodontol*. (2011) 38:532–41. doi: 10.1111/j.1600-051X.2011.01714.x
39. Maresz KJ, Hellvard A, Sroka A, Adamowicz K, Bielecka E, Koziel J, et al. *Porphyromonas gingivalis* facilitates the development and progression of destructive arthritis through its unique bacterial peptidylarginine deiminase (PAD). *PLoS Pathog*. (2013) 9:e1003627. doi: 10.1371/journal.ppat.1003627

40. Ogrendik M. Effects of clarithromycin in patients with active rheumatoid arthritis. *Curr Med Res Opin.* (2007) 23:515–22. doi: 10.1185/030079906X167642
41. Ogrendik M. Levofloxacin treatment in patients with rheumatoid arthritis receiving methotrexate. South Med J. (2007) 100:135–9. doi: 10.1097/01.smj.0000254190.54327.3b
42. Ogrendik M. Treatment of rheumatoid arthritis with ornidazole: a randomized, double-blind, placebo-controlled study. *Rheumatol Int.* (2006) 26:1132–7. doi: 10.1007/s00296-006-0145-0
43. Stein PS, Desrosiers M, Donegan SJ, Yepes JF, Kryscio RJ. Tooth loss, dementia and neuropathology in the Nun Study. *J Am Dent Assoc.* (2007) 138:1314–22. doi: 10.14219/jada.archive.2007.0046
44. Poole S, Singhrao SK, Kesavalu L, Curtis MA, Crean S. Determining the presence of periodontopathic virulence factors in short-term postmortem Alzheimer's disease brain tissue. *J Alzheimer's Dis.* (2013) 36:665–77. doi: 10.3233/JAD-121918
45. Dominy SS, Lynch C, Ermini F, Benedyk M, Marczyk A, Konradi A, et al. *Porphyromonas gingivalis* in Alzheimer's disease brains: evidence for disease causation and treatment with small-molecule inhibitors. *Sci Adv.* (2019) 5:eaau3333. doi: 10.1126/sciadv.aau3333
46. Ide M, Harris M, Stevens A, Sussams R, Hopkins V, Culliford D, et al. Periodontitis and cognitive decline in Alzheimer's disease. *PLoS ONE.* (2016) 11:e0151081. doi: 10.1371/journal.pone.0151081
47. Poole S, Singhrao SK, Chukkapalli S, Rivera M, Velsko I, Kesavalu L, et al. Active invasion of *Porphyromonas gingivalis* and infection-induced complement activation in ApoE-/- mice brains. *J Alzheimer's Dis.* (2014) 43:67–80. doi: 10.3233/JAD-140315
48. Singhrao SK, Chukkapalli S, Poole S, Velsko I, Crean SJ, Kesavalu L. Chronic *Porphyromonas gingivalis* infection accelerates the occurrence of age-related granules in ApoE – / – mice brains. *J Oral Microbiol.* (2017) 9:1270602. doi: 10.1080/20002297.2016.1270602
49. Foschi F, Izard J, Sasaki H, Sambri V, Prati C, Müller R, et al. *Treponema denticola* in disseminating endodontic infections. *J Dent Res.* (2006) 85:761–5. doi: 10.1177/154405910608500814
50. Atarashi K, Suda W, Luo C, Kawaguchi T, Motoo I, Narushima S, et al. Ectopic colonization of oral bacteria in the intestine drives TH1 cell induction and inflammation. *Science.* (2017) 358:359–65. doi: 10.1126/science.aan4526
51. Mojon P. Oral health and respiratory infection. *J Can Dent Assoc.* (2002) 68:340–5.
52. Sun J, Zhou M, Salazar CR, Hays R, Bedi S, Chen Y, et al. Chronic periodontal disease, periodontal pathogen colonization, and increased risk of precancerous gastric lesions. *J Periodontol.* (2017) 88:1124–34. doi: 10.1902/jop.2017.160829
53. Abed J, Emgård JEM, Zamir G, Faroja M, Almogy G, Grenov A, et al. Fap2 Mediates *Fusobacterium nucleatum* Colorectal adenocarcinoma enrichment by binding to Tumor-Expressed Gal-GalNAc. *Cell Host Microbe.* (2016) 20:215–25. doi: 10.1016/j.chom.2016.07.006
54. Rubinstein MR, Wang X, Liu W, Hao Y, Cai G, Han YW. *Fusobacterium nucleatum* promotes colorectal carcinogenesis by modulating E-cadherin/β-catenin signaling via its FadA adhesin. *Cell Host Microbe.* (2013) 14:195–206. doi: 10.1016/j.chom.2013.07.012
55. Brito F, de Barros FC, Zaltman C, Carvalho ATP, Carneiro AJ de V, Fischer RG, et al. Prevalence of periodontitis and DMFT index in patients with Crohn's disease and ulcerative colitis. *J Clin Periodontol.* (2008) 35:555–60. doi: 10.1111/j.1600-051X.2008.01231.x
56. Habashneh RA, Khader YS, Alhumouz MK, Jadallah K, Ajlouni Y. The association between inflammatory bowel disease and periodontitis among Jordanians: a case-control study. *J Periodontal Res.* (2012) 47:293–8. doi: 10.1111/j.1600-0765.2011.01431.x
57. Blasco-Baque V, Garidou L, Pomié C, Escoula Q, Loubieres P, Le Gall-David S, et al. Periodontitis induced by *Porphyromonas gingivalis* drives periodontal microbiota dysbiosis and insulin resistance via an impaired adaptive immune response. *Gut.* (2017) 66:872–85. doi: 10.1136/gutjnl-2015-309897
58. Arimatsu K, Yamada H, Miyazawa H, Minagawa T, Nakajima M, Ryder MI, et al. Oral pathobiont induces systemic inflammation and metabolic changes associated with alteration of gut microbiota. *Sci Rep.* (2015) 4:4828. doi: 10.1038/srep04828
59. Morris JF, Sewell DL. Necrotizing pneumonia caused by mixed infection with *Actinobacillus actinomycetemcomitans* and *Actinomyces israelii*: case report and review. *Clin Infect Dis.* (1994) 18:450–2. doi: 10.1093/clinids/18.3.450
60. Tan L, Wang H, Li C, Pan Y. 16S rDNA-based metagenomic analysis of dental plaque and lung bacteria in patients with severe acute exacerbations of chronic obstructive pulmonary disease. *J Periodontal Res.* (2014) 49:760–9. doi: 10.1111/jre.12159
61. Kimizuka R, Kato T, Ishihara K, Okuda K. Mixed infections with *Porphyromonas gingivalis* and *Treponema denticola* cause excessive inflammatory responses in a mouse pneumonia model compared with monoinfections. *Microbes Infect.* (2003) 5:1357–62. doi: 10.1016/j.micinf.2003.09.015
62. Saito T, Shimazaki Y, Sakamoto M. Obesity and periodontitis. *N Engl J Med.* (1998) 339:482–3. doi: 10.1056/NEJM199808133390717
63. D'Aiuto F, Sabbah W, Netuveli G, Donos N, Hingorani AD, Deanfield J, et al. Association of the metabolic syndrome with severe periodontitis in a large U.S. population-based survey. *J Clin Endocrinol Metab.* (2008) 93:3989–94. doi: 10.1210/jc.2007-2522
64. Furusho H, Miyauchi M, Hyogo H, Inubushi T, Ao M, Ouhara K, et al. Dental infection of *Porphyromonas gingivalis* exacerbates high fat diet-induced steatohepatitis in mice. *J Gastroenterol.* (2013) 48:1259–70. doi: 10.1007/s00535-012-0738-1
65. Yoneda M, Naka S, Nakano K, Wada K, Endo H, Mawatari H, et al. Involvement of a periodontal pathogen, *Porphyromonas gingivalis* on the pathogenesis of non-alcoholic fatty liver disease. *BMC Gastroenterol.* (2012) 12:16. doi: 10.1186/1471-230X-12-16
66. Han YW, Fardini Y, Chen C, Iacampo KG, Peraino VA, Shamonki JM, et al. Term stillbirth caused by oral *Fusobacterium nucleatum*. *Obstet Gynecol.* (2010) 115(2 Pt 2):442–5. doi: 10.1097/AOG.0b013e3181cb9955
67. Han YW, Houcken W, Loos BG, Schenkein HA, Tezal M. Periodontal disease, atherosclerosis, adverse pregnancy outcomes, and head-and-neck cancer. *Adv Dent Res.* (2014) 26:47–55. doi: 10.1177/0022034514528334
68. Nibali L, D'Aiuto F, Griffiths G, Patel K, Suvan J, Tonetti MS. Severe periodontitis is associated with systemic inflammation and a dysmetabolic status: a case-control study. *J Clin Periodontol.* (2007) 34:931–7. doi: 10.1111/j.1600-051X.2007.01133.x
69. Lösche W, Karapetow F, Pohl A, Pohl C, Kocher T. Plasma lipid and blood glucose levels in patients with destructive periodontal disease. *J Clin Periodontol.* (2000) 27:537–41. doi: 10.1034/j.1600-051x.2000.027008537.x
70. Schenkein HA, Bradley JL, Purkall DB. Anticardiolipin in porphyromonas gingivalis antisera causes fetal loss in mice. *J Dent Res.* (2013) 92:814–8. doi: 10.1177/0022034513497959
71. Geerts SO, Nys M, De MP, Charpentier J, Albert A, Legrand V, et al. Systemic release of endotoxins induced by gentle mastication: association with periodontitis severity. *J Periodontol.* (2002) 73:73–8. doi: 10.1902/jop.2002.73.1.73
72. Forner L, Larsen T, Kilian M, Holmstrup P. Incidence of bacteremia after chewing, tooth brushing and scaling in individuals with periodontal inflammation. *J Clin Periodontol.* (2006) 33:401–7. doi: 10.1111/j.1600-051X.2006.00924.x
73. Hajishengallis G, Liang S, Payne MA, Hashim A, Jotwani R, Eskan MA, et al. Low-abundance biofilm species orchestrates inflammatory periodontal disease through the commensal microbiota and complement. *Cell Host Microbe.* (2011) 10:497–506. doi: 10.1016/j.chom.2011.10.006
74. Meyer DH, Fives-Taylor PM. The role of *Actinobacillus actinomycetemcomitans* in the pathogenesis of periodontal disease. *Trends Microbiol.* (1997) 5:224–8. doi: 10.1016/S0966-842X(97)01055-X
75. Liu H, Redline RW, Han YW. *Fusobacterium nucleatum* induces fetal death in mice via stimulation of TLR4-mediated placental inflammatory response. *J Immunol.* (2007) 179:2501–8. doi: 10.4049/jimmunol.179.8.5604-c
76. Tribble GD, Lamont RJ. Bacterial invasion of epithelial cells and spreading in periodontal tissue. *Periodontol 2000.* (2010) 52:68–83. doi: 10.1111/j.1600-0757.2009.00323.x
77. Riviere GR, Riviere KH, Smith KS. Molecular and immunological evidence of oral Treponema in the human brain and their association with Alzheimer's disease. *Oral Microbiol Immunol.* (2002) 17:113–8. doi: 10.1046/j.0902-0055.2001.00100.x

78. Hajishengallis G. Periodontitis: from microbial immune subversion to systemic inflammation. *Nat Rev Immunol.* (2015) 15:30–44. doi: 10.1038/nri3785
79. Jusko M, Potempa J, Karim AY, Ksiazek M, Riesbeck K, Garred P, et al. A metalloproteinase karilysin present in the majority of *Tannerella forsythia* isolates inhibits all pathways of the complement system. *J Immunol.* (2012) 188:2338–49. doi: 10.4049/jimmunol.1101240
80. Popadiak K, Potempa J, Riesbeck K, Blom AM. Biphasic effect of gingipains from *Porphyromonas gingivalis* on the human complement system. *J Immunol.* (2007) 178:7242–50. doi: 10.4049/jimmunol.178.11.7242
81. Maekawa T, Krauss JL, Abe T, Jotwani R, Triantafilou M, Triantafilou K, et al. *Porphyromonas gingivalis* manipulates complement and TLR signaling to uncouple bacterial clearance from inflammation and promote dysbiosis. *Cell Host Microbe.* (2014) 15:768–78. doi: 10.1016/j.chom.2014.05.012
82. Taxman DJ, Swanson K V., Broglie PM, Wen H, Holley-Guthrie E, Huang MT-H, et al. *Porphyromonas gingivalis* mediates inflammasome repression in polymicrobial cultures through a novel mechanism involving reduced endocytosis. *J Biol Chem.* (2012) 287:32791–9. doi: 10.1074/jbc.M112.401737
83. Gur C, Ibrahim Y, Isaacson B, Yamin R, Abed J, Gamliel M, et al. Binding of the Fap2 protein of *Fusobacterium nucleatum* to human inhibitory receptor TIGIT protects tumors from immune cell attack. *Immunity.* (2015) 42:344–55. doi: 10.1016/j.immuni.2015.01.010
84. Hayashi C, Madrigal AG, Liu X, Ukai T, Goswami S, Gudino C V., et al. Pathogen-mediated inflammatory atherosclerosis is mediated in part via Toll-like receptor 2-induced inflammatory responses. *J Innate Immun.* (2010) 2:334–43. doi: 10.1159/000314686
85. Slocum C, Coats SR, Hua N, Kramer C, Papadopoulos G, Weinberg EO, et al. Distinct lipid a moieties contribute to pathogen-induced site-specific vascular inflammation. *PLoS Pathog.* (2014) 10:e1004215. doi: 10.1371/journal.ppat.1004215
86. Delbosc S, Alsac J-M, Journe C, Louedec L, Castier Y, Bonnaure-Mallet M, et al. *Porphyromonas gingivalis* participates in pathogenesis of human abdominal aortic aneurysm by neutrophil activation. Proof of concept in rats. *PLoS ONE.* (2011) 6:e18679. doi: 10.1371/journal.pone.0018679
87. Carrion J, Scisci E, Miles B, Sabino GJ, Zeituni AE, Gu Y, et al. Microbial carriage state of peripheral blood dendritic cells (DCs) in chronic periodontitis influences DC differentiation, atherogenic potential. *J Immunol.* (2012) 189:3178–87. doi: 10.4049/jimmunol.1201053
88. Wang M, Shakhatreh M-AK, James D, Liang S, Nishiyama S-I, Yoshimura F, et al. Fimbrial proteins of porphyromonas gingivalis mediate in vivo virulence and exploit TLR2 and complement receptor 3 to persist in macrophages. *J Immunol.* (2007) 179:2349–58. doi: 10.4049/jimmunol.179.4.2349
89. Sharma A, Novak EK, Sojar HT, Swank RT, Kuramitsu HK, Genco RJ. *Porphyromonas gingivalis* platelet aggregation activity: outer membrane vesicles are potent activators of murine platelets. *Oral Microbiol Immunol.* (2000) 15:393–6. doi: 10.1034/j.1399-302x.2000.150610.x
90. Nakayama K. *Porphyromonas gingivalis* cell-induced hemagglutination and platelet aggregation. *Periodontol 2000.* (2010) 54:45–52. doi: 10.1111/j.1600-0757.2010.00351.x
91. Miyakawa H, Honma K, Qi M, Kuramitsu HK. Interaction of *Porphyromonas gingivalis* with low-density lipoproteins: implications for a role for periodontitis in atherosclerosis. *J Periodontal Res.* (2004) 39:1–9. doi: 10.1111/j.1600-0765.2004.00697.x
92. Qi M, Miyakawa H, Kuramitsu HK. *Porphyromonas gingivalis* induces murine macrophage foam cell formation. *Microb Pathog.* (2003) 35:259–67. doi: 10.1016/j.micpath.2003.07.002
93. Pan Y, Teng D, Burke AC, Haase EM, Scannapieco FA. Oral bacteria modulate invasion and induction of apoptosis in HEp-2 cells by *Pseudomonas aeruginosa. Microb Pathog.* (2009) 46:73–9. doi: 10.1016/j.micpath.2008.10.012
94. Li Q, Pan C, Teng D, Lin L, Kou Y, Haase EM, et al. *Porphyromonas gingivalis* modulates *Pseudomonas aeruginosa*-induced apoptosis of respiratory epithelial cells through the STAT3 signaling pathway. *Microbes Infect.* (2014) 16:17–27. doi: 10.1007/978-3-662-43883-1
95. Flynn KJ, Baxter NT, Schloss PD. Metabolic and community synergy of oral bacteria in colorectal cancer. *mSphere.* (2016) 1:e00102-16. doi: 10.1128/mSphere.00102-16
96. Kinane DF, Riggio MP, Walker KF, MacKenzie D, Shearer B. Bacteraemia following periodontal procedures. *J Clin Periodontol.* (2005) 32:708–13. doi: 10.1111/j.1600-051X.2005.00741.x
97. Bian T, Li L, Lyu J, Cui D, Lei L, Yan F. Human beta-defensin 3 suppresses *Porphyromonas gingivalis* lipopolysaccharide-induced inflammation in RAW 264.7 cells and aortas of ApoE-deficient mice. *Peptides.* (2016) 82:92–100. doi: 10.1016/j.peptides.2016.06.002
98. Lyu J, Bian T, Chen B, Cui D, Li L, Gong L, et al. Beta-defensin 3 modulates macrophage activation and orientation during acute inflammatory response to *Porphyromonas gingivalis* lipopolysaccharide. *Cytokine.* (2017) 92:48–54. doi: 10.1016/j.cyto.2016.12.015
99. Pulendran B, Kumar P, Cutler CW, Mohamadzadeh M, Van Dyke T, Banchereau J. Lipopolysaccharides from distinct pathogens induce different classes of immune responses *in vivo*. *J Immunol.* (2001) 167:5067–76. doi: 10.4049/jimmunol.167.9.5067
100. Stoll LL, Denning GM, Weintraub NL. Potential role of endotoxin as a proinflammatory mediator of atherosclerosis. *Arterioscler Thromb Vasc Biol.* (2004) 24:2227–36. doi: 10.1161/01.ATV.0000147534.69062.dc
101. Deleon-Pennell KY, de Castro Brás LE, Lindsey ML. Circulating *Porphyromonas gingivalis* lipopolysaccharide resets cardiac homeostasis in mice through a matrix metalloproteinase-9-dependent mechanism. *Physiol Rep.* (2013) 1:e00079. doi: 10.1002/phy2.79
102. DeLeon-Pennell KY, de Castro Brás LE, Iyer RP, Bratton DR, Jin Y-F, Ripplinger CM, et al. P. gingivalis lipopolysaccharide intensifies inflammation post-myocardial infarction through matrix metalloproteinase-9. *J Mol Cell Cardiol.* (2014) 76:218–26. doi: 10.1016/j.yjmcc.2014.09.007
103. de Maat MP, Kluft C. Determinants of C-reactive protein concentration in blood. *Ital Hear J.* (2001) 2:189–95.
104. Noack B, Genco RJ, Trevisan M, Grossi S, Zambon JJ, De Nardin E. Periodontal infections contribute to elevated systemic C-reactive protein level. *J Periodontol.* (2001) 72:1221–7. doi: 10.1902/jop.2000.72.9.1221
105. Loos BG, Craandijk J, Hoek FJ, Dillen PMEW, Van Der Velden U. Elevation of systemic markers related to cardiovascular diseases in the peripheral blood of periodontitis patients. *J Periodontol.* (2000) 71:1528–34. doi: 10.1902/jop.2000.71.10.1528
106. Sahingur SE, Sharma A, Genco RJ, De Nardin E. Association of increased levels of fibrinogen and the −455G/A fibrinogen gene polymorphism with chronic periodontitis. *J Periodontol.* (2003) 74:329–37. doi: 10.1902/jop.2003.74.3.329
107. Ebersole JL, Machen RL, Steffen MJ, Willmann DE. Systemic acute-phase reactants, C-reactive protein and haptoglobin, in adult periodontitis. *Clin Exp Immunol.* (1997) 107:347–52. doi: 10.1111/j.1365-2249.1997.270-ce1162.x
108. Ricklin D, Reis ES, Lambris JD. Complement in disease: a defence system turning offensive. *Nat Rev Nephrol.* (2016) 12:383–401. doi: 10.1038/nrneph.2016.70
109. Ricklin D, Hajishengallis G, Yang K, Lambris JD. Complement: a key system for immune surveillance and homeostasis. *Nat Immunol.* (2010) 11:785–97. doi: 10.1038/ni.1923
110. Silasi-Mansat R, Zhu H, Popescu NI, Peer G, Sfyroera G, Magotti P, et al. Complement inhibition decreases the procoagulant response and confers organ protection in a baboon model of *Escherichia coli* sepsis. *Blood.* (2010) 116:1002–10. doi: 10.1182/blood-2010-02-269746
111. Wijnstok NJ, Twisk JWR, Young IS, Woodside J V, McFarlane C, McEneny J, et al. Inflammation markers are associated with cardiovascular diseases risk in adolescents: the Young Hearts project 2000. *J Adolesc Health.* (2010) 47:346–51. doi: 10.1016/j.jadohealth.2010.04.008
112. Andrukhov O, Ulm C, Reischl H, Nguyen PQ, Matejka M, Rausch-Fan X. Serum cytokine levels in periodontitis patients in relation to the bacterial load. *J Periodontol.* (2011) 82:885–92. doi: 10.1902/jop.2010.100425
113. Duarte PM, da Rocha M, Sampaio E, Mestnik MJ, Feres M, Figueiredo LC, et al. Serum levels of cytokines in subjects with generalized chronic and aggressive periodontitis before and after non-surgical periodontal therapy: a pilot study. *J Periodontol.* (2010) 81:1056–63. doi: 10.1902/jop.2010.090732
114. Schenkein HA, Koertge TE, Brooks CN, Sabatini R, Purkall DE, Tew JG. IL-17 in sera from patients with aggressive periodontitis. *J Dent Res.* (2010) 89:943–7. doi: 10.1177/0022034510369297

115. Brito LCW, DalBó S, Striechen TM, Farias JM, Olchanheski LR, Mendes RT, et al. Experimental periodontitis promotes transient vascular inflammation and endothelial dysfunction. *Arch Oral Biol.* (2013) 58:1187–98. doi: 10.1016/j.archoralbio.2013.03.009
116. Matsuda Y, Kato T, Takahashi N, Nakajima M, Arimatsu K, Minagawa T, et al. Ligature-induced periodontitis in mice induces elevated levels of circulating interleukin-6 but shows only weak effects on adipose and liver tissues. *J Periodontal Res.* (2016) 51:639–46. doi: 10.1111/jre.12344
117. Liuzzo G, Trotta F, Pedicino D. Interleukin-17 in atherosclerosis and cardiovascular disease: the good, the bad, and the unknown. *Eur Heart J.* (2013) 34:556–9. doi: 10.1093/eurheartj/ehs399
118. Gelderblom M, Weymar A, Bernreuther C, Velden J, Arunachalam P, Steinbach K, et al. Neutralization of the IL-17 axis diminishes neutrophil invasion and protects from ischemic stroke. *Blood.* (2012) 120:3793–802. doi: 10.1182/blood-2012-02-412726
119. Higashi Y, Goto C, Hidaka T, Soga J, Nakamura S, Fujii Y, et al. Oral infection-inflammatory pathway, periodontitis, is a risk factor for endothelial dysfunction in patients with coronary artery disease. *Atherosclerosis.* (2009) 206:604–10. doi: 10.1016/j.atherosclerosis.2009.03.037
120. Lundberg K, Kinloch A, Fisher BA, Wegner N, Wait R, Charles P, et al. Antibodies to citrullinated alpha-enolase peptide 1 are specific for rheumatoid arthritis and cross-react with bacterial enolase. *Arthritis Rheum.* (2008) 58:3009–19. doi: 10.1002/art.23936
121. Gully N, Bright R, Marino V, Marchant C, Cantley M, Haynes D, et al. *Porphyromonas gingivalis* peptidylarginine deiminase, a key contributor in the pathogenesis of experimental periodontal disease and experimental arthritis. *PLoS ONE.* (2014) 9:e100838. doi: 10.1371/journal.pone.0100838
122. Suwannalai P, Trouw LA, Toes REM, Huizinga TWJ. Anti-citrullinated protein antibodies (ACPA) in early rheumatoid arthritis. *Mod Rheumatol.* (2012) 22:15–20. doi: 10.3109/s10165-011-0486-8
123. Konig MF, Abusleme L, Reinholdt J, Palmer RJ, Teles RP, Sampson K, et al. Aggregatibacter actinomycetemcomitans-induced hypercitrullination links periodontal infection to autoimmunity in rheumatoid arthritis. *Sci Transl Med.* (2016) 8:369ra176. doi: 10.1126/scitranslmed.aaj1921
124. Schenkein HA, Berry CR, Burmeister JA, Brooks CN, Barbour SE, Best AM, et al. Anti-cardiolipin antibodies in sera from patients with periodontitis. *J Dent Res.* (2003) 82:919–22. doi: 10.1177/154405910308201114
125. Chen Y-W, Nagasawa T, Wara-Aswapati N, Ushida Y, Wang D, Takeuchi Y, et al. Association between periodontitis and anti-cardiolipin antibodies in Buerger disease. *J Clin Periodontol.* (2009) 36:830–5. doi: 10.1111/j.1600-051X.2009.01467.x
126. Perschinka H, Mayr M, Millonig G, Mayerl C, van der Zee R, Morrison SG, et al. Cross-reactive B-cell epitopes of microbial and human heat shock protein 60/65 in atherosclerosis. *Arterioscler Thromb Vasc Biol.* (2003) 23:1060–5. doi: 10.1161/01.ATV.0000071701.62486.49
127. Foteinos G, Afzal AR, Mandal K, Jahangiri M, Xu Q. Anti-heat shock protein 60 autoantibodies induce atherosclerosis in apolipoprotein E-deficient mice via endothelial damage. *Circulation.* (2005) 112:1206–13. doi: 10.1161/CIRCULATIONAHA.105.547414
128. Ford PJ, Gemmell E, Hamlet SM, Hasan A, Walker PJ, West MJ, et al. Cross-reactivity of GroEL antibodies with human heat shock protein 60 and quantification of pathogens in atherosclerosis. *Oral Microbiol Immunol.* (2005) 20:296–302. doi: 10.1111/j.1399-302X.2005.00230.x
129. Sandal I, Karydis A, Luo J, Prislovsky A, Whittington KB, Rosloniec EF, et al. Bone loss and aggravated autoimmune arthritis in HLA-DRβ1-bearing humanized mice following oral challenge with Porphyromonas gingivalis. *Arthritis Res Ther.* (2016) 18:249. doi: 10.1186/s13075-016-1143-6
130. Dutzan N, Kajikawa T, Abusleme L, Greenwell-Wild T, Zuazo CE, Ikeuchi T, et al. A dysbiotic microbiome triggers Th17 cells to mediate oral mucosal immunopathology in mice and humans. *Sci Transl Med.* (2018) 10:eaat0797. doi: 10.1126/scitranslmed.aat0797
131. Kugyelka R, Kohl Z, Olasz K, Mikecz K, Rauch TA, Glant TT, et al. Enigma of IL-17 and Th17 cells in rheumatoid arthritis and in autoimmune animal models of arthritis. *Mediators Inflamm.* (2016) 2016:1–11. doi: 10.1155/2016/6145810
132. Bedoya SK, Lam B, Lau K, Larkin J. Th17 cells in immunity and autoimmunity. *Clin Dev Immunol.* (2013) 2013:1–16. doi: 10.1155/2013/986789
133. Borilova Linhartova P, Kastovsky J, Lucanova S, Bartova J, Poskerova H, Vokurka J, et al. Interleukin-17A Gene Variability in Patients with Type 1 Diabetes Mellitus and Chronic Periodontitis: Its Correlation with IL-17 Levels and the Occurrence of Periodontopathic Bacteria. *Mediators Inflamm.* (2016) 2016:1–9. doi: 10.1155/2016/2979846
134. de Aquino SG, Talbot J, Sônego F, Turato WM, Grespan R, Avila-Campos MJ, et al. The aggravation of arthritis by periodontitis is dependent of IL-17 receptor A activation. *J Clin Periodontol.* (2017) 44:881–91. doi: 10.1111/jcpe.12743
135. de Aquino SG, Abdollahi-Roodsaz S, Koenders MI, van de Loo FAJ, Pruijn GJM, Marijnissen RJ, et al. Periodontal pathogens directly promote autoimmune experimental arthritis by inducing a TLR2- and IL-1-driven Th17 response. *J Immunol.* (2014) 192:4103–11. doi: 10.4049/jimmunol.1301970
136. Sato K, Takahashi N, Kato T, Matsuda Y, Yokoji M, Yamada M, et al. Aggravation of collagen-induced arthritis by orally administered *Porphyromonas gingivalis* through modulation of the gut microbiota and gut immune system. *Sci Rep.* (2017) 7:6955. doi: 10.1038/s41598-017-07196-7
137. Eskan MA, Jotwani R, Abe T, Chmelar J, Lim J-H, Liang S, et al. The leukocyte integrin antagonist Del-1 inhibits IL-17-mediated inflammatory bone loss. *Nat Immunol.* (2012) 13:465–73. doi: 10.1038/ni.2260
138. Potempa J, Mydel P, Koziel J. The case for periodontitis in the pathogenesis of rheumatoid arthritis. *Nat Rev Rheumatol.* (2017) 13:606–20. doi: 10.1038/nrrheum.2017.132
139. Munenaga S, Ouhara K, Hamamoto Y, Kajiya M, Takeda K, Yamasaki S, et al. The involvement of C5a in the progression of experimental arthritis with *Porphyromonas gingivalis* infection in SKG mice. *Arthritis Res Ther.* (2018) 20:247. doi: 10.1186/s13075-018-1744-3
140. Miyajima S, Naruse K, Kobayashi Y, Nakamura N, Nishikawa T, Adachi K, et al. Periodontitis-activated monocytes/macrophages cause aortic inflammation. *Sci Rep.* (2015) 4:5171. doi: 10.1038/srep05171
141. Cheng W-C, van Asten SD, Burns LA, Evans HG, Walter GJ, Hashim A, et al. Periodontitis-associated pathogens P. gingivalis and A. actinomycetemcomitans activate human CD14 + monocytes leading to enhanced Th17/IL-17 responses. *Eur J Immunol.* (2016) 46:2211–21. doi: 10.1002/eji.201545871
142. Kato T, Yamazaki K, Nakajima M, Date Y, Kikuchi J, Hase K, et al. Oral administration of *Porphyromonas gingivalis* alters the gut microbiome and serum metabolome. *mSphere.* (2018) 3:e00460–18. doi: 10.1128/mSphere.00460-18
143. Levy M, Kolodziejczyk AA, Thaiss CA, Elinav E. Dysbiosis and the immune system. *Nat Rev Immunol.* (2017) 17:219–32. doi: 10.1038/nri.2017.7
144. Bienenstock J, McDermott M, Befus D, O'Neill M. A common mucosal immunologic system involving the bronchus, breast and bowel. *Adv Exp Med Biol.* (1978) 107:53–9. doi: 10.1007/978-1-4684-3369-2_7
145. Wang J, Li F, Wei H, Lian Z-X, Sun R, Tian Z. Respiratory influenza virus infection induces intestinal immune injury via microbiota-mediated Th17 cell–dependent inflammation. *J Exp Med.* (2014) 211:2683. doi: 10.1084/jem.20140625
146. Ruane D, Brane L, Reis BS, Cheong C, Poles J, Do Y, et al. Lung dendritic cells induce migration of protective T cells to the gastrointestinal tract. *J Exp Med.* (2013) 210:1871–88. doi: 10.1084/jem.20122762
147. Quan FS, Compans RW, Kang SM. Oral vaccination with inactivated influenza vaccine induces cross-protective immunity. *Vaccine.* (2012) 30:180–8. doi: 10.1016/j.vaccine.2011.11.028
148. Tulic MK, Piche T, Verhasselt V. Lung-gut cross-talk: evidence, mechanisms and implications for the mucosal inflammatory diseases. *Clin Exp Allergy.* (2016) 46:519–28. doi: 10.1111/cea.12723
149. Grainger JR, Wohlfert EA, Fuss IJ, Bouladoux N, Askenase MH, Legrand F, et al. Inflammatory monocytes regulate pathologic responses to commensals during acute gastrointestinal infection. *Nat Med.* (2013) 19:713–21. doi: 10.1038/nm.3189
150. Askenase MH, Han S-JJ, Byrd AL, Morais da Fonseca D, Bouladoux N, Wilhelm C, et al. Bone-marrow-resident NK cells prime monocytes

for regulatory function during infection. *Immunity*. (2015) 42:1130–42. doi: 10.1016/j.immuni.2015.05.011
151. Griseri T, McKenzie BS, Schiering C, Powrie F. Dysregulated hematopoietic stem and progenitor cell activity promotes interleukin-23-driven chronic intestinal inflammation. *Immunity*. (2012) 37:1116–29. doi: 10.1016/j.immuni.2012.08.025
152. Faraco G, Brea D, Garcia-Bonilla L, Wang G, Racchumi G, Chang H, et al. Dietary salt promotes neurovascular and cognitive dysfunction through a gut-initiated TH17 response. *Nat Neurosci.* (2018) 21:240–9. doi: 10.1038/s41593-017-0059-z
153. Croxford AL, Lanzinger M, Hartmann FJ, Schreiner B, Mair F, Pelczar P, et al. The cytokine GM-CSF drives the inflammatory signature of CCR2+ monocytes and licenses autoimmunity. *Immunity*. (2015) 43:502–14. doi: 10.1016/j.immuni.2015.08.010
154. Krieg a M, Love-Homan L, Yi a K, Harty JT. CpG DNA induces sustained IL-12 expression *in vivo* and resistance to *Listeria monocytogenes* challenge. *J Immunol.* (1998) 161:2428–34.
155. Siracusa MC, Saenz SA, Tait Wojno ED, Kim BS, Osborne LC, Ziegler CG, et al. Thymic stromal lymphopoietin-mediated extramedullary hematopoiesis promotes allergic inflammation. *Immunity*. (2013) 39:1158–70. doi: 10.1016/j.immuni.2013.09.016
156. Katayama Y, Battista M, Kao W-M, Hidalgo A, Peired AJ, Thomas SA, et al. Signals from the sympathetic nervous system regulate hematopoietic stem cell egress from bone marrow. Cell. (2006) 124:407–21. doi: 10.1016/j.cell.2005.10.041
157. Maryanovich M, Zahalka AH, Pierce H, Pinho S, Nakahara F, Asada N, et al. Adrenergic nerve degeneration in bone marrow drives aging of the hematopoietic stem cell niche. *Nat Med*. (2018) 24:1–10. doi: 10.1038/s41591-018-0030-x
158. Lucas D, Scheiermann C, Chow A, Kunisaki Y, Bruns I, Barrick C, et al. Chemotherapy-induced bone marrow nerve injury impairs hematopoietic regeneration. *Nat Med.* (2013) 19:695–703. doi: 10.1038/nm.3155
159. Courties G, Herisson F, Sager HB, Heidt T, Ye Y, Wei Y, et al. Ischemic stroke activates hematopoietic bone marrow stem cells. Circ Res. (2015) 116:407–17. doi: 10.1161/CIRCRESAHA.116.305207
160. Liu Q, Jin W-N, Liu Y, Shi K, Sun H, Zhang F, et al. Brain ischemia suppresses immunity in the periphery and brain via different neurogenic innervations. *Immunity*. (2017) 46:474–87. doi: 10.1016/j.immuni.2017.02.015
161. Gadani SP, Walsh JT, Zheng J, Kipnis J, Smirnov I. The glia-derived alarmin IL-33 orchestrates the immune response and promotes recovery following CNS injury. *Neuron.* (2015) 85:703–9. doi: 10.1016/j.neuron.2015.01.013
162. Kim ND, Luster AD. The role of tissue resident cells in neutrophil recruitment. *Trends Immunol.* (2015) 36:547–55. doi: 10.1016/j.it.2015.07.007
163. Walsh JT, Hendrix S, Boato F, Smirnov I, Zheng J, Lukens JR, et al. MHCII-independent CD4+ T cells protect injured CNS neurons via IL-4. *J Clin Invest.* (2015) 125:699–714. doi: 10.1172/JCI76210
164. Filiano AJ, Xu Y, Tustison NJ, Marsh RL, Baker W, Smirnov I, et al. Unexpected role of interferon-γ in regulating neuronal connectivity and social behaviour. *Nature.* (2016) 535:425–9. doi: 10.1038/nature18626
165. Vainchtein ID, Chin G, Cho FS, Kelley KW, Miller JG, Chien EC, et al. Astrocyte-derived interleukin-33 promotes microglial synapse engulfment and neural circuit development. *Science*. (2018) 359:1269–73. doi: 10.1126/science.aal3589
166. Borovikova L V, Ivanova S, Zhang M, Yang H, Botchkina GI, Watkins LR, et al. Vagus nerve stimulation attenuates the systemic inflammatory response to endotoxin. *Nature.* (2000) 405:458–62. doi: 10.1038/35013070
167. Pavlov VA, Parrish WR, Rosas-Ballina M, Ochani M, Puerta M, Ochani K, et al. Brain acetylcholinesterase activity controls systemic cytokine levels through the cholinergic anti-inflammatory pathway. *Brain Behav Immun*. (2009) 23:41–5. doi: 10.1016/j.bbi.2008.06.011
168. Cunin P, Caillon A, Corvaisier M, Garo E, Scotet M, Blanchard S, et al. The tachykinins substance P and hemokinin-1 favor the generation of human memory Th17 cells by inducing IL-1 , IL-23, and TNF-Like 1A expression by monocytes. *J Immunol.* (2011) 186:4175–82. doi: 10.4049/jimmunol.1002535
169. Pereira MMA, Mahú I, Seixas E, Martinéz-Sánchez N, Kubasova N, Pirzgalska RM, et al. A brain-sparing diphtheria toxin for chemical genetic ablation of peripheral cell lineages. *Nat Commun.* (2017) 8:14967. doi: 10.1038/ncomms14967
170. Cardoso V, Chesné J, Ribeiro H, García-Cassani B, Carvalho T, Bouchery T, et al. Neuronal regulation of type 2 innate lymphoid cells via neuromedin U. *Nature*. (2017) 549:277–81. doi: 10.1038/nature23469
171. Méndez-Ferrer S, Lucas D, Battista M, Frenette PS. Haematopoietic stem cell release is regulated by circadian oscillations. *Nature.* (2008) 452:442–7. doi: 10.1038/nature06685
172. Hanoun M, Maryanovich M, Arnal-Estapé A, Frenette PS. Neural regulation of hematopoiesis, inflammation, and cancer. *Neuron*. (2015) 86:360–73. doi: 10.1016/j.neuron.2015.01.026
173. Vasamsetti SB, Florentin J, Coppin E, Stiekema LCA, Zheng KH, Nisar MU, et al. Sympathetic neuronal activation triggers myeloid progenitor proliferation and differentiation. *Immunity*. (2018) 49:93–106.e7. doi: 10.1016/j.immuni.2018.05.004
174. Yamazaki S, Ema H, Karlsson G, Yamaguchi T, Miyoshi H, Shioda S, et al. Nonmyelinating schwann cells maintain hematopoietic stem cell hibernation in the bone marrow niche. *Cell.* (2011) 147:1146–58. doi: 10.1016/j.cell.2011.09.053
175. McCulloch L, Smith CJ, McColl BW. Adrenergic-mediated loss of splenic marginal zone B cells contributes to infection susceptibility after stroke. *Nat Commun.* (2017) 8:15051. doi: 10.1038/ncomms16151
176. Prass K, Meisel C, Höflich C, Braun J, Halle E, Wolf T, et al. Stroke-induced immunodeficiency promotes spontaneous bacterial infections and is mediated by sympathetic activation reversal by poststroke T helper cell type 1-like immunostimulation. *J Exp Med.* (2003) 198:725–36. doi: 10.1084/jem.20021098
177. Wong CHY, Jenne CN, Lee W-Y, Leger C, Kubes P. Functional innervation of hepatic iNKT cells is immunosuppressive following stroke. *Science*. (2011) 334:101–5. doi: 10.1126/science.1210301
178. Chesné J, Cardoso V, Veiga-Fernandes H. Neuro-immune regulation of mucosal physiology. *Mucosal Immunol.* (2018) 12:10–20. doi: 10.1038/s41385-018-0063-y
179. Veiga-Fernandes H, Mucida D. Neuro-immune interactions at barrier surfaces. *Cell.* (2016) 165:801–11. doi: 10.1016/j.cell.2016.04.041
180. Yoo BB, Mazmanian SK. The enteric network: interactions between the immune and nervous systems of the gut. *Immunity*. (2017) 46:910–26. doi: 10.1016/j.immuni.2017.05.011
181. Gabanyi I, Muller PA, Feighery L, Oliveira TY, Costa-Pinto FA, Mucida D. Neuro-immune interactions drive tissue programming in intestinal macrophages. *Cell.* (2016) 164:378–91. doi: 10.1016/j.cell.2015.12.023
182. Klose CSN, Mahlakõiv T, Moeller JB, Rankin LC, Flamar A-L, Kabata H, et al. The neuropeptide neuromedin U stimulates innate lymphoid cells and type 2 inflammation. *Nature.* (2017) 549:282–6. doi: 10.1038/nature23676
183. Wallrapp A, Riesenfeld SJ, Burkett PR, Abdulnour R-EE, Nyman J, Dionne D, et al. The neuropeptide NMU amplifies ILC2-driven allergic lung inflammation. *Nature.* (2017) 549:351–6. doi: 10.1038/nature24029
184. Oetjen LK, Mack MR, Feng J, Whelan TM, Niu H, Guo CJ, et al. Sensory neurons co-opt classical immune signaling pathways to mediate chronic itch. *Cell.* (2017) 217–28. doi: 10.1016/j.cell.2017.08.006
185. Trompette A, Gollwitzer ES, Pattaroni C, Lopez-Mejia IC, Riva E, Pernot J, et al. Dietary fiber confers protection against Flu by shaping Ly6c–patrolling monocyte hematopoiesis and CD8+T cell metabolism. *Immunity*. (2018) 48:992–1005. doi: 10.1016/j.immuni.2018.04.022
186. Jung S. Macrophages and monocytes in 2017: macrophages and monocytes: of tortoises and hares. *Nat Rev Immunol.* (2018) 18:85–6. doi: 10.1038/nri.2017.158
187. van der Meer JWM, Joosten LAB, Riksen N, Netea MG. Trained immunity: a smart way to enhance innate immune defence. *Mol Immunol.* (2015) 68:40–4. doi: 10.1016/j.molimm.2015.06.019
188. Ginhoux F, Guilliams M. Tissue-resident macrophage ontogeny and homeostasis. *Immunity*. (2016) 44:439–49. doi: 10.1016/j.immuni.2016.02.024

189. Davies LC, Jenkins SJ, Allen JE, Taylor PR. Tissue-resident macrophages. *Nat Immunol.* (2013) 14:986–95. doi: 10.1038/ni.2705
190. Mitroulis I, Ruppova K, Wang B, Chen L-S, Grzybek M, Grinenko T, et al. Modulation of myelopoiesis progenitors is an integral component of trained immunity. *Cell.* (2018) 172:147–61. doi: 10.1016/j.cell.2017.11.034
191. Netea MG, Joosten LABB, Latz E, Mills KHGG, Natoli G, Stunnenberg HG, et al. Trained immunity: a program of innate immune memory in health and disease. *Science.* (2016) 352:aaf1098. doi: 10.1126/science.aaf1098
192. Takizawa H, Boettcher S, Manz MG. Demand-adapted regulation of early hematopoiesis in infection and inflammation. *Blood.* (2012) 119:2991–3002. doi: 10.1182/blood-2011-12-380113
193. Bekkering S, Arts RJW, Novakovic B, Kourtzelis I, van der Heijden CDCC, Li Y, et al. Metabolic induction of trained immunity through the mevalonate pathway. *Cell.* (2018) 172:135–146.e9. doi: 10.1016/j.cell.2017.11.025
194. Quintin J, Saeed S, Martens JHA, Giamarellos-Bourboulis EJ, Ifrim DC, Logie C, et al. Candida albicans infection affords protection against reinfection via functional reprogramming of monocytes. *Cell Host Microbe.* (2012) 12:223–2. doi: 10.1016/j.chom.2012.06.006
195. Saeed S, Quintin J, Kerstens HHD, Rao NA, Aghajanirefah A, Matarese F, et al. Epigenetic programming of monocyte-to-macrophage differentiation and trained innate immunity. *Science.* (2014) 345:1251086 doi: 10.1126/science.1251086
196. Nagasawa T, Kobayashi H, Aramaki M, Kiji M, Oda S, Izumi Y. Expression of CD14, CD16 and CD45RA on monocytes from periodontitis patients. *J Periodontal Res.* (2004) 39:72–8. doi: 10.1111/j.1600-0765.2004.00713.x
197. Nicu EA, Van Der Velden U, Everts V, Loos BG. Expression of FcγRs and mCD14 on polymorphonuclear neutrophils and monocytes may determine periodontal infection. *Clin Exp Immunol.* (2008) 154:177–86. doi: 10.1111/j.1365-2249.2008.03751.x
198. Carneiro VMA, Bezerra ACB, Guimarães M do CM, Muniz-Junqueira MI. Decreased phagocytic function in neutrophils and monocytes from peripheral blood in periodontal disease. *J Appl Oral Sci.* (2012) 20:503–9. doi: 10.1590/S1678-77572012000500002
199. Payne JB, Peluso Jr. JF, Nichols FC. Longitudinal evaluation of peripheral blood monocyte secretory function in periodontitis-resistant and periodontitis-susceptible patients. *Arch Oral Biol.* (1993) 38:309–17. doi: 10.1016/0003-9969(93)90138-C
200. Gill N, Wlodarska M, Finlay BB. The future of mucosal immunology: Studying an integrated system-wide organ. *Nat Immunol.* (2010) 11:558–60. doi: 10.1038/ni0710-558
201. McDermott MR, Bienenstock J. Evidence for a common mucosal immunologic system. I. Migration of B immunoblasts into intestinal, respiratory, and genital tissues. *J Immunol.* (1979) 122:1892–8.
202. Tacket CO, Losonsky G, Nataro JP, Cryz SJ, Edelman R, Kaper JB, et al. Onset and duration of protective immunity in challenged volunteers after vaccination with live oral cholera vaccine CVD 103-HgR. *J Infect Dis.* (1992) 166:837–41. doi: 10.1093/infdis/166.4.837
203. Chen SC, Jones DH, Fynan EF, Farrar GH, Clegg JC, Greenberg HB, et al. Protective immunity induced by oral immunization with a rotavirus DNA vaccine encapsulated in microparticles. *J Virol.* (1998) 72:5757–61.
204. Singh V, Sadler R, Heindl S, Llovera G, Roth S, Benakis C, et al. The gut microbiome primes a cerebroprotective immune response after stroke. *J Cereb Blood Flow Metab.* (2018) 38:1293–8. doi: 10.1177/0271678X18780130
205. Sampson TR, Debelius JW, Thron T, Janssen S, Shastri GG, Ilhan ZE, et al. Gut microbiota regulate motor deficits and neuroinflammation in a model of Parkinson's disease. *Cell.* (2016) 167:1469–80. doi: 10.1016/j.cell.2016.11.018
206. Kigerl KA, Hall JCE, Wang L, Mo X, Yu Z, Popovich PG. Gut dysbiosis impairs recovery after spinal cord injury. *J Exp Med.* (2016) 213:2603–20. doi: 10.1084/jem.20151345
207. Sze MA, Dimitriu PA, Hayashi S, Elliott WM, McDonough JE, Gosselink J V, et al. The lung tissue microbiome in chronic obstructive pulmonary disease. *Am J Respir Crit Care Med.* (2012) 185:1073–80. doi: 10.1164/rccm.201111-2075OC
208. Spencer SP, Wilhelm C, Yang Q, Hall JA, Bouladoux N, Boyd A, et al. Adaptation of innate lymphoid cells to a micronutrient deficiency promotes type 2 barrier immunity. *Science.* (2014) 343:432–7. doi: 10.1126/science.1247606
209. Hall JA, Cannons JL, Grainger JR, Dos Santos LM, Hand TW, Naik S, et al. Essential role for retinoic acid in the promotion of CD4+ T cell effector responses via retinoic acid receptor alpha. *Immunity.* (2011) 34:435–47. doi: 10.1016/j.immuni.2011.03.003
210. Furusawa Y, Obata Y, Fukuda S, Endo TA, Nakato G, Takahashi D, et al. Commensal microbe-derived butyrate induces the differentiation of colonic regulatory T cells. *Nature.* (2013) 504:446–50. doi: 10.1038/nature12721
211. Nadjsombati MS, McGinty JW, Lyons-Cohen MR, Jaffe JB, DiPeso L, Schneider C, et al. Detection of succinate by intestinal tuft cells triggers a type 2 innate immune circuit. *Immunity.* (2018) 49:33–41.e7. doi: 10.1016/j.immuni.2018.06.016
212. Rothhammer V, Borucki DM, Tjon EC, Takenaka MC, Chao C-C, Ardura-Fabregat A, et al. Microglial control of astrocytes in response to microbial metabolites. *Nature.* (2018) 557:724–8. doi: 10.1038/s41586-018-0119-x
213. Olson CA, Vuong HE, Yano JM, Liang QY, Nusbaum DJ, Hsiao EY. The gut microbiota mediates the anti-seizure effects of the ketogenic diet. *Cell.* (2018) 173:1728–41. doi: 10.1016/j.cell.2018.04.027
214. Sharon G, Sampson TR, Geschwind DH, Mazmanian SK. The central nervous system and the gut microbiome. *Cell.* (2016) 167:915–32. doi: 10.1016/j.cell.2016.10.027
215. Trompette A, Gollwitzer ES, Yadava K, Sichelstiel AK, Sprenger N, Ngom-Bru C, et al. Gut microbiota metabolism of dietary fiber influences allergic airway disease and hematopoiesis. *Nat Med.* (2014) 20:159–66. doi: 10.1038/nm.3444
216. Thorburn AN, McKenzie CI, Shen S, Stanley D, Macia L, Mason LJ, et al. Evidence that asthma is a developmental origin disease influenced by maternal diet and bacterial metabolites. *Nat Commun.* (2015) 6:7320. doi: 10.1038/ncomms8320
217. Maji A, Misra R, Dhakan DB, Gupta V, Mahato NK, Saxena R, et al. Gut microbiome contributes to impairment of immunity in pulmonary tuberculosis patients by alteration of butyrate and propionate producers. *Environ Microbiol.* (2018) 20:402–19. doi: 10.1111/1462-2920.14015
218. McAleer JP, Kolls JK. Contributions of the intestinal microbiome in lung immunity. *Eur J Immunol.* (2018) 48:39–49. doi: 10.1002/eji.201646721
219. Abt MC, Osborne LC, Monticelli LA, Doering TA, Alenghat T, Sonnenberg GF, et al. Commensal bacteria calibrate the activation threshold of innate antiviral immunity. *Immunity.* (2012) 37:158–70. doi: 10.1016/j.immuni.2012.04.011
220. Yu X, Shahir A-M, Sha J, Feng Z, Eapen B, Nithianantham S, et al. Short-chain fatty acids from periodontal pathogens suppress histone deacetylases, EZH2, and SUV39H1 to promote Kaposi's sarcoma-associated herpesvirus replication. *J Virol.* (2014) 88:4466–79. doi: 10.1128/JVI.03326-13
221. Lu R, Meng H, Gao X, Xu L, Feng X. Effect of non-surgical periodontal treatment on short chain fatty acid levels in gingival crevicular fluid of patients with generalized aggressive periodontitis. *J Periodontal Res.* (2014) 49:574–83. doi: 10.1111/jre.12137
222. Abe K. Butyric acid induces apoptosis in both human monocytes and lymphocytes equivalently. *J Oral Sci.* (2012) 54:7–14. doi: 10.2334/josnusd.54.7
223. Cueno ME, Saito Y, Ochiai K. Periodontal disease level-butyric acid amounts locally administered in the rat gingival mucosa induce ER stress in the systemic blood. *Microb Pathog.* (2015) 94:70–5. doi: 10.1016/j.micpath.2015.10.021
224. Kilian M, Chapple ILC, Hannig M, Marsh PD, Meuric V, Pedersen AML, et al. The oral microbiome - an update for oral healthcare professionals. *Br Dent J.* (2016) 221:657–66. doi: 10.1038/sj.bdj.2016.865
225. Duncan C, Dougall H, Johnston P, Green S, Brogan R, Leifert C, et al. Chemical generation of nitric oxide in the mouth from the enterosalivary circulation of dietary nitrate. *Nat Med.* (1995) 1:546–51. doi: 10.1038/nm0695-546
226. Bryan NS, Loscalzo J. *Nitrite and Nitrate in Human Health and Disease.* Cham: Springer International Publishing (2017). doi: 10.1007/978-3-319-46189-2

227. Kapil V, Haydar SMA, Pearl V, Lundberg JO, Weitzberg E, Ahluwalia A. Physiological role for nitrate-reducing oral bacteria in blood pressure control. *Free Radic Biol Med.* (2013) 55:93–100. doi: 10.1016/j.freeradbiomed.2012.11.013
228. Bondonno CP, Liu AH, Croft KD, Considine MJ, Puddey IB, Woodman RJ, et al. Antibacterial mouthwash blunts oral nitrate reduction and increases blood pressure in treated hypertensive men and women. *Am J Hypertens.* (2015) 28:572–5. doi: 10.1093/ajh/hpu192
229. Lundberg JO, Govoni M. Inorganic nitrate is a possible source for systemic generation of nitric oxide. *Free Radic Biol Med.* (2004) 37:395–400. doi: 10.1016/S0891-5849(04)00348-X

Conflict of Interest Statement: The authors declare that the research was conducted in the absence of any commercial or financial relationships that could be construed as a potential conflict of interest.

frontiers in Immunology

REVIEW
published: 29 November 2019
doi: 10.3389/fimmu.2019.02530

Mucosal Immunity and the FOXO1 Transcription Factors

Dana T. Graves and Tatyana N. Milovanova*

Department of Periodontics, School of Dental Medicine, University of Pennsylvania, Philadelphia, PA, United States

FOXO1 transcription factors affect a number of cell types that are important in the host response. Cell types whose functions are modulated by FOXO1 include keratinocytes in the skin and mucosal dermis, neutrophils and macrophages, dendritic cells, Tregs and B-cells. FOXO1 is activated by bacterial or cytokine stimulation. Its translocation to the nucleus and binding to promoter regions of genes that have *FOXO* response elements is stimulated by the MAP kinase pathway and inhibited by the PI3 kinase/AKT pathway. Downstream gene targets of FOXO1 include pro-inflammatory signaling molecules (TLR2, TLR4, IL-1β, and TNF-α), wound healing factors (TGF-β, VEGF, and CTGF) adhesion molecules (integrins-β1, -β3, -β6, $\alpha_v\beta_3$, CD11b, CD18, and ICAM-1), chemokine receptors (CCR7 and CXCR2), B cell regulators (APRIL and BLYS), T-regulatory modulators (Foxp3 and CTLA-4), antioxidants (GPX-2 and cytoglobin), and DNA repair enzymes (GADD45α). Each of the above cell types are found in oral mucosa and modulated by bacteria or an inflammatory microenvironment. FOXO1 contributes to the regulation of these cells, which collectively maintain and repair the epithelial barrier, formation and activation of Tregs that are needed to resolve inflammation, mobilization, infiltration, and activation of anti-bacterial defenses in neutrophils, and the homing of dendritic cells to lymph nodes to induce T-cell and B-cell responses. The goal of the manuscript is to review how the transcription factor, FOXO1, contributes to the activation and regulation of key leukocytes needed to maintain homeostasis and respond to bacterial challenge in oral mucosal tissues. Examples are given with an emphasis on lineage specific deletion of *Foxo1* to explore the impact of FOXO1 on cell behavior, inflammation and susceptibility to infection.

Keywords: bacteria, bone loss, forkhead, gingiva, immune, mucosa, periodontal disease, periodontitis

OPEN ACCESS

Edited by:
Avi-Hai Hovav,
Hebrew University of Jerusalem, Israel

Reviewed by:
Richard Lamont,
University of Louisville, United States
Nicolas Dutzan,
University of Chile, Chile

****Correspondence:***
Dana T. Graves
dtgraves@upenn.edu

Specialty section:
This article was submitted to Mucosal Immunity, a section of the journal Frontiers in Immunology

Received: *25 June 2018*
Accepted: *11 October 2019*
Published: *29 November 2019*

Citation:
Graves DT and Milovanova TN (2019) Mucosal Immunity and the FOXO1 Transcription Factors. Front. Immunol. 10:2530. doi: 10.3389/fimmu.2019.02530

Forkhead box-O (FOXO) transcription factors were first identified in Drosophila melanogaster (1). There are four members of this family in mammals, three of which (FOXO1, FOXO3, and FOXO4) have conserved sequence homologies while FOXO6 is more distantly related (2). FOXO proteins regulate cell survival and apoptosis, proliferation, energy metabolism, oxidative stress responses, and its mutations are closely linked to cancer formation (1, 3). FOXO1, FOXO3, and FOXO4 often have common target genes and function. However, there are differences that are related to interaction with different co-activators and co-repressors. For example, global *Foxo1* deletion in mice is embryonically lethal in contrast to global ablation of *Foxo3* or *Foxo4*, which is not. The biological functions of FOXOs can overlap but are not necessarily redundant. FOXOs act primarily as transcription factors following translocation to the nucleus but can sometimes have "off target" effects as co-regulators in the nucleus or by binding to other proteins in the cytoplasm (4).

FOXOs are controlled at several levels including expression, nuclear translocation, DNA binding and interaction with other proteins. FOXOs have four primary domains with the following functions: (a) DNA binding, (b) nuclear localization, (c) nuclear export, and (d) transactivation. FOXOs recognize two consensus response elements: a Daf-16 binding site (5′-GTAAA (T/C)AA) and an insulin-response element (5′-(C/A)(A/C)AAA(C/T)AA) (1). The core DNA sequence 5′-(A/C)AA(C/T)A is recognized by all FOXO-family members. FOXO post-translational modification involves acetylation, phosphorylation, ubiquitination, methylation, and glycosylation (1). The modifications affect nuclear translocation or exit from the nucleus, DNA binding, and interaction with co-repressors and co-activators (5). Kinases/phosphatases and acetylases/deacetylases modulate shuttling of FOXOs to and from the nucleus. FOXO1 nuclear localization and resulting transcriptional activity is downregulated by phosphorylation from insulin stimulation via the phosphoinositide-3-kinase/AKT pathway or conversely, up-regulated by phosphorylation at different aminoacids through RAS/mitogen-activated protein kinase activity (1). Deacetylation of FOXO1 typically enhances nuclear localization and activity while they are reduced by acetylation (6). Generally, the level of FOXO1 nuclear localization is proportional to its activity. However, we have found that high glucose increases FOXO1 nuclear localization but reduces induction of specific genes (TGF-β and VEGF) by reducing its binding to the promoter regions despite increased nuclear localization (7–10). In fact, FOXO1 can bind to specific molecules to act as part of a co-repressor or co-activator complex (11). In this regard it is not always simple to predict the impact of FOXO1 on a given activity since its function his highly modified by post-translational modification and interaction with other partners.

FOXOs play a key role in maintaining homeostasis and in adapting to environmental changes (2). Since FOXO1 is the best studied of the FOXO family it is the focus of this review. FOXO1 may have an important role in regulating several aspects of mucosal immunity by affecting dendritic cells (12), macrophage and neutrophil recruitment and activation (13–15), as well as T-helper cell and B-lymphocyte development and function (16–18). FoxO1 also affects immune responses by controlling cytokine production (19) and protecting hematopoietic stems cells from oxidative stress (20). In addition, FOXO1 regulates important aspects of keratinocyte function and potentially has a role in maintaining or repairing epithelial barrier function (21, 22). Surprisingly FOXO1 can have a specific effect under normal conditions and opposite effect in other conditions such those in diabetes and can have cell specific responses (21, 23). Thus, it is often difficult to predict the impact of FOXO1 and its role under various conditions. These studies demonstrate the complex nature of FOXO1 and its responsiveness to the cellular microenvironment, suggesting that it is highly regulated by epigenetic factors such as high glucose or those where oxidative stress is high. This is likely to be a fruitful area of future research.

Abbreviations: FOXO 1, Forkhead box protein O1; TNF alpha, Tumor Necrosis factor alpha; TGF beta, transforming Growth factor; VEGF, Vascular Endothelial Growth factor; CTGF, Connective Tissue Growth Factor; APRIL, A-proliferation-inducing ligand; BLYS, B-lymphocyte Stimulator; ICAM-1, Intercellular Adhesion Molecule; GPX2, Glutathione peroxidase 2; GADD45a, Growth Arrest And DNA Damage Inducible Alpha; CCR7-C, C chemokine receptor type 7; Il-6, Interleukin 6; RANKL, Receptor activator of nuclear factor kappa-B ligand; DCs, Dendritic cells; Ly, Lymphocyte antigen; ROS, Reactive oxygen species; HO-1, Heme oxygenase 1; PD-L1, Programmed death-ligand 1; TLR, Toll like receptor; PDL-cells, periodontal ligament cells.

PERIODONTAL DISEASE PATHOGENESIS

Periodontal disease is an inflammatory disease that is initiated by bacteria that forms a biofilm on the tooth surface and includes gingivitis consisting of gingival inflammation but not bone loss and periodontitis that leads to a net loss of bone (24–26). Periodontitis is recognized as the most prevalent lytic bone disorder in humans and the most common cause of tooth loss in adults in developed countries. In addition, periodontal disease, particularly periodontitis is linked to other chronic diseases such as rheumatoid arthritis, cardiovascular disease, and insulin resistance associated with type 2 diabetes (26). When bacteria or their products encounter leukocytes the host response is activated. Although periodontal disease is considered a destructive process it should be kept in mind that it represents corollary damage resulting from an effective host response that limits spread of bacteria (27–29). This concept is supported by findings that a combined *TLR2/TLR4* deletion that impairs the host response reduces periodontal bone resorption but increases systemic dissemination of oral bacteria (27). Another line of evidence that supports this conclusion is the limited colonization of gingival tissues by bacteria, indicative of the effectiveness of the host response in clearing bacteria despite the continual presence of bacteria in the gingival sulcus (28). However, when the host response is sufficiently compromised bacteria can invade the gingival tissues effectively (28). Further support comes from studies which demonstrate that there is very little damage caused directly by periodontal pathogens *in vivo* and that most of the damage occurs indirectly from the host response (29, 30). Thus, under typical conditions the bacteria are not sufficiently robust compared to the host defense and are prevented from colonizing gingival connective tissues and directly causing damage (27–29). A key component of the transition from gingivitis to periodontitis is the movement of inflammation from a sub-epithelial compartment toward bone (31). The proximity of inflammatory mediators to osteocytes/osteoblasts and PDL cells leads to the induction of RANKL by these cells as well as inhibition of coupled bone formation and periodontal bone loss (32, 33). Several mechanisms may facilitate this transition including a bacterial dysbiosis, bacterial penetration to connective tissue, ineffective removal of bacteria or their products, inadequate function of several cell types including neutrophils and dendritic cells, lack of adequate stimulation of Th2 and T-regulatory lymphocyte responses, hyper-activation of a Th1 and Th17 responses and failure to down regulate inflammation through various mechanisms (34–41). The importance of an adequate host response to bacterial challenge has been shown by increased

susceptibility to periodontitis in mice with genetic deletion of specific genes that regulate leukocyte recruitment such as *Icam-1, P-selectin, Beta2-integrin/CD18*; recognition of bacteria by *TLR2, TLR4, Lamp-2*; immune modulation by *Cxcr2, Ccr4, IL-10, OPG, IL1RA, TNF-α receptor, IL-17 receptor, Socs3, Foxo1*; and deletion of genes that encode proteolytic enzymes including *Mmp8 and Plasmin* (42). The adaptive immune response produces inflammatory mediators that stimulate apoptosis in osteoblasts through a mechanism involving activation of FOXO1 in osteoblasts and suppression of coupled bone formation, an important component of periodontal bone loss (19, 39).

KERATINOCYTES AND FOXO1

An epithelial barrier separates the gingival connective tissue from the external environment and protects it from bacterial colonization (43). It consists primarily of keratinocytes, which are separated from the connective tissue by a basement membrane. Epithelial cells produce cell to cell junctions, inflammatory cytokines, and elaborate anti-microbial peptides that limit bacterial invasion (44). *In vitro*, oral bacteria are able to pass the epithelial barrier via different paths: *Porphyromonas gingivalis* (*Pg*) can invade by intracellular spread from epithelial cell to epithelial cell, *Aggregatibacter* actinomycetemcomitans (*Aa*), and Fusobacterium nucleatum (*Fn*) move between epithelial cells. In contrast, Streptococcus gordonii (*Sg*) is predominantly associated with the superficial cell layer (45). Transcription factors such as FOXO1 play important roles the response of keratinocytes to perturbation by bacteria or wounding (22, 46–48). *Porphyromonas gingivalis* stimulates an increase in FoxO1 expression and has multiple effects on gingival epithelium including a loss of barrier function (47). FOXO1 is needed for keratinocytes to maintain expression of integrins beta-1, beta-3, and beta-6, which may be critical to maintaining barrier function (47). FOXO1 has also been shown to mediate keratinocyte responses to bacteria. For example, FOXO1 mediates *Porphyromonas gingivalis*-stimulated expression of antioxidants (catalase, superoxide dismutase, and peroxiredoxin 3) (48). *Porphyromonas gingivalis* activates FOXO1 by inducing the production of ROS, which in turn stimulates JNK activation and presumably stimulates FOXO1 nuclear localization (48). Surprisingly, knockdown of FOXO1 under basal conditions increases IL-1β production suggesting that FOXO1 in the absence of an inflammatory stimulus acts to restrain inflammation (48). Short-term exposure of keratinocytes to *Porphyromonas gingivalis* reduces apoptosis, while long-term exposure increases keratinocyte cell death. *Porphyromonas gingivalis*-stimulated apoptosis under the latter conditions is FOXO1 dependent (47).

Several classes of genes expressed by keratinocytes are FOXO1 dependent including keratin-1, -10, -14, and involucrin, which are expressed in differentiated keratinocytes (47). Similarly, genes that maintain barrier function such as integrin beta-1, -3, and -6 are FOXO1 regulated (47). Thus, FOXO1 affects several genes that affect keratinocyte behavior that potentially modulate barrier function and are needed for cell to cell adhesion or adhesion to matrix proteins.

Upon wounding keratinocytes respond quickly to re-epithelialize the wounded surface. Wound healing increases FoxO1 nuclear-localization in keratinocytes to promote re-epithelialization (49). TGF- β is quickly released upon wounding. FoxO1 mediates the effect of TGF-β on keratinocytes (50) and FoxO1 is needed to upregulate TGF-β expression in keratinocytes during wound healing suggesting a reciprocal relationship (49). TGF-β promotes epithelial migration to cover the wound surface and without adequate TGF-β signaling re-epithelialization is compromised. Other components in epithelial cell migration are induced by FoxO1 during wounding including integrin-β3 and -β6 and MMP-3 and -9. Furthermore, FOXO1 promotes re-epithelialization by increasing resistance to oxidative stress through the induction genes with anti-oxidant activity [e.g., glutathione peroxidase 2 (GPX-2) and cytoglobin] and which repair damaged DNA (e.g., growth arrest and DNA damage inducible 45α, GADD45α) (49). This is significant since high levels of ROS interfere with keratinocyte function and compromise re-epithelialization (49). In the absence of FOXO1 keratinocyte apoptosis is also increased during healing and associated with increased oxidative stress (49). **Figure 1** presents a summary of FOXO1 downstream gene targets and their potential effect on keratinocyte function.

The above functions of FOXO1 have been shown to occur in re-epithelialization of the wounded skin. Studies have also demonstrated that FoxO1 is required for mucosal re-epithelialization. FOXO1 expression in keratinocytes is needed for repair of injured mucosa under normal conditions. In a diabetic environment FOXO1 has the opposite effect as shown by improved migration of mucosal keratinocytes and improved re-epithelialization in diabetic mice with keratinocyte specific *Foxo1* ablation (7). A potential mechanism involves the altered expression of FOXO1 downstream target genes based on glycemic levels. For example, hyperglycemia *in vivo* and in high glucose *in vitro* increase FOXO1 interactions response elements in chemokine CCL20 and interleukin-36γ promoters that increase transcription in a FOXO1-dependent manner. High levels of CCL20 and IL-36γ stimulated by high glucose interfere with keratinocyte migration. Thus, in high glucose FOXO1 fails to induce TGF-β, which can enhance keratinocyte migration and instead causes excessive production of CCl20 and IFNγ, which inhibit migration (7). Thus, the glucose environment changes the activity of FOXO1 so that it promotes mucosal epithelialization under normal conditions but causes a shift in its induction of downstream targets that at to inhibit re-epithelialization.

FoxO1 activity in keratinocytes may also affect the underlying connective tissue. It has been shown that expression of VEGF in keratinocytes is dependent on *Foxo1* (9) since its deletion reduces VEGF expression and keratinocyte-stimulated angiogenesis in the underlying connective tissue *in vivo*. Furthermore, FOXO1 induces TGF-β and CTGF in keratinocytes and *Foxo1* ablation in keratinocytes reduces the number of mesenchymal stem cells and fibroblasts *in vivo* (51). These results suggest that FOXO1 is an important transcription factor in epithelium that participates in connective healing by the production of growth factors such as VEGF, TGF-β, and CTGF. In contrast, the role of FOXO1 in organizing the mucosal keratinocyte response to microbial challenge is not as well understood although it is evident that

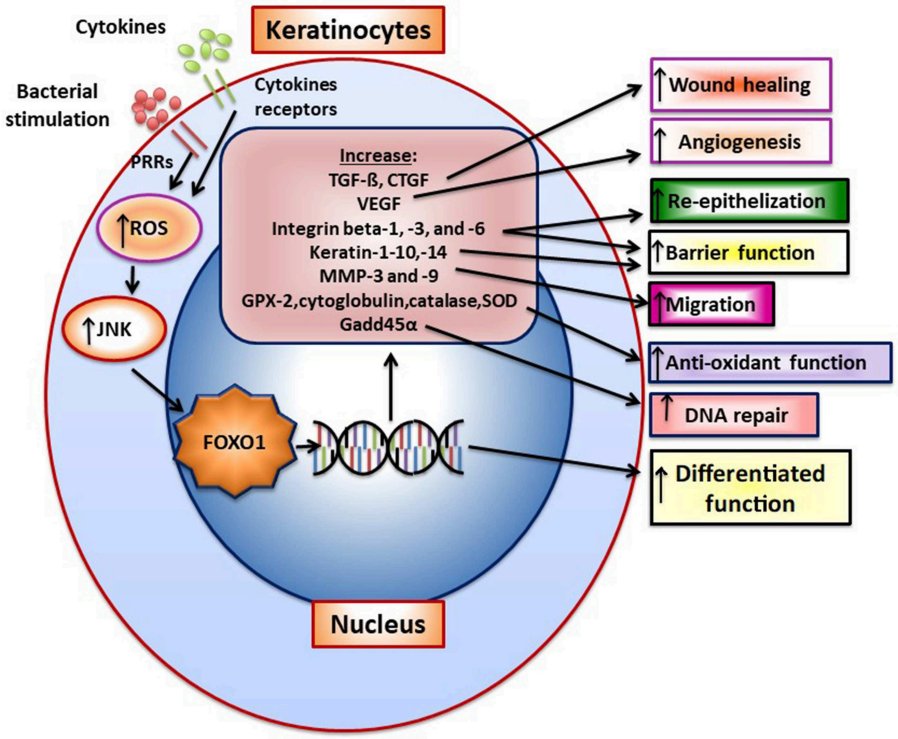

FIGURE 1 | FOXO1 is activated in keratinocytes to induce gene expression that modulates keratinocyte behavior. FoxO1 induces the expression of genes that affect keratinocyte function such as TGF-ß, VEGF, CTGF, integrins beta-1, -3, -6, Keratin-1, -10, -14, antioxidants GPX-2, cytoglobin, catalase and superoxide dismutase, and a DNA repair enzyme, Gadd45α. Bacteria through pattern recognition receptors or cytokine stimulation induces formation of reactive oxygen species that activate components of the MAP kinase pathway such as JNK, which stimulate FoxO1 nuclear localization where FoxO1 modulates gene transcription.

FOXO1 is induced by bacterial challenge (44, 48). Future research may provide insight into the potential regulation of barrier function by FOXO1 as well as clarify its regulation of the inflammatory response of keratinocytes to microbes *in vivo* and potential anti-microbial functions.

DENDRITIC CELLS AND FOXO1

Dendritic cells (DCs) are antigen-presenting cells, which capture, process and present antigens to lymphocytes to initiate and regulate the adaptive immune response (38). Microbial products can stimulate dendritic cells (DC) through toll-like receptors (TLRs) to enhance T-cell activation (52, 53). Trafficking of DC through lymphatic vessels is an essential aspect of protection by clearing bacteria and promoting protective immune responses (54). There is increased DC trafficking to lymph nodes and to the gingiva in response to the accumulation of dental plaque (55) and a decrease following periodontal treatment (56). In one of the few cause and effect studies, ablation of Langerhans cells and Langerhans$^+$ dendritic cells resulted in reduced numbers of Tregs, elevated production of RANKL, and enhanced alveolar bone loss during experimental periodontitis (57). In contrast, a more specific deletion of mucosal Langerhans cells had no effect on *Porphyromonas gingivalis* induced periodontitis but did enhance the production of Th17 cells (58). The authors in the latter report suggest that neither Langerhans cells nor Th17 cells play a major role in *Porphyromonas gingivalis* induced periodontal bone loss in the mouse model.

Bacteria activate FOXO1 in DC by inducing its nuclear localization through the MAPK pathway (12). FOXO1 affects several aspects of DC function. FOXO1 directly or indirectly participates in several aspects of DC stimulation of T- and B-lymphocytes through its effect on bacterial phagocytosis, lymphocyte migration, and homing as well as DC-lymphocyte binding. It is needed for DC phagocytosis of bacteria as *FOXO1* specific deletion in DCs inhibits bacterial phagocytosis (12). In addition, it affects DC migration and DC binding to lymphocytes (12). DC homing to lymph nodes is a key early aspect of the adaptive immune response. After engaging bacteria, DCs in the mucosa move to regional lymph nodes where they interact with lymphocytes. FOXO1 plays a key role in DC homing to lymph nodes through upregulation of CCR7. CCR7 is a chemokine receptor that responds to ligands expressed in lymph nodes to direct DC-lymph node homing. In addition, FOXO1 upregulates expression of ICAM-1. ICAM-1 is needed for DC binding to lymphocytes and formation of an immune synapse that activates lymphocytes. FOXO1 is able to bind to response elements in the promoters of ICAM-1 and CCR7 consistent with direct transcriptional regulation (12). Transfection with ICAM-1 and CCR7 expression vectors rescues impaired DC function

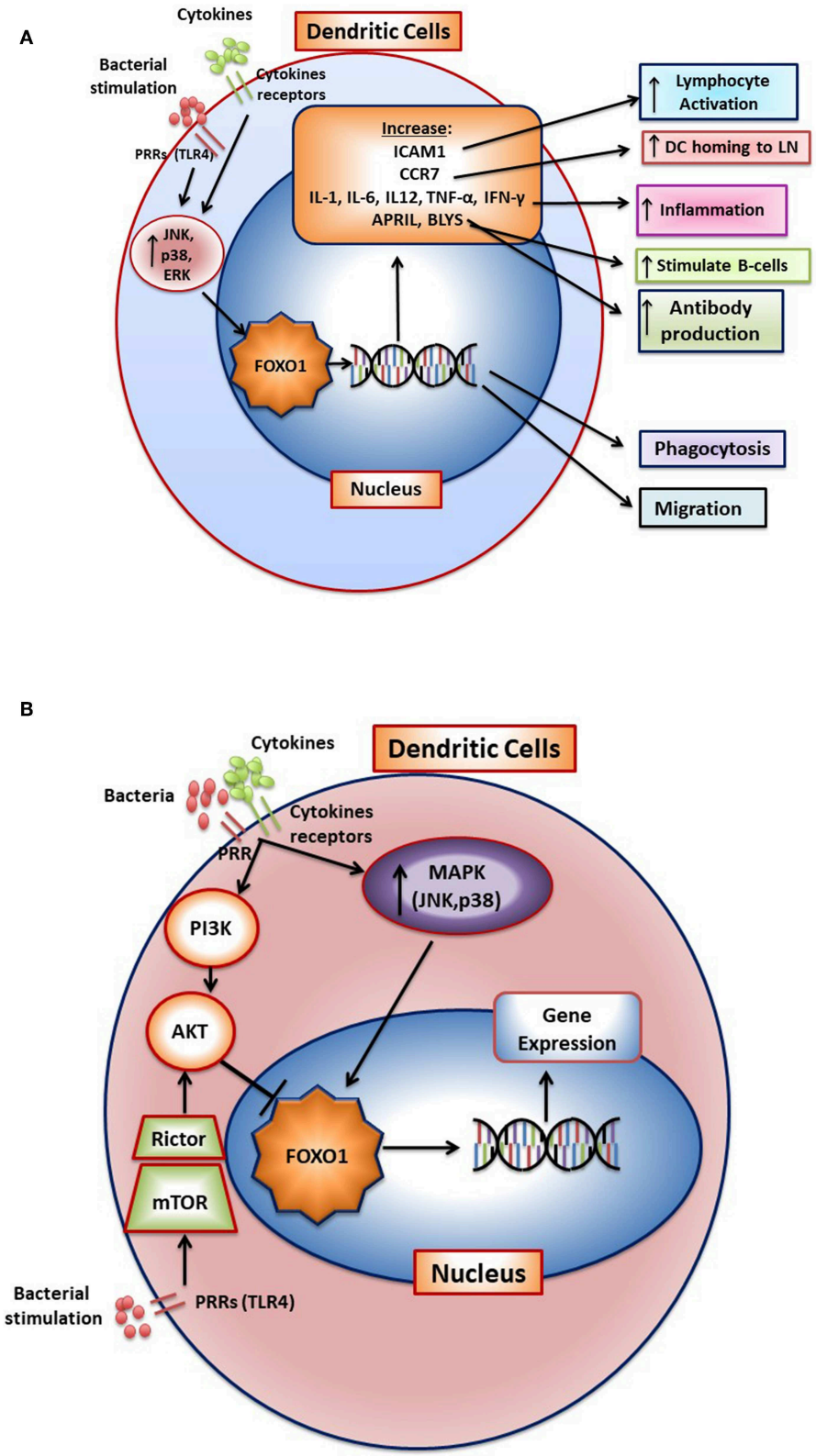

FIGURE 2 | FOXO1 regulates activation and function of dendritic cells. **(A)** FoxO1 nuclear localization is stimulated by activation of the MAP kinase pathway (JNK, p38, and ERK). In the nucleus FOXO1 affects DC function by increasing expression of genes such as ICAM1, CCR7, APRIL, BLYS, IL-1-β, IL-6, IL12, IFN-γ, TNF-α, and

(Continued)

FIGURE 2 | αvβ3. The change in gene expression promotes DC homing to the lymph nodes, antigen presentation, DC activation of T-and B- cells, and inflammation. **(B)** Cytokine receptors and pattern recognition receptors such as toll-like receptors (TLRs) stimulate activation of FOXO1 through the MAP kinase pathway. Activated FOXO1 can bind to the promoter region of target genes and regulate transcription. AKT is a major downstream target of PI3K that functions as a negative regulator of FOXO1. Stimulation of mTOR activates AKT to inhibit FoxO1 activity, which has been proposed to prevent a hyperinflammatory response.

in vivo and *in vitro* in *Foxo1* deleted DCs demonstrating their functional significance. FOXO1 downstream gene targets and their impact on DC function are summarized in **Figure 2A**. The linkage between FOXO1, DC and the capacity of DC to stimulate adaptive immunity is reinforced by evidence that bacteria-specific antibody production *in vivo* is impaired by lineage specific *Foxo1* ablation in DC (12). When FOXO1 is over-expressed *in vitro*, DCs produce high levels of IL-12, IL-6, and TNF-α and when *Foxo1* is deleted DCs have reduced capacity to produce inflammatory cytokines (59). Thus, FOXO1 regulates expression of inflammatory cytokines in DCs as does AKT1, which inhibits FOXO1 activity (58–64).

Bacteria and their products increase FOXO1 expression and activation in DCs by signaling through TLRs (59–61). Oral infection stimulates DC migration to cervical lymph nodes and induces antibody production *in vivo* (59). Recent experiments have demonstrated that periodontitis lesions are characterized by neutrophils and T-helper cells (36, 65). Deletion of *Foxo1* specifically in DCs reduces DC homing to lymph nodes induced by periodontal pathogens and reduces the production of specific antibody in response to their oral inoculation (59). The up-regulation of adaptive immunity is in part dependent upon FOXO1 regulation of APRIL and BLYS (see **Figure 2A**). This is significant since APRIL and BLYS are needed for stimulation of B-cells to form plasma cells (59). In addition, oral infection stimulates DC migration to mucosal epithelium. This migration is reduced by DC-specific *Foxo1* ablation (59). Interestingly, reduced DC homing to lymph nodes and periodontal tissues caused by lineage specific *Foxo1* deletion in DCs increases periodontal inflammation and susceptibility to periodontitis (59). The enhanced susceptibility is most likely through reduced humoral immunity, suggesting an important protective role for adaptive immunity in protecting periodontal tissues from microbial dysbiosis. The decreased antibody protection against bacteria in turn, may lead to an increased innate immune response that mediates periodontal tissue destruction. The latter is supported by findings that specific ablation of *Foxo1* in DC is linked to increased IL-1β and IL-17 levels, greater RANKL expression and osteoclast formation and more bone loss (59). In addition, DC-specific ablation of *Foxo1* in aged mice reduces anti-*Porphyromonas gingivalis* IgG1 and is associated with greater periodontal bone loss (62).

Stimulation of DC with bacteria such as *Porphyromonas gingivalis* or LPS induces a significant increase in FOXO1 activation as reflected by increased nuclear localization. Moreover, bacteria-induced FOXO1 nuclear localization is blocked by inhibitors of p38, JNK, and ERK. The inhibition of all three MAP kinase components is more effective than any one of them alone. However, the regulation of FOXO1 activity is more complex. In addition to stimulating FOXO1, TLR4 signaling can indirectly inhibit FoxO1 activation (63). In this scenario, LPS stimulation in DC activates mTOR and subsequently stimulates AKT, which inhibits FOXO1 activity. The activation of AKT in dendritic cells may prevent a hyperinflammatory response by deactivating FOXO1 (60). In addition, AKT has been reported to induce dendritic cell proliferation and survival (64). The activation of FOXO1 through the MAP kinase pathway and inhibition of FOXO1 through mTOR induced AKT signaling is shown in **Figure 2B**. These studies suggest that FOXO1 and AKT1 interact to modulate inflammatory responses in DC *in vivo*. It remains to be proven whether this occurs *in vivo* and whether AKT1 functions in DC to down-regulate FOXO1 or whether it primarily modulates DC function through phosphorylation of other downstream targets such as mTor or GSK-3.

LYMPHOCYTES AND FOXO1

Lymphocytes play important protective and destructive roles in periodontitis (25). B-lymphocytes are the predominant leukocyte in chronic inflammatory periodontal lesions and differentiate to plasma cells that produce antibody (36). There is no consensus on whether the development of antibodies in periodontitis is protective, although some studies have shown that a deficient Th2 response is associated with increased susceptibility to periodontitis (25). Similarly, the deletion of B-cells in mice have led to inconsistent results (36). Increased Th2 and Treg lymphocyte production is generally associated with resistance to periodontitis or resolution of periodontal inflammation (66). Th2 lymphocytes produce anti-inflammatory cytokines such as IL-4 and IL-10 and antibodies that may be protective (25). T-regulatory lymphocytes suppress inflammation by production of cytokines such TGF-β and IL-10. In experimental periodontitis adoptive transfer of Tregs inhibits periodontal disease susceptibility (67). Development of chronic periodontitis is linked to Th1 lymphocytes that produce IFNγ and IL-1-β and Th17 lymphocytes that produce IL-17A (68). Inflammation is problematic because it inhibits coupled bone formation that occurs after an episode of periodontal bone loss (39). In addition, RANKL, which plays an essential role in periodontal bone resorption has other properties besides stimulating osteoclastogenesis and is needed to form germinal centers in lymph nodes and may be important in enhancing formation of Tregs in inflamed bone (69).

FOXO1 plays an important role in adaptive immunity. FOXO1 affects lymphocyte development, homing, cytokine expression, and gene recombination (70). It modulates the formation of Tregs B-lymphocytes and is instrumental in maintaining hematopoietic stem cells (71, 72). Antibody class-switch by B-cells is also FOXO1 dependent (73). It exerts these effects through transcriptionally inducing key downstream target genes including L-selectin and sphingosine-1-phosphate

receptor 1 (S1pr1) for homing and IL-7 receptor-α that promotes survival of naive T-cells. FOXO1 promotes the formation of T-regulatory cells and B-lymphocytes (71, 72). The formation and function of Tregs is negatively affected by *Foxo1* ablation as mice with lineage specific *Foxo1* deletion have substantially reduced Tregs and those that are formed have diminished viability and function (70, 74). Furthermore, in the absence of FOXO1 TGF-β stimulated Tregs formation is reduced and Th1 cells increased (75). FOXO1 binds to the *Foxp3* and cytotoxic T-lymphocyte antigen 4 (*Ctla4*) promoters to induce their transcription (70). AKT inhibits FOXO1 and reduced AKT activity is needed for FOXO1 to induce Treg formation. Moreover, inflammatory conditions may stimulate the PI3K/AKT pathway and inhibit formation of Tregs (76). A summary of FOXO1 and its role in Tregs is shown in **Figure 3**. Studies of FOXO1 function in dendritic cells demonstrate that FOXO1 protects against bacteria induced periodontitis through upregulation of dendritic cell activity. However, they have not yet addressed whether FOXO1 induces formation and activity of specific $CD4^+$ T-helper cell phenotypes or the formation and activity of $CD8^+$ lymphocytes that may affect resistance or susceptibility to periodontal disease.

MONOCYTES/MACROPHAGES AND FOXO1

Monocytes are mobilized to the peripheral tissue by infection. Macrophages exist in different forms, classically pro-inflammatory M1 macrophages and anti-inflammatory/pro-healing M2 macrophages (77). M1 macrophages are generated when exposed to IFNγ, TNF–α, IL-1, and IL-6 while M2 macrophages are induced by IL-4, IL-10, and IL-13 (77). It is thought that there is a continuum between M1 and M2 macrophages, that most are not purely M1 or M2 and that they can be programmed to change M1 and M2 phenotypes. A third M3 macrophage phenotype has been proposed that results from incomplete macrophage reprogramming (77). These intermediate M3 polarization states may prevent an excessive response resulting from macrophage polarization. FOXO1 and its function in macrophages is summarized in **Figure 4**.

When exposed to bacteria, M1 macrophages secrete inflammatory cytokines that directly or indirectly stimulate osteoclast formation as well as proteases that degrade connective tissue matrix. IL-1β and TNF-α produced by monocytes/macrophages are highly expressed during induction of periodontal disease (78). The conversion from the gingivitis to periodontitis and recruitment of inflammatory cells in close proximity to bone is blocked by IL-1 and TNF-α blockers demonstrating the importance of these macrophage products in the destructive process (31). However, at later stages macrophage also contribute to the resolution of inflammation through the removal of apoptotic neutrophils and stimulate repair (37). This reflects the conversion from the M1 to the M2 phenotype. FOXO1 and its function in macrophages is summarized in **Figure 4**.

TLRs stimulate FOXO1 activity in macrophages (79). FoxO1 activation in macrophages is pro-inflammatory as it increases IL-1β production (80). FOXO1 binds to response elements in the IL-1β promoter to increase transcriptional activity (80). FOXO1 also binds to DNA response elements of a number of genes in the TLR

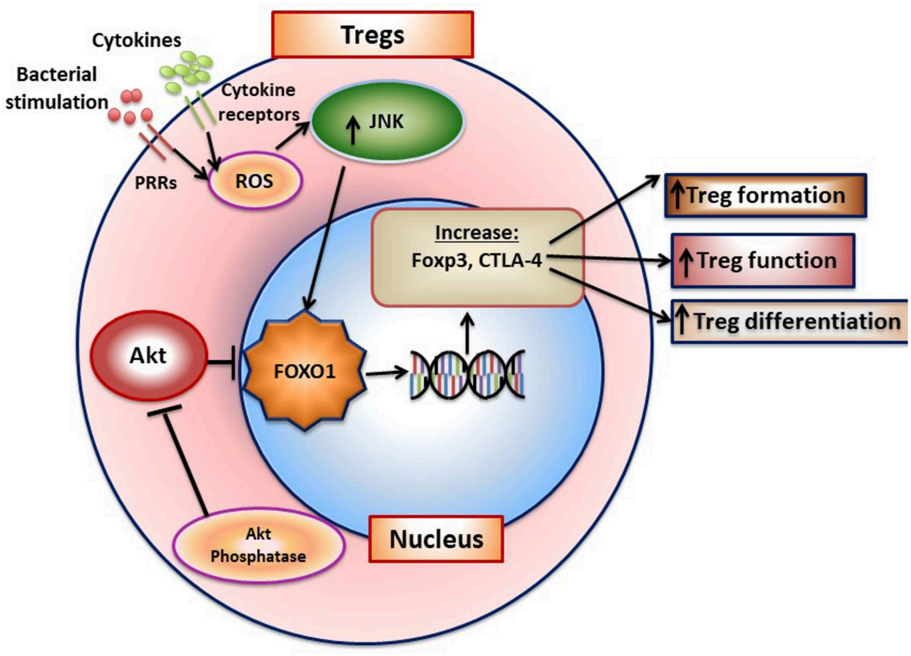

FIGURE 3 | FOXO1 regulates formation of T-regulatory cells. FoxO1 induces Foxp3, CTLA-4, IL-10, and TGF-β to enhance Treg formation and function. Activation of AKT phosphatase blocks AKT activation, which functions to increase FOXO1 nuclear localization to maintain Treg function.

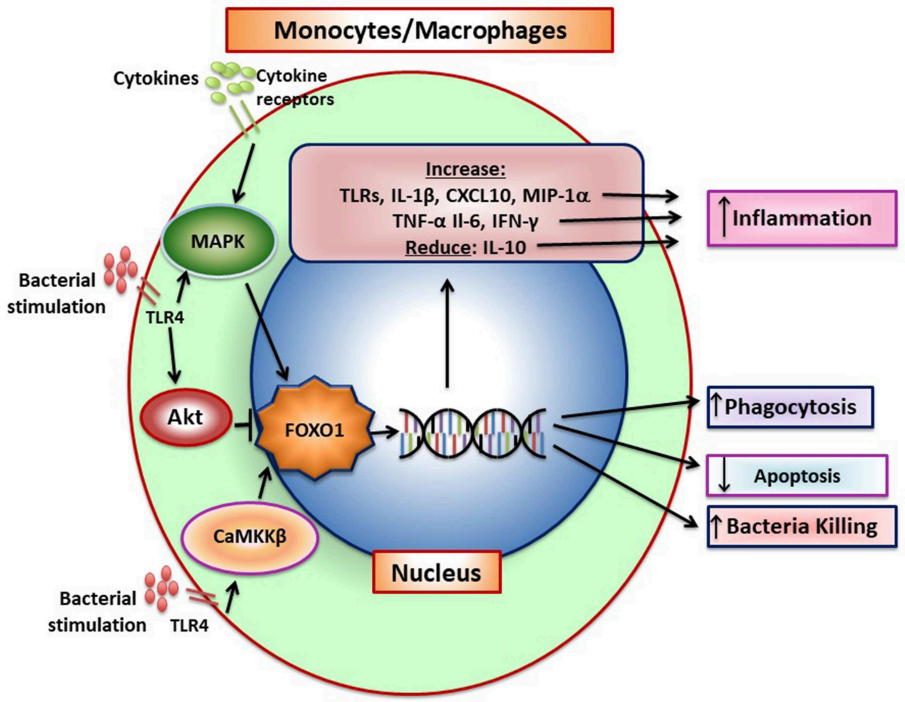

FIGURE 4 | FOXO1 increases production of inflammatory mediators by monocytes/macrophages. Pattern recognition receptors and cytokine receptor stimulation induces FOXO1 activity. FoxO1 increases expression of TLRs, IL-1β, CXCL10, MIP-1α, TNF-α, IL-6, and IFN-γ and can also reduce IL-10, which combined, increase inflammation. Pattern recognition receptors such as TLR4 can induce CaMKKβ that leads to increased FOXO1 nuclear localization and activation, which has been linked to increased bacterial killing. In addition, FOXO1 can act to increase phagocytosis and reduce apoptosis. There is conflicting data on FOXO1 and macrophage polarization. In tumor-associated macrophages FOXO1 is reported to increase the M1 phenotype but in asthma to increase the M2 phenotype.

signaling pathway including TLR4 itself to enhance inflammation (14). Thus, FOXO1 can enhance TLR4 stimulated expression of IL-1β, Cxcl10, and MIP1α through upregulation of molecules in the TLR4 pathway as well as induce their transcription directly. FOXO1 may also protect macrophages from apoptosis to increase their survival in an inflammatory environment and enhance inflammation (81). Hyperglycemia may further increase the macrophage inflammatory phenotype by reducing the capacity of FoxO1 to stimulate IL-10 expression (13).

The effect of FOXO1 on macrophage polarization has been controversial and may depend upon specific conditions. *Foxo1* deletion in myeloid cells has been shown to reduce M1 and increases M2 polarization in macrophages (79). As a result, these experiments suggest that FOXO1 in macrophages promotes M1 polarization in concert with its pro-inflammatory function. Consistent with this hypothesis, tumor associated macrophages that have reduced FOXO1 expression exhibit increased M2 polarization, which is thought to enhance tumor growth (82). However, it has also been reported that in response to LPS, M2 macrophages exhibit increased FOXO1 expression and FOXO1 binds to the IL-10 promoter in M2 macrophages more efficiently than it does in M1 macrophages (13). Thus, under these experimental conditions FOXO1 promotes M2 macrophage formation by inducing IL-10, Arg1, Fizz1, and interleukin-13 receptor alpha 1 (IL-13Ra1) (13).

FOXO1 activity may affect macrophage function by modulating autophagy (83). Autophagy has been proposed as a mechanism by which macrophages deal with intracellular pathogens to enhance their killing (84). When macrophages are challenged with *E. coli* there is an increase in cellular calcium levels that promotes autophagy and anti-bactericidal activity that is stimulated by calcium/calmodulin dependent protein kinase β (CaMKKβ). CaMKKβ leads to increased FOXO1 nuclear localization (83). When *Foxo1* is knocked down there is a significant reduction in autophagy.

Although FOXO1 is pro-inflammatory in macrophages it may also limit a hyper-inflammatory response by inducing AKT that in turn inactivates FOXO1 (14). It has been proposed that TLR4 activation stimulates PI3 kinase activity, which in turn phosphorylates AKT to induce FOXO1 phosphorylation and its transit from the nucleus to the cytoplasm to deactivate it. A similar mechanism has been proposed in dendritic cells as described above and in Brown et al. (60). Taken together, it is possible that insulin has an anti-inflammatory effect by inducing AKT activity and inhibiting FOXO1. FOXO1 may also augment the innate immune response by affecting myeloid cells. Genetic ablation of *Foxo1*, *Foxo3*, and *Foxo4* in myeloid cells results in an expansion of granulocyte/monocyte progenitors (81). The increased formation of these progenitors is likely due to an inhibitory effect of FOXOs on cell-cycle progression that is lost when the FOXOs are deleted. The precise role of FOXO1 in

macrophages has not been settled and it may depend on the conditions tested. The interpretation of these studies is also limited by a lack of *in vivo* studies with more specific deletion of *Foxo1* in monocytes/macrophages. The role of FOXO1 in macrophage function is summarized in **Figure 4**.

NEUTROPHILS AND FOXO1

Neutrophils are the predominant leukocyte recruited to the gingiva by bacteria or their products that have crossed the epithelial barrier and entered the connective tissue. One hypothesis for the development of periodontal disease is an inadequate neutrophil defense that that leads to greater inflammation and periodontal destruction (85). Neutrophil polymorphonuclear leukocytes (PMNs) phagocytose and kill microbes and remove subcellular particles (85). Following an acute inflammatory response the removal of apoptotic neutrophils is needed to resolve inflammation; a failure to remove apoptotic neutrophils interferes with resolution and leads to prolonged inflammation (86). Neutrophils and their products are responsible for much of the destruction of periodontal connective tissue and may also contribute to loss of epithelial barrier by inducing micro-ulceration.

Bacteria induce FOXO1 activation in neutrophils through TLR2 and TLR4, which is linked to FOXO1 deacetylation and stimulation by reactive oxygen species (15). TLR2 and TLR4 signaling stimulate FOXO1 nuclear localization. The nuclear localization is dependent on formation of ROS since inhibitors that block formation of ROS or NOS reduce FOXO1 activation. Moreover, bacteria-induced FOXO1 nuclear localization is also dependent on deacetylation since Sirt1 and histone deacetylase inhibitors reduce FOXO1 nuclear localization. The latter is consistent with findings that acetylation and phosphorylation of FOXO1 at specific sites block its translocation to the nucleus (6). In addition to responding to TLR2/TLR4 signaling, FOXO1 may act as a feed forward loop to enhance inflammation. This is based on findings that over-expression of FOXO1 increases upregulation of TLR2/4 and enhances neutrophil mediated inflammation by increasing inflammatory cytokine expression (e.g., TNF and IL-1) (15). An important component in the response of neutrophils to infection is the mobilization of neutrophils from bone marrow to the vasculature and migration to infected sites (87). *Foxo1* ablation in neutrophils interferes with neutrophil mobilization, which is mechanistically linked to FOXO1 induction of the chemokine CXCR2 (15). When *Foxo1* is ablated in neutrophils there is a significant reduction in neutrophil mobilization that coincides with reduced bacterial

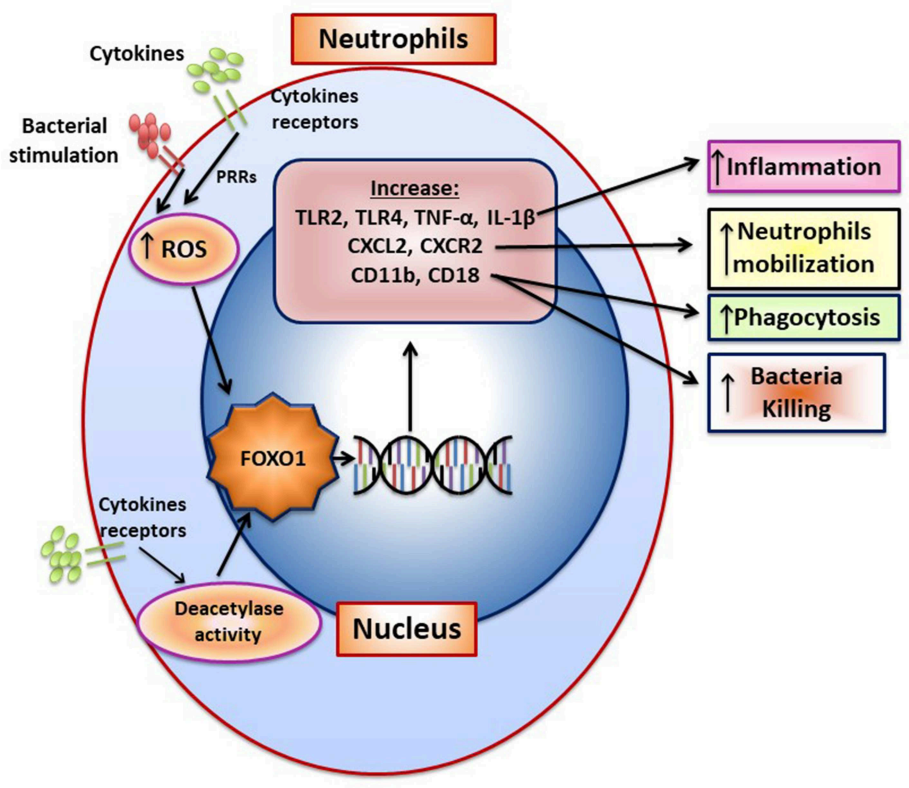

FIGURE 5 | FOXO1 increases neutrophil mobilization and function. The formation of ROS and NOS induced by pattern recognition and cytokine receptors increase FOXO1 nuclear localization and activity. FOXO1 nuclear localization is also stimulated by deacetylation due to deacetylase activity. FOXO1 increases expression of TLR2, TLR4, TNF, and IL-1β to increase inflammation. CXCL2 and CXCR2 are induced by FOXO1 and are associated with enhanced neutrophil mobilization resulting from infection. CD11b and CD18 are integrins that are induced by FOXO1 and facilitate migration, phagocytosis, and bacterial killing.

clearance and a reduced capacity of neutrophils to phagocytose and kill bacteria *in vitro* (15). The impact of FOXO1 on phagocytosis is tied to its regulation of CD11b, which along with CD18 captures bacteria to facilitate phagocytosis (15). A summary of FOXO1 downstream target genes and their impact on neutrophil function is shown in **Figure 5**.

In summary, FOXO1 is activated by bacteria or their products in several sub-classes of myeloid cells and lymphocytes as well as keratinocytes. These cell types are important in mucosal immunity. FOXO1 has the potential to play an important role in maintaining homeostasis in periodontal tissues and in the response to bacterial challenge. Alterations in FOXO1 function have a significant effect of periodontal disease susceptibility and due to FOXO1 regulation of leukocyte function. These studies indicate that FOXO1 plays an important role in the host defense and suggest potential mechanisms through up regulation of cellular activity. A limitation of many of the above studies is lack of lineage-specific demonstration of *Foxo1* deletion in each cell type or sub-set to better define its activities.

AUTHOR CONTRIBUTIONS

DG conceived this review. DG wrote the first draft of the manuscript and DG and TM edited it. Both authors contributed to manuscript revision, read, and approved the submitted version.

FUNDING

This work was supported by NIH grants R01DE017732 and R01DE021921.

REFERENCES

1. Wang Y, Zhou Y, Graves DT. FOXO transcription factors: their clinical significance and regulation. *Biomed Res Int.* (2014) 2014:925350. doi: 10.1155/2014/925350
2. Tsuchiya K, Ogawa Y. Forkhead box class O family member proteins: the biology and pathophysiological roles in diabetes. *J Diabetes Investig.* (2017) 8:726–34. doi: 10.1111/jdi.12651
3. Coomans de. Brachene A, Demoulin JB. FOXO transcription factors in cancer development and therapy. *Cell Mol Life Sci.* (2016) 73:1159–72. doi: 10.1007/s00018-015-2112-y
4. Iyer S, Ambrogini E, Bartell SM, Han L, Roberson PK, de Cabo R, et al. FOXOs attenuate bone formation by suppressing Wnt signaling. *J Clin Invest.* (2013) 123:3409–19. doi: 10.1172/JCI68049
5. Daitoku H, Sakamaki J, Fukamizu A. Regulation of FoxO transcription factors by acetylation and protein-protein interactions. *Biochim Biophys Acta.* (2011) 1813:1954–60. doi: 10.1016/j.bbamcr.2011.03.001
6. Qiang L, Banks AS, Accili D. Uncoupling of acetylation from phosphorylation regulates FoxO1 function independent of its subcellular localization. *J Biol Chem.* (2010) 285:27396–401. doi: 10.1074/jbc.M110.140228
7. Xu F, Othman B, Lim J, Batres A, Ponugoti B, Zhang C, et al. Foxo1 inhibits diabetic mucosal wound healing but enhances healing of normoglycemic wounds. *Diabetes.* (2015) 64:243–56. doi: 10.2337/db14-0589
8. Zhang C, Ponugoti B, Tian C, Xu F, Tarapore R, Batres A, et al. FOXO1 differentially regulates both normal and diabetic wound healing. *J Cell Biol.* (2015) 209:289–303. doi: 10.1083/jcb.201409032
9. Jeon HH, Yu Q, Lu Y, Spencer E, Lu C, Milovanova T, et al. FOXO1 regulates VEGFA expression and promotes angiogenesis in healing wounds. *J Pathol.* (2018) 245:258–64. doi: 10.1002/path.5075
10. Zhang C, Feinberg D, Alharbi M, Ding Z, Lu C, O'Connor JP, et al. Chondrocytes promote vascularization in fracture healing through a FOXO1-dependent mechanism. *J Bone Miner Res.* (2019) 34:547–56. doi: 10.1002/jbmr.3610
11. Jogdand GM, Mohanty S, Devadas S. Regulators of Tfh cell differentiation. *Front Immunol.* (2016) 7:520. doi: 10.3389/fimmu.2016.00520
12. Dong G, Wang Y, Xiao W, Pacios Pujado S, Xu F, Tian C, et al. FOXO1 regulates dendritic cell activity through ICAM-1 and CCR7. *J Immunol.* (2015) 194:3745–55. doi: 10.4049/jimmunol.1401754
13. Chung S, Ranjan R, Lee YG, Park GY, Karpurapu M, Deng J, et al. Distinct role of FoxO1 in M-CSF- and GM-CSF-differentiated macrophages contributes LPS-mediated IL-10: implication in hyperglycemia. *J Leukoc Biol.* (2015) 97:327–39. doi: 10.1189/jlb.3A0514-251R
14. Fan W, Morinaga H, Kim JJ, Bae E, Spann NJ, Heinz S, et al. FoxO1 regulates Tlr4 inflammatory pathway signalling in macrophages. *EMBO J.* (2010) 29:4223–36. doi: 10.1038/emboj.2010.268
15. Dong G, Song L, Tian C, Wang Y, Miao F, Zheng J, et al. FOXO1 regulates bacteria-induced neutrophil activity. *Front Immunol.* (2017) 8:1088. doi: 10.3389/fimmu.2017.01088
16. Dengler HS, Baracho GV, Omori SA, Bruckner S, Arden KC, Castrillon DH, et al. Distinct functions for the transcription factor Foxo1 at various stages of B cell differentiation. *Nat Immunol.* (2008) 9:1388–98. doi: 10.1038/ni.1667
17. Kerdiles YM, Stone EL, Beisner DR, McGargill MA, Ch'en IL, Stockmann C, et al. Foxo transcription factors control regulatory T cell development and function. *Immunity.* (2010) 33:890–904. doi: 10.1016/j.immuni.2010.12.002
18. Yusuf I, Zhu X, Kharas MG, Chen J, Fruman DA. Optimal B-cell proliferation requires phosphoinositide 3-kinase-dependent inactivation of FOXO transcription factors. *Blood.* (2004) 104:784–7. doi: 10.1182/blood-2003-09-3071
19. Behl Y, Siqueira M, Ortiz J, Li J, Desta T, Faibish D, et al. Activation of the acquired immune response reduces coupled bone formation in response to a periodontal pathogen. *J Immunol.* (2008) 181:8711–8. doi: 10.4049/jimmunol.181.12.8711
20. Ponugoti B, Dong G, Graves DT. Role of forkhead transcription factors in diabetes-induced oxidative stress. *Exp Diabetes Res.* (2012) 2012:939751. doi: 10.1155/2012/939751
21. Xiao E, Graves DT. Impact of diabetes on the protective role of FOXO1 in wound healing. *J Dent Res.* (2015) 94:1025–6. doi: 10.1177/0022034515586353
22. Tsitsipatis D, Klotz LO, Steinbrenner H. Multifaceted functions of the forkhead box transcription factors FoxO1 and FoxO3 in skin. *Biochim Biophys Acta.* (2017) 1861:1057–64. doi: 10.1016/j.bbagen.2017.02.027
23. Eijkelenboom A, Burgering BM. FOXOs: signalling integrators for homeostasis maintenance. *Nat Rev Mol Cell Biol.* (2013) 14:83–97. doi: 10.1038/nrm3507
24. Graves DT, Li J, Cochran DL. Inflammation and uncoupling as mechanisms of periodontal bone loss. *J Dent Res.* (2011) 90:143–53. doi: 10.1177/0022034510385236
25. Alvarez C, Monasterio G, Cavalla F, Córdova LA, Hernández M, Heymann D, et al. Osteoimmunology of oral and maxillofacial diseases: translational applications based on biological mechanisms. *Front Immunol.* (2019) 18:166426. doi: 10.3389/fimmu.2019.01664
26. Beck JD, Papapanou PN, Philips KH, Offenbacher S. Periodontal medicine: 100 years of progress. *J Dent Res.* (2019) 98:1053–62. doi: 10.1177/0022034519846113
27. Chukkapalli SS, Velsko IM, Rivera-Kweh MF, Larjava H, Lucas AR, Kesavalu L. Global TLR2 and 4 deficiency in mice impacts bone resorption, inflammatory markers and atherosclerosis to polymicrobial infection. *Mol Oral Microbiol.* (2017) 32:211–25. doi: 10.1111/omi.12165

28. Sanavi F, Listgarten MA, Boyd F, Sallay K, Nowotny A. The colonization and establishment of invading bacteria in periodontium of ligature-treated immunosuppressed rats. *J Periodontol.* (1985) 56:273–80. doi: 10.1902/jop.1985.56.5.273
29. Liu R, Bal HS, Desta T, Behl Y, Graves DT. Tumor necrosis factor-alpha mediates diabetes-enhanced apoptosis of matrix-producing cells and impairs diabetic healing. *Am J Pathol.* (2006) 168:757–64. doi: 10.2353/ajpath.2006.050907
30. Assuma R, Oates T, Cochran D, Amar S, Graves D. IL-1 and TNF antagonists inhibit the inflammatory response and bone loss in experimental periodontitis. *J Immun.* (1998) 160:403–9.
31. Graves D, Delima A, Assuma R, Amar S, Oates T, Cochran D. Interleukin-1 and tumor necrosis factor antagonists inhibit the progression of inflammatory cell infiltration toward alveolar bone in experimental periodontitis. *J Periodontol.* (1998) 69:1419–25. doi: 10.1902/jop.1998.69.12.1419
32. Pacios S, Xiao W, Mattos M, Lim J, Tarapore RS, Alsadun S, et al. Osteoblast lineage cells play an essential role in periodontal bone loss through activation of nuclear factor-kappa B. *Sci Rep.* (2015) 5:16694. doi: 10.1038/srep16694
33. Zheng J, Chen S, Albiero ML, Vieira GHA, Wang J, Feng JQ, et al. Diabetes activates periodontal ligament fibroblasts via NF-kappaB. *In vivo J Dent Res.* (2018) 97:580–8. doi: 10.1177/0022034518755697
34. Xiao E, Mattos M, Vieira GHA, Chen S, Correa JD, Wu Y, et al. Diabetes enhances IL-17 expression and alters the oral microbiome to increase its pathogenicity. *Cell Host Microbe.* (2017) 22:120–8 e124. doi: 10.1016/j.chom.2017.06.014
35. Baek KJ, Ji S, Kim YC, Choi Y. Association of the invasion ability of *Porphyromonas gingivalis* with the severity of periodontitis. *Virulence.* (2015) 6:274–81. doi: 10.1080/21505594.2014.1000764
36. Hajishengallis G, Korostoff JM. Revisiting the Page & Schroeder model: the good, the bad and the unknowns in the periodontal host response 40 years later. *Periodontol 2000.* (2017) 75:116–51. doi: 10.1111/prd.12181
37. Van Dyke TE. Pro-resolving mediators in the regulation of periodontal disease. *Mol Aspects Med.* (2017) 58:21–36. doi: 10.1016/j.mam.2017.04.006
38. Song L, Dong G, Guo L, Graves DT. The function of dendritic cells in modulating the host response. *Mol Oral Microbiol.* (2018) 33:13–21. doi: 10.1111/omi.12195
39. Xiao W, Li S, Pacios S, Wang Y, Graves DT. Bone remodeling under pathological conditions. *Front Oral Biol.* (2016) 18:17–27. doi: 10.1159/000351896
40. Griffen AL, Beall CJ, Campbell JH, Firestone ND, Kumar PS, Yang ZK, et al. Distinct and complex bacterial profiles in human periodontitis and health revealed by 16S pyrosequencing. *ISME J.* (2012) 6:1176–85. doi: 10.1038/ismej.2011.191
41. Abusleme L, Dupuy AK, Dutzan N, Silva N, Burleson JA, Strausbaugh LD, et al. The subgingival microbiome in health and periodontitis and its relationship with community biomass and inflammation. *ISME J.* (2013) 7:1016–25. doi: 10.1038/ismej.2012.174
42. de Vries TJ, Andreotta S, Loos BG, Nicu EA. Genes critical for developing periodontitis: lessons from mouse models. *Front Immunol.* 8:1395. doi: 10.3389/fimmu.2017.01395
43. Kimball JR, Nittayananta W, Klausner M, Chung WO, Dale BA. Antimicrobial barrier of an *in vitro* oral epithelial model. *Arch Oral Biol.* (2006) 51:775–83. doi: 10.1016/j.archoralbio.2006.05.007
44. Fujita T, Yoshimoto T, Kajiya M, Ouhara K, Matsuda S, Takemura T, et al. Regulation of defensive function on gingival epithelial cells can prevent periodontal disease. *Jpn Dent Sci Rev.* (2018) 54:66–75. doi: 10.1016/j.jdsr.2017.11.003
45. Dickinson BC, Moffatt CE, Hagerty D, Whitmore SE, Brown TA, Graves DT, et al. Interaction of oral bacteria with gingival epithelial cell multilayers. *Mol Oral Microbiol.* (2011) 26:210–20. doi: 10.1111/j.2041-1014.2011.00609.x
46. Hameedaldeen A, Liu J, Batres A, Graves GS, Graves DT. FOXO1, TGF-beta regulation and wound healing. *Int J Mol Sci.* (2014) 15:16257–69. doi: 10.3390/ijms150916257
47. Li S, Dong G, Moschidis A, Ortiz J, Benakanakere MR, Kinane DF, et al. *P. gingivalis* modulates keratinocytes through FOXO transcription factors. *PLoS ONE.* (2013) 8:e78541. doi: 10.1371/journal.pone.0078541
48. Wang Q, Sztukowska M, Ojo A, Scott DA, Wang H, Lamont RJ. FOXO responses to *Porphyromonas gingivalis* in epithelial cells. *Cell Microbiol.* (2015) 17:1605–17. doi: 10.1111/cmi.12459
49. Ponugoti B, Xu F, Zhang C, Tian C, Pacios S, Graves DT. FOXO1 promotes wound healing through the up-regulation of TGF-beta1 and prevention of oxidative stress. *J Cell Biol.* (2013) 203:327–43. doi: 10.1083/jcb.201305074
50. Gomis RR, Alarcon C, He W, Wang Q, Seoane J, Lash A, et al. A FoxO-Smad synexpression group in human keratinocytes. *Proc Natl Acad Sci USA.* (2006) 103:12747–52. doi: 10.1073/pnas.0605333103
51. Zhang C, Lim J, Liu J, Ponugoti B, Alsadun S, Tian C, et al. FOXO1 expression in keratinocytes promotes connective tissue healing. *Sci Rep.* (2017) 7:42834. doi: 10.1038/srep42834
52. Gaddis DE, Michalek SM, Katz J. Requirement of TLR4 and CD14 in dendritic cell activation by Hemagglutinin B from *Porphyromonas gingivalis*. *Mol Immunol.* (2009) 46:2493–504. doi: 10.1016/j.molimm.2009.05.022
53. Su H, Yan X, Dong Z, Chen W, Lin ZT, Hu QG. Differential roles of *Porphyromonas gingivalis* lipopolysaccharide and *Escherichia coli* lipopolysaccharide in maturation and antigen-presenting functions of dentritic cells. *Eur Rev Med Pharmacol Sci.* (2015) 19:2482–92.
54. Berggreen E, Wiig H. Lymphangiogenesis and lymphatic function in periodontal disease. *J Dent Res.* (2013) 92:1074–80. doi: 10.1177/0022034513504589
55. Moughal NA, Adonogianaki E, Kinane DF. Langerhans cell dynamics in human gingiva during experimentally induced inflammation. *J Biol Buccale.* (1992) 20:163–7.
56. Dereka XE, Tosios KI, Chrysomali E, Angelopoulou E. Factor XIIIa+ dendritic cells and S-100 protein+ Langerhans' cells in adult periodontitis. *J Periodont Res.* (2004) 39:447–52. doi: 10.1111/j.1600-0765.2004.00764.x
57. Arizon M, Nudel I, Segev H, Mizraji G, Elnekave M, Furmanov K, et al. Langerhans cells down-regulate inflammation-driven alveolar bone loss. *Proc Natl Acad Sci USA.* (2012) 109:7043–8. doi: 10.1073/pnas.1116770109
58. Bittner-Eddy PD, Fischer LA, Kaplan DH, Thieu K, Costalonga M. Mucosal langerhans cells promote differentiation of Th17 cells in a murine model of periodontitis but are not required for *Porphyromonas gingivalis*-driven alveolar bone destruction. *J Immunol.* (2016) 197:1435–46. doi: 10.4049/jimmunol.1502693
59. Xiao W, Dong G, Pacios S, Alnammary M, Barger LA, Wang Y, et al. FOXO1 deletion reduces dendritic cell function and enhances susceptibility to periodontitis. *Am J Pathol.* (2015) 185:1085–93. doi: 10.1016/j.ajpath.2014.12.006
60. Brown J, Wang H, Suttles J, Graves DT, Martin M. Mammalian target of rapamycin complex 2 (mTORC2) negatively regulates Toll-like receptor 4-mediated inflammatory response via FoxO1. *J Biol Chem.* (2011) 286:44295–305. doi: 10.1074/jbc.M111.258053
61. Arjunan P, El-Awady A, Dannebaum RO, Kunde-Ramamoorthy G, Cutler CW. High-throughput sequencing reveals key genes and immune homeostatic pathways activated in myeloid dendritic cells by *Porphyromonas gingivalis* 381 and its fimbrial mutants. *Mol Oral Microbiol.* (2016) 31:78–93. doi: 10.1111/omi.12131
62. Wu Y, Dong G, Xiao W, Xiao E, Miao F, Syverson A, et al. Effect of aging on periodontal inflammation, microbial colonization, and disease susceptibility. *J Dent Res.* (2016) 95:460–6. doi: 10.1177/0022034515625962
63. Zaal A, Nota B, Moore KS, Dieker M, van Ham SM, Ten Brinke A. TLR4 and C5aR crosstalk in dendritic cells induces a core regulatory network of RSK2, PI3Kbeta, SGK1, and FOXO transcription factors. *J Leukoc Biol.* (2017) 102:1035–54. doi: 10.1189/jlb.2MA0217-058R
64. Weichhart T, Saemann MD. The PI3K/Akt/mTOR pathway in innate immune cells: emerging therapeutic applications. *Ann Rheum Dis.* (2008) 67(Suppl 3):iii70–4. doi: 10.1136/ard.2008.098459
65. Wilensky A, Mizraji G, Tabib Y, Sharawi H, Hovav AH. Analysis of leukocytes in oral mucosal tissues. *Methods Mol Biol.* (2017) 1559:267–78. doi: 10.1007/978-1-4939-6786-5_18
66. Engel, D. Lymphocyte function in early-onset periodontitis. *J Periodontol.* (1996) 67(Suppl 3S):332–6. doi: 10.1902/jop.1996.67.3s.332
67. Araujo-Pires AC, Vieira AE, Francisconi CF, Biguetti CC, Glowacki A, Yoshizawa S, et al. IL-4/CCL22/CCR4 axis controls regulatory T-cell

migration that suppresses inflammatory bone loss in murine experimental periodontitis. *J Bone Miner Res.* (2015) 30:412–22. doi: 10.1002/jbmr.2376
68. Chen XT, Chen LL, Tan JY, Shi DH, Ke T, Lei LH. Th17 and Th1 lymphocytes are correlated with chronic periodontitis. *Immunol Invest.* (2016) 45:243–54. doi: 10.3109/08820139.2016.1138967
69. Francisconi CF, Vieira AE, Azevedo MCS, Tabanez AP, Fonseca AC, Trombone APF, et al. RANKL triggers Treg-mediated immunoregulation in inflammatory osteolysis. *J Dent Res.* (2018) 97:917–27. doi: 10.1177/0022034518759302
70. Ouyang W, Liao W, Luo CT, Yin N, Huse M, Kim MV, et al. Novel Foxo1-dependent transcriptional programs control T(reg) cell function. *Nature.* (2012) 491:554–9. doi: 10.1038/nature11581
71. Bothur E, Raifer H, Haftmann C, Stittrich AB, Brustle A, Brenner D, et al. Antigen receptor-mediated depletion of FOXP3 in induced regulatory T-lymphocytes via PTPN2 and FOXO1. *Nat Commun.* (2015) 6:8576. doi: 10.1038/ncomms9576
72. Hawse WF, Sheehan RP, Miskov-Zivanov N, Menk AV, Kane LP, Faeder JR, et al. Cutting edge: differential regulation of PTEN by TCR, Akt, and FoxO1 controls $CD4^+$ T cell fate decisions. *J Immunol.* (2015) 194:4615–9. doi: 10.4049/jimmunol.1402554
73. Dominguez-Sola D, Kung J, Holmes AB, Wells VA, Mo T, Basso K, et al. The FOXO1 transcription factor instructs the germinal center dark zone program. *Immunity.* (2015) 43:1064–74. doi: 10.1016/j.immuni.2015.10.015
74. Rao RR, Li Q, Gubbels Bupp MR, Shrikant PA. Transcription factor Foxo1 represses T-bet-mediated effector functions and promotes memory CD8(+) T cell differentiation. *Immunity.* (2012) 36:374–87. doi: 10.1016/j.immuni.2012.01.015
75. Harada Y, Harada Y, Elly C, Ying G, Paik JH, DePinho RA, et al. Transcription factors Foxo3a and Foxo1 couple the E3 ligase Cbl-b to the induction of Foxp3 expression in induced regulatory T cells. *J Exp Med.* (2010) 207:1381–91. doi: 10.1084/jem.20100004
76. Clarke EV, Tenner AJ. Complement modulation of T cell immune responses during homeostasis and disease. *J Leukoc Biol.* (2014) 96:745–56. doi: 10.1189/jlb.3MR0214-109R
77. Malyshev I, Malyshev Y. Current concept and update of the macrophage plasticity concept: intracellular mechanisms of reprogramming and M3 macrophage "switch" phenotype. *Biomed Res Int.* (2015) 2015:341308. doi: 10.1155/2015/341308
78. Salvi GE, Brown CE, Fujihashi K, Kiyono H, Smith FW, Beck JD, et al. Inflammatory mediators of the terminal dentition in adult and early onset periodontitis. *J Periodont Res.* (1998) 33:212–25. doi: 10.1111/j.1600-0765.1998.tb02193.x
79. Wang YC, Ma HD, Yin XY, Wang YH, Liu QZ, Yang JB, et al. Forkhead box O1 regulates macrophage polarization following staphylococcus aureus infection: experimental murine data and review of the literature. *Clin Rev Allergy Immunol.* (2016) 51:353–69. doi: 10.1007/s12016-016-8531-1
80. Miao H, Ou J, Zhang X, Chen Y, Xue B, Shi H, et al. Macrophage CGI-58 deficiency promotes IL-1beta transcription by activating the SOCS3-FOXO1 pathway. *Clin Sci.* (2015) 128:493–506. doi: 10.1042/CS20140414
81. Tsuchiya K, Westerterp M, Murphy AJ, Subramanian V, Ferrante AW Jr, Tall AR, et al. Expanded granulocyte/monocyte compartment in myeloid-specific triple FoxO knockout increases oxidative stress and accelerates atherosclerosis in mice. *Circ Res.* (2013) 112:992–1003. doi: 10.1161/CIRCRESAHA.112.300749
82. Yang JB, Zhao ZB, Liu QZ, Hu TD, Long J, Yan K, et al. FoxO1 is a regulator of MHC-II expression and anti-tumor effect of tumor-associated macrophages. *Oncogene.* (2018) 37:1192–204. doi: 10.1038/s41388-017-0048-4
83. Liu X, Wang N, Zhu Y, Yang Y, Chen X, Chen Q, et al. Extracellular calcium influx promotes antibacterial autophagy in *Escherichia coli* infected murine macrophages via CaMKKbeta dependent activation of ERK1/2, AMPK and FoxO1. *Biochem Biophys Res Commun.* (2016) 469:639–45. doi: 10.1016/j.bbrc.2015.12.052
84. Jati S, Kundu S, Chakraborty A, Mahata SK, Nizet V, Sen M. Wnt5A signaling promotes defense against bacterial pathogens by activating a host autophagy circuit. *Front Immunol.* (2018) 9:679. doi: 10.3389/fimmu.2018.00679
85. Herrmann JM, Meyle J. Neutrophil activation and periodontal tissue injury. *Periodontol 2000.* (2015) 69:111–27. doi: 10.1111/prd.12088
86. Mark Bartold P, Van Dyke TE. Host modulation: controlling the inflammation to control the infection. *Periodontol 2000.* (2017) 75:317–29. doi: 10.1111/prd.12169
87. Wang J, Arase H. Regulation of immune responses by neutrophils. *Ann N Y Acad Sci.* (2014) 1319:66–81. doi: 10.1111/nyas.12445

Conflict of Interest: The authors declare that the research was conducted in the absence of any commercial or financial relationships that could be construed as a potential conflict of interest.

frontiers in Immunology

MINI REVIEW
published: 08 January 2020
doi: 10.3389/fimmu.2019.03001

Neutrophil Subsets in Periodontal Health and Disease: A Mini Review

*Josefine Hirschfeld**

Department of Periodontology, Birmingham Dental School and Hospital, Birmingham, United Kingdom

Neutrophils are amongst the most abundant immune cells within the periodontal tissues and oral cavity. As innate immune cells, they are first line defenders at the tooth-mucosa interface, and can perform an array of different functions. With regard to these, it has been observed over many years that neutrophils are highly heterogeneous in their behavior. Therefore, it has been speculated that neutrophils, similarly to other leukocytes, exist in distinct subsets. Several studies have investigated different markers of neutrophils in oral health and disease in recent years in order to define potential cell subsets and their specific tasks. This research was inspired by recent advancements in other fields of medicine in this field. The aim of this review is to give an overview of the current evidence regarding the existence and presence of neutrophil subsets and their possible functions, specifically in the context of periodontitis, gingivitis, and periodontal health.

Keywords: phenotypal marker, cell function and behavior, subset, neutrophils, cluster of differentiation, periodontitis

OPEN ACCESS

Edited by:
Avi-Hai Hovav,
Hebrew University of Jerusalem, Israel

Reviewed by:
Octavio Alberto Gonzalez,
University of Kentucky, United States
Michael Glogauer,
University of Toronto, Canada

***Correspondence:**
Josefine Hirschfeld
j.hirschfeld@bham.ac.uk

Specialty section:
This article was submitted to Mucosal Immunity, a section of the journal Frontiers in Immunology

Received: *04 September 2018*
Accepted: *06 December 2019*
Published: *08 January 2020*

Citation:
Hirschfeld J (2020) Neutrophil Subsets in Periodontal Health and Disease: A Mini Review. Front. Immunol. 10:3001. doi: 10.3389/fimmu.2019.03001

INTRODUCTION

Neutrophils are found in high abundance within the periodontal tissues and oral cavity. They typically migrate from local capillaries within the periodontal tissues toward the gingival crevice, following the highest concentration of a chemotactic gradient (1). The permanent presence of microbial and biofilm-derived chemotactic and pro-inflammatory factors attract neutrophils from the circulation into the tissues, where they become activated. Once in the gingival crevice, neutrophils are washed into the oral cavity. Even under healthy conditions, neutrophils constantly infiltrate the periodontium, although in lower numbers than during inflammation. Activated neutrophils have the aim to eliminate or reduce the microbial/antigenic load. The mechanisms by which they contribute to homeostasis and defense are (a) phagocytosis, the ingestion, and intracellular decomposition of antigens, (b) degranulation, the intra- or extracellular release of granule contents such as enzymes and antimicrobial peptides, (c) intra- or extracellular release of reactive oxygen species (ROS), which are directly cytotoxic to microbes but also to host cells, and (d) the formation of neutrophil extracellular traps (NETs), by which neutrophils release decondensed chromatin decorated with histones and granule contents into the extracellular space where they trap microorganisms. All of these processes are closely related, as effective internal degradation of microbes requires intracellular ROS release and degranulation, and as NET formation is usually preceded by ROS formation and accompanied by degranulation (2–5).

Neutrophils are well-researched cells of the innate immune system and yet, new discoveries have been constantly made. Neutrophils are widely believed to be the key cell that mediates tissue destruction and have been described as double-edged swords of immunity. In the periodontium, whilst absence of proper neutrophil function, as seen in some hereditary diseases, like Papillon-Lefèvre syndrome, leads to deleterious periodontal inflammation with severe tissue damage and tooth loss (6), neutrophil hyperactivity is equally associated with tissue damage (7). It has been long

noted that neutrophils are heterogeneous in their behavior and perform vastly different functions. For example, only a proportion of neutrophils forms NETs, where the size of that proportion depends upon the stimulus and its concentration (8, 9). Therefore, the question has been raised whether distinct neutrophil subsets may exist and more attention has been given to the research of this possibility.

Potential pro- and anti-inflammatory roles of neutrophil subsets have been demonstrated in recent models of ischaemia-related injury, trauma, cancer, sepsis, and inflammatory diseases (10, 11). Within the oral cavity, different neutrophil subsets and pro-inflammatory neutrophil phenotypes in periodontitis have also been proposed. This mini review aims at summarizing and discussing the current evidence regarding the presence of potential neutrophil subsets and phenotypes in the context of oral health and disease. Those studies are highlighted which have carried out biomarker analysis along with functional assays (**Table 1**).

IDENTIFICATION OF NEUTROPHILS AND NEUTROPHIL SUBSETS

Traditionally, neutrophils can be readily identified by their typical nuclear shape, in combination with histological hematoxylin and eosin staining (23). Furthermore, on human neutrophils isolated from different sites and in different states of health and activation, 141 cluster of differentiation (CD) markers have been described (24). Mostly, CD11b (integrin subunit alpha M adhesion molecule), CD14 (pattern recognition co-receptor), CD15 (a molecule expressed in the granulocytic series past the myeloblast stage), CD16 (Fc gamma receptor (FcγR) IIIb, low-affinity immunoglobulin (Ig) G receptor), and CD62L (L-selectin, a cell adhesion molecule) (25, 26) have been used individually or in combination to identify pure human neutrophil populations (24). Moreover, several receptors on the neutrophil surface initiate the phagocytic signaling pathway. Phagocytosis is significantly enhanced by the presence of opsonins such as antibodies or complement factors on the microbial surface. Receptors specific for the Fc-region of antibodies include CD64 (FcγRI), CD32 (FcγRIIa), CD16, and CD89 (FcαR, IgA receptor) (27). Furthermore, neutrophils recognize complement-opsonized microorganisms using the complement receptors (CRs) CD35 (CR1), CD11b/CD18 (CR3), and CD11c/CD18 (CR4) (27).

Leliefeld et al. showed that during acute inflammation, a subset of $CD16^{bright}/CD62L^{dim}$ hyper-segmented human neutrophils displayed normal phagocytosis, associated with a remarkably poor capacity to contain bacteria intracellularly (28). Conversely, $CD16^{dim}$-banded neutrophils were the only neutrophil subset that adequately contained bacteria. The authors concluded that these results were indicative of a clear neutrophil heterogeneity in their antimicrobial capacity. Several markers of neutrophil degranulation have also been reported. The surface markers are CD63 (primary/azurophilic granules), CD15 and CD66b (secondary/specific granules) as well as CD11b (tertiary/gelatinase granules) and CD13, CD14, CD18, CD45 (quaternary/secretory granules) (29). Another glycoprotein detected within specific granules is Olfactomedin-4 (OLFM4). OLFM4 mRNA has been detected in progenitor neutrophils. However, the protein is only detected in 20–25% of peripheral blood neutrophils (30), suggesting that its expression is regulated by translation mechanisms that lead to functional heterogeneity (31).

The markers described above are not exclusive to neutrophils and have been reported on other cells also, such as macrophages, B- and T-lymphocytes (32). A marker specific to neutrophils is CD177, a glycoprotein expressed on the neutrophil plasma membrane as well as on the membrane of their specific granules (33). However, the proportion of $CD177^+$ neutrophils varies amongst individuals, some displaying bimodal (high and no CD177) or trimodal (high, intermediate, and no CD177) expression. Approximately 1–10% of humans show a complete absence of $CD177^+$ cells. This has been attributed to the allelic frequency of a mutation in the CD177 gene (31). Due to its heterogeneity, this marker may not be reliable for quantification purposes, but it delineates PMN populations reliably in those individuals who express it. Neutrophil granules have also been used to describe distinct phenotypes: during acute and chronic inflammation a population of neutrophils, which co-sediments with peripheral blood mononuclear cells (PBMCs), has been reported. Typically, circulating neutrophils are separated from PBMCs by gradient centrifugation, as neutrophils have a higher density than PBMCs. Therefore, this neutrophil population has been termed low-density neutrophils (LDNs) (34).

Neutrophils are classically implicated in inflammation, but have some pro-resolving properties also. Firstly, their role as apoptotic cells in the macrophage-mediated resolution of inflammation is believed to be crucial (35). In this process, apoptotic neutrophils induce a suppression of nuclear factor kappa B signaling in macrophages, and therefore a reduction in the release of pro- but not anti-inflammatory cytokines from these cells (36). Secondly, neutrophils are co-producers of the pro-resolving lipid mediators lipoxins and maresin-1 (37, 38).

Thirdly, an immunosuppressive and pro-tumorigenic neutrophil type (N2) has been described previously (39). It features a reduction in Fas-ligand expression, down-regulation of the pathways associated with antigen processing, and a dependency on tissue growth factor beta (TGF-β) signaling (40, 41). Earlier, a similar neutrophil subset with T cell-suppressive properties had been described by Pillay et al. which was mainly based on CD16 and CD62L expression patterns along with nuclear morphology and suppression of T cell proliferation after stimulation with lipopolysaccharide (42). Interestingly, these populations also displayed differences in their survival time and ROS release. Lastly, neutrophils contribute to tissue repair and remodeling, as they produce not only matrix metalloproteinases (MMPs) removing tissue debris at the site of injury, but also tissue inhibitors of MMPs (TIMPs), preventing tissue damage by MMPs, as well as growth factors and pro-angiogenic factors (43). Indeed, a pro-angiogenic neutrophil subset has been observed in human healing wounds. It is characterized by the markers CXCR4, vascular endothelial growth factor receptor 1 (VEGFR1), and integrin alpha subunit

TABLE 1 | Overview of papers, which have described neutrophil subsets both by their marker expressions and their specific cell functions in the context of oral health and inflammation.

References	Neutrophil test populations, oral health status, and control samples	Neutrophil markers described in the test population	Functional properties of population
Wilton et al. (12)	Gingival crevicular fluid neutrophils from healthy donors vs. blood neutrophils	Defective or low CD35	Impaired phagocytosis
Van Dyke et al. (13)	Blood neutrophils from patients with aggressive periodontitis vs. periodontally healthy donors	$CD11b^{low}$	Impaired chemotaxis
Nemoto et al. (14)	Blood neutrophils from patients with aggressive periodontitis vs. periodontally healthy donors	$CD16^{low}$, $CD11a^{high}$, $CD11b^{high}$	Impaired chemotaxis
Miyazaki et al. (15)	Blood neutrophils from patients with chronic periodontitis vs. blood neutrophils	$CD16^{low}$, $CD32^{low}$	Impaired phagocytosis
Kobayashi et al. (16)	Blood neutrophils from patients with chronic periodontitis vs. periodontally healthy donors	CD16b allotype $NA2^{low}$	Impaired phagocytosis and ROS release in response to IgG-opsonized bacteria
Kobayashi et al. (17)	Gingival crevicular fluid neutrophils from patients with chronic periodontitis vs. blood neutrophils	$CD89^{high}$, $CD64^{high}$, $CD16b^{low}$, $CD32a^{low}$	Impaired phago-cytosis of IgG-opsonized bacteria
Fine et al. (18)	Oral neutrophils from patients with chronic periodontitis vs. Para1 and Para2 neutrophils	$CD10^{high}$, $CD63^{high}$, $CD64^{high}$, $CD66a^{high}$ $CD11b^{high}$, $CD18^{high}$, $CD55^{high}$	Increased phagocytosis, NET formation, ROS release, and degranulation
Fine et al. (18)	Oral neutrophils (Para2) from healthy donors vs. Para1 neutrophils	$CD55^{high}$, $CD63^{high}$, $CD170^{low}$, $CD16^{low}$, FSC-A^{low}, SSC-A^{low}	Increased phagocytosis, NET formation, and unstimulated ROS release
Rijkschroeff et al. (19)	Oral neutrophils from healthy donors vs. blood neutrophils	$CD16^{high}$, $CD11b^{high}$, $CD63^{high}$, $CD66b^{high}$	Increased unstimulated ROS release
Rijkschroeff et al. (20)	Oral neutrophils from edentulous donors vs. dentate donors with no or mild forms of periodontitis	$CD16^{high}$ $CD11b^{low}$, $CD63^{low}$, $CD66b^{low}$	Decreased unstimulated ROS release
Moonen et al. (21)	Oral neutrophils from healthy donors vs. blood neutrophils	$fMLPR^{low}$	Impaired chemotaxis, increased phagocytosis, and unstimulated NET release

Periodontitis in these studies was diagnosed according to the 1999 classification system (22).

CD49d. This subset represented ∼3% of total circulating neutrophils (44). These neutrophils produced significantly higher amounts of MMP-9 than pro-inflammatory neutrophils, which was thought to contribute extracellular matrix remodeling at these healing sites, rather than to the extracellular matrix damage mediated by activated inflammatory neutrophils (45).

POSSIBLE NEUTROPHIL SUBSETS IN PERIODONTAL HEALTH AND INFLAMMATION

Neutrophils have been identified by means of surface marker detection in high numbers in periodontal tissues (46), gingival crevicular fluid (GCF) (47) and in the oral cavity (24, 27). The presence of oral neutrophils in edentulous subjects has also been demonstrated, suggesting that neutrophils can transmigrate the oral mucosa directly (20). Neutrophils have also been identified within supragingival dental biofilms by means of their CD177 marker (48), indicating that oral PMNs are incorporated into oral biofilms. The functions of those neutrophil surface markers described in the context of periodontal diseases and lined out in **Table 1** are explained in **Table 2**.

Since the 1970s, neutrophil markers in relation to cell function have been investigated in the context of oral health and disease. In 1977, Wilton et al. discovered that only half of the GCF-derived neutrophils isolated from healthy donors expressed the complement receptor C3bR (CD35) and that this led to impaired phagocytosis compared to blood neutrophils (12). However, this assay was based on the assumption that zymosan particles had adsorbed complement factor C3b from serum rather than on identification of CD35. They also reported that the "Fc receptor system" was unimpeded. Later on, in 2000, Kobayashi et al. reported impaired phagocytosis and ROS release in response to IgG-opsonized *Porphyromonas gingivalis* and that these peripheral blood neutrophils from patients with periodontitis displayed a specific FcγRIIIb allotype (NA2) (16). They further reported that GCF-derived neutrophils from these patients had increased FcαRI and FcγRI levels and lower FcγRIIa and FcγRIIIb levels than blood neutrophils, leading to the same impairment of phagocytosis (15, 17).

A neutrophil subset with defective chemotaxis in aggressive periodontitis (Grade 3 periodontitis, according to the 2017 classification scheme (49) was described by Van Dyke et al. (13, 50). The marker, which was diminished on blood-derived neutrophils in these studies, was CD11b (formerly glycoprotein 110), a molecule associated with neutrophil adhesion. Interestingly, the same group reported a diminished capacity of the labeled chemotactic factor N-formylmethionyl-leucyl-phenylalanine (fMLP) to bind to neutrophils in individuals

TABLE 2 | Overview of the physiological functions of the neutrophil surface proteins and markers described in **Table 1**.

Neutrophil surface marker	Name of surface marker	Function of surface marker
CD10	Membrane metallo-endopeptidase	Cleaves peptides and inactivates several peptide hormones. Involved in neutrophil degranulation.
CD11a, CD11b	Integrin subunits alpha L and alpha M	Mediates leukocyte intercellular adhesion and trans-endothelial migration. Mediates adherence of neutrophils to stimulated endothelium, phagocytosis of complement-coated particles, and degranulation.
CD16	Fc fragment of IgG low affinity receptors IIIa and IIIb	Phagocytosis and clearing of antigen-antibody complexes. Only FcγRIIIb is expressed on neutrophils.
CD18	Integrin subunit beta 2	Combines with multiple different alpha chains to enable cell adhesion and cell-surface mediated signaling during immune responses and cell migration.
CD32, CD32a	Fc fragment of IgG low-affinity receptors II (general) and IIa	Phagocytosis and clearing of antigen-antibody complexes. FcγRIIa is found on phagocytic cells and co-regulates degranulation, FcγRIIb is expressed on B cells and FcγRIIc on a variety of immune cells.
CD35	Complement C3b/C4b receptor 1	Receptors of complement activation. Cellular binding to particles and immune complexes that have activated complement. Involved in neutrophil degranulation.
CD55	Decay accelerating factor for complement	Regulates the complement cascade. Binding to complement proteins accelerates their decay, thereby disrupting the cascade and reducing damage to host cells. Involved in neutrophil degranulation.
CD63	Tetraspanin-30	Mediates signal transduction in the regulation of cell development, growth and motility, and activation including degranulation. Forms complexes with integrins.
CD64	Fc fragment of IgG high-affinity receptor Ia	Phagocytosis and clearing of antigen-antibody complexes.
CD66a, CD66b	Carcinoembryonic antigen related cell adhesion molecule 1 and 8	Cell-cell adhesion, differentiation and arrangement of tissue structure, angiogenesis, apoptosis, tumor suppression, and modulation of immune responses including neutrophil degranulation.
CD89	Fc fragment of IgA receptor	Interacts with IgA-opsonized targets and triggers phagocytosis, antibody-dependent cell-mediated cytotoxicity, release of inflammatory mediators, and neutrophil degranulation.
CD170	Sialic acid binding Ig-like lectin 5	Inhibits the activation of several cell types including neutrophils, involved in cell adhesion, and neutrophil degranulation.
fMLPR (FPR)	Formyl peptide receptor	Receptor for formyl peptides including fMLP. Enhances neutrophil migration and degranulation.

Source: NCBI (25).

with periodontitis, although the receptors themselves appeared to be functional (51, 52). In line with this finding, a 1997 study by Nemoto et al. demonstrated that blood-derived neutrophils from a similar patient cohort had low CD16, but higher CD11b and CD11b expression levels, and also showed impaired chemotactic capabilities (14). An inability of blood neutrophils from periodontitis patients to migrate in a directional manner and an unresponsiveness to fMLP has also been described elsewhere (53). Furthermore, a hyperactive and hyper-reactive neutrophil phenotype has been reported previously by different groups (7, 54, 55), particularly with regard to ROS release. Although this phenotype has been attributed to higher levels of circulating bacterial products and pro-inflammatory cytokines originating from the periodontium, there is a possibility that these neutrophils may belong to a distinct subset as indicated by later studies, which are described below.

Technological developments over the past decades, particularly with regard to immunofluorescence and flow cytometry methods, have facilitated research of neutrophil markers and subsets, and have led to new insights in recent years. Much attention has been given to oral neutrophils isolated by means of mouth rinsing protocols. A large body of this work has been accomplished by Glogauer and co-workers, who compared neutrophil surface markers in oral and blood neutrophils, as well as in different health and disease states. In 2012, this group identified an oral neutrophil subset in healthy patients that expresses CD3, usually known as a T-cell receptor (56). Although specific interactions between neutrophils and T cells were not investigated in this paper, the finding corroborates the notion that neutrophils act as a bridge between the innate and adaptive immune systems. In 2016, they identified CD11b, CD16, and CD66b as markers that are consistently expressed on neutrophils independent of the cell location, level of activation and periodontal disease state (24), using high-throughput flow cytometry against a panel of 374 known CD antibodies. Furthermore, they newly identified neutrophil surface markers, which had not previously been described. These were CDw198 (C-C chemokine receptor 8), CDw199 (C-C chemokine receptor 9), CD322 (junctional adhesion molecule B, usually known to be localized at tight junctions of endothelial and epithelial cells and to be involved in adhesion and leukocyte transendothelial migration [(25) as well as CD328 sialic acid-binding Ig-like lectin 7, an adhesion molecule (25)].

In the same year, this group reported a CD marker signature indicative of cell activation, which was expressed at much higher levels on oral neutrophils in periodontitis than on healthy oral neutrophils, therefore allowing the distinction between para- and pro-inflammatory neutrophil subsets (18). The para-inflammatory phenotype was defined as neutrophils in an intermediary state that allows them to interact with the oral microflora without eliciting a marked inflammatory response, thus contributing to homeostasis.

The markers that were up-regulated on oral neutrophils of periodontitis patients were placed into three categories: markers of activation and degranulation (CD10, CD63, CD64, and CD66a), adhesion receptors (CD11b and CD18) and complement inhibitors (CD55).

The pro-inflammatory phenotype of periodontitis oral neutrophils was confirmed by elevated degranulation, phagocytosis, ROS production, and NET formation. In oral health, the authors observed two different populations of oral neutrophils. These differed in their size and granularity profile, in their expression of specific CD markers, production of ROS, and NET formation. The oral neutrophil phenotype present only in health had a forward scatter and side scatter profile similar to naïve blood neutrophils, and these cells were in a lower state of activation. At the same time, the other, more activated population showed higher expression of CD55 and CD63, whilst having decreased levels of inhibitory receptor CD170 and CD16. The authors concluded that a drop in CD16 in this population is likely a consequence of phagocytosis, and therefore is consistent with elevated phagocytic activity of this activated cell population.

Recently, in 2018, the same group reported that the surface expression of CD63, CD11b, CD16, and CD14 indicates an activation state in oral neutrophils (57), as the presence of these markers implies degranulation, adhesion and antigen recognition processes. They found that oral neutrophil activation was reduced in experimental gingivitis despite higher cell numbers, compared to those seen in health and during the resolution phase. Circulatory neutrophils, on the other hand, were shown to be activated during gingivitis onset as shown by the markers CD55, CD63, CD11b, and CD66a. Also in 2018, this group further characterized the morphology of the para-inflammatory health-associated phenotype described in 2016, and compared it to the naïve morphology of blood neutrophils as well as to the pro-inflammatory phenotype of oral neutrophils in periodontitis (58). They revealed that pro-inflammatory neutrophils in periodontitis showed less granulation, lighter cytoplasms and higher amounts of nuclear euchromatin, as assessed by electron microscopy, compared to the para-inflammatory oral health neutrophils. The periodontitis oral neutrophils also contained more phagosomes with and without undigested bacteria. Neutrophils in gingival tissues displayed naïve morphology when viewed in the blood vessels and gradually showed pro-inflammatory morphological changes as they traveled toward the epithelium.

Another group of researchers led by Nicu and Loos, have also been investigating oral neutrophils by their surface markers (19). They described that in oral neutrophils from healthy donors without additional stimulation, these cells were more activated than circulatory neutrophils, as indicated by higher expression of CD11b, CD63, and CD66b, and elevated constitutive ROS release. The authors concluded that oral neutrophils are in a more mature stage of their life cycle compared with peripheral blood neutrophils, but that they are still responsive to stimulation. Two years later, they published data regarding oral neutrophils from periodontitis patients, and reported that CD11b was elevated in these neutrophils compared to those from healthy controls (59), confirming results from the Glogauer group. Interestingly, this group also investigated oral neutrophils in edentulous patients and found that they expressed low levels of all three activation markers and low constitutive ROS release (20). In a recent publication, these researchers characterized oral neutrophils as terminally migrated cells and reported that oral neutrophils had lost their ability to migrate in a coordinated directional manner (21). They showed that the fMLP receptor, crucial for fMLP-mediated chemotaxis, was detectable in only half of the neutrophils, compared to blood neutrophils. They reasoned that the fMLP receptor was saturated with fMLP from the oral environment and that therefore neutrophils were desensitized to fMLP. In future studies, it would be interesting to investigate whether these receptors are indeed saturated or expressed to a lesser level, as this would give further hints toward a possible novel phenotype of oral neutrophils.

CONCLUSION

There is a multitude of reports confirming that blood, tissue, and oral neutrophils act in heterogeneous manners, and that different neutrophil populations and phenotypes exist. It is currently not clear, however, whether neutrophils of the periodontium and oral cavity express or lack certain surface markers in response to stimuli and activation, or whether true subsets exist that shape the specific response of these cells. For example, during the process of transmigration, neutrophils substantially alter their surface marker expression pattern toward higher expression of integrins, chemokines and proteases, and also show delayed apoptosis (10). In this context, the changes in these measurable markers is likely due to their momentary activity rather than reflecting a specific cell subset. At the same time, certain markers such as CD177 appear to be more influenced by the genetic background than by stimuli and cell function. It is also important to consider that oral neutrophils are terminally migrated cells, are under high osmotic stress conditions in saliva compared to blood (60) and are exposed to a high load of microbes, antigens and toxins. These conditions are likely to influence measurable neutrophil parameters, such as granularity, size, release of substances, and possibly the expression of surface markers.

On the other hand, in several systemic diseases, more evidence has been gathered with regard to the existence of true subsets. Studies in the context of oral health and inflammation need to be undertaken bringing together observations of distinct neutrophil populations, markers and behaviors. For example, future studies may be aimed at co-localizing specific CD markers and indicators of neutrophil activity, such as hyper-citrullinated histone for NET formation, or at investigating the influence of different stimuli that activate neutrophils upon the CD marker profile. In many previous studies, flow cytometry has been employed as the main method of neutrophil marker detection, which is a highly suitable tool for this type of research. However, few studies have reported these data in accordance with the MIFlowCyt guidelines proposed by Lee et al. (61). A lack of information regarding gating strategies, instrument settings, and color compensation

methods, makes it difficult to critically appraise these data and to reproduce experiments. Therefore, in future studies, these guidelines for reporting flow cytometry data should be adhered to by researchers, which can also help to make data from different research groups more comparable. This seminal field of research has the potential to identify neutrophil populations in the future, which could be utilized as targets in translational research and raise new therapeutic possibilities.

AUTHOR CONTRIBUTIONS

JH conceptualized and wrote the article, and prepared the tables.

FUNDING

This work was supported by the Academy of Medical Sciences (SGL019/1024).

REFERENCES

1. Barros SP, Williams R, Offenbacher S, Morelli T. Gingival crevicular fluid as a source of biomarkers for periodontitis. *Periodontology.* (2016) 70:53–64. doi: 10.1111/prd.12107
2. Brinkmann V, Reichard U, Goosmann C, Fauler B, Uhlemann Y, Weiss DS, et al. Neutrophil extracellular traps kill bacteria. *Science.* (2004) 303:1532–5. doi: 10.1126/science.1092385
3. Segal AW. How neutrophils kill microbes. *Ann Rev Immunol.* (2005) 23:197–223. doi: 10.1146/annurev.immunol.23.021704.115653
4. Nishinaka Y, Arai T, Adachi S, Takaori-Kondo A, Yamashita K. Singlet oxygen is essential for neutrophil extracellular trap formation. *Biochem Biophys Res Commun.* (2011) 413:75–9. doi: 10.1016/j.bbrc.2011.08.052
5. Palmer LJ, Cooper PR, Ling MR, Wright HJ, Huissoon A, Chapple IL. Hypochlorous acid regulates neutrophil extracellular trap release in humans. *Clin Exp Immunol.* (2012) 167:261–8. doi: 10.1111/j.1365-2249.2011.04518.x
6. Roberts H, White P, Dias I, Mckaig S, Veeramachaneni R, Thakker N, et al. Characterization of neutrophil function in Papillon-Lefevre syndrome. *J Leukoc Biol.* (2016) 100:433–44. doi: 10.1189/jlb.5A1015-489R
7. Matthews JB, Wright HJ, Roberts A, Cooper PR, Chapple ILC. Hyperactivity and reactivity of peripheral blood neutrophils in chronic periodontitis. *Clin ExpImmunol.* (2007) 147:255–64. doi: 10.1111/j.1365-2249.2006.03276.x
8. Kenny EF, Herzig A, Krüger R, Muth A, Mondal S, Thompson PR, et al. Diverse stimuli engage different neutrophil extracellular trap pathways. *eLife.* (2017) 6:e24437. doi: 10.7554/eLife.24437.032
9. De Bont CM, Koopman WJH, Boelens WC, Pruijn GJM. Stimulus-dependent chromatin dynamics, citrullination, calcium signalling and ROS production during NET formation. *Biochim Biophys Acta Mol Cell Res.* (2018) 1865:1621–9. doi: 10.1016/j.bbamcr.2018.08.014
10. Beyrau M, Bodkin JV, Nourshargh S. Neutrophil heterogeneity in health and disease: a revitalized avenue in inflammation and immunity. *Open Biol.* (2012) 2:120134. doi: 10.1098/rsob.120134
11. Garley M, Jabłonska E. Heterogeneity among neutrophils. *Arch Immunol Ther Ex.* (2018) 66:21–30. doi: 10.1007/s00005-017-0476-4
12. Wilton JM, Renggli HH, Lehner T. The role of Fc and C3b receptors in phagocytosis by inflammatory polymorphonuclear leucocytes in man. *Immunology.* (1977) 32:955–61.
13. Van Dyke TE, Wilson-Burrows C, Offenbacher S, Henson P. Association of an abnormality of neutrophil chemotaxis in human periodontal disease with a cell surface protein. *Infect Immun.* (1987) 55:2262–7.
14. Nemoto E, Nakamura M, Shoji S, Horiuchi H. Circulating promyelocytes and low levels of CD16 expression on polymorphonuclear leukocytes accompany early-onset periodontitis. *Infect Immun.* (1997) 65:3906–12.
15. Miyazaki A, Kobayashi T, Suzuki T, Yoshie H, Hara K. Loss of Fc gamma receptor and impaired phagocytosis of polymorphonuclear leukocytes in gingival crevicular fluid. *J Periodontal Res.* (1997) 32:439–46. doi: 10.1111/j.1600-0765.1997.tb00556.x
16. Kobayashi T, Van Der Pol WL, Van De Winkel JG, Hara K, Sugita N, Westerdaal NA, et al. Relevance of IgG receptor IIIb (CD16) polymorphism to handling of Porphyromonas gingivalis: implications for the pathogenesis of adult periodontitis. *J Periodontal Res.* (2000) 35:65–73. doi: 10.1034/j.1600-0765.2000.035002065.x
17. Kobayashi T, Yamamoto K, Sugita N, Van Spriel AB, Kaneko S, Van De Winkel JG, et al. Effective in vitro clearance of Porphyromonas gingivalis by Fc alpha receptor I (CD89) on gingival crevicular neutrophils. *Infect Immun.* (2001) 69:2935–42. doi: 10.1128/IAI.69.5.2935-2942.2001
18. Fine N, Hassanpour S, Borenstein A, Sima C, Oveisi M, Scholey J, et al. Distinct oral neutrophil subsets define health and periodontal disease states. *J Dent Res.* (2016) 95:931–8. doi: 10.1177/0022034516645564
19. Rijkschroeff P, Jansen IDC, Van Der Weijden FA, Keijser BJF, Loos BG, Nicu EA. Oral polymorphonuclear neutrophil characteristics in relation to oral health: a cross-sectional, observational clinical study. *Int J Oral Sci.* (2016) 8:191–8. doi: 10.1038/ijos.2016.23
20. Rijkschroeff P, Loos BG, Nicu EA. Impaired polymorphonuclear neutrophils in the oral cavity of edentulous individuals. *Eur J Oral Sci.* (2017) 125:371–8. doi: 10.1111/eos.12367
21. Moonen CG, Hirschfeld J, Cheng L, Chapple IL, Loos BG, Nicu EA. Oral neutrophils characterized: chemotactic, phagocytic, and neutrophil extracellular trap (NET) formation properties. *Front Immunol.* (2019) 10:635. doi: 10.3389/fimmu.2019.00635
22. Armitage GC. Development of a classification system for periodontal diseases and conditions. *Ann. Periodontol.* (1999) 4:1–6. doi: 10.1902/annals.1999.4.1.1
23. Peckham M, Knibbs A, Paxton S. *Histology Guide*. Universtiy of Leeds, UK: Faculty of Biological Sciences (2003). Available online at: https://www.histology.leeds.ac.uk/blood/blood_wbc.php (accessed December 06, 2019).
24. Lakschevitz FS, Hassanpour S, Rubin A, Fine N, Sun C, Glogauer M. Identification of neutrophil surface marker changes in health and inflammation using high-throughput screening flow cytometry. *Exp Cell Res.* (2016) 342:200–9. doi: 10.1016/j.yexcr.2016.03.007
25. NCBI (1988). *Gene*. Bethesda, MD: National Library of Medicine (US): National Center for Biotechnology Information. Available online at: https://www.ncbi.nlm.nih.gov/gene/ (accessed December 06, 2019).
26. Nakayama F, Nishihara S, Iwasaki H, Kudo T, Okubo R, Kaneko M, et al. CD15 expression in mature granulocytes is determined by alpha 1,3-fucosyltransferase IX, but in promyelocytes and monocytes by alpha 1,3-fucosyltransferase IV. *J Biol Chem.* (2001) 276:16100–6. doi: 10.1074/jbc.M007272200
27. Rijkschroeff P, Loos BG, Nicu EA. Oral polymorphonuclear neutrophil contributes to oral health. *Curr Oral Health Rep.* (2018) 5:211–20. doi: 10.1007/s40496-018-0199-6
28. Leliefeld PHC, Pillay J, Vrisekoop N, Heeres M, Tak T, Kox M, et al. Differential antibacterial control by neutrophil subsets. *Blood Adv.* (2018) 2:1344–55. doi: 10.1182/bloodadvances.2017015578
29. Naegelen I, Beaume N, Plançon S, Schenten V, Tschirhart EJ, Bréchard S. Regulation of neutrophil degranulation and cytokine secretion: a novel model approach based on linear fitting. *J Immunol Res.* (2015) 2015:817038. doi: 10.1155/2015/817038
30. Clemmensen SN, Bohr CT, Rørvig S, Glenthøj A, Mora-Jensen H, Cramer EP, et al. Olfactomedin 4 defines a subset of human neutrophils. *J Leukoc Biol.* (2012) 91:495–500. doi: 10.1189/jlb.0811417
31. Deniset JF, Kubes P. Neutrophil heterogeneity: Bona fide subsets or polarization states? *J Leukoc Biol.* (2018) 103:829–38. doi: 10.1002/JLB.3RI0917-361R
32. Minnema-Luiting J, Vroman H, Aerts J, Cornelissen R. Heterogeneity in immune cell content in malignant pleural mesothelioma. *Int J Mol Sci.* (2018) 19:1041. doi: 10.3390/ijms19041041
33. Goldschmeding R, Van Dalen CM, Faber N, Calafat J, Huizinga TW, Van Der Schoot CE, et al. Further characterization of the NB 1 antigen as a variably expressed 56-62 kD GPI-linked glycoprotein of plasma membranes

and specific granules of neutrophils. *Br J Haematol*. (1992) 81:336–45. doi: 10.1111/j.1365-2141.1992.tb08237.x
34. Carmona-Rivera C, Kaplan MJ. Low-density granulocytes: a distinct class of neutrophils in systemic autoimmunity. *Semin Immunopathol*. (2013) 35:455–63. doi: 10.1007/s00281-013-0375-7
35. El Kebir D, Filep JG. Targeting neutrophil apoptosis for enhancing the resolution of inflammation. *Cells*. (2013) 2:330–48. doi: 10.3390/cells2020330
36. Marwick JA, Mills R, Kay O, Michail K, Stephen J, Rossi AG, et al. Neutrophils induce macrophage anti-inflammatory reprogramming by suppressing NF-κB activation. *Cell Death Dis*. (2018) 9:665. doi: 10.1038/s41419-018-0710-y
37. Brezinski ME, Serhan CN. Selective incorporation of (15S)-hydroxyeicosatetraenoic acid in phosphatidylinositol of human neutrophils: agonist-induced deacylation and transformation of stored hydroxyeicosanoids. *PNAS*. (1990) 87:6248–52. doi: 10.1073/pnas.87.16.6248
38. Abdulnour R-EE, Dalli J, Colby JK, Krishnamoorthy N, Timmons JY, Tan SH, et al. Maresin 1 biosynthesis during platelet-neutrophil interactions is organ-protective. *PNAS*. (2014) 111:16526–31. doi: 10.1073/pnas.1407123111
39. Cuartero MI, Ballesteros I, Moraga A, Nombela F, Vivancos J, Hamilton JA, et al. N2 neutrophils, novel players in brain inflammation after stroke: modulation by the PPARγ agonist rosiglitazone. *Stroke*. (2013) 44:3498–508. doi: 10.1161/STROKEAHA.113.002470
40. Fridlender ZG, Sun J, Kim S, Kapoor V, Cheng G, Ling L, et al. Polarization of tumor-associated neutrophil phenotype by TGF-beta: "N1" versus "N2" TAN. *Cancer Cell*. (2009) 16:183–94. doi: 10.1016/j.ccr.2009.06.017
41. Prame Kumar K, Nicholls AJ, Wong CHY. Partners in crime: neutrophils and monocytes/macrophages in inflammation and disease. *Cell Tissue Res*. (2018) 371:551–65. doi: 10.1007/s00441-017-2753-2
42. Pillay J, Kamp VM, Van Hoffen E, Visser T, Tak T, Lammers J-W, et al. A subset of neutrophils in human systemic inflammation inhibits T cell responses through Mac-1. *J Clin Invest*. (2012) 122:327–36. doi: 10.1172/JCI57990
43. Wang J. Neutrophils in tissue injury and repair. *Cell Tissue Res*. (2018) 371:531–9. doi: 10.1007/s00441-017-2785-7
44. Massena S, Christoffersson G, Vagesjo E, Seignez C, Gustafsson K, Binet F, et al. Identification and characterization of VEGF-A-responsive neutrophils expressing CD49d, VEGFR1, and CXCR4 in mice and humans. *Blood*. (2015) 126:2016–26. doi: 10.1182/blood-2015-03-631572
45. Christoffersson G, Vagesjo E, Vandooren J, Liden M, Massena S, Reinert RB, et al. VEGF-A recruits a proangiogenic MMP-9-delivering neutrophil subset that induces angiogenesis in transplanted hypoxic tissue. *Blood*. (2012) 120:4653–62. doi: 10.1182/blood-2012-04-421040
46. Dutzan N, Konkel JE, Greenwell-Wild T, Moutsopoulos NM. Characterization of the human immune cell network at the gingival barrier. *Mucosal Immunol*. (2016) 9:1163–72. doi: 10.1038/mi.2015.136
47. Suzuki T, Sugita N, Yoshie H, Hara K. Presence of activated eosinophils, high IgE and sCD23 titers in gingival crevicular fluid of patients with adult periodontitis. *J Periodontal Res*. (1995) 30:159–66. doi: 10.1111/j.1600-0765.1995.tb01268.x
48. Hirschfeld J, Dommisch H, Skora P, Horvath G, Latz E, Hoerauf A, et al. Neutrophil extracellular trap formation in supragingival biofilms. *Int J Med Microbiol*. (2015) 305:453–63. doi: 10.1016/j.ijmm.2015.04.002
49. Caton JG, Armitage G, Berglundh T, Chapple ILC, Jepsen SS. A new classification scheme for periodontal and peri-implant diseases and conditions - Introduction and key changes from the 1999 classification. *J Clin Periodontol*. (2018) 45(Suppl 20):S1–8. doi: 10.1111/jcpe.12935
50. Van Dyke TE, Warbington M, Gardner M, Offenbacher S. Neutrophil surface protein markers as indicators of defective chemotaxis in LJP. *J Periodontol*. (1990) 61:180–4. doi: 10.1902/jop.1990.61.3.180
51. Van Dyke TE, Levine MJ, Tabak LA, Genco RJ. Reduced chemotactic peptide binding in juvenile periodontitis: a model for neutrophil function. *Biochem Biophys Res Commun*. (1981) 100:1278–84. doi: 10.1016/0006-291X(81)91962-8
52. Van Dyke TE, Zinney W, Winkel K, Taufiq A, Offenbacher S, Arnold RR. Neutrophil function in localized juvenile periodontitis. Phagocytosis, superoxide production and specific granule release. *J Periodontol*. (1986) 57:703–8. doi: 10.1902/jop.1986.57.11.703
53. Roberts HM, Ling MR, Insall R, Kalna G, Spengler J, Grant MM, et al. Impaired neutrophil directional chemotactic accuracy in chronic periodontitis patients. *J Clin Periodontol*. (2015) 42:1–11. doi: 10.1111/jcpe.12326
54. Fredriksson MI, Gustafsson AK, Bergstrom KG, Asman BE. Constitutionally hyperreactive neutrophils in periodontitis. *J Periodontol*. (2003) 74:219–24. doi: 10.1902/jop.2003.74.2.219
55. Johnstone AM, Koh A, Goldberg MB, Glogauer M. A hyperactive neutrophil phenotype in patients with refractory periodontitis. *J Periodontol*. (2007) 78:1788–94. doi: 10.1902/jop.2007.070107
56. Lakschevitz FS, Aboodi GM, Glogauer M. Oral neutrophils display a site-specific phenotype characterized by expression of T-cell receptors. *J Periodontol*. (2013) 84:1493–503. doi: 10.1902/jop.2012.120477
57. Wellappuli NC, Fine N, Lawrence HP, Goldberg M, Tenenbaum HC, Glogauer M. Oral and blood neutrophil activation states during experimental gingivitis. *JDR Clin Trans Res*. (2018) 3:65–75. doi: 10.1177/2380084417742120
58. Borenstein A, Fine N, Hassanpour S, Sun C, Oveisi M, Tenenbaum HC, et al. Morphological characterization of para- and proinflammatory neutrophil phenotypes using transmission electron microscopy. *J Periodontal Res*. (2018) 53:972–82. doi: 10.1111/jre.12595
59. Nicu EA, Rijkschroeff P, Wartewig E, Nazmi K, Loos BG. Characterization of oral polymorphonuclear neutrophils in periodontitis patients: a case-control study. *BMC Oral Health*. (2018) 18:149–149. doi: 10.1186/s12903-018-0615-2
60. Villiger M, Stoop R, Vetsch T, Hohenauer E, Pini M, Clarys P, et al. Evaluation and review of body fluids saliva, sweat and tear compared to biochemical hydration assessment markers within blood and urine. *Eur J Clin Nutr*. (2018) 72:69–76. doi: 10.1038/ejcn.2017.136
61. Lee JA, Spidlen J, Boyce K, Cai J, Crosbie N, Dalphin M, et al. MIFlowCyt: the minimum information about a Flow Cytometry Experiment. *Cytometry A*. (2008) 73:926–30. doi: 10.1002/cyto.a.20623

Conflict of Interest: The author declares that the research was conducted in the absence of any commercial or financial relationships that could be construed as a potential conflict of interest.

Advantages of publishing in Frontiers

OPEN ACCESS
Articles are free to read for greatest visibility and readership

FAST PUBLICATION
Around 90 days from submission to decision

HIGH QUALITY PEER-REVIEW
Rigorous, collaborative, and constructive peer-review

TRANSPARENT PEER-REVIEW
Editors and reviewers acknowledged by name on published articles

Frontiers
Avenue du Tribunal-Fédéral 34
1005 Lausanne | Switzerland

Visit us: www.frontiersin.org
Contact us: frontiersin.org/about/contact

REPRODUCIBILITY OF RESEARCH
Support open data and methods to enhance research reproducibility

DIGITAL PUBLISHING
Articles designed for optimal readership across devices

FOLLOW US
@frontiersin

IMPACT METRICS
Advanced article metrics track visibility across digital media

EXTENSIVE PROMOTION
Marketing and promotion of impactful research

LOOP RESEARCH NETWORK
Our network increases your article's readership